MITNE-182

Copy 5

CORE DESIGN FOR A SMALL HTGR

by

Arnaldo A.T. Ribeiro

David D. Lanning

Department of Nuclear Engineering
MASSACHUSETTS INSTITUTE OF TECHNOLOGY
138 Albany Street
Cambridge, Massachusetts 02139

October 1975

CORE DESIGN FOR A SMALL HTGR

by

Arnaldo Aloisio Telles Ribeiro

Submitted to the Department of Nuclear Engineering on
October 23, 1975 in partial fulfillment of the requirements
for the degree of Doctor of Philosophy

ABSTRACT

A conceptual design for a small (300 MWth) High Temperature Gas-Cooled Reactor (HTGR) total energy system was made to provide both heat and electricity to large U. S. Army bases by 1985. The major emphasis was on the nuclear design but thermal hydraulics and vessel internals were also discussed.

The economic ground rules for the fuel cycle cost calculation are quite different from those of commercial plants: the Army will not pay carrying charges on their fuel, will not receive credit for bred U^{233} and will pay consumed U^{235} after irradiation. Under those conditions the lowest fuel cycle cost corresponds to the longest possible batch.

The High Enrichment (HE) and Low Enrichment (LE) fuels were selected, among other possible options, for a more detailed investigation based on practical reasons; the HE fuel consists in a mixture of uranium containing 93% of U^{235} as the fissile material and Th^{232} as the fertile material; the LE fuel consists in uranium enriched in U^{235} (enrichments examined vary from 11 to 30%). A nuclear comparison between these two types of fuel under the same restrictions of maximum excess of reactivity and choice of burnable poison was made. The HE fuel was found to have two advantages for the present type of economy: a 43.4% longer batch and a 12.8% lower average consumption of U^{235} per day.

The HE chosen as the fuel to use in the Army HTGR, was optimized to a 4.8 full power year-batch. The control rod (CR) requirements were minimized to approximately one dollar reactivity per CR pair by optimizing the lumped burnable poison design and by using 12 extra CR pairs evenly distributed in the replaceable side reflector. To obtain such a long batch without reaching any of the coated fuel particle failure limits some special fuel configurations had to be developed. For the Final Reference Design, FRD, the simplest and less expensive configuration was chosen: a single fuel region core with the burnable poison in the bottom reflector.

Another configuration, called Parfait, consisting of having a fertile only region in the center of the otherwise single zone core and also containing LBP in the bottom reflector, was shown to permit a slightly longer batch (~4.5% longer) than the FRD. This is possible because its maximum fuel centerline temperature and fast neutron flux on the coated fuel particles are lower than those of the FRD. It is probable that an optimized Parfait configuration will be more economical than the FRD, but the advantage, if any, will be marginal and for a first batch the simplest design was prefered.

ACKNOWLEDGEMENTS

The author wishes to thank the expert guidance and kindness of his advisor, Professor D. D. Lanning.

Thanks are also due to Professor M. J. Driscoll, general manager of HTGR/GT project (and also reader of this thesis) who provided valuable assistance and discussions among other students on the project.

Computer calculations for this work were performed at the MIT Information Processing Center with financial support under a research contract between MIT and the U. S. Army. Mrs. Virginia Miethe Forsberg and Rachel Morton supplied assistance in communicating with the computer and Cindi Mitaras very ably handled the typing of this work.

Financial support by CNEN, Comissao Nacional de Energia Nuclear, Brazil, is sincerely acknowledged.

The author is also grateful to his wife, Denise, for her encouragement and companionship and also for her help in the preparation of the figures for this report.

TABLE OF CONTENTS

LIST OF TABLES

LIST OF FIGURES

CHAPTER I

INTRODUCTION

I.1 Foreword

Since June of 1974, MIT has been engaged in a sponsored research to develop a conceptual design of a small (~300 MWth) High Temperature Gas-cooled Reactor (HTGR) total energy system for the U. S. Army. The ground rules of the conceptual design state that the system is to start supplying both heat and electricity for large Army bases by 1985. This thesis project constitutes the part of the design research dealing with the reactor and with emphasis in the nuclear design. The design is described in sufficient depth to permit its use by the contracting agency as the basis for discussion with a reactor vendor.

As explained in Chapter 5 of the final report dated May 1975 (Ref.82), it was decided at the outset to specify Fort Saint Vrain (FSV) type fuel for the HTGR/GT(*) unit. The same practical reasons leading to this decision, i.e., commercial procedure and industrial base helped narrowing the options for the fuel-cycle and particle design. An essential feature of this HTGR/GT nuclear design is the fact that the Army does not pay carrying charges on their fuel; the optimum refueling interval becomes the longest possible, because, that minimizes shut down periods and consequently the fuel cycle cost of the plant.

By using nuclear methods and cross sections developed and validated by GA for the FSV core (modified to account for the HTGR/GT smaller carbon-to-uranium ratio) a reference design was developed for a 300 MWth HTGR batch

---

(*)High Temperature Gas-cooled Reactor/Indirect cycle Gas-Turbine (see Ref. 32).

core with enough reactivity for 4.8 full power years (6 calendar years assuming a 0.8 load factor).

There follows a summary description of the HTGR/GT reference design and the organization of this report.

1.2 Summary Description

The HTGR/GT is a high-temperature gas-cooled type of reactor cooled by helium, graphite moderated and using a U-235/Th fuel cycle. The core arrangement and fuel element are of the same basic design as in FSV. Table 1.2-1 gives a comparison of the important design and performance parameter in FSV and in the HTGR/GT.

1.2.1 Reactor Core

The reactor core consists of 133 fuel columns, each column is composed of 4 fuel elements together with top and bottom reflector elements. (1.5 elements in each reflector.) Surrounding the active core there are 48 columns of replaceable reflector elements and then the permanent reflector having the external side with a circular form concentric with the vessel (see Figure 1.2.1-1). The core is divided into 19 refueling regions consisting of a central control element column and 6 adjacent standard element columns (see Figure 1.2.1-2.) Core heat is removed by upward helium flow in the reflector and downward helium flow in the core. The coolant flow for each region of the core is adjusted by selective reduction of the coolant channel diameter of the upper 2/3 of the top reflector graphite blocks.

The fuel material is a mixture of 93.15% enriched uranium and thorium oxides in the form of small spheres ($\sim$700 μm) coated with the pyrolytic carbon and silicon carbide. The fuel particles are bonded together with a graphite binder to form fuel rods. The fuel rods are stalked and sealed in individual fuel holes in the graphite elements. The number of fuel and coolant holes in the elements is summarized in Table 1.2-1 and the matrix arrangement is shown in Figure 1.2.1-2.

TABLE 1.2-1

COMPARISON OF FSV AND HTGR/GT CORE DESIGN PARAMETERS

	FSV	HTGR/GT
Reactor core output, MW(Th)	851	300
Core dimensions, dia/ht,ft	19.5/15.6	14.3/10.4
Number of fuel elements/columns	1482/247	532/133
Primary coolant flow, 10 lbs/hr	3.39	0.8 x 2 = 1.6
Primary coolant inlet pressure, psig	688	394
Avg. coolant temp., reactor inlet, °F	762	953
Avg. coolant temp., reactor outlet, °F	1445	1500
Core orifices	37 variable	3 fixed orifice zones
Maximum fast fluence(E>0.18 Mev)10^{21} nvt	8	8
Avg. power density, watts/cc	6.3	6.34
Fuel life, full power years	4.8	4.8
Number of refueling regions	37	Batch refueled
Element (hexagonal prism): across flats/length, in	14.17/31.2	
Fuel holes per element, std/control	210/120	
Fuel hole diam., in	0.5	
Coolant channels per element, std/control	108/57	
Coolant channel dia., in	0.625	
Reflector thickness, cm. top/bottom/side	118.9/118.9/135.9	118.9/118.9/73.2
Max. fuel burnup, MWD/T	100,000	106 x 10^3
Max. fuel centerline temperature, °F	2300	2100

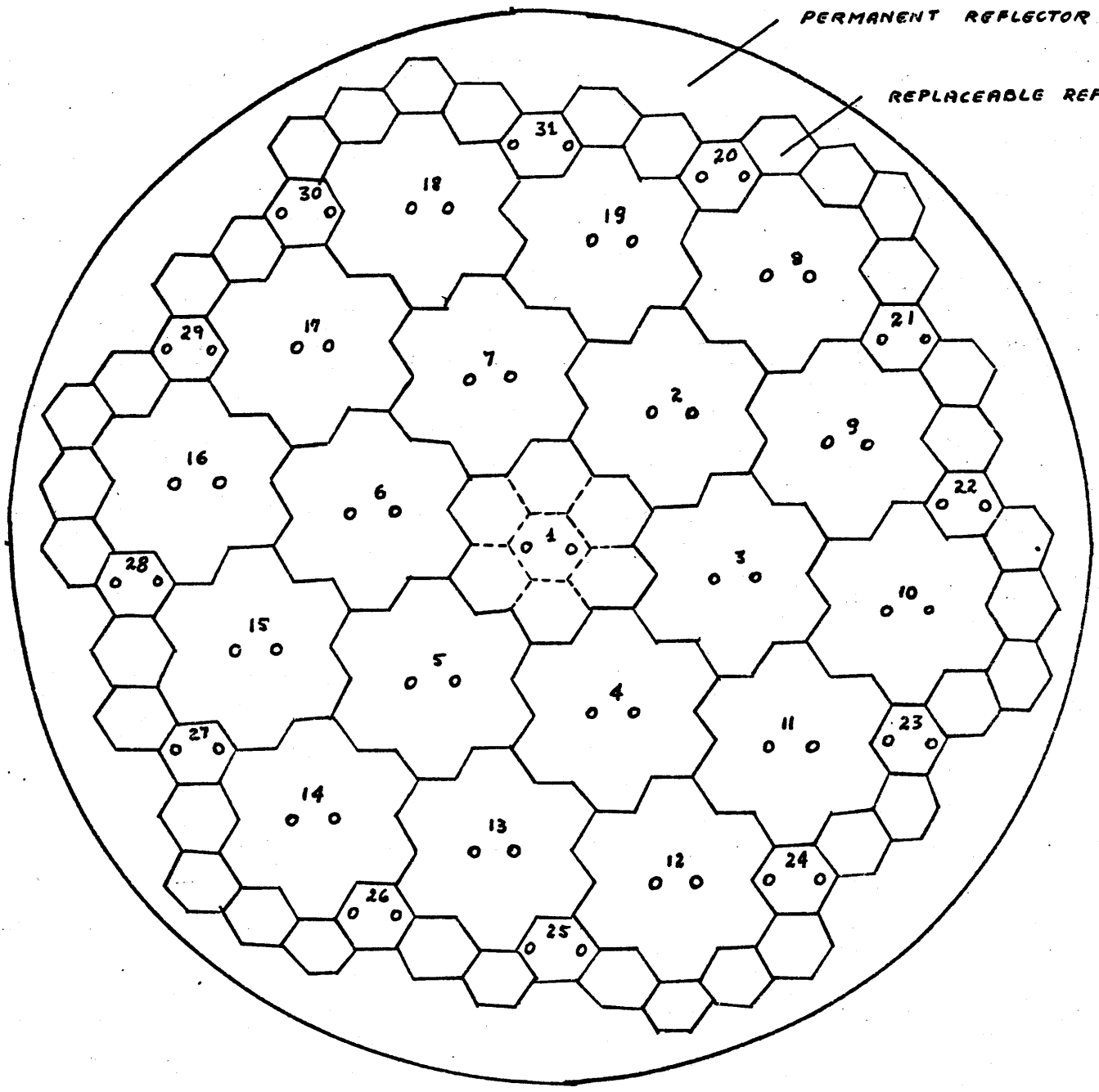

FIG. 1.2.1-1 HORIZONTAL SECTION THROUGH THE HTGR/GT CORE

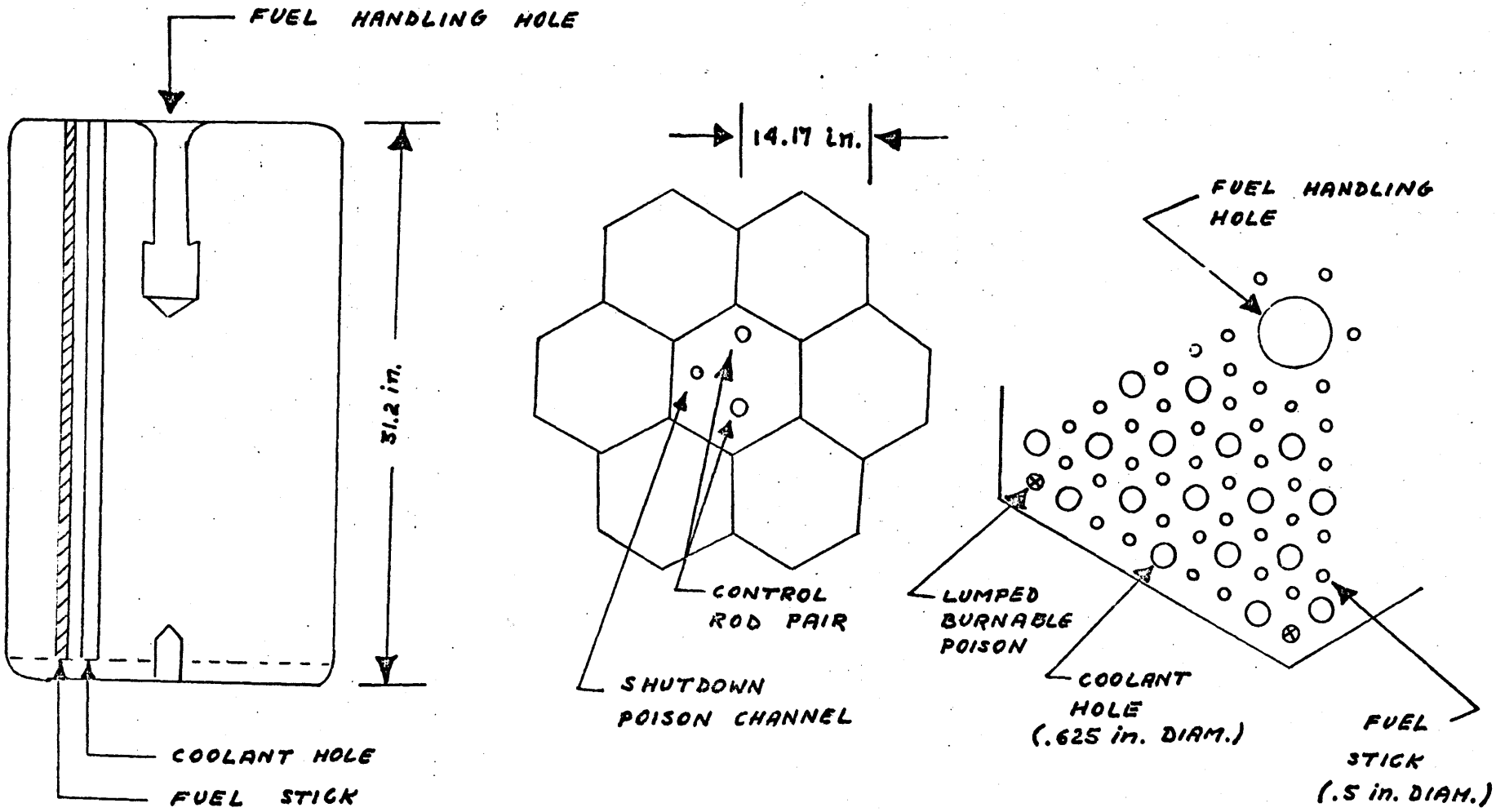

FIG. 1.2.1-2 FUEL ELEMENT DESIGN

1.2.2 Reactor Vessel Internals

The core is located and supported within the reactor vessel by three structures; the core support structure, the permanent side reflector and boronated shield, and the core lateral restrain structure (see Figure 1.2.2-1).

Each refueling region is supported by a single graphite core support block (see Figure 1.2.2-1), which is, in turn, supported by three graphite posts. The top and bottom ends of the posts have spherical seats to allow for differential horizontal movement.

The permanent side reflector is composed of graphite blocks shaped to make the transition from the removable hexagonal reflector blocks to the circular form of the thermal shield, insulation and vessel walls. The reflector's function is to reduce core neutron leakage and the fast flux and gamma exposure of the reactor vessel.

The thermal shield is a metal-clad boronated graphite assembly immediately surrounding the permanent side reflector; its function is to reduce the thermal neutron flux to the reactor vessel. The insulation function is to maintain the steel vessel wall temperature below 700°F.

The core lateral restraint structure has evenly spaced spring assemblies which span the thermal shield and the vessel walls. The spring assemblies keep the mass of graphite in the core, the core support floor, and the permanent side reflector firmly located in the core cavity. They also diminish the effects of seismic impact loads.

1.2.3 Reactivity Control Systems

Reactor control is provided by 62 control rods, (CR), operated in pairs by 31 control rod drives. The drives are located above the center

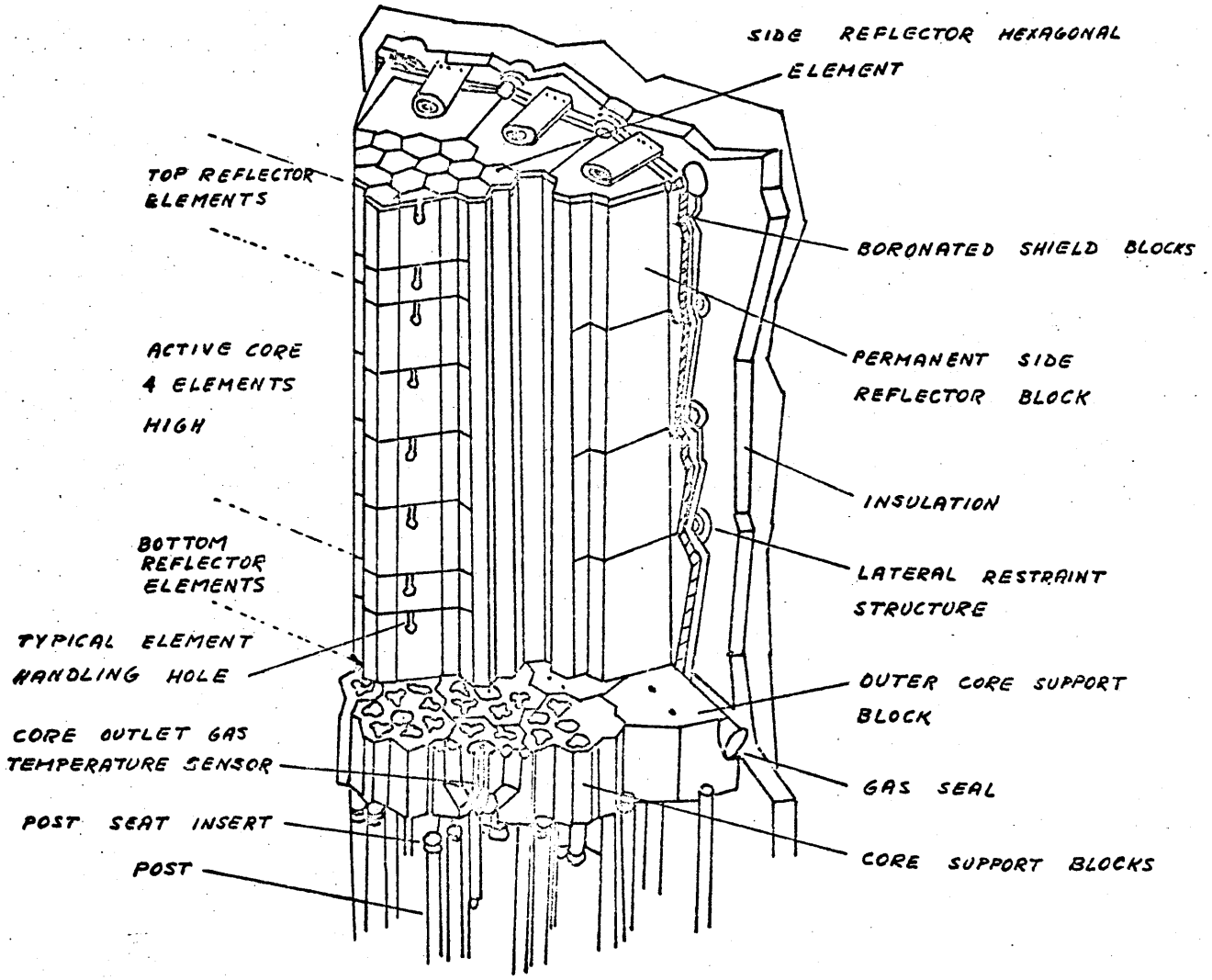

FIG. 1.2.2-1 HTGR/GT CORE ARRANGEMENT

column of each control element column; 19 in the 19 core refueling regions and 12 evenly spaced in the temporary reflector (see Figure 1.2.1-1). The CR drives can be hydraulic as used in Peach Bottom. The flexible cables and drumm employed in FSV are not adequate in a steel vessel design where blowdown conditions are much more severe than in PCRV design and the higher coolant velocities could damage the CR driven by flexible steel cables (see Section 6.2.3). Each individual CR is composed of articulated segments, each consisting of a metal container filled with boron carbide dispersed in a graphite matrix.

A manually actuated reserve shutdown system, utilizing boronated graphite spheres, is provided for back up shutdown capability. The spheres, which are contained in hoppers located in the refueling penetrations, are released into a channel in the control element column by rupture discs actuated by gas pressure. The reserve shutdown system is sufficient by itself to shut down the hot operating reactor to room temperature without the use of control rods.

1.3 Organization of this Report

This thesis project constitutes the part of the HTGR/GT design research dealing with the reactor and with emphasis in the nuclear design. It is organized in the following manner:

Chapter 1: This report is introduced. A summary description of the final design is given.

Chapter 2: The codes and calculational methods used are introduced and evaluated.

Chapter 3: A model is established for comparison between the High Enriched Uranium (HE) and Low Enriched Uranium (LE) fuel batches . The results favoring HE are checked against possible errors; sensitivity studies are made.

Chapter 4: The possible particle failure mechanisms and the HTGR/GT performance requirements are discussed. An accessment for a possible particle design is attempted.

Chapter 5: The nuclear design of the core is described and discussed in greater detail.

Chapter 6: Steel and prestressed concrete reactor vessel (PCRV) are compared. The internals design are discussed.

Chapter 7: Conclusions and Recommendations.

CHAPTER 2

CALCULATIONAL METHODS AND EVALUATIONS

The major emphasis of this thesis research project was on the core design; for that reason this chapter is divided in two sections: the first dealing with methods for the design of the core and the second with methods used outside the core.

2.1 Core Design Methods

The core design of a nuclear reactor is not a straightforward matter. It requires several interrelated steps in an iterative manner. Ideally one could identify the steps as in Table 2.1-1 (over simplified), but in practice not all the iteration can be included in order to speed up the results and be able to produce a reference design in a one year time required. For the HTGR/GT core design the following steps were made (organization by sections inside brackets).

1. Several fuel type possibilities were examined; the High Enrichment (HE) with thorium as a fertile fuel and Low Enrichment (LE) with U^{238} as the fertile fuel were selected for further investigation (see Chapter 3).

2. Two 4 group cs sets were obtained (see Section 2.1.1), one for HE and another for LE studies.

3. Two burnup codes were used at the initial stages of the HE vs LE comparison: CITATION (Ref. 10) and 2DB (Ref. 22). CITATION was found to be prefered (see Section 2.1.2). The abstracts and some input examples for those codes can be found in Appendix B.

TABLE 2.1-1

STEPS IN A CORE DESIGN

1. Identify suitable fuel cycles.
2. Obtain a cross section (cs) set for each of the fuel cycles. If using a small number of groups, 4 for instance, the cs sets will be quite sensitive to nuclides concentration (iterative), fuel rods size etc.
3. Choose a burnup code.
4. Establish a model for comparing the fuel cycles
5. With the help of the developed cs set and burnup code analyse the fuel cycles with the established model.
6. Study the sensitivity of results to possible errors in the cs sets or changes in the model. Decide in favor of one of the fuel cycles for more detailed analysis.
7. Optimize the core design for the chosen fuel observing the performance limits of the coated fuel particles (see Chapter 4).

4. A simple model to compare LE and HE was developed. For the same initial fissile inventory HE was shown to produce a higher reactivity lifetime (see Chapter 3) and chosen for more detailed analysis.

5. Some detailed calculations were made to compare the calculational methods with GA methods and experimental results. The FSV HTGR core design was used for the comparison and the GA results were reproduced within a very small error by using the 4 group HE cs set and CITATION (see Section 2.1.3). The successful completion of this step was taken to be proof that the calculational methods could be used for the detailed HTGR/GT core design optimization (Chapter 5).

2.1.1 Cross Section Sets

Ideally a cs set for each fuel type should have been obtained, but in practice that would have been too time consuming. In the HE case the only code available at MIT, the GGC-3 (Ref.101) is written for a UNIVAC machine and is not operable at MIT's IBM (several months would have been necessary to debug the code). In the LE case there are several codes available to obtain few group cs set: LEOPARD (Ref. 88), LASER (Ref. 89) and ANISN (Ref. 79). These codes can not be used for HE fuel because the resonance region for Th^{232} is different from that of U^{238} and the energy structure in them, chosen for good reproduction of U^{238} neutronic properties, is not adequate for Th^{232}.

Thanks to the cooperation of personnel from Dragon and GA "right from the shelve" LE and HE cs sets were available. Those cs sets were not completely appropriate to the HTGR/GT design; they were obtained for the fissile contents (or c/u ratio) typical of 1 year refueling intervals. Nevertheless they were acceptable for a preliminary design and the HE vs LE comparison described in Chapter 3 was carried with them. This approach was chosen for the most efficient use of the given time.

The HE fuel proved better than the LE one as expected from a previous bibliographic survey (Refs. 12, 48, 51 and 52) and the comparison is shown to be meaningful in section 2.1.1.2, despite its anavoidable inconsistencies.

The comparison was made then with:(a) the cs sets, at operating temperature, typical of 1000 MWe Dragon Project for LE and FSV (c/u=4000) for HE, see Section 2.1.1.1;(b) use of unselfshield natural B burnable poison in both cases;(c) unrodded single zone representation of the core in RZ geometry.

After the choice of the HE fuel, the following improvements were made on the HE cs set:

1. Correction for the HTGR/GT lower than FSV c/u ratio

The range of c/u ratios needed for the HTGR/GT batch studies goes from about 1200 to 2200. By inspection in the HE sets for c/u = 5000, and c/u = 4000 it was observed that the changes in cs for groups 1, 2 and 3 (fast groups) is very small or non-existant for all nuclides except for Th in the 2nd group, but in this only case the change was caused by

a difference in the Th concentration in the fuel rods of the c/u = 5000 and c/u = 4000 sets (changing the self-shielding factor);no changes were thought to be necessary then for groups 1, 2 and 3. It was also observed that there is an approximately 5% decrease in the thermal group cs (group 4) with the 20% decrease in c/u ratio (from 5000 to 4000) due to the spectrum hardening.

At first without available information a new set of thermal group cs at operating temperature was obtained by linear extrapolation to c/u = 1370 (see Table 2.1.1-1) and some runs with sensitivity purposes were prepared with those extrapolated cs (Chapter 3).

Some time later Dr. Marshall was consulted about this procedure and he offered to send an additional cs set for the range of c/u ratio needed for the HTGR/GT batch studies. No changes were necessary for groups 1, 2 and 3 and the changes for group 4 are summarized in Table 2.1.1-1. The σ_{f4}^{25} could always be taken for any c/u value from Fig. 5 of Ref. 26 (reproduced here as Fig. 2.1.1-1). The cs used in the detailed design described in Chapter 5 were those recommended in Dr. Marshall's letter.

2. Use of lumped burnable poison (LBP)

The B^{10} cs are used instead of those of natural B and a depletion varied self-shielding factor is applied (Section 2.1.3 and Chapter 5).

3. The control rod (CR) homogenized cs for FSV

The CR homogenized cs for the two types of CR used in FSV were obtained from GA (see Section 2.1.3) and used in some CR configuration studies described in Section 5.2.

TABLE 2.1.1-1

THERMAL GROUP CS'S CHANGED FOR THE DIFFERENT C/U

	Ref. 38 cs at oper. temp.		Our estimate	Dr. Marshall's letter for C/U=1800	
	C/U=5000	C/U=4000	hot C/U=1371	room temp.	oper. temp.
fission U235	193.409	184.431	160.828(*)	186.	158.
capture U^{235}	36.5109	34.9264	30.7607	34.35	29.93
fission U^{233}	236.089	233.738	227.557	-----	-----
capture U^{233}	27.6037	28.1339	29.5278	33.39	29.81
capture nat B	295.187	284.048	254.764	-----	-----
capture Th^{232}	2.68306	2.56462	2.25324	2.600	2.190
capture B^{10}	1490.91	1434.64	-----	1457	1257
capture Xe^{135}	9.65579×10^5	8.94178×10^5	-----	1.028×10^6	$.6645 \times 10^6$
capture Sm^{149}	2.79655×10^4	2.60679×10^4	-----	2.892×10^4	1.987×10^4

(*) By linear extrapolation. From Fig. 2.1.1-1 this value is 151 barns

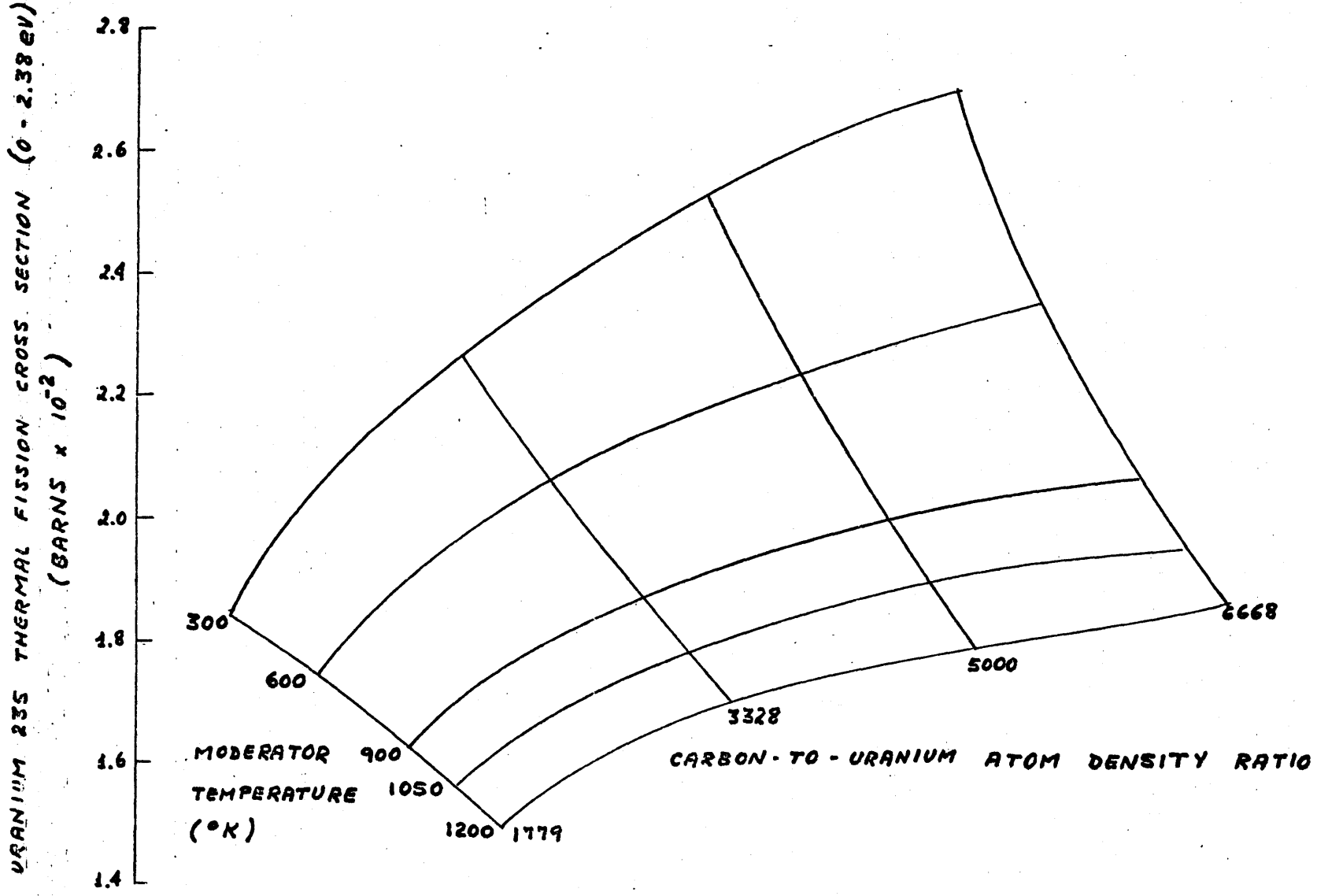

FIG. 2.1.1-1 EFFECTIVE URANIUM-235 THERMAL FISSION CROSS SECTION

The following is a description and an evaluation of the two cs sets as used in the comparison in Chapter 3. The sensitivity of results to errors in the sets is also studied in Chapter 3.

2.1.1.1 Description of the cs sets

HE cs set:

The HE cs set (Ref. 38) is a 4 group set for 2 c/u ratios (5000 with $(N_{Th})_{rod}$ = 1.25 x 10^{-3} atoms/bcm, typical of Fulton and 4000 with $(N_{Th})_{rod}$ = 1.5 x 10^{-3} atoms/lb cm ,typical of FSV at 300°K (room) and at 1060°K (operating). The structure of the groups is compared to that of the LE set in Table 2.1.1.1-1 and the nuclides included are compared to those included in the LE set in Table 2.1.1.1-2. The set was generated at GA by the code GGC-5 using basic data from a GAM data tape for fast group and a GATHER data tape for the thermal (Ref. 26).

LE cs set:

The LE cs set is a 4 group set for a typical mid-cycle composition for the 1000 MW dragon project at operating temperature. The energy structure of the groups and the nuclides included are summarized respectively in Tables 2.1.1.1-1 and 2.1.1.1-2.

2.1.1.2 Evaluation of the cs sets

For a meaningful comparison between HE and LE the two respective cs sets must be equivalent or near equivalent. The sense of the word "equivalent" employed here will become clearer as the reader progresses through this section.

TABLE 2.1.1.1-1

ENERGY STRUCTURE OF THE HE AND LE 4-GROUP CS SETS

Group	HE	LE
1	E > .183 MeV	E > .183 Mev
2	17.6 eV < E < .183 MeV	961 eV < E < .183 MeV
3	2.38 eV < E < 17.6 eV	1.86 eV < E < 961 eV
4	E < 2.38 eV	E < 1.86 eV

TABLE 2.1.1.1-2

NUCLIDES IN THE HE AND LE CS SETS

Category	Common nuclides	Only in He	Only in LE
Fissile	U^{235}, Pu^{239}, Pu^{241}	U^{232}, U^{233}	---
Fertile	U^{238}, Pu^{240}	Th^{232}, U^{234}	---
Intermediate	Np^{239}	Pa^{233}, Pa^{231}	
Other	U^{236}, Pu^{242}, N_p^{237}, nat B	B^{10}	O, Dummy mat.
Structural	C, Si, CREF	----	----
Fission Products	Mo^{95}, Tc^{99}, Rh^{103}, Xe^{131}, Xe^{135}	NSAG23	Kr^{83}, Zr^{95} dummy
	Cs^{133}, Nd^{143}, Nd^{145}, Pm^{147}, Pm^{148} Sm^{149}, Sm^{150}, Sm^{151}, Sm^{152}, Eu^{153} Eu^{154}, Eu^{155}	NSAG25	Mo^{97}, Ru^{101} Rh^{105}, Pd^{105} Pd^{108}, Ag^{109}, Cd^{113} I^{131}, Xe^{133}, Cs^{134} Xe^{136}, Pr^{141}, Pr^{143} Nd^{144}, Nd^{146}, Sm^{147} Sm^{148}, Gd^{155}, Gd^{156} Gd^{157}, FP U^{235} chain 40

In the LE fuel most of the fast absorption is in the U^{238} resonance region and in the HE fuel it is in the Th^{232} resonance region. For that reason the cs for those two nuclides are treated quite differently in the LE and HE cs sets. On the other hand if one performs a depletion calculation in a batch not having U^{238} and Th^{232} the results should be the same if the two sets are equivalent.

With regard to U^{238} and Th^{232}, their absorption cs are multiplied by a self-shielding factor (U^{238} in the LE and Th^{232} in the HE cs sets). The method used to determine the self-shielding factors must be shown to be equivalent in the two sets (see Section 2.1.1.2.1). The other point where an equivalence can be checked is the scattering matrix, in which case Age theory consistency was tested. The results and comments for the performed tests are summarized in the subsections that follow.

2.1.1.2.1 Testing the Self-Shielding Equivalence

The equivalence test that follows is based on a semi empirical method to predict resonance self-shielding of heavy nuclides developed in Ref. 60; from this Ref. 60, the effective resonance integral (RI_{eff}) is given by:

$$RI_{eff} = [1 - f(Z,N)]RI_{\infty} + f(Z,N)RI_{\infty}\left[1 + \frac{NR}{S/4V}\right]^{-1/2} , \quad (2.1.1.2.1\text{-}1)$$

where:

$f(Z,N)$ = .95 for U^{238} and Th^{232} (resolved fraction of the resonance integral),

RI_{∞} = $\begin{cases} 272 \text{ barns for } U^{238} \\ 77 \text{ barns for } Th^{232} \end{cases}$ Infinite resonance integral,

$\left[1 + \frac{NR}{S/4V}\right]^{-1/2}$ = self-shielding factor applicable to the resolved part of the resonance integral,

R = $\begin{cases} 11600 \text{ barns for } U^{238} \\ 3800 \text{ barns for } Th^{232} \end{cases}$ pseudo resonance parameter,

N = nuclide number density (U^{238} or Th^{232}) in the fuel rod,

S = external area of the fuel rod, and

V = volume of the fuel rod

The values of RI_{eff} and N/S/4V for FSV and Dragon are calculated in Table 2.1.1.2.1-1.

It can be easily shown that the resonance integral in a lethargy interval Δu is given by $\sigma \Delta u$. The self-shielding factors used in the LE and HE cs sets can then be checked against the values calculated in Table 2.1.1.2.1-1:

a) LE: The resolved resonance region of U^{238} is from 1.86 eV to 961 eV ($\Delta u = 6.25$) which corresponds to group 3 in the LE set; the U^{238} abs. cs for this group (From Ref. 39) is 10.171 barns $\therefore$ Resolved part of RI_{eff} = (10.171 barns)(6.25) = 63.57 barns.

b) HE: The resolved resonance region of Th^{232} is from 17.6 eV to 961 eV ($\Delta u = 4$) which corresponds to part of group 2 in the HE set; the Th^{232} abs. cs in this region can be taken from Fig. 3 of Ref. 26 as 8.75 barns (see Fig. 2.1.1.2.1-1): Resolved part of RI_{eff} = (8.75 barns)(4) = 35 barns.

The values of RI_{eff} for the resolved part of the resonance region used by GA and Dragon are larger than the ones given in Table 2.1.1.2.1-1 as calculated by the method in Ref. 60. The ratios of calculated values

Table 2.1.1.2.1-1 N/S/4V for FSV and Dragon

	FSV	Dragon
N, atoms/barn cm (Th^{232} or U^{238})	1.5×10^{-3}	1.355×10^{-3}
D, Fuel pin diam., in./cm	.491/1.247	.551/1.4
N/S/4V = ND, atoms/barn	1.871×10^{-3}	1.897×10^{-3}
Resolved part of RI_{eff}, barns	29.36	53.87

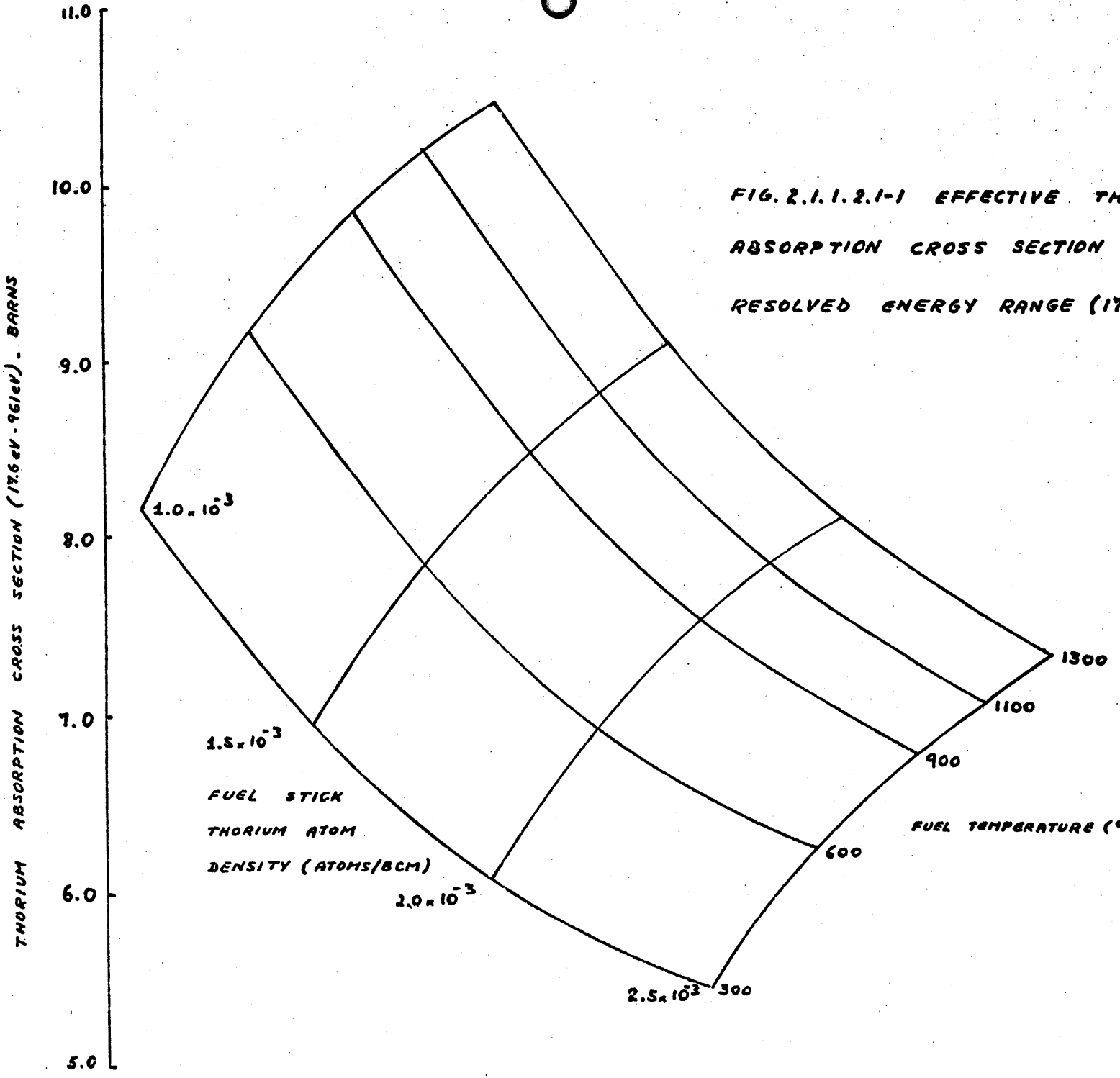

FIG. 2.1.1.2.1-1 EFFECTIVE THORIUM ABSORPTION CROSS SECTION IN THE RESOLVED ENERGY RANGE (17.6 TO 961 eV)

are 63.57/53.87 = 1.18 for Dragon and 35129.36 = 1.192 for FSV. This comparison indicates that the self-shielding methods used by GA and Dragon are equivalent.

2.1.1.2.2 Testing the Scattering Matrix Equivalence

In a 4 group structure, only downscattering from group i to group i + 1 is considered in the scattering matrix. In this case Fermi Age Theory yields:

$$\sigma_{i,i+1} = (\xi/\Delta u_i)\ \sigma_{si} \qquad (2.1.1.2.2\text{-}1)$$

Since ξ = .158 for carbon independently of fuel type or group, it can be written

$$(\sigma_{i,i+1}\ \Delta u_i/\sigma_{si})_{LE} \equiv (\sigma_{i,i+1}\ \Delta u_i/\sigma_{si})_{HE} \quad . \qquad (2.1.1.2.2\text{-}2)$$

This equivalence is not verified for groups 2 and 3 (see Table 2.1.1.2.2-1). The reason is that Age theory is not valid in energy ranges of strong absorption. The LE resonances in group 3 and the HE resonances in group 2 decrease the relative scattering probability making $(\sigma_{i,i+1}\Delta u_i/\sigma_{si}) < .158$. In group 1, that includes the source, $(\sigma_{1,2}\ \Delta u_1/\sigma_{s1}) > .158$ but the LE and HE values are equivalent. The equivalence of the total effect of groups 2 and 3 can be approximately checked by collapsing them into a single group called (2+3) scattering to group 4:

$$\sigma_{(2+3),4} = (\xi/\Delta u_{(2+3)})\ \sigma_{s(2+3)}, \qquad (2.1.1.2.2\text{-}3)$$

TABLE 2.1.1.2.2-1

DOWNSCATTERING CS CHECK UP

	LE					HE				
i	ΔU_i	$\sigma_{i,i+1}$	$\sigma_{i,i}$	σ_{Si}	$(\sigma_{i,i+1}\Delta U_i/\sigma_{Si}$	ΔU_i	$\sigma_{i,i+1}$	$\sigma_{i,i}$	σ_{Si}	$(\sigma_{i,i+1}\Delta U_i/\sigma_{Si})$
1	4.406	.1950	2.656	2.851	.3014	4.406	.1967	2.668	2.865	.3025
2	5.249	.1372	4.466	4.603	.1565	9.249	.0626	4.605	4.668	.1240
3	6.247	.0999	4.610	4.710	.1325	2.001	.3664	4.383	4.750	.1544
2 + 3	11.496	.0641	4.597	4.661	.1580	11.250	.0658	4.617	4.683	.1580
4	--	--	4.700	4.700	--	--	--	4.614	4.614	--

$$\sigma_{s(2+3),4} = \frac{\int_{2+3} \sigma_s(E)\phi(E)dE}{\int_{2+3}\phi(E)dE} \simeq \frac{\int_{2+3} \sigma_s(E)\frac{dE}{E}}{\int_{2+3}\frac{dE}{E}} = \frac{\sigma_{s2}\,\Delta U_2 + \sigma_{s3}\,\Delta U_3}{\Delta U_2 + \Delta U_3} \quad , \qquad (2.1.1.2.2\text{-}4)$$

$$\sigma_{(2+3),(2+3)} = \sigma_{s(2+3)} - \sigma_{(2+3),4} \quad . \qquad (2.1.1.2.2\text{-}5)$$

The conclusion is then that the scattering matrices are equivalent in the LE and HE sets.

It is important to mention that a mistake was found in the HE scattering matrix in Ref. 38. In this reference there is a complete scattering matrix for graphite including upscattering from group 4 to 3; in Ref. 26 it was said that in a 4 group structure GA did not use upscattering. Asked about this inconsistency by the phone, Dr.Davison from GA informed that Ref. 38 was in error. For the reasons to be explained in Appendix B an effective downscattering cs from group 2 to 3 was defined as

$$(\sigma_{23})_{eff} = \sigma_{23}^{Ref.38} + \sigma_{43}^{Ref.38}\,(\phi_4/\phi_2), \qquad (2.1.1.2.2\text{-}6)$$

and σ_{43} was eliminated. From the cs in Ref. 38 and using a typical $\phi_4/\phi_2 = .39$:

$$(\sigma_{23})_{eff} = 6.07321 \times 10^{-2} + (4.69641 \times 10^{-3}) \times (.39) = 6.25637 \times 10^{-2} \text{ barns};$$

this is the value used in Table 2.1.1.2.2-1.

2.1.1.2.3 Depletion runs without U^{238} and Th^{232}

The use of depletion runs without U^{238} and Th^{232} helped in the detection of input errors in the initial stages of the project. The final results of the CITATION runs are summarized in Table 2.1.1.2.3-1.

Table 2.1.1.2.3-1 Depletion Results Without U^{238} and Th^{232}

Time (days)	N_{25} in 10^{-5} nuc/bcm		N_B in 10^{-5} nuc/bcm		N_{Xe} in 10^{-10} nuc/bcm		k_{eff}	
	LE	HE	LE	HE	LE	HE	LE	HE
0	4.86		1.709		3.5		1.2538	1.2857
100	4.617	4.621	1.620	1.627	3.800	3.754	1.2069	1.2491
360	3.994	4.008	1.394	1.417	3.557	3.514	1.1560	1.2043
720	3.141	3.166	1.076	1.118	3.080	3.040	1.0896	1.1437

This Table clearly shows that the two sets are not equivalent. At BOL when only U^{235}, not B, C, Si and Xe are present, $(k_{eff})_{HE} - (k_{eff})_{LE} = + 0.03190$; after 720 days of operation and with F.P. build up this difference increased to + 0.05409 despite the fact that the LE nat. B conc. became lower than that of the HE set (the differences found in N_{25} and N_{xe} have a too small effect to be considered here).

The use of constant with time nat. B abs. cs in the HE vs LE comparison described in Chapter 3 (the B cs's in the two sets were at first thought to be averaged in time effective values but they were really unself-shielded nat. B abs. cs) was a mistake. If we neglect the small abs. in B^{11} the nat. B abs. cs for group i is given by

$$\sigma_{ai}^{B} = \frac{N_{B10}\,\sigma_{ai}^{B10}}{N_{B10} + N_{B11}} \qquad (2.1.1.2.3\text{-}1)$$

As B^{10} is being depleted it is obvious that σ_{ai}^{B} should decrease; the correct procedure, would have been to calculate σ_{ai}^{B10} from Eq. (2.1.1.2.3-1) and use always N_{B10} and σ_{ai}^{B10} in any depletion calculation. The effect of this mistake in the k_{eff} vs time curve can be seen in Fig. 2.1.3.3-3. For the HE vs LE comparison this error is of little importance since both types of run had it. In Table 2.1.1.2.3-2 the percent absorption in each nuclide in the HE and LE runs without U^{238} and Th^{232} is shown.

It is probable that the nat. B absorption cs's in the LE set are slightly high (explaining $(k_{eff})_{LE} < (k_{eff})_{HE}$ at BOL and $(N_B)_{LE} < (N_B)_{HE}$ with depletion) and that some differences in the FP treatments are responsible for the higher k_{eff} decrease rate with time in the LE runs. The depletion runs without U^{238}, Th^{232} and nat. B (see Table 2.1.1.2.3-3) present further evidence of this.

TABLE 2.1.1.2.3-2

PERCENT ABSORPTION IN LE AND HE RUNS WITHOUT U^{238} AND Th^{232} AFTER 990 DAYS (INITIAL CONC. OF TABLE 2.1.1.2.3.-1)

	% absorp. LE	% absorp. HE
U235	57.49	60.68
U236	2.90	2.81
NP237	0.79	0.69
BORON	21.63	22.46
CARBON	0.85	0.79
SILICON	0.40	0.43
XE148	1.69	1.84
SM149	1.26	1.60
XE133	2.25	---
NSAG25	---	0.76
FIS PRO-40	0.33	---
All others	10.55	7.94
Total abs. in FP	16.03	12.14

TABLE 2.1.1.2.3-3

DEPLETION RESULTS WITHOUT U^{238}, Th^{232} AND NAT. B

Time	N_{25} in 10^{-5} nuc/bcm		N_{xe} in 10^{-10} nuc/bcm		k_{eff}	
(days)	LE	HE	LE	HE	LE	HE
0	.4000		3.5		1.216168	1.198740
100	.2020	.2020	3.191	3.037	1.082805	1.108994

Even though the cs sets differ, as shown in Chapter 3, the difference favoring HE is larger than the inherent differences between the sets. Thus sufficient information was obtained to choose the HE fuel and proceed with the HE set detailed adjustment, described in Section 2.1.3, for the final nuclear design described in Chapter 5. Nevertheless several trials to adjust the LE cs to reproduce HE results were made. Some of those trials are important for the sensitivity studies and are described in Appendix C.

2.1.1.2.4 Conclusions

The self-shielding of the fertile materials was found to be equivalent in LE and HE within the uncertainties of the method employed. The scattering matrix can also be considered equivalent with due allowance for Fermi Age Theory lack of precision in the presence of neutrons sources or sinks.

The runs without U^{238} and Th^{232} and those without U^{238}, Th^{232} and nat. B can not be considered equivalent in the LE and HE sets. In part this inconsistency can be attributed to the fact that the spectrom in those runs is very much different from the spectrum used to calculate the HE and LE cs sets. In fact, even for the complete runs the cs sets are not completely adequate because the c/u ratio had been decreased in relation to that of the original sets to increase the reactivity lifetime. Anyway the difference found between the sets is smaller than the difference favoring the HE fuel.

2.1.2 Burnup Code

The burnup code completely adequate to our problem and operable at MIT is CITATION (Ref. 10). Because 2DB (Ref. 22) is an easier code to use and requires less memory it was decided to analyze the possibility of its employment.

Although the 2DB code is a code specifically written for fast reactor burnup calculations it could be used with some minor input tricks (see Appendix B) in the preliminary static runs to determine range of compositions for the HTGR/GT. In the depletion runs there was a large difference between the 2DB and CITATION results. The reason was that 2DB uses a lumped fictitious fission product, not having any provision for yields from fission. No input trick could be found to compensate for the absence of regular fission products and the idea of using 2DB was abandoned. CITATION was the code used in all burnup calculations included in this report.

2.1.3 Comparison with Some of GA Results on the FSV Design

After having established the calculational methods it is necessary to determine how well they can be expected to calculate the power distribution and k_{eff} of the rodded core and the unrodded k_{eff} variation with depletion. The tools to be used are: CITATION, the four group HE cs set (with homogenized CR cs) and the CITATION resonance shielding correlation (NS = 10 in Section 000 for the LBP). It was decided to check these methods by trying to reproduce some of GA calculations for the FSV design; specifically GA reference design 12 calculations were used for this check up. The calculations necessary to the CITATION input preparations are developed in Appendix A.

2.1.3.1 Relative Power Density Distribution per Region Comparison

The relative power density per region, represented in Fig. 2.1.3.1-1, was obtained by GA for one certain HM leading, CR configuration and lumped burnable poison (LBP) distribution as specified in Appendix A.1. Each interior hexagonon in this figure represents a fuel region composed of seven hexagonal prisms as shown in Fig. 2.1.3.1-2. A more detailed cross sectional view of the FSV core, which has been used as the bases for the calculations, is shown in Fig. 2.1.3.1-3. It was possible to obtain the relative power density distribution for 3 different assumptions relative to the LBP (see Appendix A.1); the results are compared to those of GA in Table 2.1.3.1-1.

2.1.3.2 Relative Axial Power Profile Comparison

For exactly the same core description originating Fig. 2.1.3.1-1 the relative axial power profile as determined by GA is shown in Fig. 2.1.3.2-1.

The FSV core was represented in RZ geometry for a CITATION input as in Fig. 2.1.3.2-2. The appropriate compositions and dimensions were determined in Appendix A.2 and are summarized in Table 2.1.3.2-1.

The most important results in the computer output are:

1. k_{eff} = .99474 (the corresponding xy value for LBP2 was k_{eff} = 1.0187 as in Table 2.1.3.1-1)
2. The average power densities in each zone. Knowing the volumes of each zone the power produced in the upper and lower halves of the core can be determined and compared with GA's value from Table A.1-2 in Table 2.1.3.2-2.

KEY :

TOP - CR - CONTROL ROD INSERTED

MIDDLE - REGION NUMBER

BOTTOM - RELATIVE POWER DENSITY

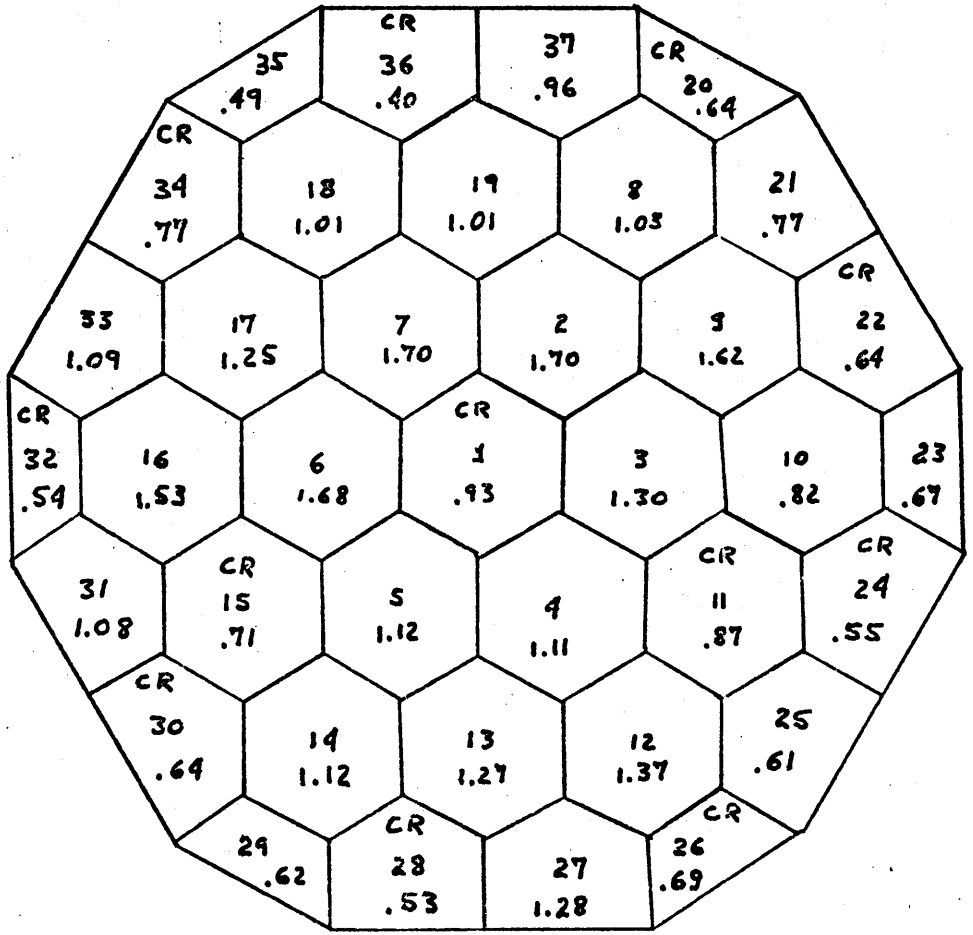

FIG. 2.1.3.1-1 FSV RELATIVE POWER DISTRIBUTION PER REGION

ONE CENTRAL CONTROL ELEMENT : 120 FUEL HOLES , 57 COOLANT CHANNELS
SIX ADJACENT STANDARD ELEMENTS : 210 FUEL HOLES , 108 COOLANT CHANNELS EACH

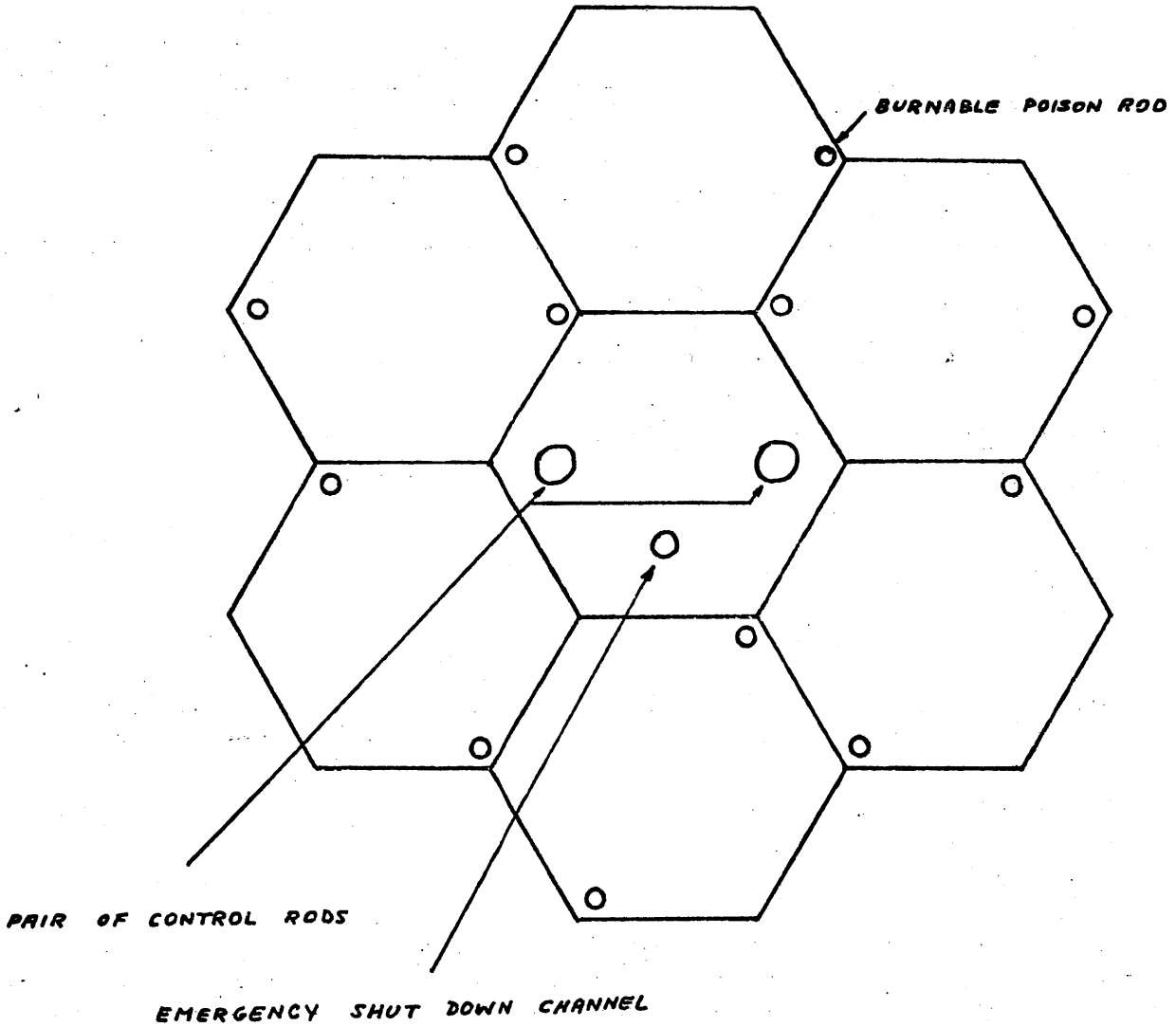

FIG. 2.1.3.1-2 FSV FUEL REGION

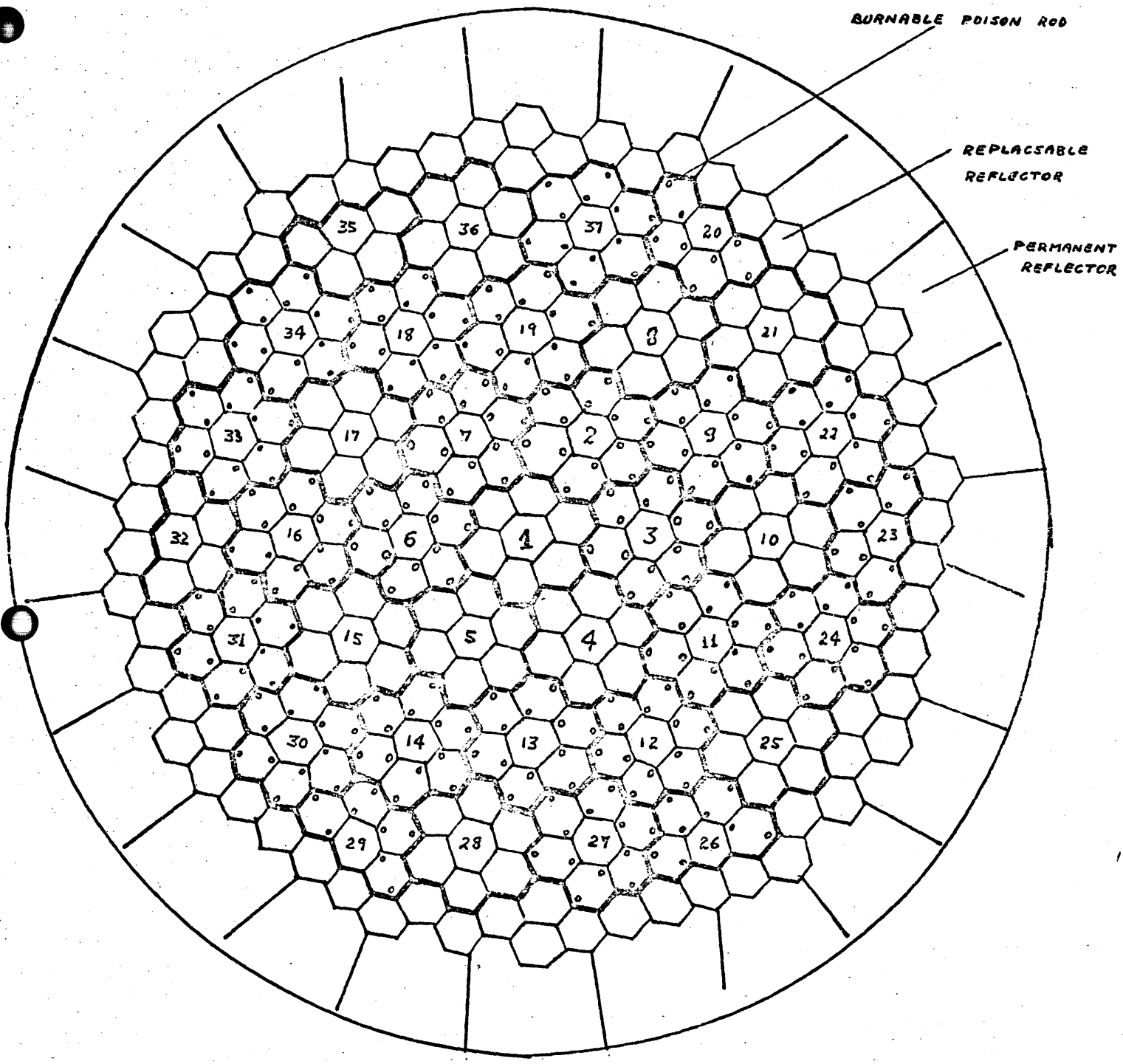

FIG. 2.1.3.1-3 FSV CORE CROSS SECTION VIEW

TABLE 2.1.3.1-1

RADIAL POWER DISTRIBUTION AND k_{eff} COMPARISON WITH GA VALUES FROM FIG. 2.1.3.1-1

	LBP1	LBP2	LBP3	GA
k_{eff}	1.0092	1.0187	1.00962	1.0039
Relative power in internal region				
1	.85 G	.86 G	.87 G	.93
2	1.71 G	1.75 G	1.73 G	1.70
3	1.32 G	1.34 G	1.33 G	1.30
4	1.12 G	1.10 G	1.11 G	1.11
5	1.06 G	1.05 G	1.07 G	1.12
6	1.67 G	1.70 G	1.70 G	1.68
7	1.65 G	1.70 G	1.68 G	1.70
8	1.10 G	1.09 G	1.11 G	1.03
9	1.74 G	1.75 G	1.75 G	1.68
10	.74 G-F	.73 G-F	.73 G-F	.82
11	.87 G	.87 G	.87 G	.87
12	1.64 F-B	1.60 F	1.57 F	1.37
13	1.34 G	1.32 G	1.31 G	1.27
14	1.01 G-F	1.01 G-F	1.01 G-F	1.12
15	.63 F	.63 F	.64 G-F	.71
16	1.64 G	1.66 G	1.66 G	1.53
17	1.24 G	1.27 G	1.29 G	1.25
18	.90 F	.92 G-F	.92 G-F	1.01
19	.97 G	1.00 G	.99 G	1.01
Rating:				
G=good agreement less than 10% misfit	14G, 2G-F 2F, 1F-B	14G, 3G-F 2F	14G, 4G-F 1F	
F = fair, from 10% to 20% misfit				
B = bad, misfit larger than 20%				

Table 2.1.3.1-1 (Continued)

Relative power in periphery regions:	LBP1	LBP2	LBP3	GA
20	.79 F-B	.76 F	.77 F	.64
21	.78 G	.76 G	.77 G	.77
22	.57 G-F	.58 G-F	.58 G-F	.64
23	.56 F	.55 F-B	.55 F-B	.67
24	.49 F	.50 G-F	.50 G-F	.55
25	.67 G	.63 G	.63 G	.61
26	.93 B	.88 B	.85 F-B	.69
27	1.45 F	1.40 G-F	1.36 G	1.28
28	.47 G-F	.46 G-F	.46 G-F	.53
29	.53 F	.53 F	.53 F	.62
30	.53 F-B	.55 F	.55 F	.64
31	1.06 G	1.06 G	1.06 G	1.08
32	.59 G	.58 G	.58 G	.54
33	1.09 G	1.11 G	1.11 G	1.09
34	.69 G-F	.72 G	.72 G	.77
35	.42 F	.42 F	.43 F	.49
36	.34 F	.35 F	.35 F	.40
37	1.01 G	1.00 G	1.01 G	.96

Ratings in periphery	6G; 3G-F; 6F 2F-B; 1B	7G; 4G-F; 5F 1F-B; 1B	8G; 3G-F; 5F 2F-B
Total ratings	20G; 4G-F; 8 F 3F-B; 1B	21G; 7G-F; 7F; 1F-B; 1B	22G; 7G-F; 6F 2F-B

FIG. 2.1.3.2-1 FSV RODDED AXIAL POWER DISTRIBUTION AT BOL WITH 13 CONTROL ROD PAIRS COMPLETELY INSERTED

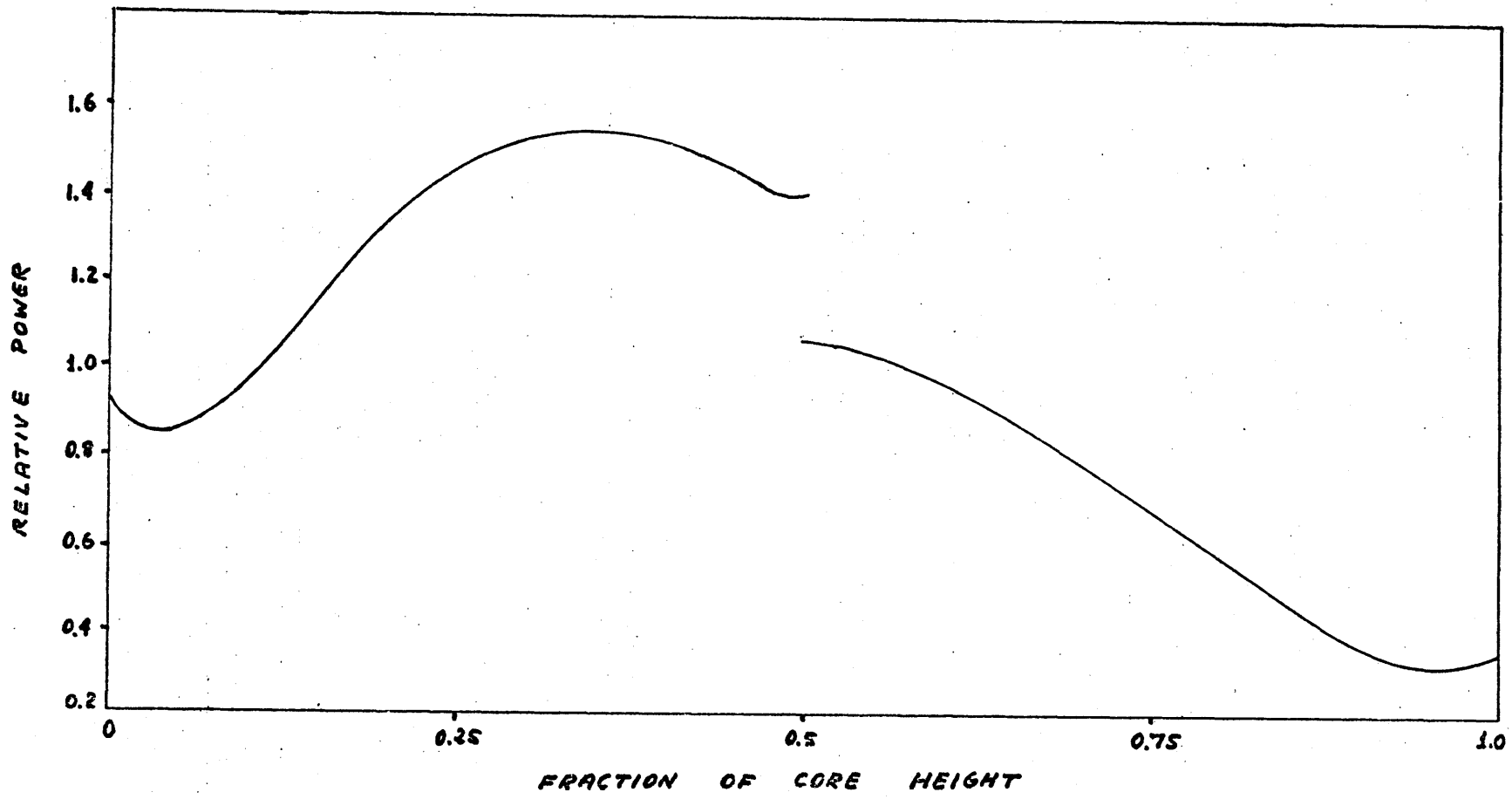

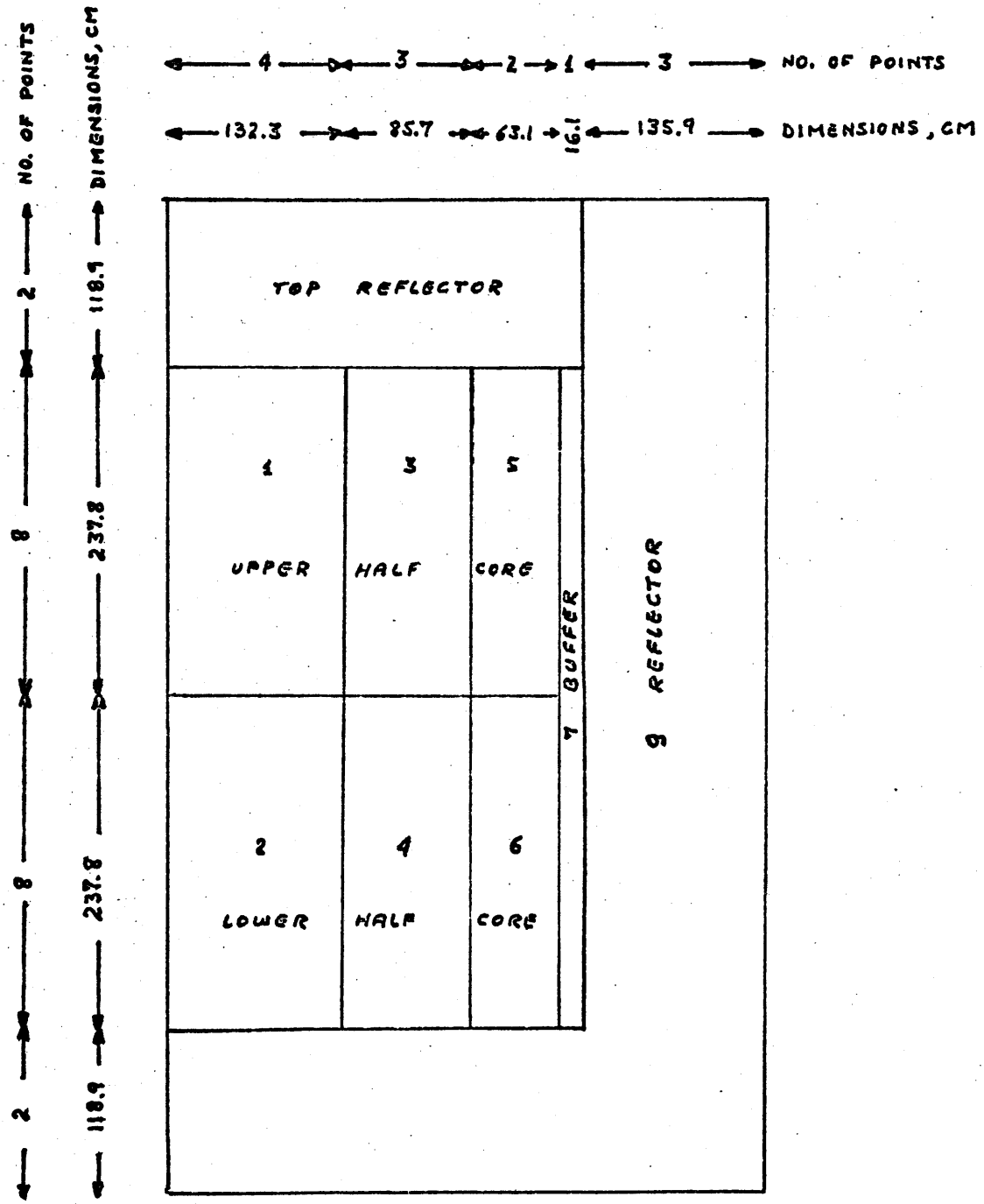

FIG. 2.1.3.2-2 FSV CORE REPRESENTATION IN RZ GEOMETRY

TABLE 2.1.3.2-1

NUCLIDE ATOMIC DENSITIES PER ZONE IN FIG. 2.1.3.2-2, 10^{-5} ats/bcm

Zone	N_C	N_{Si}	N_{25}	N_{28}	N_{02}	N_{B10}^{LBP2}	N_{CR1}	N_{CR2}
1	6190.	73.7	1.434	.1066	32.37	.01665	3.271	--
2	6190.	73.7	1.065	.0791	28.15	.01665	3.271	--
3	6190.	73.7	1.590	.1181	32.55	.01942	5.725	--
4	6190.	73.7	1.180	.0877	28.45	.01942	5.725	--
5	6190.	73.7	1.878	.1396	34.65	.02470	--	9.674
6	6190.	73.7	1.417	.1053	30.72	.02470	--	9.674
7	6190.	73.7	.8664	.0644	32.38	--	--	24.56
8	8594.	--	--	--	--	--	22.9	--
9	8876.	--	--	--	--	--	--	--

TABLE 2.1.3.2-2

POWER PRODUCTION IN THE UPPER AND LOWER HALVES OF THE FSV CORE

	Zone	Volume in 10^6cc	Power density w/cc	Total power in each half, MW Our results	GA
UPPER HALF	1	13.08	13.81		
	3	22.43	9.53	540.3	566.3
	5	23.53	5.68		
	half 7	6.96	1.80		
LOWER HALF	2	13.08	7.56		
	4	22.43	5.18	301.7	275.7
	6	23.53	3.15		
	half 7	6.96	1.80		

3. Point power densities at 16 axial locations for several radial positions. The relative average axial power distributions could then be obtained and is compared with that of Fig. 2.1.3.2-1 in Fig. 2.1.3.2-3.

2.1.3.3 Reactivity Variation with Depletion Curves Comparison

For the same core description, i.e. Figs. 2.1.3.1-1 and 2.1.3.2-1, except for the CR's, the unrodded k_{eff} variation as a function of operating time as determined by GA, is shown in Fig. 2.1.3.3-1.

The FSV core was represented in RZ geometry for a CITATION input as in Fig. 2.1.3.3-2 with the initial composition as in Table 2.1.3.3-1. The appropriate dimensions and compositions were easily deduced from those in Fig. 2.1.3.2-1 and Table 2.1.3.2-1. Nevertheless several trials were necessary before a satisfactory match between our results and those of GA could be obtained. The most important of those trials are summarized below and compared to GA's results in Fig. 2.1.3.3-3:

Curve 1

Calculated by using basically the same data used in the HE vs LE batch comparison given in Chapter 3.

Curve 2

Calculated by using unshielded nat. B as in Curve 1 but correcting the FP chain specifications of Pm, Sm and Eu (See Fig. 2.1.3.3-4).

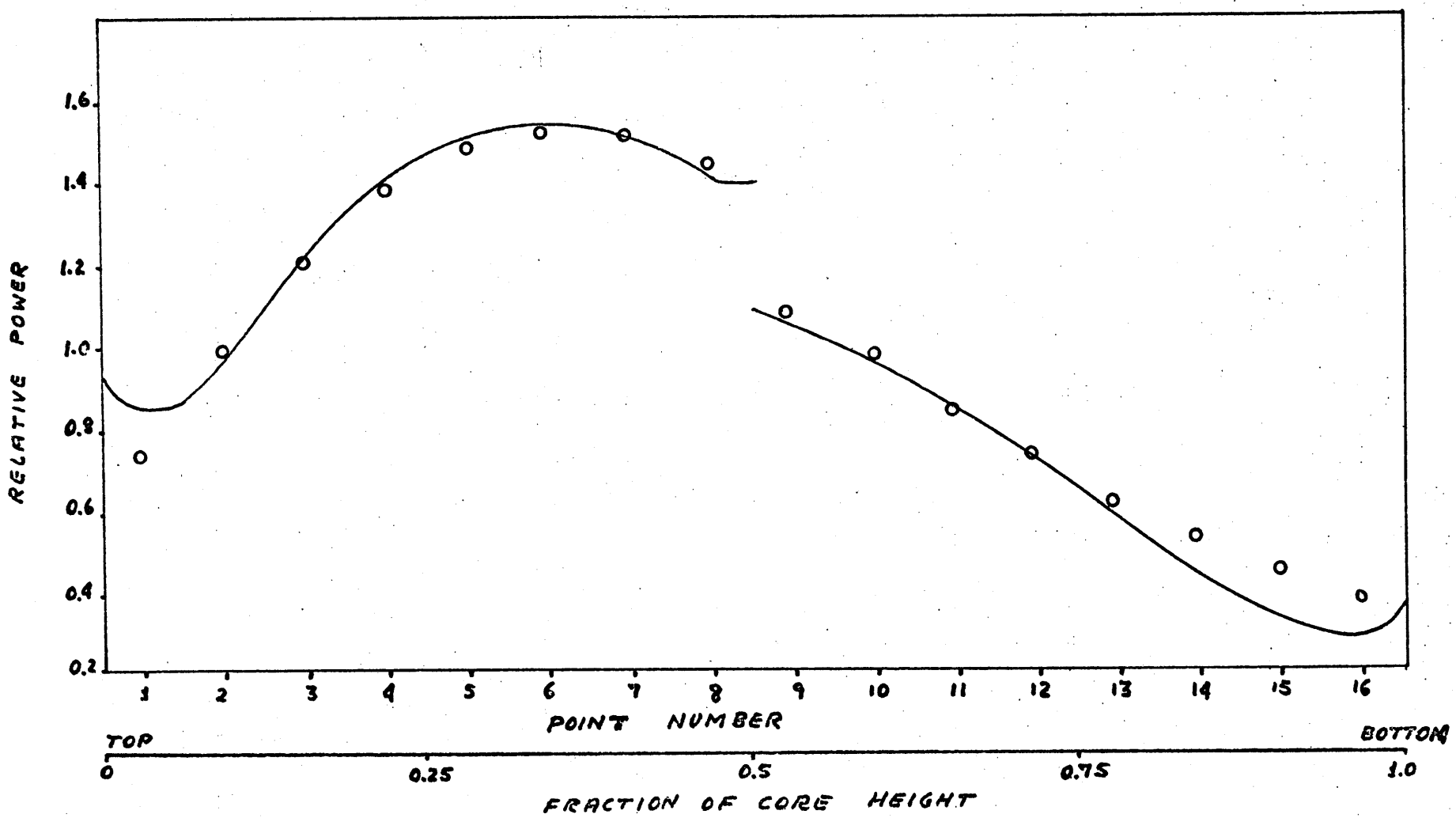

FIG. 2.1.3.2-3 FSV RELATIVE AXIAL POWER DISTRIBUTION OBTAINED AT MIT

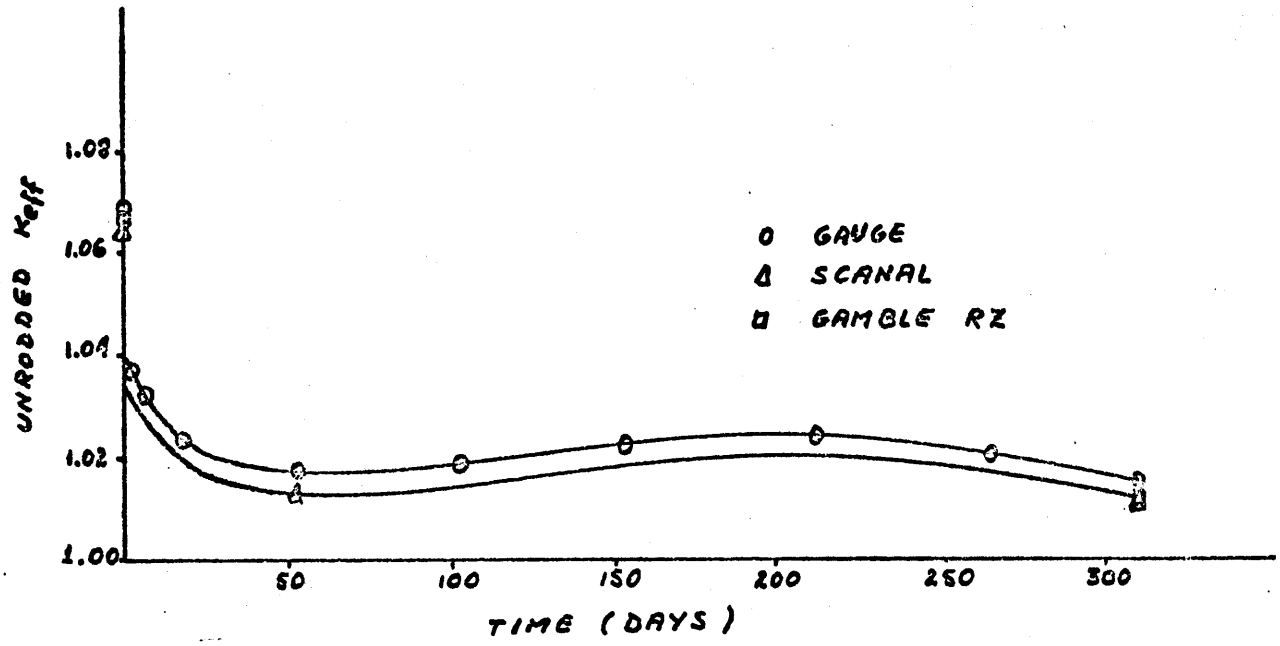

FIG. 2.1.3.3-1 FSV K_{eff} VS. TIME FOR THE UNRODDED CORE

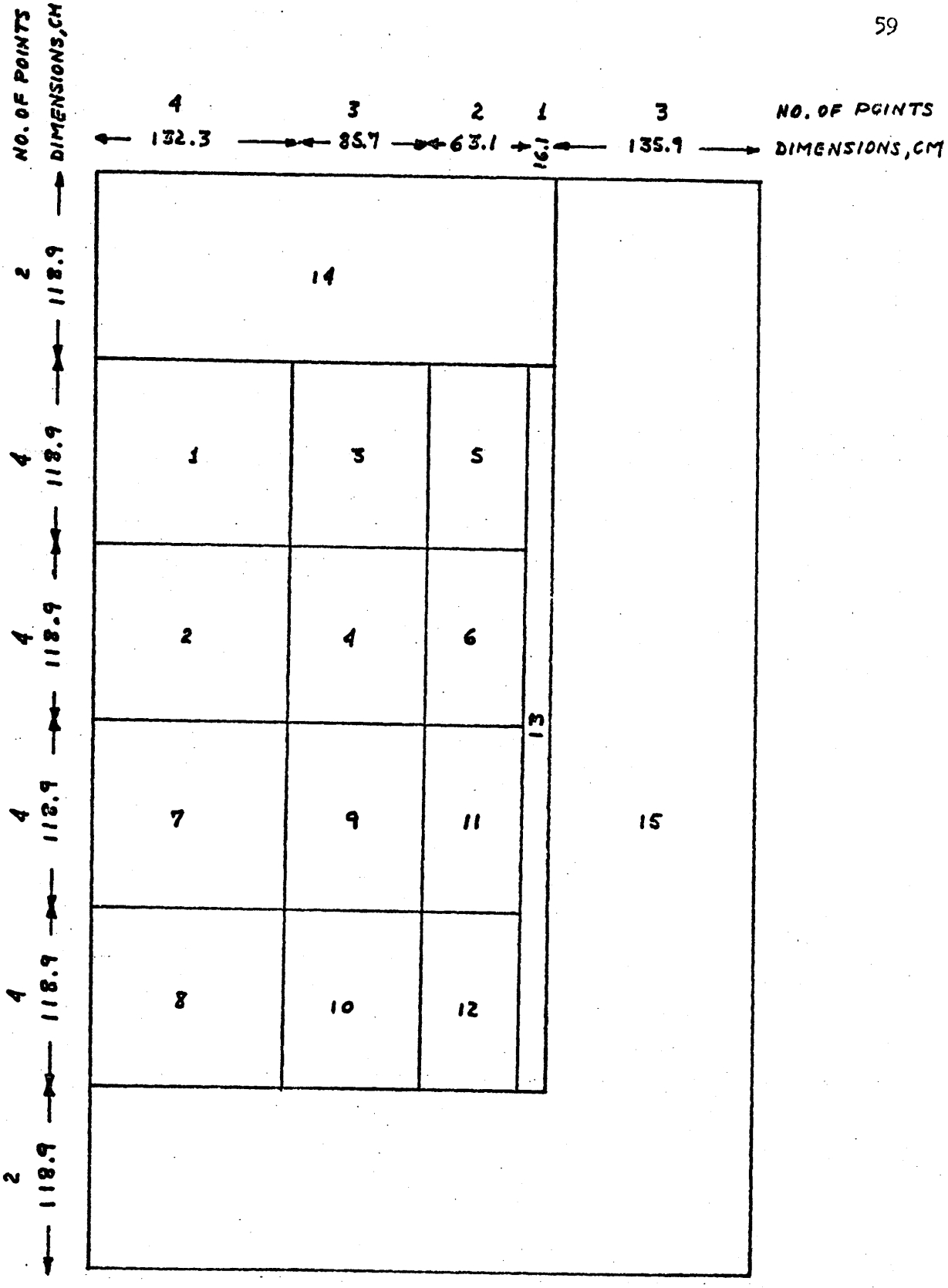

FIG. 2.1.3.3-2 FSV CORE REPRESENTATION IN RZ GEOMETRY FOR CITATION DEPLETION RUNS

TABLE 2.1.3.3-1

NUCLIDE ATOMIC DENSITIES PER ZONE IN FIG. 2.1.3.3-2, 10^{-5} ATOM/BCM

Zone	N_C	N_{Si}	N_{25}	N_{28}	N_{02}	N_{B10}^{LBP2}	N_{CR1}	N_{CR2}
1,2	6190.	73.7	1.434	.1066	32.37	.01665	3.271	--
7,8	6190.	73.7	1.065	.0791	28.15	.01665	3.271	--
3,4	6190.	73.7	1.590	.1181	32.55	.01942	5.725	--
9,10	6190.	73.7	1.180	.0877	28.45	.01942	5.725	--
5,6	6190.	73.7	1.878	.1396	34.65	.02470	--	9.674
11,12	6190.	73.7	1.417	.1053	30.72	.02470	--	9.674
13	6190.	73.7	.8664	.0644	32.38	--	--	24.56
14	8594.	--	--	--	--	--	22.9	--
15	8876.	--	--	--	--	--	--	--

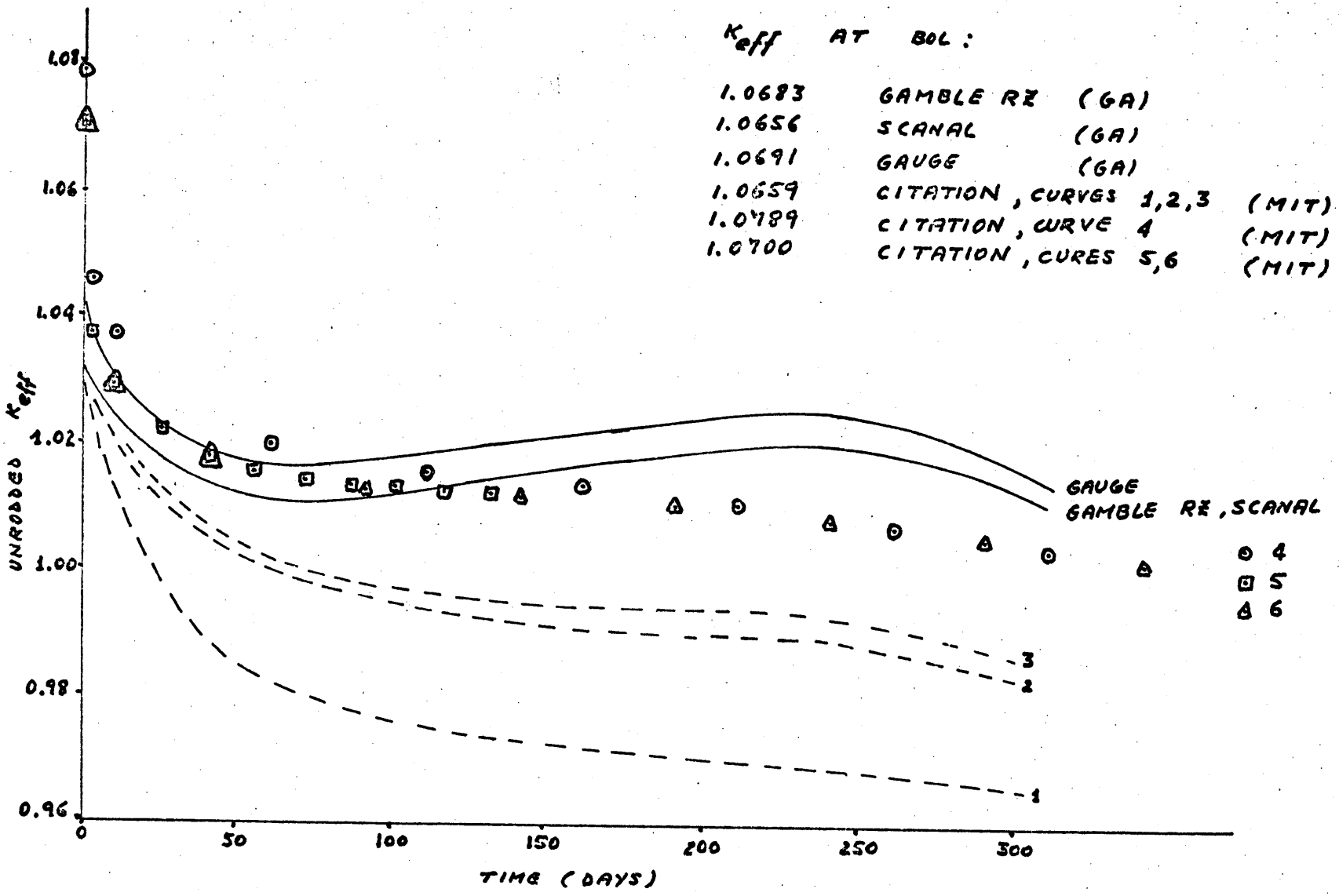

FIG. 2.1.3.3-3 FSV K_{eff} VS TIME CURVES OBTAINED AT MIT

Pm , Sm AND Eu CHAINS AS IN CURVE 1 OF FIG. 2.1.3.3-3

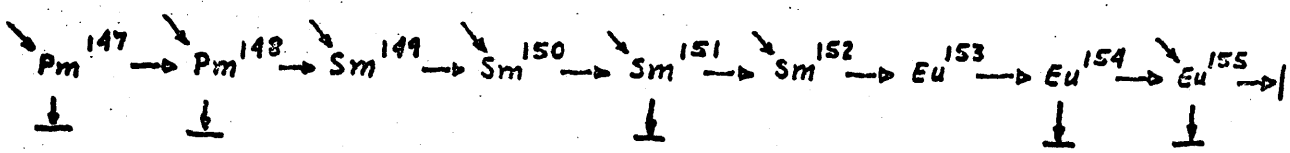

Pm , Sm AND Eu CHAINS AS IN THE OTHER CURVES OF FIG.2.1.3.3-3

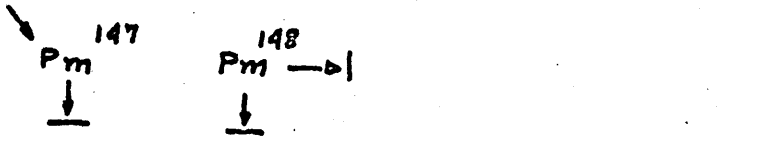

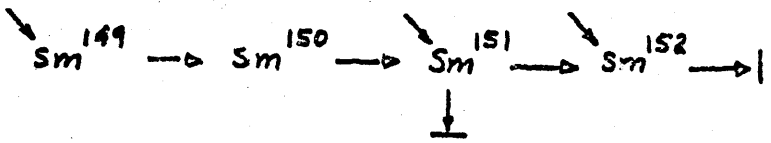

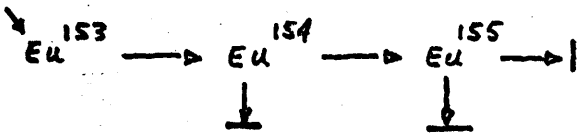

FIG. 2.1.3.3-4 CHAIN SPECIFICATIONS FOR Pm , Sm AND Eu

Curve 3

Everything as in Curve 2 but with correction in cs sets of U^{234} and Nd^{145} (they were wrongly taken at room temperature instead of operating temperature).

Curve 4

All corrections made and using depletion dependent LBP cs (see Appendix A.3.3); only one LBP cs set for the whole core; the B^{10} conc. was taken as 6/7 of the one recommended by Dr. Marshall (called LBP3) (*).

Curves 5 and 6

All corrections made and using 3 sets of LBP cs according to depletion region positioning in the core. Curve 5 uses depletion time steps of 15 days and curve 6 uses 50 day steps. There is a small difference in the k_{eff} not easily seen in Fig. 2.1.3.3-3: (a) at 40 days $(k_{eff})_5 = 1.018395$ and $(k_{eff})_6 = 1.017969$.

(*) The 6/7 factor was introduced here, but later removed (see Section 2.1.3.4), because there is LBP in only 6 of the 7 elements of a region.

2.1.3.4 Conclusions

The comparison of the relative power density distribution, per region, showed that for most of the regions our results are within less than a ± 10% variation from the GA results. From Table 2.1.3.1-1 it can be seen that the best approximation is that of LMP3. It is obvious that the difference comes from the way of representing the periphery regions. On the other hand there is no point in trying to further improve the representation since the present HTGR/GT design does not contain a buffer zone.

The relative axial power profile comparison in Table 2.1.3.2-2 and Fig. 2.1.3.2-3 show very good agreement between our results and those of GA.

The k_{eff} of RZ runs is always somewhat smaller than the corresponding XY values. The reason for that is the presence of CR in the top reflector not taken into account in the XY runs.

The results of the reactivity variation with depletion curve comparisons are:

1. Curves 4, 5 and 6 are within less than 1% difference to GA curves. Curve 4 is a little less in agreement than curve 5 and 6 but not so much as to justify the use of the more expensive runs with 3 cs sets (e.g. curves 5 and 6), so in the depletion runs for the HTGR/GT only one cs set for the whole core was used.

2. The use of the CITATION resonance shielding correlation is satisfactory (see also Table A.3.3.1-1).

3. The best BOL k_{eff} match for those unrodded RZ runs was obtained for LBP3 (Curves 5 and 6). The use of LBP2 or another one based on $N_{B10} = (6/7)(N_{B10})_{LBP's}$ (Curve 4) yield a too high k_{eff}. Because LBP3 yields the best results in the RZ unrodded depletion runs and also in the XY static rodded ones, it was adopted for all the HTGR/GT runs.

Some time after the conclusion of those comparison depletion runs a small error in the volume calculation of zone 5, 6, 11 and 12 was noted. This error caused a 0.5% error in the densities for those regions; the effect on k_{eff} is very small and the runs were not repeated. The concentrations in Tables 2.1.3.2-1 and 2.1.3.3-1 and the dimensions in Figs. 2.1.3.2-2 and 2.1.3.3-2 are correct; the slight mistake can be seen in the input example in Appendix B.

Another concern could be the use of Eq. A.3.3-2 for much higher concentrations of B^{10} in LBP rods than the concentration used in FSV, as is necessary for the long batches studied for the HTGR/GT design (LBP 2 to 3 times more concentrated). Consulted about that on the phone Dr. Marshall assured us that the constants in Eq. A.3.3-2 need not be changed, being valid for a very broad range of B^{10} concentrations in the LBP rod.

2.2 Design Methods Outside the Core

This present section is an evaluation of the calculational methods employed for the vessel internals design (section 6.2).

It was necessary to specify an upper limit for the fast neutron fluence (E>1 MeV for this case) in the HTGR/GT steel vessel wall. This limit is based on neutron radiation induced embrittlement of the steel and is investigated with the help of Charpy-v notch impact experiments (see Fig. 2.2-1). The value specifyed for the fine grain BWR steel vessels is 10^{19} n/cm^2 in 40 years (page 6.14 of Ref. 76). In the HTGR/GT the vessel exposure temperature is some 200°F above that of BWR's which has the effect of reducing the radiation embrittlement. The reasoning applied to explain this response theoretically is that with higher temperature the ability of displaced atoms to return to a vacancy site is enhanced, thereby relieving part of the damage (Ref. 97). This effect is quite significant as can be seen in Fig. 2.2-2. The same 10^{19} m/cm^2 fast fluence limit was then adopted for the HTGR/GT with a larger safety margin.

Once decided, the maximum nvt limit, it was necessary to verify if the fast neutron fluence in the HTGR/GT vessel wall was below this maximum specified limit of 10^{19} n/cm^2. This calculation was performed with the help of the ANISN transport code (Ref. 79) and of a coupled neutron and γ ray 40 group cs set (Ref. 80), with the energy structure as in Table 2.2-1. The computer output also provides the data for the γ heating calculation in the vessel wall. ANISN is a one dimensional code and the HTGR/GT was represented in one dimension for the preparation

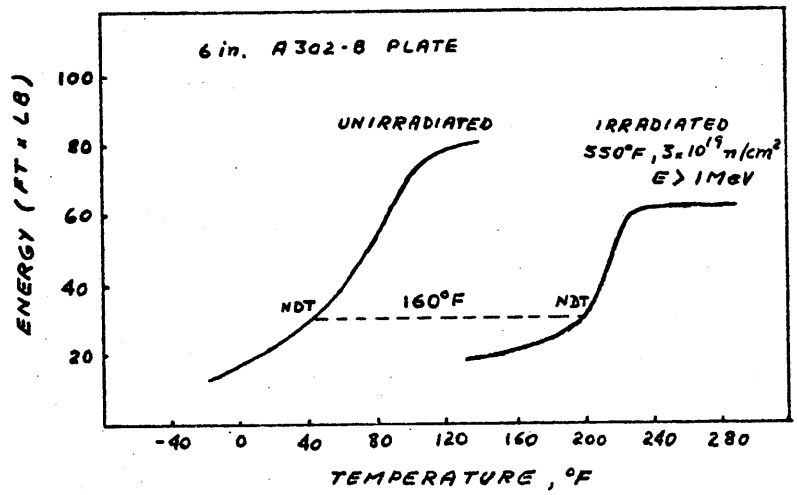

FIG. 2.2-1 TYPICAL CHARPY-V NOTCH IMPACT DATA FOR IRRADIATED A 302-B STEEL

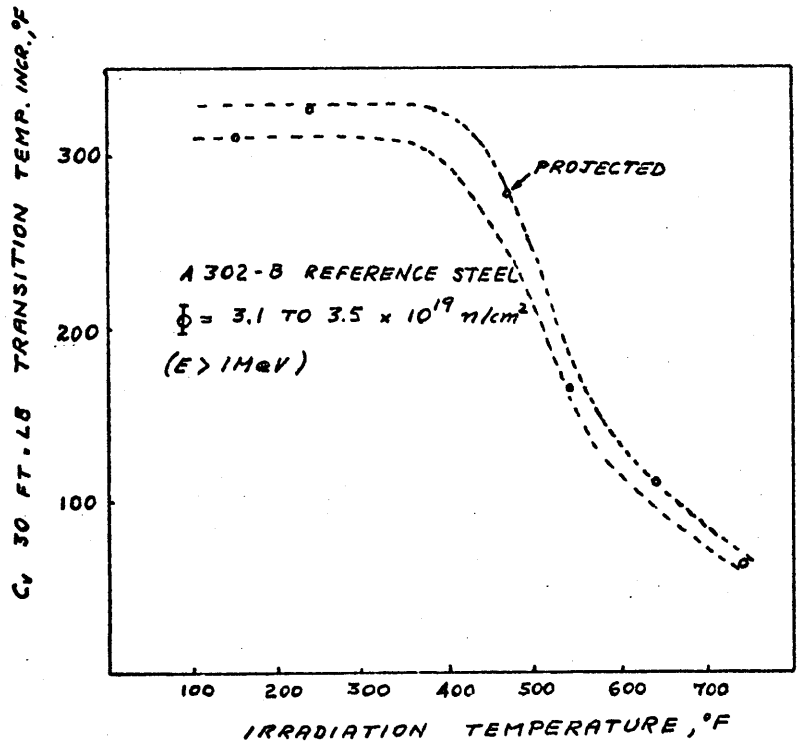

FIG. 2.2-2 EFFECT OF IRRADIATION TEMPERATURE ON TRANSITION TEMPERATURE INCREASE FOR AN A 302-B REFERENCE STEEL

TABLE 2.2-1

ENERGY STRUCTURE OF THE 22 NEUTRON GROUPS AND 18 γ GROUPS USED IN THE ANISN RUNS

A. Neutron groups

Group no.	1	2	3	4	5	6	7	8	9	10	11	12	13
max. energy (MeV)	15.0	12.2	10.0	8.18	6.36	4.96	4.06	3.01	2.46	2.35	1.83	1.11	0.55

Group no.	14	15	16	17	18	19	20	21	22
max. energy (eV)	111,000	3,350	583	101	29.0	10.7	3.06	1.12	0.414

B. γ groups

Group no.	1	2	3	4	5	6	7	8	9
ave. energy (MeV)	9.00	7.25	5.75	4.50	3.50	2.75	2.25	1.83	1.50

Group No.	10	11	12	13	14	15	16	17	18
ave. energy (MeV)	1.165	0.90	0.70	0.50	0.35	0.25	0.15	0.075	0.030

of the ANISN input as in Fig. 2.2-3. The description and composition of the 6 zones in Fig. 2.2-3 is given in Table 2.2-2. Several comments can be made about this representation:

A) Neutron source. The number of neutrons produced per sec in a 1 cm thick slice of the core is required. The average production of neutrons in the whole core is given by

$$(300\ \text{Mwth})(1\ \text{fission}/200\ \text{MeV})(1\ \text{MeV}/1.6\text{x}10^{-19}\ \text{MW}\cdot\text{sec})(2.43\text{n}/\text{fission}) =$$

$$2.277 \times 10^{19}\ \text{n/sec}\ .$$

The neutron production in the 1 cm thick central radial layer is:

$$(2.277\text{x}10^{19}\ \text{n/sec})(1.3\ \text{axial peak/ave. power})/(317.0\ \text{cm}) =$$

$$.9339 \times 10^{17}\ \text{n/cm sec.}$$

To add an extra conservatism the input source of neutrons was also multiplied by the radial power peaking factor 1.21, that is, 1.13×10^{17} n/cm sec. The output point to point neutron flux in n/cm^2sec can be considered to have a 21% safety margin.

B) Core composition. Only C and Si are considered. For neutron transport calculations it is a good approximation to neglect the U and Th presence in the core since C/U $\simeq$ 2000 and C/Th $\simeq$ 200; so, the fast neutron fluence in the vessel wall should be unaffected by this approximation. Most of the γ's produced in the core originated from U and Th neutron capture, but because the γ mean free path is small (approximately 2 cm in Fe and 20 cm in C) the core γ's contribution to the vessel γ flux is negligible.

C) Absence of boron in the thermal shield. Boron is used in the thermal shield to decrease the thermal neutron flux (and γ production) in the vessel wall (see section 2.2.2). The ANISN runs were performed without B in the thermal shield which contributes even more to the

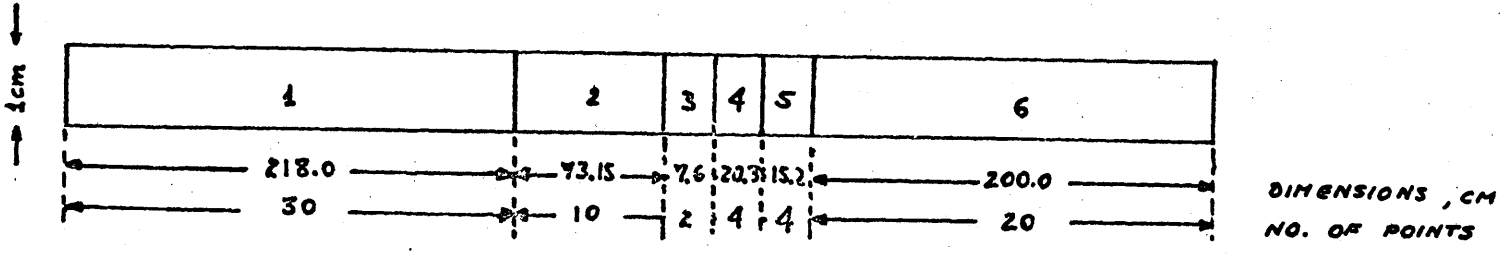

FIG. 2.2-3 HTGR/GT ONE DIMENSIONAL REPRESENTATION FOR THE ANISN INPUT PREPARATION

TABLE 2.2-2

HTGR/GT COMPOSITION AND NEUTRON SOURCE FOR THE ANISN CALCULATION OF THE NEUTRON AND γ FLUXES IN THE VESSEL WALL

Zone No.	Zone Name	Composition in 10^{-5} ats/bcm	comments
1	core	$N_C = 6190.$; $N_{Si} = 73.7$	neutron source = 1.13×10^{17} n/cmsec
2	side reflector	$N_C = 8884.\ (1-\alpha)$	$\alpha = 0.2$ or 0.4 (porosity)
3	thermal shield	$N_{Fe} = 8487.$	
4	insulator	$N_C = 8884.$	
5	vessel wall	$N_{Fe} = 8487.$	
6	concrete	$N_H = 692.6$; $N_o = 2290.0$; $N_{Si} = 2000.$	

the conservatism of the fast flux and γ heating calculation.

D) Concrete close to the vessel wall. The concrete biological shield is going to be located some 2 or 3 feet away from the vessel to permit cooling of the walls, but with respect to reflection of the fast neutron flux it can be treated as if it had a boundary with the vessel wall.

E) Diffusion coefficient to use for the graphite reflector. For the ANISN input, the graphite atom density was calculated as

$$N_C = (8884.0 \times 10^{-5} \text{ ats/bcm})(1-\alpha) \ , \qquad (2.2\text{-}1)$$

where α is the average graphite porosity. Since the diffusion coefficient is inversely proportional to the atom density, the relation between the diffusion coefficient of the compact moderator, D_M, and that of a moderator with a porosity α, D_α, is (neglecting transport effects):

$$D_\alpha/D_M = 1/(1-\alpha) \ . \qquad (2.2\text{-}2)$$

The final HTGR/GT reflector design consists of eleven 2 in. diameter coolant holes per graphite element leading to a 20% porosity reflector. There is evidence that for such relatively large diameter holes an anisotropic effect will occur making the diffusion coefficient in the direction of the neutron flux gradient (radial direction) higher than the value calculated from Eq. 2.2-2. In Ref. 96, for instance, it was found experimentally for the case of 2.25 in. diameter void tubes in heavy water, in a 16% porosity array, $D_\alpha = 1.29\ D_M$ in the radial direction instead of $1.19\ D_M$ as if calculated from Eq. 2.2-2.

The diffusion coefficients in graphite and heavy water are very similar, being 0.84 cm and 0.87 cm respectively in the pure state. Although in the heavy water case the diameter of the holes is larger than those of the HTGR/GT graphite reflector, the possible consequences of having a

$$\frac{1.29 - 1.19}{1.29} \times 100\% = 7.75\%$$

higher diffusion coefficient than the value used in our calculations is analysed here.

The flux decreases exponentially with distance in the reflector. If the first 12 neutron groups (see section 2.2.1) are collapsed at the core lateral surface and at the reflector external surface, an attenuation coefficient $\underline{a}$ for the reflector thickness $\underline{x}$ can be defined and evaluated from the ANISN output by

$$\frac{\left(\sum_{1}^{12} \phi_i\right)_{\text{refl. ext. surf.}}}{\left(\sum_{1}^{12} \phi_i\right)_{\text{core surf.}}} = e^{-ax} = \frac{3.312 \times 10^{10}}{2.407 \times 10^{13}} = 1.376 \times 10^{-3}. \qquad (2.2\text{-}3)$$

The attenuation coefficient $\underline{a}$ can be approximately taken as proportional to the inverse of the collapsed diffusion coefficient, so if D_α is 7.75% higher than the value used in ANISN, the flux in the vessel would be 60% higher than the value calculated from the ANISN output:

$$\frac{\left(\sum_{1}^{12} \phi_i\right)_{1.0775D_\alpha}}{\left(\sum_{1}^{12} \phi_i\right)_{D_\alpha \text{ANISN}}} = \frac{e^{-ax/1.0775}}{e^{-ax}} = 1.6 \quad . \qquad (2.2\text{-}4)$$

Since the limit fast fluence on the vessel wall is more than 10 times higher than the value calculated from the ANISN output (see section 2.2.1), the anisotropic correction does not change the conclusions derived in section 2.2.1 which were based on calculations using Eq. 2.2-1.

This possibility of a 7.75% higher diffusion coefficient for the graphite reflector would also have the effect of decreasing the k_{eff} by increasing the leakage term. The effect of a 20% increase in the side reflector porisity in the k_{eff} was found to be 0.3% on the CITATION runs; since this effect is due to the 20% decrease in D, the effect of a 7.75% increase in D due to anisotropy can be estimated as 0.166% on k_{eff} assuming linear dependence.

The 22 neutron groups and 18 γ group values are printed in the ANISN output for the midpoint of each of the 70 intervals required in the input. From this print out the fast fluence and γ heating in the vessel wall were calculated.

2.2.1 Maximum fast fluence in the vessel wall

The neutron flux with energy above 1 MeV at a given point x in the vessel wall can be conservatively calculated as the summation over the first 12 neutron groups (see Table 2.2-1):

$$\phi(x,\ E > 1\ \text{MeV}) = \sum_{i=1}^{12} \phi_i(x,E_i)\ . \qquad (2.2.1\text{-}1)$$

From a plot of the four points in the vessel wall it is possible to extrapolate the value of the maximum flux above 1 MeV (see Fig. 2.2.1-1).

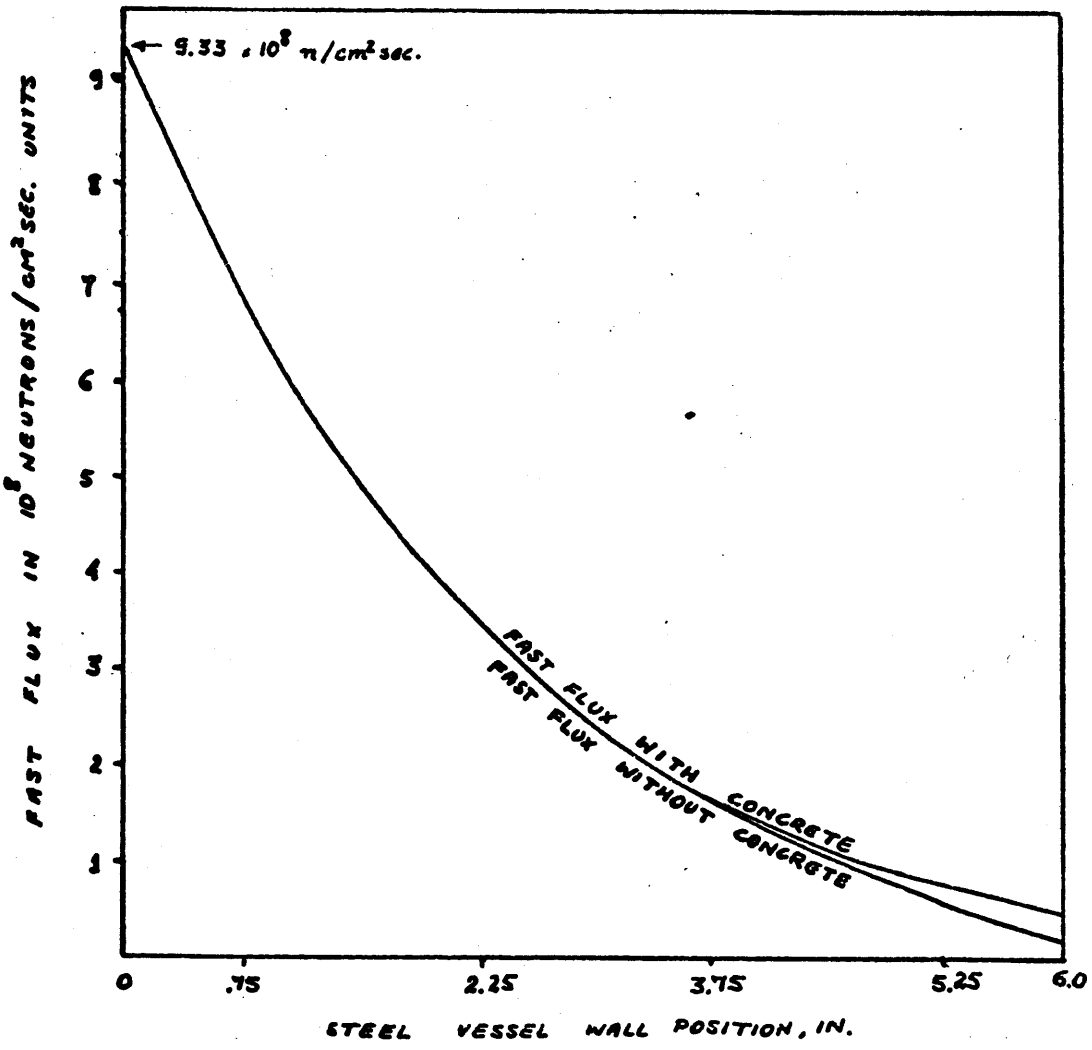

FIG. 2.2.1-1 FAST FLUX DISTRIBUTION IN THE VESSEL WALL FOR THE 20% POROSITY REFLECTOR CASE

The maximum nvt after 30 years can then be calculated as

$$\bar{nvt}(30 \text{ years}) = (9.46 \times 10^{8} \text{ sec})[\phi(0, E > 1 \text{ MeV})] = 0.088 \times 10^{19} \text{ n/cm}^2 , \quad (2.2.1\text{-}2)$$

for the case of the reflector with $\alpha = 0.2$. The concrete shield causes just a 2% increase in the fast flux at the internal vessel surface (can not be seen in the scale of Fig. 2.2.1-1).

2.2.2 Gamma Heating in the Vessel Wall

In section 6.2.1.1 the power density in the vessel wall due to γ heating is calculated. The power density at a point α in. distant from the internal vessel surface is given by

$$q'''(x) = (12.1 \text{ BTU/hr in}^3) e^{-(0.6327 \text{ in}^{-1})x} . \quad (2.2.2\text{-}1)$$

The total heat generation per unit area can be calculated as

$$q'' = \int_0^6 q'''(x)dx = 18.702 \text{ BTU/hr cm}^2 = 2693 \text{ BTU/hr ft}^2 . \quad (2.2.2\text{-}2)$$

The γ heating calculated for the PCRV liner and thermal barrier in the Delmarva PSAR (Ref. 32) varies from 500 to 4000 BTU/hr ft^2 as the boronated thermal shield varies from 3 in. to 0. The heat generation profile in the HTGR/GT vessel wall determined with ANISN, the 18 γ groups and the approximations stated before for the preparation of the ANISN input, is thus in agreement with similar calculations performed by GA personnel for the Delmarva PSAR (Ref. 32).

CHAPTER 3
SELECTION OF FUEL TYPE

During the first two months (June and July, 1974) of this one year project, a bibliographic survey on possible fuel types was made. The principal options analysed were: a) High-Enrichment (HE) - U^{235} / $Th^{232} \rightarrow U^{233}$; b) Low-Enrichment (LE) - U^{235} / $U^{238} \rightarrow PU$; c) PU / $Th^{232} \rightarrow U^{233}$; d) PU / $U^{238} \rightarrow PU$; e) U^{233} / $Th^{232} \rightarrow U^{233}$.

The HE and LE fuels were selected for a more detailed investigation based on the fact that they are the only ones with sufficient commercial experiences and industrial base for use in a plant designed to start in 1985. The other options have certain advantages and may be tried later at the time they become commercially available: the use of Pu instead of U^{235} has the desirable features of providing a longer batch lifetime and lower reactivity swing (Refs. 12 and 25); the use of U^{233} instead of U^{235} or Pu has the advantage of a better conversion ratio due to a higher value of η in the thermal spectrum.

Recent analysis of LE cycles for large commercial HTGR's appear to be converging on the consensus that this cycle is less economic than the HE cycle if HE fuel is available at present prices (Refs. 12, 48, 51, 85). Work carried in Europe on the LE cycle has shown that optimum fuel loadings are such that fuel burnup lifetimes are about 25 percent shorter than for the HE cycle (Refs. 12 and 40). Waiver of

carrying charges on U^{235} should then enhance the HE economic advantage for the HTGR/GT Army base application. Also, for the long batch case the HE fuel was expected to prove to be better. Nevertheless, several depletion runs were produced to compare these two fuels in this present case. There follows a description of the comparison model and an analysis of the results pointing to the selection of the HE fuel.

3.1. Model for Comparison

The objective of the model is to get a meaningful comparison between the two fuels and preliminary information for a refined design, based on the winning fuel, at a low computation cost. With that in mind the HTGR/GT core was represented as in Fig. 3.1-1. All the runs were unrodded and the presence of control rods in the top reflector was neglected; very long depletion intervals (180 days) were employed for cheaper runs. In order to compare the two fuels in the same conditions the following constraints were imposed in the HE and LE depletion runs:

1. Same depletion intervals in HE and LE runs.
2. The max. hot excess reactivity to be controlled by the CR would be 0.11 Δk. This choice had to be arbitrary at this stage, but it was based on Peach Bottom experience [k_{eff} (hot, clean, BOL) = 1.11, 2.2 full power years batch]. The CR requirements are discussed more completely in Chapter 5.
3. The burnable poison to be used in both cases is natural B. In Section 2.1.1.2.3 it is shown that the natural B depletion calculation in the comparison runs is not entirely correct but the error introduced is small and affects LE and HE runs in the same way; the k_{eff} decreases too fast with time in both cases. In the HE runs of Chapter 5 this error is removed and the burnable poison design is optimized.
4. In the FSV design with the maximum fuel compactation permitted by the present day technology, the average

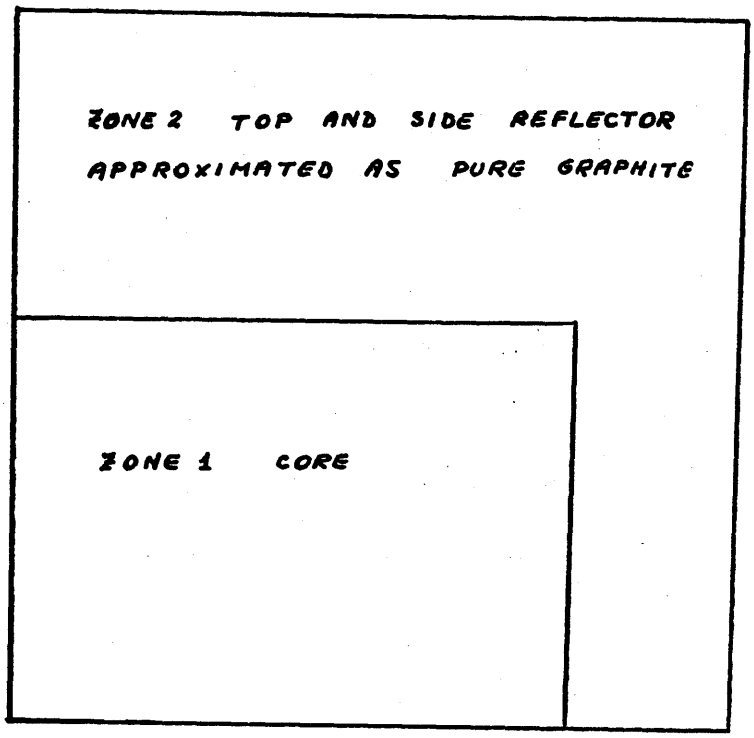

FIG. 3.1-1 MODEL FOR THE HE AND LE FUEL COMPARISON

homogenized HM density in the core is about 39.2×10^{-5} HM atoms /b cm. Since the FSV fuel element was chosen from the outset, this establishes the following limit:

$$(N_{02} + N_{25} + N_{28})_{LE \text{ or } HE} \leq 39.2 \times 10^{-5} \text{ atoms/b cm.} \quad (3.1\text{-}1)$$

Actually slightly higher values are possible with larger fuel particles (see Chapter 4), but the results are not very sensitive to variations in the total HM content.

Before starting the more expensive depletion runs, the adequate range of concentrations for $k_{eff} \simeq 1.11$ was determined by trial and error with very inexpensive static runs using 2DB most of the time.

3.2 Results Obtained

Several depletion runs were performed with the LE and HE fuels by varying the enrichment and natural boron content within the constraints specified in section 3.1. Some of those runs were made with slight changes in the cs for sensitivity study purposes. Some small errors were detected and corrected in the initial runs, and the difference between the correct and wrong results were also used for the sensitivities reported in Section 3.3. The objective of those sensitivity studies is to determine the effect of cs uncertainties or calculational approximation methods used in the HE vs LE comparison results described here.

In Table 3.2-1 the best LE and HE results are summarized; some intermediate and wrong runs are exemplified. The inputs for the best LE and HE runs can be found in the Appendix B.

The results show that HE has two basic advantages for the present type of economy (Section 3.4): a) much higher reactivity lifetime; b) lower U^{235} average consumption per day of operation. The advantage of producing more fissile material (U^{233} which is about 2 times more expensive than Pu) can not be realized (see Sections 3.4 and 4.3.1) directly; nevertheless, the better neutronics of U^{233} in a thermal reactor makes the U^{235} consumption, and the loss of reactivity

Table 3.2-1 HE vs. HE comparison

run no.	Fuel Type	Initial Conc. in 10^{-5} nuc./b cm N_{25}	N_{28}	N_{02}	N_B	kg U^{235} burned	kg Pu^{239} produced
1	HE Wrong	4.200	.316	34.68	.6347	385.21	2.73
2	HE Cor.	4.200	.316	34.68	.6347	374.45	2.63
3	LE Wrong	4.513	34.69	--	1.400	357.88	53.63
4	LE Cor.	4.513	34.69	--	1.400	--	--
5	LE Cor.	4.513	34.69	--	.3974	193.8	78.2
6	LE Cor.	4.513	11.09	--	1.619	252.18	30.5
7	LE Cor.	6.417	32.78	--	.8197	256.04	89.06

The errors in the HE set 1 were: a) the graphite conc: The correct value is $N_c = 6.19 \times 10^{-2}$ atoms/b cm instead of 6.22×10^{-2} atoms/b cm; b) Use of upscattering cs, but σ_{23} is the same in runs 1 and 2. The error in the LE set was the use of the HE graphite scattering matrix instead of that of LE (see Table 2.1.1.2.2-1). The importance of this is that $(\sigma_{34})_{HE} \approx 3.7(\sigma_{34})_{LE}$ and the use of $(\sigma_{34})_{HE}$ in the LE set would greatly increase the resonance escape probability and thus k_{eff} in the LE runs.

Table 3.2-1 (cont'd)

Run No.	kg U^{233} produced	Clean k_{eff}	BOL k_{eff} w/equil.Xe	Reactivity lifetime days	Enrichm. of Uranium	$\frac{N_{fissile}}{N_{fertile}}$
1	148.38	1.10996	1.09000	1128.28	93%	.12
2	141.92	1.10763	1.08749	1086.21	93%	.12
3	--	1.1147	1.09663	1089.00	11.5%	.13
4	--	--	0.90995	--	11.5%	.13
5	--	1.11127	1.0907	540.0	11.5%	.13
6	--	1.11474	1.09955	638.3	28.9%	.42
7	--	--	1.10848	665.2	16.4%	.20

Table 3.2-1 (cond't)

Run No.	$\frac{\text{kg } U^{235}}{\text{burn. day}}$	Loss of reac. per day*, $10^{-4}d^{-1}$
1	.3414	.7977
2	.3447	.8055
3	.3286	.8873
4	--	--
5	.3589	1.680
6	.3951	1.560
7	.3849	1.631

*After Xe build up

per unit time, lower in the HE than in the LE fuel.*

Although the HE fuel was expected to have some advantage over the LE fuel due to the better neutronics of U^{233} as compared to Pu^{239} in a thermal neutron spectrum, the results in Table 3.2-1 showing such a big advantage for the HE fuel came as a surprise. It seems that a major part of the difference in reactivity lifetime can be caused by a lack of equivalence between the HE and LE sets favoring the HE fuel. This matter is analysed in Section 3.3.

---

*The Army will pay for U^{235} consumed and will not receive per fissile material produced (Section 3.4).

3.3. Sensitivity Studies

In this section the sensitivity of results to possible lack of equivalence between the HE and LE cs sets and to possible errors introduced by the model is calculated. The sensitivity studies are organized into two sections:

3.3.1. Individual sensitivity studies - the sensitivity of results to changes in the following parameters is investigated: a) Number of depletion zones; b) Size of depletion intervals; c) down scattering matrix; d) Total HM content; e) Self-shielding factor; f) Leakage; g) U^{235} and B cs (through depletion runs without U^{238} and Th^{232} and runs without U^{238}, Th^{232} and B); h) Fission product (FP) build up; i) Carbon-to-uranium (c/u) ratio.

3.3.2. Global effects of the sensitivity studies on the HE vs LE comparison - The combined effect of the several parameter uncertainties in the comparison results described in Section 3.2 is calculated.

3.3.1. Individual sensitivity studies

3.3.1.1. Number of depletion zones

In the small unrodded single zone core model used, the power density had always, at any depletion interval, its maximum in the center in all runs. The use of a single depletion zone averages the fissile content in core causing the more depleted center to have a fissile content larger than it truly has. Because the "Importance" of the fuel in the center is larger than in the periphery, the k_{eff} will decrease

less with depletion if one single depletion zone is used. Since this approximation was made for both LE and HE, the use of a larger number of depletion zones should not alter the relative comparison; the difference between using 1 and 9 depletion zones in the HE set can be seen in Table 3.3.1.1-1.

Table 3.3.1.1-1. Sensitivity of results to the no. of depletion zones

No. of Zones	(N_{25} N_{28} N_{02} N_8)x 10^5 nuc./b cm				$(k_{eff})_{BOL}$ after Xe	batch life days	cost of run (US$)
1	4.2	.316	34.68	.6347	1.089998	1128.28	15.86
9					1.089810	1053.12	20.57

3.3.1.2. Size of the depletion intervals

For a given composition the code is used to determine the values of k_{eff} and relative fluxes as given by solving the diffusion equations. The absolute value of the fluxes are determined such that the required power in the reactor is achieved:

$$\text{Power} = \sum_j \sum_{i=1}^{4} \gamma_j N_j \sigma_{fi}^j \phi_i, \quad (3.3.2.1)$$

where the summation over j refers to the fissile nuclides, γ_j being the energy released in the reactor per fission of nuclide j. The general burnup equation for a stable fissile nuclide j can be written as:

$$\frac{dN_j}{dt} = \sum_{i=1}^{4} N_j \sigma_{ai}^{j} \phi_i + \lambda_m N_m + \sum_{i=1}^{4} N_n \sigma_{ci}^{n} \phi_i . \quad (3.3.2\text{-}2)$$

At each depletion step the flux is maintained constant and if one performs the group summations, Eq 3.3.2-2 can be written as:

$$\frac{dN_j}{dt} = -N_j \sigma_a^j \phi + \lambda_m N_m + N_n \sigma_c^n \phi = f(t) . \quad (3.3.2\text{-}3)$$

The new concentration after a time step Δt, N_j^{k+1}, can be found iteratively by:

$$N_j^{k+1} = N_j^k + \frac{\Delta t}{2} (f^k + f^{k+1}) . \quad (3.3.2\text{-}4)$$

In the case of U^{235} at BOL, for instance, the burnup equation reduces to

$$\frac{dN_{25}}{dt} = -N_{25} \sigma_a^{25} \phi , \quad (3.3.2\text{-}5)$$

whose analytical solution is

$$N_{25}(t) = N_{25}(0) \varepsilon^{-\sigma_a^{25} \phi t} . \quad (3.3.2\text{-}6)$$

In this simple case it is easy to determine analytically the value to be found by iteration:

$$N_{25}^1 = N_{25}^0 \frac{1 - \frac{\sigma_a^{25} \phi \Delta t}{2}}{1 + \frac{\sigma_a^{25} \phi \Delta t}{2}} . \quad (3.3.2\text{-}7)$$

A typical value of $\sigma_a^{25}\ \phi$ is 6.52×10^{-9} sec^{-1} and it is easy to determine the values of N_{25} after 180 days by Eq. 3.3.2-6 ($N_{25}^1 = .90357 N_{25}^0$), by Eq. 3.3.2-7 ($N_{25}^1 = .90349\ N_{25}^0$) and by Eq. 3.3.2-7 in two subsequent steps of 90 days each ($N_{25}^2 = .90355\ N_{25}^0$). It is seen that the effect of using 180 days time steps is to slightly increase the fissile burnup. In Ref. 52 the relative error in U^{235} feed requirements due to finite time steps is calculated and plotted in Fig. 8, reproduced here as Fig. 3.3.1.2-1.

The effect of this fissile burnup increase is to decrease k_{eff}, as can be observed in curves 5 and 6 of Fig. 2.1.3.3-3.

Since the same large depletion intervals were used for LE and HE and the effect has the same direction in both cases and is only a small change anyway, we conclude that the size of the depletion steps is not important for these comparisons.

3.3.1.3 Down Scattering Matrix

From Table 3.2-1 a 0.48% increase in N_c plus inclusion of upscattering ($\sigma_{43} = 4.6964 \times 10^{-3}$ barns) cause a 0.23% increase in the HE BOL k_{eff} and a 42 days longer batch. It is easy to see that the upscattering contribution is by far the most important of them:

$$\Delta\Sigma_{43} = N_c \Delta\sigma_{43}^c = (6190. \times 10^{-5} \text{ats/bcm})(4.6964 \times 10^{-3} \text{ barns}),$$

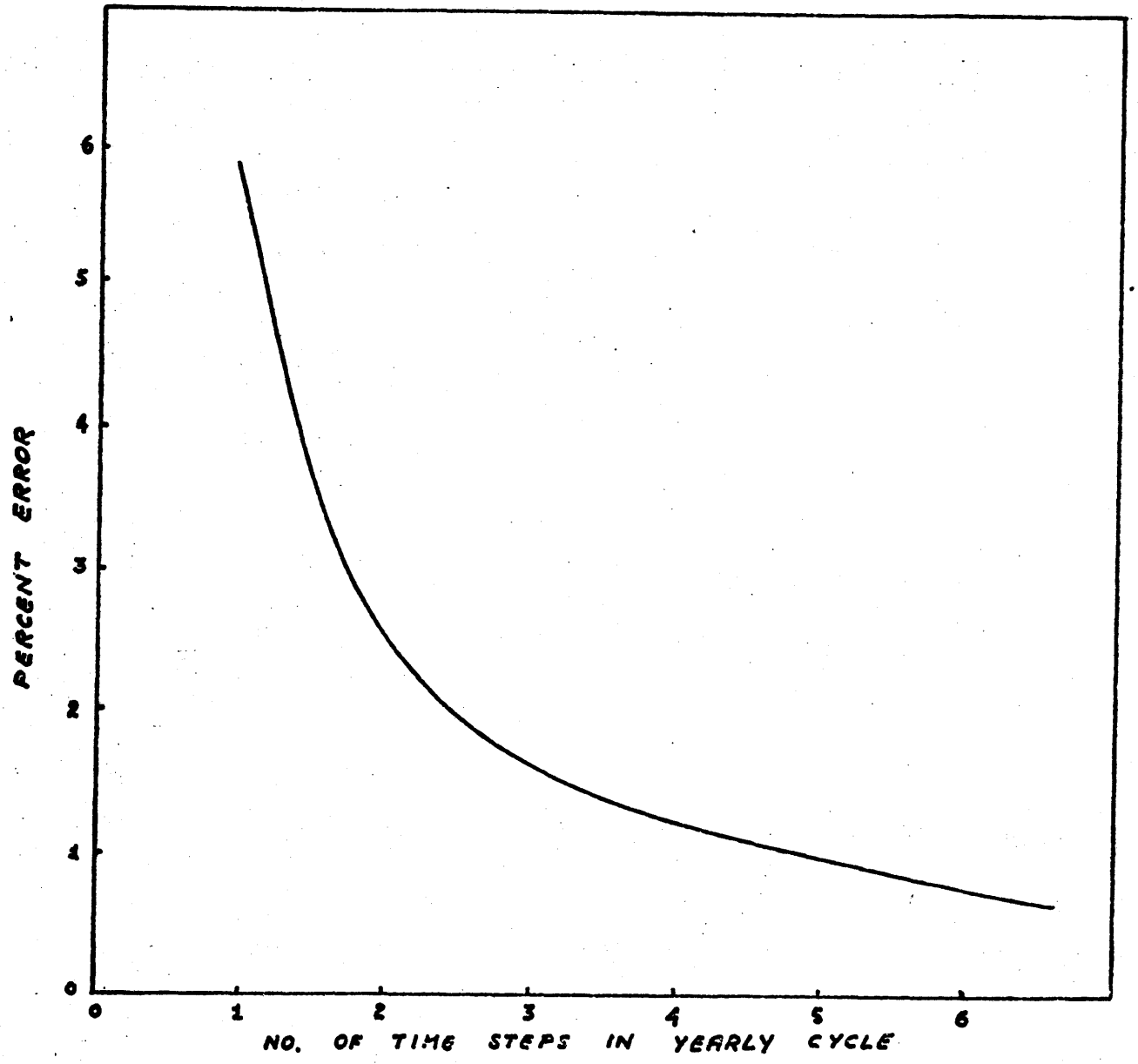

FIG. 3.3.1.2-1 ERROR IN U-235 FEED REQUIREMENTS DUE TO FINETE NUMBER OF TIME STEPS IN DEPLETION CALCULATIONS

$$\Delta\Sigma_{23} = \Delta N_c \, \sigma_{23} = (0.03 \times 10^{-5} \text{atoms/bcm})(6.256 \times 10^{-2} \text{barns}).$$

Since the change in σ_{23} given by Eq. 2.1.1.2.2-6 was introduced to compensate for the absence of upscattering cs, this 0.23% reactivity increase due to inclusion of upscattering (at constant σ_{23}) can be also related to a change in σ_{23}. From Eq. 2.1.1.2.2-6:

$$\frac{\Delta\sigma_{23}}{\sigma_{23}} = \frac{6.256 - 6.073}{6.256} = 0.0293, \quad (3.3.1.3\text{-}1)$$

that is, a 2.93% change in σ_{23} causes a 0.23% change in k_{eff} and a 42 days change in the reactivity lifetime.

Also from Table 3.2-1 a 270% increase in the LE σ_{34} causes a 20.5% increase in the LE BOL k_{eff} and makes the LE loss of reactivity per day comparable to those of HE runs.

3.3.1.4 Total HM Content

By comparing runs 5,6 and 7 of Table 3.2-1 it can be seen that it is advantageous to use the highest possible HM content because then the most neutrons are absorbed in the fertile material. Essentially it is like substituting BP by fertile material and thus increasing the fissile productions, decreasing the U^{235} burnup and necessary $N_{fissile}/N_{fertile}$; the loss of reactivity per day increases with the BP removal though. It can also be observed that the sensitivity of results to changes in the total HM content is relatively small.

3.3.1.5 Self-Shielding Factor

If there was a 25% under estimation in the Th^{232} self-shielding factor, σ_{a2}^{02} would have been equal to 5.0 barns instead of 4.0058 as it is in the HE set. Table 3.3.1.5-1 compares the HE results with these two values of σ_{a2}^{02}.

Table 3.3.1.5-1 Sensitivity of HE results to a 25% error in σ_{a2}^{02}.

run	Atom densities in 10^{-5} atoms/bcm (N_{25}	N_{28}	N_{02}	N_3)	σ_{a2}^{02} barns	k_{eff} (after xe)	Reac. lifetime days	$\Delta k/\Delta t$ $10^{-4} d^{-1}$
1	4.200	.316	34.68	.6347	4.0058(cor)	1.0900	1128.3	.7977
2	4.200	.316	34.68	.6347	5.0000(wr)	1.0327	360.0	.9072
3.	5.369	.316	34.68	.6347	5.0000(wr)	1.0916	1409.7	.6498

It was already shown in Chapter 2 that the self-shielding treatments in the LE and HE sets were reasonably equivalent and a 25% misfit is not to be expected. It is interesting to note that the HE $\Delta k_{eff}/\Delta t$ value for σ_{a2}^{02} = 5 barns is still smaller than those of LE runs, so it would just require to increase the $N_{fissile} / N_{fertile}$ ratio to increase the BOL k_{eff} and the HE runs would still look better. This point is illustrated by run no. 3 of Table 3.3.1.5-1 (run 3 is not particable because N_{25}/N_{28} >93/7).

It was shown in Section 2.1.1.2.1 that there is a 1.2% difference between the self-shielding calculations for the Th in the HE set and U^{238} in the LE set. The effect of

a 1.2% decrease in σ_{a3}^{28} is shown in Table 3.3.1.5.2.

Table 3.3.1.5-2 Sensitivity of LE results to a 1.2% decrease in σ_{a3}^{28}.

Atom densities in 10^{-5} atoms /bcm	σ_{a3}^{28} barns	k_{eff}	Reac. life days	$\Delta k/\Delta t$ 10^{-4}/d
N_{25} N_{28} N_B				
6.417 32.78 0.8197	10.171 (cor.)	1.1085	665.2	1.631
	10.049 (wrong)	1.1115	683.3	1.632

3.3.1.6 Leakage

The carbon cs used in the reflector in the LE runs are the same as those for the core in the absence of an appropriate set. Leakage in LE runs are 3% higher than in HE runs, but the effect of this difference in k_{eff} is very small because leakage is about 2 orders of magnitude smaller than absorption.

Of course the reflector thickness used in both the LE and HE runs was the same in this comparison (side reflector thickness = 53.5 in as in FSV), but it had to be decreased for the HE detailed runs because of the steel vessel size diameter limitation to 21ft (see Chapter 6). Some static 2DB runs showed that for side reflector thicknesses in excess of some 60 cm the thickness has no noticeable effect on the k_{eff}.

3.3.1.7 U^{235} and nat. B cs

The effect of changes in the U^{235} and B cs was examined in depletion runs without Th^{232} and U^{238} and in depletion runs without Th^{232}, U^{238} and B (see Section 2.1.1.2.3). Several small changes in B and U^{235} LE absorption cs were tried with the objective of obtaining a BOL k_{eff} and a reactivity lifetime comparable to those of the HE runs without success (see Appendix C). The reason for that, indicated in Chapter 2, is again summarized here: the FP absorption is not equivalent in the two sets being higher in the LE set and making $\Delta k/\Delta t$ higher in LE runs; the $\Delta k/\Delta t$ value can be made equal by making the LE nat. B depletion a little faster, but then the LE BOL k_{eff} gets even lower. The sensitivities of several parameters to the small cs changes tried in depletion runs without Th^{232} and U^{238} are shown in Table 3.3.1.7-1. The neutron spectrum sensitivity to those changes is treated in Appendix C.

Table 3.3.1.7-1 Comparison of Several modified LE runs with HE*

	LE1	LE2	LE3	LE4	HE
Abs. in U^{235}	.68879	.67815	.68058	.68056	.69485
Prod. in U^{235}	1.25375	1.23596	1.24079	1.24086	1.28565

*All runs without Th^{232} and U^{238} and with N_{25}=4.86 x 10^{-5}, N_B = 1.709 x 10^{-5} and N_{Xe} = 3.5 x 10^{-10} atoms/^{25} bcm. The meaning of LE1, LE2, LE3 and LE4 can be found in Appendix C.

(Prod /abs) in U^{235}	1.8200	1.8230	1.8231	1.8233	1.8503
Abs. in B	2.5122	.26227	.25972	.25972	.23650
Prod. in U^{235}/abs. in U^{235}+B	1.3338	1.3143	1.3196	1.3198	1.3804
k_{eff} at BOL	1.2538	1.2360	1.2408	1.2409	1.2857
Reactivity lifetime, days	1169.6	1213.9	1214.5	1214.8	1413.5
$(\Delta k/\Delta t) \times 10^4$ $days^{-1}$	2.170	1.944	1.982	1.983	2.021

3.3.1.8 Fission product build up

After 990 days the percentage of absorption in F.P. is 12.14% in HE and 16.03% in LE in the runs without Th^{232} and U^{238}. Those percentages are much lower in a typical complete run: 8.36% in HE after 990 days (complete LE runs do not last so long); after 630 days the FP absorption is 7.23% in LE and 6.52% in HE typical complete runs.

The HE set has two fictitious FP: the NSAG23 (with yield 1 from U^{233} and 0 for any other fissile nuclide) and NSAG25 (with yield 1 from U^{235} and 0 for any other fissile nuclide). If the yield is 1.5 instead 1 in both cases, the difference in k_{eff} after 860 days is only 0.25%.

The k_{eff} as a function of time sensitivity to changes in the FP chains can be seen by comparing curves 1 and 2 in Fig. 2.1.3.3-3. In this same figure a comparison between curves 2 and 3 shows the effect of large decreases in the absorption cs of U^{234} and Nd^{145}. In fact most of the increase in k_{eff} is due to U^{234}. Except for Sm^{149} and Xe^{135} the sensitivity to errors in the FP cs is very low.

3.3.1.9 Carbon to uranium ratio

The carbon to uranium (U^{235} + U^{238}) atom density ratio, c/u, is the most adequate correlation parameter to identify the different HE cs sets treated in this thesis. The carbon to heavy metal atom density ratio, C/HM, is a constant (see Eq. 3.1-1) and the carbon to thorium atom density ratio, C/Th, has a much lower variation with composition than C/U. Also, since the uranium enrichment in U^{235} is fixed in 93%, the C/U information is enough to determine the HE BOL HM composition. In the LE set the C/U and C/HM are equal and information about enrichment is necessary to determine the composition.

The C/U ratio for which the cs sets used in this chapter were determined are about 4000 in the HE case and 387 with ∿8% enriched uranium in the LE case. Nevertheless, these sets were used for C/U ratios of 1500 in HE runs and 158 (with ∿ 15% enrichment) or 387 (with 29% enrichment) in LE runs.

The necessary cs corrections for the lower C/U in the HE set are discussed in Chapter 2, and are incorporated in the more detailed HE runs described in Chapter 5. The sensitivity to the corrections in the HE set was not large (see Table 3.3.1.9-1, and note that the important parameter $\Delta k/\Delta t$ remains approximately the same) and the LE cs set was not corrected for the lower C/U and (or) higher enrichment because it became evident that such a correction would not alter

significantly the results of the comparison.

Table 3.3.1.9-1 Sensitivity to carbon-to-uranium (C/U) changes in the HE cs set*

C/U	BOL k_{eff}	Reac. lifetime days	$(\Delta k/\Delta t)$ $x10^{-4}d^{-1}$	$\Delta N_{25}/\Delta t$ kg/d	$\Delta N_B/\Delta t$ kg/d
4000	1.08749	1086.2	.8055	.344	.00246
1371	1.07744	972.2	.7965	.350	.00253

3.3.2 Global effects of the sensitivity studies on the HE vs LE comparison

The objective of this section is to combine the effects of the several parameter uncertainties (Section 3.3.1) to determine the global effect of possible lack of equivalence between the cs sets or possible errors introduced by the model on the comparison results described in Section 3.2.

In Section 3.3.1 it was shown that the model dependent parameters (no. of depletion zones, size of depletion intervals and total HM content) affect the HE and LE results in the same way and have just a small influence in them. All the other sensitivities studied were related to the lack of equivalence between the HE and LE cs sets. Rather than trying to estimate the effect of differences in FP build up, U^{235}

---

*The initial concentrations were: N_{25}= 4.2, N_{28} = .316, N_{02} = 34.68, N_B = .6347 in 10^{-5} atoms/b cm units. The CS for C/U = 1371 are from our estimate in Table 2.1.1-1.

and natural B depletion, down scattering matrix, leakage and differences in cs due to changes in C/U or enrichment, their total effect on the reactivity lifetime comparison is here considered the difference between LE and HE reactivity lifetimes in runs without Th^{232} and U^{238}. From Table 3.3.1.7-1 $\Delta k/\Delta t$ is $2.170 \times 10^{-4} d^{-1}$ for the original LE set (LE1) and $2.021 \times 10^{-4} d^{-1}$ for HE. Considering that the maximum excess reactivity after equilibrium Xe is 0.09 in both LE and HE runs the error in reactivity lifetime calculations due to nuclides other than Th^{232} and U^{238} is given by:

$$\delta t_1 = (0.09)\left[\frac{2.170 - 2.021}{(2.021)(2.170)}\right] \times 10^4 d = 30.5 \text{ days.}$$

To calculate the total effect of possible lack of equivalence between the cs sets on the reactivity lifetime it is still necessary to add to δt_1 the reactivity lifetime uncertainties due to uncertainties in the U^{238} and Th self-shielding factor calculations. To estimate the maximum uncertainty in these calculations reference is made to the HE cs set evaluation contained in Ref. 32 (see Table 3.3.2-1). According to this evaluation the uncertainty in the cs is below 10%. Because the present comparison was carried in a C/U much lower than the one they were prepared for (or a much higher enrichment in the LE case), a 20% uncertainty is here assumed in the self-shielding factor calculations. From Table 3.3.1.5-1 a 25% change in σ_{a2}^{o2} causes a change in $\Delta k/\Delta t$

from $0.7977 \times 10^{-4} d^{-1}$ to $0.9072 \times 10^{-4} d^{-1}$. Supposing linear variation with cs change the uncertainty in reactivity lifetime due to Th^{232} self shielding factor uncertainty is

$$\delta t_2 = (0.09)(20/25)\left[\frac{0.9072 - 0.7977}{(0.9072)(0.7977)}\right] \times 10^4 d = 108d;$$

Table 3.3.2-1 HE cs set evaluation in Ref. 32

A. Core k_{eff} for homogeneous critical assemblies

Assembly	C/U	Calculated k_{eff}	Measured k_{eff}
1	5000	1.023 ± 0.005	1.013 ± 0.003
2	2500	1.017 ± 0.005	1.014 ± 0.003
3	1718	1.013 ± 0.005	1.013 ± 0.003
4	859	1.012 ± 0.005	1.013 ± 0.003
5	432	1.019 ± 0.005	1.016 ± 0.003

B. Analysis of the reactivity coefficient measurements in the HTGR critical assemblies 2 to 5:

Nuclide	B	U^{235}	U^{233}	U^{238}	U^{236}	Np^{237}	Th^{232}
accuracy in calculated reaction rates	±2	±2	±4	+2to+5	+3to+5	+2to-10	+2to+5

C. The Analysis for assembly 1 indicates a consistent overestimate of 10% in worth.

From Table 3.3.1.5-2 and supposing again linear variation with cs change the uncertainty in reactivity lifetime due to U^{238} self-shielding uncertainty is

$$\delta t_3 = (0.09)(20/1.2)\left[\frac{1.632-1.631}{(1.631)(1.632)}\right] \times 10^4 d = 5.6d.$$

The total uncertainty, due to lack of equivalence between the cs sets, in the difference in reactivity lifetime between HE and LE runs is given by $\delta t_1 + \delta t_2 + \delta t_3 = 144.1$ days. From Table 3.2-1 the difference in reactivity lifetime between HE and LE (runs 2 and 6) is

$$(0.09)\left[\frac{1.560-0.8055}{(1.560)(0.8055)}\right] \times 10^4 d = 540.4 \text{ days;}$$

which shows that the difference in reactivity lifetime favoring HE is considerably higher than the uncertainty due to the possible lack of equivalence between the two sets.

3.4. Fuel Cycle Economic Evaluation

An economic assessment of alternative total energy systems for large military installations has been made by Metcalfe (Ref. 86). This section is a summary of his most important findings and with emphasis on the fuel cycle economics.

The groundrules for the economic analysis performed by Metcalfe are summarized in Table 3.4-1. Costs of electricity and thermal energy (utility hot water at 380°F) produced for large military bases by nuclear and fossil-fired power plants in the 100MWe size range for 1985 plant start-up have been estimated in 1985 dollars, levelized over plant life. The HTGR/Brayton unit was shown to produce total energy products more economically than the PWR (23.9 mills/kwhr and 2.45 $/MBTU versus 30.3 mills/kwhr and 2.93 $/MBTU, respectively). Breakeven fuel costs for comparable fossil-fired steam-electric power plants were found to be 8 $/bbl for oil, 12 $/ton for coal, and 116¢/1000 scf for natural gas. Oil-fired gas turbine units were found to have breakeven fuel costs of 17$/bbl for oil. Synthetic Natural Gas, SNG, fired gas turbine units fueled by on-site coal gasification facilities were found to have breakeven fuel costs of 30 $/ton of coal.

Parametric and sensitivity studies have been conducted to examine the effect of size (50 to 200 MWe), annual cost of money (8-12%), plant lifetime (20 to 40 years), plant start-up date (1980-1990) and plant capacity factor (40-80%).

TABLE 3.4-1

GROUNDRULES FOR ECONOMIC ANALYSIS

REFERENCE BASE CASE

Loads Served	100MWe Plus Approximately 200 MWth Supplied to the Thermal Utility
Plant Types	Nuclear: HTGR/Brayton, PWR/Rankine Fossil: Coal, Oil and Gas-Fired Rankine Oil-Fired Gas Turbine
Site	AEC's "Middletown",USA
Construction Period	Nuclear: 7 Years Fossil: 5 Years
Date of Operation	1985
Cooling	Mechanical Draft Wet Cooling Towers
Environmental	Near Zero Rad Waste Systems for Nuclear Plants; SO_x Removal Systems for Coal Units
Work Week	40 Hours, No Overtime
Cost of Money	10%
Escalation	8% Labor 5% Materials

Single Unit on Site

80% Plant Operating Capacity Factor

30 Year Plant Lifetime

PRIMARY VARIATIONS

Vary Plant Rating - 50, 100, 150, 200, 1000 MWe
(Thermal Demand Approximately Equal to Twice the Electric Power Demand)

Table 3.4-1 (Cont'd)

SENSITIVITY STUDIES

Plant Power Rating - 100 MWe

(1) Vary Cost of Money - 8, 10, 12%

(2) Vary Plant Lifetime - 20, 30, 40 Years

(3) Vary Plant Start-up Date - 1980, 1985, 1990

(4) Vary Plant Capacity Factor - 40, 60, 80%

Note: Underlining (___) indicates reference value.
Oil-Fired Gas Turbine system examined for 100 MWe only.
Gas-Fired Rankine system examined for base case only.

The Brayton cycle HTGR system is demonstrated to be economically superior to the other nuclear and fossil-fired options for total energy applications. The SNG-fired gas turbine system with on-site coal gasification capability is identified as a strong contender for the proposed application in the event that low-priced coal is locally available.

The capital costs were estimated with the aid of the CONCEPT III computer program(Ref. 95) and are summarized in Table 3.4-2. In the case of the nuclear units, capital costs accounts for roughly two-thirds of the cost of energy produced. The remaining third of the energy generation cost is roughly evenly split between nuclear fuel and operating/maintenance costs.

Government agencies and installations which use nuclear fuel (principally government laboratories and military reactors, at present) apply unique accounting practices in calculating their nuclear fuel cycle costs. Under government ownership the basic fuel cycle cost parameters consist of burn-up charges for the U^{235} consummed (Enriched uranium is obtained from the government, and payment for fuel is made following irradiation upon return of the fuel to the government supplier.), fabrication charges, reprocessing and reconversion charges (including spent fuel shipping), and carrying charges (on cash expenditures but not on the fuel). Also, in direct contrast to the usual commercial practice no credit is taken for bred fissile material and no carrying charges are assessed

TABLE 3.4-2
CAPITAL COST ESTIMATES

1. Concept III Capital Cost Estimates

(A) Reference Base Case

Plant Rating (MWe)	HTGR	PWR	COAL	OIL	GAS
50	2380	2355	1622	1343	1276
100	1686	1668	1172	935	872
150	1410	1395	999	783	723
200	1252	1237	902	700	642
1000	704	695	577	432	384

(B) Sensitivity Studies (100 MWe)

Parameter Changed To	HTGR	PWR	COAL	OIL
1980 Start-up[a]	1332	1318	926	754
1990 Start-up[b]	2179	2155	1517	1190
8% Interest	1605	1588	1123	896
12% Interest	1767	1747	1222	974

Note: All costs are given in $/kwe, 1985 dollars except:

[a]Cost is in 1980 dollars.
[b]Cost is in 1990 dollars.

Table 3.4-2 (Cont'd)

2. Captial Cost Estimates in 1974 Dollars

Plant Rating (MWe)	HTGR	PWR	COAL	OIL	GAS
50	1568	1546	1007	840	817
100	1111	1095	727	584	540
150	930	915	620	490	449
200	825	812	560	438	396
1000	464	456	358	270	232

Note: All costs are given in $/kwe for reference base case.

on the fuel while it is in user custody.

The HE and LE fuel cycle costs (batch parameters summarized in Table 3.4-3) were compared under those economic conditions. Using the payment schedule and HTGR fuel processing costs presented in Tables 3.4-4 and 3.4-5 respectively the fuel cycle costs for LE and HE were calculated and are summarized in Table 3.4-6. This comparison shows that the LE fuel cycle is about 40% more expensive than the HE one.

TABLE 3.4-3

FUEL CYCLE PARAMETERS

FOR HIGH AND LOW ENRICHMENT FUELS

	High Enrichment	Low Enrichment
Unit Rating (MWe)	100	100
(MWt)	286	286
Full Power Batch Core Lifetime (yr)	3.1	1.8
Beginning-of-Life Core Values		
Enrichment (%)	93	16
Enrichment Charges ($/gm-$U^{235}$)	14.33	13.13
End-of-Life Core Values		
Enrichment (%)	87	13
Enrichment Charges ($/gm-$U^{235}$)	14.28	12.88
U^{235} Consumed (kg) During Batch Core Lifetime	349	232
Total Heavy Metal Inventory (kg)	6295	6435
Average Burnup Rate (gm-U^{235}/MW-day)(a)	1.078	1.234

(a) At BOL all the power production is due to U^{235}. At the EOL $\sim$ 35% of the HE power is due to U^{233} and $\sim$ 24% of the LE power due to Pu^{239}. For that reason the average U^{235} burnup in the HE is lower than in the LE batch.

Note: All costs are given in 1974 dollars.

TABLE 3.4-4

PAYMENT SCHEDULE

FOR GOVERNMENT-OWNED BASIS

Process	Payment Due
Enrichment	100% due 12 months after discharge
Reprocessing and Reconversion	100% due 12 months after discharge
Uranium Credit[a]	100% due 12 months after discharge
Shipping[b]	100% due 6 months after discharge
Fabrication	10% per month due from 14 to 6 months and 10% due 4 1/2 months before insertion

[a]Credit for unburned U^{235}; no credit for bred fissile material (Pu^{239}, U^{233}).

[b]Negligible error results when shipping payment is assumed due 12 months after discharge to facilitate calculations.

TABLE 3.4-5

HTGR FUEL PROCESSING COSTS AS A FUNCTION OF UNIT RATING

	Cost ($/kg-HM) For Unit Rating of	
Cost Component	1000MWe	100MWe
Fabrication	200	256
Shipping	17	22
Reprocessing and Reconversion	135	173

Note: All costs are given in 1974 dollars.

TABLE 3.4-6

HTGR/GT FUEL CYCLE COSTS

FOR HIGH AND LOW ENRICHMENT FUELS

	High Enrichment	Low Enrichment
Unit Rating (MWe)	100	100
Full Power Batch Core Lifetime (yr)	3.1	1.8
Component Costs (thousand dollars)		
Burnup Charges	5,535	3,585
Fabrication Charges (Including carrying charges)	2,575	2,329
Reprocessing, Reconversion and Shipping Charges	1,228	1,255
Total Cost (thousand dollars)	9,338	7,169
Annual Cost[a] (mills/kwhr)	3.52	4.97

[a]Levelized overfuel residence period at 80% capacity factor.

Note: All costs are given in 1974 dollars for the reference base case HTGR.

After optimization (Chapter 5) the HE reactivity lifetime increased to 4.8 full power years and a new fuel cycle cost calculation was made. The optimized HE fuel cycle parameters necessary for this new fuel cycle cost calculation are presented in Table 3.4-7.

In 1985 dollars, the 100MWe HTGR fuel cycle cost levelized over a 30 year plant lifetime at 10% cost of money and constant plant capacity factor of 80% was found to be 6.04 mills/kwhr using the parameters in Table 3.4-7, the payment schedule as in Table 3.4-4 and the HTGR fuel costs as in Table 3.4-8.

Some comments should be made about the way to obtain the HTGR fuel processing costs. Current estimates for HTGR fuel processing costs were obtained for a 1000MWe HTGR. LWR experience has shown that the individual fuel cycle charges per kw generated increase as reactor rating decreases. It was necessary to scale down the 1000MWe costs to represent the 100 MWe HTGR values. In the absence of reliable small HTGR fuel cycle data, the same percentage change in charges as a function of plant rating existent for PWR's was assumed for HTGR plants (see Table 3.4-5). The fabrication costs quoted are based on the GA fuel design involving two different particle sizes (see Chapter 4). By choosing an intermediate single sized particle, a ten-fold decrease in particle fabrication charges might be achieved. However, this particle will have a large amount of U^{233} mixed with U^{235} after

TABLE 3.4-7

HTGR FUEL CYCLE PARAMETERS AFTER OPTIMIZATION

PARAMETER	VALUE
Unit Rating (MWe)	100
(MWt)	286
Full Power Batch Core Lifetime (Yr)	4.8
Refueling Interval (Yr)	6.0[a]
Beginning-of-Life Core Values	
Enrichment (%)	93
U^{235} (Kg)	740
U^{233} (Kg)	0
Total Heavy Metal (Kg)	6824
End-of-Life Core Values	
Enrichment (%)	86
U^{235} (Kg)	275
U^{233} (Kg)	154
Average Burnup Rate (Gm U^{235}/MW-day)	0.93

[a] At 80% plant capacity factor.

TABLE 3.4-8

HTGR FUEL PROCESSSING COSTS

Year	Separative Work Cost	UF_6	Fabrication	Shipping	Reprocessing and Reconversion
1985	113.14	34.73	437.85	30.45	239.47
1990	128.01	42.25	558.81	35.30	277.61
1995	144.83	51.40	713.20	40.92	321.83
2000	163.86	62.54	910.25	47.44	373.09
2005	185.39	76.09	1161.70	55.00	432.51
2010	209.76	92.58	1482.70	63.76	501.40
2015	237.32	112.63	1892.30	73.91	581.26
2020	268.51	137.03	2415.10	85.68	673.84
2025	303.79	166.72	3082.40	99.33	781.16
Annual Escalation Rate:	2 1/2%	4%	5%	3%	3%

Note: All costs are given in dollars per kilogram heavy metal.

irradiation, and one could therefore expect a penalty (of unknown magnitude) for reprocessing.

3.5 Summary and Conclusions

The HE and LE fuels were selected, among several other possible options, for a more detailed investigation based on the fact that they are the only ones with sufficient commercial experience and industrial base for use in a plant design to start in 1985. With the objective of getting a meaningful comparison between the two fuels and preliminary information for a refined design, based on the winning fuel, at a low computation cost, a simplified model was developed. The results obtained (see Table 3.2-1) show that HE has two basic advantages for the present type of economy:
a) a 48.4% longer batch for the some maximum excess of reactivity constraint; b) a 12.8% lower U^{235} average consumption per day (comparison between runs 2 and 6 of Table 3.2-1).

An analysis of the possible consequences of lack of equivalence between the cs sets or possible errors introduced by the model on the reactivity lifetime calculations was made. It was concluded that the uncertainties in the calculations were smaller than the differences in reactivity lifetime favoring HE.

An economical evaluation of the two fuel cycles was summarized from Metcalfe (Ref. 86). The annual fuel cycle cost of HE fuel was found to be about 40% cheaper than that of the LE (3.52 compared with 4.97 mills /kwhr, 1974 dollars). The HE fuel cycle cost after optimization (Chapter 5) was found to be 6.04 mills / kwhr in 1985 dollars, or 2.12 mills/ kwhr in 1974 dollars supposing a 10% annual inflation rate.

CHAPTER 4

FUFL PARTICLES DESIGN

In the first chapter of this report the fuel compacts and particles to be used in the HTGR/GT core were briefly described. In this chapter a more detailed discussion of the subject is made: first some parameters of interest are defined ; then the particle failure mechanisms are discussed; the fuel type is selected among the possible options; finally, respecting the design requirements in Table 1.2-1, an assessment for a possible particle design is made.

4.1 General Coated Fuel Particle Information

The use of coated fuel particles in HTGR's has been extremely varied. In Fig. 4.1-1 the typical dimensions and compositions of a coated particle are given. The choice of an optimum design is conditioned by the design requirements; the range of values for the design variables is constrained by the current state of the art in coated particle and fuel compact manufacture. For the discussion in this chapter the nomenclature from Ref. 34 is adopted. For convenience the most important definitions are reproduced here:

ν = reactor core volume fraction occupied by fuel rod compacts ;

f = fraction of fuel rods occupied by coated particle ;

ρ = theoretical metal density of oxide or carbide fuel ($8.1\ g/cm^3$ for Th in ThC_2 or ThO_2, and $9.6\ g/cm^3$ for U in UC_2 or UO_2) ;

ρ_m = heavy metal density required in loaded fuel rods as established from reactor design and fuel materials performance considerations ;

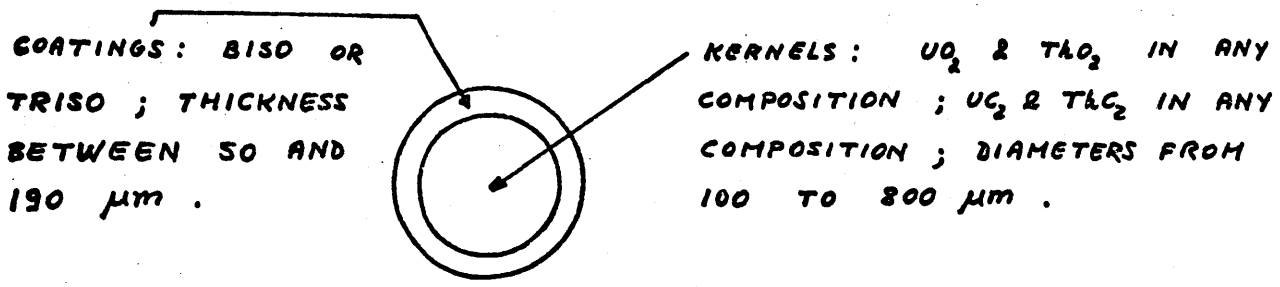

FIG. 4.1-1 TYPICAL DIMENSIONS AND COMPOSITIONS OF A COATED FUEL PARTICLE

R = mean thermal power rating of the fuel, MWth per kg of fissile material;

h = mean thermal power density of the core, $MW(th)/m^3$;

ε = feed enrichment of fissile fuel (LE) ;

N = ratio of fertile to fissile atoms (HE) ;

d = mean duration of the fuel life, days ;

p = internal porosity in the fuel kernel ;

r = radius of internal kernel ;

t = thickness of the coatings .

The heavy metal loading requirement of fuel rods on the LE and HE fuel is given respectively by

$$\rho_m = h/R\varepsilon\nu \qquad (4.1\text{-}1)$$

and

$$\rho_m = (N+1)h/R\nu \ . \qquad (4.1\text{-}2)$$

This quantity can also be expressed as a function of particle parameters as:

$$\rho_m = \rho f(1-p)\left[\frac{r^3}{(r+t)^3}\right] \ . \qquad (4.1\text{-}3)$$

Table 4.1-1 compares the above parameters and design limits for several HTGR designs.

Several types of kernels have been employed. Depending on the fabrication process the kernels can be obtained with controlled density: compacts (plasma-torch melted or sintered with $p \simeq 0$) or porous with p as high as 0.5.

TABLE 4.1-1

FUEL PARTICLE PARAMETERS AND DESIGN LIMITS IN SEVERAL HTGR DESIGNS.

	Dragon	FSV	Fulton
Peak fast neutron fluence (E> .183MeV,n/cm^2)	4.8 x 10^{21}	8 x 10^{21}	8 x 10^{21}
Peak temperature, °F	2280	2300	2580
Full power residence time, days	1000	1752	1168
Peak burnup, %FIMA	10 (demand)	Fissile: 30	Fissile: 75
	15 to 20 (perform)	Fertile: 8	Fertile: 7.5
Power density, w/cc	8.0	6.3	8.4
HM conc in compacts (ρ_m),g/cc	0.8 to 1.0	∿.7	∿ .7
kernel composition	UO_2	Fiss: ThC_2/UC_2 (4.25/1)	Fiss: UC_2
		Fert: ThC_2	Fert: ThO_2
kernel diameter, μm	800	Fiss: 100-300	Fiss: 200
		Fert: 300-600	Fert: 500
Kernel porosity	20%	Fiss & fert below 10%	Fiss & Fert below 10%
Coating type, total thickness (μm)	TRISO,190	Fiss: TRISO, 130	Fiss: TRISO, 170
		Fert: TRISO, 130	Fert: BISO, 160

Several types of coatings have been tried: purely metallic ones, oxide based ones (BaO, BeO, $A\ell_2O_3$) and carbides (SiC, ZrC). The coatings based on PyC (**BISO** and **TRISO** - see Fig. 4.1-2 for description and properties) really stand out from its competitors (Ref. 74). A possible variation in the TRISO coating is the substitution of SiC by ZrC. When Dr. Shimokawa from JAERI visited at MIT in 1974, he mentioned that this substitution was under studies in Japan (see, for instance, Ref. 83).

As for the binder matrix, there is basically two principal types of compactation processes (description from Ref. 74):

1) Overcoating of the particle with graphite powder treated with thermosetting resins; pressing to the desired form at 100°C to 150°C; high-temperature heat treatment (850°C) and degassing of the compact at about 1800°C.

2) Injection molding process. A close-packed bed of particle is bonded with a viscous mixture of pitch and graphite powder (low density matrix of 0.6 to 0.9 g/cm^3); by warm molding and extrusion matrix densities of the order of 1.4 to 1.75 g/cm^3 can be obtained. In any case a stage of carbonization and degassing follows.

Process 1 has some advantages over process 2: a) a more isotropic fuel body which, having a low permeability, contributes positively to the fission products retention; b) the individual overcoating isolates the effect of an individual particle failure. On the other hand it can only be used for relatively large particles ($2r \simeq 500\ \mu m$) and yields low values of f (around .35). The particles for FSV were produced by process 2 with the objective of getting a higher packing fraction

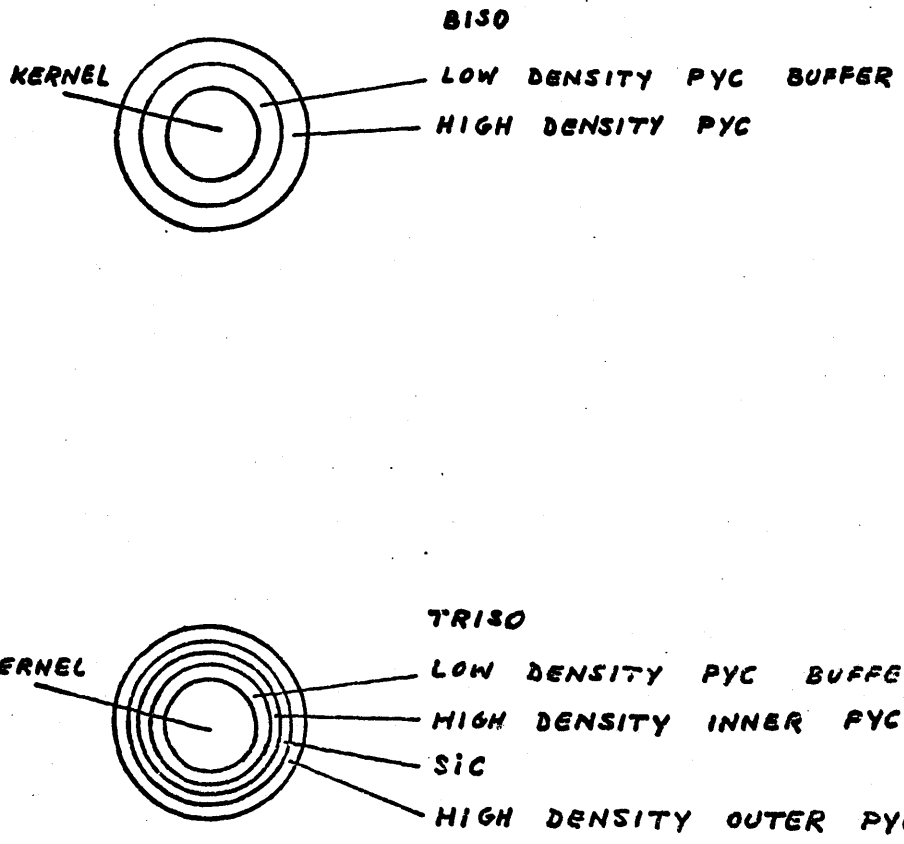

THE BUFFER LAYER ABSORBS FP RECOILS AND PROVIDES VOID VOLUME FOR THE ACCUMULATION OF GASEOUS FP AND FUEL KERNEL SWELLING. THE HIGH DENSITY PYC IS A PRESSURE VESSEL FOR THE GASEOUS FP AND THE SiC LAYER DETAINS SOLID FP DIFFUSION

FIG. 4.1-2 BISO AND TRISO COATING CHARACTERISTICS

in the initial FSV core. Four sizes of particles were used with the result of f = .62. The use of process 2 with single size particle of $2r < 500$ μm would normally still permit a f = .55 to .60.

4.2 Particle Failure Mechanisms

There are basically two kinds of coated particle failure mechanisms: mechanical and chemical.

4.2.1 Mechanical Failure

As fuel depletes gaseous FP are formed and exert an increasing pressure on the coating. The fast neutron dose on the outer PyC layer induces a shrinkage of this layer and compression of the internal layers of the coating. The total stress in the coating can be represented as a sum of these two components:

$$\sigma_t(T) = \sigma_1(BU,T) + \sigma_2(nvt,T) \ , \qquad (4.2\text{-}1)$$

where

$\sigma_1(BU,T)$ - stress caused by a burnup BU at a temperature T ;

$\sigma_2(nvt,T)$- stress caused by a fast neutron fluence nvt at a temperature T .

The stress to rupture curve for a certain particle design is determined from experiments and with the help of mathematical models. An example of such a curve is shown in Fig. 4.2.1-1. The stress to rupture by fission products pressure alone is determined by "accelerated experiments" (use of highly enriched particle thus artificially eliminating the fast fluence effect) and the stress to rupture by fast fluence alone is determined by irradiation of a dummy coated particle (no fuel inside - observe only fast nvt effect on the coating).

Presently PyC coatings resistant up to a fast fluence of 8×10^{22} n/cm^2 can be fabricated, but it will not sustain the SiC in the TRISO coating adequately. The practical limit for the PyC being used in the TRISO coating is 8×10^{21} n/cm^2 for neutrons with energy above 0.18 MeV.

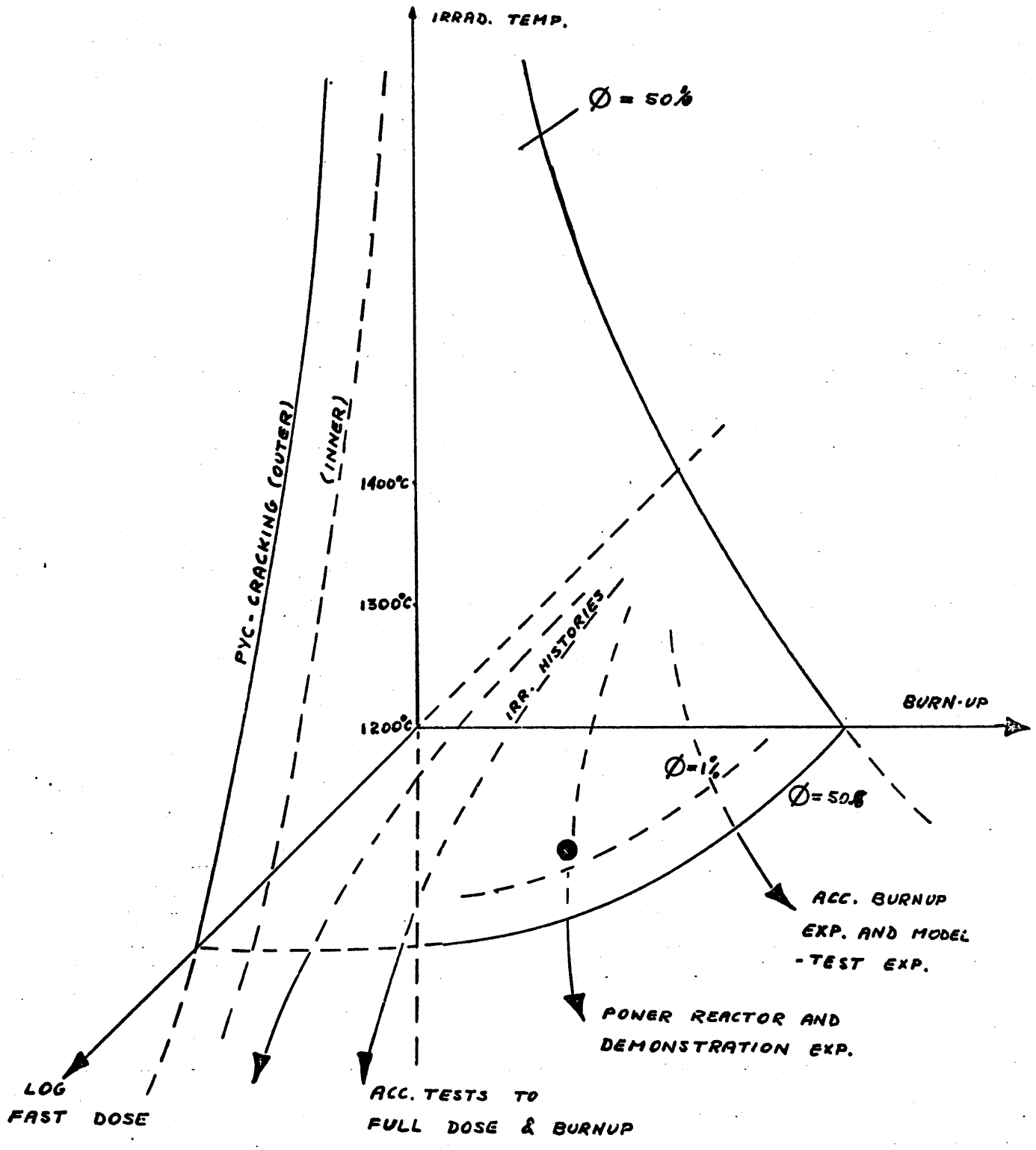

FIG. 4.2.1-1 COATED PARTICLE MECHANICAL PERFORMANCE DIAGRAM (FROM OECD DRAGON PROJECT)

The burnup limit is not so rigid. The pressure caused by the gaseous FP build up (and O_2, CO and CO_2 in the case of oxide fuels) is proportional to the fuel density, BU and temperature and inversely proportional to the porosity of the fuel. If the design requires a higher burnup in the particles, the excess gaseous FP production can be acomodated by either increasing the porosity of the particle or the coating thickness (the buffer layer is increased to absorb the kernel diameter increase and to provide more space for gaseous FP and the high density part of the coating has also to be thicker to withstand the higher pressure). In either case, ρ_m necessarily decreases. In the early Dragon designs ρ_m would range from 1.0 to 2.0 g of HM/cc and BU was limitting. Nowadays their designs require ρ_m in the 0.7 to 0.8g/cc range in which case the gaseous FP pressure can always be maintained below the acceptable limits and the maximum fast fluence is always the limit reached first (Ref. 85).

In the HTGR/GT case, ρ_m = 0.713 g/cc and the preliminary accessments for a single oxide fuel particle design in section 4.3 show by comparison with Dragon's particle that BU should not be limitting in the HTGR/GT either.

4.2.2 Chemical Failure

There are two chemical failure mechanisms:

A. Spearhead attack

B. Kernel migration in a temperature gradiente, also called amoeba effect.

The first of these mechanisms is considered relatively unimportant nowadays and is included here for historical reasons. In the early irradiation tests a progressive erosion initiating in the inner layers and eventually reaching the outermost was detected. This effect was called "spearhead attack" and was originated by microcracks in the inner coating caused by FP recoil. This problem was eliminated with the introduction of a buffer zone of porous PyC between the kernel and the more dense coating. It is known that a superficial buffer density of 2.82 mg/cm^2 is necessary to stop the most energetic FP particles and thus a minimum buffer layer thickness to prevent "spearhead attack" can be calculated. In each case, even for very porous .08 g/cm^3 PyC, an approximately 35 μm thick buffer layer is enough to eliminate the spearhead attach problem.

The mechanism of kernel migration can be described in 3 steps: 1) carbon from the buffer layer is absorbed in the hot side of the kernel; 2) diffusion of the C to the cold side of the kernel; 3) Rejection of C in the cold side as graphite. The net effect is the kernel migration in the temperature gradient advancing through the hottest side of the buffer layer. The design bases at GA is to require that the worse particle will not present a kernel migration to more than 40% of the buffer layer thickness in normal power; the remaining 60% is to account for transients. The particle is assumed to fail if the kernel migrates through the whole buffer layer (Ref. 35). Such a high degree of conservatism reflects the still high uncertainty in the failure prediction by the amoeba effect mechanism.

The irradiation of kernel has little influence on the kernel migration velocity and the size of the kernel has no influence at all; this is because the increase in distance for the carbon to travel is compensated by an increase in the temperature gradient across the kernel. Increasing the buffer layer thickness helps relieve the problem, though.

The kernel migration coefficient (KMC), in $°Kcm^2/sec$, is defined as:

$$KMC = T^2 \frac{(dx/dt)}{(dT/dx)} \quad , \qquad (4.2.2\text{-}1)$$

where:

T - kernel temperature in °K ;

dx/dt - velocity of migration of the kernel in cm/sec ;

dT/dx - $(T_{hot} - T_{cold})$/diameter of the kernel in °K/cm .

The KMC for a defined particle design has a temperature dependence of the form

$$KMC = Ae^{-B/T} \quad , \qquad (4.2.2\text{-}2)$$

where A and B are two empirical constants determined for each case by fitting experimental data. Taking the decimal logarithm of Eq. (4.2.2-2) comes:

$$Log_{10}KMC = Log_{10}A - (0.4343B)\frac{1}{T} \quad . \qquad (4.2.2\text{-}3)$$

This Equation is plotted for several kernel types in Fig. 4.2.2-1 (from Fig. 3 of Ref. 21 and Fig. F.1.2-5 of Ref. 35).

All curves from this figure were taken from Fig. 3 of Ref. 21 except in the case of UC_2 where a disagreement exists with the PSAR for Fulton Generating Station (Ref. 35).

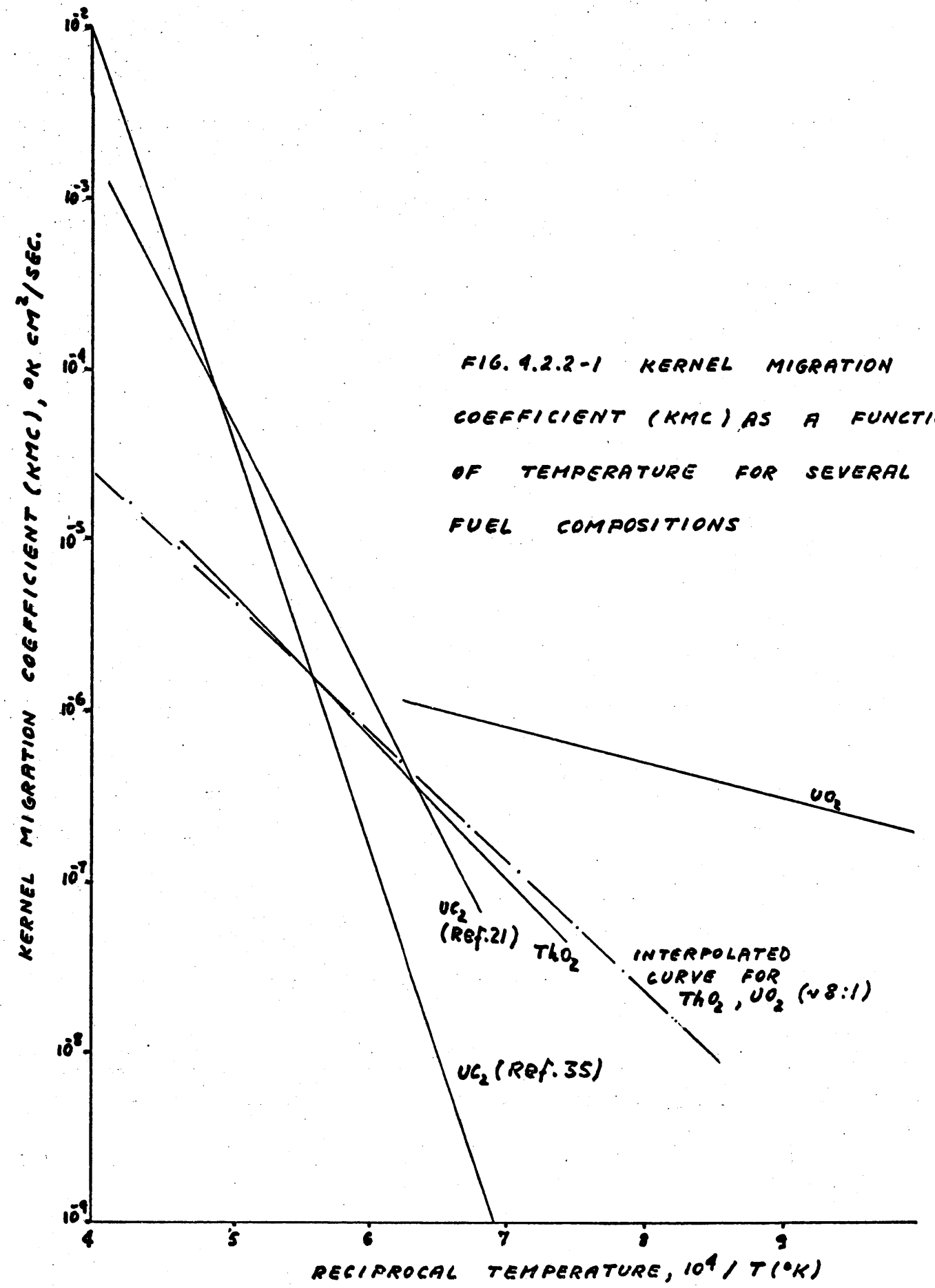

FIG. 4.2.2-1 KERNEL MIGRATION COEFFICIENT (KMC) AS A FUNCTION OF TEMPERATURE FOR SEVERAL FUEL COMPOSITIONS

In the Fulton design two separate particles are employed; a fissile particle containing only 93% enrichment U and a fertile one containing only Th. Initially both particles were going to be oxides but in the case of U the carbide was prefered on the basis of the curve from Fig. F.1.2-5 of Ref. 35 because its KMC is smaller than that of UO_2 for T_{CL} = 2580°F (1415°C), max. fuel temperature in Fulton, in this curve and it is not in the curve from Ref. 21.

There is no curve for ThC_2 in Fig. 4.2.2-1 but the information from all sources is that kernel migration is fairly fast in ThC_2 (5 to 10 times faster than in UC_2) and the fertile kernels in Delmarva and Fulton are composed of ThO_2. At temperatures below 1200°C the KMC of ThC_2 and of ThO_2 are comparable or slightly favoring ThC_2.

In section 4.3 the use of a single particle type consisting of a mixture of Th and U oxides (approximate properties of 8 to 1) is advised for the HTGR/GT. In this case the KMC for the HTGR/GT fuel particle can be approximately taken as a linear interpolation between the ThO_2 and UO_2 curves (see dashed line in Fig. 4.2.2-1).

The maximum temperature gradient in a fuel element is near the periphery and the maximum temperature is in the centerline. However, the kernel migration velocity is calculated using the highest KMC (at T_{CL}) and the steepest temperature gradient (at the fuel periphery). In Table 4.2.2-1 the max. velocity of migration and buffer zone required thickness are calculated for several temperatures and assuming a 4.8 full power years residence time. Of course there is a limit on how much one can increase the buffer thickness. This limit is dictated by the required ρ_m in the core.

For the maximum HTGR/GT T_{CL} of less than 2100°F in any of the designs discussed in Chapter 5 the required buffer thicknesses are relatively low and the HM loading requirements can be easily met (see section 4.3)

Table 4.2.2-1

Velocity of Migration and Required Buffer Layer Thickness for Several T_{CL} Values and a 4.8 Years Residence Time*

Assumed T_{CL}			KMC	dx/dt	min. buffer thickness
°F	°C	°K	10^{-8} °K cm^2/sec	10^{-12} cm/sec	μm
1900	1038	1311	3.5	3.48	13.2
2000	1093	1366	7.0	6.41	24.2
2100	1149	1422	12.0	10.15	38.4
2200	1204	1477	20.0	15.68	59.3
2300	1260	1533	28.0	20.37	77.0

(*) The temperature gradient assumed was dT/dx = 171°K/cm and the same GA design bases were employed to determine the minimum required buffer layer thickness.

4.3 Fuel Specifications

After selection of the HE fuel type (see Chapter 3) it was necessary to specify the coated fuel particle system, that is, decide between using a homogeneous or a heterogeneous system (i.e., separate fissile and fertile particles). For the decided system the kernel and coating composition and dimensions were specified.

4.3.1 Homogeneous vs. Heterogeneous Particle System

In a system were the fissile particles are partially or totally separated from the fertile ones, the burnup in the fissile particles is much higher than the average burnup of the system. This can be shown with the following approximate development. Let:

U_{25} mass of U^{235} in tons ;

x fraction of U^{235} in total U ;

Th mass of Th^{232} in tons ;

Th_1 mass of Th^{232} in fissile particles only, tons ;

E_{23} Thermal energy produced by U^{233} in Mwth ;

E_{25} thermal energy produced by U^{235} in MWth ;

BU_H homogeneous system burnup or ave. BU in a heterogeneous system ;

BU_F BU in the fissile particles of a heterogeneous system .

Neglecting fissions from Th^{232} and U^{238} one can write:

$$BU_F = \frac{E_{25} + (Th_1/Th)E_{23}}{(U_{25}/x) + Th_1} \quad , \qquad (4.3.1\text{-}1)$$

and

$$BU_H = \frac{E_{25} + E_{23}}{(U_{25}/X) + Th} \quad . \qquad (4.3.1\text{-}2)$$

Dividing Eq. (4.3.1-1) by Eq. (4.3.1-2), it results:

$$\frac{BU_F}{BU_H} = \frac{[E_{25} + (Th_1/Th)E_{23}][(U_{25}/X) + Th]}{[(U_{25}/X) + Th_1][E_{25} + E_{23}]} = \frac{[E_{25}+(Th_1/Th)E_{23}](U_{25}+ XTh)}{(U_{25}+ X\ Th_1)(E_{25} + E_{23})} \qquad (4.3.1\text{-}2)$$

Defining now Θ, R and γ as:

$$\alpha = Th_1/U_{25} \quad , \qquad (4.3.1\text{-}4)$$

$$\beta = U_{25}/Th \quad , \qquad (4.3.1\text{-}5)$$

and

$$\gamma = E_{23}/E_{25} \, , \qquad (4.3.1\text{-}6)$$

it follows that

$$U_{25} + X\ Th_1 = U_{25}(1 + X\alpha) \quad , \qquad (4.3.1\text{-}7)$$

$$U_{25} + X\ Th = U_{25}[1 + (X/\beta)] \, , \qquad (4.3.1\text{-}8)$$

$$Th_1/Th = \alpha\beta \quad , \qquad (4.3.1\text{-}9)$$

and

$$E_{25} + E_{23} = E_{25}(1 + \gamma) \quad . \qquad (4.3.1\text{-}10)$$

By substituting Eqs. (4.3.1-7), (4.3.1-8), (4.3.1-9) and (4.3.1-10) into Eq. (4.3.1-3) it follows:

$$\frac{BU_F}{BU_H} = \left(\frac{1 + \alpha\beta\gamma}{1 + \gamma}\right)\left(\frac{\beta + X}{\beta}\right)\left(\frac{1}{1 + X\alpha}\right). \qquad (4.3.1\text{-}11)$$

The values of ✖, α and β in FSV are respectively 0.93, 4.25 and 0.045. The value of γ can be estimated through the conversion ratio, C, definition. The conversion ratio is defined as the number of fissile nuclei produced from fertile material to the number of fissile material consumed in fission and non fission reactions. If Pu production and consumption is neglected, C can be approximated as

$$C \simeq \frac{U_{23} \text{ produced}}{U_{25} \text{ consumed} + U_{23} \text{ consumed}} \quad . \qquad (4.3.1\text{-}12)$$

The equation for γ can be approximated as

$$\gamma = \frac{E_{23}}{E_{25}} \simeq \frac{U_{23} \text{ consumed}}{U_{25} \text{ consumed}} \quad , \qquad (4.3.1\text{-}13)$$

and if this equation is substituted into Eq. 4.3.1-12 for the equilibrium cycle where the production and consumption of U_{23} is the same, there results:

$$C = \frac{\gamma}{\gamma + 1} \quad , \qquad (4.3.1\text{-}14)$$

or

$$\gamma = \frac{C}{1 - C} \quad . \qquad (4.3.1\text{-}15)$$

In the equilibrium cycle with bred fuel recycle, C = 0.66 (Ref. 51) and γ = 1.94 from Eq. 4.2.1-15. If the values of x, α and β are substituted into Eq. 4.3.1-11, it follows that

$$\frac{BU_F}{BU_H} = \left(\frac{1 + 0.191\gamma}{1 + \gamma}\right)(4.38) \quad . \qquad (4.3.1\text{-}16)$$

The ratio BU_F/BU_H would only be equal to 1 for $\gamma = 20.7$ (or C = 0.95); as γ decreases the ratio BU_F/BU_H increases approaching 4.38 assymptotically. For $\gamma = 1.94$, $BU_F/BU_H = 2.04$ and the fissile particle has to be designed for a much larger BU than the fertile particle thus requiring a higher coating to kernel ratio. The conclusion is that for everything else the same, the homogeneous system permits a higher HM loading than the heterogeneous system. It is interesting to note that in FSV the fissile particles contain some Th^{232} (Th_1); in the most recent design, Fulton Generating Station, the separation is complete (Ref. 35), that is, the fissile particles contain only UC_2 ($\alpha = 0$), and BU_F/BU_H increases relative to FSV. In Fulton BU_F = 75% FIMA and for the fertile particles BU = 7.5% FIMA.

The objective of using a heterogeneous system is to allow separation of the particles in a reprocessing plant and recuperation of the U^{233} produced free from U^{236} contaminant. As explained in section 3.4 there will be no credit for U^{233} produced in the HTGR/GT case, thus there is no incentive to separate the particles.

It was decided to recommend the homogeneous system of particles because then burnup problems could be more easily covered by the particle design. Also, the use of single intermediate sized kernel particle would permit the compactation by the process 1 described in section 4.1.

4.3.2 Coating Selection

The function of the particle coating is to confine the dangerous products of the nuclear fission. According to the danger and ease with which those nuclides can escape the kernel and buffer layer, they may

be classified in the following order (Ref. 74):

(1) noble gas (Kr,xe);

(2) the halogen group (I);

(3) metallic elements capable of migrating, such as alkaline, (Cs, Sr, Ba), lanthanides (Ce), and U and Th themselves;

(4) imobile species (Zr)

Historically the first really successful coatings to be produced were of the BISO type (see Fig. 4.1.2). The high density PyC external layer was found to be extremely impermeable to gas. The solid FP at high temperature can migrate slowly through the PyC, though. For that reason the possibility of using an outer extra carbide layer was considered. Some of the carbides tried were Zr, Si, Nb and Ta carbides. The SiC is presently accepted in the United States and England as the best choice. Being highly fragile the SiC is sustained by an external high density layer of PyC. This combination of PyC/SiC/PyC is called TRISO (see Fig. 4.1-2) and came as an improvement over the BISO. With SiC the retention of solid FP such as Ba, Cs, Sr and Ce increases by a factor of up to three orders of magnitude.

The BISO coating is less expensive and can be used for low BU particles as the fertile particles in heterogeneous particle systems. For the high BU HTGR/GT particles the proper coating to use is the TRISO.

4.3.3 Kernel Composition

The Th to U atoms ratio in the final reference design (Chapter 5) is 34.68/4.516 = 7.7. A choice must be made between using a mixture of carbides or a mixture of oxides of Th and U in the kernel. The following aspects were observed:

A) Fabrication. The cost is about equal but the U,Th contamination in the coating layers can be kept in a lower level with oxides

B) Fission products retention. Oxides are certainly better than carbides; oxides have a much higher retention of Sr (100 times) and rare earths than carbides.The retention of Cs and Ba is the same but the possible Ba getter (Al_2O_3 forming $BaAl_2O_4$) and Cs getter ($Al_2O_3 + SiO_2$) are more dilutable in an oxide kernel.

C) Amoeba effect. At the HTGR/GT maximum T_{C_L} of about 2100°F the KMC should be about the same in a Th,U carbides or oxides mixture.

D) Internal Pressure build-up. The internal pressure build up is about 25% larger in the oxides due to the production of O_2, CO and CO_2 with fission. This disadvantage can be partially offset with the use of oxigen getters such as SiC.

E) Future perspectives. It looks like oxides have a better chance of improvement. Not only because of research around items B and D, but also due to the fact that oxides were prefered in several other HTGR programs.

Because of the higher FP retention and of the brighter future prospects it was decided to use a mixture of ThO_2 and UO_2 (7.7:1 proportions) in the HTGR/GT kernels.

4.3.4 Preliminary Particles Design

In all designs discussed in Chapters 3 and 5 the total HM homogenized atom density was 39.2×10^{-5} HM atoms/bcm, which corresponds to $\rho_m = .713$ g/cm^3. The UO_2 density is 9.6 g/cm^3 and that of ThO_2 is 8.1 g/cm^3; the density of the UO_2, ThO_2 mixture will be taken as

$$\rho = \frac{(g.6g/cc)(4.52) + (8.1g/cc)(34.68)}{39.2} = 8.3g/cc \ .$$

Assuming compactation by process 1 of section 4.1, the fraction of fuel rods occupied by coated particles will be about f = 0.35. Substituting these values of ρ_m, ρ and f into Eq. 4.1-3 it results:

$$(1-\rho)\left[\frac{r}{(r+t)}\right]^3 = 0.245 \ . \qquad (4.3.4\text{-}1)$$

It is not the intention of this section to make a final decision on the particle design, but only to indicate that a conservative design is possible by comparing with other designs for similar maximum conditions in the core, showing that a design observing Eq. 4.3.4-1 is possible.

The estimated average burnup in the HTGR/GT is given in Table 4.3.4-1, in MWD/T and in %FIMA. For the Final Reference Design described in Chapter 5, the maximum burnup was estimated to be 106 x 10^3 MWD/T or 10.9 %FIMA. The maximun T_{C_L} is about 2100°F and the peak nvt below 8 x 10^{21} n/cm^2 in the HTGR/GT.

Since the HTGR/GT particle size should be comparable to that of Dragon and the maximum T_{C_L} and BU is not too different in those two designs, a possible HTGR/GT particle design is here proposed based on the Dragon particle design. Let us assume that the maximum pressure build up is the same in the two particle designs so that the coating thickness of Dragon could be maintained at the HTGR/GT. In this case, it can be written

Table 4.3.4-1

Average Burnup Calculation for the HTGR/GT

A. HM inventory in the core

	U^{235}	U^{238}	Th^{232}
mass in kg	775.7	59.1	6,323.0
no. of atoms in 10^{27} atom units	1.957	.7495	16.41

B. Average BU in MWD/T after 4.8 years (1752 days) of full 300 MWth power operation:

$$\text{ave. BU} = \frac{(300\ \text{MW})(1752\text{D})}{(6323 + 775.7 + 59.1) \times 10^{-3}\text{T}} = 74{,}430\ \text{MWD/T}$$

C. Average BU in %FIMA after 4.8 years (1.514×10^{8} sec) of full 300 MWth power operation :

$$\text{ave BU} = (1.514 \times 10^{8}\ \text{sec})(300\ \text{MW})(1\ \text{fis./}\ 200\ \text{MeV})(1\ \text{MeV}/$$

$$1.6 \times 10^{-19}\ \text{MW sec})(100\%\ )/(1.987 + .1495 +$$

$$16.41) \times 10^{27}\ \text{ats} = 7.65\%\ \text{FIMA}$$

$$\left[\frac{\rho_m(1-p)(BU)(T_L)}{p}\right]_{Dragon} = \left[\frac{\rho_m(1-p)(BU)(T_L)}{p}\right]_{HTGR/GT}, \qquad (4.3.4\text{-}2)$$

or

$$\frac{(0.9)(.80)(10)(2280+460)}{0.2} = \frac{(0.713)(1-p)(10.9)(2100+460)}{p}. \qquad (4.3.4\text{-}3)$$

The HTGR/GT porosity from Eq. 4.3.4-3 is p = .167. To be conservative a value of 0.2 will be assumed.

The thickness of all high density TRISO layers will be maintained. The buffer layer thickness from Table 4.2.2-1 at 2100°F is 40 μm, so that the total layer thickness will be t = 195 μm. The kernel radius from Eq. 4.3.4-1 for p = 0.2 and t = 195 μm is 403.3 μm. The results of all those calculations are summarized in Table 4.3.4-2.

It is concluded that in a homogeneous system with ρ_m = 0.713 g/cc the FP build up and amoeba effect problems in the proposed HTGR/GT design can be easily engineered out with proper design of the coated fuel particle. The fast neutron fluence is the real limiting factor in the HTGR/GT design.

TABLE 4.3.4-2

COATED PARTICLE DESIGN SPECIFICATIONS FOR DRAGON AND FOR THE HTGR/GT

	Dragon	HTGR/GT	Comments
Kernel			
composition	UO_2	ThO_2,UO_2	Proportion of 7.7ThO_2 to 1 UO_2
diameter, μm	800	806	From Eq. 4.3.4-1 with p=0.2 and t = 195 μm
porosity	20%	20%	From conservative use of Eq. 4.3.4-3
Buffer			
thickness,μm	35	40	2100°F in Table 4.2.2-1
density, g/cc	1.1	1.1	Maintaining the Dragon value
Seal			
thickness,μm	20	20	Maintaining the Dragon value
density, g/cc	1.6	1.6	" " " "
Inner PyC			
thickness,μm	45	45	" " " "
density, g/cc	1.8	1.8	" " " "
SiC			
thickness,μm	35	35	" " " "
density, g/cc	≥3.2	≥3.2	" " " "
Outer PyC			
thickness,μm	55	55	" " " "
density, g/cc	1.8	1.8	" " " "

CHAPTER 5

HTGR/GT NUCLEAR DESIGN

5.1 Introduction

A summary description of the reference core design is given in section 1.2. The reasoning and design methods employed to arrive at this reference design are discussed below in more detail.

The first major decision was to refuel the entire core in a batch refueling cycle. In the absence of carrying charges the high inventory cost of a batch core does not increase the fuel cycle cost; thus, the longest possible batch, satisfying safety requirements, becomes the most economical by minimizing shut down periods. Even if carrying charges were considered, use of a batch core would have been strongly advised in this small plant size where the capital cost accounts for 2/3 of the total energy cost and the fuel cycle cost and operating cost divide equally the remaining third (section 3.4). In such a case the use of a batch core should be considered for its practical advantages, namely:

A. Allows acceptable burnup of the entire batch.

B. Simplicity of design of refueling programming. The batch fueling cycle is much simpler than the more economical scattered refueling schemes. In scattered refueling there is always power peaking problems requiring the employment of several enrichment zones and careful refueling programming. Even the use of a single enrichment batch is here possible due to the small size of the core; the BOL power peaking is not large and decreases all the time with depletion.

These advantages are well recognized and there is experience in the commercial use of batch cores in similar situations, i.e., Peach Bottom (Ref. 11) and JAERI (Ref. 84). Once the decision was taken in favor of batch loading, the LE and HE batches were compared (see Chapter 3) and HE batch loading was chosen.

The operating conditions had to be decided in a very early stage of the project:

A) The coolant pressure and temperature conditions were determined after power cycle optimization (Ref. 82);

B) The average power density (PD) is used to determine the size of the reactor and the average fuel centerline temperature; for a given composition it will also determine the average burnup and nvt in the core, and it is then very much related with the maximum residence time of the coated fuel particles in the reactor. Capital cost considerations point towards the use of higher PD's (smaller vessel) and fuel cycle cost considerations towards lower PD's (longer batches). The sensitivity of the capital costs to the size of the core is lower than the sensitivity of the fuel cycle cost to the refueling intervals and the PD should be as low as practical. The maximum diameter of shop fabricated steel vessels is about 21 ft. (Chapter 6 discusses the choice of a steel vessel instead of a PCRV) which limits the PD to a minimum of about the level of the PD in FSV if the optimum height to diameter ratio (approximately 0.9, Table 9-2 of Ref. 29) is assumed in the core.

Having decided the power density, the volume of the 300 MWth HTGR/GT was determined. To maintain the same FSV fuel element design and have a near optimum height to diameter ratio, two options were possible for the core arrangement: a) columns of 4 graphite elements; b) columns of 5 graphite elements each. The 4 elements column is more adequate having a larger diameter and permitting a greater number of CR (reactivity control was expected to be a problem) and a smaller pressure drop. The only concern in this larger diameter option was if the side reflector was thick enough to shield the vessel wall from the fast neutron flux to maintain the fast fluence below the acceptable limits (see section 2.2) which was proven with the help of the transport code ANISN (Ref. 79).

The situation could then be summarized as follows:

1. The coolant conditions, the PD and core configuration (see Fig. 1.2.1-1) were chosen.
2. The maximum temperature, burnup and fast fluence in the coated fuel particles were estimated to be of the same level of FSV. In FSV the coated fuel particles remain in the reactor for 6 calendar years (4.8 full power years assuming a 0.8 load factor) with annual shuffling and refueling of 1/6 of the core. The HTGR/GT has lower peaking factors but the particles in the middle (highest flux) remain always in the middle. A 4.8 full power years batch was then established as the HTGR/GT design aim.

3. For conservatism all compositions tried had their HM content below 39.2×10^{-5} atoms/b cm (Eq. 3.1-1); in Chapter 4 it is shown that for the HTGR/GT case the use of single larger particles is probably more adequate than the FSV particle design. In this case slightly higher HM contents may be achievable, but there is not much room for improvement and the results are not very sensitive to the HM contents (Chapter 3), so this constraint is not limiting.

The optimum composition and CR requirements for a 4.8 year-batch was to be determined. Basically the optimum composition should minimize the possibility of coated fuel particle failure. In Chapter 4 it was seen that the three failure controlling parameters are the maximum burnup, nvt and T_{ℓ}. To quickly analyse the merits of the several cases treated, some short cuts to rapidly estimating these parameters are necessary:

1) Burnup: In all cases the total power is 300 MWth, the residence time is 1752 days (4.8 years) and the HM density is 39.2×10^{-5} atoms/bcm. Because the range of composition is small and the atomic weights are nearly the same the total amount of HM in the core can be taken as 7.158 tons (even the Parfait configurations, in section 5.2.2, have approximately this value. The average burnup, BU_{ave}, can be calculated as:

$$BU_{ave} = \frac{(300\ \text{MWth})(1752\text{D})}{7.158\ \text{T}} = 73{,}428\ \text{MND/T} \quad . \qquad (5.1\text{-}1)$$

The average power density in the core is 6.34 w/cc and the peak power density can be taken from the computer output. Because the

peak power density vary very little with time and is located at approximately the same spot the maximum burnup, BU_{max}, can be conservatively estimated as

$$BU_{max} = (BU_{ave}) \frac{(\frac{PD_{max}}{6.34})_{EOL} + (\frac{PD_{max}}{6.34})_{EOL}}{2} \quad . \qquad (5.1\text{-}2)$$

2) Maximum fast fluence: The fast fluence during a time t in a position r, z is given by:

$$nvt(r,z) = \int_o^t \phi_1(r,z,t)dt \qquad (5.1\text{-}3)$$

The fast flux distribution $\phi_1(r,z,t)$ (neutron flux with E > 0.183Mev) is always proportional to the power density distribution because the power density is proportional to the number of fissions/ cm^3sec (if one neglects the small difference in fission energy of the fissile materials - see Eq. 3.3.2-1) and the number of fissions times the fraction of the fission spectrum with energy larger than 0.183 Mev must be proportional to ϕ_1. For the same reasons given above in item 1 the maximum nvt after 4.8 years can be calculated as:

$$nvt_{max} = \frac{(\bar{\phi}_1 \frac{PD_{max}}{6.34})_{BOL} + (\bar{\phi}_1 \frac{PD_{max}}{6.34})_{EOL}}{2} 1.51 \times 10^8 \text{ sec} , \qquad (5.1\text{-}4)$$

where $\bar{\phi}_1$ is the average flux in the core for group 1 taken from the computer output (in all outputs there is a point by point PD distribution and average fluxes by region print out). In long batches like ours the final composition is very much different from the

initial one. In particular the fissile inventory decreases to about half its initial value and according to Eq. 3.3.2-1 the flux must increase. In fact the thermal flux increases a lot, but $\bar{\phi}_1$ remains approximately constant as it must since the average power is independent of time and composition. The values of $\bar{\phi}_1$ for several of the designs tried are summarized in Table 5.1-1. If BOL $\bar{\phi}_1$ and EOL $\bar{\phi}_1$ are substituted by an average in time value (see Table 5.1-1), Eq. 5.1-4 can be written as:

$$nvt_{max} = (1.514 \times 10^8 \times \bar{\phi}_1 \text{ sec}) \left[\frac{(PD'_{max}/6.34)_{BOL} + (PD_{max}/6.34)_{EOL}}{2} \right]. \quad (5.1\text{-}5)$$

3) Maximum fuel centerline temperature: For this calculation the simplest approach is first to calculate the coolant temperature profile in the center region and from there to calculate the T_ℓ profile. The numbers and model used here are explained in more detail in Ref. 87. The increase in the center region coolant temperature in going from point i to i+1 is given by:

$$PD_i A \, \Delta Z_i = m \, c_p (T_{i+1} - T_i) \quad (5.1\text{-}6)$$

where:

m = 22.047 lb/sec average mass flow rate per region;

c_p = 1.2416 BTU/lb°F = 1309.0 W-sec/lb°F;

A = 7859.9 cm^2 center region area;

PD_i = power density in w/cc at point i from CITATION for the center column;

Table 5.1-1

Average Values of the Fast Flux in the Core of Several Cases

Design (*)	Bol $\bar{\phi}_1$ x 10^{-13} n/cm^{2}sec	BOL $\bar{\phi}_1$ x 10^{-13} n/cm^{2}sec	Ave. in time $\bar{\phi}_1$ x 10^{-13} n/cm^{2}sec
RD1	3.13	3.38	3.26
RD2	3.16	3.41	3.29
RD3	3.36	3.45	3.41
RD4	3.37	3.58	3.48
RD5	3.29	3.58	3.44
RD6	3.40	3.60	3.50
RD7	3.50	3.61	3.56
RD8	3.42	3.62	3.52
RD9	3.53	3.62	3.58
PARF2	3.10	3.62	3.36

(*) These designs are discussed in section 5.3

T_i = coolant temperature to be determined (the starting point is 964.2°F at the entrance);

ΔZ_i = 317.0 cm/number of axial intervals; in the preliminary runs of section 5.2, 9 intervals were used and ΔZ_i = 35.22 cm which is an approximation since the CITATION intervals are not all of the same size.

Substitution of the numerical values into Eq. 5.1-6 yields

$$T_{i+1} = T_i + (9.586)\ PD_i \quad , \tag{5.1-7}$$

for 9 axial intervals. The fuel centerline temperature can be calculated from

$$(T_\ell)_i = T_i + q_i\ \Delta Z_i R_i \quad , \tag{5.1-8}$$

where:

q_i = heat generation in an individual fuel pin of the central region. Since any region has 1380 fuel pins, q_i = $PD_i A/1380$;

R_i = resistance to heat transfer at temperature typical of point i. Note that the product $\Delta Z_i R_i$ is really independent of ΔZ_i:

$$R_1 \Delta Z_i = \{\frac{1}{4\pi\ k_f\ \Delta Z_i} + \frac{\ell n[(r+g)/r]}{2\pi\ k_g\ \Delta Z_i} + \frac{\ell n[r+g+c)/(r+g)]}{2\pi\ k_c\ \Delta Z_i} +$$

$$+ \frac{1}{2\pi h\ \Delta Z_i (r+g+c)}\} \Delta Z_i \quad , \tag{5.1-9}$$

where:

k_f = 4.0 BTU/ft°F hr = .0385 w-sec/cm° F sec = fuel thermal conductivity ;

k_g = .17 to .22 BTU/ft°F hr = (1.6 to 2.1) x 10^{-3} w/cm°F = Helium gap thermal conductivity ;

k_c = 16.0 BTU/ft°F hr = .154 w/cm°F = graphite thermal conductivity ;

h = 75 to 95 BTU/hr ft^2°F = .0237 to .0300 w/cm^2°F = heat transfer coefficient ;

r = .2455 in = .6236 cm = fuel pin radius ;

g = .0045 in = .0114 cm = Helium gap thickness ;

c = .1775 in = .4509 cm = distance from fuel hole to coolant hole.

It is seen that the variation of the above parameters with temperature is very small and an average ΔZR = 8.1 cm°F/w can be used at any i. Eq. 5.1-8 then becomes :

$$(T_\ell)_i = T_i + (46.14°F\ cm^3/w)PD_i \ . \qquad (5.1\text{-}10)$$

Axial power shape would produce a T_ℓ. It can be shown that an inlet peaked exponential independent of axial position in the channel (see Ref. 3), that is, for a given average power density and axial power shape, would allow the minimum maximum T_ℓ possible; on the other hand a flat axial power would minimize the peak burnup and fast fluence.

In the FSV design GA used 2 axial zones for a good compromise between those conflicting interests (see Table 2.1.3.2-1 and Fig. 2.1.3.2-1). In the HTGR/GT the radial power peaking factor is naturally low due to the small size of the core and the maximum T_{ℓ} is below 2300°F (maximum fuel centerline temperature in FSV) even for a completely flat axial power shape. Also, the lack of fuel shuffling makes the maximum BU and nvt for a certain power peak reached in a batch core higher than corresponding values for a core where fuel shuffling is employed. An axial power shape such as that of ESV (axial peaking factor = 1.56 from Fig. 2.1.2.2-1) for instance, would have been unacceptable for the HTGR/GT. If just a single zone was employed in the HTGR/GT the presence of CR in the top reflector would make the power peak in the core bottom reflector interface. This peak is very high (see section 5.3.2) and can not be tolerated; three different configurations were shown to eliminate this problem in section 5.3.2.

As for the XY power distribution, the problem is the relatively high CR requirements associated with a high excess of reactivity core necessary for a long batch. With only 19 CR pairs in the core the worth of each pair would have been too high making it difficult to maintain a low peaking power factor. For that reason 12 extra CR pairs were added to the temporary reflector (see section 5.2). Also, the CR requirements were decreased after LBP optimization (see section 5.3.1.3).

The HTGR/GT nuclear design discussion is organized in this

chapter in the following way:

Section 5.1 Introduction. The design problems are mentioned; simplified equations to quickly estimate the maximum BU, nvt and T_{ℓ} are developed; the organization of Chapter 5 is given.

Section 5.2 Control Rod Configuration Studies. The maximum permissible k_{eff} using FSV CR design is calculated for several compositions.

Section 5.3 Unrodded Composition Optimization. Several static and depletion runs in RZ geometry with increasing complexity are discussed. The runs with 8 or less core depletion zones are called preliminary runs, having 6 to 7 points in the radial and 8 points in the axial direction inside the core and are discussed in Section 5.3.1; the runs to determine the Final Reference Design, FRD, were made with 12 core depletion zones, each zone having at least 16 mesh points, and are treated in section 5.3.2 .

5.2 Control rod (CR) configuration studies

The objective of the CR configuration studies was to determine the maximum allowable hot excess of reactivity in the HTGR/GT if the FSV periphery type of CR pairs (Table A.1-4B) were employed. As a by product the worth of the CR and the region peaking factors in some near critical configurations were also calculated.

The 19 core and 12 reflector CR locations in the HTGR/GT are shown in Fig.1.2.1-1. Since the HTGR/GT core has homogeneous composition and all CR configurations tried were symmetrical, the core could be represented by using 1/4 of core symmetry (see Fig. 5.2-1). In all cases the rods were either completely in or completely out which yields a maximum region peaking factor of about 1.4 in the near critical configurations. This value is about 15% higher than the values found in the unrodded RZ depletion runs used to calculate the maximum BU's, nvt's and T_{ℓ}'s (section 5.3). In those RZ representations the radial peaking is about 1.21; the insertion of CR should increase somewhat the peaking factor, but this effect is expected to be offset by the fact that CR programming will change the peak location from time to time. Also, a more careful CR programming with partial CR insertion should decrease the 1.4 value found with the rods completely in or completely out. As a result no factor was introduced to correct the values found in section 5.3.

The first group of CR configuration runs was made with the CS for c/u = 4000; the configurations and k_{eff} obtained are summarized in Table 5.2-1. From this table the following worths can be calculated:

A) Total CR bank worth = 0.22 ΔK or 0.007 Δk/rod pair

B) Average worth few rods in is ∿0.008 Δk in the core and 0.007 Δk in the reflector.

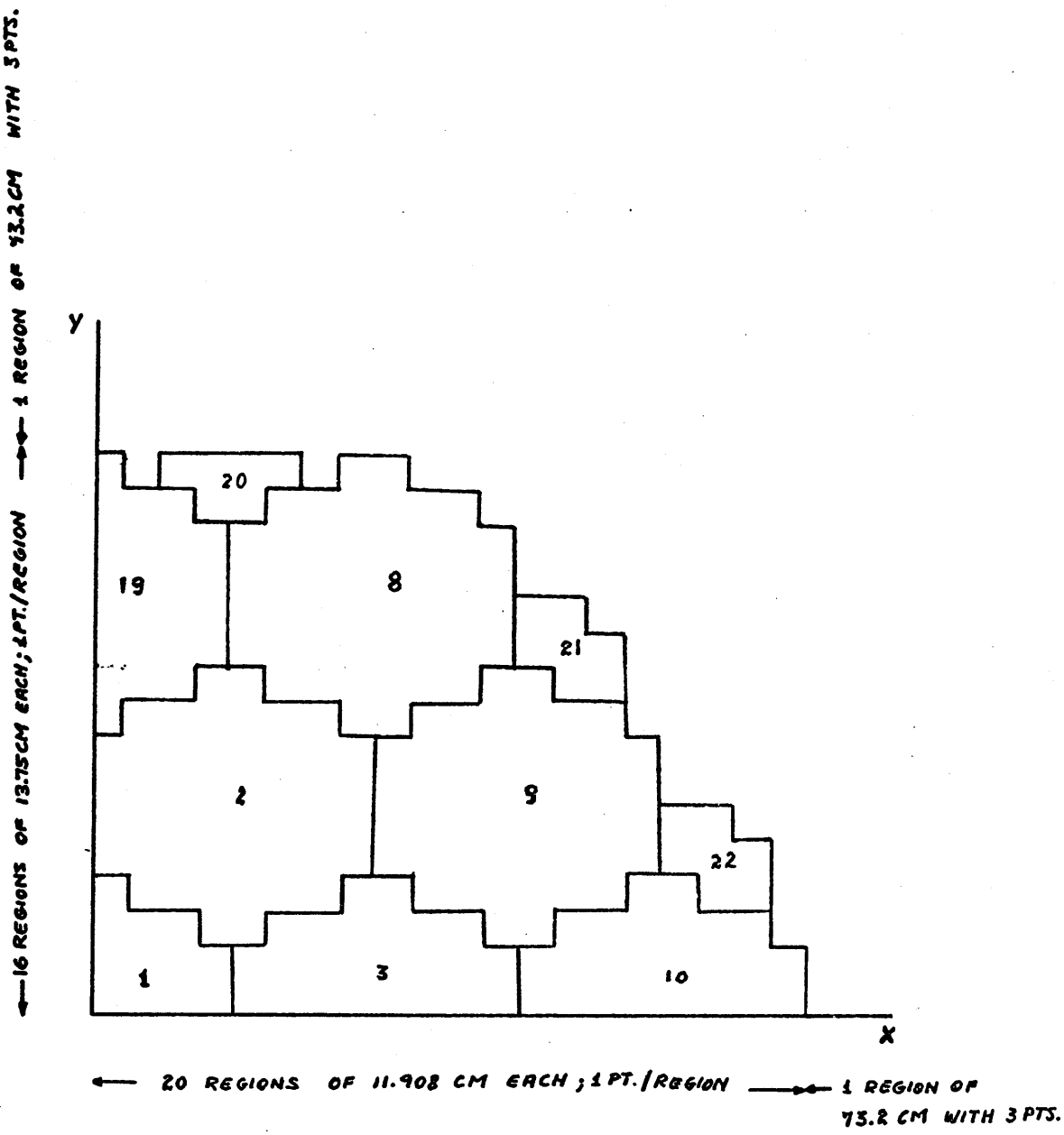

FIG. 5.2-1 HTGR/GT 1/4 OF CORE REPRESENTATION IN XY GEOMETRY FOR THE PREPARATION OF A CITATION INPUT

Table 5.2-1 Summary of CR configurations with N_{25}=2.92, N_{28}=.220, N_{02}=36.06 and N_{8}=.4417 (in 10^{-5} atom/bcm)

Run No.	Regions With CR Inserted	Temperature	k_{eff}
1	1,8,9,10,11,12,14,15,16,17,18	Hot	.99387
2	None	Hot	1.08234
3	2,3,4,5,6,7	Hot	1.03032
4	2,3,4,5,6,7 + 12 REF. CR	Hot	.94711
5(*)	2,3,4,5,6,7 + 12 REF. CR	Hot	.95046
6	2,3,4,5,6,7 + 12 REF. CR	Cold	1.00869
7	All rods	Cold	.89650
8	None	Cold	1.11652
9	Only the central CR out	Cold	.94167

(*)This and the next runs had the correction in the graphite δ_{23} given by Eg. 2.1.1.2.2-1. The difference between runs 4 and 5 give the sensitivity to the change. The cs used in these 9 runs were still for c/u=4000.

Table 5.2-2 Summary of CR configurations with N_{810}=.1218 10^{-5} atoms/bcm (see section 5.3) and N_{25} given in the table (*)

Run No.	N_{25}	Region With CR Inserted	Temperature	k_{eff}
1	3.847	Only the central CR out	Cold	.99553
2	3,847	All rods	Cold	.95006
3	3.847	None	Cold	1.20204
4	4.548	All rods	Cold	.99925
5	4.548	Only the central CR out	Cold	1.03039
6	4.548	None	Cold	1.24551
7	4.548	None	Hot	1.19799

(*)The U^{238} and Th^{232} atom densities can be determined from equallity 3.1-1 and by knowing that N_{28}=7 N_{25}/93. The cs used in those runs were for c/u=1800.

C) Worth of the central CR pair = 0.0452 Δk (all other pairs inserted). The central CR pair is always the most reactive and it is interesting to note that the worth of a CR pair with all the others inserted is much larger than its worth when just a few rods are in, as in the case of a near critical configuration for instance.

D) Temperature defect = 0.05823 Δk (loss of core reactivity in going from cold to hot full power condition with the central CR pair stucked out).

It is important to realize that the actual values of the k_{eff}'s for the composition in Table 5.2-1 are really somewhat smaller than the values in the table because the XY runs did not take into account the top reflector CR and LBP in the bottom reflector. Assuming that the differences between the k_{eff}'s from the XY runs and the k_{eff}'s from the corresponding RZ runs (taken as correct) is the same independent of temperature, the corrections in the XY k_{eff}'s would cancel out in the following worth calculations, since all the worths above were calculated as the difference between XY k_{eff}'s from Table 5.2-1.

The CR worths listed above can be used to estimate the maximum controllable correct RZ hot k_{eff} and the maximum controllable excess of reactivity:

$$\text{temperature effect:} \quad (k_{eff})_{cold} - (k_{eff})_{hot} = 0.05823\ \Delta k; \qquad (5.2\text{-}1)$$

$$\text{shut down margin:} \quad (k_{eff})_{cold} - 0.22\ (\text{total control worth}) = 1.0 - 0.0452\ (\text{stuck rod allowance}). \qquad (5.2\text{-}2)$$

By solving Eqs. 5.2-1 and 5.2-2 for $(k_{eff})_{hot}$, the maximum allowable hot excess of reactivity $= (k_{eff})_{hot} - 1.0 = 0.1166\ \Delta k$.

After correction for c/u ratio and use of B^{10} concentration and self-shielded cs, the same procedure described above was repeated for some other compositions. The configurations and XY k_{eff}'s obtained for two other compositions are summarized in Table 5.2-2.

The total CR bank worth was verified to increase with increased U^{235} content and for $N_{25}=4.548 \times 10^{-5}$ atoms/bcm the maximum controllable hot excess of reactivity was calculated to be 0.1576 Δk (much higher than 0.1166 Δk for $N_{25}=2.92 \times 10^{-5}$ atoms/bcm). The final optimized 4.8 full power year-batches have fissile contents in the (4.2 to 4.548) $\times 10^{-5}$ atoms/bcm range (see section 5.3), which means that hot k_{eff}'s in the 1.15 neighborhood in the optimized runs could still be controlled by the CR type under study in this section. After LBP optimization (section 5.3.1.3) the long life batches were obtained with maximum hot unrodded k_{eff}'s well below the lower limit of controllability 1.1166 at any time in the life.

5.3 Unrodded composition optimization

All the studies to optimize the composition were made with the help of CITATION and represents the HTGR/GT core in RZ geometry. The merits of each composition were analyzed with respect to minimum burnup, nvt, T_{GL} and CR requirements.

The results of a depletion run can vary considerably with the number of depletion zones and mesh size specified in the input. Since the thermal diffusion length calculated for the HTGR/GT core is about 9 cm, the mesh size for adequate representation of the flux and PD should be somewhat smaller than this amount. By analyzing the relative form of the flux in the core it can be seen that the use of 3 radial regions and 4 axial regions in a total of 12 core depletion zones should suffice for our purposes. This is proven in section 2.1.3.3.

Unfortunately, a computer run with such a detailed representation is costly and to perform all runs till optimum in that fashion would have been too expensive. Actually most of the runs were performed with very little detail with the objective of obtaining preliminary information (section 5.3.1) thus reducing the number of necessary detailed runs and saving computational expenses.

5.3.1 Preliminary studies

At first several compositions were tried using LBP rods of the same size and B^{10} content as those of FSV, but having 6 rods per element instead of 2:

A) Using LBP in the reflector to increase the reactivity lifetime. The use of LBP in the side reflector considerably increased the radial

peaking and the idea was rejected, but the LBP addition to the bottom reflector proved beneficial. The first composition and configuration with LBP in the bottom reflector was called Reference Design 1, ^{RD1}, and is discussed in section 5.3.1.1 together with RD2, a new version of RD1 with lower fissile content.

B) Parfait configurations. The Parfait concept (see section 5.3.1.2) is to have a central fertile region in the core with the idea of getting a higher conversion ratio and reactivity lifetime and of decreasing the power peaking factors. In our trials the already approved bottom reflector LBP was also incorporated. The Parfait configurations are described and compared with RD1 in section 5.3.1.2. The second Parfait trial proved better than RD1.

Next came the LBP optimization (section 5.3.1.3) abandoning the FSV LBP rod design. These studies to determine the optimum B^{10} concentration in the LBP, and number of LBP rods were made in single zone cores for the RD2 composition.

5.3.1.1 Discussion of RD1 and RD2

The RZ representation of the HTGR/GT as prepared for the CITATION in the RD1 and RD2 cases is shown in Fig. 5.3.1.1-1. Both RD1 and RD2 have 6 LBP rods per element, one at each corner, in the core and 12 LBP rods per element in the reflector; in appendix A.3.3.2 the calculations necessary to represent those LBP rods in the CITATION input is exemplified for the Final Reference Design (FRD). Table 5.3.1.1-1 provides the composition per zone for the unrodded RD1 and RD2.

The RD1 was the first calculation with LBP in the bottom reflector.

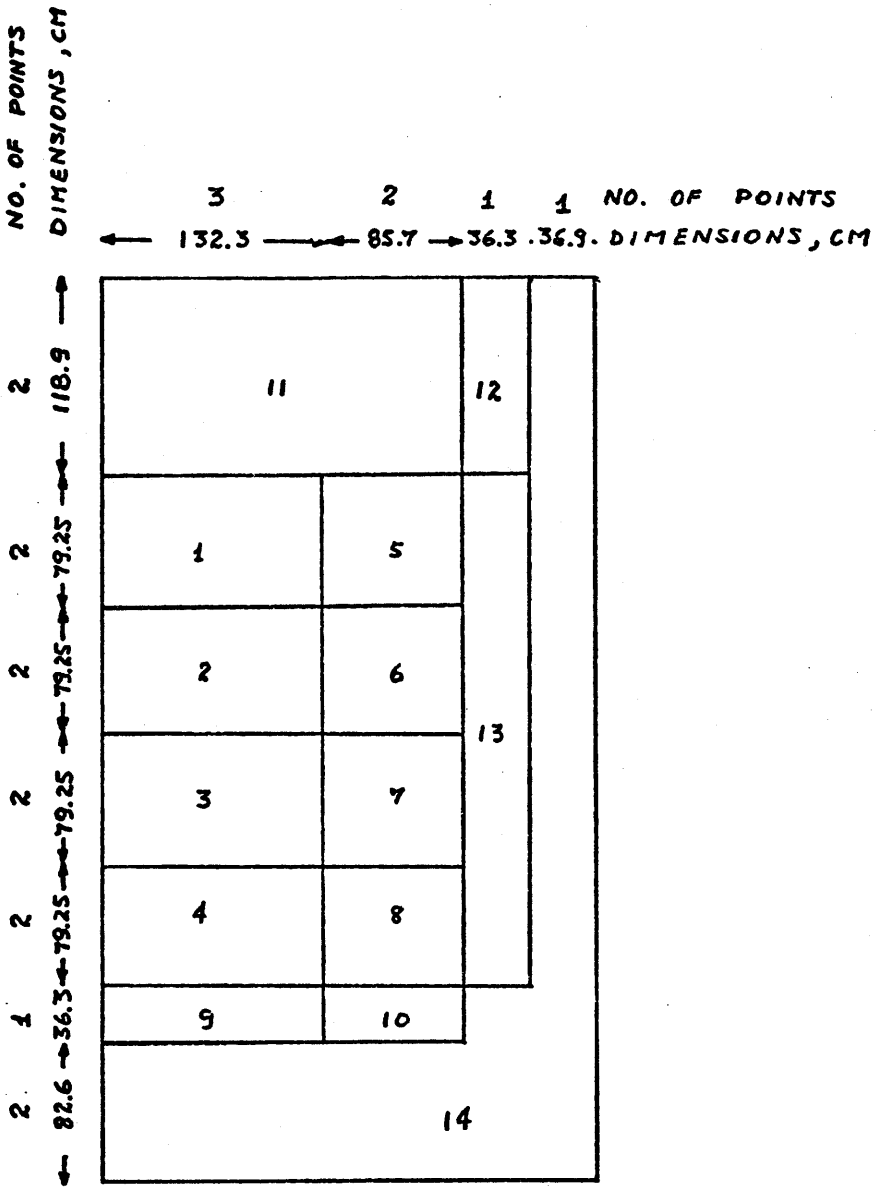

FIG. 5.3.1.1-1 HTGR/GT RZ REPRESENTATION FOR THE CITATION INPUT TO RD1, RD2 AND PARF1

Table 5.3.1.1-1 Atom Densities (in 10^{-5} atoms/bcm) Per Zone (*) in RD1, RD2 and PARF1

Zones	Volume 10^6 cm^3	HM atom densities in 10^{-5} atom/bcm								
		RD1			PARF1			RD2		
		N_{25}	N_{28}	N_{02}	N_{25}	N_{28}	N_{02}	N_{25}	N_{28}	N_{02}
1,4,5,6,7,8	38.613	4.548	.342	34.31	5.575	.420	33.21	4.200	.316	34.68
2,3	8.716	4.548	.342	34.31	---	---	39.20	4.200	.316	34.68

(*)Refer to Fig. 5.3.1.1-1. In all designs N_{810}=.1218 in zones 1 to 8 and .2436 in zones 9 and 10 (10^{-5} atoms /bcm units).

Table 5.3.1.1-2 Point Power Density (w/cc) in the RD1 Central Column

Equi-spaced points from entrance	1	2	3	4	5	6	7	8
RD1, BOL	5.55	7.71	9.38	10.2	10.1	9.15	7.34	5.01
RD1 without LBP in the bot. refl., BOL	4.47	6.44	8.07	9.18	9.69	9.59	8.89	8.23
RD1, 1330 days	5.10	6.91	7.27	7.77	7.85	7.77	7.77	7.39

The power density point to point in the central column for RD1 and for RD1 without LBP in the bottom reflector are compared in Table 5.3.1.1-2. The slight tilt in the axial power profile towards the center obtained with the addition of B^{10} to the bottom reflector decreased the maximum T_{GL} by 125°F. This effect can be seen in Fig. 5.3.1.1-2 which was obtained with the code HEATING-II by Stengle (Ref. 87) by using the BOL data in Table 5.3.1.1-2. Note that both curves are below the FSV limit of 2300°F. With depletion the center channel power decreases thus also decreasing the T_{GL}. In the RD1 and RD2 designs the bottom reflector LBP is completely spent in about 800 days and the center channel point power densities with and without bottom reflector B^{10} are very similar (see the points for RD1 in Table 5.3.1.1-2).

The BU_{max} and nvt_{max} do not benefit with the addition of B^{10} to the bottom reflector. Those values increase about 3% due to the higher peaking with LBP: 101,330 to 104,268 MWD/T and 6.79 to 6.99 x 10^{21} n/cm^2.

The k_{eff} vs. time curves for RD1 and RD2 are represented in Fig. 5.3.1.1-3. From the two RD1 curves it can be seen that the addition of B^{10} to the bottom reflector saves .0089 Δk in the CR requirements for the same reactivity lifetime.

The only T_{GL} profiles calculated with temperature dependent parameters by the HEATING-II code to appear in this thesis are those two shown in Fig. 5.3.1.1-2. All the future T_{GL} profiles were calculated from Eqs. 5.1-7 and 5.1-10. The error introduced by the use of temperature averaged parameters can be estimated by repeating the BOL T_{GL} calculation for RD1 with Eqs. 5.1-7 and 5.1-10 and comparing with the values from Fig. 5.3.1.1-2. The method used to calculate T_{GL} is illustrated in Fig. 5.3.1.1-4 and the comparison with the values from Fig. 5.3.1.1-2 is

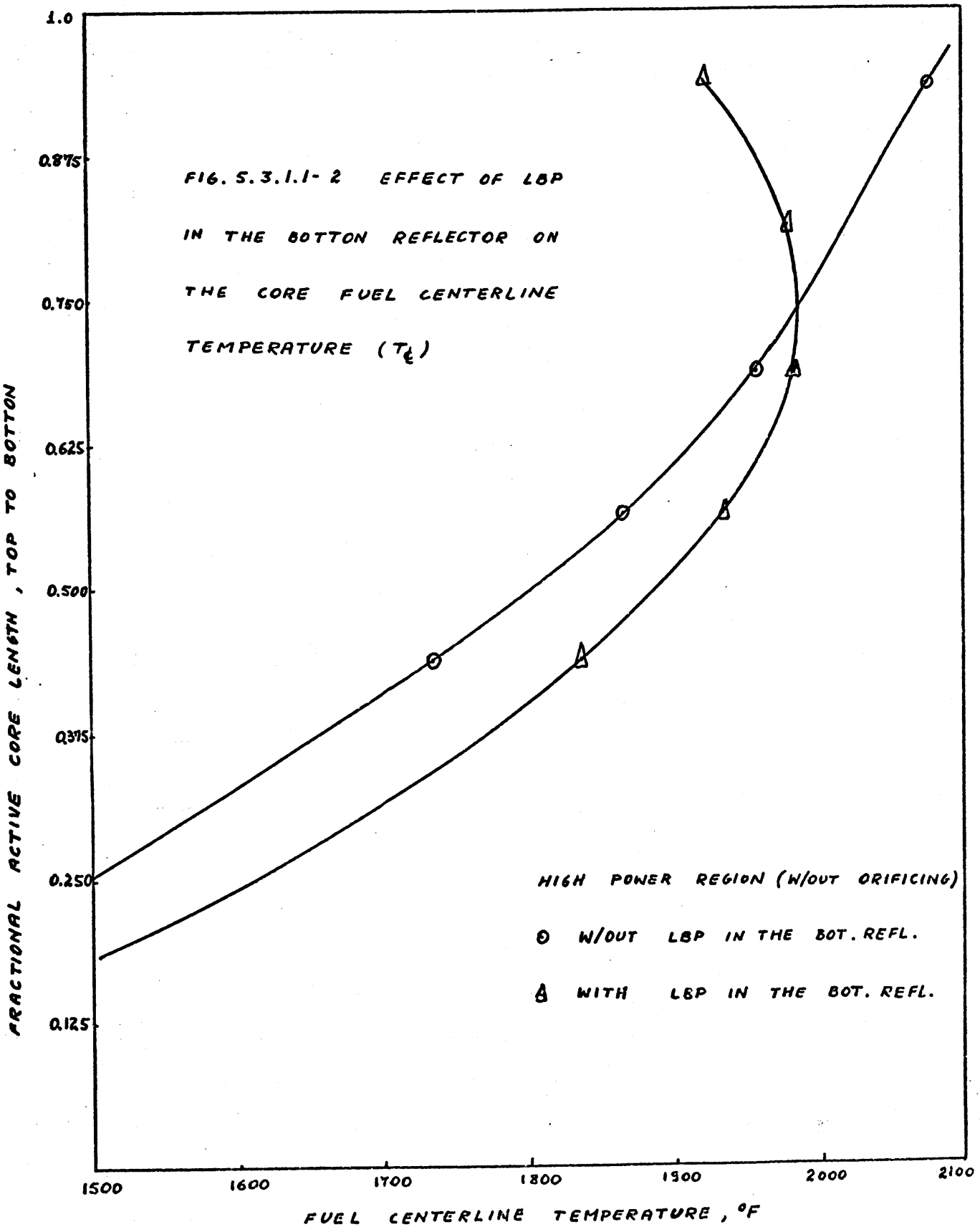

FIG. 5.3.1.1-2 EFFECT OF LBP IN THE BOTTON REFLECTOR ON THE CORE FUEL CENTERLINE TEMPERATURE (T_ℓ)

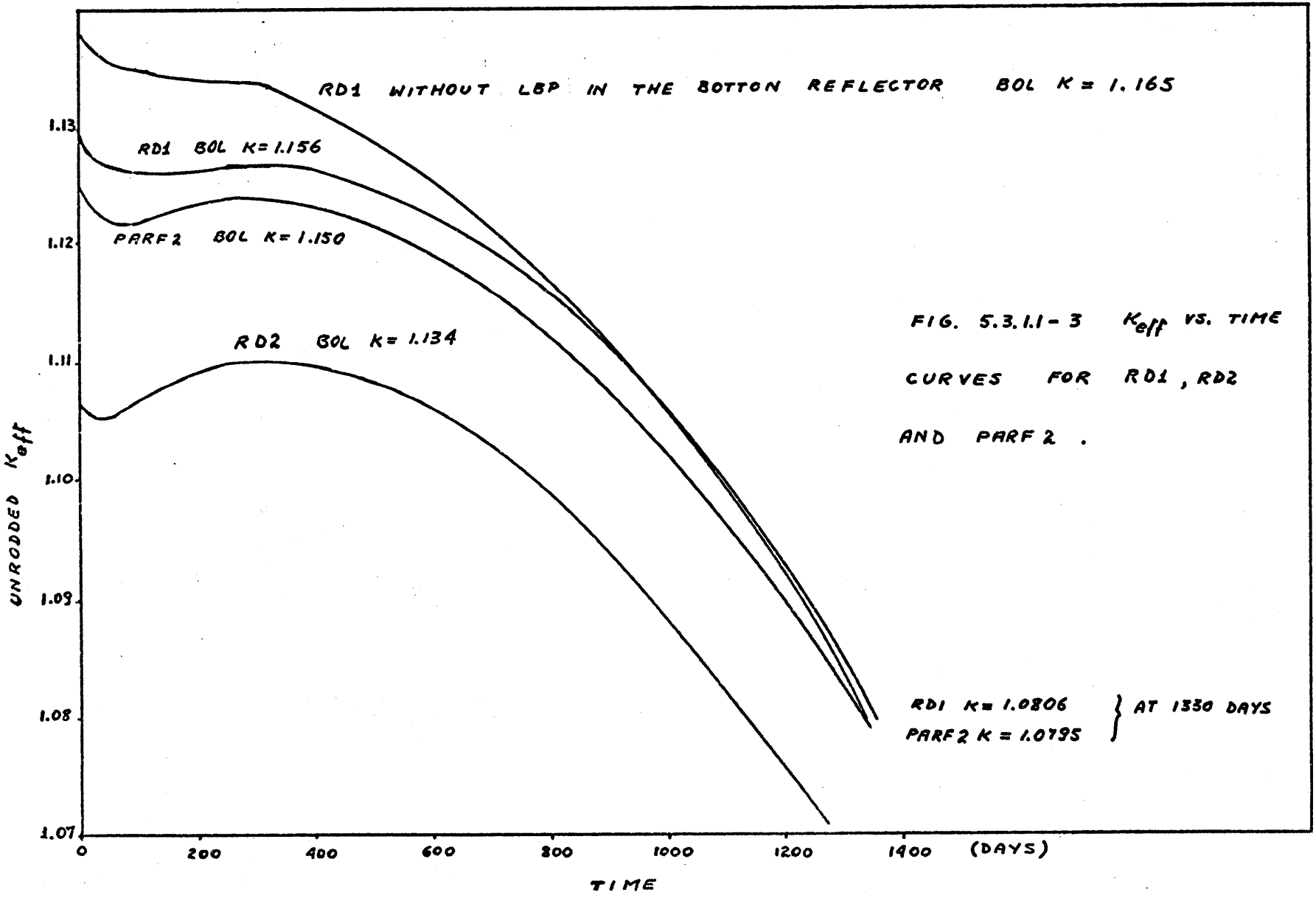

FIG. 5.3.1.1-3 K_{eff} VS. TIME CURVES FOR RD1, RD2 AND PARF 2.

RD1 K= 1.0806 } AT 1330 DAYS
PARF2 K = 1.0795 }

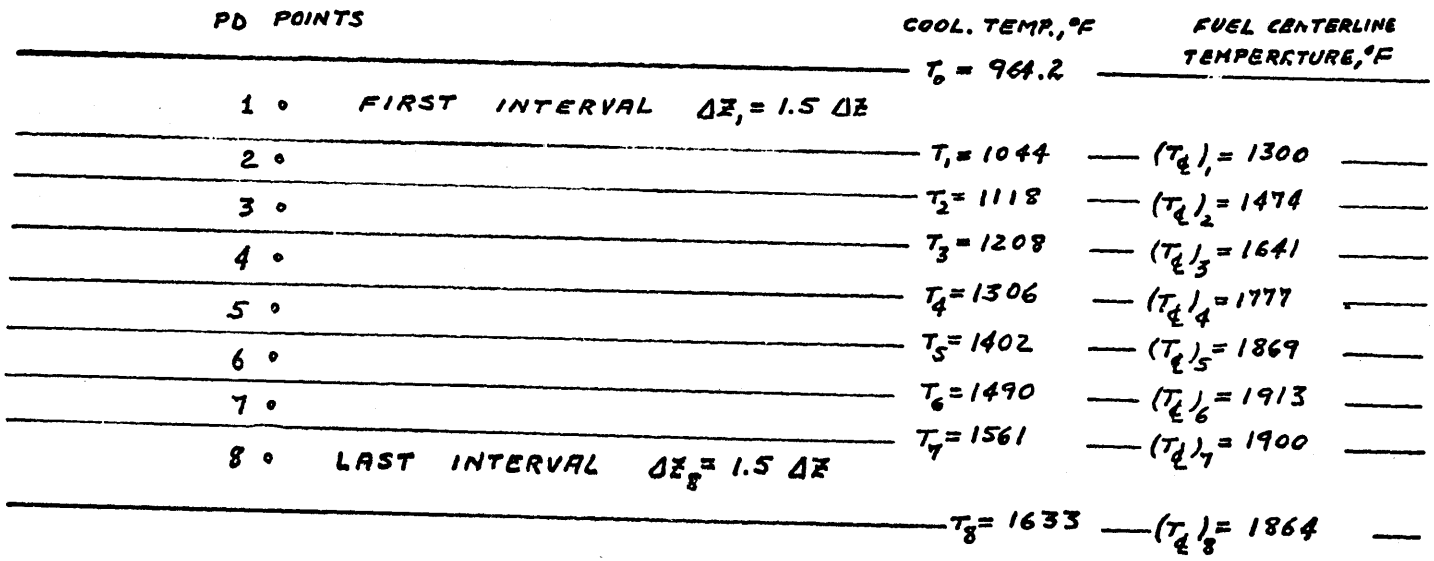

FIG. 5.3.1.1-4 MODEL TO ILLUSTRATE THE T_ℓ CALCULATION FOR RDI USING EQS. 5.1-7 AND 5.1-10

summarized in Table 5.3.1.1-3. It is seen that the approximate equations underestimate the temperature difference between the fuel centerline and the coolant $[(T_{CL})_1-T_i]$; at the maximum T_{CL} the underestimation is 17%. For that reason the maximum T_{CL} for the FRD was taken as 2100°F (Table 1.2-1) and the buffer layer thickness was designed for 2100°F (Table 4.2.2-1), although the T_{CL} value calculated in section 5.3.2 is only 1982°F (see Fig. 5.3.2.4-1 for FRD8≡FRD).

The more detailed runs described in section 5.3.2 evidenced the existence of a 15w/cc PD peak in the core-bottom reflector interface when a pure graphite bottom reflector was employed. The maximum T_{CL} in this case is well above the 2100°F calculated by Stengle with the data from Table 5.3.1.1-2, and pure graphite bottom reflector in single zone core designs were demonstrated to be unacceptable.

5.3.1.2 Parfait configurations

The Parfait concept consists in having a central fertile region in the core with the idea of getting a higher conversion ratio and reactivity lifetime and of decreasing the power peaking factor. This concept has been examined for LMFBR's in the past and was then called the Parfait Blanket Concept. The concept retained the external axial and radial blankets of a conventional fast reactor, but also employed a disc-shaped internal blanket region inserted at the core midplane.

Ducat (Ref. 8) identified some significant advantages of the Parfait Blanket Concept relative to the conventional design: a) the parfait configuration had a 25% smaller peak fast flux; b) axial and radial flux flattening contributing to a 7.6% reduction in the peak fuel burnup; c) 25% reduction in the burnup reactivity swing thus reducing the

Table 5.3.1.1-3 Comparison of T_{C_L} for RD1 as Calculated by Eqs. 5.1-7 and 5.1-10 and as Computed by HEATING-II

Calculation With Eqs. 5.1-7 and 5.1-10				Value From Fig. 5.3.1.1-2
i	PDi	T_i	$(T_{C_L})_i$	$(T_{C_L})_i$
	W/cc	^oF	^oF	^oF
1	5.55	1044	1300	---
2	7.71	1118	1474	---
3	9.38	1208	1641	---
4	10.2	1306	1777	1890
5	10.1	1402	1869	1960
6	9.15	1490	1913	1990
7	7.34	1561	1900	1970
8	5.01	1633	1864	1880

CR requirements.

Although the HTGR is a completely different type of reactor, these advantages found for the LMFBR could well exist also for the HTGR/GT. It was then decided to examine the interest in using a fertile region (with Th^{232} instead of U^{238}) in the center of the HTGR/GT. The HTGR/GT configurations containing fertile only regions in the center were called Parfait configurations (PARF) in this report.

Two Parfait configurations having about the same fissile content of RD1 were tried: PARF1, described in Table 5.3.1.1-1 and Fig. 5.3.1.1-1 and PARF2, described in Table 5.3.1.2-1 and Fig. 5.3.1.2-1.

The reactivity lifetime obtained with PARF1 is slightly better then that of RD1 but the power distribution was unacceptable. The results clearly indicated that the size of the fertile region (zones 2 and 3 of Fig. 5.3.1.1-2 corresponding to the 98 central graphite blocks of the core) had been exaggerated and that B^{10} should not be added to the fertile region. In PARF2 the fertile region consisted only on the 7 central graphite blocks of the third plane of elements counting from the top (zone 3 of Fig. 5.3.1.2-1). As a result the PD distribution obtained was very good (see Table 5.3.1.2-2) yielding a maximum BU of 101 GWD/T a maximum nvt of $7 \times 10^{21} n/cm^2$ and a much lower T_{C_L} profile (see Table 5.3.1.2-3) than that of RD1. The bottom reflector LBP B^{10} content of RD1, RD2 and PARF2 is almost completely spent after some 800 days; as already explained in section 5.3.1.1, the single zoned core T_{C_L} profile (case of RD1 and RD2) becomes unacceptable in that situation; that is not the case for a Parfait configuration, though.

In section 5.3.2 it is shown that for single zone core designs there is just a narrow range of possible B^{10} or Th^{232} concentrations in

Table 5.3.1.2-1 PARF2 composition in 10^{-5} atoms/bcm units

Zones	N_{25}	N_{28}	N_{02}	N_{Si}	N_C	N_{B10}	N_{CR}
1,2,4,5,6,7,8	4.548	.342	34.31	73.3	6190.	.1218	---
3	---	---	39.20	73.7	6190.	---	---
9,10	---	---	---	---	8797.	.2436	---
11	---	---	---	---	8635.	---	30.43
12	---	---	---	---	8594.	---	53.25
13	---	---	---	---	8594.	---	---
14	---	---	---	---	8876.	---	---

Table 5.3.1.2-2 PARF2 power density distribution in W/CC

BOL						1330 days					
middle regions		periphery regions				middle regions		periphery regions			
5.76	5.69	5.45	4.76	4.09	3.84	5.20	5.17	5.21	4.58	3.95	3.69
7.92	7.85	7.59	6.68	5.80	5.53	7.01	6.97	7.06	6.24	5.43	5.18
9.09	9.08	8.99	8.01	6.99	6.71	7.29	7.27	7.49	6.67	5.85	5.63
9.13	9.25	9.40	8.54	7.51	7.25	7.79	7.75	7.97	7.15	6.30	6.10
0.003	0.005	8.97	8.28	7.34	7.12	3.64	3.53	8.07	7.25	6.40	6.21
5.86	0.004	7.90	7.36	6.50	6.37	3.62	3.51	8.01	7.17	6.3]	6.11
4.10	4.16	4.31	3.96	3.52	3.44	7.54	7.51	7.66	6.74	5.81	5.38

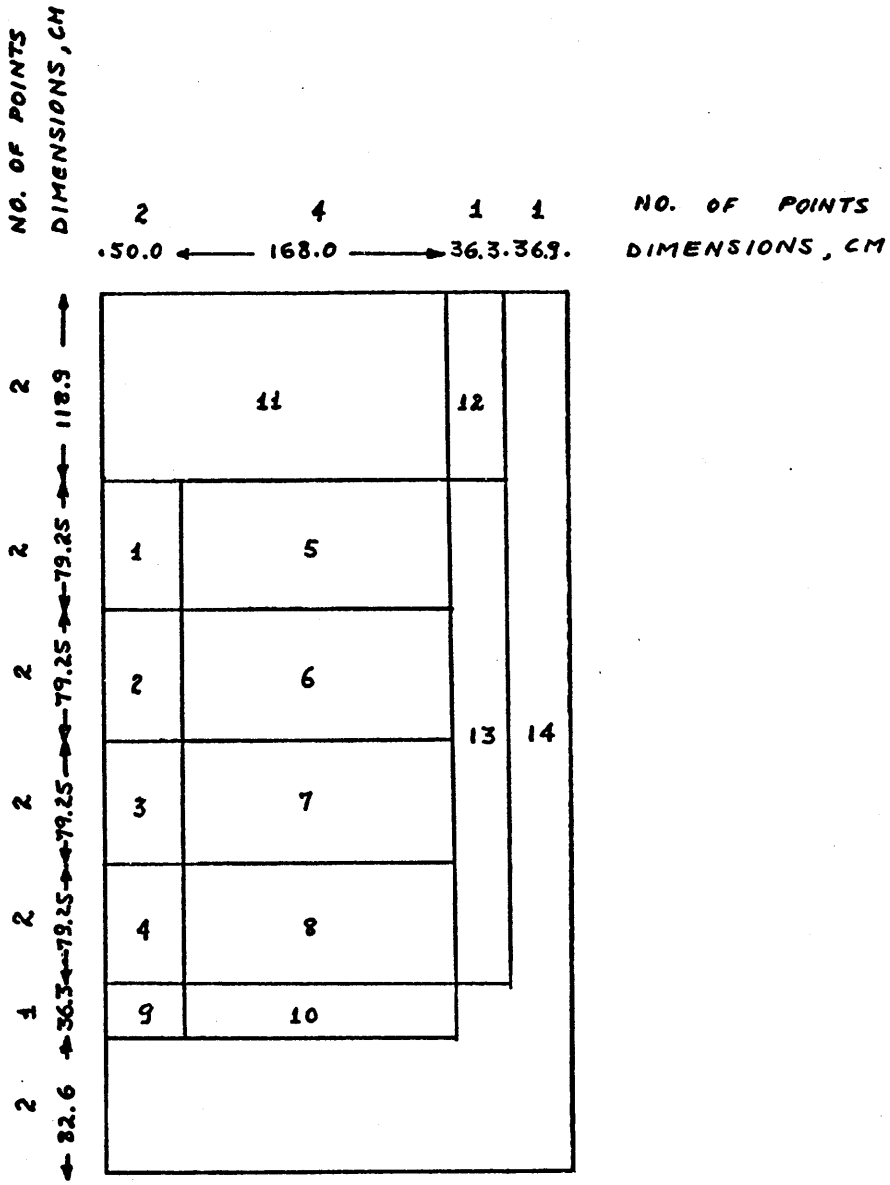

FIG. 5.3.1.2-1 HTGR/GT RZ REPRESENTATION FOR THE CITATION INPUT TO PARF2

Table 5.3.1.2-3 PARF2 T_{C_L} Profile in the Hottest Channel at BOL and After 1330 Days

	BOL				1330 Days		
i	PD_i	T_i	$(T_{C_L})_i$	i	PD_i	T_i	$(T_{C_L})_i$
1	5.45	1016.4	1268	1	5.21	1014.1	1254
2	7.59	1089.2	1439	2	7.06	1081.8	1408
3	8.99	1175.4	1590	3	7.49	1153.6	1499
4	9.40	1265.5	1699	4	7.97	1230.0	1598
5	8.97	1351.5	1765	5	8.07	1307.4	1680
6	7.90	1427.2	1792	6	8.01	1384.2	1754
7	6.32	1487.8	1779	7	8.03	1461.1	1832
8	4.31	1529.1	1728	8	7.66	1534.6	1888

the bottom reflector; below that range the concentration is not enough to prevent the power peaking at the core-bottom reflector interface at the EOL; above the range the fast fluence in the center of the core is above the maximum limit of 8×10^{21} n/cm^2. In Parfait configurations there is not such a problem.

With respect to CR requirements, Fig. 5.3.1.1-3 shows that PARF2 requires slightly less poison control than RD1 for the same reactivity lifetime.

5.3.1.3 LBP optimization

The objective of lumping the burnable poison is to decrease its depletion rate by decreasing its effective absorption cs by a self-shielding effect. By varying the diameter and B^{10} atom density in the LBP rod the self-shielding factor g can be varied, where:

$$g = \frac{1}{1+(1.514)(LBPN_{B10}\sigma_{a4}^{B10}r)+(0.684)(LBPN_{B10}\sigma_{a4}^{B10}r)^2} \quad , \qquad (5.3.1.2\text{-}1)$$

and:

σ_{a4}^{B10} - unshielded thermal group absorption CS of B^{10} (1257 barns at 1050°K),

r - radius of the LBP rod (0.515 cm in FSV), and

$LBPN_{B10}$ - B^{10} atom density in the LBP rod.

The optimum size and initial B^{10} concentration are the ones producing the k_{eff} vs. time curve with the least CR requirements and with k_{eff} approaching unity at the required residence time. There will always be an optimum size and B^{10} concentration for a certain residence time. At the

EOL the LBP should have a negligible worth, otherwise too much LBP was added thus unnecessarily increasing the fissile inventory in the core. In the runs reported in sections 5.3.1.1 and 5.3.1.2 the worth of the LBP was becoming negligible too soon; that was to be expected since the FSV LBP rods being used in those runs were optimized for one year refueling intervals. This present section treats the LBP optimization to 4.8 full power year -batches. In the LBP optimization studied only the number of LBP rods per element and B^{10} concentration in the rods were varied. The size of the LBP rods used in FSV was maintained and the maximum number of rods per element was 6 (one per corner) so that the FSV fuel element could be used without any changes.

The computer runs to determine the optimum were necessarily expensive, being depletion runs for 1752 days. Nevertheless, some savings were made by using the simplest possible RZ representation of the HTGR/GT unrodded core (see Fig. 5.3.1.3-1).

All the LBP distributions were tried for the fissile content of RD2 (see a summary of the LBP distribution trials in Table 5.3.1.3-1). The k_{eff} vs. time curves obtained for the LBP distribution trials are shown in Fig. 5.3.1.3-2.

With respect to CR requirements RD6, RD7, RD8 and RD9 are completely acceptable. The amount of B^{10} in the bottom reflector LBP rods; x=3, looks excessive, though. Not only the fast flux in the center of the reactor becomes too high, but also by the EOL the remaining B^{10} is still too high showing very little reactivity gain from the BOL to the EOL condition.

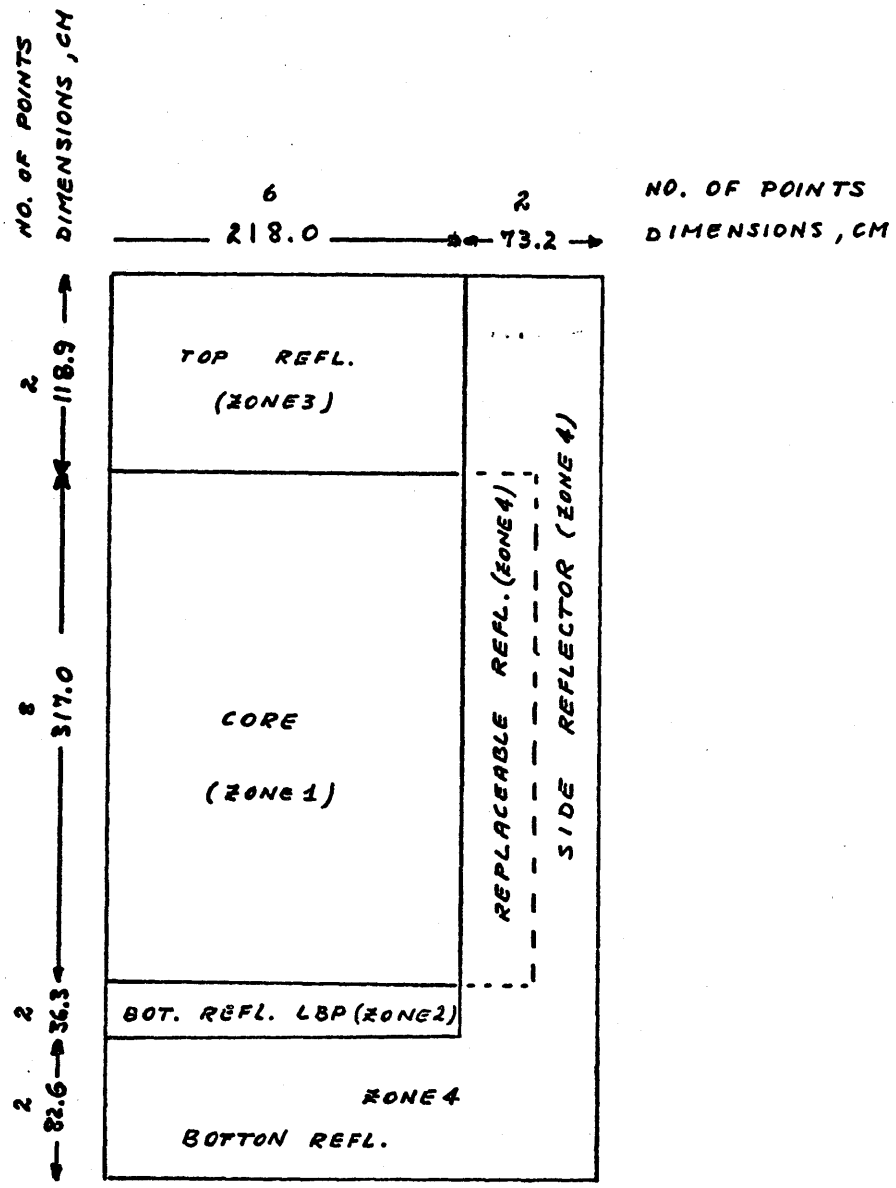

FIG. 5.3.1.3-1 HTGR/GT CORE IN RZ GEOMETRY FOR THE LBP OPTIMIZATION RUNS

Table 5.3.1.3-1 LBP Configurations for $N_{25}=4.200 \times 10^{-5}$ Atoms/bcm

Design Name	n_c	x_c	$(N_{B10})_C$	g_c	n_{BR}	x_{BR}	$(N_{B10})_{BR}$	g_{BR}
RD2	6	1	0.1217	0.7740	12	1	0.2435	0.7740
RD3	6	1.5	0.1826	0.6778	12	1.5	0.3654	0.6778
RD4	5	2	0.2029	0.6147	9	3	0.5478	0.4986
RD5	4	2.2	0.1786	0.5885	9	3	0.5478	0.4986
RD6	5	2.5	0.2536	0.5523	9	3	0.5478	0.4986
RD7	6	2.5	0.3043	0.5523	9	3	0.5478	0.4986
RD8	5	2.7	0.2739	0.5298	9	3	0.5478	0.4986
RD9	6	2.7	0.3287	0.5298	9	3	0.5478	0.4986

Definitions:

n_c - no. of LBP rods per graphite element in the core

n_{BR} - no. of LBP rods per graphite element in the bottom refl.

x_c - B^{10} conc. in the core LBP rods/B^{10} conc. in the FSV LBP rods

x_{BR} - B^{10} conc. in the bottom refl. LBP rods/B^{10} conc. in the FSV LBP rods

$(N_{B10})_C$ - B^{10} conc. in 10^{-5} atoms/bcm in the core

$(N_{B10})_{BR}$ - B^{10} conc. in 10^{-5} atoms/bcm in the bottom reflector

g_c - initial self-shielding factor for the LBP in the core

g_{BR} - initial self-shielding factor for the LBP in the bottom refl.

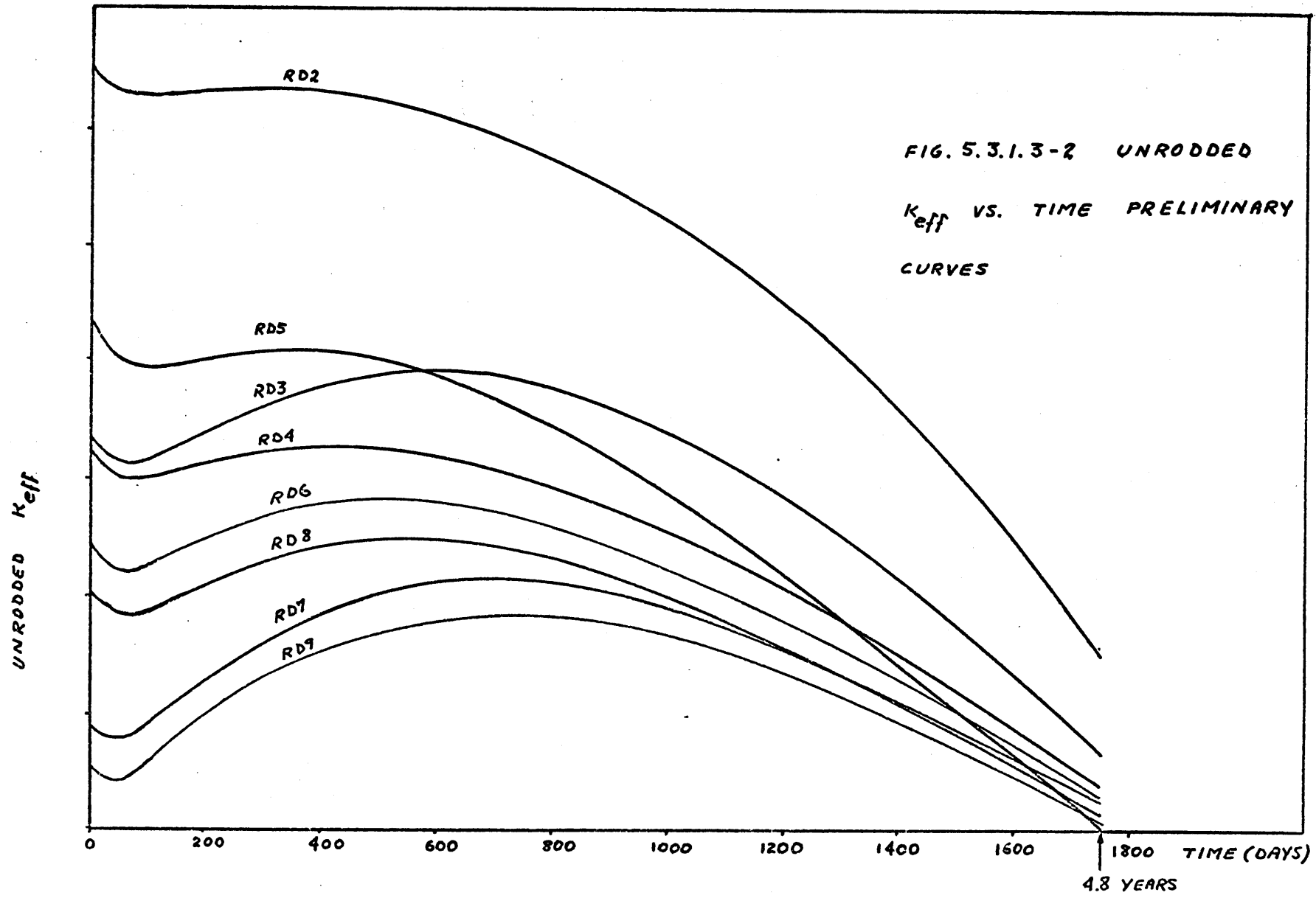

FIG. 5.3.1.3-2 UNRODDED K_{eff} VS. TIME PRELIMINARY CURVES

5.3.1.4 Preliminary conclusions

Satisfactory k_{eff} vs. time curves can be obtained with $x_c > 2$ and n_c = 5 or 6 without need for any reactivity gain from the bottom reflector LBP. The value x_R = 3 was identified as excessive and x_R=1 as too small.

From Tables 5.1-1 and 5.3.1.3-1 it is observed that the average fast flux increases with the amount of B^{10} and decreases with the fissile amount present in the core. This behavior was to be expected of course. For a constant power an increase in the fissile content would allow a lower value of the flux according to Eq. 3.3.2-1; the addition of B^{10}, whose thermal group absorption CS, σ_{a4}^{B10}, is more than one thousand times larger than σ_{a1}^{B10}, hardens the spectrum (note that the insertion of CR would not have this same effect because there the thermal group CS is much more self-shielded - see Table A.1-4).

The maximum T_{C_L} in all unrodded preliminary runs is below 2300°F even if no LBP is added to the bottom reflector. The obvious development would have been to remove all the B^{10} from the bottom reflector. The more detailed runs (section 5.3.2) showed that this is impossible because when all bottom reflector LBP is removed a large power peak (unrevealed in large mesh runs) appears in the core-bottom reflector boundary.

5.3.2 Detailed design studies

The objective of this section is to present the most detailed HTGR/GT depletion runs to be treated in this thesis. The HTGR/GT core was represented in RZ geometry as in Fig. 5.3.2-1 for these more detailed design studies. A total of eight designs were tried: FRD1(*),FRD2,...FRD8. The input characteristics of the eleven computer runs necessary to analyze those eight dsigns are summarized in Table 5.3.2-1. The eight design trials

---

* FRD1 ≡ Final Reference Design trial no. 1.

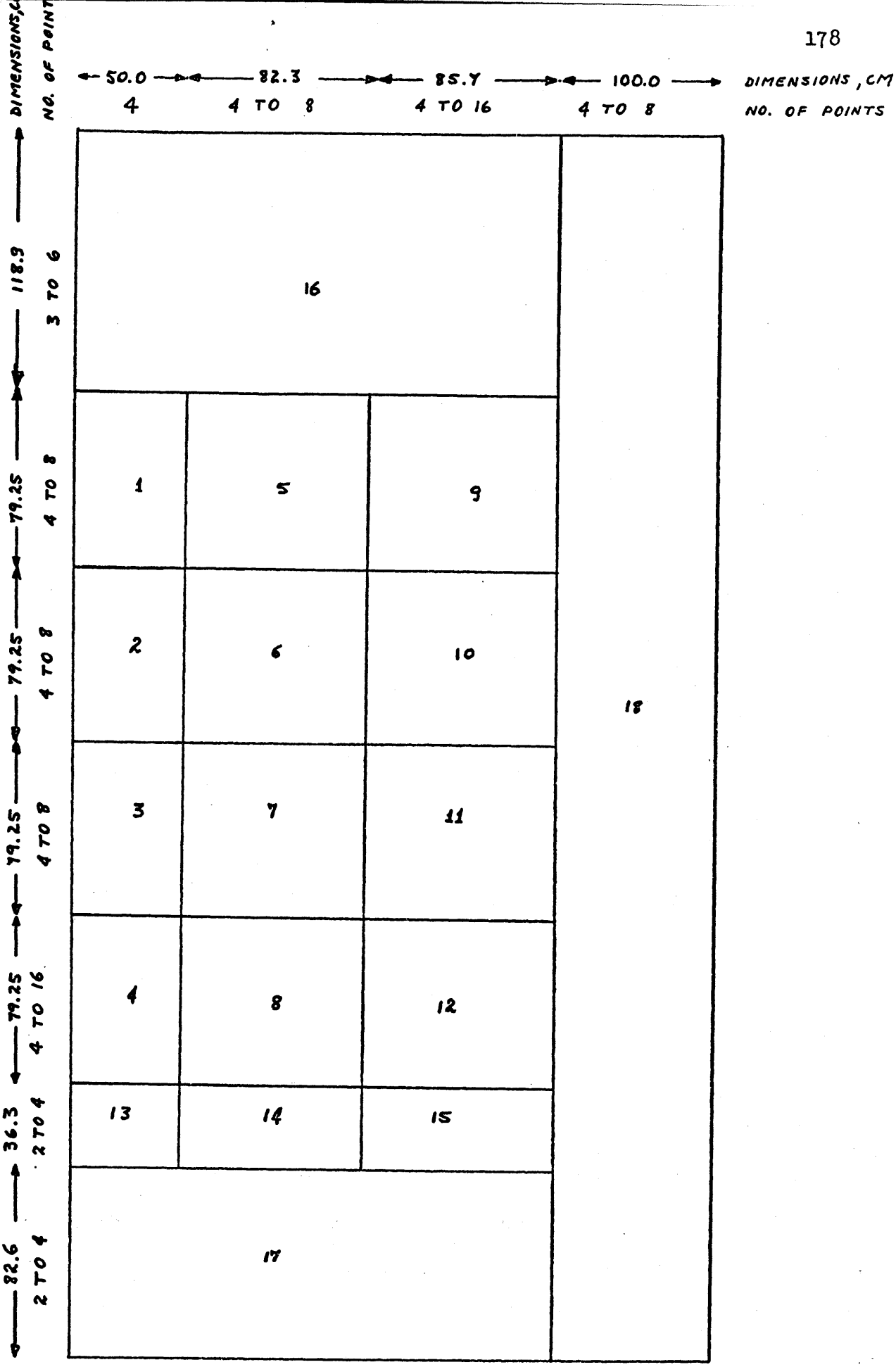

FIG. 5.3.2-1 HTGR/GT RZ REPRESENTATION FOR THE FRD CITATION RUNS

Table 5.3.2-1 Final Reference Design input characteristics (*)

run no.	Design	run type	no. of points per zone (refer to Fig. 5.3.2-1) radial direction points (center to periphery)				axial direction points (top to bottom)						
1	FRD1	depletion	4	4	4	4	3	4	4	4	4	2	2
2	FRD2	static	4	4	4	4	3	4	4	4	4	2	2
3	FRD3	depletion	4	4	4	4	3	4	4	4	4	2	2
4	FRD4	depletion	4	4	4	4	3	4	4	4	4	2	2
5	FRD4	static	4	8	16	8	6	8	8	8	16	4	4
6	FRD5	depletion	4	4	4	4	3	4	4	4	4	2	2
7	FRD6	depletion	4	4	4	4	3	4	4	4	4	2	2
8	FRD7	static	4	8	16	8	6	8	8	8	16	4	4
9	FRD8	static	4	8	8	6	6	8	8	8	16	4	4
10	FRD7	depletion	4	8	8	6	6	8	8	8	12	4	4
11	FRD8	depletion	4	8	8	6	6	8	8	8	12	4	4

(*) Some other runs not appearing in this table were made with specific objectives. Those objectives were to determine the k_{eff} sensitivity to variations in the side reflector porosity and thickness.

are presented in Table 5.3.2-2.

The first 5 designs could not be accepted because they violated the particle limits of operation. The remaining of this section is devoted to a detailed analysis of the results obtained for FRD6, FRD7 and FRD8. This analysis consists in comparing the reactivity lifetime and CR requirements maximum $_{nvt}$, BU and T_{C_L} for those three designs.

5.3.2.1 Reactivity lifetime and CR requirements

The k_{eff} variation with time for FRD6, FRD7 and FRD8 is presented in Fig. 5.3.2.1-1. It can be seen that in any case the maximum k_{eff} is well below the maximum controllable reactivity level seen in section 5.2. It is also interesting to note that if the curves in Fig. 5.3.2.1-1 were normalized for the same EOL k_{eff} the maximum k_{eff} reached in FRD6, FRD7 and FRD8 would have been approximately the same.

5.3.2.2 Maximum $_{nvt}$

The maximum nvt in a coated particle after 4.8 years of full power operation is given by

$$\text{max. nvt} = (1.513 \times 10^{8}\text{sec}) \times \text{max. ave. } \phi_1 \quad , \qquad (5.3.2.2\text{-}1)$$

where max. ave. ϕ_1 is the maximum first group neutron flux averaged in time. This value is found by inspection in the computer output (see Table 5.3.2.2-1). For all cases the max. ave. ϕ_1 was located at the BOL maximum. The maximum nvt values calculated with Eq. 5.3.2.2-1 are: 7.64×10^{21} n/cm^2 for FRD6, 7.79×10^{21} n/cm^2 for FRD7 and 7.97×10^{21} n/cm^2 for FRD8; all below the maximum limit of 8×10^{21} n/cm^2.

Table 5.3.2-2 Final Reference Design (FRD) Trials (*)

Design	Characteristics			Comments
	x_C	n_R	x_R	
FRD1	2.5	6	2.5	The max. $nvt=8.55\times10^{21}$ n/cm^2; low reactivity lifetime ~1610 days ∴ rejected.
FRD2	2.5	6	2.5	Parfait; the limits are observed but there is not enough reactivity lifetime ∴ rejected.
FRD3	2.3	6	2.0	The max. $nvt=8.33\times10^{21}$ n/cm^2 ∴ rejected.
FRD4	2.3	0	---	The results looked very good on run 4, but run 5 (see Table 5.3.2-1) showed a 15 w/cc PD peak at the core-bottom reflector interface ∴ rejected.
FRD5	2.3	0	---	To suppress the PD peak in the core bottom reflector interface Th^{232} was added ($N_{02}=39.2\times10^{-5}$ atoms/bcm) to the bottom reflector. The Th^{232} amount was excessive resulting in a too high peak in the center of the core ∴ rejected.
FRD6	2.3	6	2.0	Parfait; $N_{02}=39.2\times10^{-5}$ in zone 3; all other core zones have $N_{25}=4.548$, $N_{28}=0.342$, and $N_{02}=34.31$. Very good results.
FRD7	2.3	0	---	With $N_{02}=20.0\times10^{-5}$ atoms/bcm in the bottom reflector. Very good results.
FRD8	2.3	3	1.8	Very good results.

(*)Except in Parfait configurations (FRD2 and FRD6), all designs have homogeneous composition in zones 1 to 12. This composition is $N_{25}=4.2$, $N_{28}=0.316$, $N_{02}=34.68$, $N_c=6190$, and $N_{Si}=73.7$ (units of 10^{-5} atoms/bcm) and each graphite element has 6 LBP rods ($n_c=6$).

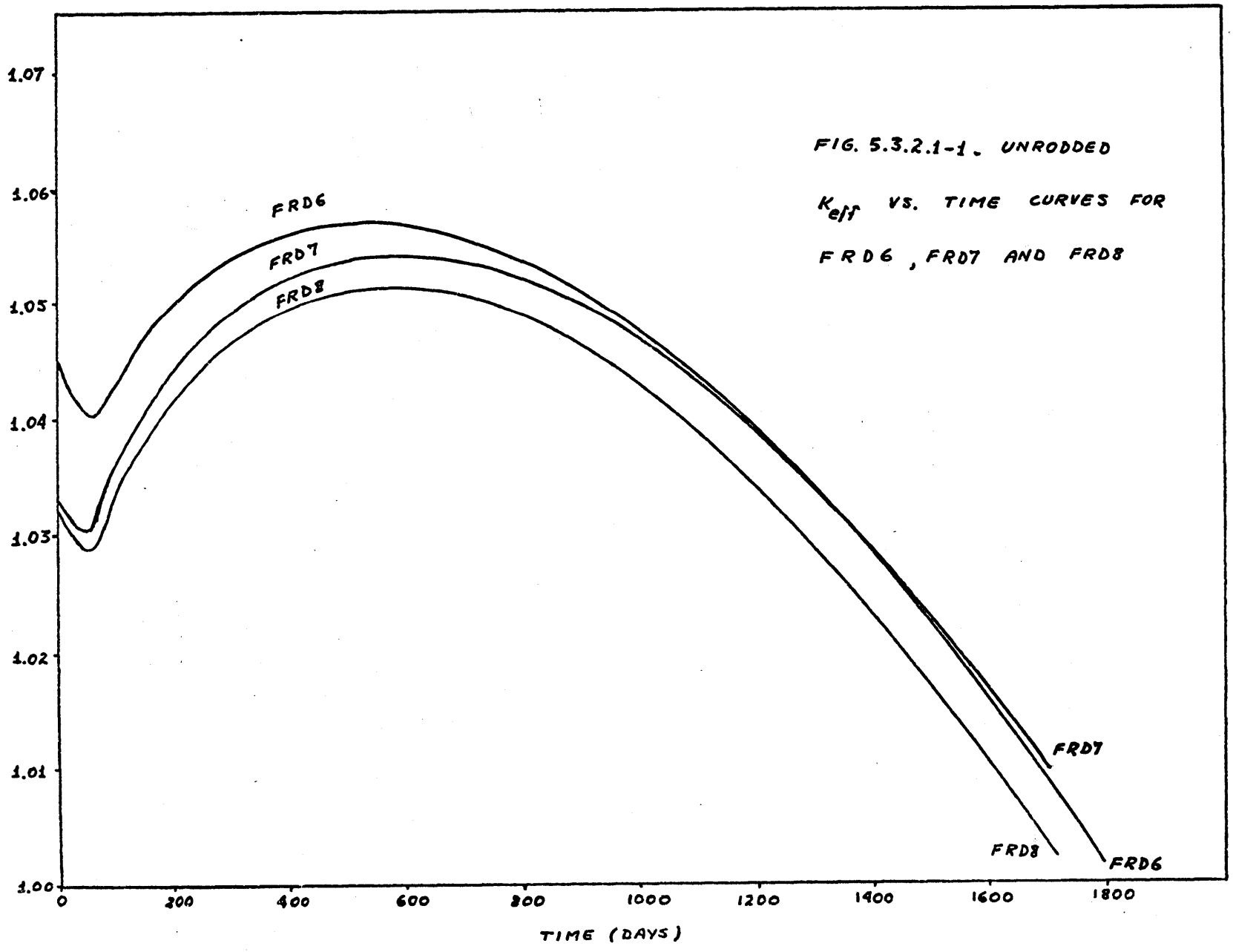

FIG. 5.3.2.1-1. UNRODDED K_{eff} VS. TIME CURVES FOR FRD6, FRD7 AND FRD8

Table 5.3.2.2-1 Maximum First Group Neutron Flux Averaged in Time (max. ave. ϕ_1) for FRD6, FRD7 and FRD8

	FRD6		FRD7		FRD8	
	Max. BOL at 5,10 (*)	Max. EOL at 5,11	Max. BOL at 1,24	Max. EOL at 5,22	Max. BOL at 1,24	Max. EOL at 5,22
BOL ϕ_1, 10^{13} n/cm^2 sec	5.314	5.231	5.670	5.407	5.712	5.466
EOL ϕ_1, 10^{13} n/cm^2 sec	4.791	4.838	4.628	4.686	4.826	4.890
AVE ϕ_1, 10^{13} n/cm^2 sec	5.05	5.03	5.15	5.05	5.27	5.18

(*)Location of the max. at point 5,10 means the 5th radial point (from center to periphery) and 10th axial point (from top to bottom). Refer to Fig. 5.3.2-1 and Table 5.3.2-1.

The lowest nvt value for the Parfait design is in part due to the location of its fertile region in zone 3 and in part due to its higher fissile content. Another interesting point is the variation of ϕ_1 with time: the average ϕ_1 increases slightly with fissile depletion but the maximum ϕ_1 decreases with time due to the power flattening The lowest decrease in maximum ϕ_1 with time is in FRD6 and the highest is in FRD7 (see Table 5.3.2.2-1). The larger decrease in maximum ϕ_1 with time for the FRD7 is due to the fact that at EOL part of the power is produced at the bottom reflector in this case and so the PD and ϕ_1 at the center should decrease slightly more. In FRD6 the maximum ϕ_1 and PD are immediately above the fertile region all time; at BOL this maximum is lower than single zone cores due to the ∿0 power fertile region; at EOL the fertile region PD is about 5 w/cc and the PD and ϕ_1 distribution in FRD6 is not much different from single core designs.

In all the FRD runs the fuel rods were treated as if having the same length as the graphite elements. Actually the fuel rods are about 1.8 in. smaller. Since the maximum PD and nvt is always near the core midplane, where there is also a boundary between graphite elements, there was some concern about the possibility of a local power (and flux) peaking in the fuel rod extremes. A one dimensional CITATION run was made, with a very fine mesh spacing, (68 points in the 31.2 in. long graphite element) to check this possibility. It was found out that there is effectively a local PD peak at the fuel rod-graphite interface (this local PD peak is about 15% higher than the values found for axially homogenized fuel elements), but there is no fast flux peak at the fuel-graphite interface, so the maximum nvt values calculated in the FRD runs are not affected. The effect of this local power peaking in the maximum BU calculations is

certainly smaller than 15% because the fuel will deplete more near the graphite interface and the local peak will tend to disappear with time. Nevertheless the fuel kernel was designed with a porosity more than 15% higher than the required for the FRD BU.

5.3.2.3 Maximum BU

The maximum BU in the coated particles after 1752 days of full power operation (4.8 years) is given by

$$BU_{max} = BU_{ave} \text{ (max. ave. PD/6.34 w/cc)} \quad , \qquad (5.3.2.3\text{-}1)$$

where max. ave. PD is the maximum PD averaged in time. As the max. ave. ϕ_1, this value is found by inspection in the computer outputs (see Table 5.3.2.3-1). The average BU was shown to be 73,428 MWD/T in section 5.1 and with the values of max. ave. PD from Table 5.3.2.3-1, BU_{max} can be calculated as 110 x 10^3 MWD/T for FRD6, 104.10^3 MWD/T for FRD7 and 106 x 10^3 MWD/T for FRD8. As mentioned in Chapter 4 those values are not excessive in a single particle system. The lower average PD in FRD7 is due to the bottom reflector power contribution at the EOL. It is also interesting to note that the fertile region in zone 3 in FRD6 decreases the maximum ϕ_1 but increases the maximum PD. A comparison between FRD7 and FRD8 near the core-bottom reflector interface shows that the fertile bottom reflector decreases the PD at the interface less efficiently than the boronated reflector but it decreases the fast flux more efficiently. That is to be expected of course if the bottom reflector macroscopic absorption cs for FRD7 and FRD8 are analyzed.

Table 5.3.2.3-1 Maximum PD averaged in time (max. ave. PD) for FRD6, FRD7 and FRD8

	FRD6		FRD7		FRD8	
	max BOL at 2,11	max EOL at 1,11	max BOL at 1,24	max EOL at 5,22	max BOL at 1,24	max EOL at 5,22
BOL PD, W/CC	10.48	10.45	10.21	9.827	10.28	9.834
EOL PD, W/CC	8.530	8.579	7.796	8.102	8.096	8.369
Ave. PD, W/CC	9.51	9.51	9.00	8.96	9.19	9.10

Actually the maximum BU in FRD6, FRD7 and FRD8 should be slightly higher than the values found in the FRD run due to the local PD peak in the fuel rod-graphite interface (see section 5.3.2.2). This fact was taken into account in the fuel particle specifications by designing a porosity more than 15% higher than the value required for the FRD BU (see section 4.3.4).

5.3.2.4 Maximum T_{CL}

The equation to calculate T_{i+1} (Eq. 5.1-7) deduced in section 5.1 had to be slightly changed to account for the differences in ΔZ_i; $(T_{CL})_i$ can still be calculated from Eq. 5.1-10 since the value 46.14°F cm^3/W is independent of ΔZ_i.

To calculate T_{i+1} in run 7 of Table 5.3.2-1 for FRD6, ΔZ_i=317.0 cm/17 = 18.65 cm for any i, so:

$$T_{i+1}=T_i+4.793°F/(W/cc)(PD_i) \quad . \qquad (5.3.2.4\text{-}1)$$

To calculate T_{i+1} in runs 10 and 11 for FRD7 and FRD8, ΔZ_i=(79.25 cm) x (3)/25 =9.51 cm for the first 25 intervals on the first 3 core graphite elements and ΔZ_i = (79.25 cm)/13 = 6.096 cm for the last 13 intervals in the last core graphite block, so:

$$T_{i+1}=T_i+(2.444°F/W/CC)(PD_i) \text{ for } i = 7 \text{ to } 30, \qquad (5/3/2/4\text{-}2)$$

and

$$T_{i+1}=T_i+(1.567°F/(w/cc)(PD_i) \text{ for } i = 31 \text{ to } 42. \qquad (5.3.2.4\text{-}3)$$

In the three designs studied the B^{10} or Th^{232} in the bottom

reflector at the EOL is still enough to prevent the power peak at the core-bottom reflector interface and the highest T_{CL} is found at the BOL. For that reason the T_{CL} profile calculation is here shown only for the BOL situation. In this case the P.D. in the bottom reflector in FRD7 can be neglected. The starting point for all calculations was coolant inlet temperature equal to 964.2°F and the calculational procedure was made as illustrated in Fig. 5.3.1.2-2 (see Table 5.3.2.4-1).

In Fig. 5.3.2.4-1 the T_{CL} for FRD6, FRD7 and FRD8 hottest channels are plotted. The best profile is that of FRD6, mostly due to its heavily B^{10} loaded bottom reflector (that required also a higher fissile content in the core). The curve of FRD8 is better than that of FRD7 because B^{10} is more efficient than Th^{232} in suppressing the PD peaking at the core-bottom reflector interface.

5.3.2.5 Other considerations

If the limit conditions are observed (case of design FRD6, FRD7 and FRD8) some other considerations such as cost and simplicity are in order. Taking FRD8 (the simplest) as a standard, FRD6 would require 8% more fissile material and two different orders for fuel and FRD7 would also require two different orders for fuel and even though the fissile content is the same, about 5% more Th is necessary in FRD7 for the bottom reflector.

5.3.2.6 Summary and conclusions

Three different designs were examined in detail for the HTGR/GT. They were all shown to have acceptable CR requirements, maximum $BU_{,nvt}$ and T_{CL}. FRD6 has the lowest maximum $_{nvt}$ and T_{CL} and FRD7 the lowest

Table 5.3.2.4-1 T_{CL} profile calculation for FRD6, FRD7 and FRD8 at the hottest channel at BOL.

A. T_{CL} calculation for FRD6 (along column 5)

Point	4	5	6	7	8	9	10	11	12	13	14
PD, W/CC	4.81	5.91	7.17	8.24	9.05	9.54	9.73	9.68	9.76	9.37	8.79
T, °F	999	1028	1063	1102	1146	1196	1238	1285	1332	1376	1415
T_{CL}, °F	1221		1394			1632			1782	1806	1825

Point	15	16	17	18	19
PD, W/CC	8.07	7.01	6.09	5.10	4.39
T, °F	1457	1491	1520	1544	1576
T_{CL}, °F	1829	1814	1801	1779	1779

B. T_{CL} calculation for FRD7 (along column 1)

Point	7	8	9	10	11	12	13	14	15	16	17
PD, W/CC	4.50	4.47	4.90	5.47	6.06	6.64	7.18	7.69	8.16	8.58	8.96
T, °F	981	992	1004	1017	1032	1049	1066	1085	1105	1126	1148
T_{CL}, °F	1189			1269			1397			1522	

Point	18	19	20	21	22	23	24	25	26	27	28
PD, W/CC	9.29	9.57	9.80	9.98	10.11	10.19	10.21	10.18	10.09	9.95	9.97
T, °F	1170	1194	1218	1242	1267	1292	1317	1342	1366	1391	1414
T_{CL}, °F							1788	1812		1850	

Point	29	30	31	32	33	34	35	36	37	38	39
PD, W/CC	9.53	9.24	8.95	8.71	8.44	8.16	7.85	7.54	7.23	6.94	6.74
T, °F	1438	1472	1493	1507	1520	1533	1545	1557	1568	1519	1590
T_{CL}, °F		1898		1909	1909	1910	1907	1905	1902	1899	1901

Point	40	41	42
PD, W/CC	6.72	7.11	8.34
T, °F	1600	1612	1632
T_{CL}, °F	1910	1930	2017

T_{ℓ} Calculation for FRD8 (along column 1)

Point	7	8	9	10	11	12	13	14	15	16
PD,w/cc	4.60	4.57	5.01	5.59	6.19	6.77	7.32	7.84	8.30	8.73
T_{ℓ},°F	981	993	1005	1019	1034	1050	1068	1087	1108	1129
T_{ℓ},°F	1193			1276			1406			1532

Point	17	18	19	20	21	22	23	24	25	26
PD,w/cc	9.10	9.43	9.71	9.93	10.10	10.21	10.27	10.28	10.23	10.12
T_{ℓ} °F	1151	1174	1198	1222	1247	1272	1297	1322	1347	1372
T_{ℓ},°F			1646			1743		1796	1819	1839

Point	27	28	29	30	31	32	33	34	35	36
PD,w/cc	9.96	9.75	9.48	9.16	8.85	8.59	8.30	8.00	7.67	7.34
T_{ℓ},°F	1396	1420	1443	1477	1497	1511	1524	1536	1548	1560
T_{ℓ},°F	1856		1880	1900	1905	1908	1908	1905	1902	1899

Point	37	38	39	40	41	42
PD,w/cc	7.00	6.69	6.44	6.36	6.63	7.62
T_{ℓ},°F	1571	1581	1591	1601	1612	1630
T_{ℓ},°F	1894	1890	1888	1894	1918	1982

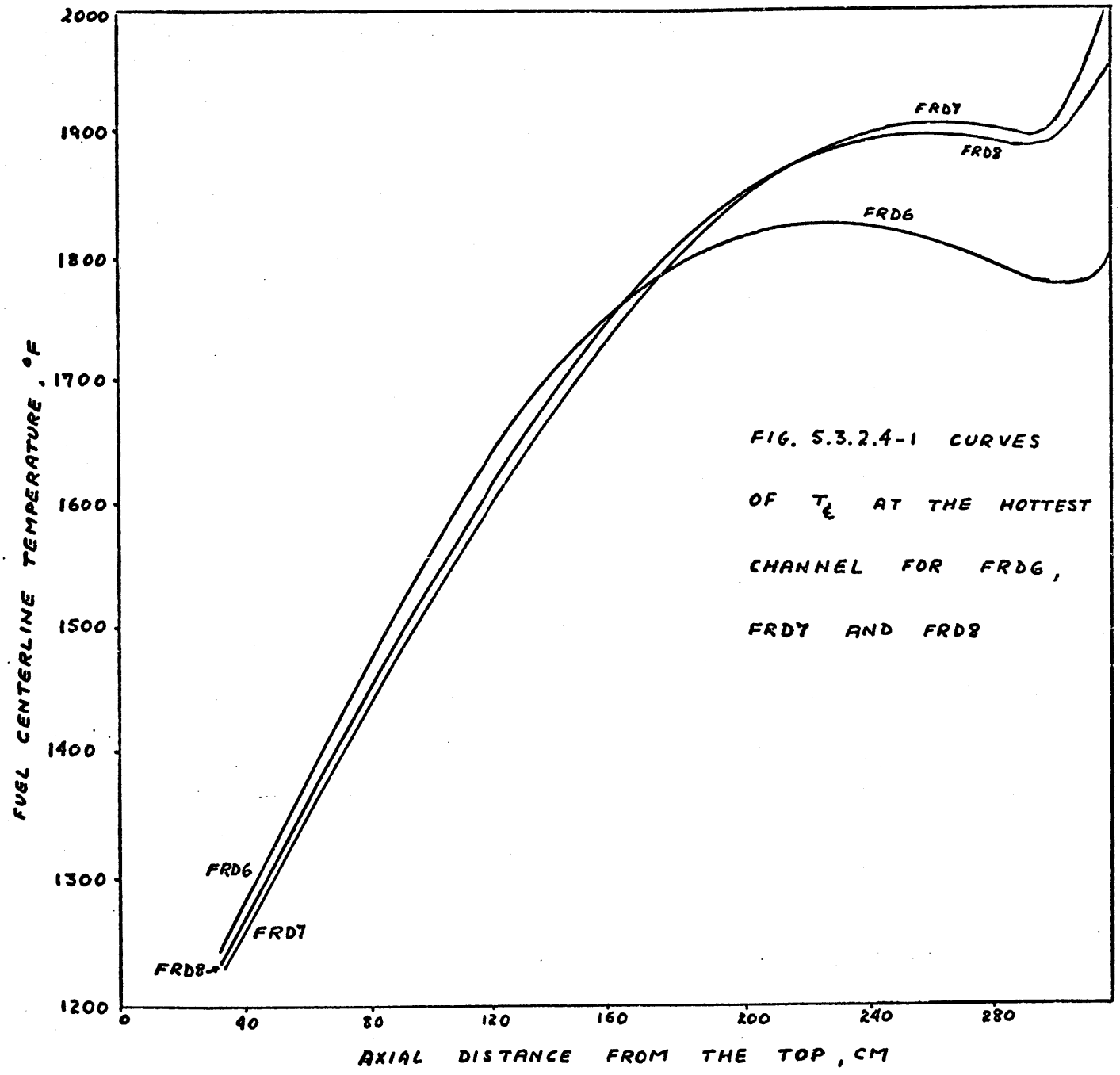

FIG. 5.3.2.4-1 CURVES OF T_ℓ AT THE HOTTEST CHANNEL FOR FRD6, FRD7 AND FRD8

maximum BU and CR requirements. FRD8 is the simplest and less expensive and is kind of average between FRD6 and FRD7 in the above comparison being in the same level of overall reliability.

The FRD8 was thus chosen as the Final Reference Design, FRD, for the HTGR/GT.

CHAPTER 6

REACTOR VESSEL AND INTERNALS

In this chapter a description of the choice of the reactor vessel type, steel vessel or Prestressed Concrete Reactor Vessel (PCRV), and the design of the vessel internals which is to a certain extent dependent on the vessel choice, is made.

6.1 Reactor Vessel Choice

6.1.1 Discussion

There are three practical ways in which a pressure vessel may be constructed. The first consists of a steel pressure vessel which contains the core and is connected to other components in the energy conversion system through piping and duct work. The second way uses a PCRV as the primary pressure boundary and is also connected to the energy conversion system through piping and ducts. The third way contains the entire He loop and all major components in that loop in a PCRV; this last choice is known as the "Integral Design".

Throughout the history of the reactor program in the United States, steel pressure vessels have been used. This is true in the case of all Light Water Reactors (LWR) which have been designed, the Liquid Metal Fast Breeder Reactor (LMFBR) pressure vessel, and the gas cooled reactor at Peach Bottom. The safety record of these vessels is excellent and the ASME pressure vessel code for nuclear plants has long been established.

The PCRV has recently entered the field of reactor pressure vessels and has gained great respect based on its desirable

characteristics and good operating experience. The PCRV connected to the energy conversion system is considered less economical than the use of steel vessels or integral design PCRV (Ref. 90). The main advantage of the integral design is the high standard of safety achieved by containing the whole gas pressure circuit in a vessel which cannot fail suddenly but could only progress in small steps towards failure, thereby giving warning. The compact grouping of the plant and the fact that the structural thickness of the concrete fulfills the necessary shielding against radiation, give a high degree of economy.

The European work on concrete reactor vessels started about 1955 (Ref. 91). G1 and G2 in the Marcoul reactor were the first and second PCRV's and were constructed by the French. Since then the vessels have been getting larger and larger. The English have built vessels with internal diameters between 60 and 100 ft. and from 60 to 120 ft. high. All the European PCRV reactors are gas reactors and with the exception of GI they are of the integrated type. The safety of these vessels has been found to be so good that the secondary containment vessel was deamed as unnecessary. The Swedish and Germans have designed BWR's enclosed in PCRV with internal pressures of 1232 and 1418 psi respectively but they were not constructed yet.

In the United States the HTGR program was a little delayed relative to that of the European's and GA is the only American manufacturer of HTGR's. The first American HTGR to be constructed

was the 40 MWe prototype reactor Peach Bottom. This reactor started operation in 1967 and was recently decomissioned after an excellent operational record, with less than 5% lifetime forced outage rate. Peach Bottom used a steel pressure vessel (see Fig. 6.1.1-1) and its main design features are summarized in Table 6.1.1-1. The second GA HTGR, FSV, is a 330 MWe power plant using a PCRV integral design (see Fig. 6.1.1-2) and its main design features are also summarized in Table 6.1.1-1 together with those of Peach Bottom and the two more recent large commercial plants.

Typically the PCRV has been associated with large power plant cores. A great effort was made in the United States to develop steel power plant pressure vessels of large enough size to house LWR cores up to 1,500 MWe. Steel vessel diameters of above approximately 21 ft. (for 1,000 MWe BWR) can not be shop fabricated because it is then too large to ship. Site fabrication of a steel vessel is not impossible, however, the economics would then greatly favor PCRV. In an HTGR the power density is much lower than in PWR's or even BWR's because the slowing down length is longer in graphite than water and He has a lower density than water. In fact, the 21 ft. diameter for a 1,000 MWe BWR can just barely house the 100 MWe HTGR/GT; in particular the design of the HTGR/GT reflector (see section 6.2.2) became a major concern, and only after it was proven that it was thick enough to maintain the fast neutron flux in the vessel walls below the maximum limit could the steel vessel be considered as a competitor with the PCRV. For that reason all

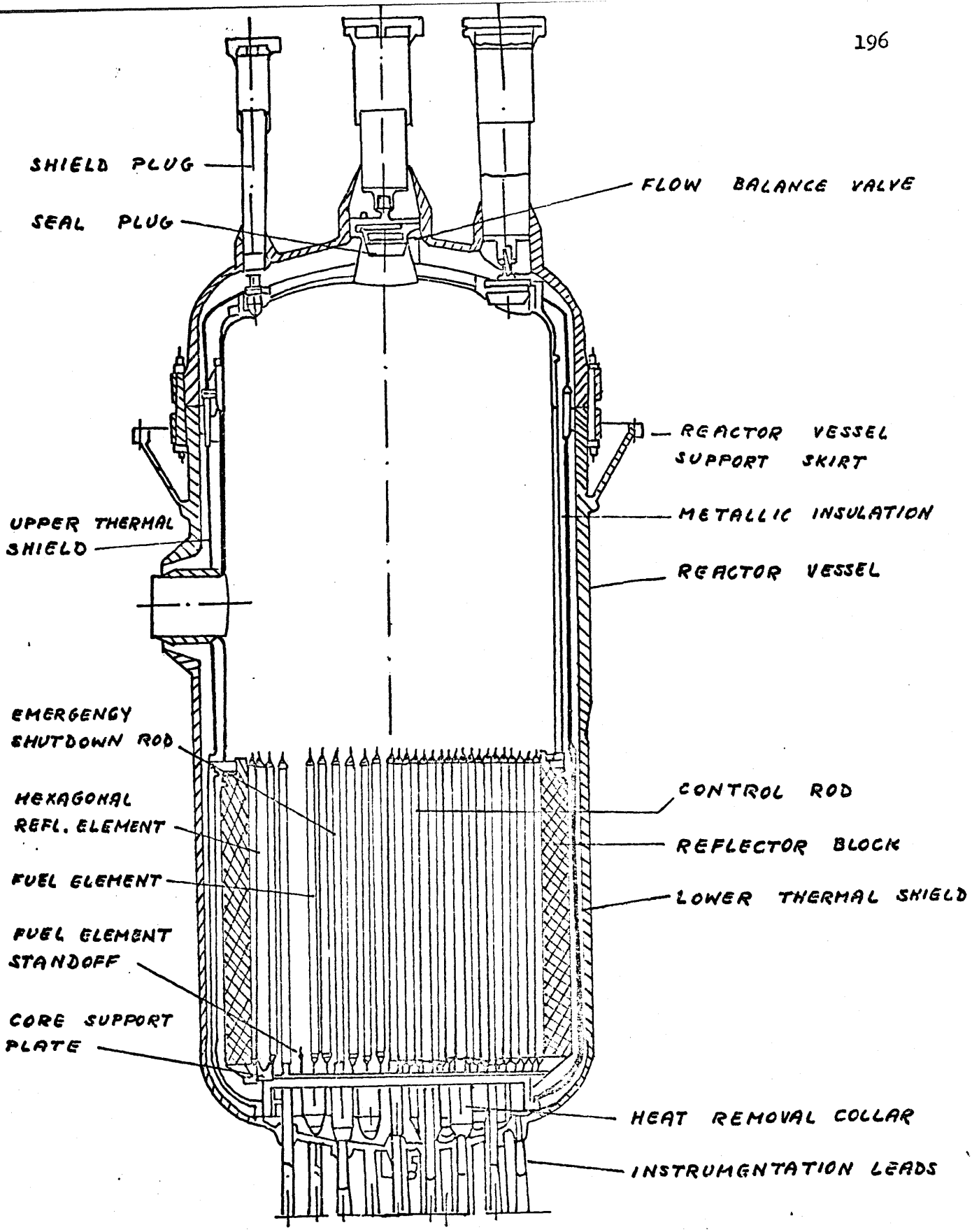

FIG. 6.1.1-1 VERTICAL SECTION OF PEACH BOTTOM-1

TABLE 6.1.1-1 HTGR REACTOR PLANT PARAMETERS

Construction Schedule	Peach Bottom	Fort St. Vrain	Delmarva-SCE 770 MW Unit 1 / Unit 2		Phila.Elec. 1160 MW Unit 1/Unit 2	
Site work started	2-62	4-68	5-74/5-76	5-76/5-76	6-75	6-75
Plant acceptance	5-67	9-73	1-79/6-81	1-81/6-82	6-81	6-83
Capacity						
Net electrical output, MW	40	330	767.1*		1156.7*	
Gross generation, MW	44.5	342	780.5		1174.7*	
Overall station of efficiency, %	34.8	38.8	38.4		38.6	
Net heat rate, Btu/kw-hr	9810	8800	8898		8851	
Plant auxiliary power, MW	4.5	12	13.4		18.0	
Design life of plant, yrs	Prototype	30	40		40	

*Assumed 2.25 in. Hg turbine backpressure

Reactor Core	Peach Bottom	Fort St. Vrain	Delmarva-SCE 770 MW	Phila.Elec. 1160 MW
Reactor Core output, MW(t)	115	851	2000	3000
Net NSS output, MW(t)	113.1	842	1981.2	2978.3
Core dimensions, dia/hgt, ft.	9.16/7.5	19.5/15.6	23.2/20.8	27.8/20.8
NSS helium inventory, lbs.	1000	8900	13,500	19,500
Number of fuel elements/columns	804/N/A	1482/247	2744/343	3944/493
Primary coolant flow, (10^6)lbs/hr	0.492	3.39	7.48	11.23
Primary coolant inlet pressure, psig	305	688	710	710
Avg. coolant temp., reactor inlet, F	650	762	606	606
Avg. coolant temp., reactor outlet, F	1380	1445	1366	1366
Core pressure drop, psi	3.2	8.4	9.7	10.0
Core orifices	N/A	37 variable	55 variable	73 variable 18 fixed
Total initial neutron flux, nv	1.7×10^{14}	1.8×10^{14}	2.4×10^{14}	2.4×10^{14}
Maximum Fast fluence (E > 0.18 mev), nvt	4.3×10^{21}	8×10^{21}	8×10^{21}	8×10^{21}

Reactor Core	Peach Bottom	Fort St. Vrain	Delmarva-SCE 770 MW	Phila.Elec. 1160 MW
Avg. power density , kW(t)/liter	8.3	6.3	8.1	8.4
Region peaking factor (radial max.)	N/A	1.83	1.6	1.6
Temperature defect, initial core,beginning of cycle, Δp	0.071	0.070	0.058	0.058
Isothermal temp.coefficient at 930 C,initial core beginning of cycle, Δp/deg °C	-5.4×10^{-5}	-3.8×10^{-5}	-4.3×10^{-5}	-4.3×10^{-5}
Neutron lifetime, initial core, beginning of cycle, sec	2.1×10^{-4}	2.4×10^{-4}	3.5×10^{-4}	3.5×10^{-4}
Average heat flux,BTU/hr-ft	70,000	45,000	62,000	65,000
Max.heat flux,BTU/hr-ft	111,000	140,000	177,000	185,000
Fuel life, full power years	2.2	4.8	3.2	3.2
Fraction of core replaced each year (80% capacity)	Prototype	1/6	1/4	1/4
Avg. conversion ratio (equilibrium)	0.44	0.62	0.66	0.66

Reactor Core	Peach Bottom	Fort St. Vrain	Delmarva-SCE 770 MW	Phila.Elec. 1160 MW
U-233 power fraction, equilibrium cycle (end of cycle)				
no recycle	0.34	0.47	0.51	0.51
recycle	N/A	0.54	0.59	0.59
Fuel and Thermal Data				
Fuel material	(← Th/U^{235} [93% enriched]/U^{233} [recycle] →)			
Fuel form	Coated particles in graphite compacts/sleeves	Coated particles in cylindrical pitch-bonded fuel rods structurally maintained by hexagonal graphite blocks		
Burnable poison material	Rh_{103}	B_4C in C	B_4C in C	B_4C in C
Number of refueling regions, full/partial	Batch refueled	37	37/18	61/24
Element (hexagonal across flats), in.	N/A	14.0	14.17	14.17
Element (length), in.	144	31	31.22	31.22
Fuel holes per element, std/control	N/A	210/120	132/76	132/76
Fuel rod diameter, in.	2.74 (compact)	0.491	0.619	0.619

Fuel and Thermal Data	Peach Bottom	Fort St. Vrain	Delmarva-SCE 770 MW	Phila.Elec. 1160 MW
Fuel Hole diameter, in.	N/A	0.5	0.624	0.624
Coolant channel diameter, in.	N/A	0.625	0.826	0.826
Coolant channels per element, std/control	N/A	108/57	72/43	72/43
Permanent reflector thickness, cm. top/bottom/side (mean)	68.58/68.88/61	118.9/118.9/135.89	118/.9/118.9/106.68	46.8/46.8/42
Replaceable reflector lifetime yrs.	N/A	8	8	8
Total quantity of uranium (U^{235})/ thorium, kg (initial core)	220/1450	882/19,458	1125/26,100	1583/37,500
Total weight reactor graphite, (10^6) lbs.	0.17	1.44	1.69	2.19
Average fuel burnup, MWd/tonne	60,000	100,000	94,000	98,000
Max. fuel center-line temp. (short term), F	2430	2300	2421	2467
Avg. fuel temp., F	1700	1500	1612	1634
Fuel melting point, F	4440	4440	4440	4440
Avg. moderator temp., F	1600	1380	1348	1362

Fuel and Thermal Data	Peach Bottom	Fort St. Vrain	Delmarva-SCE 770 MW	Phila.Elec. 1160 MW
Fuel handling equipment Handling machine height, ft-in./weight, tons	34/9	44/163	37-6/77	37-6/77
Transfer cask height, ft-in./weight, tons	29/70	N/A	11-4/47	11-4/47
Auxiliary service cask height, ft-in./weight,tons	33-5/22	44/70	37-6/73	37-6/73
Annual estimated refueling hours	400 (triennial)	170	233-288	298-368
Minimum men required for refueling	7	10	13	13

FUEL PARTICLE PARAMETERS

	PEACH BOTTOM		FORT ST. VRAIN			Delmarva-SCE 770 MW		Phila.Elec. 1160 MW
	U-235 Makeup	U-233 Recycle	1st Core	U-235 Makeup	U-233 Recycle	1st Core	U-235 Makeup	U-233 Recycle
FISSILE Kernel Composition	ThC_2/ UC_2(5.5:1)	No recycle planned	ThC_2/ UC_2(4.25:1)	ThC_2/ UC_2(4.25:1)	No recycle planned prior to 1984	UC_2	UC_2	ThC_2/ UC_2(4.25:1
Diameter, μm	250-450		100-300	100-300		200	200	350
Density, %	>90		>90	>90		>90	>90	>90
Coating								
Type	BISO		TRISO	TRISO		TRISO	TRISO	TRISO
Total thickness/μm	90-155		130	130		170	170	200

FUEL PARTICLE PARAMETERS

	PEACH BOTTOM		FORT ST. VRAIN			Delmarva-SCE 770 MW		Phila.Elec. 1160 MW
	U-235 Makeup	U-233 Recycle	1st Core	U-235 Makeup	U-233 Recycle	1st Core	U-235 Makeup	U-233 Recycle
FERTILE Kernel Composition	ThC_2/ UC (18.5:1)	N/A	ThC2	ThC_2/		ThO_2	ThO_2	ThO_2
Diameter, μm	300-500		300-600	300-600		500	500	500
Density, %	>90		>90	>90		>90	>90	>90
Coating								
Type	BISO		TRISO	TRISO		BISO	BISO	BISO
Total thickness, μm	75-130		130	130		160	160	160
Coating Composition								
BISO								
Inner buffer layer	(		Low density pyrolytic carbon					)
Outer pyro layer	(		High density isotropic pyrolytic carbon					)
TRISO								
Inner buffer layer			Low density pyrolytic carbon					)
Inner pyro layer	(		High density isotropic pyrolytic carbon					)
SIC layer	(		Silicon carbide					)
Outer pyro layer	(		High density isotropic pyrolytic carbon					)

Reactor Vessel	Peach Bottom	Fort St. Vrain	Delmarva-SCE 770 MW	Phila. Elec. 1160 MW
Type	Steel pressure vessel ASTM A 212 GrB	(Prestressed Concrete Reactor Vessel (PCRV) Single cavity	) (Multiple Cavity	)
Internal clearance dimensions, (ID x IH) ft-in.	14 x 35	31 x 75	32-8 x 47-4	37 x 47-4
PCRV support height, ft.	N/A	33	15	15
Max. external dimensions, (OD x OH) ft-in.	14-5 x 35-5	64 x 106	94 x 91-6	100 x 91-6
Min. PCRV wall thickness, ft-in.	N/A	9	17-6	17-6
Normal working pressure, psig	335	688	710	710
Design pressure, psig (setting of second relief valve)	450	845	765	765
No. vertical prestress tendons	N/A	90	264	336
Wires per vertical tendon	N/A	170	169	169
Post-tensioning force per vertical tendon (initial jacking), tons	N/A	700	700	700

Reactor Vessel	Peach Bottom	Fort St. Vrain	Delmarva-SCE 770 MW	Phila. Elec. 1160 MW
No. circumferential tendons or channels	N/A	310 (tendons)	24 (channels)	24 (channels)
Wire layers per channel	N/A	N/A	11-17	11-17
Volume of concrete in PCRV and PCRV support, cu yds	N/A	6975	20,000	22,000
Weight reinforcing steel in PCRV and PCRV support tons	N/A	600	1050	1200
Average concrete design compressive strength, psi	N/A	10,700*	6500	6500
Linear thickness, core cavity/penetrations, in.	N/A	0.75/0.75	0.75/0.5	0.75/0.5
Linear temp. normal (avg) hot spot, F	N/A	130/200	150/250	150/250
Thermal barrier	N/A	Ceramic fiber blankets/blocks covered by carbon steel or nickel alloy plates		

*Actual-design value was 6500 psi

Reactor Vessel	Peach Bottom	Fort St. Vrain	Delmarva-SCE 770 MW	Phila. Elec. 1160 MW
PCRV Penetrations				
Upper head wells				
He purification	N/A	8	8	8
Neutron detectors	N/A	6	6	6
Material surveillance	N/A	8 (sidewall)	2	2
Reflector storage	N/A	N/A	3	2
Control rod storage	N/A	N/A	3	4
Upper head penetrations				
Auxiliary cooling loops	N/A	N/A	2	3
Control rod drive/refueling	N/A	37	49/55	73/85
Safety relief valve	N/A	1 (sidewall)	2	2
Pressure measurement	N/A	6 (sidewall)	6	6
Filter absorbers	N/A	2	2	2
Nuclear instrumentation/ refueling	N/A	N/A	2	2
Steam generator/circulator	N/A	N/A	4	6
Gas seal buffers	N/A	4	6	6
Spares	N/A	1 (access)	1	1
Botton head penetrations				
Steam generator piping	N/A	12	16	24
Gas sample	N/A	4	4	4
Spares	N/A	1 (access)	3	3
Helium Circulators (each)				
Type	Horiz.single-stage centrifugal	(Axial flow compressor with driver)		
Dimensions, (length x dia) ft-in.	12-6 x 7-4	22 x 3-4	21 x 6-6	21 x 6-6

Reactor Vessel	Peach Bottom	Fort St. Vrain	Delmarva-SCE 770 MW	Phila. Elec. 1160 MW
Bearings	Oil lubricated	(	Water lubricated	)
Drive	Motor driven	(	Single-stage steam turbine	)
Flow control	(		Variable speed	)
Number of circulators	2	4	4	6
Steam flow, including bypass, ($10^{}$) lb/hr	N/A	1.395	1.332	1.332
Speed (rpm)	3200	9550	7050	7050
Circulating capacity, ($10^{}$) lb/hr	0.246	0.8725	1.87	1.87
Static press. rise (helium) psi	7.5	14	20.71	20.71
Total component cooling requirements for all circulators				
At operating conditions (10^6)BTU/hr	N/A	4.0	4.4	6.6
During refueling, (10^6) BTU/hr	N/A	2.0	3.6	5.4
Compressor inlet temp., F	626	742	721	721

Reactor Vessel	Peach Bottom	Fort St. Vrain	Delmarva-SCE 770 MW	Phila. Elec. 1160 MW
Weight (each) lb	N/A	20,000	21,000	21,000
Power, hp	2500	5200	16,270	16,270
NSS power to drive each circulator, MW(t)	N/A	3.9	11.1	11.1
Thermal power returned to NSS from each circulator, MW(t)	1.5	3.1	10.6	10.6
Steam Generators (per module)				
Type	Forced recirculation	Once through, helical-coil with integral reheat; carbon steel, chrome-moly, Incoloy 625 & 800		
No. of steam generator modules	2	12	4	6
Dimensions, (ht x dia)ft-in.	30 x 8	25-7 x 5-6	69-9 x 12-8	69-9 x 12-8
Module dry weight assembled, lbs.	127,000 34,500 (drum)	100,200	465,000	465,000
Heat transfer, main steam/ reheat, (10^{6}) BTU/hr	199/NA	209/34.7	1456/278	1456/278

Steam Generators (per module)	Peach Bottom	Fort St. Vrain	Delmarva-SCE 770 MW	Phila. Elec. 1160 MW
Heat losses from NSS heat transfer system, MW(t)	7.8	7.5	17.1	19
Bulk gas inlet temp. F	1298	1427	1366	1366
Coolant mass flow, (10^6) lbs/hr	0.246	0.284	1.883	1.883
Superheater steam flow, (10^6) lbs/hr	0.185	0.192	1.349	1.349
Superheater outlet press, psig/temp, F	1480/1005	2500/1000	2500/955	2500/955
Reheater steam flow, (10^6) lbs/hr	N/A	0.187	1.331	1.331
Reheater inlet press., psig/temp, F	N/A	638/673	631/637	631/637
Reheater outlet press., psig/temp, F	N/A	600/1002	574/1002	574/1002
Feedwater press., psig/temp, F	1580/428	3100/403	3150/370	3150/370

Reactivity Control Systems	Peach Bottom	Fort St. Vrain	Delmarva-SCE 770 MW	Phila. Elec. 1160 MW
Type	Control rods/Emergency shutdown cannisters			
Dimensions (OL/OD) ft-in.	N/A	25-3/1-10	31-9/1-9	31-9/1-9
Control rods	36/19 emergency	37 pair	49 pair	73 pair
Emergency shutdown cannisters	55	37	49	73
Active control rod length, in.	90	186	250	250
Absorber material	B C/graphite			
Minimum control rod lifetime, yrs	4	4	4	4
Canning material	Graphite	(	Incoloy 800	)
Shape	Cylindrical	(	Hollow Cylindrical	)
Drive (normal)	Hydraulic	(	Electric motor/cable and drum	)
Scram method rods	Hydraulic electric	(	Gravity	)
Cannisters	(		Gravity	)
Equil.control rod worth (all rods hot),% K	24	20	23.6	23.3
Scram insertion time,sec	0.8	180	22±3	22±3
Minimum rod withdrawal time,min	N/A	3	4	5

HTGR Auxiliary Systems Core Auxiliary Cooling System	Peach Bottom	Fort St. Vrain	Delmarva-SCE 770 MW	Phila. Elec. 1100 MW
Core aux.circulators, no.	N/A	0*	2	3
Compressor type	N/A	Water-turnine	(Single-stage axial flow)	
Drive type	N/A	Pelton-wheel	(Electric motor)	
Helium flow rate (each) lb/hr Depressurized PCRV	N/A	34,200 @ 0 psig, 500 F	80,000 @ 8.5 psig,450F	60,000 @ 8.5 psig, 450 F
Pressurized PCRV	N/A	374,400 @ 545 psig, 500 F	236,000 @ 710 psig,600F	176,500 @ 710 psig, 600 F
Core aux. heat exchangers,no.	N/A	0(use st.gen.)	2	3
Type	N/A	N/A	(Helical tube,pressurized water)	
Feedwater flow rate (each), lb/hr	N/A	N/A	871,000	653,000
Total core auxiliary cooling system heat load,(10)Btu/hr,				
Normal operation	N/A	N/A	29.0	29.1
Emergency-pressurized PCRV	N/A	N/A	232.0	346.0
Emregency-depressurized PCRV	N/A	N/A	117.3	176.0

*Use existing main circulators

Auxiliary Systems Requirements	Peach Bottom	Fort St. Vrain	Delmarva-SCE 770 MW	Phila. Elec. 1160 MW
Total NSS electrical load, Kva				
Normal operation at full power	N/A	850	955	1237
Normal refueling shutdown	N/A	850	1117	1439
Design basis accident	N/A	350	1956	2876
Total auxiliary boiler steam (@ 200 psig,600F), lbs/hr	N/A	45,000	150,000	195,000
Helium Purification System				
Type	(High-temperature charcoal bed filter adsorber, purification cooler/moisture separator, molecular sieve dryer, LN cooler, low-temperature charcoal adsorber, hydrogen getter (titanium)			
System capability		Two 100% independent trains		
Flow per train, lbs/hr		935	2000	2000
PCRV Cooling System Heat Load, (10^6)Btu/hr,Normal operation	N/A	12.1	37.0	51.0
Refueling	N/A	2.4	8.0	10.0

Turbine Generator	Peach Bottom	Fort St. Vrain	Delmarva-SCE 770 MW	Phila. Elec. 1160 MW
Type	Tandem-compound, double-flow	Cross compound	(Tandem-compound, four flow) single	Two half-size
Generator rating, Mva	52	380	867	676
TSV pressure, psig/temp,F	1450/1000	2400/1000	2400/950	2400/950
IP cylinder TSV press, psig/temp. F	N/A	555.5/1000	554/1000	553.2/1000
Vacuum, in. Hg	1.5	2.5	2.25	3.5
No. H.P. feedwater htrs (per tubing)	2	2	0	0
No. L.P. feedwater htrs (per tubing)	2	3	3	3
Condensor (per tubing)				
Type	Single-pass, divided water-box	Two-pass divided water-box	(Single pressure, single-pass three shell)	
Duty, (10^9) Btu/hr	0.25	1.67	4.04	3.04
Hotwell capacity, gal	1,500	10,000	26,000	20,700

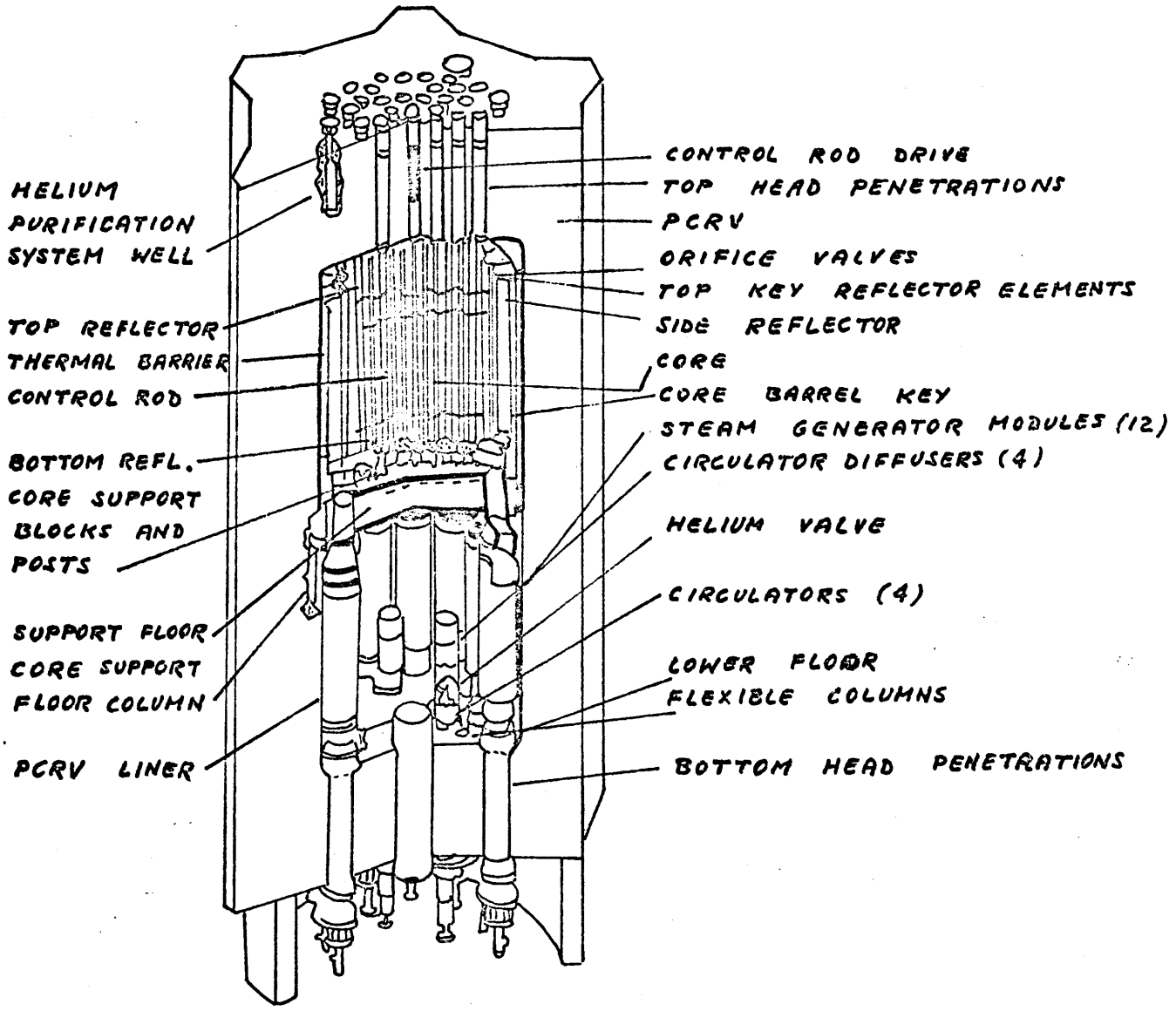

FIG. 6.1.1-2 THE FSV REACTOR ARRANGEMENT

commercial HTGR's constructed in the world employ PCRV's. This is reversed in the case of small prototypes with diameters smaller than 21 ft. where steel vessels have been preferred (see Table 6.1.1-2).

In order to make an adequate comparison of the steel vs PCRV pressure boundary the following aspects were examined: safety, economy, maintainability and flexibility.

6.1.1.1 Safety Analysis

One of the points which greatly favors use of a PCRV is the safety aspects of this vessel. When a PCRV is constructed the concrete is put into compression by the prestressed tendons. The tension in the tendons is just great enough to ensure that there will be no point in the concrete which is under tension when the vessel is pressurized. To do this a great number of tendons are applied with circumferential, longitudinal, and end slab stresses. The real safety advantage becomes apparent when one considers tendon failure, that is, should one tendon fail, the vessel will not fail catastrophically. In fact the GA 1,000 MWe reference design has 8,000 tendons, 4,000 of which must fail before there is vessel failure. Another safety advantage of having so many tendons is that one may be removed without affecting plant operation and in this way constant maintenance may be practiced with no interruption of plant service. A point of concern in relation to PCRV's is that concrete loses its properties if its temperature is too high. Therefore adequate cooling of the thermal barrier is required, which means that a separate cooling system is necessary for this task and loss of this coolant will result in immediate core shutdown and could lead to PCRV failure.

Table 6.11-2 Summary Description of Small HTGR Reactors

	Peach Bottom I	Fort St. Vrain	Dragon	AVR	Geesthacht II	JAERI-- VHTR	THTR
1. Power Conversion	Indirect Rankine	Indirect Rankine	Indirect	Indirect Rankine	Direct Brayton	Rankine/ Brayton	Indirect Rankine
2. Rated Output (MWt/MWe)	115.5/40	842/330	20/-	49/13.2	65/24	50/4.5 (Indirect) /7.0 (Direct)	750/300
3. Net Eff. (%)	34.6	39.2	NA	27	37	21.36(Direc.)	40
4. Core Dimensions (ft.), Dia/Ht	9.16/7.5	19.5/15.6	3.5/8.3	9.8/9.8	8.1/6.9	15.3/8.2	18.3/ 19.7
Power Density (KW/liter)	8.3	6.3	14	2.3	6.4	4.7	6.0
Outlet Temp. (°F)	1380	1445	1382	1562	1355	1382	1382
Coolant Flow	Up	Down	Up	Up	Up	Down	Down
5. Reactor Vessel	Steel	PVRV	Steel	Steel	Steel	Steel	PCPV
Dimensions (ft), Dia./Ht	14/35	49/106 (Inside)	11.5/58	19/82.4	13/32.5	16.8/36.1	52/50 (Inside)
Operating Pressure (psig)	335	688	294	131	368	569	588
6. Containment	Vertical Cylindrical Steel Shell	NA	Steel Shell (Inner) Concrete (Outer)	Steel Cylinder	Concrete Building	Cylindrical Concrete Structure	NA
Dimensions (ft), Dia./Ht	100/162	76x120/161 (Outside)	66/106 (Inner)	52.5/134.5	100x100/ 140	114.8/213	81/83 (Outside)
Operating Pressure (psig)	-.2~8	-.2	10(Inner) .5(Outer)	.3	0	0	NA
7. Primary System Control Rod Drives	Hydraulic	Electrical Cable and Drum Type	Electrical Gear Box Wire, Drum	Pneumatic Slip on Guide Rails	Hydraulic	Electrical Magnetic Clutch and Drum	Pneumatic

Table 6.1.1-2 Continued

	Peach Bottom I	Fort St. Vrain	Dragon	AVR	Geesthacht II	JAERI--VHTR	THTR
Circulators	Centrifugal Blowers driven by 1.402 MW/ 3600 RPM Motors	Axial Flow Circulators driven by Exhaust Steam from HP Turbine	Six Blowers; Variable-frequency Squirrel--cage Motors rated 100 h.p. at 1200 r.p.m.	Two Blowers driven by Electrical Motor	NA	Centrifugal Horizontal Circulators driven by Induction Motor (Indirect)	Electric Motor driven Blower
Ducting	Concentric	NA	Concentric	NA	Concentric	Concentric	NA
8. Emergency Shutdown	Thermally Released Absorbers	Releasing Boron Carbide Spheres by Gravity Fall	None	Charging Graphite Spheres Containing Boron into Core	Reactor Scram and Shut-down of the Turbine	Boron Balls	Long-Stroke Pneumatic Absorber Rod Drive System
9. Emergency Shutdown	Natural Convection Cooling	Provision for Flooding Evaporator and Super-heater of Steam Generator	Guaranted Electrical Supplies, Natural Circulation in Cooling Circuit	Heat Loss through Vessel Walls	He and N_2 Emergency Cooling Systems (2)	Emergency Core Cooling System (5% of Full Flow)	Rupture-Safe PCPV
10. References	PI, D2	P4,D4,P5	D5, R1	D6	B1	J1,I2,S6	M10

The maximum credible accident in a PCRV is the failure of a refueling port (about 100 in^2 area) and the maximum credible accident in a steel vessel system occurs with a double-ended rupture of the largest pipe in the primary system. In the HTGR/GT steel vessel final design, where concentric pipes are employed (see section 6.2) the worst case consists in the rupture of the external inlet pipe (~1756 in^2), that is, the blowdown following the accident is much faster in the steel vessel case. However, due to the large heat capacity of the graphite moderator, the blowdown velocity is not critical in the emergency core cooling design of HTGR's. Once subcriptical several hours will pass before thermal margins would be exceeded. The difference in the blowdown time is therefore not an important consideration in the temperature reached during such a loss of coolant accident, that is, it is not important if the blowdown occurs quickly (some seconds) as in the case of the steel vessel pipe rupture or somewhat slower (approximately 1 hour) as in the case of the failed refueling port. In either case the core heat up transient is so long that the actual time duration of the blowdown is insignificant. However, the extremely high flowrates encountered in the steel vessel blowdown require careful analysis (see section 6.2). The shutdown and emergency cooling systems for the HTGR/GT steel vessel final design and accident analysis were discussed by Shin (Ref. 82), and because safety is such an important topic, some of his findings will be briefly summarized here.

A. Shutdown and Emergency Cooling Systems

The following modes of energy removal from the primary coolant are provided:

Operational:	Normal	--	use of gas turbine loops via 1HX units
Shutdown:	Normal	--	use of GT loops in shutdown mode
			use of shutdown cooler loop on secondary side of 1HX
	Auxiliary	--	use of purification system
	Ultimate	--	use of heat leakage through reactor vessel, removed by reactor cavity and/or containment air cooling systems

Post-Accident (Primary System Blowdown)

Same modes as during shutdown.

If all shutdown cooling modes are operational the maximum decay heat rate can be accomodated without an increase in fuel temperature; if only one (and the least effective) of the several redundant paths is operational, the fuel temperature increase will be less than 300°F before the heatup transient is turned around ... hence the fuel will not exceed its normal full power operating temperature.

B. Accident Analysis

Several accident possibilities were categorized. The primary system blowdown was found to be by far the most serious one. There are various factors which both mitigate and aggravate this accident with respect to the present design, as noted in Table 6.1.1.1-1.

Upon receipt of a low primary system pressure signal an automatic scram would occur; if not, then the operator could initiate emergency scram and allow the boron shot to enter the core. Because there is ample time to bring into action the various modes of shutdown heat removal, the more immediate problem is to avoid ingress of air into the hot core because of the danger of graphite oxidation ... i.e., a graphite fire. To avoid that problem sufficient make up helium is injected to keep primary system pressure slightly above that of the containment atmosphere.

Ample inert gas exists for injection into the primary system to maintain a differential pressure: the entire primary helium inventory and the entire turbine plant helium inventory (both including reserve storage); in addition the nitrogen from the liquid nitrogen system used for the cryogenic absorbers is available at the discretion of the station staff.

The prohibition against air in the core is not absolute: a small amount (<5 vol. %) can be tolerated at high temperatures (99), and below about 900^{o}F the graphite is cold enough to reduce the reaction rate to a tolerable level (100). Thus it is only

TABLE 6.1.1.1-1

Factors Affecting the HTGR/GT Blowdown Accident

Mitigating

1. Indirect cycle removes turbine/compressor-generated missiles as accident initiators.
2. Pressure is lower than PCRV-Type HTGR's (400 vs ~ 700 psia), hence lower flow for a given break size: mass flow through break is proportional to product of primary pressure and break area.
3. Satisfactory primary system blower performance after depressurization is more readily assured than that of direct cycle Turbomachinery with respect to providing adequate flow through core.
4. Service pressure of steel vessel and piping (400 psia) is much lower than for PWR's (~2,000 psia).
5. Unlike Fort St. Vrain, the present reactor is contained; unlike Geesthacht, two main coolant loops are provided.

Aggravating

1. Large vessel and duct dimensions compared to Peach Bottom, Dragon, AVR (but not other gas-cooled reactors).
2. No easy way to limit rupture flow areas to ~100 sq. in. as in integral/PCRV Type HTGR's. Hence more rapid blowdown is possible.
3. Containment inerting not using (in contrast to Peach Bottom).

during the interim period between blowdown and cooldown that caution is necessary.

Assuming that overheating and oxidation are avoided, blowdown will release on the order of several hundred curies of activity into the containment, consisting of primary circuit circulating activity and a small percentage of volatiles deabsorbed from the primary circuit surfaces. This can easily be handled by the off-gas treatment system.

6.1.1.2 Cost Comparison

An Attempt to determine the cost of both steel and integral concrete pressure boundary designs was made in the Fall of 1973 (Ref. 6). The PCRV integral system was found to be about 30% cheaper but the difference was small compared with the total cost of the plant and with the uncertainties involved in such an estimate.

The total cost of the plant was calculated by Metcalfe (Ref. 86) to be about 111 U.S. millions $\pm$ 18% 1974 dollars (see section 3.4) and the cost of the steel vessel was estimated as $7,600,000 in 1972 (Ref. 92) which is $9,196,000 in 1974 dollars assuming a 10% inflation rate.

6.1.1.3 Maintainability and Flexibility

The non integral design (with steel vessel) is certainly much easier to design and to maintain than the integral one. It is also much more flexible permitting several modifications on the initial design. This plant is the first of a kind and with any new plant

many design changes may be encountered in the future. Some of these may come about due to increases in technology and some through better plant design.

The flexibility problem favors the non-integral system design in first of a kind plants, but once the design has been established and future improvements are not required, this advantage becomes trivial. The ease of maintenance is an all time advantage though.

6.1.2 Conclusions

It was decided, after weighing the above factors, that the steel vessel should be used in the first generation army reactor. The ease of maintenance and plant flexibility consideration play a major role in this decision. Since this plant is first of a kind, many plant layouts and choice of system equipment will be made before a final design is completed. The economy initially slightly favoring PCRV suffered a change of position when design progressed towards the employment of an indirect Brayton Cycle in which case the PCRV would have to be very big to house the very large intermediate heat exchangers (He on both loops).

The safety comparison favored a PCRV but steel vessel performance has been found to be reliable in LWR's and in Peach Bottom.

6.2 Vessel Internals

Whenever possible the internals of FSV were maintained. The use of a steel vessel instead of a PCRV and of a single zone batch of long reactivity lifetime made necessary a few modifications though. For that reason the following angles are treated separately:

a) Vessel Wall Temperature - As can be seen in Table 6.2-1 the steel mechanical properties start to fall down at about 700 to 800°F; the concrete has to be maintained below 212°F in order not to loose water. In the PCRV there is an insulation between the reflector and the steel liner and an extra cooling system for the steel liner and adjacent concrete. In the HTGR/GT steel vessel case it is enough to isolate the vessel walls. To have a lower temperature in the reflector the coolant passes first through the reflector and then in the core (see Fig. 6.2-1). The insulation of the vessel is treated in section 6.2.1.

b) Reflector Design - The max. steel vessel internal diameter shop fabricated is 251 in. (20.92 ft. for a 1075 MWe BWR). It is specified for a max. fast nvt (E>1MeV) of 10^{19} n/cm^2 in 40 years (from page 6.14 of Ref. 76). The reflector thickness is limited by the size of the vessel which brings a design problem treated in section 6.2.2. The max. nvt limit in PCRV is only 2×10^{18} n/cm^2 (Ref. 73) but in the PCRV that is no size limitation and the reflector can be as thick as economically desirable.

c) CR Drive Problem - In a steel vessel blowdown the coolant mass flow rate is much faster than in a PCRV blowdown. In section 6.2.3

Table 6.2-1

Maximum Allowable Stress Values in Tension for Carbon and Low-alloy Steel, in Pounds per Square Inch, Class UCS*

Material & Specification No.	Grade	Nominal Composition	P No.	Spec. min. tensile	For metal temperatures not exceeding °F							
					-20 60 650	700	750	800	850	900	950	1000
Plate Steels: Carbon Steels												
SA 7			1	60,000	12,650							
SA 113	C		1	48,000	11,050							
SA 201	A	C, Si	1	55,000	13,750	13,250	12,050	10,200	8,350	6,500	4,500	2,500
SA 201	B	C, Si	1	60,000	15,000	14,350	12,950	10,800	8,650	6,500	4,500	2,500
SA 212	A	C, Si	1	65,000	16,250	15,500	13,850	11,400	8,950	6,500	4,500	2,500
SA 212	B	C, Si	1	70,000	17,500	16,600	14,750	12,000	9,250	6,500	4,500	2,500
SA 283	A		1	45,000	10,350							
SA 283	B		1	50,000	11,500							
SA 283	C		1	55,000	12,650							
SA 283	D		1	60,000	12,650							
SA 285	A		1	45,000	11,250	11,000	10,250	9,000	7,750	6,500		
SA 285	B		1	50,000	12,500	12,100	11,150	9,600	8,050	6,500		
SA 285	C		1	55,000	13,750	13,250	12,050	10,200	8,350	6,500		
SA 300			1									

*From the 1962 edition of the ASME Boiler and Pressure Vessel Code, Unfired Pressure Vessels.

Table 6.2-1 (Continued)

Maximum Allowable Stress Values in Tension for Carbon and Low-alloy Steel, in Pounds per Square Inch, Class UCS*

Material Specification No.	Grade	Nominal Composition	P No.	Spec. min. tensile	For metal temperatures not exceeding °F							
					-20 to 650	700	750	800	850	900	950	1000
Low-alloy steels												
SA 202	A	Cr, Mn, Si	4	75,000	18,750	17,700	15,650	12,600	9,550	6,500	4,500	2,500
SA 202	B	Cr, Mn, Si	4	85,000	21,250	19,800	17,700	12,800	9,900	6,500	4,500	2,500
SA 203	A, D	2½ and 3½ Ni	4	65,000	16,250	15,500	13,850	11,400	8,950	6,500	4,500	2,500
SA 203	B, E	2½ and 3½ Ni	4	70,000	17,500	16,600	14,750	12,000	9,250	6,500	4,500	2,500
SA 204	A	C, ½ Mo	3	65,000	16,250	16,250	16,250	15,650	14,400	12,500	10,000	6,250
SA 204	B	C, ½ Mo	3	70,000	17,500	17,500	17,500	16,900	15,000	12,750	10,000	6,250
SA 204	C	C, ½ Mo	3	75,000	18,750	18,750	18,750	18,000	15,900	13,000	10,000	6,250
SA 302	A	Mn, ½ Mo	3	75,000	18,750	18,750	18,750	18,000	15,900	13,000	10,000	6,250
SA 302	B	Mn, ½ Mo	3	80,000	20,000	20,000	20,000	19,100	16,800	13,250	10,000	6,250
SA 357		5 Cr, ½ Mo	5	60,000		13,400	13,100	12,800	12,400	11,500	10,000	7,300
SA 387	A	½ Cr, ½ Mo	3	65,000	16,250	16,250	16,250	15,650	14,400	12,500	10,000	6,250
SA 387	B	1 Cr, ½ Mo	4	60,000	15,000	15,000	15,000	14,750	14,200	13,100	11,000	7,500
SA 387	C	1¼ Cr, ½ Mo-Si	4	60,000	15,000	15,000	15,000	15,000	14,400	13,100	11,000	7,800
SA 387	D	2¼ Cr, 1 Mo	5	60,000	15,000	15,000	15,000	15,000	14,400	13,100	11,000	7,800
SA 353	A	9 Ni	10	90,000	22,500							
SA 353	B	9 Ni	10	95,000	23,750							

*From the 1962 edition of the ASME Boiler and Pressure Vessel Code, Unfired Pressure Vessels.

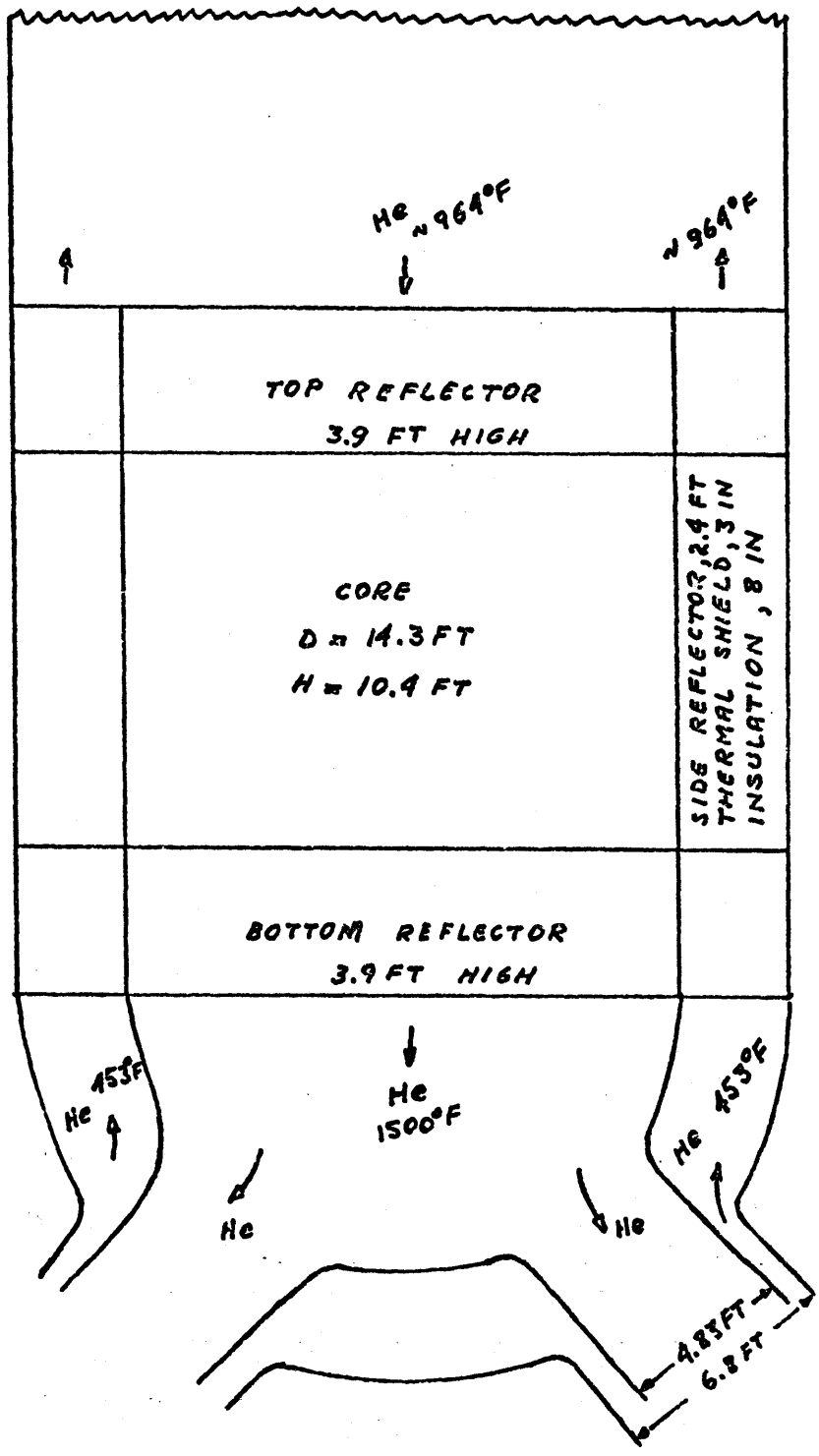

FIG. 6.2-1 COOLANT FLOW IN THE HTGR/GT

it is shown that with flexible steel cables the CR may be ejected from the core or be damaged in a steel vessel blowdown. For that reason the flexible steel cable drives used in FSV should not be advised for the HTGR/GT.

d) Inlet and Outlet Ducts - Since those ducts must be very large to cut pressure losses and there are two primary loops, it is necessary to use concentric tubes as demonstrated in Fig. 6.2-1. This is a common practice in the case of steel vessel HTGR's as can be seen in Table 6.1.1-2. The diameter of those tubes is also treated in section 6.2.3.

e) Longer Reactivity Lifetime - As discussed in Chapter 5 the HTGR/GT design includes 12 CR pairs in the side reflector for larger reactivity control and LBP in the bottom reflector to get a lower T_{C_L} and some increase in reactivity lifetime without increasing the CR requirements.

f) Core Orificing - From the cumulative heat transferred to coolant values in the CITATION outputs it was felt that the use of fixed orifices in the HTGR/GT core were appropriate. This problem was treated in detail in Stengle's MS thesis (Ref. 87) and is here summarized in section 6.2.4

6.2.1 Vessel Wall Temperature and Thermal Stress

The final material and mechanical specifications for the insulator and steel vessel are out of the scope of this thesis. Nevertheless a rough estimate of the temperature and thermal stress in the vessel walls is made with some reasonable assumptions to demonstrate feasibility.

The following assumptions were made:

a) About 2% of the heat generated by fission in the core is really absorbed by the coolant in the reflector. Then the He temperature increase in the reflector is from 953°F to 964°F (includes n and γ heating in the reflector plus conduction from the core).

b) The temperature increase from the coolant to the reflector graphite is ~8°F. This comes from the fact that this increase is ~400°F in the hottest part of the core. The highest temperature in the reflector should then be 972°F. The objective of items a and b is just to establish a conservatively high max. temperature for the reflector.

c) The vessel wall and insulator can be treated as slabs as in Fig. 6.2.1-1. This is standard procedure for large diameter cylindrical equipment.

d) All the heat produced in the vessel wall is due to γ radiation. This comes from the ANISN output (see Sections 2.2 and 6.2.1.1) values for the neutron and γ fluxes and values for the neutron and energy absorption cs. The γ heating is about 2 orders of magnitude larger than the neutron heating.

e) The γ heating in the insulator can be neglected. The exact insulator composition is not known, but most thermal insulator materials are rather porous and have low γ absorption cs compared to iron (c for instance has energy absorption cs 10 times smaller in most groups). A specific insulator had to be assumed to be able to perform a temperature distribution and thermal stress

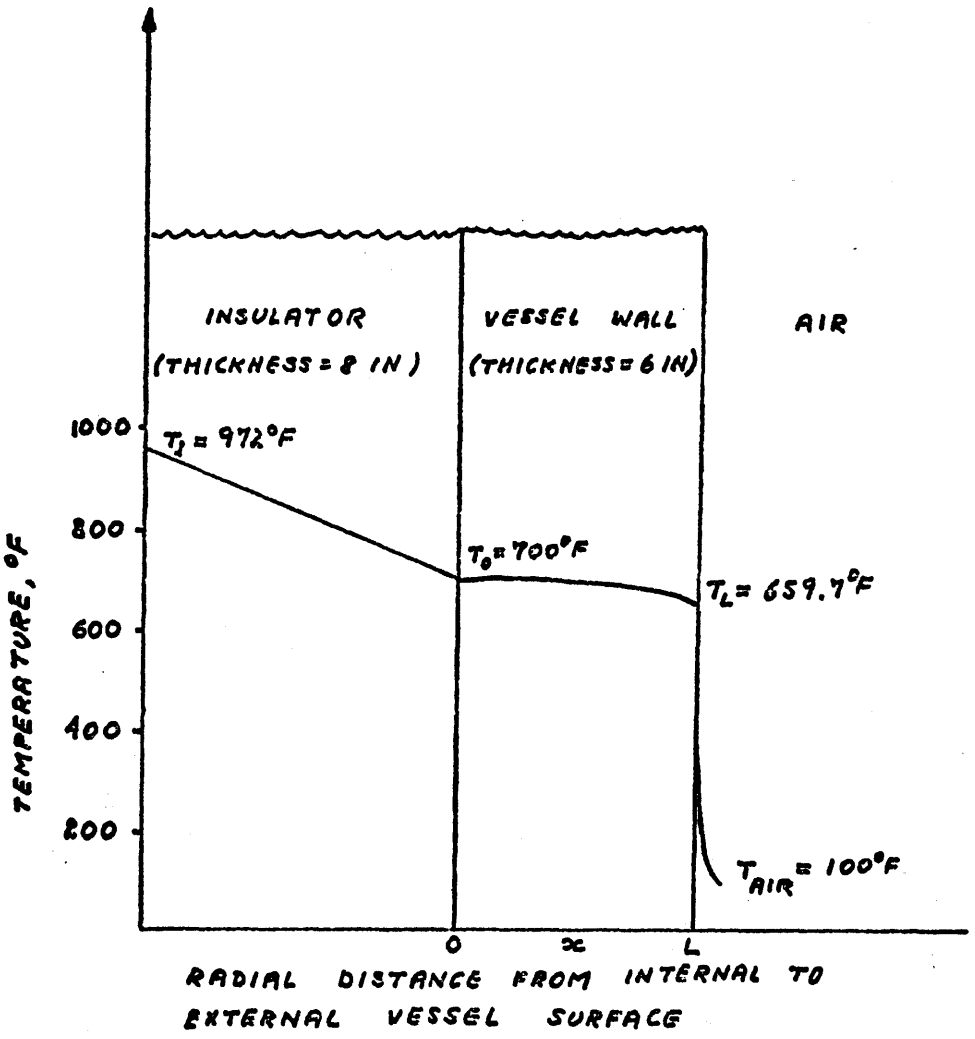

FIG. 6.2.1-1 RADIAL TEMPERATURE PROFILE IN THE INSULATOR AND VESSEL WALL

calculation. The chosen insulator was the 12 lb/ft^3 density "Refrasil" produced by H.I. Thompson Fiberglass Co. This material maintains its properties at high temperatures (~1,500^{o}F) and withstand high neutron and γ fluences. Its average thermal conductivity in the 1,000^{o}F to 600^{o}F range is ~0.5 Btu-in/hr ft^2 ^{o}F.

f) Also a steel vessel type had to be assumed. For its relatively low cost and high max. allowable stress the low alloy steel SA302 Gr.B was chosen and a summary of its pertinent properties are summarized in Table 6.2.1-1.

6.2.1.1 Temperature Distribution

The heat conduction equation for a slab with heat generation (vessel wall) is:

$$\frac{d^2T}{dx^2} + \frac{\dddot{q}(x)}{k_v} = 0 \qquad (6.2.1.1\text{-}1)$$

The $\dddot{q}(x)$ was determined with the help of the 18 γ group ANISN output. The value at $x=0$ is calculated in Table 6.2.1.1-1 and the value at $0 < x < L$ was assumed as

$$\dddot{q}(x) = q(0)e^{-ax}, \qquad (6.2.1.1\text{-}2)$$

where the attenuation coefficient, $a = .6327$ in^{-1}, was determined also from the ANISN output as the best value to fit the exponential decay of the γ fluxes.

TABLE 6.2.1-1

Properties of Low Alloy Steel SA 302 Gr. B

Thermal Conductivity, k_v	2.362 BTU/hr in ^{o}F
Attenuation Coefficient, a	0.6327 in^{-1}
Thermal Expansion Coefficient, α	6.0 x 10^{-6} in/^{o}F
Young Modulus, E	3.0 x 10^{7} psi/in
Poison Ratio, ν	0.3

TABLE 6.2.1.1-1

Determination of γ Power Density at Internal Vessel Wall from ANISN Output Data

γ Group	Mean Energy (MeV)	σ_a (barns)	ϕ (10^{11} γ/cm^2 sec) (**)	$\sigma_a \bar{E} \phi$ (*) (10^{11} MeV b γ/cm^2 sec)
1	9.00	1.628	0.573	8.396
2	7.25	1.243	5.916	53.314
3	5.75	0.959	3.030	16.708
4	4.50	0.741	2.384	7.949
5	3.50	0.577	2.719	5.491
6	2.75	0.461	1.659	2.103
7	2.25	0.389	1.771	1.550
8	1.83	0.330	1.548	0.935
9	1.50	0.283	1.742	0.739
10	1.125	0.234	2.204	0.601
11	0.90	0.190	1.728	0.295
12	0.70	0.154	2.358	0.254
13	0.50	0.116	7.713	0.447
14	0.35	0.089	4.246	0.132
15	0.25	0.077	6.727	0.129
16	0.15	0.105	7.771	0.122
17	0.075	0.330	0.792	0.020
18	0.030	3.04	0.005	0.000
				99.185

(*) The iron atom density is N_{Fe} = 8487. x 10^{-5} atoms/bcm The summation of $N_{Fe}\ \sigma_a \bar{E} \phi$ for the 18 γ groups yields 8.418 x 10^{11} MeV/sec cm^3 or $\dddot{q}$ = 0.1347 w/cm^3 = 7.531 BTU/hr in^3.

(**) The values are at x = 0.75 in., so $\dddot{q}(0.75) = \dddot{q}(0)e^{-a0.75}$ = 7.531 BTU/hr in^3 ∴ $\dddot{q}(0)$ = 12.10 BTU/hr in^3.

The solution of Eq. 6.2.1.1-1 is:

$$T(x) = -\frac{\dddot{q}(0)/k_v}{a^2} e^{-ax} + c_1 x + c_2. \qquad (6.2.1.1\text{-}3)$$

The constants c_1 and c_2 can be expressed as a function of T_o and T_L, the temperature at the vessel internal and external surfaces (yet to be determined) respectively, if one requires:

$$T = T_o \quad \text{at} \quad x = 0,$$

and

$$T = T_L \quad \text{at} \quad x = L.$$

The constants are:

$$c_1 = -\left[(T_o - T_L) + \frac{\dddot{q}(0)/k_v}{a^2}(1 - e^{-aL})\right]/L, \qquad (6.2.1.1\text{-}4)$$

and

$$c_2 = T_o + \frac{\dddot{q}(0)/k_v}{a^2}. \qquad (6.2.1.1\text{-}5)$$

To determine T_o and T_L the continuity of the heat flow is required at the two vessel wall surfaces:

a) Insulator - vessel wall interface:

$$k_{ins.} \frac{972^{\circ}F - T_o}{8 \text{ in}} = -k_v \left(\frac{dT(x)}{dx}\right)_{x=0} = -k_v \left[\frac{\ddot{q}(0)/k_v}{a} + c_1\right]; \qquad (6.2.1.1\text{-}6)$$

b) Vessel Wall - air interface:

$$-k_v \left(\frac{dT(x)}{dx}\right)_{x=L} = h_{air} (T_L - T_{air}) \qquad (6.2.1.1\text{-}7)$$

or $$-k_v\left[\frac{(q'''(0)/k_v)e^{-aL}}{a} + c_1\right] = h_{air}(T_L - T_{air}), \qquad (6.2.1.1\text{-}8)$$

where h_{air} is the heat transfer coefficient of air. If no forced air circulation is made h_{air} can be correlated by (Ref. 93):

$$\frac{Nu_H}{4\sqrt{Gr_H/4}} = \frac{0.902\ Pr^{1/2}}{(0.861 + Pr)^{1/4}}\ , \qquad (6.2.1.1\text{-}9)$$

where:

Pr = Prandt Number = $c_p\mu/k$; (6.2.1.1-10)

Nu_H = Nusselt Number = hH/k ; (6.2.1.1-11)

Gr_H = Grashof Number = $gH^3\beta(T_L - T_{air})/(\mu/\rho)^2$; (6.2.1.1-12)

H - Height of the vessel wall, assumed 45 ft. ;

g - Gravity acceleration ;

$\beta = -\ 1/\rho\ (\partial\rho/\partial T)_p$ expansion coefficient . (6.2.1.1-13)

Supposing air at 100°F (Ref. 93, Table E.3):

k = 0.016 BTU/hr ft°F,

Pr = 0.706,

$g\beta/(\mu/\rho)^2$ = 1.8/ft^3°F,

and $$h_{air} = (3.425 \times 10^{-3})(T_L - 560^{\circ}R)^{0.25}\ \frac{BTU}{hr\ ft^{2\circ}R}\ . \qquad (6.2.1.1\text{-}14)$$

Substitution of Eq. 6.2.1.1-14 into Eq. 6.2.1.1-8 and numerical solution by trial and error of the system formed by Eqs. 6.2.1.1-6 and 6.2.1.1-8 show that h_{air} achieved with natural convection is not enough to keep the vessel temperature below 700°F. With forced convection h_{air} in the range of 2 to 50 BTU/hr ft^{2}°F (Ref. 93) are possible and adequate cooling is at hand. The minimum necessary value of h can be obtained by making T_o = 700°F in Eqs. 6.2.1.1-6 and 6.2.1.1-8 and calculating h_{air} and T_L; after substitution by numerical values on these two Eqs. , there results:

$$(4.34 \times 10^{-4})(1532^{\circ}R - 1160^{\circ}R) = (1160^{\circ}R - T_L)(0.3937) - 14.20, \quad (6.2.1.1\text{-}15)$$

and

$$(4.495 \text{ BTU/in}^2\text{hr}) + (0.3937 \text{ BTU/in}^2\text{hr}^{\circ}R)(1160^{\circ}R - T_L) = h(T_L - 560^{\circ}R). \quad (6.2.1.1\text{-}16)$$

From those two Eqs. , T_L = 1119.7°R and $(h_{air})_{min}$ = 0.0364 BTU/hr in^2 °R = 5.24 BTU/hr ft^2 °R.

6.2.1.2 Thermal Stress in the Vessel Wall

The static thermal stress in an infinite slab can be calculated from (Ref. 9 4):

$$\sigma_y(x) = \sigma_z(x) =$$

$$\frac{\alpha E}{1-\nu}\left[-T(x) + \frac{1}{L}\int_o^L T(x)dx + \frac{12[x-(L/2)]}{L^3}\int_o^L T(x)\left[x - \frac{L}{2}\right]dx\right], \quad (6.2.1.2\text{-}1)$$

The temperature distribution comes from Eq. 6.2.1.1-3 after substitution by numerical values:

$$T(x) = 1160^{\circ}R + (12.80^{\circ}R)(1 - e^{-0.6327x}) - (8.802^{\circ}R/in)x \quad (6.2.1.2\text{-}2)$$

It is observed that T(x) is almost constant and with good approximation an average between $T_o = 1160^{\circ}R$ and $T_L = 1119.7^{\circ}R$ can be used in the integrals of Eqs. 6.2.1.2-1 to obtain:

$$\sigma_y(x) = \sigma_y(x) = \frac{\alpha E}{1-\nu}\left[1139.9^{\circ}R - T(x)\right] . \quad (6.2.1.2\text{-}3)$$

Substituting the values for α, E and ν from Table 6.2.1-1 the maximum thermal stress (at x = 0 or 6) is found to be 5194 psi which is well below the max. permissible level of 20,000 psi for this type of steel.

6.2.2 Reflector Design

The increase in coolant temperature in passing through the core and reflector is given by:

$$\Delta T = Q/\dot{m}\, c_p \quad , \quad (6.2.2\text{-}1)$$

where:

$Q = 300$ MWth $= 284.3 \times 10^3$ BTU/sec, core heat generation rate ;

$\dot{m} = 418.89$ lb/sec = He coolant mass flow rate ; $C_p = 1.2416$ BTU/lb$^{\circ}$F = He specific heat (almost constant with temperature). This and all other He physical properties were obtained with the code HELIUM (Ref. 78).

The coolant temperature increase calculated with Eq. 6.2.2-1 is 546.7°F, of which, 2% assumed in the side reflector pass (from 953°F to 964°F as in Fig. 6.2-1). To calculate the friction pressure drop and heat transfer coefficient in the core and reflector the following equations were used:

$$\dot{m} = \rho_1 A_1 v_1 = \rho_2 A_2 v_2 \ , \qquad (6.2.2\text{-}2)$$

$$A_i = n_i \pi D_i^2/4 \ , \qquad (6.2.2\text{-}3)$$

$$Re_i = D_i v_i \rho_i / \mu_i = 4\dot{m}/\pi n_i D_i \mu_i \ , \qquad (6.2.2\text{-}4)$$

$$\Delta p_i = \frac{.184}{Re_i^{.2}} \frac{L}{D_i} \frac{\rho_i v_i^2}{2g_c} = a_i / n_i^{1.8} D_i^{4.8} \ , \qquad (6.2.2\text{-}5)$$

$$Nu_i = (0.023)(Re_i^{.8})(Pr_i^{.4}) = h_i D_i / k_i \ , \qquad (6.2.2\text{-}6)$$

where:

$i = 1,2$ index 1 for the core and index 2 for the reflector ;

ρ - He density ;

v - Velocity ;

A - Cross flow area ;

D - diameter of one coolant channel ;

n - Number of coolant channels ;

μ - Viscosity of He ;

Re - Reynolds no. ;

L - 218.4 in. length of a coolant channel ;

g_c - 386.4 lb_m in/sec lb_f ;

$a_1 = .6036 \times 10^7$ - use D in in. and get ΔP_1 in psi from Eq. 6.2.2-5

$a_2 = .5074 \times 10^7$ - use D in in. and get ΔP_2 in psi from Eq. 6.2.2-6

Nu - Nusselt no.

Pr - Prandt no.

Table 6.2.2-1 summarizes these parameter values for the conditions in the core and reflector. The core design is discussed in Chapter 5; this section deals with the side reflector design.

For the best choice of parameters in the reflector the following conflicting interests have to be considered:

a) Heat Transfer - large η, low D

b) Fast Neutron Flux Barrier & k_{eff} - low porosity, that is, low η and D

c) Neutron Streaming - D must be low compared with the reflector thickness to prevent neutron streaming out.

d) Low Pressure Drop - large n and D, specially D (see Eq. 6.2.2-5)

The reflector is composed of a temporary part (48 columns immediately surrounding the core) and a permanent part. The temporary part is replaced each refueling time, that is, at 6 year intervals. The permanent part stays for the whole life of the plant and provides the transition from the hexagonal prisms to the cylindrical form of the thermal shield, insulator and vessel walls.

Set n_2' be the no. of coolant holes per graphite element and α_2 be the void fraction or porosity in the reflector. Given the area of a graphite element as 173.99 in^2 and for D_2 in in. one must have:

TABLE 6.2.2-1

Parameter Values for Conditions in the Core and Reflector

Symbol	ρ	η	D	A	V	μ	Re	Δp	Pr	k
Name	density	----	diam.	area	He veloc.	Viscosity	Reynolds	Pres. Drop	Prandt	He core
Units	10^{-6} lb/in^3	----	in.	in^2	in/sec	10^{-6} lb/sec.in.	----	psi	----	10^{-6} BTU/in. sec ^{o}F
Core	52.546	13,395	.625	4109.5	1939.8	2.419	26,336	2.15	.650	4.621
Reflector	61.053	?	?	?	?	2.1505	?	?	.653	4.089

$$\alpha_2 = (n_2'\pi D_2/4)/173.99 \quad . \qquad (6.2.2\text{-}7)$$

The total side reflector area is 18,136.65 in.^{2} of which (48)(173.99 in.^{2}) = 8351.52 in.^{2} in the temporary part. Then η_2' and η_2 are related by

$$\eta_2 = [48 + (9785.13/173.99)]n_2' = 104.24n_2' \quad . \qquad (6.2.2\text{-}8)$$

Several values for n_2', D_2 and α_2 were tried. The fast flux on the vessel wall was determined for $\alpha = 0.2$ and $\alpha = 0.4$ with the help of the transport code ANISN. The calculational method is described in section 2.2 and an input example for the use of ANISN is given in Appendix B. The results of these trials are summarized in Table 6.2.2-2 together with the estimated effect of α on k_{eff} obtained in CITATION runs.

Since the max. nvt was below 1 x 10^{19} neutrons/cm^2 in all trials and the values of h are not important in the reflector the optimum is economical. Values of D_2 above 2 in. were excluded to avoid neutron streaming.

The pumping power required for a certain friction pressure drop in the reflector is given by

$$W_{p2} = \Delta p_2 \dot{m}/\rho_2$$

$$= \Delta p_2[418.89 \text{ lb/sec}/61.053 \times 10^{-6} \text{lb/in}^3](1.13\times10^{-7} \text{MW/lb}_f \text{ in.})$$

$$= (0.775 \text{ MW/psi})\ \Delta p_2. \qquad (6.2.2\text{-}9)$$

TABLE 6.2.2-2

Side Reflector Design Possibilities

Symbol	α_2	η_2'	D_2	Δp_2	v	Re	Nu	h	nvt (30yr)
Name	Porosity		Diam.	Pres. Drop	He Veloc.	Reynolds	Nusselt	Heat Tr. Coeff.	Fast Fluence
Units	--	--	in.	psi	in./sec.	--	--	10^{-4} BTU/sec.in.^{2o}R	10^{-19} neutrons/cm^2
1	0.05	11	1	15.79	7,566	214,800	357.5	14.6	--
2	0.20	11	2	0.57	1.892	107,400	205.4	4.20	0.088
3	0.20	108	0.64	2.19	1.892	34,368	82.5	5.27	0.088
4	0.40	22	2	0.16	0.946	54,073	118.6	2.42	0.440

A 20% decrease in the reflector C no. density (20% increase in α) caused a 0.3% decrease in k_{eff}.

Taking trial 2 as reference in Table 6.2.2-2 a comparison with trials 3 and 4 can be made in terms of MW requirements in the following way:

Trial 3: requires [(2.19 - 0.57)(0.775)]=1.26 MWe more than 2.

Trial 4: requires [(0.57 - 0.16)(0.775)]=0.32 MWe less than 2 for pumping and [(0.3%)(300 MWth]=0.9 MWth more to account for the increased leakage.

Based in these results trial 2 was chosen as reflector best design. It also has an extra advantage over trial 4 which is its larger safety margin in the max. allowable fast fluence in the vessel.

6.2.3 Control Rod Drive Specification

In the case of a rupture in one of the two inlet reactor tubes the He flow out of the reactor would be chocked with a critical max. mass flow rate given by (Ref. 55):

$$\dot{m}_{max.} = \frac{A_R p_o}{RT_o} \sqrt{2 g_c J c_p T_o \left[(r_p)^{2/\gamma} - (r_p)^{\frac{\gamma+1}{\gamma}} \right]}, \qquad (6.2.3\text{-}1)$$

where:

γ = $c_p/c_v = 1.66$;

J = 778.16 ft-lb_f/BTU ;

g_c = 32.17 lb_m ft/lb_f sec^2 ;

c_p = 1.24 BTU/lb_m ^oR ;

T_o = 1413^oR (see discussion below). He temperature inside the vessel;

p_o = 400 lb_f/in^2 ;

R = 1545.08 (ft. lb_f/lb mole ^oR)(1 lb mole/4 lb_m) ;

r_p = $[2/(\gamma+1)]^{\gamma/(\gamma-1)}$ = 0.49 = critical pressure ratio ;

A_R = rupture area .

Substitution of the numerical values into Eq. (6.2.3-1) yields:

$$\dot{m}_{max} = (2.214\ lb_m/sec\ in^2)A_R \ . \qquad (6.2.3\text{-}2)$$

The conservative use of T_o = 1413^oR requires some explanation. The HTGR/GT is designed with concentric inlet and outlet tubes as in Fig. 6.2-1. If the internal tube breaks there is no blowdown; if the internal and external tubes break together the flow in the core and side reflector will be in the down direction; if first the external tube bringing He at 1413^oR to the reactor breaks, then there is a flow reversal in the core and possibility of CR ejection or damage. In this last case the mass flow rate in the core would become equal to the blowdown mass flow rate given by Eq. (6.2.3-2) and using Eq. 6.2.2-5 the core pressure drop would be

$$\Delta p_1 = 1.714 \times 10^{-4}\ A_R^{1.8} \ . \qquad (6.2.3\text{-}3)$$

To prevent CR ejection one must have

$$\Delta p_1 < \rho_{CR}\ L_{CR} \ , \qquad (6.2.3\text{-}4)$$

where :

ρ_{CR} = 156 lb_m/ft^3 = 0.0903 lb_m/in^3 CR set density estimate from data in Ref. 32;

L_{CR} = 124.8 in. in the core + 24.2 in. of shock absorber = 149 in. (length of CR).

The max. rupture area to prevent CR ejection can be found by substitution of Eq. 6.2.3-4 into Eq. 6.2.3-3:

$$(A_R)_{max} \cong 524 \text{ in.}^2 \quad . \tag{6.2.3-5}$$

As mentioned in section 6.1 the max. rupture area in a PCRV is about 100 in^2 (refueling port hole failure) and so there is no possibility of CR ejection in a blowdown. In the steel vessel case the max. rupture area is that of inlet tube which must have a much larger area than 529 in^2 to cut down pumping expenses. Suppose for instance that the primary circulation loop is 80 ft. long; the friction Δp in one primary loop is then given by

$$\Delta p_L = 4.27 \times 10^6 / A_R^{2.4} \quad , \tag{6.2.3-6}$$

and the pumping power is given by

$$w = \Delta p_e \frac{\dot{m}}{2}/\rho = 1.7 \times 10^{13}/A_R^{2.4} \text{ lb}_f \text{ in/sec}$$

$$= 1.921 \times 10^6 \text{ MW}/A_R^{2.4} \quad , \tag{6.2.3-7}$$

for A_R in in.^{2}. If A_R = 524 in.^{2}, w = 0.57 MW/loop; it was then decided to use A_R = 2638 in.^{2} (w = 0.012MW/loop), as in Fig. 6.2-1, and not advise the use of flexible steel cable drives. Some other possibilities are the hydraulic drive as in Peach Bottom or the magnetic one as used in PWR's.

6.2.4 Core Orificing

Stengle (Ref. 87) has shown that a simple orifice arrangement, achieved by varying the diameter of the coolant channels in the upper 2/3 of the top reflector blocks, can maintain the coolant outlet temperatures to within $\pm$ 60°F of the mixed mean coolant outlet temperature of 1,500°F throughout the core life. This compares with a $\pm$ 250°F range in the unorificed core. Additionally, the max. T_{C_L} is reduced to 1,900°F, a decrease of 200°F from the value in the unorificed core.

These benefits of orificing are accomplished at the cost of a 38% increase in the core-related pumping power requirement.

This section comments the work of Stengle in the lights of the final design requirements.

The total coolant flow in the core is 1.508 x 10^6 lb_m/hr. In the unorificed core the pressure drop is the same in each of the 19 regions (see Fig. 1.2.1-1) and the mass flow rate is approximately the same in each region. The pressure drop in the core and end reflectors was found to be 2.51 psi.

The side reflector pressure drop calculated by Stengle is for the 40% porosity reflector design that was later abandoned. The correct pressure drop in the reflector is 0.57 psi as in Table 6.2.2-2 (only friction, because the acceleration pressure drop is negligible in the reflector). The total pressure drop in the unorificed core is then 2.51 + 0.57 = 3.08 psi.

The core was divided into 3 orifice zones:

a) Inner Zone - consists only of the central region (region 1).

b) Middle Zone - consists of the 6 regions surrounding the central region (regions 2 to 7).

c) Outer Zone - consists of the 12 peripheral regions (regions 8 to 19).

Based on the radial PD distribution showed in Fig. 6.2.4-1, the unorificed flow distribution presented in Table 6.2.4-1 was obtained. Note that the acceleration pressure drop in the inner channels is larger than in the peripheral ones due to the different exit temperature produced by unequal radial heat generation rates. Since the pressure drop in all coolant channels through the active core and top and bottom reflectors must be equal (the small difference in Table 6.2.4-1 is due to approximation in iterative calculation of the mass flow rates per channel), the friction pressure drops are lower in the interior channels.

The radial PD distribution obtained with the more detailed FRD (Final Reference Design) runs is slightly different from that

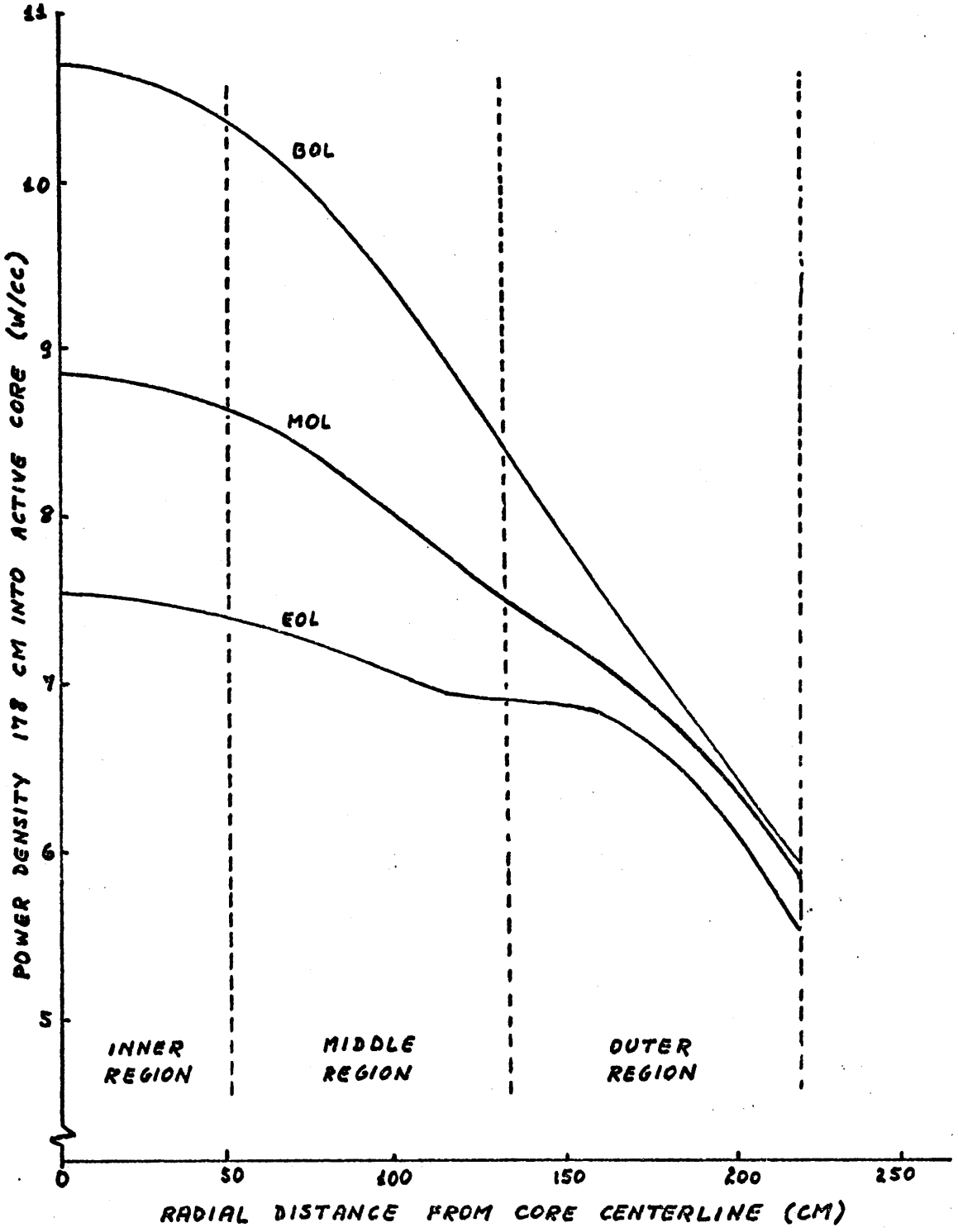

FIG. 6.2.4-1 HTGR/GT RADIAL POWER PROFILES AS USED IN REF. 87

TABLE 6.2.4-1

Flow Distribution for the Unorificed Core

Region	Total Heat Generation Rate Per Region (BTU/hr)	Flow Rate Per Region (lbm/hr)	Pressure Drop Friction (psi)	Pressure Drop Acceleration (psi)	Total (psi)
Beginning-of-Life					
nner (section 1)	7.167×10^7	7.380×10^4	2.300	0.210	2.510
iddle (sections 2-7)	6.431×10^7	7.625×10^4	2.311	0.194	2.505
uter (sections 9-19)	4.767×10^7	8.139×10^4	2.367	0.155	2.522
End-of-Life					
nner	6.143×10^7	7.700×10^4	2.322	0.188	2.510
iddle	5.761×10^7	7.850×10^4	2.342	0.179	2.521
uter	5.166×10^7	7.994×10^4	2.341	0.164	2.505

of Fig. 6.2.4-1 (employed by Stengle in his calculations) and is shown in Fig. 6.2.4-2. For the purpose of mass flow rate per zone calculations, Fig. 6.2.4-1 suffice.

The orifice arrangement was designed by Stengle to give an outlet temperature of 1,500°F from each core region for the average lifetime condition. From Fig. 6.2.4-1 and Eq. 6.2.2-1 the required mass flow rates per region were determined:

a) Inner Region - 9.719×10^4 lb_m/hr.

b) Middle Region - 8.976×10^4 lb_m/hr.

c) Outer Region - 7.269×10^4 lb_m/hr.

Total mass flow rate $\dot{m} = [9.719 + (8.976)(6) + (7.269)(12)] \times 10^4$ lb_m/hr

$= 1.508 \times 10^6$ lb_m/hr.

The total pressure drops in the active core and bottom reflector are 2.973 psi, 2.574 psi and 1.754 psi for the inner, middle and outer zone respectively. The total plenum-to-plenum pressure drop, Δp_t, must be the same for all channels, so additional pressure drops for the middle and outer region channels are required to bring their totals up to the total for the inner region. The use of orifices is the standard approach for achieving this result. It is recommended that the core be orificed by selectively reducing the coolant channel diameter in the upper 2/3 of the top reflector (the top reflector consists of one and a half graphite elements; the upper first element is going to be orificed). The inner region coolant hole diameter is maintained equal to 0.625 in. which would

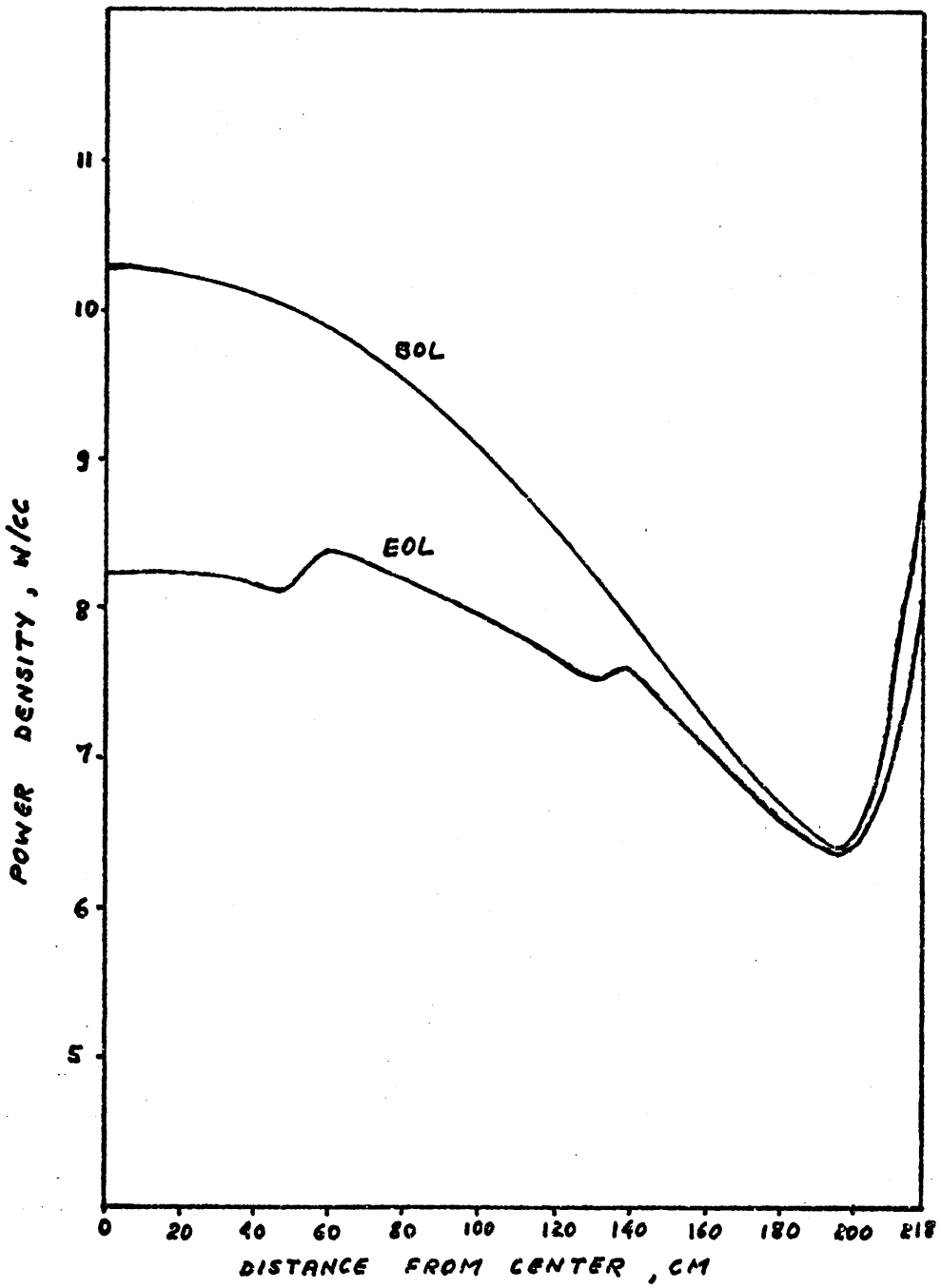

FIG. 6.2.4-2 FRD8 RADIAL POWER PROFILE AT THE HOTTEST RON

yield a 0.563 psi pressure drop in the top reflector and thus $\Delta p_t = 0.563 + 2.973 = 3.54$ psi. The total pressure drop in the orificed core design is then 3.54 + 0.57 = 4.11 psi which is 33% higher than that of the unorificed core. The new diameter to use in the upper 2/3 of the top reflector so that $\Delta p_t = 3.54$ psi in all channels is 0.52 in. in the middle zone and 0.412 in. in the outer zone.

Having the mass flow rate and the axial power density distribution per region Stengle determined the max. T_{C_L} with the help of the code HEATING II. The value found was 200°F less than the equivalent value for an unorificed core. The PD distribution used in his runs was that from Table 5.3.1.2-4 which is not accurate nor the final one. Nevertheless the 200°F difference can be taken as representative of the difference between orificing or not the core.

The core pumping power requirements can be calculated from

$$w_{core} = \sum_{j=1}^{4} \Delta p_j \dot{m}_j/\rho_j \quad , \qquad (6.2.4\text{-}1)$$

where the index j is for the inner zone, middle zone, outer zone and side reflector. For the unorificed core $w_{core} = 2.47$ MWe and for the orificed core it is equal to 3.42 MWe, a 38% increase. This increase of 0.95 MWe pumping power requirement would cost ~21.1 thousand dollars per year at a 0.8 load factor and 19 mills/kw hr cost of electric energy.

The employment of the top reflector orificing described in this section is strongly advised here for the first batch of this first of a kind reactor. The installation cost is essentially equal to unorificed top reflector blocks and the increase in pumping power costs is perfectly justified by the higher safety margin. Depending on the results of the first batch the use of core orificing may be judged unnecessary in which case the second batch would use ordinary top reflector blocks and preserve all the other features described in this report.

CHAPTER 7

SUMMARY, CONCLUSIONS AND RECOMMENDATIONS

7.1 Summary and Conclusions

Since June of 1974, M.I.T. has been engaged in a sponsored research to develop a conceptual design of a small (300 MWth) High Temperature Gas-cooled Reactor (HTGR) total energy system for the U.S. Army. The ground rules of the conceptual design state that the system is to start supplying both heat and electricity for large Army bases by 1985. This thesis project constitutes the separate part of the design research dealing with the reactor and with emphasis on the nuclear design. The part of the research dealing with the secondary loop has progressed to the recommendation of the use of an intermediary helium loop and to a gas turbine, GT, operating in a Brayton cycle (Ref. 82) and for that reason the whole project is referred to as HTGR/GT.

The High Enrichment (HE) and Low Enrichment (LE) fuels were selected, among several other possible options, for a more detailed investigation based on the fact that they are the only ones with sufficient commercial experience and industrial base for use in a plant design to start in 1985.

An essential feature of the HTGR/GT nuclear design is the peculiar way in which its fuel cycle cost is calculated. Under Government ownership the basic fuel cycle cost parameters consist of burnup charges for the U^{235} consumed (enriched uranium is obtained from the Government, and payment for fuel is made following irradiation upon return of the fuel to the government suppliers), fabrication charges,

reprocessing and reconversion changes (including spent fuel shipping), and carrying changes (on cash expenditures but not on the fuel). Also, in direct contrast to the usual commercial practice, no credit is taken for bred fissile material and no carrying charges are assessed on the fuel while it is in user custody. In the absence of fuel carrying charges the high inventory cost of a batch core does not increase the fuel cycle cost and the longest possible batch, satisfying safety requirements, becomes the most economical by minimizing shut down periods.

The core arrangement and operating conditions had to be decided in a very early stage of the project:

A) The average power density (PD) is used to determine the size of the reactor and the average fuel centerline temperature; for a given composition it will also determine the average burnup and nvt in the core and it is then very much related with the maximum residence time of the coated fuel particles in the reactor. Capital cost considerations point towards the use of higher PD's (smaller vessel) and fuel cycle considerations towards lower PD's (longer batches). The sensitivity of the capital costs to the size of the core is lower than the sensitivity of the fuel cycle cost to the refueling intervals and the PD should be as low as practical. The maximum diameter of shop fabricated steel vessels is about 21 ft. (the HTGR/GT includes the use of a steel vessel instead of a PCRV) which limits the PD to a minimum of about the level of the PD in FSV if the optimum height to diameter ratio of about 0.9 is assumed in the core. The same fuel element design of FSV (see Figure 1.2.1-2) was maintained in the HTGR/GT and to have a near optimum height to diameter ratio in the core, two options were possible

for the core arrangement: a) columns of 4 graphite elements; b) columns of 5 graphite elements. The 4 element-column is more adequate having a larger core diameter and permitting a greater number of control rods (reactivity control was expected to be a problem) and a smaller pressure drop. The HTGR/GT core will consist of 133 fuel columns; each column composed of 4 fuel elements together with top and bottom reflector elements, 1.5 elements in each reflector (see Fig. 1.2.2-1). Surrounding the active core there are 48 columns of replaceable reflector elements and then the permanent reflector having the external side with a circular form concentric with the vessel (see Fig. 1.2.1-1).

B) The coolant pressure and temperature condition were determined after power cycle optimization (Ref. 82). The important design and performance parameters for the HTGR/GT are compared to those of FSV in Table 1.2-1.

A simplified calculational model was developed with the objective of getting a meaningful comparison between the HE and LE fuel as well as preliminary information for a refined design, based on the winning fuel, at a low computational cost. This model included the use of a single depletion zone unrodded core and the same constraints were imposed for the HE and LE depletion runs, namely: a) use of the same depletion code: CITATION (Ref. 10); b) same depletion intervals; c) the maximum hot excess of reactivity to be controlled by control rods (CR) would be 0.11 Δk; d) same burnable poison: natural boron; e) the maximum homogenized heavy metal (HM) concentration in the core is 39.2×10^{-5} HM atoms/ barn cm.

Before starting the more expensive CITATION depletion runs, the adequate range of concentrations for $k_{eff} = 1.11$ was determined by trial and error with very inexpensive static runs using 2DB (Ref. 22). The results obtained with the simplified model (Table 3.2-1) show that HE has two basic advantages for the HTGR/GT type of economy: a) a 48.4% longer batch for the same maximum excess of reactivity constraint; b) a 12.8% lower U^{235} average consumption per day (comparison between runs 2 and 6 of Table 3.2-1).

An analysis of the possible consequences of lack of equivalence between the HE and LE cross section (CS) sets or possible errors introduced by the model on the reactivity lifetime calculations was made. It was concluded that the uncertainties in the calculations are smaller than the difference in reactivity lifetime favoring HE, however if the uncertainties are compounded in favor of the LE, the difference

between the two fuels becomes small.

An economical evaluation of the two fuel cycles was made by Metcalfe (Ref. 86) with the data from Table 3.2-1. The annual fuel cycle cost of the HE fuel was found to be about 40% cheaper than that of the LE (see Table 3.4-6).

The HE fuel was then optimized to batches of 4.8 full power years (see the full cycle parameters for 6 calendar year batch in Table 3.4-6) by using lumped burnable poison (LBP) rods of the same diameter as those of Fort Saint Vrain (FSV) but having 2.3 times more B^{10} and by loading 6 rods of LBP per graphite element instead of 2. For this optimized design Metcalfe calculated the fuel cycle cost to be 2.12 mills/kwhr.

The calculational methods were established, involving the use of the computer code CITATION (Ref. 10) to give a diffusion theory solution with a four group cs set representation. The calculational methods were tested by comparison to GA results on the FSV design. The differences between results were on the order of uncertainties in the measured values; less than 1% in the k_{eff} vs. time curves and less than 10% in XY power density (PD) distribution for the internal regions.

The fuel particle system was also investigated; the possibility of using either a homogeneous or a heterogeneous (fissile and fertile particles separated) was compared; the composition of the kernel (carbides or oxides); size of particles; thickness of the coatings. A homogeneous system composed of 806μ kernel diameter TRISO coated particles with mixed oxide kernels was considered the best choice (see Table 4.3.4-2). This system would not be burnup limited and the present

design would withstand temperatures up to 2100°F without danger of [illegible] effect and fast neutron fluences of up to 8×10^{21} n/cm^2.

The small HTGR/CT core has an inherently low radial power peaking factor allowing the use of a single enrichment zone. The presence of control rods (CR) in the top reflector tends to tilt the axial power shape towards the bottom and in a single zone core and pure graphite bottom reflector there is a large power peak at the core-bottom reflector interface that would elevate the T_{ℓ} above 2100°F and the maximum nvt above 8×10^{21} n/cm^2 in this core-bottom reflector interface region. Several designs having B^{10} or Th^{232} in the bottom reflector were tried to suppress that peak (see Fig. 5.2.2-1 and Table 5.3.2-2). There is just a narrow range of concentrations that can be used. Above that range the fast nvt in the center of the core gets above 8×10^{21} n/cm^2; below the range the Th^{232} or B^{10} content is not enough to prevent the power peaking at the interface. Three different designs were shown to be feasible:

FRD6 = A heavily loaded bottom reflector with LBP but having a fertile region near the center (Parfait configuration) to prevent the center nvt to get above 8×10^{21} n/cm^2;

FRD7 = Single zone core with Th^{232} in the bottom reflector;

FRD8 = Single zone core with LBP in the bottom reflector.

These three designs had acceptable CR requirements (see Fig. 5.3.2.1-1), maximum fast nvt below the 8×10^{21} n/cm^2 limit (see Table 5.3.2.2-1), maximum T_{ℓ} below 2100°F (see Fig. 5.3.2.4-1) and comparable maximum BU in the range of 104 to 110 GWD/T. Considerations of cost and

simplicity were then taken into account. Taking FRD8, the simplest, as a standard, FRD6 would require approximately 8% more fissile material and two different orders for fuel; FRD7 would also require two orders for fuel and even though the fissile content is the same, about 5% more Th is necessary in FRD7 for the bottom reflector (see Table 5.3.2-2).

For a 4.8 full power years batch the simplest and most economical design is FRD8, chosen as the Final Reference Design (FRD) for the HTGR/GT. However a Parfait design, like FRD6, has strong possibilities for a still longer batch. That comes from the fact that in FRD6, the two most important limitting factors, the maximum nvt and T_ϵ were well below the maximum permissible values. Another possible variation of FRD6, not studied in this report, would have been to substitute the LBP in the bottom reflector by Th^{232}.

Early in the project a comparison was made between PCRV's and steel vessels. The steel vessel was chosen for this small reactor application because of its greater flexibility and maintainability. The economy initially slightly favoring the PCRV suffered a switch over when design progressed towards the employment of an indirect Brayton cycle in which case the PCRV would have to be very big to house the very large intermediate gas-to-gas heat exchangers.

The use of a steel vessel instead of a PCRV and of a single zone batch core of long reactivity lifetime made it necessary to design a few modifications on the FSV basic internals design:

a) Vessel wall cooling system. In the PCRV case the concrete has to be maintained at a temperature below 212°F in order not to loose water;

there is an insulation between the reflector and the steel liner and an extra water cooling system for the steel liner and adjacent concrete. In the steel vessel case it is enough to maintain the vessel wall temperature below 700°F. This can be done by using insulation between the reflector and vessel walls (see Fig. 6.2.1-1) and by cooling the external vessel wall with forced convection air.

b) Reflector design. To be able to maintain a lower temperature in the vessel walls the coolant flow passes first in the reflector (up flow) and then in the core (down flow) instead of in parallel as in the FSV design; the coolant flow in the HTGR/GT side reflector is then equal to the flow in the core (see Fig. 6.2-1). The helium properties for the reflector design calculations were obtained with the computer code HELIUM (Ref. 77).

The thickness of the HTGR/GT side reflector was limited to 2.4 feet by the maximum practical steel vessel diameter of approximately 21 feet. The maximum permissible fast fluence in the vessel walls is 10^{19} n/cm^2 in 40 years, and it was calculated, with the help of the transport code ANISN (Ref. 79), that a 2.4 foot-thick graphite reflector with less than 40% porosity would be enough. The higher the porosity, the lower the pressure drop across the reflector and the higher the neutron leakage. An optimum 20% porosity was determined by requiring that the coolant hole diameter should not exceed 2 in. (a limit based on anisotropy and neutron streaming problems).

c) CR drive. In a steel vessel, blowdown due to accidental coolant pipe rupture may lead to mass flow rates which are much faster than those predicted for a PCRV blowdown. It was shown in section 6.2.3 that the use of flexible cables, as used in FSV, is not adequate in a steel vessel design. A good alternative seems to be the hydraulic CR drive, as used in Peach Bottom.

d) Inlet and outlet ducts. The inlet and outlet ducts are concentric in the HTCR/GT design (see Fig. 6.2-1), a common practice in HTGR steel vessel designs. The objective is to decrease the possibility and the consequences of a blowdown.

e) CR in the side reflector. The maximum excess of reactivity to control in the HTGR/GT is about 0.15 Δk higher than in FSV and the number of CR pairs in the active core is 19 as compared to 37 in FSV. As a result it was decided to add 12 extra pairs to the temporary reflector to reduce the necessary worth per CR pair (see Fig. 1.2.1-2).

Some CR configuration studies were made with CR pairs of the type used in the FSV periphery regions (two CR designs are employed in FSV: a) CR containing 38% of natural boron in the 19 interior regions; b) CR containing 48% of natural boron in the 18 periphery regions). The objective was to determine the maximum hot excess of reactivity controllable by this CR pair design. For the range of fissile concentrations treated in this report the maximum varies from 0.1166 to 0.1576 Δk, with due allowance for temperature effect and stuck rod criteria, as the U^{235} atom density goes from (2.92 to 4.548) x 10^{-5} atoms/barn cm. From Fig. 5.3.2.1-1 (add approximately 0.025 Δk to account for Xe

decay in a shut down event at any time) it can be seen that with this CR design the safety margin will be at least 0.038 Δk. In these CR configuration studies it was also seen that the worth of a CR pair in the core is about 10% higher than those in the reflector and it is about 0.008 Δk.

f) Core orificing. The coolant mass flow rate for each zone of the core is adjusted by selective reduction of the coolant channel diameter of the upper 2/3 of the top reflector graphite blocks. The use of the more expensive variable orificing employed in FSV was not deemed necessary for the HTGR/GT because its change in radial power shape with time is relatively small (see Fig.6.2.4-2).

7.2 Recommendations

It was seen that the Parfait core FRD6, or a possible variation of it obtained by substitution of its bottom reflector LBP by Th^{232}, have good possibilities for longer batches. A study of these two types of Parfait for longer batches is recommended. In the investigations performed for this report, no especial cs were used to represent Th^{232} in the central fertile region or bottom reflector, that is, the same $\overset{c}{cs}$ set used for the core was used although the neutron spectrum in the fertile only regions is completely different from that of the core. If the Parfait configurations are going to be further analysed in the future, attention to this point is also recommended.

Another point requiring attention is the possibility of cross flow from the reflector to the core due to the coolant pressure differential between the side reflector and the core. Two possible ways of avoiding this problem are the use of metal coolant tube, in the reflector, or the design of partial core barrels separating the core from the side reflector between the graphite blocks.

Appendix A

Calculations necessary for the preparation of some important computer inputs

A.1. Calculations for the preparation of the CITATION input to obtain the FSV relative power density distribution per region.

The relative power density distribution as obtained by GA is shown in Fig. 2.1.3.1-1. The HM loading per region for this figure is summarized in Table A.1-1 (from Table 2.3 of Ref. 68); the detail for composition 13 is shown in Fig. A.1-1 and the BOL CR configuration is given in Table A.1-2 (from Table 2.5 of Ref. 68); the necessary burnable poison specifications and locations came separately by request in a letter from Dr. Marshall (consultor for the HTGR/GT at GA) and are summarized in Table A.1-3; the 4 group homogenized CR CS set, also sent by Dr. Marshall, are reproduced in Table A.1-4.

To prepare a CITATION input to reproduce the results of Fig. 2.1.3.1-1 it is first necessary to determine the nuclide densities per region; for the 19 interior regions this is a straightforward problem with results almost independent of the calculational model, but the treatment of the periphery region and buffer zone (composition 13) requires careful analysis. There are several different ways by which the periphery region can be represented:

(1) By brute force: each periphery region would be decoupled in two regions, one with its composition from 1 to 12 and the other with composition 13; 55 regions would have been necessary in this case.

(2) Elimination of the buffer region by obtaining a homogenized mixture of compositions (1 to 12 and 13) in each of the regions 20 to 37; 37 fuel regions would have been necessary in this case.

Table A.1-1 Adjusted Fuel Loading, Initial FSV Core (*)

Composition	Location(refueling region)	U(kg)	Th(kg)
1 (upper half)	(1,4,5,8,10,15,17,21,25, 28,32,35,36)	105.6	2,905
2 (lower half)		80.5	2,596
3 (upper half)	(2,6,7)	39.2	636
4 (lower half)		28.9	544
5 (upper half)	(9,11,12,14,16,19)	88.8	1,324
6 (lower half)		65.9	1,158
7 (upper half)	(20,23,24,26,27,30,31, 34,37)	111.6	1,446
8 (lower half)		84.4	1,287
9 (upper half)	(3,13,18)	36.2	720
10 (lower half)		25.8	599
11 (upper half)	(22,29,33)	32.1	549
12 (lower half)		23.7	474
13	Outer ring of 5 rows of fuel holes and complete CR element at the core-reflector interface (see Fig. A.1-1)	50.5	1,733
		773.2	15,971

(*) From Table 2.3 of Ref. 68.

FIG. A.1-1 COMPOSITION 13 LOCATION ON THE FSV CORE

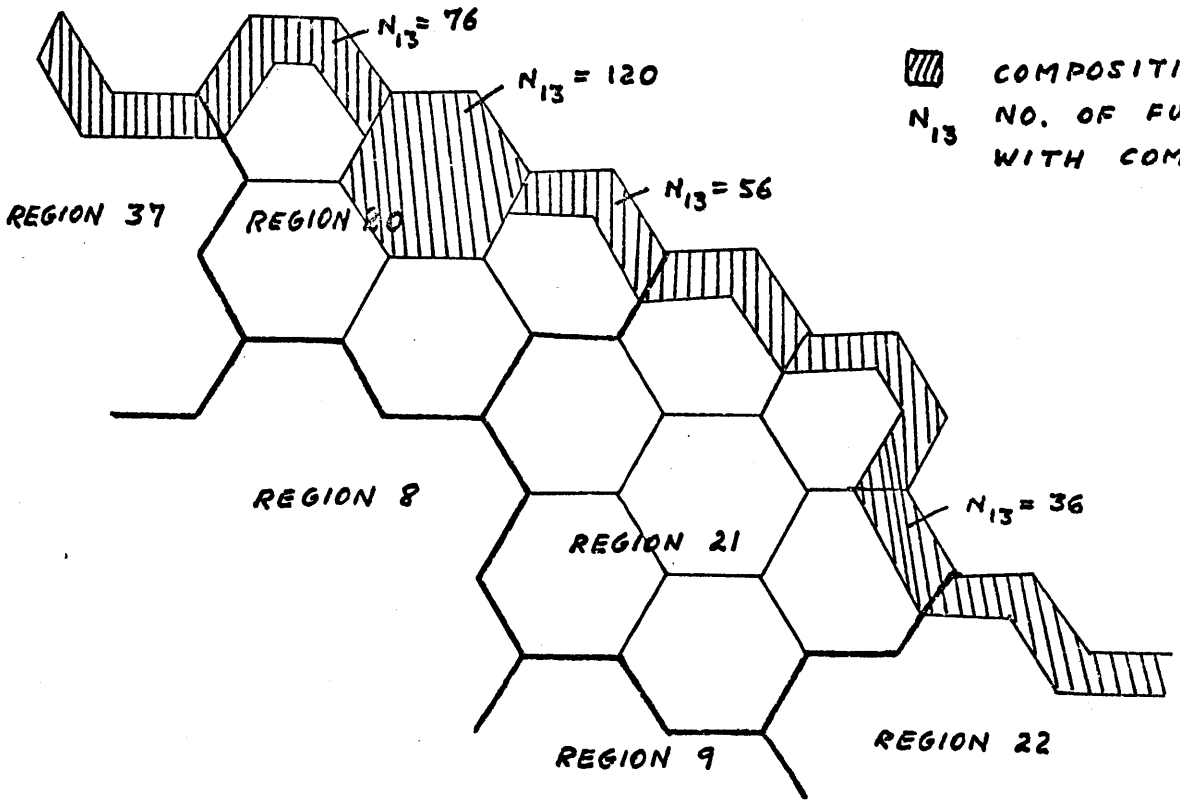

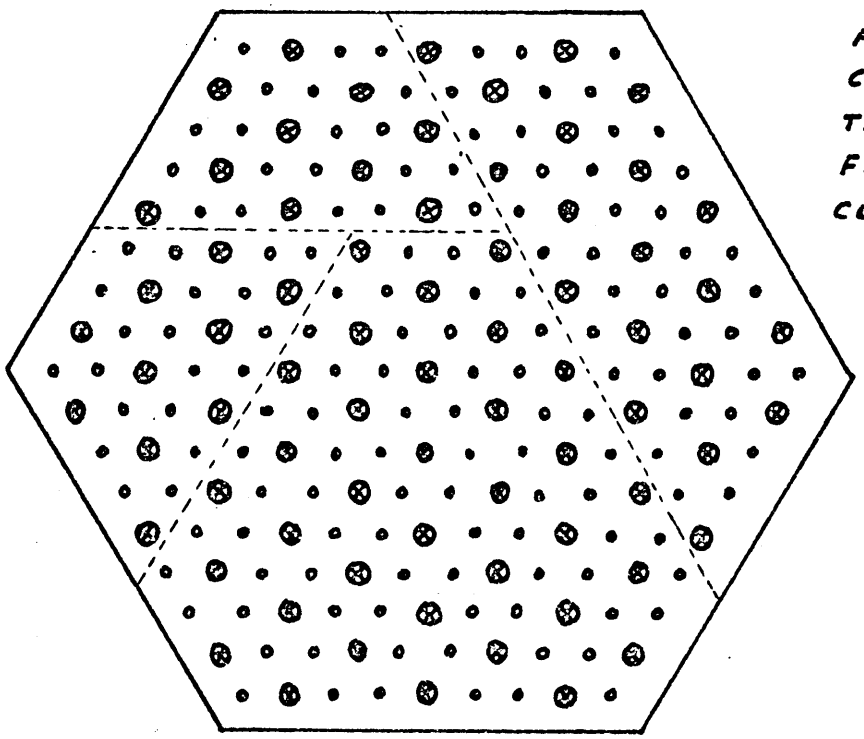

FUEL ELEMENT AT THE CORE REFLECTOR INTERFACE: THE FIRST 5 FUEL ROWS FROM THE INTERFACE HAVE COMPOSITION 13

- FUEL STICK
- COOLANT HOLE

TABLE A.1-2 DEPLETION INPUT AND RESULTS OBTAINED WITH SCANAL (*)

	Core Half	0 EFPD	2 EFPD	2 EFPD[a]	5 EFPD	10 EFPD	10 EFPD[a]	50 EFPD
Input:								
Rods inserted	Top	13	13	7	7	7	4	4
	Bottom	13	13	7	7	7	1	1
Power Function	Top	.6726						
	Bottom	.3274						
Power, MW	Top	566.3		551.2	540.0		536.9	489.4
	Bottom	275.7		290.8	302.0		305.1	383.6
Output:								
k_{eff}	Top	1.0039	1.0039	1.0070	1.0224	1.0179	1.0307	1.0179
	Bottom	0.9918	0.9649	0.9904	0.9865	0.9832	1.0191	1.0105
	Fever	1.0039	0.9721	0.9953	0.9909	0.9869	1.0073	0.9964
Power Function	Top							
	Bottom							
Power, MW	Top	566.3	551.2	541.5	540.0	536.9	472.8	459.4
	Bottom	275.7	290.8	300.5	302.0	305.1	369.3	382.6
Control rods inserted (refueling region)	Top	1 11,15,19, 22,28,34, 20,26,32, 24,30,36	idem	1 11,15,19, 22,28,34	idem	idem	1 11,15,19	idem
	Bottom	1 11,15,19, 22,28,34, 20,26,32, 24,30,36	idem	1 11,15,19, 22,28,34	idem	idem	1	idem

TABLE A.1-2 (continued)

	Core half	103.5 EFPD	207 EFPD	310.5 EFPD
Input:				
Rods inserted	Top	4	4	4
	Bottom	1	1	1
Power function	Top			
	Bottom			
Power, MW	Top	459.4	466.7	463.5
	Bottom	382.6	375.1	373.5
Output:				
k_{eff}	Top	1.0189	1.0212	1.0124
	Bottom	1.0096	1.0133	1.0101
	Fever	0.9964	0.9989	0.9929
Power Function	Top			
	Bottom			
Power, MW	Top	466.9	463.5	446.9
	Bottom	375.1	378.5	395.1
Control rods inserted (refueling region)	Top	idem	idem	idem
	Bottom	idem	idem	idem

Table A.1-3 Lumped Burnable Poison (LBP) Specifications

for FSV Design that Produced Fig. 2.1.3.1-1

LBP pin radius	.515 cm
Volume fraction of one LBP rod/element	$.7365 \times 10^{-4}$
Initial B^{10} density in the LBP rod	.025g nat. B/cc = 1.3928×10^{-3} $\frac{\text{atoms nat B}}{\text{burn cm}} \rightarrow 2.755 \times 10^{-4} \frac{\text{ats B}}{\text{bcm}}$
Initial LBP self-shielding factor, g	g = .748 (**)

(*) This value, from Dr. Marshall's letter, is slightly different from the value obtained from the LBP rod dimensions provided in Table 2.8 of Ref. 4. There is LBP rods in the following regions: (a) Interior: 2, 3, 6, 7, 9, 11, 12, 13, 14, 16, 18 and 19 (with 12 LBP rods each disposed as in Fig. 2.1.3.1-2, b) Periphery: 20, 22, 23, 24, 26, 27, 29, 30, 31, 33, 34 and 37 (regions 20, 23, 26 and 29 have 8 LBP rods each and the rest have 12 each, but all requires special treatment because of the buffer layer of composition 13 shown in Fig. A.1-1).

(**) The factor g is given by

$$g = \frac{1}{1 + (1.514)(\Sigma_a r) + (.684)(\Sigma_a r)2} \quad \text{where } r = .515 \text{ cm}$$

Table A.1-4 Four Group CR Homogenized (in the region) Absorption CS

A. The 19 interior CR pairs with 38% nat B → 1.60×10^{-3} atoms B/bcm in the control element or $.229 \times 10^{-3}$ atoms B/bcm in a fuel region (1 control and 6 standard elements). This type is called CR1.

Group	1	2	3	4
Σ_a^{CR1}, in 10^{-4} cm^{-1}	.229	5.40	12.44	11.46
σ_a^{CR1}, in barns	.1	2.36	5.44	5.01

B. The 18 periphery CR pairs with 48% nat B (2.13×10^{-3} atoms/bcm in the control element or $.304 \times 10^{-3}$ atoms B/bcm/region) → CR2.

Group	1	2	3	4
Σ_a^{CR}, in 10^{-4} cm^{-1}	.30	6.14	12.51	11.55
σ_a^{CR}, in barns	.1	2.02	4.11	3.79

(3) The following intermediate approach was used: consider the 37 regions with compositions 1 to 12; consider a region 38 with composition 13 in standard elements; consider regions 39, 40, 41, 42, 43 and 44 with composition 13 in control elements. The XY representation of this model for CITATION input is shown in Fig. A.1.-2 . In Fig. A.1-3 the dimensions of those interface regions are calculated and the necessary approximations for the preparation of Fig. A.1-2 are pointed out.

Heavy metal (HM) nuclide density calculations

Regions 1 to 19 have each 210 x 6 + 120 = 1380 fuel pins (fp); regions 20, 23, 26, 29, 32 and 35 have each 210 x 2 + (210 - 56) + (210 - 76) = 708 fp without composition 13 (see Fig. A.1-1); regions 21, 22, 24, 25, 27, 28, 30, 31, 33, 34, 36 and 37 have each 210 x 3 + (210 - 36) + (210 -56) + (210 - 76) + 120 = 1212 fp without composition 13; regions 20 to 37 have [6(56 + 76 + 120) + 12 (36 + 56 + 76)] = 3528 fp with composition 13. With this information it is easy to determine the total number of half length fp for each composition.

Let n_i be the number of half length fp with a certain composition j in region i. The total number of half fp with composition j, T_j, is given by

$$T_j = \sum_i n_i \quad . \qquad \text{(A.1-1)}$$

The values of n_i and T_j are summarized in Table A.1-5.

For any region i (i = 1 to 44) where the composition is j, Th^{232} atomic density will be given by:

X DIRECTION : 1 REGION OF 135.9 CM WITH 3 MESH POINTS AT EACH SIDE OF THE 50 11.908 CM CENTRAL REGIONS (WITH ONE MESH POINT PER REGION)

Y DIRECTION : 1 REGION OF 135.9 CM WITH 3 MESH POINTS AT EACH SIDE OF THE 44 13.75 CM CENTRAL REGIONS (WITH ONE MESH POINT PER REGION)

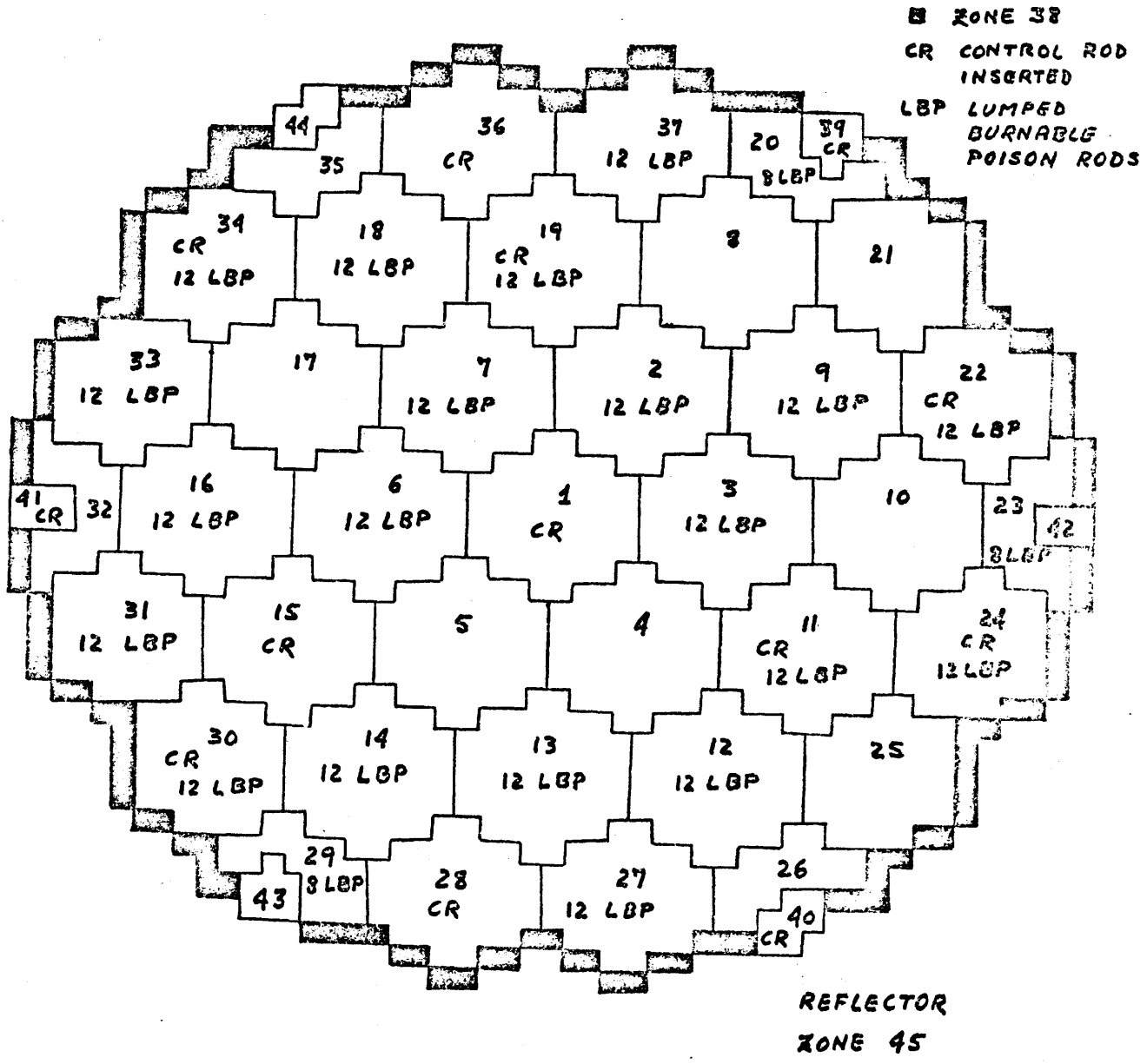

FIG. A.1-2 FSV CORE REPRESENTATION IN XY GEOMETRY FOR CITATION INPUT

FIG. A.1-3 DIMENSIONS OF REGIONS AT THE CORE REFLECTOR INTERFACE IN FSV XY CITATION REPRESENTATION

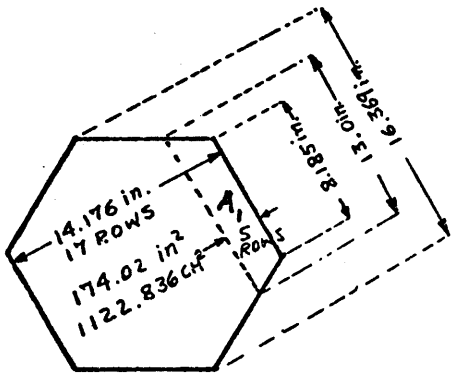

UNIT OF AREA IN FIG. A.1-2 : 11.908 CM × 13.75 CM = 163.735 CM^2 .

A_1 = 284.91 CM^2 ∴ 1.74 UNITS

A_2 = (5/17)(14.176)(8.185)(2) = 68.25 in^2 = 440.3 CM^2
∴ 2.69 UNITS

A_3 = 613.07 CM^2 ∴ 3.74 UNITS

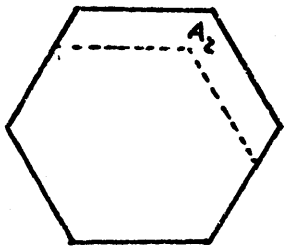

REGION 38 : 1) INTERFACE WITH REGIONS 21, 22, 24, 25, 27, 28, 30, 31, 33, 34, 36 AND 37 : $(A_1 + A_2 + A_3)$ / 163.735 CM^2 = 8.17 UNITS AT EACH INTERFACE ; 2) INTERFACE WITH REGIONS 20, 23, 26, 29, 32 AND 35 : $(A_2 + A_3)$ / 163.735 CM^2 = 6.43

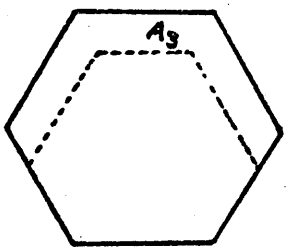

REGIONS 39 TO 44 : EACH REGION IS A COMPLETE CR ELEMENT WHOSE AREA IS 1/7 OF A STANDARD INTERNAL FUEL REGION (1 TO 19). SINCE EACH STANDARD REGION HAS 48 UNITS, ANY REGION FROM 39 TO 44 HAS 48/7 ≅ 7 UNITS OF AREA .

REGIONS 21, 22, 24, 25, 27, 28, 30, 31, 33, 34, 36 AND 37 : $[(1122.836\ CM^2)(7) - (A_1 + A_2 + A_3)]$ / 163.735 CM^2 = 39.8

REGIONS 20, 23, 26, 29, 32 AND 35 : $[(1122.836\ CM^2)(4) - (A_2 + A_3)]$ / 163.735 CM^2 = 21

Table A.1-5 Values of n_i and T_j

A. Values of n_i

n_i = 1380 for i = 1 to 19

n_i = 708 for i = 20,23,26,29,32 and 35

n_i = 1212 for i = 21,22,24,25,27,28,30,31,33,34,36 and 37

n_i = 2808 for i = 38

n_i = 120 for i = 39,40,41,42,43 and 44

B. Values of T_j, $[U(kg)]_j$ and $[Th(kg)]_j$ and associated i

j	i	$[U(kg)]_j$	$[Th(kg)]_j$	T_j
1	1,4,5,8,10,15,17 21,25,28,32,35,36	105.6	2905	15,924
2	1,4,5,8,10,15,17 21,25,28,32,35,36	80.5	2596	15,924
3	2,6,7	39.2	636	4,140
4	2,6,7	28.9	544	4,140
5	9,11,12,14,16,19	88.8	1324	8,280
6	9,11,12,14,16,19	65.9	1158	8,280
7	20,23,24,26,27,30, 31,34,37	111.6	1446	9,396
8	20,23,24,26,27,30, 31,34,37	84.4	1287	9,396
9	3,13,18	36.2	720	4,140
10	3,13,18	25.8	599	4,140
11	22,29,33	32.1	549	3,132
12	22,29,33	23.7	474	3,132
13	38,39,40,41,42,43,44 (upper half)	25.25	866.5	3,528
13	38,39,40,41,42,43,44 (lower half)	25.25	866.5	3,528

$$(N_{o2})_i = \{(Th(kg)]_j n_i/T_j\} \ (10^3 g/kg)(6.023x10^{23} at/atg)(1\ atg/232g)(10^{-24} cm^2/b) /V_i \quad , \qquad (A.1\text{-}2)$$

where V_i is the volume of half region i. For any interior region, $V_i = 1.8686 \times 10^6$ cm^3 (i = 1 to 19), and for the periphery region V_i = (1.8686×10^6)[area of region i/area of an interior region = $7.86 \times 10^3 cm^2$].

Interior regions (i = 1 to 19; $V_i = 1.8686 \times 10^6$ cm^3):

$$(N_{02})_i = \{(Th(kg)]_j/T_j\} x\ n_i \times 1.3893 \times 10^{-6} \quad . \qquad (A.1\text{-}3)$$

Analogously and remembering that 93% of U(kg) is U^{235} and 7% is U^{238}, it follows:

$$(N_{25})_i = \{[U(kg)]_j/T_j\} \times n_i \times 1.2754 \times 10^{-6} \quad , \qquad (A.1\text{-}4)$$

and

$$(N_{28})_i - \{[U(kg)]_j/T_j\} \times n_i \times 9.4783 \times 10^{-8} \quad . \qquad (A.1\text{-}5)$$

Regions 21, 22, 24, 25, 27, 28, 30, 31, 33, 34, 36 and 37:

$$V_i = (1.8686 \times 10^6 \text{ cm}^3)(\frac{6521.56}{7859.85}),$$

$$(N_{02})_i = \{[Th(kg)]_j/T_j\} n_i \times 1.6744 \times 10^{-6} \quad , \qquad (A.1\text{-}6)$$

$$(N_{25})_i = \{[U(kg)]_j/T_j\} n_i \times 1.5374 \times 10^{-6} \quad , \qquad (A.1\text{-}7)$$

and

$$(N_{28})_i = \{[U(kg)]_j/T_j\}\, n_i \times 1.1426 \times 10^{-7} \quad . \qquad \text{(A.1-8)}$$

Regions 20, 23, 26, 29, 32 and 35: $V_i = (1.8686 \times 10^6\ cm^3)(3437.96/7859.85)$,

$$(N_{02})_i = \{[Th(kg)]_j/T_j\} \times n_i \times 3.1762 \times 10^{-6} \quad , \qquad \text{(A.1-9)}$$

$$(N_{25})_i = \{[U(kg)]_j/T_j\} \times n_i \times 2.9162 \times 10^{-6} \quad , \qquad \text{(A.1-10)}$$

and

$$(N_{28})_i = \{[U(kg)]_j/T_j\} \times n_i \times 2.1674 \times 10^{-7} \quad . \qquad \text{(A.1-11)}$$

Region 38: $V_{38} = \{[12(A_1+A_2+A_3) + 6(A_2+A_3)]/7.86 \times 10^3\}(1.8686 \times 10^6 cm^3)$

$= 5.32 \times 10^6 cm^3$,

$$(N_{02})_{38} = \{[Th(kg)]_{13}/T_{13}\}\, n_i \times 4.8789 \times 10^{-7} = 33.65 \times 10^{-5} \text{ atoms/bcm}, \qquad \text{(A.1-12)}$$

$$(N_{25})_{38} = \{[U(kg)]_{13}/T_{13}\}\, n_{38} \times 4.4808 \times 10^{-7} = .9004 \times 10^{-5} \text{ atoms/bcm}, \qquad \text{(A.1-13)}$$

and

$$(N_{28})_{38} = \{[U(kg)]_{13}/T_{13}\}\, n_{38} \times 3.3294 \times 10^{-8} = 6.691 \times 10^{-7} \text{ atoms/bcm}. \qquad \text{(A.1-14)}$$

Regions 39, 40, 41, 42, 43, 44: $V_i = 1.8686 \times 10^6 cm^3/7 = .2669 \times 10^6 cm^3$,

$$(N_{02})_i = \{[Th(kg)]_{13}/T_{13}\}\, n_i \times 9.7269 \times 10^{-6} = 28.66 \times 10^{-5} \text{ atoms/bcm}, \qquad \text{(A.1-15)}$$

$$(N_{25})_i = \{[U(kg)]_{13}/T_{13}\}\, n_i \times 8.9306 = .7672 \times 10^{-5} \text{ atoms/bcm}, \qquad \text{(A.1-16)}$$

and

$$(N_{28})_i = \{[U(kg)]_{13}/T_{13}\}\, n_i \times 6.6372 \times 10^{-7} = 5.701 \times 10^{-7} \text{ atoms/bcm}. \qquad \text{(A.1-17)}$$

With the values of $[U(kg)]_j$, $[Th(kg)]_j$, T_j and n_i from Table A.1-5, the HM nuclide atomic densities were calculated by the equation above and summarized in Table A.1-6.

Burnable poison density calculation

Three types of input burnable poison were prepared:

(1) Using the LBP rods dimensions specified in Table 2.8 of Ref. 69: .405 in. diameter, 26 in. of length for which case the volume fraction of a lump per graphite element is 6.168×10^{-4}. Wrong use of natural B atomic density and unself-shielded CS. Let this be called LBP1 for reference.

(2) Same as LBP1, but using B^{10} atomic density and shielded thermal CS. Let this be called LBP2.

(3) Use of B^{10} atomic density and shielded CS but the volume fraction as given by Dr. Marshall, called LBP3.

The calculation for LBP2 are exemplified below and the CITATION output results for LBP1, LBP2 and LBP3 are compared in Table A.1-7.

Regions 1, 4, 5, 8, 10, 15, 17, 21, 25, 28, 32, 35 and 36 have $N_{BIO} = 0$.

Regions 2, 3, 6, 7, 9, 11, 12, 13, 14, 16, 18 and 19 have 12 LBP rods each, so the B^{10} atom density in these regions is given by:

$$B_{BIO} = (2.755 \times 10^{-4} \text{ atoms } B^{10}/\text{bcm})(6.168 \times 10^{-4})(12/7) = 2.913 \times 10^{-7}.$$

Regions 22, 24, 27, 30, 31, 33, 34 and 37 have 12 LBP rods each but the region volume fraction should be multiplied by $\{(1122.836 \times 7)/[(1122.836 \times 7) - (A_1+A_2+A_3)]\} = 1.2052$ to compensate for the smaller volume of those

Table A.1-6 Atom Densities per Region in FSV (*)

Rod Comp.	Regions	N_{oz} Up	N_{oz} Bot.	N_{oz} Ave.	N_{25} Up	N_{25} bot.	N_{25} Ave.	N_{28} Up	N_{28} bot.	N_{28} Ave.	N_{B10} as LBP2	N_{B10}^{CR} up=bo
1-2	4,5,8,10,17	34.97	31.25	33.11	1.167	.8897	1.028	.0867	.0661	.0764	-----	-----
1-2	1,15	34.97	31.25	33.11	1.167	.8897	1.028	.0867	.0661	.0764	-----	22.9
1-2	21,25	37.02	33.08	35.05	1.236	.9419	1.089	.0918	.0700	.0809	-----	-----
1-2	28,36	37.02	33.08	35.05	1.236	.9419	1.089	.0918	.0700	.0809	-----	36.67
1-2	32-35	41.02	36.66	38.84	1.369	1.044	1.207	.1018	.0776	.0897	-----	-----
3-4	2,6,7	29.45	25.19	27.32	1.666	1.229	1.448	.1238	.1913	.1076	.02913	-----
5-6	9,12,14,16	30.65	26.81	28.73	1.888	1.401	1.645	.1403	.1041	.1222	.02913	-----
5-6	11,19	30.65	26.81	28.73	1.888	1.401	1.645	.1403	.1041	.1222	.02913	22.9
7-8	27,31,37	31.23	27.80	29.52	2.213	1.674	1.944	.1645	.1244	.1445	.035107	-----
7-8	24,30,34	31.23	27.80	29.52	2.213	1.674	1.944	.1645	.1244	.1445	.035107	36.67
7-8	20,23,26	34.60	30.80	32.70	2.452	1.855	2.154	.1823	.1378	.1601	.044399	-----
9-10	3,13,18	33.34	27.74	30.54	1.539	1.097	1.318	.1144	.0815	.0980	.02913	-----
11-12	22	35.57	30.71	33.14	1.910	1.410	1.660	.1419	.1048	.1235	.035107	36.67
11-12	33	35.57	30.71	33.14	1.910	1.410	1.660	.1419	.1048	.1235	.035107	-----
11-12	29	39.42	34.03	36.73	2.116	1.562	1.839	.1573	.1161	.1367	.044399	-----
13	38	-----	-----	33.65	-----	-----	.9002	-----	-----	.0669	-----	-----
13	39,40,41	-----	-----	28.66	-----	-----	.7672	-----	-----	.0570	-----	213.0
13	42,43,44	-----	-----	28.66	-----	-----	.7672	-----	-----	.0570	-----	-----

(*)In all zones N_C=6190.x10^{-5} and N_{Si}=73.7x10^{-5} ats/bcm. In the reflector the only nuclide present is graphite in the concentration of 8876.x10^{-5} ats/bcm (region 45). All densities as expressed in units of 10^{-5} atoms/bcm.

(+)For interior regions (1 to 19) use CR1 CS set and for periphery regions (20 to 44) use CR2 CS set from Table A.1-4.

regions (see Figs. A.1-1 and A.1-3):

$$N_{BIO} = (2.913 \times 10^{-7} \text{ atoms } B^{10}/\text{bcm})(1.2052) = 3.5107 \times 10^{-7} \text{ atoms/bcm.}$$

Regions 20, 23, 26 and 29 have 8 LBP rods and 4 graphite elements each, but two of those elements are slightly smaller than the regular ones (see Figs. A.1-1 and A.1-3); N_{BIO} is given by:

$$N_{BIO} = (2.755 \times 10^{-4} \text{ atoms } B^{10}/\text{bcm})(6.168 \times 10^{-4})8/4\{(1122.836 \times 4)/[(1122.836 \times 4) - (A_2 + A_3)]\}$$

$$\therefore N_{BIO} = 4.4399 \times 10^{-7} \text{ atoms/bcm.}$$

Control rod density calculation

All regions have $N_{CR} = 0$ except regions 1, 11, 15, 19, 22, 24, 28, 30, 34, 36, 39, 40 and 41. From Table A.1-4:

Regions 1, 11, 15 and 19: $N_{CR1} = 22.9 \times 10^{-5}$ atoms/bcm ;

Regions 22, 24, 28, 30, 34 and 36: $N_{CR2} = [213.0 \times 10^{-5}/7](1.2052)$
$= 36.673 \times 10^{-5}$ atoms/bcm ;

Regions 39, 40 and 41: $N_{CR2} = 213.0 \times 10^{-5}$ atoms/bcm.

With the average values of HM and CR atomic densities in Table A.1-6 three CITATION runs were obtained: one with LBP1, another with LBP2 and another with LBP3 (see inputs in App. B). The outputs yield the k_{eff} and power density in the 44 regions required. To obtain Table A.1-7 the following steps are necessary:

(1) Determine the average power density. In this case 6.437 W/CC was the calculated value; it is slightly above the FSV real core power

Table A.1-7 Radial Power Distribution and k_{off} Comparison with GA Values from Fig. 2.1.3-1

	LBP1	LBP2	LBP3	GA
k_{off}	1.0092	1.0187	1.00962	1.0039
Relative power in internal regions:				
1	.85G	.86G	.87G	.93
2	1.71G	1.75G	1.73G	1.70
3	1.32G	1.34G	1.33G	1.30
4	1.12G	1.10G	1.11G	1.11
5	1.06G	1.05G	1.07G	1.12
6	1.67G	1.70G	1.70G	1.68
7	1.65G	1.70G	1.68G	1.70
8	1.10G	1.09G	1.11G	1.03
9	1.74G	1.75G	1.75G	1.68
10	.74G-F	.73G-F	.73G-F	.82
11	.87G	.87G	.87G	.87
12	1.64F-B	1.60F	1.57F	1.37
13	7.34G	1.32G	1.31G	1.27
14	1.01G-F	1.01G-F	1.01G-F	1.12
15	.63F	.63F	.64G-F	.71
16	1.64G	1.66G	1.66G	1.53
17	1.24G	1.27G	1.29G	1.25
18	.90F	.92G-F	.92G-F	1.01
19	.97G	1.00G	.99G	1.01
Rating:	14G, 2G-F	14G, 3G-F	14G, 4G-F	
see Table 2.1.3.1-1	2F, 1F-B	2F	1F	

Table A.1-7 (continued)

Relative Power in Periphery Regions:		LBP1		LBP2		LBP3		GA
20		1.10		1.04		1.06		
} 20 eff		} .79 F-B		} .76 F		} .77 F		.64
39		.17		.19		.19		
21	21 eff	.84	.78 G	.81	.76 G	.83	.77 G	.77
22	22 eff	.59	.57 G-F	.60	.58 G-F	.60	.58 G-F	.64
23		.67		.67		.67		
} 23 eff		} .56 F		} .55 F		} .55 F		.67
42		.29		.29		.29		
24	24 eff	.49	.49 F	.50	.50 G-F	.50	.50 G-F	.55
25	25 eff	.70	.67 G	.66	.63 G	.66	.63 G	.61
26		1.32		1.23		1.20		
} 26 eff		} .93 B		} .88 B		} .85 F-B		.69
40		.21		.23		.23		
27	27 eff	1.64	1.45 F	1.58	1.40 G-F	1.54	1.36 G	1.28
28	28 eff	.46	.47 G-F	.46	.46 G-F	.46	.46 G-F	.53
29		.62		.62		.62		
} 29 eff		} .53 F		} .53 F		} .53 F		.62
43		.31		.31		.31		
30	30 eff	.54	.53 F-B	.56	.55 F	.56	.55 F	.64
31	31 eff	1.17	1.06 G	1.17	1.06 G	1.17	1.06 G	1.08
32		.76		.73		.74		
} 32 eff		} .59 G		} .58 G		} .58 G		.54
41		.19		.22		.23		
33	33 eff	1.21	1.09 G	1.23	1.11 G	1.23	1.11 G	1.09
34	34 eff	.73	.69 G-F	.77	.72 G	.77	.72 G	.77
35		.44		.45		.46		
} 35 eff		} .42 F		} .42 F		} .43 F		.49
44		.30		.30		.31		

Table A.1-7 (continued)

Relative Power in Periphery Regions:	LBP1	LBP2	LBP3	GA
36 36 eff	.31 .34 F	.32 .35 F	.32 .35 F	.40
37 37 eff	1.11 1.01 G	1.10 1.00 G	1.11 1.01 G	.96
38	.49	.48	.48	
Ratings	6G,3G-F,6F 2F-B,1B	7G,4G-F,6F, 1F-B	8G,3F-G,6F 1F-B	
Total ratings	20G,5G-F,8F, 3F-B,1B	21G,7G-F,8F, 1F-B	22G,7G-F,7F, 1F-B	

density (PD = 6.3 W/CC) because the area in the representation in Fig. A.1-2 is a little lower than that of FSV due to some approximations in passing to XY geometry.

(2) Find the ratio PD/Average PD for the 44 regions.

(3) For the 19 internal regions that is all; for the others a composed value has to be determined:

Regions 21, 22, 24, 25, 27, 28, 30, 31, 33, 34, 36 and 37 combine with 38 in the 5:1 proportion (their area relationship) to determine 21 eff., 22 eff., etc. to compare with GA's values; e.g.: in LBP3, $(\text{PD ratio})_{21}$ = .83, $(\text{PD ratio})_{38}$ = .48. $\therefore$ $(\text{PD ratio})_{21\text{eff}}$ = [(.83) x 5 + .48]/6 = .77.

Regions 20, 23, 26, 29, 32 and 35 combine with 38 and respectively 39, 42, 40, 43, 41 and 44 in the proportion 20:6:7 to determine 20 eff., 23 eff., etc. to compare with GA's values; e.g.: in LBP1, $(\text{PDratio})_{20}$ = 1.10, $(\text{PD ratio})_{39}$ = .17 and $(\text{PD ratio})_{38}$ = .49 $\therefore$ $(\text{PD ratio})_{20\text{eff}}$ = [(1.10) x (20) + (.48)(6) + (.17)(7)]133 = .79.

(4) Rate the results: G (within 10% of GA's value), F (between 10% and 20% away from GA's value) and B (more than 20% difference to GA's value.

A.2 Calculations for the preparation of the CITATION input to obtain the FSV relative axial power profile.

The FSV core was represented in RZ geometry for a CITATION input as in Fig. 2.1.3.2-2. The appropriate compositions and dimensions were determined from Table A.1-6 and Fig. A.1-2 in the following way:

(1) Zones 1 and 2 were determined by making a cylinder with the same volume as refueling regions 1 to 7 of Fig. A.1-2 and finding an average composition for the upper (zone 1) and lower (zone 2) halves of this cylinder from the atomic densities in Table A.1-6 (in 10^{-5} atoms/bcm):

$$(N_{25})_1 = \frac{(1.666)(3) + (1.167)(3) + (1.539)}{7} = 1.434 \quad ,$$

$$(N_{25})_2 = \frac{(1.229)(3) + (.890)(3) + (1.097)}{7} = 1.065 \quad ,$$

$$(N_{28})_1 = \frac{(.1238)(3) + (.0867)(3) + (.1144)}{7} = .1066 \quad ,$$

$$(N_{28})_2 = \frac{(.0913)(3) + (.0661)(3) + (.0815)}{7} = .0791 \quad ,$$

$$(N_{02})_1 = \frac{(29.45)(3) + (34.97)(3) + (33.34)}{7} = 32.37 \quad ,$$

$$(N_{02})_2 = \frac{(25.19)(3) + (31.25)(3) + (27.74)}{7} = 28.15 \quad ,$$

$$(N_{BIO})_1 = (N_{BIO})_2 = \frac{(.02913)(4)}{7} = .01665 \quad \text{(as LBP2)} \ ,$$

and

$$(N_{CRI})_1 = (N_{CRI})_2 = 22.9/7 = 3.271 \quad .$$

(2) Zones 3 and 4 were determined by making an annulus with the same volume as zones 8 to 19 of Fig. A.1-2 and finding an average composition for the upper (zone 3) and lower (zone 4) halves of this annulus from the atomic densities in Table A.1-6 (in 10^{-5} atoms/bcm):

$$(N_{25})_3 = \frac{(1.167)(4) + (1.888)(6) + (1.539)(2)}{12} = 1.590 \quad ,$$

$$(N_{25})_4 = \frac{(.890)(4) + (1.401)(6) + (1.097)(3)}{12} = 1.180 \quad ,$$

$$(N_{28})_3 = \frac{(.0867)(4) + (.1403)(6) + (.1144)(2)}{12} = .1181 \quad ,$$

$$(N_{28})_4 = \frac{(.0661)(4) + (.1041)(6) + (.0815)(2)}{12} = .0877 \quad ,$$

$$(N_{02})_3 = \frac{(34.97)(4) + (30.65)(6) + (33.34)(2)}{12} = 32.55 \quad ,$$

$$(N_{02})_4 = \frac{(31.25)(4) + (26.81)(6) + (27.74)(2)}{12} = 28.45 \quad ,$$

$$(N_{BIO})_3 = (N_{BIO})_4 = \frac{(.02913)(8)}{12} = .01942 \quad ,$$

and

$$(N_{CRI})_3 = (N_{CRI})_4 = \frac{(22.9)(3)}{12} = 5.725 \quad .$$

(3) Analogously zone 5 and 6 correspond to fuel regions 20 to 37 in Fig. A.1-2; the internal radius of the annulus is 218.0 cm (external radius of zones 3 and 4) and the external radius can be determined from the data in Fig. A.1-3 with the help of Eq. A.2-1:

$$[\underbrace{(1122.84)(7)-(A_1+A_2+A_3)}_{6521.59}]x12+[\underbrace{(1122.84)(4)-(A_2+A_3)}_{3437.975}]x6=\pi(r^2-218.0^2) \qquad (A.2\text{-}1)$$

$$\therefore \quad r = \sqrt{(98.887x10^3/\pi)+218.0^2}=281.1 \quad .$$

$$(N_{25})_5= [(2.213)(6)+(1.236)(4)+(1.910)(2)](6521.59)+[(2.452)(2)+(1.369)(2)+2.116](3437.98)/98.887 \times 10^3 = 1.878$$

$$(N_{25})_6=([1.674)(6)+(.9419)(4)+(1.410)(2)](.06595)+[(1.855)(3)+(1.044)(2)+1.562](.03477) = 1.417 \quad ,$$

$$(N_{28})_5=[(.1645)(6)+(.0918)(4)+(.1419)(2)](.06595)+[(.1823)(3)+(.1018)(2)+.1573](.03477) = .1396 \quad ,$$

$$(N_{28})_6=[(.1244)(6)+(.0700)(4)+(.1048)(2)](.06595)+[(.1378)(3)+(.0776)(2)+.1161](.03477)= .1053 \quad ,$$

$$(N_{02})_5=[(31.23)(6)+(37.02)(4)+(35.57)(2)](.06595)+[(34.60)(3)+(41.02)(2)+39.42](.03477) = 34.65 \quad ,$$

$$(N_{02})_6=[(27.80)(6)+(33.08)(4)+(30.71)(2)](.06595)+[(30.80)(3)+(36.66)(2)+34.03](.03477) = 30.72 \quad ,$$

$(N_{BIO})_5=(N_{BIO})_6=(.035107)(8)(.06595)+(.044399)(4)(.03477) = .02470$,

and

$$(N_{CR2})_5 = (N_{CR2})_6 = (36.67)(4)(.06595) = 9.674 \quad .$$

(4) Zone 7 was determined by making an annulus with the same volume as zones 38 to 44 (composition 13), taking the dimensions from Fig. A.1-3 and using the equation:

$$(12)(A_1+A_2+A_3)+(6)(A_2+A_3+1122.84)=29.219\times10^3= (r^2-281.1^2) \qquad (A.2\text{-}2)$$

$\therefore$ r = 297.2 cm,

$$(N_{25})_7=\frac{[12A_1+18(A_2+A_3)]\times(.9002)+(6)(1122.84)(.7672)}{29.219\times10^3}=.8664, \qquad (A.2\text{-}3)$$

$$(N_{28})_7=\frac{(22.38)(.0669)+(5.737)(.0570)}{29.219}=.0644, \qquad (A.2\text{-}4)$$

$$(N_{02})_7=\frac{(22.38)(33.65)+(6.737)(28.66)}{29.219}=32.38, \qquad (A.2\text{-}5$$

and

$$(N_{CR2})_7=(213.0)(3)(1122.84)/29.219\times10^3=24.56. \qquad (A.2\text{-}6$$

(5) Reflector zones: the thicknesses of FSV were maintained in the top, bottom and side reflector. All the CR are located in the top reflector and to simplify the input a single top reflector region was assumed with $N_{CR1}=22.9\times10^{-5}$ atoms/bcm.

A.3 Calculations for the preparation of the CITATION input to obtain the FSV k_{eff} vs. time curve.

All the runs were made in RZ geometry for which case the calculations to determine the BOL compositions were exemplified in Appendix A.2.. For the depletion runs being treated here it is also necessary to specify the FP yields from fission, decay constants, chains by decay and capture and the CITATION resonance shielding correlation.

A.3.1 F.P. yields from fission

The F.P. yields from fission were taken mostly from Refs. 28 and 36. The yields for the long lived and stable FP are summarized in Table A.3.1-1. NSAG23 and NSAG25 are fission product aggregates for U^{233} and U^{235} fission respectively [NSAG stands for "non-saturated (F.P.) aggregate"]; they represent all the stable FP not treated explicitly in the burnup calculations. The only FP from the HE set (see Table 2.1.1.1-2) missing in Table A.3.1-1 are Xe^{135} (no. 58 in the CITATION input), Pm^{148} (no. 65), Sm^{150} (no. 68), Eu^{154} (no. 72) and Eu^{155} (no. 73) because they are not directly produced from fission, with the exception of Xe^{135} that is not stable . The yield of Xe^{135} directly from fission is very small ($\sim$.003) but since it is produced from Te^{135} after 2 fast β^- decays and Te^{135} has a relatively high yield, Xe^{135} here is treated as if directly produced with yields .060 (from U^{233}), .064 (from U^{235}) and .072 (from Pu^{237}); those numbers were taken from Ref. 32.

There is not much information about fission yields from other HM outside U^{233}, U^{235}, Pu^{239}, Th^{232} and U^{238}, however most of the FP are produced by fission of U^{233}, U^{235} and Pu^{239} and the results have low

Table A.3.1-1 Stable and Long Lived F.P. Yields From Fission

No. in the CITATION Input	Nuclide	Yield from fission of U^{238}	U^{235}	Pu^{229}
39	$_{42}Mo^{95}$	.062	.0627	.057
85	$_{43}To^{99}$	.048	.0606	.061
50	$_{45}Rh^{103}$	.016	.0300	.057
53	$_{54}Xe^{131}$	.037	.0293	.032
55	$_{55}Cs^{133}$	.062	.0659	.054
60	$_{60}Nd^{143}$	.052	.0598	.061
61	$_{60}Nd^{145}$	.030	.0395	.041
63	$_{61}Pm^{147}$	.017	.0238	.026
67	$_{62}Sm^{149}$	.0062	.0113	.017
69	$_{62}Sm^{151}$	.0026	.0045	.010
70	$_{62}Sm^{152}$	.0017	.00285	.0075
71	$_{63}Eu^{153}$	.00095	.0015	.0043
86	NSAG23	1	0	0
87	NSAG25	0	1	0

sensity to the assumption employed to estimate the yields for those other HM. In our case the yields for those other HM were determined in the following manner:

Pu^{241} - repeat values from Pu^{239}

U^{232} - repeat values from U^{233}

Th^{232} - from Ref. 31 or 37 or fast fission of U^{235}

U^{238} - from Ref. 31 or 37 or fast fission of U^{235}

Pa^{231}, Pa^{233}, U^{234} -repeat values from Th^{232}

U^{236}, Np^{237}, Pu^{240}, Pu^{242} - repeat values from U^{238}

The complete list of yields from fission can be seen in the CITATION input examples for depletion runs in the Appendix B.

A.3.2 Decay constants and nuclide chain specification

Because not all nuclides are being represented, certain approximations in the complete chains are necessary. Fig. A.3.2-1 presents the nuclide chains as appearing in the CITATION inputs. The decay constants for the radiactive nuclides are summarized in Table A.3.2-1.

After some unexpected results and an examination in the sub-routines of MIT version of CITATION it was found out that its option for the use of $\sigma(n,2n)$ was not working properly. This option is needed in two cases: (a) Th^{232} producing Pa^{231}, which yields U^{232} by β^- decay; and (b) U^{233} producing U^{232}. In the first case it was very simple to represent $\sigma(n,2n)$ as a fraction of σ_f (CITATION has a partial capture option in section 036 permitting to represent the formation of Pa^{231} atoms as a

FIG. A.3.2-1 NUCLIDE CHAIN SPECIFICATIONS

A. Th^{232} CHAIN

THE VOIDS CORRESPOND TO NUCLIDES NOT IN THE HE SET

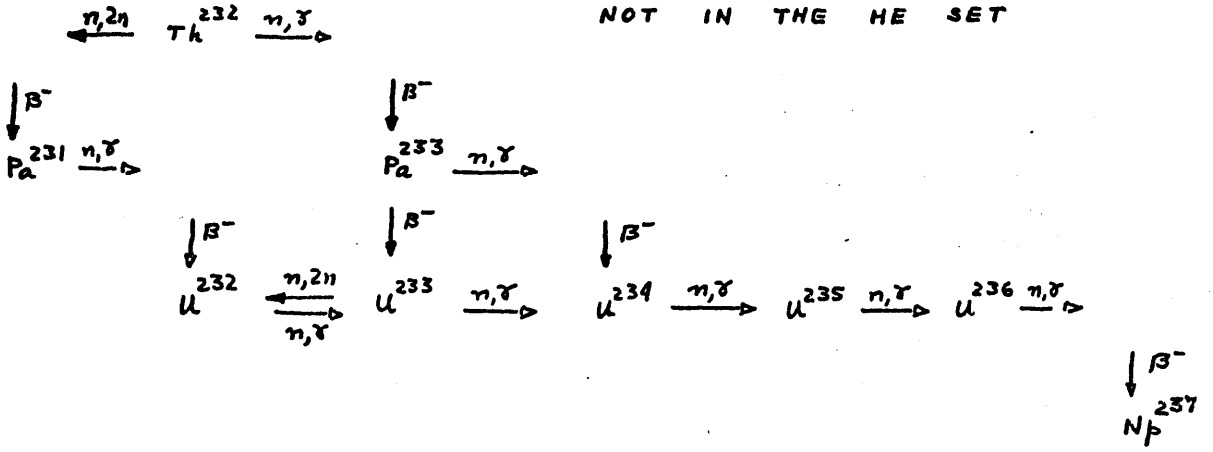

CITATION INPUT STRUCTURE OF THE Th^{232} CHAIN

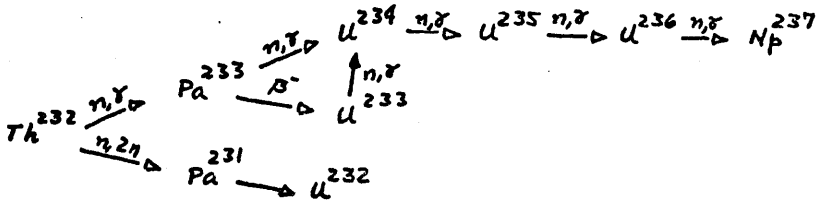

B. U^{238} CHAIN

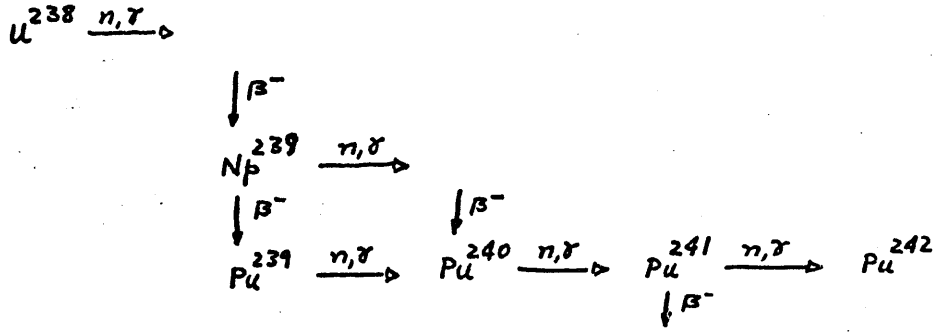

CITATION INPUT STRUCTURE OF THE U^{238} CHAIN

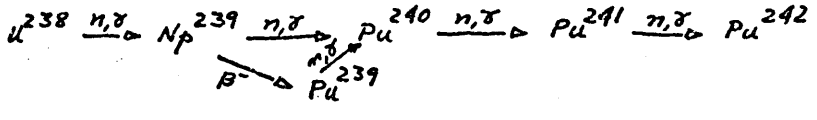

FIG. A.3.2-1 (CONT'D)

C. FISSION PRODUCT CHAINS

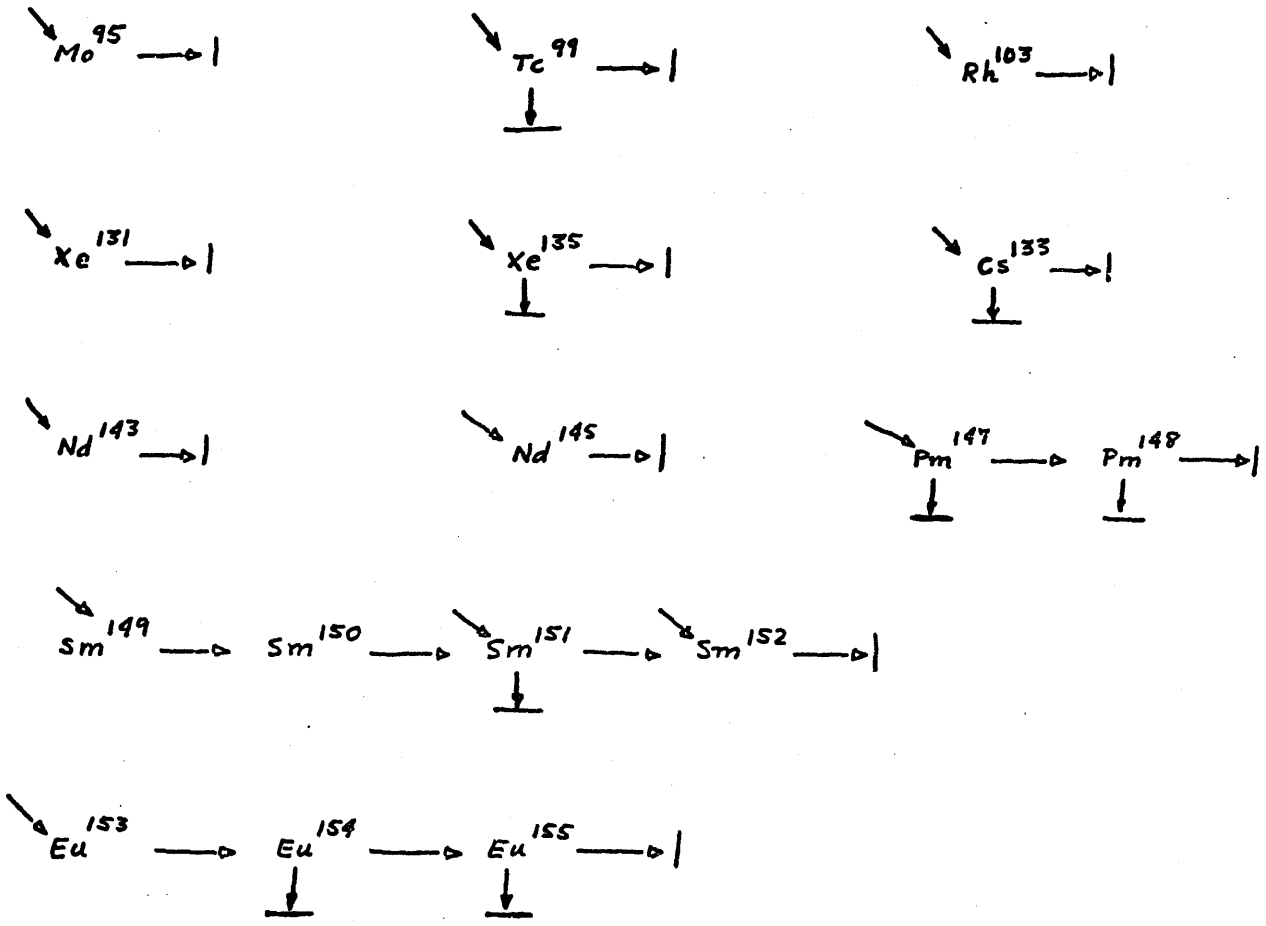

Table A.3.2-1 Decay Constants in sec^{-1}

No. in the CITATION Input	Nuclide	Decay Constant in sec^{-1}
85	Te^{99}	1.04×10^{-12}
58	Xe^{135}	2.102×10^{-5}
63	Pm^{147}	8.378×10^{-9}
65	Pm^{148}	1.480×10^{-6}
69	Sm^{151}	2.361×10^{-10}
72	Eu^{154}	2.813×10^{-9}
73	Eu^{155}	1.210×10^{-8}
7	Pa^{233}	2.971×10^{-7}
13	Np^{239}	3.414×10^{-6}
16	Pu^{241}	1.539×10^{-9}

fraction of the number of fissions in Th^{232}) because both are non-zero only in the first group, thus the fraction of atoms of Pa^{231} formed per fission is independent of the flux. Some hand calculations showed that the amount of U^{232} was not important for criticality calculations and since its amount as a radioactive contaminant can always be estimated if needed it was decided to remove U^{232} from the HE set in the more recent runs.

A.3.3 CITATION resonance shielding correlation

The B^{10} concentration in the LBP rods decreases enormously with time and thus the resonance self shielding effect tends to disappear with depletion. At GA the effective thermal capture as of B^{10} is continually recalculated by the equations:

$$(\sigma^{BIO}_{a4})_{eff} = (\sigma^{BIO}_{a4})\, g \quad , \tag{A.3.3-1}$$

and

$$g = \frac{1}{1+(1.514)(\Sigma_{a4}r)+(.684)(\sigma_{a4}r)^2} \quad . \tag{A.3.3-2}$$

In the CITATION code this effect is taken into account by using the option N5 = 10 in section 000 of nuclide 105 (SELF SH BP). This option asks the code to use its resonance shielding correlation; the broad energy group CS must be supplied at two atomic densities, which can be known with the help of Eqs. A.3.3-1 and A.3.3-2. The procedure is as follows:

Given $(\sigma^{BIO}_{a4})^0_{eff}$ for initial homogenized density $(N_{BIO})^0$ and $(\sigma^{BIO}_{a4})^t_{eff}$ for homogenized density $(N_{BIO})^t$ at any time t, calculate an effective infinitive dilution CS,

$$\sigma_{a\infty} = \sigma^t\sigma^o \left[\frac{N^o\sigma^o - N^t\sigma^t}{N^o(\sigma^o)^2 - N^t(\sigma^t)^2}\right] \quad , \qquad \text{(A.3.3-3)}$$

and a density correlating parameter

$$N^* = \frac{N^o(\sigma^o)^2}{4\,\sigma_{a\infty}\,[\sigma_a - \sigma^o]} \quad . \qquad \text{(A.3.3-4)}$$

In the cs's for B^{10}, set NS = 10, $\sigma^{BIO}_{a4} = \sigma_{a\infty}$ and $\sigma_{x4} = N^*$. The implemented equations are:

$$(\sigma^{BIO}_{a4})_{eff} = Y\,\sigma_{a\infty} \quad , \qquad \text{(A.3.3-5)}$$

where, given

$$C = N^*/N_{BIO} \quad , \qquad \text{(A.3.3-6)}$$

$$Y = 2[\sqrt{C(C+1)} - C] \quad . \qquad \text{(A.3.3-7)}$$

Several different cases were treated. In this appendix the most important calculations performed are exemplified.

A.3.3.1 FSV depletion runs comparison

The initial B^{10} conc. in the LBP rod and in the fuel regions are known. The initial g and $(\sigma^{BIO}_{a4})_{eff}$ are calculated in Table A.1-3. The other value at a time t cannot be known before hand; a typical midcycle value was assumed for $(N_{BIO})^t$ and for this value g and $(\sigma^{BIO}_{a4})_{eff}$ were calculated and so determining $\sigma_{a\infty}$ and N*. This first single set of values of $\sigma_{a\infty}$ and N* for the whole core originated curve 4 of Fig. 2.1.3.3-3. One

wonders how well the CITATION correlation can calculate $(\sigma^{BIO}_{a4})_{eff}$ as a function of time. In Table A.3.3.1-1 the values of $(\sigma^{BIO}_{a4})_{eff}$ as calculated by GA equation and by the CITATION correlation are compared.

Since the values of $\sigma_{a\infty}$ and N* depend on N^o_{BIO} as well as on N^t_{BIO}, and N^t_{BIO} varies a great deal from region to region, it was decided to calculate 3 sets of CS for B^{10} according to the region in the core (see Table A.3.3.1-2). This representation originated curves 5 and 6 of Fig. 2.1.3.3-3.

A.3.3.2 HTGR/GT reference design

In the Final Reference Design, FRD, or FRD8 as described in Chapter 5:

(a) In the core: $n_c = 6$, $x_c = 2.3$ (6 LBP rods per element and 2.3 times more B^{10} per rod than the quantity used in FSV),

$$\sigma^{BIO}_{a4} = 1257 \text{ barns} \quad \text{for C/U} = 1800,$$
$$(N^o_{LBP})_{FSV} = 2.755 \times 10^{-4} \text{ ats/bcm } (B^{10} \text{ conc. in FSV LBP rod}),$$
$$(N^o_{LBP})_{HTGR/GT} = x(N^o_{LBP})_{FSV}, \qquad \text{(A.3.3.2-1)}$$

Vol. of LBP rod/vol. of graphite element $= 7.365 \times 10^{-4}$,

$$(N^o_{elem.}) = (2.3)(2.755 \times 10^{-4} \text{ ats/bcm})(6)(7.365 \times 10^{-4}) = .28 \times 10^{-5} \text{ ats/bcm},$$

$$(\Sigma_{a4}r)_o = (2.3)(2.755 \times 10^{-4} \text{ atoms/bcm})(1257\text{6})(.515 \text{ cm}) = .4102,$$

and $(\Sigma_{a4}r)_t$ was typically taken at a time such that $(\Sigma_{a4}r)_t = (\Sigma_{a4}r)_o/5$.

Table A.3.3.1-1 σ_{a4}^{B10} as Calculated by GA Equation and by CITATION Resonance Shielding Correlation

t(days)	0	10	60	160	260	310
N_{B10} x10^{-6} atoms/bcm(+)	.1988	.1771	.1256	.0756	.0493	.0404
g	.748	.771	.829	.8918	.9275	.9400
Y	.703	.721	.773	.8391	.8836	.9009
$(\sigma_{a4}^{B10})_{eff}$ by GA	1073.11	1106.12	1189.59	1279.41	1330.64	1348.56
$(\sigma_{a4}^{B10})_{eff}$ by CITATION	1073.03	1101.10	1180.00	1280.76	1348.74	1375.07

(+)Those values correspond to zone 2 of Fig. 2.1.3.3-2 in the output corresponding to curve 4 of Fig. 2.1.3.3-3.

Table A.3.3.1-2 Calculation of $G_{a\infty}$ and N* for 3 Groups of Zones of Fig. 2.1.3.3-2

Group of Zones	1,2,7.8	3,4,9,10	5,6,11,12
N_{B10}^{o} in 10^{-6} atoms/bcm	.2319	.2705	.3440 (*)
N_{B10}^{t} in 10^{-6} atoms/bcm	.0533	.0742	.1099 (**)
$(\sigma_{a4}^{B10})_{eff}$ at BOL by GA	← 1073.11 barns →		
g at t=310 days	.9220	.8927	.8482
$(\sigma_{a4}^{B10})_{eff}$ at 310 days by GA	1322.67	1282.12	1216.82
$\sigma_{a\infty}$ by Eq. A.3.3-3	1456.56	1416.55	1317.01
N* by Eq. A.3.3-4	1.1953×10^{-7}	1.6013×10^{-7}	3.083×10^{-7}

(*)Using LBP3

(**)Average value for each group of zones from the output corresponding to curve 4 of Fig. 2.1.3.3-3 at t=310 days.

From Eqs. A.3.3-2 and A.3.3-1, σ^o = 724.025 b and σ^t = 1113.56 b. From Eq. A.3.3-3, $\sigma_{a\infty}$ = 1463.32 barns and from Eq. A.3.3-4, N* = 3.39206 x 10^{-7}.

(b) In the bottom reflector: n_R = 3, α_R = 1.8, $(\Sigma_{a4}r)_o$ = 0.321 $\rightarrow g_o$ = .6435 $\rightarrow \sigma^o$ = 807.571 b, $(\Sigma_{a4}r)_t = (\Sigma_{a4}r)_o/5 \rightarrow g_t$ = .9091 $\rightarrow$ σ^t = 1142.71 b, $\sigma_{a\infty}$ = 1366.55 from Eq. A.3.3-3, N^o_{Elem} = (1.8)(3)(2.755x10^{-4} ats/bcm)(7.365x10^{-4}) = .1096 x 10^{-5} atoms/bcm, and N^* = 2.33934 x 10^{-7} from Eq. A.3.3-4.

APPENDIX B

COMPUTER CODES EMPLOYED

Four computer codes were employed in this thesis: CITATION (Ref. 10), ANISN (Ref. 79), 2DB (Ref. 22) and HELIUM (Ref. 78). The objective of this appendix is to provide an abstract for these codes and illustration of their use in this report.

B.1 CITATION

CITATION solves problems involving the finite difference representation of diffusion theory treating up to three space dimensions with arbitrary group to group scattering. Depletion problems may be solved and fuel managed for multi-cycle analysis. Extensive first order perturbation results may be obtained given microscopic data and nuclide concentration.

The solution methods used are explicit, finite difference approximations in space and time. The neutron flux eigenvalue problems are solved by direct iteration to determine the multiplication factor or the nuclide densities required for a critical system.

CITATION was the principal code used in this report. Most static criticality problems and all depletion calculations were performed by CITATION. There follows four examples of CITATION inputs and excerpts from the output of the FRD run.

CITATION INPUT TO OBTAIN THE XY RELATIVE POWER DENSITY IN FSV

```
C
C
C
      // *ARNALLO =I=SETPO1',CLASS=C,=EGION=500K
      /*MITTO USE=*(M11535,12580,...%IO)
C     /*MAIN     TIME=15,LINES=30,CARDS=20
      /*SET LOV
      /*SETUP UNIT=2314,ID=234135,S=CHV,                                    X
      /*COMM='DSINS 27514 10581 DISPACK'
      //STEP2 EXEC FORG,PROG='PV,M7514.10581.CITATION.LOAD70KC(NELIB)'
      //G.FT01F001 DD  UNIT=SYSDA,DISP=(NEW,DELETE),SPACE=(TRK,(20,10)),
      //        DCB=(RECFM=VS,LRECL=2404,BLKSIZE=2408)
      //G.FT02F001 DD UNIT=SYSDA,DISP=(NEW,DELETE),SPACE=(TRK,(20,10)),
      //        DCB=(RECFM=VS,LRECL=3004,BLKSIZE=3008)
C     //G.FT03F001 DD UNIT=SYSDA,DISP=(NEW,DELETE),SPACE=(TRK,(20,10)),
      //        DCB=(RECFM=VS,LRECL=1504,BLKSIZE=1508)
      //G.FT04F001 DD  UNIT=SYSDA,DISP=(NEW,DELETE),SPACE=(TRK,(20,10)),
C     //        DCB=(RECFM=VS,LRECL=3004,BLKSIZE=3008)
      //G.FT05F001 DD UNIT=SYSDA,DISP=(NEW,DELETE),SPACE=(TRK,(20,10)),
      //        DCB=(RECFM=VS,LRECL=1004,BLKSIZE=1008)
C     //G.FT09F001 DD UNIT=SYSDA,DISP=(NEW,DELETE),SPACE=(TRK,(20,10)),
      //        DCB=(RECFM=VS,LRECL=1504,BLKSIZE=1508)
      //G.FT10F001 DD  UNIT=SYSDA,DISP=(NEW,DELETE),SPACE=(TRK,(20,10)),
C     //        DCB=(RECFM=VS,LRECL=1504,BLKSIZE=1508,BUFNO=1)
      //G.FT11F001 DD  UNIT=SYSDA,DISP=(NEW,DELETE),SPACE=(TRK,(20,10)),
      //        DCB=(RECFM=VS,LRECL=1504,BLKSIZE=1508)
C     //G.FT12F001 DD  UNIT=SYSDA,DISP=(NEW,DELETE),SPACE=(TRK,(30,15)),
      //        DCB=(RECFM=VS,LRECL=3004,BLKSIZE=3008)
      //G.FT13F001 DD  UNIT=SYSDA,DISP=(NEW,DELETE),SPACE=(TRK,(30,15)),
C     //        DCB=(RECFM=VS,LRECL=1504,BLKSIZE=1508,BUFNO=1)
      //G.FT14F001 DD  UNIT=SYSDA,DISP=(NEW,DELETE),SPACE=(TRK,(30,15)),
      //        DCB=(RECFM=VS,LRECL=3004,BLKSIZE=3008)
C     //G.FT15F001 DD  UNIT=SYSDA,DISP=(NEW,DELETE),SPACE=(TRK,(40,20)),
      //        DCB=(RECFM=VS,LRECL=3600,BLKSIZE=7204)
      //G.FT16F001 DD  UNIT=SYSDA,DISP=(NEW,DELETE),SPACE=(TRK,(20,10)),
C     //        DCB=(RECFM=VS,LRECL=1504,BLKSIZE=1508)
      //G.FT17F001 DD  UNIT=SYSDA,DISP=(NEW,DELETE),SPACE=(TRK,(20,10)),
      //        DCB=(RECFM=VS,LRECL=1504,BLKSIZE=1508)
C     //G.FT18F001 DD  UNIT=SYSDA,DISP=(NEW,DELETE),SPACE=(TRK,(20,10)),
      //        DCB=(RECFM=VS,LRECL=1504,BLKSIZE=1508)
      //G.FT19F001 DD  UNIT=SYSDA,DISP=(NEW,DELETE),SPACE=(TRK,(20,10)),
C     //        DCB=(RECFM=VS,LRECL=1504,BLKSIZE=1508)
      //G.FT21F001 DD  UNIT=SYSDA,DISP=(NEW,DELETE),SPACE=(TRK,(20,10)),
      //        DCB=(RECFM=VS,LRECL=1504,BLKSIZE=1508)
C     //G.FT22F001 DD  UNIT=SYSDA,DISP=(NEW,DELETE),SPACE=(TRK,(20,10)),
      //        DCB=(RECFM=VS,LRECL=1504,BLKSIZE=1508,BUFNO=1)
      //G.FT23F001 DD  UNIT=SYSDA,DISP=(NEW,DELETE),SPACE=(TRK,(20,10)),
C     //        DCB=(RECFM=VS,LRECL=1504,BLKSIZE=1508)
      //G.FT24F001 DD  UNIT=SYSDA,DISP=(NEW,DELETE),SPACE=(TRK,(20,10)),
      //        DCB=(RECFM=VS,LRECL=1504,BLKSIZE=1508)
      //G.FT25F001 DD  UNIT=SYSDA,DISP=(NEW,DELETE),SPACE=(TRK,(20,10)),
      //        DCB=(RECFM=VS,LRECL=1504,BLKSIZE=1508,BUFNO=1)
C     //G.FT26F001 DD  UNIT=SYSDA,DISP=(NEW,DELETE),SPACE=(TRK,(20,10)),
      //        DCB=(RECFM=VS,LRECL=1504,BLKSIZE=1508)
      //G.FT27F001 DD  UNIT=SYSDA,DISP=(NEW,DELETE),SPACE=(TRK,(20,10)),
      //        DCB=(RECFM=VS,LRECL=1504,BLKSIZE=1508)
C     //G.FT28F001 DD  UNIT=SYSDA,DISP=(NEW,DELETE),SPACE=(TRK,(20,10)),
      //        DCB=(RECFM=VS,LRECL=1504,BLKSIZE=1508)
      //G.FT29F001 DD  UNIT=SYSDA,DISP=(NEW,DELETE),SPACE=(TRK,(20,10)),
      //        DCB=(RECFM=VS,LRECL=1504,BLKSIZE=1508)
      //G.FT30F001 DD  UNIT=SYSDA,DISP=(NEW,DELETE),SPACE=(TRK,(20,10)),
      //        DCB=(RECFM=VS,LRECL=1504,BLKSIZE=1508)
C
```

```
//G.FT31F001 DD UNIT=SYSDA,DISP=(NEW,DELETE),SPACE=(TRK,(20,10)),
//         DCB=(RECFM=VS,LRECL=1604,BLKSIZE=1608)
//G.FT32F001 DD UNIT=SYSDA,DISP=(NEW,DELETE),SPACE=(TRK,(20,10)),
//         DCB=(RECFM=VS,LRECL=1604,BLKSIZE=1608)
//G.SYSIN DD *,DCB=(RECFM=FB,LRECL=80,BLKSIZE=2000)
ARMY REACTOR
DATE : APRIL 17, 1976
000
  8
FOUR GROUP MICROSCOPIC CROSS SECTIONS ,SET 1 ,CORE
  -2   9   4   1   0   0
       0.976          0.024
      15.0+06       0.183+06          0.0           0.0
    1.5065+06     1.7547+03        17.6          2.38
     6.434-10      2.489-04     5.472+00      5.339-02
      0.0127        0.0317     1.551-06      1.022-05
0                                   0.12         0.315          1.36          3.8
0
0
  10   92235   0   0   0        J235
       235.05                  3.23-11
0
0
0
0
0

       0.0031        0.00524       0.00182       0.00066          .00052        0.00346
0
0
  1.39898+00   1.27033+00   5.40567+00   2.56026+00
  1.89305+01   1.25851+01   2.42794+01   2.43016+00
  6.27115+01   3.44455+01   7.77132+01   2.43000+00
  2.19357+02   1.24431+02   2.32064+02   2.43000+00
  3.84480+00   1.62145-01   0.0          0.0           0.0           1.03392+01
  9.56718-03   0.0          0.0          0.0           1.24010+01    3.57869-02
  0.0          0.0          0.0          1.06901+01
   5   90232   0   0   0        T-232
       232.04                  3.14-11
0
0
0
0
0

       0.1077        0.0221        0.0085        0.0021           0.0017        0.0074
0
0
  1.67250-01   3.67550-02   5.34430+00   2.40137+00
  4.00577+00   5.5-305-15   2.24742+01   0.0
  1.77341-01   0.0          1.13115+01   0.0
  2.56452+00   0.0          1.45630+01   0.0
  4.03514+00   1.-1911-01   0.0          0.0           0.0           1.84571+01
  1.13191-02   0.0          0.0          0.0           1.15838+01    5.03630-02
  0.0          0.0          0.0          1.19484+01
  12   92234   0   0   0        J234
       234.05                  3.31-11
0
0
```

```
0
0
0
                                                                    0.000475      0.00536
      0.00434      0.01519      0.00881      0.00294
0
0
  1.81243-01  5.74320-02  5.45743+00  2.90869+00
  1.22929+01  3.25206-11  3.33451+01  0.0
  6.53815+01  9.95458-11  7.78183+01  0.0
  1.05313+00  0.0         1.17433+01  0.0
  5.02555+00  2.50537-01  0.0         0.0          0.0          2.36330+01
  6.01594-02  0.0         0.0         0.0          1.24010+01   3.57869-02
  0.0         0.0         0.0         1.06901+01
 105   10510   2   0   0      SELF SH. BP
      10.013
0
0
0
0
0
0
0
0
0
  4.79423-01
  2.77019+01
  2.47949+02
  1.07311+03
 115   11510   2   0   0      CP1
      10.811
  0
  0
  0
  0
  0
  0
  0
  0
  0
     0.10+00
     2.3E+00
     5.44+00
     5.01+00
 125   12510   2   0   0      CP2
      10.811
0
0
0
0
0
0
0
0
0
     0.10+00
     2.02+00
     4.11+00
     3.79+00
```

```
     5     1612    0    0    0       CARBON
          12.011
     0
     0
     0
     0
     0
     0
     0
     0
     0
     0
       1.58799-04  0.0          2.26492+00  0.0
       2.45014-05  0.0          4.39653+00  0.0
       2.20025-04  0.0          4.45714+00  0.0
       1.27191-03  0.0          4.54142+00  0.0
       2.66809+00  1.96672-01   0.0         0.0          0.0          4.60731+00
       6.25637-02  0.0          0.0         0.0          4.38336+00   3.66401-01
       0.0         0.0          0.0         4.61394+00
       83    2612    0    0    0       CREF
          12.011
     0
     0
     0
     0
     0
     0
     0
     0
     0
       7.59581-07  0.0          1.48676+00  0.0
       3.35931-05  0.0          4.34724+00  0.0
       2.54030-04  0.0          4.12727+00  0.0
       1.35200-03  0.0          4.42375+00  0.0
       1.76473+00  2.16030-01   0.0         0.0          0.0          4.60731+00
       8.76041-02  0.0          0.0         0.0          3.73898+00   3.88029-01
       0.0         0.0          0.0         4.88181+00
       84    1428    0    0    0       SILICO
          28.086
     0
     0
     0
     0
     0
     0
     0
     0
     0
       3.53831-03  0.0          2.89543+00  0.0
       2.95549-03  0.0          1.44123+00  0.0
       1.04334-02  0.0          2.10394+00  0.0
       5.96917-02  0.0          2.15211+00  0.0
       2.42337+00  2.34022-01   0.0         0.0          0.0          1.92720+00
       1.19842-02  0.0          0.0         0.0          2.02682+00   7.26207-02
       0.0         0.0          0.0         2.09845+00
       4
     001
       0                                                              3
       1                        1                                    2          4
```

```
0
003
 0  2        ^                 0   0   0   0
0
                               842.0          1.0    2.1035-03
004
 3   135.89  1   11.908  1   11.908  1   11.908  1   11.908  1   11.908
 1   11.908  1   11.908  1   11.908  1   11.908  1   11.908  1   11.908
 1   11.908  1   11.908  1   11.908  1   11.908  1   11.908  1   11.908
 1   11.908  1   11.908  1   11.908  1   11.908  1   11.908  1   11.908
 1   11.908  1   11.908  1   11.908  1   11.908  1   11.908  1   11.908
 1   11.908  1   11.908  1   11.908  1   11.908  1   11.908  1   11.908
 1   11.908  1   11.908  1   11.908  1   11.908  1   11.908  1   11.908
 1   11.908  1   11.908  1   11.908  1   11.908  1   11.908  1   11.908
 1   11.908  1   11.908  1   11.908  3   135.89
 3   135.89  1   13.750  1   13.750  1   13.750  1   13.750  1   13.750
 1   13.750  1   13.750  1   13.750  1   13.750  1   13.750  1   13.750
 1   13.750  1   13.750  1   13.750  1   13.750  1   13.750  1   13.750
 1   13.750  1   13.750  1   13.750  1   13.750  1   13.750  1   13.750
 1   13.750  1   13.750  1   13.750  1   13.750  1   13.750  1   13.750
 1   13.750  1   13.750  1   13.750  1   13.750  1   13.750  1   13.750
 1   13.750  1   13.750  1   13.750  1   13.750  1   13.750  1   13.750
 1   13.750  1   13.750  1   13.750  3   135.89
005
45 45 45 45 45 45 45 45 45 45 45 45 45 45 45 45 45 45 45 45 45 45 45 45
45 45 45 45 45 45 45 45 45 45 45 45 45 45 45 45 45 45 45 45 45 45 45 45
45 45 45 45
45 45 45 45 45 45 45 45 45 45 45 45 45 45 45 45 45 45 45 45 45 38 38 45
45 45 45 45 45 38 38 45 45 45 45 45 45 45 45 45 45 45 45 45 45 45 45 45
45 45 45 45
45 45 45 45 45 45 45 45 45 45 45 45 45 45 45 45 45 45 45 38 38 36 36 38
38 45 45 38 38 37 37 38 38 45 45 45 45 45 45 45 45 45 45 45 45 45 45 45
45 45 45 45
45 45 45 45 45 45 45 45 45 45 45 45 45 45 44 44 38 38 38 36 36 36 36 36
36 38 38 37 37 37 37 37 37 38 39 38 38 45 45 45 45 45 45 45 45 45 45 45
45 45 45 45
45 45 45 45 45 45 45 45 45 45 45 45 45 44 44 44 35 35 36 36 36 36 36 36
36 36 37 37 37 37 37 37 37 37 20 20 20 39 39 39 45 45 45 45 45 45 45 45
45 45 45 45
45 45 45 45 45 45 45 45 45 45 38 38 38 44 44 35 35 35 36 36 36 36 36 36
36 36 37 37 37 37 37 37 37 37 20 20 20 39 39 39 38 38 45 45 45 45 45 45
45 45 45 45
45 45 45 45 45 45 45 45 45 45 34 35 35 35 35 35 35 35 36 36 36 36 36 36
36 36 37 37 37 37 37 37 37 37 20 20 20 20 39 20 20 38 45 45 45 45 45 45
45 45 45 45
45 45 45 45 45 45 45 45 45 34 34 35 35 35 35 35 35 18 18 36 36 36 36 36
36 19 19 37 37 37 37 37 37  8  8 20 20 20 20 20 20 38 38 45 45 45 45 45
45 45 45 45
45 45 45 45 45 45 45 34 34 34 34 34 34 35 35 18 18 18 18 18 18 36 36 19
19 19 19 19 19 37 37  8  8  8  8  8  8 20 20 21 21 21 21 38 38 45 45 45
45 45 45 45
45 45 45 45 45 45 34 34 34 34 34 34 34 34 18 18 18 18 18 18 18 18 19 19
19 19 19 19 19 19  8  8  8  8  8  8  8  8 21 21 21 21 21 21 21 38 45 45
45 45 45 45
45 45 45 45 45 45 34 34 34 34 34 34 34 34 18 18 18 18 18 18 18 18 19 19
19 19 19 19 19 19  8  8  8  8  8  8  8  8 21 21 21 21 21 21 21 39 45 45
45 45 45 45
45 45 45 45 45 45 34 34 34 34 34 34 34 34 18 18 18 18 18 18 18 18 19 19
19 19 19 19 19 19  8  8  8  8  8  8  8  8 21 21 21 21 21 21 21 38 45 45
```

```
45 45 45 45
45 45 45 45 45 45 34 34 34 34 34 34 34 34 18 18 18 18 18 18 18 18 19 19
19 19 19 19 19 19  8  8  8  8  8  8  8  8 21 21 21 21 21 21 21 38 45 45
45 45 45 45
45 45 45 45 45 34 38 34 34 34 34 34 34 17 17 18 18 18 18 18 18  7  7 19
19 19 19 19 19  2  2  8  8  8  8  8  8  9  9 21 21 21 21 21 21 38 38 45
45 45 45 45
45 45 45 38 38 33 33 33 33 34 34 17 17 17 17 17 17 18 18  7  7  7  7  7
 7 19 19  2  2  2  2  2  2  8  8  9  9  9  9  9  9 21 21 22 22 22 22 38
38 45 45 45
45 45 38 33 33 33 33 33 33 33 17 17 17 17 17 17 17 17  7  7  7  7  7  7
 7  7  2  2  2  2  2  2  2  2  9  9  9  9  9  9  9  9 22 22 22 22 22 22
22 38 45 45
45 45 38 33 33 33 33 33 33 33 17 17 17 17 17 17 17 17  7  7  7  7  7  7
 7  7  2  2  2  2  2  2  2  2  9  9  9  9  9  9  9  9 22 22 22 22 22 22
22 38 45 45
45 45 38 33 33 33 33 33 33 33 17 17 17 17 17 17 17 17  7  7  7  7  7  7
 7  7  2  2  2  2  2  2  2  2  9  9  9  9  9  9  9  9 22 22 22 22 22 22
22 38 45 45
45 45 38 33 33 33 33 33 33 33 17 17 17 17 17 17 17 17  7  7  7  7  7  7
 7  7  2  2  2  2  2  2  2  2  9  9  9  9  9  9  9  9 22 22 22 22 22 22
22 38 45 45
45 38 32 33 33 33 33 33 33 16 16 17 17 17 17 17 17  6  6  7  7  7  7  7
 7  1  1  2  2  2  2  2  2  3  3  9  9  9  9  9  9 10 10 22 22 22 22 22
22 23 38 45
45 38 32 32 32 33 33 16 16 16 16 16 16 17 17  6  6  6  6  6  6  7  7  1
 1  1  1  1  1  2  2  3  3  3  3  3  3  9  9 10 10 10 10 10 10 22 22 23
23 23 38 45
45 38 32 32 32 32 16 16 16 16 16 16 16 16  6  6  6  6  6  6  6  6  1  1
 1  1  1  1  1  1  3  3  3  3  3  3  3  3 10 10 10 10 10 10 10 10 23 23
23 23 38 45
45 41 41 41 32 32 16 16 16 16 16 16 16 16  6  6  6  6  6  6  6  6  1  1
 1  1  1  1  1  1  3  3  3  3  3  3  3  3 10 10 10 10 10 10 10 10 23 23
42 42 42 45
45 41 41 41 32 32 16 16 16 16 16 16 16 16  6  6  6  6  6  6  6  6  1  1
 1  1  1  1  1  1  3  3  3  3  3  3  3  3 10 10 10 10 10 10 10 10 23 23
42 42 42 45
45 38 32 32 32 32 16 16 16 16 16 16 16 16  6  6  6  6  6  6  6  6  1  1
 1  1  1  1  1  1  3  3  3  3  3  3  3  3 10 10 10 10 10 10 10 10 23 23
23 23 38 45
45 38 32 32 32 31 31 16 16 16 16 16 16 15 15  6  6  6  6  6  6  5  5  1
 1  1  1  1  1  4  4  3  3  3  3  3  3 11 11 10 10 10 10 10 10 24 24 23
23 23 38 45
45 38 32 31 31 31 31 31 31 16 16 15 15 15 15 15 15  6  6  5  5  5  5  5
 5  1  1  4  4  4  4  4  4  3  3 11 11 11 11 11 11 10 10 24 24 24 24 24
24 23 38 45
45 45 38 31 31 31 31 31 31 31 15 15 15 15 15 15 15 15  5  5  5  5  5  5
 5  5  4  4  4  4  4  4  4  4 11 11 11 11 11 11 11 11 24 24 24 24 24 24
24 38 45 45
45 45 38 31 31 31 31 31 31 31 15 15 15 15 15 15 15 15  5  5  5  5  5  5
 5  5  4  4  4  4  4  4  4  4 11 11 11 11 11 11 11 11 24 24 24 24 24 24
24 38 45 45
45 45 38 31 31 31 31 31 31 31 15 15 15 15 15 15 15 15  5  5  5  5  5  5
 5  5  4  4  4  4  4  4  4  4 11 11 11 11 11 11 11 11 24 24 24 24 24 24
24 38 45 45
45 45 38 31 31 31 31 31 31 31 15 15 15 15 15 15 15 15  5  5  5  5  5  5
 5  5  4  4  4  4  4  4  4  4 11 11 11 11 11 11 11 11 24 24 24 24 24 24
24 38 45 45
45 45 45 38 38 31 31 31 31 30 30 15 15 15 15 15 15 14 14  5  5  5  5  5
```

```
  5 13 13  4  4  4  4  4  4 12 12 11 11 11 11 11 11 25 25 24 24 24 24 38
 38 45 45 45
 45 45 45 45 45 45 38 30 30 30 30 30 30 15 15 14 14 14 14 14 14  5  5 13
 13 13 13 13 13  4  4 12 12 12 12 12 12 11 11 25 25 25 25 25 25 38 38 45
 45 45 45 45
 45 45 45 45 45 45 38 30 30 30 30 30 30 30 14 14 14 14 14 14 14 14 13 13
 13 13 13 13 13 13 12 12 12 12 12 12 12 12 25 25 25 25 25 25 25 38 45 45
 45 45 45 45
 45 45 45 45 45 45 38 30 30 30 30 30 30 30 14 14 14 14 14 14 14 14 13 13
 13 13 13 13 13 13 12 12 12 12 12 12 12 12 25 25 25 25 25 25 25 38 45 45
 45 45 45 45
 45 45 45 45 45 45 38 30 30 30 30 30 30 30 14 14 14 14 14 14 14 14 13 13
 13 13 13 13 13 13 12 12 12 12 12 12 12 12 25 25 25 25 25 25 25 38 45 45
 45 45 45 45
 45 45 45 45 45 45 38 38 30 30 30 30 30 30 14 14 14 14 14 14 14 14 13 13
 13 13 13 13 13 13 12 12 12 12 12 12 12 12 25 25 25 25 25 25 38 38 45 45
 45 45 45 45
 45 45 45 45 45 45 45 38 30 30 30 30 30 29 29 14 14 14 14 14 14 28 28 13
 13 13 13 13 13 27 27 12 12 12 12 12 12 26 26 25 25 25 25 25 25 25 38 45
 45 45 45 45
 45 45 45 45 45 45 45 45 45 38 38 29 29 29 29 29 29 14 14 28 28 28 28 28
 28 13 13 27 27 27 27 27 27 12 12 26 26 26 26 26 26 38 38 45 45 45 45 45
 45 45 45 45
 45 45 45 45 45 45 45 45 45 45 38 29 29 43 29 29 29 29 28 28 28 28 28 28
 28 28 27 27 27 27 27 27 27 27 26 26 26 26 26 26 26 38 45 45 45 45 45 45
 45 45 45 45
 45 45 45 45 45 45 45 45 45 45 38 38 43 43 43 29 29 29 28 28 28 28 28 28
 28 28 27 27 27 27 27 27 27 27 26 26 26 40 40 38 38 38 45 45 45 45 45 45
 45 45 45 45
 45 45 45 45 45 45 45 45 45 45 45 45 43 43 43 29 29 29 28 28 28 28 28 28
 28 28 27 27 27 27 27 27 27 27 26 26 40 40 40 45 45 45 45 45 45 45 45 45
 45 45 45 45
 45 45 45 45 45 45 45 45 45 45 45 45 45 45 45 38 38 38 38 28 28 28 28 28
 28 38 38 27 27 27 27 27 27 38 38 38 40 40 45 45 45 45 45 45 45 45 45 45
 45 45 45 45
 45 45 45 45 45 45 45 45 45 45 45 45 45 45 45 45 45 45 45 38 38 28 28 38
 38 45 45 38 38 27 27 38 38 45 45 45 45 45 45 45 45 45 45 45 45 45 45 45
 45 45 45 45
 45 45 45 45 45 45 45 45 45 45 45 45 45 45 45 45 45 45 45 45 45 38 38 45
 45 45 45 45 45 38 38 45 45 45 45 45 45 45 45 45 45 45 45 45 45 45 45 45
 45 45 45 45
 45 45 45 45 45 45 45 45 45 45 45 45 45 45 45 45 45 45 45 45 45 45 45 45
 45 45 45 45 45 45 45 45 45 45 45 45 45 45 45 45 45 45 45 45 45 45 45 45
 45 45 45 45
012
  1  1  1  1       1       ZONE 1
  2  2  1  1       1       ZONE 2
  3  3  1  1       1       ZONE 3
  4  4  1  1       1       ZONE 4
  5  5  1  1       1       ZONE 5
  6  6  1  1       1       ZONE 6
  7  7  1  1       1       ZONE 7
  8  8  1  1       1       ZONE 8
  9  9  1  1       1       ZONE 9
 10 10  1  1       1       ZONE10
 11 11  1  1       1       ZONE11
 12 12  1  1       1       ZONE12
 13 13  1  1       1       ZONE13
 14 14  1  1       1       ZONE14
```

```
 15 15   1   1       1          ZONE15
 16 16   1   1       1          ZONE16
 17 17   1   1       1          ZONE17
 18 18   1   1       1          ZONE18
 19 19   1   1       1          ZONE19
 20 20   1   1       1          ZONE20
 21 21   1   1       1          ZONE21
 22 22   1   1       1          ZONE22
 23 23   1   1       1          ZONE23
 24 24   1   1       1          ZONE24
 25 25   1   1       1          ZONE25
 26 26   1   1       1          ZONE26
 27 27   1   1       1          ZONE27
 28 28   1   1       1          ZONE28
 29 29   1   1       1          ZONE29
 30 30   1   1       1          ZONE30
 31 31   1   1       1          ZONE31
 32 32   1   1       1          ZONE32
 33 33   1   1       1          ZONE33
 34 34   1   1       1          ZONE34
 35 35   1   1       1          ZONE35
 36 36   1   1       1          ZONE36
 37 37   1   1       1          ZONE37
 38 38   1   1       1          ZONE38
 39 39   1   1       1          ZONE39
 40 40   1   1       1          ZONE40
 41 41   1   1       1          ZONE41
 42 42   1   1       1          ZONE42
 43 43   1   1       1          ZONE43
 44 44   1   1       1          ZONE44
 45 45   1   1      1-01        REFLECTOR
  0
 018
  10      6 12       105115125      5 83 84
 020
   1  1   0   0
   5 6190.-05 84  73.7-05 10 1.023-05  6 33.11-05 12 .0764-05115  22.9-05
   0
   2  2   0   0
   5 6190.-05 84  73.7-05 10 1.444-05  6 27.32-05 12 .1076-05105 .4060-06
   0
   3  3   0   0
   5 6190.-05 84  73.7-05 10 1.313-05  6 30.54-05 12 .0980-05105 .4060-06
   0
   4  4   0   0
   5 6190.-05 84  73.7-05 10 1.023-05  6 33.11-05 12 .0764-05
   5  5   0   0
   5 6190.-05 84  73.7-05 10 1.023-05  6 33.11-05 12 .0764-05
   6  6   0   0
   5 6190.-05 84  73.7-05 10 1.444-05  6 27.32-05 12 .1076-05105 .4060-06
   0
   7  7   0   0
   5 6190.-05 84  73.7-05 10 1.444-05  6 27.32-05 12 .1076-05105 .4060-06
   0
   8  8   0   0
   5 6190.-05 84  73.7-05 10 1.023-05  6 33.11-05 12 .0764-05
   9  9   0   0
   5 6190.-05 84  73.7-05 10 1.545-05  6 28.73-05 12 .1222-05105 .4060-06
   0
```

```
 10 10  0  0
  5 6190.-05 84  73.7-05 10 1.023-05  6 33.11-05 12 .0764-05
 11 11  0  0
  5 6190.-05 84  73.7-05 10 1.543-05  6 28.73-05 12 .1222-05105 .4060-06
115  22.9-05
 12 12  0  0
  5 6190.-05 84  73.7-05 10 1.543-05  6 28.73-05 12 .1222-05105 .4060-06
  0
 13 13  0  0
  5 6190.-05 84  73.7-05 10 1.314-05  6 30.54-05 12 .0980-05105 .4060-06
  0
 14 14  0  0
  5 6190.-05 84  73.7-05 10 1.543-05  6 28.73-05 12 .1222-05105 .4060-06
  0
 15 15  0  0
  5 6190.-05 84  73.7-05 10 1.023-05  6 33.11-05 12 .0764-05115  22.9-05
  0
 16 16  0  0
  5 6190.-05 84  73.7-05 10 1.543-05  6 28.73-05 12 .1222-05105 .4060-06
  0
 17 17  0  0
  5 6190.-05 84  73.7-05 10 1.023-05  6 33.11-05 12 .0764-05
 18 18  0  0
  5 6190.-05 84  73.7-05 10 1.314-05  6 30.54-05 12 .0980-05105 .4060-06
  0
 19 19  0  0
  5 6190.-05 84  73.7-05 10 1.543-05  6 28.73-05 12 .1222-05105 .4060-06
115  22.9-05
 20 20  0  0
  5 6190.-05 84  73.7-05 10 2.154-05  6 32.70-05 12 .1601-05105 .6188-06
  0
 21 21  0  0
  5 6190.-05 84  73.7-05 10 1.089-05  6 35.05-05 12 .0809-05
 22 22  0  0
  5 6190.-05 84  73.7-05 10 1.660-05  6 33.14-05 12 .1235-05105 .4893-06
125 36.67-05
 23 23  0  0
  5 6190.-05 84  73.7-05 10 2.154-05  6 32.70-05 12 .1601-05105 .6188-06
  0
 24 24  0  0
  5 6190.-05 84  73.7-05 10 1.944-05  6 29.52-05 12 .1445-05105 .4893-06
125 36.67-05
 25 25  0  0
  5 6190.-05 84  73.7-05 10 1.089-05  6 35.05-05 12 .0809-05
 26 26  0  0
  5 6190.-05 84  73.7-05 10 2.154-05  6 32.70-05 12 .1601-05105 .6188-06
  0
 27 27  0  0
  5 6190.-05 84  73.7-05 10 1.944-05  6 29.52-05 12 .1445-05105 .4893-06
  0
 28 28  0  0
  5 6190.-05 84  73.7-05 10 1.089-05  6 35.05-05 12 .0809-05125 36.67-05
  0
 29 29  0  0
  5 6190.-05 84  73.7-05 10 1.839-05  6 36.73-05 12 .1367-05105 .6188-06
  0
 30 30  0  0
  5 6190.-05 84  73.7-05 10 1.944-05  6 29.52-05 12 .1445-05105 .4893-06
125 36.67-05
```

```
 31 31  0  0
  5 6190.-05 84  73.7-05 10 1.944-05  6 29.52-05 12 .1445-05105 .4893-06
  0
 32 32  0  0
  5 6190.-05 84  73.7-05 10 1.207-05  6 38.84-05 12 .0897-05
 33 33  0  0
  5 6190.-05 84  73.7-05 10 1.660-05  6 33.14-05 12 .1235-05105 .4893-06
  0
 34 34  0  0
  5 6190.-05 84  73.7-05 10 1.944-05  6 29.52-05 12 .1445-05105 .4893-06
125 36.67-05
 35 35  0  0
  5 6190.-05 84  73.7-05 10 1.207-05  6 38.84-05 12 .0897-05
 36 36  0  0
  5 6190.-05 84  73.7-05 10 1.089-05  6 35.05-05 12 .0809-05125 36.67-05
  0
 37 37  0  0
  5 6190.-05 84  73.7-05 10 1.944-05  6 29.52-05 12 .1445-05105 .4893-06
  0
 38 38  0  0
  5 6190.-05 84  73.7-05 10 .9002-05  6 33.65-05 12 .0669-05
 39 39  0  0
  5 6190.-05 84  73.7-05 10 .7672-05  6 28.66-05 12 .0570-05125  213.-05
  0
 40 40  0  0
  5 6190.-05 84  73.7-05 10 .7672-05  6 28.66-05 12 .0570-05125  213.-05
  0
 41 41  0  0
  5 6190.-05 84  73.7-05 10 .7672-05  6 28.66-05 12 .0570-05125  213.-05
  0
 42 42  0  0
  5 6190.-05 84  73.7-05 10 .7672-05  6 28.66-05 12 .0570-05
 43 43  0  0
  5 6190.-05 84  73.7-05 10 .7672-05  6 28.66-05 12 .0570-05
 44 44  0  0
  5 6190.-05 84  73.7-05 10 .7672-05  6 28.66-05 12 .0570-05
 45 45  0  0
 83 9876.-05
0
999
0
/*ENDDATASET
/*
/*EOJ ********
```

CITATION INPUT TO OBTAIN THE FSV REACTIVITY VARIATION WITH TIME

```
//JA0734   JOB 1,
// *ARNAL00 STEFTA01,CLASS=A,REGION=500K
/*MITID USER=(411535,12650,,,410)
/*SPI WEEKLY
/*MAIN     TIME=15,LINES=30,CARDS=20
/*SETUP UNIT=2314,ID=234146,SER=CHV,
/*COMM='USING 47514 10541 DISPACK'
//STEP2 EXEC F20S,P20S=P2V,V2S14,10541,CITATION,LOAD70KC(NELTB),
//G.FT01F001 DD UNIT=SYSDA,DISP=(NEW,DELETE),SPACE=(TRK,(20,10)),
//         DCB=(RECFM=VS,LRECL=2404,BLKSIZE=2408)
//G.FT02F001 DD UNIT=SYSDA,DISP=(NEW,DELETE),SPACE=(TRK,(20,10)),
//         DCB=(RECFM=VS,LRECL=3004,BLKSIZE=3008)
//G.FT03F001 DD UNIT=SYSDA,DISP=(NEW,DELETE),SPACE=(TRK,(20,10)),
//         DCB=(RECFM=VS,LRECL=1504,BLKSIZE=1508)
//G.FT04F001 DD UNIT=SYSDA,DISP=(NEW,DELETE),SPACE=(TRK,(20,10)),
//         DCB=(RECFM=VS,LRECL=3004,BLKSIZE=3008)
//G.FT05F001 DD UNIT=SYSDA,DISP=(NEW,DELETE),SPACE=(TRK,(20,10)),
//         DCB=(RECFM=VS,LRECL=1004,BLKSIZE=1008)
//G.FT09F001 DD UNIT=SYSDA,DISP=(NEW,DELETE),SPACE=(TRK,(20,10)),
//         DCB=(RECFM=VS,LRECL=1504,BLKSIZE=1508)
//G.FT10F001 DD UNIT=SYSDA,DISP=(NEW,DELETE),SPACE=(TRK,(20,10)),
//         DCB=(RECFM=VS,LRECL=1504,BLKSIZE=1508,BUFNO=1)
//G.FT11F001 DD UNIT=SYSDA,DISP=(NEW,DELETE),SPACE=(TRK,(20,10)),
//         DCB=(RECFM=VS,LRECL=1504,BLKSIZE=1508)
//G.FT12F001 DD UNIT=SYSDA,DISP=(NEW,DELETE),SPACE=(TRK,(30,15)),
//         DCB=(RECFM=VS,LRECL=3004,BLKSIZE=3008)
//G.FT13F001 DD UNIT=SYSDA,DISP=(NEW,DELETE),SPACE=(TRK,(30,15)),
//         DCB=(RECFM=VS,LRECL=1504,BLKSIZE=1508,BUFNO=1)
//G.FT14F001 DD UNIT=SYSDA,DISP=(NEW,DELETE),SPACE=(TRK,(30,15)),
//         DCB=(RECFM=VS,LRECL=3004,BLKSIZE=3008)
//G.FT15F001 DD UNIT=SYSDA,DISP=(NEW,DELETE),SPACE=(TRK,(40,20)),
//         DCB=(RECFM=VS,LRECL=3500,BLKSIZE=7204)
//G.FT16F001 DD UNIT=SYSDA,DISP=(NEW,DELETE),SPACE=(TRK,(20,10)),
//         DCB=(RECFM=VS,LRECL=1504,BLKSIZE=1508)
//G.FT17F001 DD UNIT=SYSDA,DISP=(NEW,DELETE),SPACE=(TRK,(20,10)),
//         DCB=(RECFM=VS,LRECL=1504,BLKSIZE=1508)
//G.FT18F001 DD UNIT=SYSDA,DISP=(NEW,DELETE),SPACE=(TRK,(20,10)),
//         DCB=(RECFM=VS,LRECL=1504,BLKSIZE=1508)
//G.FT19F001 DD UNIT=SYSDA,DISP=(NEW,DELETE),SPACE=(TRK,(20,10)),
//         DCB=(RECFM=VS,LRECL=1504,BLKSIZE=1508)
//G.FT21F001 DD UNIT=SYSDA,DISP=(NEW,DELETE),SPACE=(TRK,(20,10)),
//         DCB=(RECFM=VS,LRECL=1504,BLKSIZE=1508)
//G.FT22F001 DD UNIT=SYSDA,DISP=(NEW,DELETE),SPACE=(TRK,(20,10)),
//         DCB=(RECFM=VS,LRECL=1504,BLKSIZE=1508,BUFNO=1)
//G.FT23F001 DD UNIT=SYSDA,DISP=(NEW,DELETE),SPACE=(TRK,(20,10)),
//         DCB=(RECFM=VS,LRECL=1504,BLKSIZE=1508)
//G.FT24F001 DD UNIT=SYSDA,DISP=(NEW,DELETE),SPACE=(TRK,(20,10)),
//         DCB=(RECFM=VS,LRECL=1504,BLKSIZE=1508)
//G.FT25F001 DD UNIT=SYSDA,DISP=(NEW,DELETE),SPACE=(TRK,(20,10)),
//         DCB=(RECFM=VS,LRECL=1504,BLKSIZE=1508,BUFNO=1)
//G.FT26F001 DD UNIT=SYSDA,DISP=(NEW,DELETE),SPACE=(TRK,(20,10)),
//         DCB=(RECFM=VS,LRECL=1504,BLKSIZE=1508)
//G.FT27F001 DD UNIT=SYSDA,DISP=(NEW,DELETE),SPACE=(TRK,(20,10)),
//         DCB=(RECFM=VS,LRECL=1504,BLKSIZE=1508)
//G.FT28F001 DD UNIT=SYSDA,DISP=(NEW,DELETE),SPACE=(TRK,(20,10)),
//         DCB=(RECFM=VS,LRECL=1504,BLKSIZE=1508)
//G.FT29F001 DD UNIT=SYSDA,DISP=(NEW,DELETE),SPACE=(TRK,(20,10)),
//         DCB=(RECFM=VS,LRECL=1504,BLKSIZE=1508)
//G.FT30F001 DD UNIT=SYSDA,DISP=(NEW,DELETE),SPACE=(TRK,(20,10)),
```

```
//          DCB=(RECFM=VS,LRECL=1500,BLKSIZE=1508)
//G.FT31F001 DD UNIT=SYSDA,DISP=(NEW,DELETE),SPACE=(TRK,(20,10)),
//          DCB=(RECFM=VS,LRECL=1500,BLKSIZE=1508)
//G.FT32F001 DD UNIT=SYSDA,DISP=(NEW,DELETE),SPACE=(TRK,(20,10)),
//          DCB=(RECFM=VS,LRECL=1504,BLKSIZE=1508)
//G.SYSIN DD *,DCB=(RECFM=FB,LRECL=80,BLKSIZE=2000)
FSV USING LSP SELF SHIELDING
DATE : APRIL 12,1975
000
  8
FOUR GR HOT MC CS . SET 1
  -2  40   4   1   0   0
        0.975        0.02+         0.0          0.0
         15.0+06     0.183+05        17.6         2.38
      1.5066+06   1.7947+03     6.472+00     5.339-02
       6.434-10    2.489-04    1.551-06     1.022-05
         0.0127       0.0317        0.12        0.315          1.36          3.8
  0
  0
  0
    8  92233   0   0   0       0233
         233.04                3.19-11
  0
  0
  0
  0
  0                                                                  .0006         .0020
        .0017         .0018         .0003         .0002
  0
  0
      2.06149+00   1.26632+00   4.92369+00   2.60514+00
      1.78841+01   1.68348+01   2.76470+01   2.50291+00
      1.14053+02   9.62624+01   1.26803+02   2.50290+00
      2.61972+02   2.3373+02    2.65875+02   2.50000+00
      2.71221+00   1.43944-01   0.0          0.0          0.0          9.79411+00
      9.78603-03   0.0          0.0          0.0          1.26968+00   5.82115-02
      0.0          0.0          0.0          4.00300+00
     10  92235   0   0   0       0235
         235.05                3.23-11
  0
  0
  0
  0
  0                                                                  .00052        0.00346
        0.0031       0.00024       0.00182       0.00066
  0
  0
      1.39898+00   1.27033+00   5.40597+00   2.56026+00
      1.89305+01   1.75651+01   2.42793+01   2.43016+00
      6.27115+01   3.43436+01   7.77132+01   2.43000+00
      2.19357+02   1.94431+02   2.32064+02   2.43000+00
      3.84490+00   1.62145-01   0.0          0.0          0.0          1.03392+01
      9.56718-03   0.0          0.0          0.0          1.24010+01   3.57869-02
      0.0          0.0          0.0          1.04901+01
     14  94239   0   0   0       0239
         239.05                3.34-11
  0
```

0
0
0
0

.0020 .0018

.0013 .0020 .0005 .0003

0
0

1.77736+00 1.70474+00 6.03665+00 3.04455+00
1.85408+01 1.04937+01 3.05325+01 2.47045+00
9.23446+01 5.43217+01 1.04597+02 2.87000+00
1.22702+03 7.56321+02 1.25699+03 2.89000+00
4.16737+00 9.19710-02 0.0 0.0 0.0 1.19819+01
1.05121-02 0.0 0.0 0.0 1.23072+01 4.52438-02
0.0 0.0 0.0 2.90700+01
16 94241 0 0 0 90241
241.06 3.37-11 .15-08

0
0
0
0
0

.00015 .00365

.00375 .0062 .0024 .0005

0
0

1.74803+00 1.65418+00 6.09200+00 3.18751+00
2.26935+01 1.55617+01 3.27885+01 3.03043+00
2.19130+02 1.43334+02 2.33332+02 3.03000+00
8.82100+02 6.05555+02 9.33552+02 3.03000+00
3.95875+00 3.85223-01 0.0 0.0 0.0 1.00844+01
1.06068-02 0.0 0.0 0.0 1.41521+01 4.98861-02
0.0 0.0 0.0 1.84520+01
81 92232 0 0 0 9232
232.04 3.1e-11 .3-09

0
0
0
0
0
0
0
0

1.01337+00 9.07250-01 9.10104+00 2.99008+00
1.82592+01 1.63743+01 3.44315+01 2.50368+00
1.65514+02 9.55003+01 1.78851+02 2.50300+00
4.20368+01 2.21143+01 5.43554+01 2.50300+00
5.72522+00 2.35249+00 0.0 0.0 0.0 1.61640+01
8.28935-03 0.0 0.0 0.0 1.32900+01 4.59685-02
0.0 0.0 0.0 1.12690+01
4 92232 0 0 0 TH232
232.04 3.1e-11

0
0
0
0

0.0017 0.0074

0.0077 0.0221 0.0045 0.0021

0
0
1.67250-01 3.57550-02 5.34430+00 2.40137+00
4.00577+00 5.54306-15 2.24742+01 0.0
1.77341-01 0.0 1.13113+01 0.0
2.56462+00 0.0 1.45530+01 0.0
4.99514+00 1.31911-01 0.0 0.0 0.0 1.84571+01
1.13191-02 0.0 0.0 0.0 1.15828+01 5.03630-02
0.0 0.0 0.0 1.19994+01
9 92234 0 0 0 1234
234.04 3.20-11
0
0
0
0
0
0
0
0
0
1.09440+00 3.62071-01 6.31656+00 2.68486+00
7.75802+00 8.04308-03 2.59327+01 2.50701+00
2.65246+02 2.33211-01 3.15471+02 2.50000+00
2.92195+01 2.54117-03 4.34557+01 2.50500+00
5.20090+00 2.10627-01 0.0 0.0 0.0 1.82281+01
6.55730-03 0.0 0.0 0.0 5.01882+01 3.67775-02
0.0 0.0 0.0 1.42402+01
12 92236 0 0 0 1236
238.05 3.31-11
0
0
0
0
0
0.000475 0.00536
0.00634 0.01519 0.00381 0.00294
0
0
1.61245-01 6.74320-02 5.45743+00 2.90869+00
1.22939+01 5.25206-11 3.53561+01 0.0
6.53815+01 9.95453-11 7.74183+01 0.0
1.05319+00 0.0 1.17433+01 0.0
5.02555+00 2.50637-01 0.0 0.0 0.0 2.36330+01
6.01594-02 0.0 0.0 0.0 1.24010+01 3.57869-02
0.0 0.0 0.0 1.06901+01
15 94240 0 0 0 01240
240.05 3.35-11
0
0
0
0
.00028 .0024
.00165 .0033 .00125 .00024
0
0
1.14039+00 3.69140-01 6.01954+00 3.10140+00
1.35124+01 1.57140-02 3.59479+01 2.90023+00

2.45916+00 0.0 1.3444[illegible]+01 0.0
1.24504+03 0.0 1.3[illegible]+03 0.0
4.71546+00 1.4[illegible]-01 0.0 0.0 0.0 2.34241+01
1.10344-02 0.0 0.0 0.0 1.09242+01 6.14572-02
0.0 0.0 0.0 1.3[illegible]+02
7 91233 0 0 0 94233
233.04 3.1[illegible]-11 .297-06

8.57691-01 6.[illegible]-01 6.41424+00 3.04249+00
1.32242+01 2.[illegible]-03 2.54552+01 2.50405+00
1.31400+02 0.0 1.43554+02 0.0
7.06072+01 0.0 [illegible]+01 0.0
4.66084+00 [illegible]-01 0.0 0.0 0.0 1.22219+01
9.06624-03 0.0 0.0 0.0 1.22051+01 4.89215-02
0.0 0.0 0.0 1.49738+01
M2 91231 0 0 0 94231
231.04 3.12-11

8.49154-01 6.[illegible]-01 6.[illegible]+00 3.04355+00
1.37944+01 2.[illegible] 2.[illegible]+01 2.50905+00
1.01969+02 [illegible] 1.1[illegible]+02 2.50000+00
3.78434+02 1.[illegible] [illegible]+02 2.50000+00
4.61971+00 [illegible]-01 0.0 0.0 0.0 1.25396+01
1.00696-02 0.0 0.0 0.0 1.20033+01 4.77146-02
0.0 0.0 0.0 2.12450+01
13 93239 0 0 0 98239
233.05 3.32-11 .341-05

1.15211+00 [illegible]-01 5.[illegible]+00 2.08879+00
1.96821+01 [illegible] [illegible]+01 2.51398+00
1.28638+02 0.0 1.41372+02 0.0
2.05751+01 0.0 [illegible]+01 0.0
4.25773+00 [illegible]-01 0.0 0.0 0.0 1.20107+01
8.24249-03 0.0 0.0 0.0 1.26998+01 3.42124-01
0.0 0.0 0.0 9.79650+00

```
  11  92235   0   0   0      U235
       236.05                3.25-11
 0
 0
 0
 0
 0                                                          .00056        .0051
          .006        .012        .008        .002
 0
 0
    5.65974-01  3.35044-01  5.49910+00  2.75489+00
    7.46001+00  0.0        2.73296+01  0.0
    1.14395+02  0.0        1.31369+02  0.0
    2.35139+00  0.0        1.43425+01  0.0
    5.10649+00  2.26632-01  0.0         0.0         0.0         1.98609+01
    7.66378-03  0.0        0.0         0.0         1.69285+01  4.54945-02
    0.0         0.0        0.0         1.19912+01
  17  94242   0   0   0      PU242
       242.06                3.34-11
 0
 0
 0
 0
 0                                                          .00028        .0024
          .00165      .0033       .00125      .00024
 0
 0
    1.16038+00  9.69180-01  6.01994+00  3.10180+00
    5.82875+00  1.57140-02  3.13415+01  2.90023+00
    4.92482+02  0.0        5.42319+02  0.0
    1.02713+01  0.0        2.10797+01  0.0
    4.71547+00  1.42095-01  0.0         0.0         0.0         2.55056+02
    7.14095-03  0.0        0.0         0.0         4.83875+01  1.44954+00
    0.0         0.0        0.0         1.08084+01
  18  93237   0   0   0      NP237
       237.05                3.28-11
 0
 0
 0
 0
 0
 0
 0
 0
    1.39713+00  9.77586-01  6.04963+00  2.68882+00
    1.50784+01  6.29623-04  4.05491+01  2.51398+00
    8.31042+01  2.34710-03  9.42499+01  2.50000+00
    1.25970+02  0.0        1.38649+02  0.0
    4.21779+00  4.34723-01  0.0         0.0         0.0         2.53869+01
    8.37754-03  0.0        0.0         0.0         1.11035+01  4.20604-02
    0.0         0.0        0.0         1.27790+01
 105  10510   1   0  10      SELF SH-ED
      10.013
 0
 0
 0
```

```
0
0
0
0
0
0
  4.79423-01  0.0          0.0          0.0          0.0
  2.77019+01  0.0          0.0          0.0          0.0
  2.47048+02  0.0          0.0          0.0          0.0
  1.45656+03  0.0          0.0          0.0          1.19530-07
 115  11510  2  0  0      C21
    10.011
0
0
0
0
0
0
0
0
    0.10+00
    2.35+00
    5.44+00
    5.01+00
 125  12510  2  0  0      C22
    10.011
0
0
0
0
0
0
0
0
    0.10+00
    2.02+00
    4.11+00
    3.79+00
   5  1612  0  0  0      CA2301
    12.011
0
0
0
0
0
0
0
0
  1.58799-04  0.0          2.24492+00  0.0
  2.45014-05  0.0          4.39558+00  0.0
  2.20025-04  0.0          4.44714+00  0.0
  1.27191-03  0.0          4.54142+00  0.0
  2.44409+00  1.44472-01    0.0          0.0          0.0          4.60731+00
  6.25637-02  0.0          0.0          0.0          4.38336+00   3.66401-01
  0.0         0.0          0.0          4.61394+00
  83  2612  0  0  0      C=EF
```

12.011
0
0
0
0
0
0
0
0
7.59590-07 0.0 1.98075+00 0.0
3.35931-05 0.0 4.39723+00 0.0
2.54030-04 0.0 4.12727+00 0.0
1.95200-03 0.0 4.68837+00 0.0
1.76473+00 2.16030-01 0.0 0.0 0.0 4.60731+00
8.76041-02 0.0 0.0 0.0 3.73898+00 3.86029-01
0.0 0.0 0.0 4.98181+00
84 1429 0 0 0 SILICO
28.086
0
0
0
0
0
0
0
0
3.58831-03 0.0 2.68548+00 0.0
2.05949-03 0.0 1.84125+00 0.0
1.04995-02 0.0 2.10594+00 0.0
5.96917-02 0.0 2.15814+00 0.0
2.42897+00 2.54022-01 0.0 0.0 0.0 1.92720+00
1.19992-02 0.0 0.0 0.0 2.02642+00 7.26207-02
0.0 0.0 0.0 2.09845+00
39 4295 0 0 0 4045
94.906
0
0
0
0
0
0
0
0
7.52166-02 0.0 4.58875+00 0.0
1.03280+01 0.0 1.36973+01 0.0
1.04288+00 0.0 6.17757+00 0.0
5.19999+00 0.0 1.21054+01 0.0
4.38372+00 1.29814-01 0.0 0.0 0.0 8.36077+00
8.52333-03 0.0 0.0 0.0 5.08261+00 5.20802-02
0.0 0.0 0.0 6.90652+00
85 4396 0 0 0 1099
98.906 .103-07
0
0
0
0

```
0
0
0
0
0
   2.14092-01  0.0          6.30933+00  0.0
   4.76617+00  0.0          1.03103+01  0.0
   6.85232+01  0.0          7.32330+01  0.0
   8.96751+00  0.0          1.33494+01  0.0
   5.96324+00  1.30107-01    0.0         0.0          0.0          5.63472+00
   1.00104-02  0.0          0.0         0.0          4.72353+00   4.62726-02
   0.0         0.0          0.0         4.58189+00
  50  45103    0   0   0       PH103
      102.91
0
0
0
0
0
0
0
0
   1.60929-01  0.0          6.03693+00  0.0
   2.42437+00  0.0          9.65454+00  0.0
   2.25313+00  0.0          7.40941+00  0.0
   1.97192+02  0.0          2.09725+02  0.0
   5.74307+00  1.32630-01    0.0         0.0          0.0          7.22225+00
   7.92122-03  0.0          0.0         0.0          5.10350+00   5.27827-02
   0.0         0.0          0.0         1.25380+01
  53  54131    0   0   0       PE131
      130.91
0
0
0
0
0
0
0
0
   7.39432-02  0.0          6.12465+00  0.0
   4.35276+00  0.0          1.16570+01  0.0
   3.78496+02  0.0          1.53446+03  0.0
   4.48910+01  0.0          4.27962+01  0.0
   5.92620+00  1.24714-01    0.0         0.0          0.0          7.21830+00
   9.49365-02  0.0          0.0         0.0          1.15787+03   9.88164-02
   0.0         0.0          0.0         3.59520+00
  58  54135    0   0   0       PE135
      134.91                           .210185-04
0
0
0
0
0
0
0
0
```

```
0.0          0.0          3.97192+00   0.0
6.24433-02   0.0          7.79442+00   0.0
6.44383+01   0.0          1.75234+02   0.0
8.94174+05   0.0          1.00424+06   0.0
3.95146+00   1.20457-01   0.0          0.0          0.0          7.70671+00
2.52700-02   0.0          0.0          0.0          1.08173+02   2.42237+00
0.0          0.0          0.0          2.00062+05
55   55133   0   0   0      CS133
     132.91
0
0
0
0
0
0
0
0
0
5.31874-02   0.0          4.89534+00   0.0
7.53006+00   0.0          1.42713+01   0.0
1.43759+02   0.0          1.50353+02   0.0
1.04744+01   0.0          1.73501+01   0.0
4.59275+00   2.4?405-01   0.0          0.0          0.0          1.07293+01
1.19252-02   0.0          0.0          0.0          6.54027+00   5.47290-02
0.0          0.0          0.0          6.87550+00
60   60143   0   0   0      N0143
     142.91
0
0
0
0
0
0
0
0
4.55259-02   0.0          5.39702+00   0.0
4.81949+00   0.0          1.06019+01   0.0
6.27799+00   0.0          2.31268+01   0.0
1.17327+02   0.0          2.28459+02   0.0
6.22336+00   3.?607?-02   0.0          0.0          0.0          5.77398+00
9.42599-03   0.0          0.0          0.0          1.86415+01   2.07327-01
0.0          0.0          0.0          1.11132+02
61   60145   0   0   0      N0145
     144.91
0
0
0
0
0
0
0
0
4.15420-02   0.0          5.37542+00   0.0
1.49038+01   0.0          4.72734+01   0.0
6.81429+01   0.0          3.44580+01   0.0
2.24455+01   0.0          3.?1863+01   0.0
6.24797+00   3.8?110-02   0.0          0.0          0.0          3.24517+01
```

```
 1.78670-02  0.0          0.0          0.0          1.61718+01  1.08238-01
 0.0         0.0          0.0          1.57350+01
 63  61147   0   0   0       SM147
     144.91                    .83-08
 0
 0
 0
 0
 0
 0
 0
 0
 2.44474-01  0.0          6.35155+00   0.0
 3.15819+01  0.0          4.65645+01   0.0
 9.33429+02  0.0          1.25507+03   0.0
 6.73366+01  0.0          8.24895+01   0.0
 5.98788+00  4.91494-02   0.0          0.0          0.0         1.49736+01
 9.02243-03  0.0          0.0          0.0          3.21587+02  5.39804-02
 0.0         0.0          0.0          1.53529+01
 65  61148   0   0   0       SM148
     147.91                    .1933-06
 0
 0
 0
 0
 0
 0
 0
 0
 0
 3.30615-01  0.0          6.45895+00   0.0
 1.71293+02  0.0          1.71293+02   0.0
 1.74935+03  0.0          1.75471+03   0.0
 1.01005+04  0.0          1.23508+04   0.0
 6.50953+00  1.15567-01   0.0          0.0          0.0         3.35360-04
 5.66464-03  0.0          0.0          0.0          5.32721+00  3.27874-02
 0.0         0.0          0.0          2.25030+03
 67  62149   0   0   0       SM149
     148.91
 0
 0
 0
 0
 0
 0
 0
 0
 0
 1.98835-01  0.0          5.16765+00   0.0
 4.13584+01  0.0          7.72113+01   0.0
 1.68563+02  0.0          1.92794+02   0.0
 2.60573+04  0.0          2.61138+04   0.0
 4.77310+00  1.95970-01   0.0          0.0          0.0         3.58492+01
 3.46061-03  0.0          0.0          0.0          2.42109+01  2.40916-02
 0.0         0.0          0.0          4.59000+01
 68  62150   0   0   0       SM150
     149.92
 0
```

```
0
0
0
0
0
0
 4.55596-02  0.0          5.03319+00  0.0
 2.23647+01  0.0          4.78458+01  0.0
 6.49879+00  0.0          1.34525+01  0.0
 3.17979+01  0.0          4.74554+01  0.0
 4.79196+00  1.95570-01   0.0         0.0          0.0         2.47010+01
 7.78119-01  0.0          0.0         0.0          6.90545+00  4.82651-01
 0.0         0.0          0.0         1.56575+01
 49  62151   0  0  0      SM151
      150.92                          .231-09
0
0
0
0
0
0
0
0
0
 4.93991-01  0.0          5.43936+00  0.0
 4.53330+01  0.0          5.75160+01  0.0
 2.01032+02  0.0          3.05780+02  0.0
 1.67528+03  0.0          1.67528+03  0.0
 4.74980+00  1.95670-01   0.0         0.0          0.0         1.21750+01
 7.96774-03  0.0          0.0         0.0          1.47080+01  3.99919-02
 0.0         0.0          0.0         0.0
 70  62152   0  0  0      SM152
      151.92
0
0
0
0
0
0
0
0
 4.64954-02  0.0          5.03398+00  0.0
 2.10657+00  0.0          1.61516+01  0.0
 1.09106+03  0.0          2.45155+03  0.0
 8.09039+01  0.0          9.60443+01  0.0
 4.79191+00  1.95670-01   0.0         0.0          0.0         1.40301+01
 1.40690-02  0.0          0.0         0.0          1.40039+03  9.54289-02
 0.0         0.0          0.0         1.52404+01
 71  63153   0  0  0      SM153
      152.92
0
0
0
0
0
0
0
0
```

```
 2.00268-01  0.0          4.70694+00  0.0
 4.53443-01  0.0          5.40331+01  0.0
 4.33324+02  0.0          4.38875+02  0.0
 1.65021+02  0.0          1.71401+02  0.0
 4.23597+00  2.20744-01   0.0         0.0          0.0          8.64056+00
 4.42356-02  0.0          0.0         0.0          1.53528+01   1.97222-01
 0.0         0.0          0.0         5.98000+00
 72  63154   0  0  0      50154
     153.42                          .28-08

 4.74072-01  0.0          7.09283+00  0.0
 3.69015+01  0.0          4.14509+01  0.0
 9.71947+01  0.0          1.02186+02  0.0
 9.85715+02  0.0          9.96231+02  0.0
 6.40000+00  2.14+07-01   0.0         0.0          0.0          4.54399+00
 5.41226-03  0.0          0.0         0.0          4.96651+00   3.27858-02
 0.0         0.0          0.0         1.05160+01
 73  63155   0  0  0      50155
     154.92                          .44-08

 1.67793-01  0.0          5.32796+00  0.0
 8.59836+01  0.0          8.33127+01  0.0
 9.07073+02  0.0          9.14483+02  0.0
 5.23723+03  0.0          5.23724+03  0.0
 6.55259+00  2.07570-01   0.0         0.0          0.0          3.32150+00
 7.60465-03  0.0          0.0         0.0          7.35235+00   5.26477-02
 0.0         0.0          0.0         0.0
 86  86120   0  0  0      MSAG23
     120.0

 2.32047-02  0.0          4.20795+00  0.0
 1.01082+00  0.0          1.25204+01  0.0
```

```
C
C
      1.06533+00  0.0          9.54010+00  0.0
      2.37243+00  0.0          1.38033+01  0.0
C     8.08244+00  1.47312-01    0.0         0.0         0.0         1.14969+01
      1.30793-02  0.0          0.0         0.0         8.38930+00  8.24094-02
      0.0         0.0          0.0         1.13309+01
C     87   87120   0   0   0       VS4625
          120.0
      0
C     0
      0
      0
C     0
      0
      0
C     0
      0
      3.92694-02  0.0          2.02124+00  0.0
C     1.05242+00  0.0          1.21935+01  0.0
      1.34484+00  0.0          9.47583+00  0.0
      1.72027+00  0.0          1.24053+01  0.0
C     7.84297+00  1.46003-01    0.0         0.0         0.0         1.11283+01
      1.23564-02  0.0          0.0         0.0         8.05436+00  7.76267-02
      0.0         0.0          0.0         1.10850+01
C     9
      FOUR.G3.YC.CS . SET 2
      -2  40   4   1   0   0
C         0.375        0.024        0.0         0.0
         15.0+06     0.14340+06       17.6        2.38
      1.5066+06   1.7947+03    6.472+00    6.339-02
C     6.434-10    2.459-08     1.561-06    1.022-05
         0.0127      0.0317       0.12        0.315       1.36        3.8
      0
C     0
      0
      8   92233   0   0   0      0233
C        233.04                  3.14-11
      0
      0
C     0
      0
      0
C                                                                  .0006       .0020
         .0017       .0018       .0003       .0002
      0
C     0
      2.06149+00  1.96632+00   4.42363+00  2.60514+00
      1.78841+01  1.56358+01   2.76870+01  2.50291+00
C     1.14053+02  9.62424+01   1.26804+02  2.50290+00
      2.61872+02  2.33733+02   2.65987+02  2.50000+00
      2.71221+00  1.49966-01   0.0         0.0         0.0         9.79411+00
C     8.78603-03  0.0          0.0         0.0         1.26968+00  5.82115-02
      0.0         0.0          0.0         4.00300+00
      10   92235   0   0   0      0235
C        235.05                  3.29-11
      0
      0
C     0
      0
      0
C
```

```
                                                                                .00052      0.00346
        0.0031        0.00524       0.00142       0.00066
 0
 0
      1.39898+00   1.27033+00   5.40597+00   2.56026+00
      1.89305+01   1.25851+01   2.42743+01   2.43016+00
      6.27115+01   3.43434+01   7.77132+01   2.43000+00
      2.19357+02   1.24431+02   2.32064+02   2.43000+00
      3.84490+00   1.22145-01   0.0          0.0          0.0          1.03392+01
      9.54719-03   0.0          0.0          0.0          1.24010+01   3.57869-02
      0.0          0.0          0.0          1.06901+01
      14   94239   0   0   0        91239
     232.05                    3.34-11
 0
 0
 0
 0
 0

                                                                                .0020       .018
        .0013         .0026         .0005         .0003
 0
 0
      1.77736+00   1.70474+00   5.03663+00   3.04455+00
      1.95408+01   1.05937+01   3.05826+01   2.87045+00
      9.23445+01   5.53217+01   1.04567+02   2.87000+00
      1.32792+03   7.56321+02   1.23699+03   2.89000+00
      4.16737+00   9.12710-02   0.0          0.0          0.0          1.19819+01
      1.05121-02   0.0          0.0          0.0          1.23072+01   4.52438-02
      0.0          0.0          0.0          2.90700+01
      16   94241   0   0   0        91241
     241.06                    3.37-11       .15-08
 0
 0
 0
 0
 0

                                                                                .00015      .00365
        .00275        .0062         .0024         .0005
 0
 0
      1.74303+00   1.55418+00   6.09200+00   3.18751+00
      2.24935+01   1.56617+01   3.27885+01   3.03043+00
      2.19130+02   1.23336+02   2.33332+02   3.03000+00
      8.42100+02   8.05585+02   9.00552+02   3.03000+00
      3.95875+00   3.65223-01   0.0          0.0          0.0          1.00844+01
      1.06048-02   0.0          0.0          0.0          1.41521+01   4.98861-02
      0.0          0.0          0.0          1.54520+01
      81   92232   0   0   0        91232
     232.04                    3.13-11       .3-09
 0
 0
 0
 0
 0
 0
 0
 0

      1.01337+00   7.07200-01   9.10106+00   2.99008+00
```

```
 1.92592+01  1.08743+01  3.44315+01  2.50328+00
 1.65514+02  4.23003+01  1.72550+02  2.50300+00
 4.20969+01  2.24163+01  5.33555+01  2.50300+00
 5.72522+00  2.35243+00  0.0         0.0         0.0         1.61640+01
 8.29925-03  0.0         0.0         0.0         1.32900+01  4.59685-02
 0.0         0.0         0.0         1.12690+01
 6  90232  0  0  0  [4232
      232.04                3.14-11
0
0
0
0
0
                                                 0.0017      0.0074
  0.0077      0.0221      0.0085      0.0021
0
0
 1.67250-01  3.57550-02  5.34430+00  2.40137+00
 4.00577+00  5.55306-15  2.24742+01  0.0
 1.77361-01  0.0         1.14113+01  0.0
 2.56462+00  0.0         1.48530+01  0.0
 4.09514+00  1.41911-01  0.0         0.0         0.0         1.84571+01
 1.13191-02  0.0         0.0         0.0         1.15838+01  5.03630-02
 0.0         0.0         0.0         1.19984+01
 9  92234  0  0  0  0234
      234.04                3.20-11
0
0
0
0
0
0
0
0
 1.09460+00  3.62071-01  6.31656+00  2.68486+00
 7.75802+00  3.04308-03  2.59927+01  2.50701+00
 2.65246+02  2.33211-01  3.15471+02  2.50000+00
 2.92195+01  2.54117-03  4.34587+01  2.50500+00
 5.20000+00  2.10527-01  0.0         0.0         0.0         1.82281+01
 6.55730-03  0.0         0.0         0.0         5.01882+01  3.67775-02
 0.0         0.0         0.0         1.42402+01
 12  92232  0  0  0  0234
      238.05                3.31-11
0
0
0
0
0
                                                 0.000475    0.00536
  0.00634     0.01519     0.00481     0.00294
0
0
 1.91245-01  3.75320-02  5.45743+00  2.90869+00
 1.22929+01  5.25295-11  3.57851+01  0.0
 6.53815+01  4.05454-11  7.79143+01  0.0
 1.05312+00  0.0         1.17433+01  0.0
 5.02555+00  2.50647-01  0.0         0.0         0.0         2.36330+01
 6.01504-02  0.0         0.0         0.0         1.24010+01  3.57869-02
```

```
 0.0          0.0          0.0          1.0?901+01
 15   24240   0   0   0       21240
      240.05                 3.3?-11
 0
 0
 0
 0
 0
                                                    .00028       .0024
      .00165        .0033        .00125       .00024
 0
 0
 1.14039+00  9.?9130-01  6.01394+00  3.10180+00
 1.35129+01  1.57140-02  3.?3?47+01  2.90023+00
 2.45916+00  0.0         1.34443+01  0.0
 1.24508+03  0.0         1.3?35?+03  0.0
 4.71546+00  1.44035-01  0.0         0.0          0.0          2.34241+01
 1.10344-02  0.0         0.0         0.0          1.09242+01   6.14572-02
 0.0         0.0         0.0         1.38460+02
  7   91233   0   0   0       24233
      233.04                 3.16-11      .297-06
 0
 0
 0
 0
 0
 0
 0
 0
 8.57591-01  6.?7?55-01  6.41424+00  3.04249+00
 1.32242+01  2.3?332-03  2.?4552+01  2.50905+00
 1.31400+02  0.0         1.?3554+02  0.0
 7.06072+01  0.0         8.?5?10+01  0.0
 4.66084+00  5.?5?12-01  0.0         0.0          0.0          1.22219+01
 9.06624-03  0.0         0.0         0.0          1.22051+01   4.89215-02
 0.0         0.0         0.0         1.49738+01
 82   91231   0   0   0       24231
      231.04                 3.12-11
 0
 0
 0
 0
 0
 0
 0
 0
 8.49154-01  ?.?0154-01  6.37723+00  3.04355+00
 1.37944+01  2.3?332-03  2.?3441+01  2.50905+00
 1.01969+02  4.?5574-05  1.14020+02  2.50000+00
 3.79484+02  1.?2??4-02  3.?0731+02  2.50000+00
 4.61071+00  9.?2?0?-01  0.0         0.0          0.0          1.25396+01
 1.00496-02  0.0         0.0         0.0          1.20033+01   4.77166-02
 0.0         0.0         0.1         2.12460+01
 13   93234   0   0   0       ?2234
      239.05                 3.32-11      .341-05
 0
 0
```

0
0
0
0
0
0

1.15211+00 9.77751-01 5.84456+00 2.68879+00
1.96821+01 6.29623-04 3.17010+01 2.51398+00
1.28638+02 0.0 1.41372+02 0.0
2.05751+01 0.0 3.03715+01 0.0
4.25773+00 4.44723-01 0.0 0.0 0.0 1.20107+01
8.24249-03 0.0 0.0 0.0 1.26998+01 3.42124-01
0.0 0.0 0.0 9.79650+00
11 92236 0 0 0 0235
236.05 3.25-11

0
0
0
0
0

.005 .012 .008 .002 .00056 .0051

0
0

5.65974-01 3.38046-01 5.83911+00 2.75469+00
7.46001+00 0.0 2.73284+01 0.0
1.14395+02 0.0 1.31364+02 0.0
2.35138+00 0.0 1.43425+01 0.0
5.10649+00 2.28632-01 0.0 0.0 0.0 1.98609+01
7.66378-03 0.0 0.0 0.0 1.69285+01 4.54945-02
0.0 0.0 0.0 1.19912+01
17 94242 0 0 0 0242
242.06 3.38-11

0
0
0
0
0

.00165 .0033 .00125 .00024 .00028 .0024

0
0

1.16038+00 9.69130-01 5.81954+00 3.10180+00
5.82875+00 1.57140-02 3.13415+01 2.90023+00
4.92482+02 0.0 5.42319+02 0.0
1.02713+01 0.0 2.10797+01 0.0
4.71547+00 1.44065-01 0.0 0.0 0.0 2.55056+02
7.14095-03 0.0 0.0 0.0 4.83875+01 1.44954+00
0.0 0.0 0.0 1.08084+01
18 93237 0 0 0 0237
237.05 3.28-11

0
0
0
0
0
0

```
      1.39713+00  4.77546-01  6.0496[illegible]+00  2.6[illegible]2+00
      1.50734+01  6.2[illegible]23-04  4.0[illegible]91+01  2.51394+00
      8.31042+01  2.[illegible]710-03  8.[illegible]93+01  2.30000+00
      1.25870+02  0.0            1.[illegible]39+02  0.0
      4.21779+00  4.[illegible]723-01  0.0          0.0          0.0          2.53869+01
      8.37754-03  0.0            0.0          0.0          1.11035+01   4.20604-02
      0.0         0.0            0.0          1.27740+01
    105   10510   1   0  10      SELF S-. 4D
        10.013
      4.79423-01  0.0            0.0          0.0          0.0
      2.77019+01  0.0            0.0          0.0          0.0
      2.47948+02  0.0            0.0          0.0          0.0
      1.41655+03  0.0            0.0          0.0          1.60130-07
    115   11510   2   0   0      CR1
        10.211
        0.10+00
        2.36+00
        5.44+00
        5.01+00
    125   12510   2   0   0      CR2
        10.211
        0.10+00
        2.02+00
        4.11+00
        3.79+00
      5   1612    0   0   0      CA-40
        10.011
```

```
 1.58789-04  0.0          2.26492+00  0.0
 2.45014-05  0.0          4.33453+00  0.0
 2.20025-04  0.0          4.48714+00  0.0
 1.27191-03  0.0          4.54142+00  0.0
 2.66809+00  1.96572-01   0.0         0.0          0.0          4.60731+00
 6.25637-02  0.0          0.0         0.0          4.38336+00   3.66401-01
 0.0         0.0          0.0         4.61394+00
 83    2412   0   0   0      OREF
   12.011
 7.59580-07  0.0          1.98075+00  0.0
 3.35031-05  0.0          4.38728+00  0.0
 2.54030-04  0.0          4.12727+00  0.0
 1.35200-03  0.0          4.54375+00  0.0
 1.75473+00  2.16030-01   0.0         0.0          0.0          4.60731+00
 8.76041-02  0.0          0.0         0.0          3.73898+00   3.88029-01
 0.0         0.0          0.0         4.88181+00
 84    1428   0   0   0      SILICO
   28.086
 3.53831-03  0.0          2.65543+00  0.0
 2.05849-03  0.0          1.34125+00  0.0
 1.04386-02  0.0          2.10994+00  0.0
 5.04917-02  0.0          2.13814+00  0.0
 2.42887+00  2.53022-01   0.0         0.0          0.0          1.92720+00
 1.19482-02  0.0          0.0         0.0          2.02682+00   7.26207-02
 0.0         0.0          0.0         2.09845+00
 90    4295   0   0   0      MOLY
   94.906
```

```
 7.52166-02  0.0          4.[illegible]+00  0.0
 1.03340+01  0.0          1.[illegible]+01  0.0
 1.04288+00  0.0          6.17757+00  0.0
 5.19994+00  0.0          1.21066+01  0.0
 4.38372+00  1.[illegible]-01  0.0  0.0  0.0  8.36077+00
 8.52933-03  0.0          0.0  0.0  5.08261+00  5.20802-02
 0.0  0.0  0.0  6.40652+00
 85  4359  0  0  0  TC 39
     98.90                .103-07

 2.14992-01  0.0          6.30833+00  0.0
 4.76617+00  0.0          1.0410?+01  0.0
 6.95232+01  0.0          7.42930+01  0.0
 4.96751+00  0.0          1.3[illegible]+01  0.0
 5.06324+00  1.30107-01  0.0  0.0  0.0  5.63472+00
 1.00104-02  0.0          0.0  0.0  4.72353+00  4.62726-02
 0.0  0.0  0.0  4.[illegible]89+00
 50  45103  0  0  0  24103
     102.91

 1.60929-01  0.0          6.03683+00  0.0
 2.42437+00  0.0          3.[illegible]+00  0.0
 2.25313+00  0.0          7.40941+00  0.0
 1.97194+02  0.0          2.[illegible]+02  0.0
 5.74307+00  1.32830-01  0.0  0.0  0.0  7.22225+00
 7.92122-03  0.0          0.0  0.0  5.10350+00  5.27827-02
 0.0  0.0  0.0  1.25380+01
 53  54131  0  0  0  2E131
     130.91

 7.33432-02  0.0          [illegible]  0.0
 4.35374+00  0.0          1.[illegible]+01  0.0
 3.78494+02  0.0          1.[illegible]+03  0.0
 4.44010+01  0.0          4.[illegible]+01  0.0
```

5.92620+00 1.24713-01 0.0 0.0 0.0 7.21830+00
9.49365-02 0.0 0.0 0.0 1.15787+03 9.88164-02
0.0 0.0 0.0 3.99520+00
59 54135 0 0 0 54135
134.91 .210165-04

0.0 0.0 3.97192+00 0.0
6.24433-02 0.0 7.79442+00 0.0
6.46393+01 0.0 1.75234+02 0.0
8.94178+05 0.0 1.0942++06 0.0
3.85146+00 1.20457-01 0.0 0.0 0.0 7.70671+00
2.52700-02 0.0 0.0 0.0 1.08173+02 2.42237+00
0.0 0.0 0.0 2.00062+05
55 55133 0 0 0 55133
132.91

5.31874-02 0.0 4.59534+00 0.0
7.53006+00 0.0 1.82713+01 0.0
1.43758+02 0.0 1.50353+02 0.0
1.04746+01 0.0 1.73501+01 0.0
4.59275+00 2.49405-01 0.0 0.0 0.0 1.07293+01
1.19252-02 0.0 0.0 0.0 6.54027+00 5.47290-02
0.0 0.0 0.0 6.87550+00
60 60143 0 0 0 60143
142.91

4.55259-02 0.0 5.35709+00 0.0
4.81649+00 0.0 1.06014+01 0.0
6.27734+00 0.0 2.51263+01 0.0
1.17327+02 0.0 2.24459+02 0.0
6.22336+00 6.42207-02 0.0 0.0 0.0 5.77398+00
9.42584-03 0.0 0.0 0.0 1.86415+01 2.07327-01
0.0 0.0 0.0 1.11132+02
61 60145 0 0 0 60145
144.91

```
  0
  0
  0
  0
  0
  0
  0
  0
  0
    4.16420-02  0.0          6.37842+00  0.0
    1.48038+01  0.0          4.72734+01  0.0
    6.81930+01  0.0          8.44680+01  0.0
    2.24455+01  0.0          3.81805+01  0.0
    6.24797+00  8.88110-02   0.0         0.0          0.0          3.24517+01
    1.78679-02  0.0          0.0         0.0          1.61718+01   1.08238-01
    0.0         0.0          0.0         1.57350+01
    63  61147    0   0   0     20147
        146.91                            .83-08
  0
  0
  0
  0
  0
  0
  0
  0
  0
    2.64474-01  0.0          6.35155+00  0.0
    3.15219+01  0.0          4.65645+01  0.0
    9.33429+02  0.0          1.25507+03  0.0
    6.73366+01  0.0          4.26895+01  0.0
    5.98788+00  9.91494-02   0.0         0.0          0.0          1.49736+01
    9.02243-03  0.0          0.0         0.0          3.21587+02   5.39804-02
    0.0         0.0          0.0         1.53529+01
    65  61148    0   0   0     29148
        147.91                           .1933-06
  0
  0
  0
  0
  0
  0
  0
  0
  0
    3.30615-01  0.0          6.95495+00  0.0
    1.71249+02  0.0          1.71295+02  0.0
    1.74935+03  0.0          1.75471+03  0.0
    1.01935+04  0.0          1.23503+04  0.0
    6.50953+00  1.14407-01   0.0         0.0          0.0          3.35360-04
    5.66444-03  0.0          0.0         0.0          5.32721+00   3.27874-02
    0.0         0.0          0.0         2.25030+03
    67  6:149    0   0   0     59149
        146.91
  0
  0
  0
  0
  0
```

```
 1.99835-01  0.0          5.16765+00  0.0
 4.13594+01  0.0          7.72113+01  0.0
 1.68553+02  0.0          1.92793+02  0.0
 2.60479+04  0.0          2.61134+04  0.0
 4.77310+00  1.95670-01   0.0         0.0          0.0          3.58492+01
 3.66051-03  0.0          0.0         0.0          2.42109+01   2.40916-02
 0.0         0.0          0.0         4.59000+01
 68   62150   0   0   0       S-150
   149.92
0
0
0
0
0
0
0
0
 4.55536-02  0.0          5.03319+00  0.0
 2.23647+01  0.0          4.78458+01  0.0
 6.48978+00  0.0          1.34525+01  0.0
 3.17979+01  0.0          4.74554+01  0.0
 4.79195+00  1.95670-01   0.0         0.0          0.0          2.47010+01
 7.78118-01  0.0          0.0         0.0          6.90545+00   4.82651-01
 0.0         0.0          0.0         1.56575+01
 69   62151   0   0   0       SM151
   150.92                                  231-09
0
0
0
0
0
0
0
0
 4.93991-01  0.0          5.43935+00  0.0
 4.53330+01  0.0          5.75160+01  0.0
 2.91032+02  0.0          3.05780+02  0.0
 1.67523+03  0.0          1.67523+03  0.0
 4.74640+00  1.95670-01   0.0         0.0          0.0          1.21750+01
 7.96774-03  0.0          0.0         0.0          1.47080+01   3.99919-02
 0.0         0.0          0.0         0.0
 70   62152   0   0   0       SM152
   151.92
0
0
0
0
0
0
0
0
 4.54054-02  0.0          5.03393+00  0.0
```

```
 2.10657+00  0.0          1.51513+01  0.0
 1.04106+03  0.0          2.15153+03  0.0
 8.08033+01  0.0          9.53443+01  0.0
 4.79141+00  1.05570-01   0.0         0.0          0.0          1.40301+01
 1.49440-02  0.0          0.0         0.0          1.40039+03   9.54289-02
 0.0         0.0          0.0         1.52404+01
 71  63153   0   0   0    50153
     152.92

 2.00264-01  0.0          4.70594+00  0.0
 4.53463+01  0.0          5.40331+01  0.0
 4.33326+02  0.0          4.58875+02  0.0
 1.45921+02  0.0          1.71401+02  0.0
 4.28597+00  2.20744-01   0.0         0.0          0.0          8.64056+00
 4.62356-02  0.0          0.0         0.0          1.53528+01   1.97222-01
 0.0         0.0          0.0         5.9+000+00
 72  63154   0   0   0    50154
     153.92                           .28-05

 4.74072-01  0.0          7.03284+00  0.0
 3.49015+01  0.0          4.16502+01  0.0
 9.71467+01  0.0          1.02183+02  0.0
 9.85715+02  0.0          9.45231+02  0.0
 6.40000+00  2.12307-01   0.0         0.0          0.0          4.54399+00
 5.41256-03  0.0          0.0         0.0          4.96651+00   3.27858-02
 0.0         0.0          0.0         1.05160+01
 73  63155   0   0   0    50155
     154.92                           .44-04

 1.47744-01  0.0          6.17543+00  0.0
 4.59835+01  0.0          5.49127+01  0.0
 4.07073+02  0.0          4.13453+02  0.0
 5.23724+03  0.0          5.27272+03  0.0
 6.55253+00  2.07257-01   0.0         0.0          0.0          3.32150+00
 7.40465-03  0.0          0.0         0.0          7.35235+00   5.26477-02
```

```
      0.0          0.0          0.0          0.0
      86   96120   0   0   0       954323
     120.0
      0
      0
      0
      0
      0
      0
      0
      0
      0
     2.82097-02  0.0          8.25795+00  0.0
     1.01082+00  0.0          1.25203+01  0.0
     1.06839+00  0.0          9.54010+00  0.0
     2.27243+00  0.0          1.34033+01  0.0
     8.08244+00  1.47312-01   0.0         0.0          0.0          1.14969+01
     1.30793-02  0.0          0.0         0.0          8.38930+00   8.24094-02
     0.0         0.0          0.0         1.13309+01
     87   97120   0   0   0       954525
     120.0
      0
      0
      0
      0
      0
      0
      0
      0
      0
     3.22594-02  0.0          8.02124+00  0.0
     1.05252+00  0.0          1.21935+01  0.0
     1.34494+00  0.0          9.47583+00  0.0
     1.72027+00  0.0          1.24053+01  0.0
     7.84297+00  1.46003-01   0.0         0.0          0.0          1.11283+01
     1.23544-02  0.0          0.0         0.0          8.05436+00   7.76267-02
     0.0         0.0          0.0         1.10650+01
     9
    FOUR GP HOT 4C CS , SET3
      -2  40   4   1   0   0
         0.976        0.024          0.0          0.0
        15.0+06       0.183+06         17.6         2.38
      1.5056+06    1.7947+03     8.472+00     8.339-02
       4.434-10     2.489-08     1.561-06     1.022-05
         0.0127       0.0317        0.12        0.315        1.36         3.8
      0
      0
      0
       8   92233   0   0   0       9233
          233.04                 3.14-11
      0
      0
      0
      0
      0
                                                            .0006        .0020
         .0017        .0018        .0003        .0002
      0
      0
```

```
 2.0514+00  1.5032+00  6.4236+00  2.0514+00
 1.7834+01  1.5548+01  2.7571+01  2.0291+00
 1.1405+02  9.8224+01  1.2504+02  2.0290+00
 2.6147+02  2.3174+02  2.8557+02  2.0000+00
 2.7122+00  1.6995-01  0.0        0.0        0.0        9.7941+00
 8.7843-03  0.0        0.0        0.0        1.2696+00  5.8211E-02
 0.0        0.0        0.0        4.0030+00
 10  92235  0  0  0  0235
 235.05                3.23-11

                                                  .00052     0.00346
     0.0031     0.00024     0.0018     0.00066

 1.3989+00  1.2703+00  5.6055+00  2.5602+00
 1.8930+01  1.6545+01  2.4274+01  2.4301+00
 6.2711+01  5.4834+01  7.7713+01  2.4300+00
 2.1935+02  1.9443+02  2.4204+02  2.4300+00
 3.8448+00  1.6215-01  0.0        0.0        0.0        1.0339+01
 9.5671E-03 0.0        0.0        0.0        1.2401+01  3.5786E-02
 0.0        0.0        0.0        1.0690+01
 14  94239  0  0  0  0239
 239.05                3.34-11

                                                  .0020      .0018
     .0013      .0020      .0005      .0003

 1.7773+00  1.7047+00  5.0366+00  3.0445+00
 1.8540+01  1.6493+01  3.0533+01  2.8704+00
 9.2344+01  8.2321+01  1.0467+02  2.8700+00
 1.2279+03  7.5832+02  1.2559+03  2.4900+00
 4.1673+00  3.1471+00  0.0        0.0        0.0        1.1981+01
 1.0512E-02 0.0        0.0        0.0        1.2307+01  4.5243E-02
 0.0        0.0        0.0        2.9070+01
 16  94241  0  0  0  0241
 241.06                3.37-11     .15-08

                                                  .00015     .00365
     .00275     .0062      .0024      .0005

 1.7480+00  1.5581+00  6.0920+00  3.1875+00
 2.2493E+01 1.9851E+01 3.2743E+01 3.0304E+00
 2.1913E+02 1.9333E+02 2.3333E+02 3.0400E+00
 8.8210E+02 7.8556E+02 9.0552E+02 3.0300E+00
 3.9587E+00 3.5322E-01 0.0        0.0        0.0        1.0084E+01
```

```
 1.06068-02  0.0          0.0          0.0          1.41521+01  4.98861-02
 0.0         0.0          0.0          1.44520+01
 81  92232   0  0  0      J232
     232.04               3.14-11      .3-09
0
0
0
0
0
0
0
0
 1.01337+00  9.07260-01   3.10106+00   2.39008+00
 1.82592+01  1.09743+01   3.44315+01   2.50328+00
 1.45514+02  9.88003+01   1.78859+02   2.50300+00
 4.20468+01  2.24183+01   5.33358+01   2.50300+00
 5.72522+00  2.36240+00   0.0          0.0          0.0         1.61640+01
 8.28925-03  0.0          0.0          0.0          1.32900+01  4.59685-02
 0.0         0.0          0.0          1.12690+01
 6  90232    0  0  0      T=232
     232.04               3.14-11
0
0
0
0
0
                                                    0.0017      0.0074
     0.0077      0.0221      0.0085      0.0021
0
0
 1.47250-01  3.57550-02   5.34430+00   2.40137+00
 4.00577+00  5.58306-15   2.24742+01   0.0
 1.77351-01  0.0          1.11115+01   0.0
 2.56462+00  0.0          1.45530+01   0.0
 4.99514+00  1.31911-01   0.0          0.0          0.0         1.84571+01
 1.13191-02  0.0          0.0          0.0          1.15838+01  5.03630-02
 0.0         0.0          0.0          1.19984+01
 9  92234    0  0  0      J234
     234.04               3.20-11
0
0
0
0
0
0
0
0
 1.03460+00  3.62071-01   5.31550+00   2.68486+00
 7.75902+00  3.04306-03   2.56927+01   2.50701+00
 2.65246+02  2.33211-01   4.15471+02   2.50000+00
 2.92195+01  2.54117-03   4.46567+01   2.50500+00
 5.20000+00  2.10627-01   0.0          0.0          0.0         1.82281+01
 6.55730-03  0.0          0.0          0.0          5.01882+01  3.67775-02
 0.0         0.0          0.0          1.42402+01
 12  92238   0  0  0      J234
     239.05               3.31-11
0
```

0.000475 0.00536

0.00634 0.01519 0.00481 0.00294

1.81245-01 5.76320-02 5.45743+00 2.90869+00
1.22929+01 5.25206-11 3.56861+01 0.0
6.53815+01 9.95552-11 7.79183+01 0.0
1.05319+00 0.0 1.17433+01 0.0
5.02555+00 2.50637-01 0.0 0.0 0.0 2.36330+01
6.01594-02 0.0 0.0 0.0 1.24010+01 3.57869-02
0.0 0.0 0.0 1.06901+01
15 94240 0 0 0 90240
240.05 3.36-11

.0002B .0024

.00165 .0033 .00125 .00024

1.15039+00 5.59120-01 5.9199+00 3.10180+00
1.35129+01 1.57140-02 3.59479+01 2.90023+00
2.45916+00 0.0 1.34443+01 0.0
1.24503+03 0.0 1.3435+03 0.0
4.71545+00 1.44045-01 0.0 0.0 0.0 2.34241+01
1.10344-02 0.0 0.0 0.0 1.09242+01 6.14572-02
0.0 0.0 0.0 1.38440+02
7 91233 0 0 0 94233
233.04 3.15-11 .297-06

8.57691-01 5.37885-01 5.4142+00 3.04249+00
1.32242+01 2.3-332-03 2.54552+01 2.50905+00
1.31400+02 0.0 1.53554+02 0.0
7.06072+01 0.0 8.5-510+01 0.0
4.6503++00 4.95713-01 0.0 0.0 0.0 1.22219+01
9.06624-03 0.0 0.0 0.0 1.22051+01 4.89215-02
0.0 0.0 0.0 1.49739+01
82 91231 0 0 0 94231
231.04 3.12-11

```
 8.49154-01  6.40156-01  5.37723+00  3.04355+00
 1.37944+01  2.49332-03  2.03441+01  2.50905+00
 1.01969+02  4.45579-06  1.14020+02  2.50000+00
 3.78424+02  1.72243-02  3.99730+02  2.50000+00
 4.61971+00  9.04366-01  0.0         0.0         0.0         1.25396+01
 1.00646-02  0.0         0.0         0.0         1.20033+01  4.77166-02
 0.0         0.0         0.0         2.12460+01
 13  93239   0   0   0      NP239
     239.05                 3.32-11     .341-05

 1.15211+00  9.77751-01  5.44456+00  2.68879+00
 1.96821+01  6.29623-04  3.17010+01  2.51378+00
 1.28634+02  0.0         1.41372+02  0.0
 2.05751+01  0.0         3.03715+01  0.0
 4.25773+00  4.34723-01  0.0         0.0         0.0         1.20107+01
 8.24244-03  0.0         0.0         0.0         1.26998+01  3.42124-01
 0.0         0.0         0.0         9.79650+00
 11  92236   0   0   0      U235
     236.05                 3.25-11

                                                 .00056      .0051
     .006        .012        .008        .002

 5.65974-01  3.35046-01  5.49910+00  2.75489+00
 7.46901+00  0.0         2.73246+01  0.0
 1.14305+02  0.0         1.31354+02  0.0
 2.35137+00  0.0         1.43423+01  0.0
 5.10645+00  2.26632-01  0.0         0.0         0.0         1.98609+01
 7.66378-03  0.0         0.0         0.0         1.69285+01  4.54945-02
 0.0         0.0         0.0         1.19912+01
 17  94242   0   0   0      U242
     242.06                 3.34-11

                                                 .00028      .0024
    .00165       .0033       .00125      .00024

 1.14034+00  9.69140-01  5.01504+00  3.10180+00
 5.92875+00  1.57140-02  3.13415+01  2.90023+00
```

```
      4.92482+02  0.0         5.42314+02  0.0
      1.02713+01  0.0         2.10797+01  0.0
      4.71547+00  1.44095-01  0.0         0.0          0.0          2.55056+02
      7.14095-03  0.0         0.0         0.0          4.83875+01   1.44954+00
      0.0         0.0         0.0         1.08084+01
      18   93237   0   0   0      MP237
     237.05                     3.23-11
    0
    0
    0
    0
    0
    0
    0
    0
      1.39713+00  9.77586-01  6.04963+00  2.68882+00
      1.50794+01  6.29623-04  4.05491+01  2.51398+00
      8.31042+01  2.98710-03  9.42498+01  2.50000+00
      1.25870+02  0.0         1.39549+02  0.0
      4.21778+00  4.34723-01  0.0         0.0          0.0          2.53869+01
      8.37754-03  0.0         0.0         0.0          1.11035+01   4.20604-02
      0.0         0.0         0.0         1.27790+01
    105   10510   1   0   10      SELF SH. HP
     10.013
    0
    0
    0
    0
    0
    0
    0
    0
      4.79423-01  0.0         0.0         0.0          0.0
      2.77013+01  0.0         0.0         0.0          0.0
      2.47948+02  0.0         0.0         0.0          0.0
      1.35554+03  0.0         0.0         0.0          2.16300-07
    115   11510   2   0   0      CR1
      10.011
    0
    0
    0
    0
    0
    0
    0
    0
    0
      0.10+00
      2.34+00
      5.44+00
      5.01+00
    125   12510   2   0   0      CR2
     10.011
    0
    0
    0
    0
```

```
        0.10+00
        2.02+00
        4.11+00
        3.79+00
     5    1612    0    0    0       CARBON
       12.011
 0
 0
 0
 0
 0
 0
 0
 0
   1.58789-04  0.0          2.25492+00  0.0
   2.45014-05  0.0          4.39654+00  0.0
   2.20025-04  0.0          4.48714+00  0.0
   1.27191-03  0.0          4.54142+00  0.0
   2.66809+00  1.95672-01    0.0         0.0          0.0          4.60731+00
   6.25637-02  0.0          0.0         0.0          4.38336+00   3.66401-01
   0.0         0.0          0.0         4.61394+00
  83    2412    0    0    0       CREF
       12.011
 0
 0
 0
 0
 0
 0
 0
 0
   7.59580-07  0.0          1.99875+00  0.0
   3.35931-05  0.0          4.38724+00  0.0
   2.54030-04  0.0          4.12727+00  0.0
   1.95200-03  0.0          4.33376+00  0.0
   1.76473+00  2.16020-01    0.0         0.0          0.0          4.60731+00
   8.76041-02  0.0          0.0         0.0          3.73898+00   3.88029-01
   0.0         0.0          0.0         4.88181+00
  84    1427    0    0    0       SILICO
       28.086
 0
 0
 0
 0
 0
 0
 0
 0
   3.59831-03  0.0          2.05544+00  0.0
   2.05949-03  0.0          1.94123+00  0.0
   1.04986-02  0.0          2.10996+00  0.0
```

```
 5.96917-02  0.0          2.1691++00  0.0
 2.42887+00  2.54022-01   0.0         0.0          0.0          1.92720+00
 1.19832-02  0.0          0.0         0.0          2.02682+00   7.26207-02
 0.0         0.0          0.0         2.09545+00
 39   4295   0.   0   0      M045
    94.906
0
0
0
0
0
0
0
0
 7.52166-02  0.0          4.59875+00  0.0
 1.03230+01  0.0          1.86973+01  0.0
 1.04238+00  0.0          6.17757+00  0.0
 5.19938+00  0.0          1.21064+01  0.0
 4.38372+00  1.24514-01   0.0         0.0          0.0          8.36077+00
 8.52933-03  0.0          0.0         0.0          5.09261+00   5.20802-02
 0.0         0.0          0.0         6.90652+00
 85   4399   0   0   0      TC99
    99.906                          .103-07
0
0
0
0
0
0
0
0
 2.14982-01  0.0          4.30833+00  0.0
 4.76617+00  0.0          1.2410++01  0.0
 6.85232+01  0.0          7.32930+01  0.0
 8.96751+00  0.0          1.32494+01  0.0
 5.96324+00  1.30107-01   0.0         0.0          0.0          5.63472+00
 1.00104-02  0.0          0.0         0.0          4.72353+00   4.62726-02
 0.0         0.0          0.0         4.98189+00
 50   45103  0   0   0      RH103
    102.91
0
0
0
0
0
0
0
0
 1.60929-01  0.0          6.03583+00  0.0
 2.42437+00  0.0          9.5545++00  0.0
 2.25313+00  0.0          7.40941+00  0.0
 1.97158+02  0.0          2.09725+02  0.0
 5.74307+00  1.32830-01   0.0         0.0          0.0          7.22225+00
 7.92122-03  0.0          0.0         0.0          5.10350+00   5.27827-02
 0.0         0.0          0.0         1.25380+01
 53   54131  0   0   0      XE131
```

```
      130.91
    0
    0
    0
    0
    0
    0
    0
    0
      7.39432-02  0.0          5.12486+00  0.0
      4.35376+00  0.0          1.16670+01  0.0
      3.78496+02  0.0          1.53545+03  0.0
      4.48910+01  0.0          4.87962+01  0.0
      5.92620+00  1.24719-01   0.0         0.0          0.0          7.21830+00
      9.49365-02  0.0          0.0         0.0          1.15787+03   9.88164-02
      0.0         0.0          0.0         3.89520+00
      SR   54135   0   0   0       XE135
      134.91                                .210185-04
    0
    0
    0
    0
    0
    0
    0
    0
      0.0         0.0          3.97192+00  0.0
      6.24433-02  0.0          7.74442+00  0.0
      6.46383+01  0.0          1.75234+02  0.0
      8.94178+05  0.0          1.08424+06  0.0
      3.85146+00  1.20457-01   0.0         0.0          0.0          7.70671+00
      2.52700-02  0.0          0.0         0.0          1.08173+02   2.42237+00
      0.0         0.0          0.0         2.00062+05
      55   55133   0   0   0       CS133
      132.91
    0
    0
    0
    0
    0
    0
    0
    0
      5.31874-02  0.0          4.44534+00  0.0
      7.53006+00  0.0          1.42713+01  0.0
      1.43759+02  0.0          1.50353+02  0.0
      1.04746+01  0.0          1.73501+01  0.0
      4.59275+00  2.49406-01   0.0         0.0          0.0          1.07293+01
      1.19252-02  0.0          0.0         0.0          6.54027+00   5.47290-02
      0.0         0.0          0.0         6.87550+00
      60   60143   0   0   0       XE143
      142.91
    0
    0
    0
    0
```

```
 4.55259-02  0.0          6.35704+00  0.0
 4.81849+00  0.0          1.0501?+01  0.0
 6.2779?+00  0.0          2.?126?+01  0.0
 1.17327+02  0.0          2.2?45?+02  0.0
 6.22336+00  ?.42076-02   0.0         0.0          0.0          5.77398+00
 9.42589-03  0.0          0.0         0.0          1.86415+01   2.07327-01
 0.0         0.0          0.0         1.11132+02
 61  60145   0   0   0    ?0145
     144.91
 4.16420-02  0.0          6.37542+00  0.0
 1.48038+01  0.0          4.72734+01  0.0
 6.81830+01  0.0          ?.44560+01  0.0
 2.24455+01  0.0          3.?1205+01  0.0
 6.24797+00  ?.??110-02   0.0         0.0          0.0          3.24517+01
 1.78679-02  0.0          0.0         0.0          1.61718+01   1.08238-01
 0.0         0.0          0.0         1.57350+01
 63  61147   0   0   0    ?M147
     146.91                           .83-08
 2.64474-01  0.0          6.35155+00  0.0
 3.15819+01  0.0          ?.65645+01  0.0
 9.33429+02  0.0          1.25507+03  0.0
 6.73366+01  0.0          ?.26995+01  0.0
 5.98798+00  9.91494-02   0.0         0.0          0.0          1.49736+01
 9.02243-03  0.0          0.0         0.0          3.21587+02   5.39804-02
 0.0         0.0          0.0         1.53529+01
 65  61148   0   0   0    ?M148
     147.91                           .1933-06
```

```
 3.30615-01  0.0          6.95895+00  0.0
 1.71249+02  0.0          1.71295+02  0.0
 1.74935+03  0.0          1.75471+03  0.0
 1.01005+04  0.0          1.23504+04  0.0
 6.50953+00  1.18807-01   0.0         0.0          0.0          3.35360-04
 5.66464-03  0.0          0.0         0.0          5.32721+00   3.27874-02
 0.0         0.0          0.0         2.25030+03
 67   62149   0   0   0      SM149
   148.91
 0
 0
 0
 0
 0
 0
 0
 0
 1.98285-01  0.0          5.16765+00  0.0
 4.13584+01  0.0          7.72113+01  0.0
 1.68563+02  0.0          1.92794+02  0.0
 2.60679+04  0.0          2.91134+04  0.0
 4.77310+00  1.95670-01   0.0         0.0          0.0          3.58492+01
 3.66061-03  0.0          0.0         0.0          2.42109+01   2.40916-02
 0.0         0.0          0.0         4.59000+01
 68   62150   0   0   0      SM150
   149.92
 0
 0
 0
 0
 0
 0
 0
 0
 4.55596-02  0.0          5.03319+00  0.0
 2.23647+01  0.0          4.78458+01  0.0
 6.49878+00  0.0          1.34525+01  0.0
 3.17979+01  0.0          4.74554+01  0.0
 4.79196+00  1.95670-01   0.0         0.0          0.0          2.47010+01
 7.78118-01  0.0          0.0         0.0          6.90545+00   4.82651-01
 0.0         0.0          0.0         1.56575+01
 69   62151   0   0   0      SM151
   150.92                              .231-09
 0
 0
 0
 0
 0
 0
 0
 0
 0
 4.93891-01  0.0          5.43936+00  0.0
 4.53230+01  0.0          5.75164+01  0.0
 2.91032+02  0.0          3.03780+02  0.0
 1.67528+03  0.0          1.67524+03  0.0
 4.74980+00  1.95670-01   0.0         0.0          0.0          1.21750+01
```

```
 7.96774-03  0.0         0.0         0.0         1.47080+01  3.99919-02
 0.0         0.0         0.0         0.0
 70  62152   0   0   0      SM152
     151.92
0
0
0
0
0
0
0
0
0
 4.64954-02  0.0         5.03393+00  0.0
 2.10657+00  0.0         1.61510+01  0.0
 1.04106+03  0.0         2.49155+03  0.0
 8.08039+01  0.0         9.50443+01  0.0
 4.79181+00  1.95670-01   0.0         0.0         0.0         1.40301+01
 1.49690-02  0.0         0.0         0.0         1.40039+03  9.54299-02
 0.0         0.0         0.0         1.52404+01
 71  63153   0   0   0      EU153
     152.92
0
0
0
0
0
0
0
0
0
 2.00268-01  0.0         4.70493+00  0.0
 4.53463+01  0.0         5.40331+01  0.0
 4.33326+02  0.0         4.48876+02  0.0
 1.65921+02  0.0         1.71901+02  0.0
 4.28597+00  2.20744-01   0.0         0.0         0.0         8.64656+00
 4.62356-02  0.0         0.0         0.0         1.53528+01  1.97222-01
 0.0         0.0         0.0         5.98000+00
 72  63154   0   0   0      EU154
     153.92                          .28-08
0
0
0
0
0
0
0
0
0
 4.74072-01  0.0         7.09288+00  0.0
 3.69015+01  0.0         4.14503+01  0.0
 9.71867+01  0.0         1.02185+02  0.0
 9.85715+02  0.0         9.96231+02  0.0
 5.40000+00  2.18807-01   0.0         0.0         0.0         4.54399+00
 5.41225-03  0.0         0.0         0.0         4.96651+00  3.27858-02
 0.0         0.0         0.0         1.05160+01
 73  63155   0   0   0      EU155
     154.92                          .44-08
0
```

```
0
0
0
0
0
0
0
  1.67799-01  0.0          6.93795+00  0.0
  8.59436+01  0.0          8.93127+01  0.0
  9.07078+02  0.0          9.14483+02  0.0
  5.23729+03  0.0          5.23729+03  0.0
  6.55258+00  2.07570-01   0.0         0.0          0.0          3.32150+00
  7.60465-03  0.0          0.0         0.0          7.35235+00   5.26477-02
  0.0         0.0          0.0         0.0
  86   86120   0   0   0       VSAG23
      120.0
0
0
0
0
0
0
0
0
  2.82097+02  0.0          8.24796+00  0.0
  1.01042+00  0.0          1.25208+01  0.0
  1.06839+00  0.0          9.54010+00  0.0
  2.27243+00  0.0          1.36033+01  0.0
  8.08244+00  1.47312-01   0.0         0.0          0.0          1.14969+01
  1.30793-02  0.0          0.0         0.0          8.38930+00   8.24094-02
  0.0         0.0          0.0         1.13309+01
  87   87120   0   0   0       VSAG25
      120.0
0
0
0
0
0
0
0
0
  3.22694-02  0.0          8.02124+00  0.0
  1.05262+00  0.0          1.21935+01  0.0
  1.34484+00  0.0          9.47683+00  0.0
  1.72027+00  0.0          1.22053+01  0.0
  7.84297+00  1.46003-01   0.0         0.0          0.0          1.11283+01
  1.23564-02  0.0          0.0         0.0          8.05476+00   7.76267-02
  0.0         0.0          0.0         1.10850+01
  4
001
  1                                                          3
  1  1                                  1                    2          4
002
  1 10  0  0  1  2  0              0          105                1
```

```
      150.0
        2.0          8.0          15.0
    1  1
003
    2       7                    1  0  0  0
                                 842.0        1.0        1.0
004
    4   132.3  3     85.7  2     66.6  1     15.9  3    135.9
    2   119.9  4    118.9  4    118.9  4    118.9  4    118.9  2    118.9
    0
005
14 14 14 14 15
    1  3  5 13 15
    2  4  6 13 15
    7  9 11 13 15
    8 10 12 13 15
   15 15 15 15 15
012
    1  2     1              CORE 1
    3  4     2              CORE 2
    5  6     3              CORE 3
    7  8     1              CORE 1
    9 10     2              CORE 2
   11 12     3              CORE 3
   14 15     1      -01     REFLECTOR
    0
018
    8 10 14 16 81     6  9 12 15     7 82 13 11    17 18105115125    5 83
   84       39 85 50 53 58 55 60 61 63 65 67 68 69 70 71 72 73 86 87
020
    1  2  0  0
105 .2319-06 10 1.434-05 12 .1066-05  6 32.37-05  5 6190.-05 84  73.7-05
    0
    3  4  0  0
105 .2706-06 10 1.590-05 12 .1181-05  6 32.55-05  5 6190.-05 84  73.7-05
    0
    5  6  0  0
105 .2877-06 10 1.888-05 12 .1403-05  6 34.82-05  5 6190.-05 84  73.7-05
    0
    7  8  0  0
105 .2319-06 10 1.065-05 12 .0791-05  6 28.15-05  5 6190.-05 84  73.7-05
    0
    9 10  0  0
105 .2706-06 10 1.180-05 12 .0877-05  6 28.45-05  5 6190.-05 84  73.7-05
    0
   11 12  0  0
105 .2877-06 10 1.424-05 12 .1193-05  6 30.48-05  5 6190.-05 84  73.7-05
    0
   13 13  0  0
   84  73.7-05 10 .4660-05 12 .0644-05  6 32.38-05  5 6190.-05
   14 14  0  0
115  22.9-05 83 8594.-05
   15 15  0  0
   83 8876.-05
    0
034
    1  3
   85 1.040-12 58 2.102-05 63 8.374-09 65 1.480-06 69 2.361-10 72 2.813-09
```

```
C
C
C
     73 1.210-08  7 2.971-07 13 3.414-06 16 1.539-09
      0
      1  3
      8 10 14 16 81  6  9 12 15  7 82 13 11 17 18
            39          .042         .0627         .057         .057         .062
          .057          .057          .057          .057         .057         .057
          .057          .057          .057          .057
            85          .048         .0606          .061         .061         .048
          .027          .027          .063          .063         .027         .027
          .063          .063          .063          .063
            50          .016          .030          .057         .057         .016
        .0016         .0016          .066          .066        .0016        .0016
          .066          .066          .066          .066
            53          .037         .0293          .032         .032         .037
          .016          .016          .032          .032         .016         .016
          .032          .032          .032          .032
            58          .060          .064          .072         .072         .060
          .065          .065          .069          .069         .065         .065
          .069          .069          .069          .069
            55          .062         .0659          .054         .054         .062
          .052          .052          .055          .055         .052         .052
          .055          .055          .055          .055
            60          .052         .0598          .061         .061         .052
        .0372         .0372         .0372         .0372        .0372        .0372
        .0372         .0372         .0372         .0372
            61          .030         .0395          .041         .041         .030
          .030          .030          .041          .041         .030         .030
          .041          .041          .041          .041
            63          .017         .0238          .026         .026         .017
          .017          .017          .026          .026         .017         .017
          .026          .026          .026          .026
            67         .0062         .0113          .017         .017        .0062
        .0062         .0062          .017          .017        .0062        .0062
          .017          .017          .017          .017
            69         .0026         .0045          .010         .010        .0026
        .0026         .0026          .010          .010        .0026        .0026
          .010          .010          .010          .010
            70         .0017        .00285         .0075        .0075        .0017
          .0017         .0017         .0075         .0075        .0017        .0017
          .0075         .0075         .0075         .0075
            71        .00095         .0015         .0043        .0043       .00095
       .00095        .00095         .0043         .0043       .00095       .00095
          .0043         .0043         .0043         .0043
            86           1.0            .0            .0           .0           .0
            .0            .0            .0            .0           .0           .0
            .0            .0            .0            .0
            87            .0           1.0            .0           .0           .0
            .0            .0            .0            .0           .0           .0
            .0            .0            .0            .0
0
0
036
  1  3 18
   7   4  -7   8   9  10  11  18
   6   6   7 209 210 211 218
   4 506-110  82  81
   6  12 -13  14  15  16  17
   5  12  13 215 216 217
   2  63  65
C
```

```
        4  67  68  69  70
        3  71  72  73
        1  39
        1  85
        1  50
        1  53
        1  58
        1  55
        1  60
        1  61
        1  86
        1  87
    0
    999
    0
    /*ENDDATASET
    /*
    /*EOJ ********
```

CITATION INPUT TO OBTAIN THE REACTIVITY VARIATION WITH TIME

IN A TYPICAL LE BATCH

```
// 'ARNALDO RIBEIRO',CLASS=A,REGION=280K
/*MITID USER=(M11535,12680,,,RIO)
/*SRI LOW
/*MAIN     TIME=15,LINES=30,CARDS=20
/*SETUP UNIT=2314,ID=234136,A=CHV,                                    X
/*COMM='USING M7514 10581 DISKPACK'
//STEP2 EXEC FORG,PROG='PV.M7514.10581.CITATION.NEWLOAD(NELIB)'
//G.FT01F001 DD UNIT=SYSDA,DISP=(NEW,DELETE),SPACE=(TRK,(20,10)),
//        DCB=(RECFM=VS,LRECL=2404,BLKSIZE=2408)
//G.FT02F001 DD UNIT=SYSDA,DISP=(NEW,DELETE),SPACE=(TRK,(20,10)),
//        DCB=(RECFM=VS,LRECL=3004,BLKSIZE=3008)
//G.FT03F001 DD UNIT=SYSDA,DISP=(NEW,DELETE),SPACE=(TRK,(20,10)),
//        DCB=(RECFM=VS,LRECL=1604,BLKSIZE=1608)
//G.FT04F001 DD UNIT=SYSDA,DISP=(NEW,DELETE),SPACE=(TRK,(20,10)),
//        DCB=(RECFM=VS,LRECL=3004,BLKSIZE=3008)
//G.FT08F001 DD UNIT=SYSDA,DISP=(NEW,DELETE),SPACE=(TRK,(20,10)),
//        DCB=(RECFM=VS,LRECL=1004,BLKSIZE=1008)
//G.FT09F001 DD UNIT=SYSDA,DISP=(NEW,DELETE),SPACE=(TRK,(20,10)),
//        DCB=(RECFM=VS,LRECL=1604,BLKSIZE=1608)
//G.FT10F001 DD UNIT=SYSDA,DISP=(NEW,DELETE),SPACE=(TRK,(20,10)),
//        DCB=(RECFM=VS,LRECL=1604,BLKSIZE=1608,BUFNO=1)
//G.FT11F001 DD UNIT=SYSDA,DISP=(NEW,DELETE),SPACE=(TRK,(20,10)),
//        DCB=(RECFM=VS,LRECL=1604,BLKSIZE=1608)
//G.FT12F001 DD UNIT=SYSDA,DISP=(NEW,DELETE),SPACE=(TRK,(30,15)),
//        DCB=(RECFM=VS,LRECL=3004,BLKSIZE=3008)
//G.FT13F001 DD UNIT=SYSDA,DISP=(NEW,DELETE),SPACE=(TRK,(30,15)),
//        DCB=(RECFM=VS,LRECL=1604,BLKSIZE=1608,BUFNO=1)
//G.FT14F001 DD UNIT=SYSDA,DISP=(NEW,DELETE),SPACE=(TRK,(30,15)),
//        DCB=(RECFM=VS,LRECL=3004,BLKSIZE=3008)
//G.FT15F001 DD UNIT=SYSDA,DISP=(NEW,DELETE),SPACE=(TRK,(40,20)),
//        DCB=(RECFM=VBS,LRECL=3600,BLKSIZE=7204)
//G.FT16F001 DD UNIT=SYSDA,DISP=(NEW,DELETE),SPACE=(TRK,(20,10)),
//        DCB=(RECFM=VS,LRECL=1604,BLKSIZE=1608)
//G.FT17F001 DD UNIT=SYSDA,DISP=(NEW,DELETE),SPACE=(TRK,(20,10)),
//        DCB=(RECFM=VS,LRECL=1604,BLKSIZE=1608)
//G.FT18F001 DD UNIT=SYSDA,DISP=(NEW,DELETE),SPACE=(TRK,(20,10)),
//        DCB=(RECFM=VS,LRECL=1604,BLKSIZE=1608)
//G.FT19F001 DD UNIT=SYSDA,DISP=(NEW,DELETE),SPACE=(TRK,(20,10)),
//        DCB=(RECFM=VS,LRECL=1604,BLKSIZE=1608)
//G.FT21F001 DD UNIT=SYSDA,DISP=(NEW,DELETE),SPACE=(TRK,(20,10)),
//        DCB=(RECFM=VS,LRECL=1604,BLKSIZE=1608)
//G.FT22F001 DD UNIT=SYSDA,DISP=(NEW,DELETE),SPACE=(TRK,(20,10)),
//        DCB=(RECFM=VS,LRECL=1604,BLKSIZE=1608,BUFNO=1)
//G.FT23F001 DD UNIT=SYSDA,DISP=(NEW,DELETE),SPACE=(TRK,(20,10)),
//        DCB=(RECFM=VS,LRECL=1604,BLKSIZE=1608)
//G.FT24F001 DD UNIT=SYSDA,DISP=(NEW,DELETE),SPACE=(TRK,(20,10)),
//        DCB=(RECFM=VS,LRECL=1604,BLKSIZE=1608)
//G.FT25F001 DD UNIT=SYSDA,DISP=(NEW,DELETE),SPACE=(TRK,(20,10)),
//        DCB=(RECFM=VS,LRECL=1604,BLKSIZE=1608,BUFNO=1)
//G.FT26F001 DD UNIT=SYSDA,DISP=(NEW,DELETE),SPACE=(TRK,(20,10)),
//        DCB=(RECFM=VS,LRECL=1604,BLKSIZE=1608)
//G.FT27F001 DD UNIT=SYSDA,DISP=(NEW,DELETE),SPACE=(TRK,(20,10)),
//        DCB=(RECFM=VS,LRECL=1604,BLKSIZE=1608)
//G.FT28F001 DD UNIT=SYSDA,DISP=(NEW,DELETE),SPACE=(TRK,(20,10)),
//        DCB=(RECFM=VS,LRECL=1604,BLKSIZE=1608)
//G.FT29F001 DD UNIT=SYSDA,DISP=(NEW,DELETE),SPACE=(TRK,(20,10)),
//        DCB=(RECFM=VS,LRECL=1604,BLKSIZE=1608)
//G.FT30F001 DD UNIT=SYSDA,DISP=(NEW,DELETE),SPACE=(TRK,(20,10)),
//        DCB=(RECFM=VS,LRECL=1604,BLKSIZE=1608)
//G.FT31F001 DD UNIT=SYSDA,DISP=(NEW,DELETE),SPACE=(TRK,(20,10)),
```

```
//         DCB=(RECFM=VS,LRECL=1604,BLKSIZE=1608)
//G.FT32F001 DD UNIT=SYSDA,DISP=(NEW,DELETE),SPACE=(TRK,(20,10)),
//         DCB=(RECFM=VS,LRECL=1604,BLKSIZE=1608)
//G.SYSIN DD *,DCB=(RECFM=FB,LRECL=80,BLKSIZE=2000)
ARMY HTGR R-Z CITATION,UNRODDED DEPLETION,NO LUMPED FP YET
DATE: OCT.12,1974
000
  8
FOUR GROUP MICROSCOPIC CROSS SECTIONS ,SET 1 ,CORE
  -2  58   4   3   0   0
      0.9817        0.0183          0.0           0.0
     10.0+06       0.183+06         961.0          1.86
   1.5066+06     1.7947+03      6.472+00      6.339-02
    6.434-10      2.489-08      1.551-06      1.022-05
      0.0127        0.0317          0.12         0.315          1.36          3.8
0
0
0
   8   92233   1   0   1       U233
      233.04                  3.18-11
0
0
0
0
0
                                                                .0006         .0020
       .0017         .0018         .0003         .0002
0
0
   2.0560+00     2.0163+00     7.7062+00     2.6746+00     1.8802-01
   5.7980+00     5.1426+00     1.7453+01     2.5102+00     1.9772-02
   7.6503+01     6.3542+01     8.9003+01     2.5100+00     1.4387-02
   2.4343+02     2.2034+02     2.5409+02     2.5000+00           0.0
  10   92235   0   0   0       U235
      235.05                  3.23-11
0
0
0
0
0
                                                               .00052        0.00346
       0.0031       0.00624       0.00182       0.00066
0
0
   1.4121+00     1.2680+00     7.7042+00     2.5614+00
   5.0980+00     3.6623+00     1.5383+01     2.4309+00
   4.6630+01     2.6788+01     5.8123+01     2.4300+00
   2.2659+02     1.9098+02     2.4086+02     2.4300+00
  5.88155+00    4.10550-01    0.0           0.0           0.0           1.02685+01
  1.64800-02    0.0           0.0           0.0           1.14787+01    1.42640-02
  0.0           0.0           0.0           1.42700+01
  14   94239   1   0   1       PU239
      239.05                  3.34-11
0
0
0
0
0
                                                                .0020         .0018
       .0013         .0020         .0005         .0003
```

```
0
0
   1.8824+00   1.7947+00   8.1659+00   3.0485+00   2.4482-01
   3.2764+00   2.3165+00   1.4589+01   2.8929+00   1.5422-01
   5.3718+01   3.0660+01   6.5477+01   2.8900+00   1.0773-02
   1.2223+03   7.7026+02   1.2325+03   2.8920+00         0.0
  16   94241   1   0   1       PU241
      241.06                 3.37-11       .15-08
0
0
0
0
0
                                                    .00015      .00365
       .00275       .0062       .0024       .0005
0
0
   1.7577+00   1.7453+00   8.0412+00   3.1861+00   2.4554-01
   5.6120+00   5.4028+00   1.6963+01   3.0327+00   1.5293-02
   9.6598+01   7.6175+01   1.1089+02   3.0300+00   1.1129-02
   9.5742+02   6.7103+02   9.6896+02   2.9690+00         0.0
  81   92232   1   0   1       U232
      232.04                 3.16-11       .3-09
0
0
0
0
0
0
0
0
0
   1.01337+00  9.07260-01  9.10108+00  2.99008+00  2.36249+00
   1.76592+01  1.03743+01  3.44315+01  2.50328+00  8.28925-03
   1.65514+02  9.88003+01  1.78850+02  2.50300+00  4.59685-02
   4.20868+01  2.24163+01  5.33556+01  2.50300+00  0.0
   6   90232   1   0   1       TH232
      232.04                 3.14-11
0
0
0
0
0
                                                    0.0017      0.0074
       0.0077       0.0221       0.0085       0.0021
0
0
   1.7114-01   3.6974-02   7.8201+00   2.4012+00   3.5173-01
   3.2741-01         0.0   1.3021+01         0.0   1.6902-02
   5.5680-02         0.0   1.5795+01         0.0   1.4217-02
   2.6470+00         0.0   1.3854+01         0.0         0.0
   9   92234   1   0   1       U234
      234.04                 3.20-11
0
0
0
0
0
0
0
```

```
0
0
   1.0352+00   8.9132-01   8.1141+00   2.6933+00   2.5041-01
   1.2236+00   6.6419-03   1.4727+01   2.5121+00   2.9184-02
   9.1160+01         0.0   1.1891+02         0.0   9.1672-03
   3.1928+01         0.0   4.1046+01         0.0         0.0
  12   92238   0   0   0       U238
      238.05                 3.31-11
0
0
0
0
0
                                                   0.000475     0.00536
     0.00634     0.01519     0.00881     0.00294
0
0
   2.4817-01   1.3980-01   7.6536+00   2.7548+00
   6.7795-01         0.0   1.4142+01         0.0
   1.0171+01         0.0   4.1742+01         0.0
   1.0690+00         0.0   1.3733+01         0.0
  7.07433+00  3.31100-01         0.0         0.0         0.0  1.34361+01
  2.79230-02         0.0         0.0         0.0  3.15618+01  9.23870-03
         0.0         0.0         0.0  1.26640+01
  15   94240   1   0   1       PU240
      240.05                 3.35-11
0
0
0
0
0
                                                    .00028       .0024
      .00165       .0033       .00125       .00024
0
0
   1.1696+00   9.7832-01   8.0132+00   3.1046+00   1.7377-01
   1.3366+00   2.5372-02   1.4981+01   2.9002+00   2.7809-02
   2.4384+01   2.0169-04   5.3063+01   2.8900+00   1.5867-02
   7.6843+02         0.0   8.2053+02         0.0         0.0
   7   91233   1   0   1       PA233
      233.04                 3.16-11      .297-06
0
0
0
0
0
0
0
0
0
   7.8302-01   5.6476-01   8.0936+00   2.7222+00   3.2856-01
   1.8393+00         0.0   1.2917+01         0.0   1.9082-02
   5.5345+01         0.0   6.7386+01         0.0   1.4084-02
   6.3504+01         0.0   7.0763+01         0.0         0.0
  82   91231   1   0   1       PA231
      231.04                 3.12-11
0
0
0
0
```

```
0
0
0
0
0
  8.39154-01  6.80158-01  6.37723+00  3.04355+00  9.08365-01
  1.39955+01  2.36859-03  2.63441+01  2.50905+00  1.00696-02
  1.01969+02  4.85979-06  1.14020+02  2.50000+00  4.77166-02
  3.78484+02  1.72863-02  3.99730+02  2.50000+00  0.0
 13   93239   1   0   1      NP239
      239.05                3.32-11      .341-05
0
0
0
0
0
0
0
0
0
   1.1624+00   9.8703-01   8.5721+00   2.6914+00   3.3337-01
   4.0120+00   1.0233-03   1.6492+01   2.5141+00   2.3395-02
   6.7609+01         0.0   8.4376+01         0.0   2.0027-02
   2.2821+01         0.0   3.2116+01         0.0         0.0
 11   92236   1   0   1      U236
      236.05                3.25-11
0
0
0
0
0
                                                   .00056      .0051
       .006        .012        .008        .002
0
0
   4.2312-01   3.5143-01   7.8550+00   2.7608+00   3.0108-01
   1.1725+00         0.0   1.4813+01         0.0   2.8938-02
   4.5331+01         0.0   7.0153+01         0.0   1.0614-02
   2.3113+00         0.0   9.1339+00         0.0         0.0
 17   94242   1   0   1      PU242
      242.06                3.38-11
0
0
0
0
0
                                                   .00028      .0024
      .00165       .0033       .00125      .00024
0
0
   1.1696+00   9.7832-01   8.0131+00   3.1046+00   2.4554-01
   1.1408+00   2.5372-02   1.4738+01   2.9002+00   2.7467-02
   1.4776+02         0.0   1.7595+02         0.0   1.1081-02
   8.3028+00         0.0   1.7416+01         0.0         0.0
 18   93237   1   0   1      NP237
      237.05                3.28-11
0
0
0
0
```

```
0
0
0
0
0
   1.1996+00   9.8703-01   1.1996+00   2.6914+00          0.0
   2.6104+00   1.0256-03   2.6104+00   2.5141+00          0.0
   5.4375+01   2.0714-03   5.4375+01   2.5000+00          0.0
   1.3946+02         0.0   1.4701+02         0.0          0.0
 105   10510   0   0   0      BURNABLE POISON
      10.811
0
0
0
0
0
0
0
0
0
   1.1754-01         0.0   2.6792+00         0.0
   1.4967+00         0.0   5.3999+00         0.0
   2.4930+01         0.0   2.8930+01         0.0
   3.0986+02         0.0   3.1359+02         0.0
  2.39311+00  1.68550-01   0.0          0.0          0.0          3.77453+00
  1.28670-01  0.0          0.0          0.0          3.90636+00   9.36370-02
  0.0         0.0          0.0          3.73000+00
 115   11510   0   0   0      CONTROL ROD
      10.811
0
0
0
0
0
0
0
0
0
   1.1754-01         0.0   2.6792+00         0.0
   1.4967+00         0.0   5.3999+00         0.0
   2.4930+01         0.0   2.8930+01         0.0
   3.0986+02         0.0   3.1359+02         0.0
  2.39311+00  1.68550-01   0.0          0.0          0.0          3.77453+00
  1.28670-01  0.0          0.0          0.0          3.90636+00   9.36370-02
  0.0         0.0          0.0          3.73000+00
   5    1612   0   0   0      CARBON
      12.011
0
0
0
0
0
0
0
0
0
   1.1988-04         0.0   2.6512+00         0.0
         0.0         0.0   4.6031+00         0.0
   8.3572-05         0.0   4.7098+00         0.0
   1.5847-03         0.0   4.7011+00         0.0
```

```
  2.65561+00  1.95000-01  0.0         0.0         0.0         4.46590+00
  1.37200-01  0.0         0.0         0.0         4.60979+00  9.99300-02
  0.0         0.0         0.0         4.69956+00
  83    2612   0   0   0      CREF                                    *
      12.011
0
0
0
0
0
0
0
0
0
   1.1988-04          0.0   2.8512+00          0.0
         0.0          0.0   4.6031+00          0.0
   8.3572-05          0.0   4.7098+00          0.0
   1.5847-03          0.0   4.7011+00          0.0
  2.65561+00  1.95000-01  0.0         0.0         0.0         4.46590+00
  1.37200-01  0.0         0.0         0.0         4.60979+00  9.99300-02
  0.0         0.0         0.0         4.69956+00
  84    1428   0   0   0      SILICO
      28.086
0
0
0
0
0
0
0
0
0
0
   3.1854-03          0.0   2.7737+00          0.0
   7.5480-04          0.0   1.8834+00          0.0
   5.1245-03          0.0   2.3042+00          0.0
   6.1842-02          0.0   1.6305+00          0.0
  2.75110+00  1.94140-02  0.0         0.0         0.0         1.84411+00
  3.85340-02  0.0         0.0         0.0         2.27804+00  2.10320-02
  0.0         0.0         0.0         1.56868+00
  39    4295   1   0   1      MO95
      94.906
0
0
0
0
0
0
0
0
0
0
   6.7979-02          0.0   6.7979-02          0.0         0.0
   8.1715-01          0.0   8.1715-01          0.0         0.0
   1.6449+01          0.0   1.6449+01          0.0         0.0
   5.5151+00          0.0   1.0143+01          0.0         0.0
  85    4399   1   0   1      TC99
      98.906                              .103-07
0
0
0
0
```

```
0
0
0
0
0
   1.4194-01          0.0   1.4194-01          0.0          0.0
   1.5957+00          0.0   1.5957+00          0.0          0.0
   2.7668+01          0.0   2.7668+01          0.0          0.0
   8.7086+00          0.0   1.7589+01          0.0          0.0
  50   45103   1   0   1      RH103
       102.91
0
0
0
0
0
0
0
0
0
   1.2898-01          0.0   1.2898-01          0.0          0.0
   2.1107+00          0.0   2.1107+00          0.0          0.0
   5.1768+00          0.0   5.1768+00          0.0          0.0
   1.5646+02          0.0   1.6060+02          0.0          0.0
  53   54131   1   0   1      XE131
       130.91
0
0
0
0
0
0
0
0
0
   4.4746-02          0.0   4.4746-02          0.0          0.0
   1.0081+00          0.0   1.0081+00          0.0          0.0
   1.1807+02          0.0   1.1807+02          0.0          0.0
   4.1838+01          0.0   4.5826+01          0.0          0.0
  58   54135   1   0   1      XE135
       134.91                            .210185-04
0
0
0
0
0
0
0
0
0
   8.3580-05          0.0   7.1928+00          0.0   9.7428-02
   4.3305-03          0.0   1.0783+01          0.0   3.3504-02
   3.5798+01          0.0   9.9249+01          0.0   4.6781-01
   8.7790+05          0.0   8.7830+05          0.0          0.0
  55   55133   1   0   1      CS133
       132.91
0
0
0
0
```

```
0
0
0
0
0
   5.7436-02          0.0    5.7436-02          0.0          0.0
   1.4250+00          0.0    1.4250+00          0.0          0.0
   5.1596+01          0.0    5.1596+01          0.0          0.0
   1.0650+01          0.0    1.7142+01          0.0          0.0
  60   60143   1   0   1       ND143
       142.91
0
0
0
0
0
0
0
0
0
   5.2516-02          0.0    5.2516-02          0.0          0.0
   8.1030-01          0.0    8.1030-01          0.0          0.0
   1.0627+01          0.0    1.0627+01          0.0          0.0
   1.2118+02          0.0    1.7953+02          0.0          0.0
  61   60145   1   0   1       ND145
       144.91
0
0
0
0
0
0
0
0
0
   8.7818-02          0.0    8.7818-02          0.0          0.0
   1.5863+00          0.0    1.5863+00          0.0          0.0
   3.9194+01          0.0    3.9194+01          0.0          0.0
   1.9778+01          0.0    3.4623+01          0.0          0.0
  63   61147   1   0   1       PM147
       146.91                                .83-08
0
0
0
0
0
0
0
0
0
   3.5537-01          0.0    3.5537-01          0.0          0.0
   5.7397+00          0.0    5.7397+00          0.0          0.0
   5.4860+01          0.0    5.4860+01          0.0          0.0
   6.7816+01          0.0    7.0944+01          0.0          0.0
  65   61148   1   0   1       PM148
       147.91                               .1933-06
0
0
0
0
```

```
0
0
0
0
0
   9.7500-01          0.0   9.7500-01          0.0          0.0
   6.5543+01          0.0   6.5543+01          0.0          0.0
   2.8097+03          0.0   2.8097+03          0.0          0.0
   8.3676+03          0.0   8.3825+03          0.0          0.0
  67   62149   1   0   1      SM149
       148.91
0
0
0
0
0
0
0
0
0
   2.2425-01          0.0   7.4170+00          0.0    9.5685-02
   4.9933+00          0.0   1.6470+01          0.0    3.4569-02
   2.7576+02          0.0   3.4764+02          0.0    1.7968-02
   2.9376+04          0.0   2.9622+04          0.0          0.0
  68   62150   1   0   1      SM150
       149.92
0
0
0
0
0
0
0
0
0
   2.0127-02          0.0   2.0127-02          0.0          0.0
   1.9777+00          0.0   1.9777+00          0.0          0.0
   6.2672+01          0.0   6.2672+01          0.0          0.0
   3.8795+01          0.0   5.3643+01          0.0          0.0
  69   62151   1   0   1      SM151
       150.92                              .231-09
0
0
0
0
0
0
0
0
0
   1.3503-01          0.0   1.3503-01          0.0          0.0
   3.9698+00          0.0   3.9698+00          0.0          0.0
   3.1890+02          0.0   3.1890+02          0.0          0.0
   2.8524+03          0.0   2.8593+03          0.0          0.0
  70   62152   1   0   1      SM152
       151.92
0
0
0
0
```

```
0
0
0
0
0
   1.0162-01          0.0    1.0162-01          0.0          0.0
   1.2033+00          0.0    1.2033+00          0.0          0.0
   2.2417+02          0.0    2.2417+02          0.0          0.0
   7.9873+01          0.0    9.4721+01          0.0          0.0
  71   63153   1   0   1       EU153
       152.92
0
0
0
0
0
0
0
0
0
   4.2748-01          0.0    4.2748-01          0.0          0.0
   6.5162+00          0.0    6.5162+00          0.0          0.0
   2.0739+02          0.0    2.0739+02          0.0          0.0
   1.4700+02          0.0    1.4700+02          0.0          0.0
  72   63154   1   0   1       EU154
       153.92                                .28-08
0
0
0
0
0
0
0
0
0
   5.1899-01          0.0    5.1899-01          0.0          0.0
   1.5620+01          0.0    1.5620+01          0.0          0.0
   3.5331+02          0.0    3.5331+02          0.0          0.0
   5.7052+02          0.0    5.7795+02          0.0          0.0
  73   63155   1   0   1       EU155
       154.92                                .44-08
0
0
0
0
0
0
0
0
0
   3.8742-01          0.0    3.8742-01          0.0          0.0
   5.6630+00          0.0    5.6630+00          0.0          0.0
   1.8222+02          0.0    1.8222+02          0.0          0.0
   5.3249+03          0.0    5.3323+03          0.0          0.0
 110   64157   1   0   1       GD-157
       157.25
0
0
0
0
```

```
0
0
0
0
0
   1.8091-01          0.0    1.8091-01          0.0          0.0
   3.9225+00          0.0    3.9225+00          0.0          0.0
   1.4227+02          0.0    1.4227+02          0.0          0.0
   3.6731+04          0.0    3.7025+04          0.0          0.0
 111   64156   1    0   1      GD-156
       156.00
0
0
0
0
0
0
0
0
0
   2.1202-01          0.0    2.1202-01          0.0          0.0
   2.0253+00          0.0    2.0253+00          0.0          0.0
   1.6918+01          0.0    1.6918+01          0.0          0.0
   4.3740+00          0.0    1.9224+01          0.0          0.0
 112   64155   1    0   1      GD-155
       155.00
0
0
0
0
0
0
0
0
0
   1.8510-01          0.0    1.8510-01          0.0          0.0
   6.5379+00          0.0    6.5379+00          0.0          0.0
   2.3039+02          0.0    2.3039+02          0.0          0.0
   8.5833+03          0.0    8.6136+03          0.0          0.0
 113   62148   1    0   1      SM-148
       148.00
0
0
0
0
0
0
0
0
0
   7.9019-02          0.0    7.9019-02          0.0          0.0
   4.1423-01          0.0    4.1423-01          0.0          0.0
   6.6671-01          0.0    6.6671-01          0.0          0.0
   3.4231+00          0.0    1.8269+01          0.0          0.0
 114   62147   1    0   1      SM-147
       147.00
0
0
0
0
```

```
0
0
0
0
0
   2.9435-01          0.0   2.9435-01          0.0          0.0
   3.2071+00          0.0   3.2071+00          0.0          0.0
   8.6340+01          0.0   8.6340+01          0.0          0.0
   3.3418+01          0.0   3.6805+01          0.0          0.0
  64   61148   1   0   1      PM-148M
       148.00
0
0
0
0
0
0
0
0
0
   9.7500-01          0.0   9.7500-01          0.0          0.0
   6.5543+01          0.0   6.5543+01          0.0          0.0
   2.8097+03          0.0   2.8097+03          0.0          0.0
   8.3676+03          0.0   8.3825+03          0.0          0.0
 116   60146   1   0   1      ND-146
       146.00
0
0
0
0
0
0
0
0
0
   3.7820-02          0.0   3.7820-02          0.0          0.0
   3.3864-01          0.0   3.3864-01          0.0          0.0
   3.3862+00          0.0   3.3862+00          0.0          0.0
   4.9445-01          0.0   1.5340+01          0.0          0.0
 117   59143   1   0   1      PR-143
       143.00
0
0
0
0
0
0
0
0
0
   8.5808-03          0.0   8.5808-03          0.0          0.0
   9.7058-02          0.0   9.7058-02          0.0          0.0
   2.2815+00          0.0   2.2815+00          0.0          0.0
   3.1238+01          0.0   3.1238+01          0.0          0.0
 118   59141   1   0   1      PR-141
       141.00
0
0
0
0
```

```
0
0
0
0
0
   1.6734-02          0.0    1.6734-02          0.0          0.0
   2.8156-01          0.0    2.8156-01          0.0          0.0
   2.5004+00          0.0    2.5004+00          0.0          0.0
   4.5642+00          0.0    8.2749+00          0.0          0.0
 119   54134   1    0   1      XE-136
       136.00
0
0
0
0
0
0
0
0
0
   5.6908-03          0.0    5.6908-03          0.0          0.0
   7.0779-02          0.0    7.0779-02          0.0          0.0
   5.0009-03          0.0    5.0009-03          0.0          0.0
   1.0686-01          0.0    4.0952+00          0.0          0.0
  56   55134   1    0   1      CS-134
       134.00
0
0
0
0
0
0
0
0
0
   1.0653-01          0.0    1.0653-01          0.0          0.0
   5.7042+00          0.0    5.7042+00          0.0          0.0
   1.5971+02          0.0    1.5971+02          0.0          0.0
   5.0665+01          0.0    5.5303+01          0.0          0.0
 120   53131   1    0   1      I-131
       131.00
0
0
0
0
0
0
0
0
0
   2.0660-02          0.0    2.0660-02          0.0          0.0
   1.4184+00          0.0    1.4184+00          0.0          0.0
   9.2652+01          0.0    9.2652+01          0.0          0.0
   2.0156+01          0.0    2.4793+01          0.0          0.0
  54   54133   1    0   1      XE-133
       133.00
0
0
0
0
```

```
0
0
0
0
0
   1.4732-02          0.0    1.4732-02          0.0          0.0
   1.1713+00          0.0    1.1713+00          0.0          0.0
   2.1961+02          0.0    2.1961+02          0.0          0.0
   8.3575+01          0.0    8.8212+01          0.0          0.0
  79   48113   1    0    1       CD-113
       113.00
0
0
0
0
0
0
0
0
0
   1.2288-01          0.0    1.2288-01          0.0          0.0
   1.6233+00          0.0    1.6233+00          0.0          0.0
   6.8277+00          0.0    6.8277+00          0.0          0.0
   1.7429+04          0.0    1.7506+04          0.0          0.0
  40   47109   1    0    1       AG-109
       109.00
0
0
0
0
0
0
0
0
0
   2.0142-01          0.0    2.0142-01          0.0          0.0
   2.7423+00          0.0    2.7423+00          0.0          0.0
   1.9195+02          0.0    1.9195+02          0.0          0.0
   3.6305+01          0.0    3.9337+01          0.0          0.0
 121   44101   1    0    1       RU-101
       101.00
0
0
0
0
0
0
0
0
0
   1.2166-04          0.0    1.2166-04          0.0          0.0
   1.3794-01          0.0    1.3794-01          0.0          0.0
   1.1026+01          0.0    1.1026+01          0.0          0.0
   2.0843+00          0.0    7.6399+00          0.0          0.0
  51   45105   1    0    1       RH-105
       105.00
0
0
0
0
```

```
0
0
0
0
0
   8.8541-04          0.0   8.8541-04          0.0          0.0
   4.2903-02          0.0   4.2903-02          0.0          0.0
   3.0253+03          0.0   3.0253+03          0.0          0.0
   9.6164+03          0.0   9.6211+03          0.0          0.0
 122    4297   1    0   1      MO-97
       97.000
0
0
0
0
0
0
0
0
0
   6.5575-02          0.0   6.5575-02          0.0          0.0
   1.0325+00          0.0   1.0325+00          0.0          0.0
   1.9703+00          0.0   1.9703+00          0.0          0.0
   8.3677-01          0.0   5.4651+00          0.0          0.0
  49    3683   1    0   1      KR-83
       83.000
0
0
0
0
0
0
0
0
0
   8.4037-02          0.0   8.4037-02          0.0          0.0
   1.9380+00          0.0   1.9380+00          0.0          0.0
   3.8965+01          0.0   3.8965+01          0.0          0.0
   7.6584+01          0.0   8.2441+01          0.0          0.0
 123   12340   1    0   1      FIS PRO-40
       40.000
0
0
0
0
0
0
0
0
0
   1.4215-02          0.0   1.4215-02          0.0          0.0
   1.3780-01          0.0   1.3780-01          0.0          0.0
   1.1094+00          0.0   1.1094+00          0.0          0.0
   4.6804-01          0.0   6.3928+00          0.0          0.0
 124    1816   1    0   1      O-16
       16.000
0
0
0
0
```

```
0
0
0
0
0
   3.3108-03          0.0    3.6923+00          0.0    1.4777-01
         0.0          0.0    3.6605+00          0.0    8.1022-02
         0.0          0.0    3.6560+00          0.0    5.8962-02
         0.0          0.0    3.2676+00          0.0          0.0
  4
001
  1                                                0                  3
  1  1     1        1     1  1     1  0  1  1
                                                                 2                4
                     1.0
002
  1  8  0  0  1  3  0
0
       100.0        260.0        180.0
  1  1     1        1     1  1     1     1  1
003
  0  2        7                    1  0  0  1
0
                                   300.         0.95          0.5
004
  4    215.5  2    169.0
  2    119.0  3    157.5
005
  2  2
  1  2
012
  1  1  1  1     1       CORE
  2  2  1  1     2       REFLECTOR
0
018
  8 10 14 16 81     6  9 12 15     7 82 13    11 17 18105115124     5 83
 84       39 85 50 53 58 55 60 61 63 65 67 68 69 70 71 72 73 49 51 40 79
 54 56 641101111121131141161171181191201211221231
020
  1  1  0  0
 10 .4513-04 12 .3469-03  5 .6222-01 84 .7370-03 58 3.500-10105 .6100-05
0
  2  2  0  0
 83 .8876-01

034
0
  1
  8 10 14 16 81  6  9 12 15  7 82 13 11 17 18
          39         .061         .063         .061         .061         .061
        .061         .061         .057         .061         .061         .061
        .061         .061         .061         .061
          85         .048         .061         .059         .052         .052
        .027         .052         .063         .052         .052         .052
        .052         .052         .052         .052
          50         .016         .030         .058         .034         .034
        .002         .034         .066         .034         .034         .034
        .034         .034         .034         .034
          53         .037         .029         .029         .029         .029
        .016         .029         .032         .029         .029         .029
```

.029	.029	.029	.029		
58	.060	.064	.072	.065	.065
.065	.065	.065	.065	.065	.065
.065	.065	.065	.065		
55	.062	.065	.053	.059	.059
.059	.059	.055	.059	.059	.059
.059	.059	.059	.059		
60	.052	.060	.063	.058	.058
.058	.058	.058	.058	.058	.058
.058	.058	.058	.058		
61	.030	.040	.042	.037	.037
.037	.037	.037	.037	.037	.037
.037	.037	.037	.037		
63	.017	.024	.029	.023	.023
.023	.023	.023	.023	.023	.023
.023	.023	.023	.023		
65	.012	.017	.023	.017	.017
.017	.017	.017	.017	.017	.017
.017	.017	.017	.017		
67	.006	.011	.019	.012	.012
.012	.012	.012	.012	.012	.012
.012	.012	.012	.012		
68	.005	.007	.014	.009	.009
.009	.009	.009	.009	.009	.009
.009	.009	.009	.009		
69	.003	.005	.012	.007	.007
.007	.007	.007	.007	.007	.007
.007	.007	.007	.007		
70	.002	.003	.008	.004	.004
.004	.004	.004	.004	.004	.004
.004	.004	.004	.004		
71	.001	.002	.004	.002	.002
.002	.002	.002	.002	.002	.002
.002	.002	.002	.002		
72	.000	.000	.003	.001	.001
.001	.001	.001	.001	.001	.001
.001	.001	.001	.001		
73	.001	.000	.002	.001	.001
.001	.001	.001	.001	.001	.001
.001	.001	.001	.001		
49	.01140	.00544	.00084	.00084	.01140
.01900	.01900	.00400	.00400	.01900	.01900
.00400	.00400	.00400	.00400		
122	.05350	.06900	.05900	.05900	.05350
.05500	.05500	.06500	.06500	.05500	.05500
.06500	.06500	.06500	.06500		
121	.03000	.05000	.06000	.06000	.03000
.00800	.00800	.06900	.06900	.00800	.00800
.06900	.06900	.06900	.06900		
51	.00500	.00950	.05000	.05000	.00500
.00070	.00070	.04000	.04000	.00070	.00070
.04000	.04000	.04000	.04000		
40	.00040	.00030	.01500	.01500	.00040
.00050	.00050	.00250	.00250	.00050	.00050
.00250	.00250	.00250	.00250		
79	.00020	.00010	.00060	.00060	.00020
.00050	.00050	.00045	.00045	.00050	.00050
.00045	.00045	.00045	.00045		
54	.05000	.06600	.05300	.05300	.05000
.04500	.04500	.05500	.05500	.04500	.04500

```
      .05500      .05500      .05500      .05500
         120      .02700      .03100      .03800      .03800      .02700
      .01000      .01000      .03100      .03100      .01000      .01000
      .03100      .03100      .03100      .03100
           56      .06000      .06000      .06900      .06900      .06000
      .05500      .05500      .06500      .06500      .05500      .05500
      .06500      .06500      .06500      .06500
         119      .06900      .06460      .05100      .05100      .06900
      .05650      .05650      .05900      .05900      .05650      .05650
      .05900      .05900      .05900      .05900
         118      .05900      .06400      .06000      .06000      .05900
      .06900      .06900      .05900      .05900      .06900      .06900
      .05900      .05900      .05900      .05900
         117      .05900      .04000      .06900      .06900      .05900
      .06500      .06500      .05500      .05500      .06500      .06500
      .05500      .05500      .05500      .05500
         116      .02300      .03070      .03600      .03600      .02300
      .04000      .04000      .04000      .04000      .04000      .04000
      .04000      .04000      .04000      .04000
         114      .01710      .01500      .02920      .02920      .01710
      .01500      .01500      .03000      .03000      .01500      .01500
      .03000      .03000      .03000      .03000
         113      .00800      .00800      .01200      .01200      .00800
      .00600      .00600      .03000      .03000      .00600      .00600
      .03000      .03000      .03000      .03000
         112      .00015      .00030      .00210      .00210      .00015
      .00005      .00005      .00100      .00100      .00005      .00005
      .00100      .00100      .00100      .00100
         111      .00005      .00013      .00120      .00120      .00005
      .00004      .00004      .00070      .00070      .00004      .00004
      .00070      .00070      .00070      .00070
         110      .00003      .00008      .00070      .00070      .00003
      .00000      .00000      .00020      .00020      .00000      .00000
      .00020      .00020      .00020      .00020
         123      1.0000      1.0000      .00000      .00000      .00000
      .00000      .00000      .00000      .00000      .00000      .00000
      .00000      .00000      .00000      .00000
0
0
036
  1  1 31
   7   6  -7   8   9  10  11  18
   6   6   7 209 210 211 218
   4 506-110  82  81
   5   6  -7 508-001  81
   6  12 -13  14  15  16  17
   5  12  13 215 216 217
   9  63  65  67  68  69  70  71  72  73
   9 114 113 267 268 269 270 271 272 273
   3 112 111 110
   2  58 119
   1 105
   1  39
   1  85
   1  50
   1  53
   1  55
   1  60
   1  61
   1  49
```

```
    1 122
    1 121
    1  51
    1  40
    1  79
    1 120
    1  54
    1  56
    1 118
    1 117
    1 116
    1 123
0
999
0
/*EOJ ********
```

CITATION INPUT FOR THE FRD RUN

```
//JK0917   JOB 1,
// 'ARNALDO RIBEIRO',CLASS=A,REGION=400K
/*MITID USER=(M12303,12680,,,DENISE)
/*SRI W
/*MAIN     TIME=15,LINES=30,CARDS=20
/*SETUP UNIT=2314,ID=234136,A=CHV,
/*COMM='USING M7514 10581 DISKPACK'
//STEP2 EXEC FORG,PROG='PV.M7514.10581.CITATION.LOAD40KC(NELTB)'
//G.FT01F001 DD UNIT=SYSDA,DISP=(NEW,DELETE),SPACE=(TRK,(20,10)),
//        DCB=(RECFM=VS,LRECL=2404,BLKSIZE=2408)
//G.FT02F001 DD UNIT=SYSDA,DISP=(NEW,DELETE),SPACE=(TRK,(20,10)),
//        DCB=(RECFM=VS,LRECL=3004,BLKSIZE=3008)
//G.FT03F001 DD UNIT=SYSDA,DISP=(NEW,DELETE),SPACE=(TRK,(20,10)),
//        DCB=(RECFM=VS,LRECL=1604,BLKSIZE=1608)
//G.FT04F001 DD UNIT=SYSDA,DISP=(NEW,DELETE),SPACE=(TRK,(20,10)),
//        DCB=(RECFM=VS,LRECL=3004,BLKSIZE=3008)
//G.FT08F001 DD UNIT=SYSDA,DISP=(NEW,DELETE),SPACE=(TRK,(20,10)),
//        DCB=(RECFM=VS,LRECL=1004,BLKSIZE=1008)
//G.FT09F001 DD UNIT=SYSDA,DISP=(NEW,DELETE),SPACE=(TRK,(20,10)),
//        DCB=(RECFM=VS,LRECL=1504,BLKSIZE=1508)
//G.FT10F001 DD UNIT=SYSDA,DISP=(NEW,DELETE),SPACE=(TRK,(20,10)),
//        DCB=(RECFM=VS,LRECL=1504,BLKSIZE=1508,BUFNO=1)
//G.FT11F001 DD UNIT=SYSDA,DISP=(NEW,DELETE),SPACE=(TRK,(20,10)),
//        DCB=(RECFM=VS,LRECL=1504,BLKSIZE=1608)
//G.FT12F001 DD UNIT=SYSDA,DISP=(NEW,DELETE),SPACE=(TRK,(30,15)),
//        DCB=(RECFM=VS,LRECL=3004,BLKSIZE=3008)
//G.FT13F001 DD UNIT=SYSDA,DISP=(NEW,DELETE),SPACE=(TRK,(30,15)),
//        DCB=(RECFM=VS,LRECL=1504,BLKSIZE=1508,BUFNO=1)
//G.FT14F001 DD UNIT=SYSDA,DISP=(NEW,DELETE),SPACE=(TRK,(30,15)),
//        DCB=(RECFM=VS,LRECL=3004,BLKSIZE=3008)
//G.FT15F001 DD UNIT=SYSDA,DISP=(NEW,DELETE),SPACE=(TRK,(40,20)),
//        DCB=(RECFM=VBS,LRECL=3600,BLKSIZE=7204)
//G.FT16F001 DD UNIT=SYSDA,DISP=(NEW,DELETE),SPACE=(TRK,(20,10)),
//        DCB=(RECFM=VS,LRECL=1604,BLKSIZE=1608)
//G.FT17F001 DD UNIT=SYSDA,DISP=(NEW,DELETE),SPACE=(TRK,(20,10)),
//        DCB=(RECFM=VS,LRECL=1604,BLKSIZE=1608)
//G.FT18F001 DD UNIT=SYSDA,DISP=(NEW,DELETE),SPACE=(TRK,(20,10)),
//        DCB=(RECFM=VS,LRECL=1604,BLKSIZE=1608)
//G.FT19F001 DD UNIT=SYSDA,DISP=(NEW,DELETE),SPACE=(TRK,(20,10)),
//        DCB=(RECFM=VS,LRECL=1604,BLKSIZE=1608)
//G.FT21F001 DD UNIT=SYSDA,DISP=(NEW,DELETE),SPACE=(TRK,(20,10)),
//        DCB=(RECFM=VS,LRECL=1604,BLKSIZE=1608)
//G.FT22F001 DD UNIT=SYSDA,DISP=(NEW,DELETE),SPACE=(TRK,(20,10)),
//        DCB=(RECFM=VS,LRECL=1604,BLKSIZE=1608,BUFNO=1)
//G.FT23F001 DD UNIT=SYSDA,DISP=(NEW,DELETE),SPACE=(TRK,(20,10)),
//        DCB=(RECFM=VS,LRECL=1604,BLKSIZE=1608)
//G.FT24F001 DD UNIT=SYSDA,DISP=(NEW,DELETE),SPACE=(TRK,(20,10)),
//        DCB=(RECFM=VS,LRECL=1604,BLKSIZE=1608)
//G.FT25F001 DD UNIT=SYSDA,DISP=(NEW,DELETE),SPACE=(TRK,(20,10)),
//        DCB=(RECFM=VS,LRECL=1604,BLKSIZE=1608,BUFNO=1)
//G.FT26F001 DD UNIT=SYSDA,DISP=(NEW,DELETE),SPACE=(TRK,(20,10)),
//        DCB=(RECFM=VS,LRECL=1604,BLKSIZE=1608)
//G.FT27F001 DD UNIT=SYSDA,DISP=(NEW,DELETE),SPACE=(TRK,(20,10)),
//        DCB=(RECFM=VS,LRECL=1604,BLKSIZE=1608)
//G.FT29F001 DD UNIT=SYSDA,DISP=(NEW,DELETE),SPACE=(TRK,(20,10)),
//        DCB=(RECFM=VS,LRECL=1604,BLKSIZE=1608)
//G.FT29F001 DD UNIT=SYSDA,DISP=(NEW,DELETE),SPACE=(TRK,(20,10)),
//        DCB=(RECFM=VS,LRECL=1604,BLKSIZE=1608)
//G.FT30F001 DD UNIT=SYSDA,DISP=(NEW,DELETE),SPACE=(TRK,(20,10)),
//        DCB=(RECFM=VS,LRECL=1604,BLKSIZE=1608)
```

```
//G.FT31F001 DD UNIT=SYSDA,DISP=(NEW,DELETE),SPACE=(TRK,(20,10)),
//        DCH=(RECFM=VS,LRECL=1504,BLKSIZE=1608)
//G.FT32F001 DD UNIT=SYSDA,DISP=(NEW,DELETE),SPACE=(TRK,(20,10)),
//        DCB=(RECFM=VS,LRECL=1504,BLKSIZE=1608)
//G.SYSIN DD *,DCH=(RECFM=FB,LRECL=80,BLKSIZE=2000)
ARMY REACTOR DEPLETION RUNS
DATE : MAY 14 , 1975
000
  8
FOUR GP MCSCOPIC CS SET 1, HOT CORE
  -2  37   4   1   0   0
       0.976        0.024          0.0          0.0
     15.0+06     0.183+06         17.6         2.38
   1.5066+06    1.7947+03     6.472+00     6.339-02
    6.434-10     2.489-08     1.551-06     1.022-05
      0.0127       0.0317         0.12        0.315          1.36          3.8
0
0
0
   9   92233   0   0   0       U233
      233.04                  3.18-11
0
0
0
0
0
                                                                .0006         .0020
       .0017        .0018        .0003        .0002
0
0
  2.06149+00  1.96632+00  4.92369+00  2.60514+00
  1.78841+01  1.58388+01  2.76870+01  2.50291+00
  1.14053+02  9.62824+01  1.26508+02  2.50290+00
  2.63548+02  2.33738+02  2.65875+02  2.50000+00
  2.71221+00  1.49986-01  0.0         0.0          0.0           9.79411+00
  8.78603-03  0.0         0.0         0.0          1.26968+00    5.82115-02
  0.0         0.0         0.0         4.00300+00
  10   92235   0   0   0       U235
      235.05                  3.23-11
0
0
0
0
0
                                                                .00052        0.00346
      0.0031      0.00624      0.00182      0.00066
0
0
  1.39898+00  1.27033+00  5.40597+00  2.56026+00
  1.89305+01  1.25851+01  2.92793+01  2.43016+00
  6.27115+01  3.43436+01  7.77132+01  2.43000+00
  1.87930+02  1.54000+02  2.32064+02  2.43000+00
  3.84480+00  1.62185-01  0.0         0.0          0.0           1.03392+01
  9.56718-03  0.0         0.0         0.0          1.24010+01    3.57469-02
  0.0         0.0         0.0         1.06901+01
  14   94239   0   0   0       PU239
      239.05                  3.34-11
0
0
0
```

```
0
0
                                                                  .0020        .0018
      .0013        .0020        .0005        .0003
0
0
  1.77736+00   1.70478+00   6.03666+00   3.04455+00
  1.85408+01   1.09937+01   3.05326+01   2.87045+00
  9.23446+01   5.63217+01   1.04697+02   2.87000+00
  1.22792+03   7.56321+02   1.25699+03   2.89000+00
  4.16737+00   9.18710-02   0.0          0.0          0.0          1.19819+01
  1.05121-02   0.0          0.0          0.0          1.23072+01   4.52438-02
  0.0          0.0          0.0          2.90700+01
  16   94241    0    0    0       PU241
      241.06                    3.37-11       .15-08
0
0
0
0
0
                                                                  .00015       .00365
      .00275       .0062        .0024        .0005
0
0
  1.74803+00   1.64418+00   6.09200+00   3.18751+00
  2.26935+01   1.58617+01   3.27885+01   3.03043+00
  2.19130+02   1.83336+02   2.33332+02   3.03000+00
  8.82100+02   6.05686+02   9.00552+02   3.03000+00
  3.95875+00   3.85223-01   0.0          0.0          0.0          1.00844+01
  1.06068-02   0.0          0.0          0.0          1.41521+01   4.99861-02
  0.0          0.0          0.0          1.84520+01
   6   90232    0    0    0       TH232
      232.04                    3.14-11
0
0
0
0
0
                                                                  0.0017       0.0074
      0.0077       0.0221       0.0085       0.0021
0
0
  1.67250-01   3.57550-02   5.34430+00   2.40137+00
  4.00577+00   5.58306-15   2.24742+01   0.0
  1.77361-01   0.0          1.18115+01   0.0
  2.19000+00   0.0          1.45630+01   0.0
  4.99514+00   1.81911-01   0.0          0.0          0.0          1.84571+01
  1.13191-02   0.0          0.0          0.0          1.15838+01   5.03630-02
  0.0          0.0          0.0          1.19984+01
   9   92234    0    0    0       U234
      234.04                    3.20-11
0
0
0
0
0
0
0
0
0
```

```
 1.09460+00  8.62071-01  6.31656+00  2.68486+00
 7.75802+00  8.04308-03  2.59927+01  2.50701+00
 2.65246+02  2.33211-01  3.15471+02  2.50000+00
 2.92185+01  2.54117-03  4.34567+01  2.50500+00
 5.20090+00  2.10627-01  0.0         0.0         0.0         1.82281+01
 6.55730-03  0.0         0.0         0.0         5.01882+01  3.67775-02
 0.0         0.0         0.0         1.42402+01
 12   92238   0   0   0      U238
     238.05                3.31-11
0
0
0
0
0
                                                 0.000475    0.00536
    0.00634     0.01519     0.00881     0.00294
0
0
 1.81245-01  6.76320-02  5.45743+00  2.90869+00
 1.22929+01  5.25206-11  3.59861+01  0.0
 6.53815+01  9.95458-11  7.78183+01  0.0
 1.05319+00  0.0         1.17433+01  0.0
 5.02555+00  2.50637-01  0.0         0.0         0.0         2.36330+01
 6.01594-02  0.0         0.0         0.0         1.24010+01  3.57869-02
 0.0         0.0         0.0         1.06901+01
 15   94240   0   0   0      PU240
     240.05                3.35-11
0
0
0
0
0
                                                 .00028      .0024
     .00165      .0033       .00125      .00024
0
0
 1.16039+00  9.69180-01  6.01994+00  3.10180+00
 1.35128+01  1.57140-02  3.69479+01  2.90023+00
 2.45916+00  0.0         1.34448+01  0.0
 1.24508+03  0.0         1.38354+03  0.0
 4.71546+00  1.44095-01  0.0         0.0         0.0         2.34241+01
 1.10344-02  0.0         0.0         0.0         1.09242+01  6.14572-02
 0.0         0.0         0.0         1.38460+02
  7   91233   0   0   0      PA233
     233.04                3.16-11     .297-06
0
0
0
0
0
0
0
0
 8.57691-01  6.97885-01  6.41424+00  3.04249+00
 1.32242+01  2.38332-03  2.54552+01  2.50905+00
 1.31400+02  0.0         1.43654+02  0.0
 7.06072+01  0.0         8.55810+01  0.0
 4.66084+00  8.95712-01  0.0         0.0         0.0         1.22213+01
 9.06624-03  0.0         0.0         0.0         1.22051+01  4.89215-02
```

```
C
C
C     0.0           0.0           0.0           1.49738+01
      82   91231     0    0    0      PA231
           231.04                   3.12-11
      0
      0
C     0
      0
      0
      0
C     0
      0
      0
      0
C     8.49154-01    6.80158-01    6.37723+00    3.04355+00
      1.37944+01    2.38332-03    2.63441+01    2.50905+00
C     1.01969+02    4.85979-06    1.14020+02    2.50000+00
      3.78484+02    1.72883-02    3.99730+02    2.50000+00
      4.61971+00    9.08365-01    0.0           0.0           0.0           1.25396+01
C     1.00696-02    0.0           0.0           0.0           1.20033+01    4.77166-02
      0.0           0.0           0.0           2.12460+01
      13   93239    0    0    0      NP239
           239.05                   3.32-11       .341-05
      0
      0
C     0
      0
      0
      0
C     0
      0
      0
      0
C     1.15211+00    9.77751-01    5.84456+00    2.68879+00
      1.96821+01    6.29623-04    3.17010+01    2.51398+00
C     1.28638+02    0.0           1.41372+02    0.0
      2.05751+01    0.0           3.03716+01    0.0
      4.25773+00    4.34723-01    0.0           0.0           0.0           1.20107+01
C     8.24249-03    0.0           0.0           0.0           1.26908+01    3.42124-01
      0.0           0.0           0.0           9.79550+00
      11   92236    0    0    0      U236
           236.05                   3.25-11
C     0
      0
      0
C     0
      0
C                                                                .00056        .0051
           .006          .012          .008          .002
      0
C     0
      5.65974-01    3.35046-01    5.89910+00    2.75489+00
      7.46001+00    0.0           2.73286+01    0.0
C     1.14395+02    0.0           1.31369+02    0.0
      2.35138+00    0.0           1.43425+01    0.0
      5.10649+00    2.26632-01    0.0           0.0           0.0           1.98609+01
C     7.66378-03    0.0           0.0           0.0           1.69285+01    4.54945-02
      0.0           0.0           0.0           1.19912+01
      17   94242    0    0    0      PU242
           242.06                   3.38-11
      0
      0
C     0
```

```
0
0
                                                                .00028        .0024
      .00165         .0033        .00125        .00024
0
0
  1.16038+00   9.69180-01   6.01994+00   3.10180+00
  5.82875+00   1.57140-02   3.13415+01   2.90023+00
  4.92482+02   0.0          5.42319+02   0.0
  1.02713+01   0.0          2.10797+01   0.0
  4.71547+00   1.44095-01   0.0          0.0          0.0          2.55056+02
  7.14095-03   0.0          0.0          0.0          4.83875+01   1.44954+00
  0.0          0.0          0.0          1.08094+01
  18   93237    0    0    0       NP237
       237.05                    3.28-11
0
0
0
0
0
0
0
0
0
  1.39713+00   9.77586-01   6.04963+00   2.68852+00
  1.50744+01   6.29623-04   4.05491+01   2.51398+00
  8.31042+01   2.98710-03   9.42498+01   2.50000+00
  1.25870+02   0.0          1.38549+02   0.0
  4.21778+00   4.34723-01   0.0          0.0          0.0          2.53869+01
  8.37754-03   0.0          0.0          0.0          1.11035+01   4.20604-02
  0.0          0.0          0.0          1.27790+01
 105   10510    1    0   10       SELF SH. RP
       10.013
0
0
0
0
0
0
0
0
0
  4.79423-01   0.0          0.0          0.0          0.0
  2.77019+01   0.0          0.0          0.0          0.0
  2.47948+02   0.0          0.0          0.0          0.0
  1.46332+03                                         3.39206-07
 125   12510    2    0    0       CH2
       10.811
0
0
0
0
0
0
0
0
0
       0.10+00
       2.02+00
       4.11+00
```

```
        3.79+00
   5     1612    0    0    0       CARBON
         12.011
0
0
0
0
0
0
0
0
0
  1.58789-04  0.0          2.26492+00  0.0
  2.45014-05  0.0          4.39658+00  0.0
  2.20025-04  0.0          4.48714+00  0.0
  1.27191-03  0.0          4.54142+00  0.0
  2.66809+00  1.96672-01   0.0         0.0          0.0         4.60731+00
  6.25637-02  0.0          0.0         0.0          4.38336+00  3.66401-01
  0.0         0.0          0.0         4.61394+00
  84     1428    0    0    0       SILICO
         28.086
0
0
0
0
0
0
0
0
0
  3.58831-03  0.0          2.68648+00  0.0
  2.05849-03  0.0          1.94125+00  0.0
  1.04986-02  0.0          2.10994+00  0.0
  5.96917-02  0.0          2.15814+00  0.0
  2.42887+00  2.54022-01   0.0         0.0          0.0         1.42720+00
  1.19882-02  0.0          0.0         0.0          2.02682+00  7.26207-02
  0.0         0.0          0.0         2.09845+00
  39     4295    0    0    0       MO95
         94.906
0
0
0
0
0
0
0
0
0
  7.52166-02  0.0          4.58875+00  0.0
  1.03280+01  0.0          1.86973+01  0.0
  1.04288+00  0.0          6.17757+00  0.0
  5.19988+00  0.0          1.21064+01  0.0
  4.38372+00  1.29814-01   0.0         0.0          0.0         8.36077+00
  8.52933-03  0.0          0.0         0.0          5.08261+00  5.20802-02
  0.0         0.0          0.0         6.90652+00
  85     4399    0    0    0       TC99
         98.906                          .103-07
0
0
0
```

```
0
0
0
0
0
0
  2.14982-01  0.0          6.30833+00  0.0
  4.76617+00  0.0          1.04109+01  0.0
  6.85232+01  0.0          7.32930+01  0.0
  8.96751+00  0.0          1.38494+01  0.0
  5.96324+00  1.30107-01   0.0         0.0          0.0          5.63472+00
  1.00104-02  0.0          0.0         0.0          4.72353+00   4.62726-02
  0.0         0.0          0.0         4.88189+00
  50   45103   0   0   0      RH103
       102.91
0
0
0
0
0
0
0
0
0
0
  1.60929-01  0.0          6.03583+00  0.0
  2.42437+00  0.0          9.65454+00  0.0
  2.25313+00  0.0          7.40941+00  0.0
  1.97188+02  0.0          2.09726+02  0.0
  5.74307+00  1.32830-01   0.0         0.0          0.0          7.22225+00
  7.92122-03  0.0          0.0         0.0          5.10350+00   5.27827-02
  0.0         0.0          0.0         1.25380+01
  53   54131   0   0   0      XE131
       130.91
0
0
0
0
0
0
0
0
0
0
  7.39432-02  0.0          6.12486+00  0.0
  4.35376+00  0.0          1.16670+01  0.0
  3.78496+02  0.0          1.53646+03  0.0
  4.48910+01  0.0          4.87962+01  0.0
  5.92620+00  1.24719-01   0.0         0.0          0.0          7.21830+00
  9.49365-02  0.0          0.0         0.0          1.15787+03   9.99164-02
  0.0         0.0          0.0         3.89520+00
  58   54135   0   0   0      XE135
       134.91                           .210185-04
0
0
0
0
0
0
0
0
0
```

```
  0.0           0.0           3.97192+00   0.0
  6.24433-02    0.0           7.79442+00   0.0
  6.46383+01    0.0           1.75234+02   0.0
  6.64500+05    0.0           1.09424+06   0.0
  3.85146+00    1.20457-01    0.0          0.0          0.0          7.70671+00
  2.52700-02    0.0           0.0          0.0          1.08173+02   2.42237+00
  0.0           0.0           0.0          2.00062+05
  55   55133    0   0   0        CS133
      132.91
0
0
0
0
0
0
0
0
0
0
  5.31874-02    0.0           4.89534+00   0.0
  7.53006+00    0.0           1.82713+01   0.0
  1.43758+02    0.0           1.50353+02   0.0
  1.04746+01    0.0           1.73501+01   0.0
  4.59275+00    2.49405-01    0.0          0.0          0.0          1.07293+01
  1.19252-02    0.0           0.0          0.0          6.54027+00   5.47290-02
  0.0           0.0           0.0          6.87550+00
  60   60143    0   0   0        ND143
      142.91
0
0
0
0
0
0
0
0
0
0
  4.55259-02    0.0           6.35709+00   0.0
  4.81949+00    0.0           1.06019+01   0.0
  6.27798+00    0.0           2.51268+01   0.0
  1.17327+02    0.0           2.28459+02   0.0
  6.22336+00    8.82076-02    0.0          0.0          0.0          5.77398+00
  9.42589-03    0.0           0.0          0.0          1.86415+01   2.07327-01
  0.0           0.0           0.0          1.11132+02
  61   60145    0   0   0        ND145
      144.91
0
0
0
0
0
0
0
0
0
0
  4.16420-02    0.0           6.37842+00   0.0
  1.48038+01    0.0           4.72734+01   0.0
  6.81880+01    0.0           8.44680+01   0.0
  2.24455+01    0.0           3.81805+01   0.0
  6.24797+00    8.85110-02    0.0          0.0          0.0          3.24517+01
  1.78679-02    0.0           0.0          0.0          1.61718+01   1.08238-01
```

```
  0.0           0.0           0.0           1.57350+01
  63   61147    0   0   0        PM147
      146.91                                .83-08
0
0
0
0
0
0
0
0
0
0
  2.64474-01    0.0           6.35155+00    0.0
  3.15819+01    0.0           4.65645+01    0.0
  9.33429+02    0.0           1.25507+03    0.0
  6.73366+01    0.0           8.26895+01    0.0
  5.98788+00    9.91994-02    0.0           0.0           0.0           1.49736+01
  9.02243-03    0.0           0.0           0.0           3.21587+02    5.39804-02
  0.0           0.0           0.0           1.53529+01
  65   61148    0   0   0        PM148
      147.91                                .1933-06
0
0
0
0
0
0
0
0
0
0
  3.30615-01    0.0           6.95895+00    0.0
  1.71289+02    0.0           1.71295+02    0.0
  1.74935+03    0.0           1.75471+03    0.0
  1.01005+04    0.0           1.23502+04    0.0
  6.50953+00    1.18807-01    0.0           0.0           0.0           3.35360-04
  5.66464-03    0.0           0.0           0.0           5.32721+00    3.27874-02
  0.0           0.0           0.0           2.25030+03
  67   62149    0   0   0        SM149
      148.91
0
0
0
0
0
0
0
0
0
0
  1.98885-01    0.0           5.16765+00    0.0
  4.13584+01    0.0           7.72113+01    0.0
  1.68563+02    0.0           1.92798+02    0.0
  1.98700+04    0.0           2.41138+04    0.0
  4.77310+00    1.95670-01    0.0           0.0           0.0           3.59492+01
  3.66061-03    0.0           0.0           0.0           2.42109+01    2.40916-02
  0.0           0.0           0.0           4.59000+01
  68   62150    0   0   0        SM150
      149.92
0
0
0
```

```
0
0
0
0
0
  4.55596-02  0.0          5.03319+00  0.0
  2.23667+01  0.0          4.78458+01  0.0
  6.49878+00  0.0          1.34525+01  0.0
  3.17979+01  0.0          4.74554+01  0.0
  4.79196+00  1.95670-01   0.0         0.0          0.0          2.47010+01
  7.78118-01  0.0          0.0         0.0          6.90545+00   4.82651-01
  0.0         0.0          0.0         1.56575+01
  69   62151   0   0   0      SM151
       150.92                              .231-09
0
0
0
0
0
0
0
0
0
  4.93891-01  0.0          5.43936+00  0.0
  4.53330+01  0.0          5.75160+01  0.0
  2.91032+02  0.0          3.05780+02  0.0
  1.67528+03  0.0          1.67528+03  0.0
  4.74980+00  1.95670-01   0.0         0.0          0.0          1.21750+01
  7.96774-03  0.0          0.0         0.0          1.47080+01   3.99919-02
  0.0         0.0          0.0         0.0
  70   62152   0   0   0      SM152
       151.92
0
0
0
0
0
0
0
0
0
  4.64954-02  0.0          5.03398+00  0.0
  2.10657+00  0.0          1.61516+01  0.0
  1.08106+03  0.0          2.48155+03  0.0
  8.08039+01  0.0          9.60443+01  0.0
  4.79181+00  1.95670-01   0.0         0.0          0.0          1.40301+01
  1.49680-02  0.0          0.0         0.0          1.40039+03   9.54289-02
  0.0         0.0          0.0         1.52404+01
  71   63153   0   0   0      EU153
       152.92
0
0
0
0
0
0
0
0
0
```

```
  2.00268-01  0.0          4.70698+00  0.0
  4.53463+01  0.0          5.40331+01  0.0
  4.33326+02  0.0          4.48876+02  0.0
  1.65921+02  0.0          1.71901+02  0.0
  4.28597+00  2.20744-01   0.0         0.0          0.0          8.64056+00
  4.62356-02  0.0          0.0         0.0          1.53528+01   1.97222-01
  0.0         0.0          0.0         5.98000+00
  72   63154   0   0   0       EU154
       153.92                              .28-08
0
0
0
0
0
0
0
0
0
  4.74072-01  0.0          7.09288+00  0.0
  3.69015+01  0.0          4.14509+01  0.0
  9.71867+01  0.0          1.02186+02  0.0
  9.85715+02  0.0          9.96231+02  0.0
  6.40000+00  2.18807-01   0.0         0.0          0.0          4.54399+00
  5.41226-03  0.0          0.0         0.0          4.96651+00   3.27858-02
  0.0         0.0          0.0         1.05160+01
  73   63155   0   0   0       EU155
       154.92                              .44-08
0
0
0
0
0
0
0
0
0
  1.67799-01  0.0          6.92795+00  0.0
  8.59836+01  0.0          8.93127+01  0.0
  9.07078+02  0.0          9.14463+02  0.0
  5.23729+03  0.0          5.23729+03  0.0
  6.55258+00  2.07570-01   0.0         0.0          0.0          3.32150+00
  7.60465-03  0.0          0.0         0.0          7.35235+00   5.26477-02
  0.0         0.0          0.0         0.0
  86   86120   0   0   0       NSAG23
       120.0
0
0
0
0
0
0
0
0
0
  2.82097-02  0.0          8.25796+00  0.0
  1.01082+00  0.0          1.25208+01  0.0
  1.06839+00  0.0          9.54010+00  0.0
  2.27243+00  0.0          1.36033+01  0.0
  8.08244+00  1.47312-01   0.0         0.0          0.0          1.14969+01
  1.30793-02  0.0          0.0         0.0          8.38930+00   8.24094-02
```

```
  0.0           0.0           0.0           1.13309+01
  87   87120    0   0   0      NSAG25
       120.0
0
0
0
0
0
0
0
0
  3.22694-02   0.0           8.02124+00    0.0
  1.05282+00   0.0           1.21935+01    0.0
  1.34484+00   0.0           9.47583+00    0.0
  1.72027+00   0.0           1.28053+01    0.0
  7.84297+00   1.46003-01    0.0           0.0           0.0           1.11293+01
  1.23564-02   0.0           0.0           0.0           8.05436+00    7.76267-02
  0.0          0.0           0.0           1.10850+01
  9
FOUR GP MCSCOPIC CS SET 2. HOT REFLECTOR
  -2   3   4   1   0   0
       0.976         0.024          0.0           0.0
     15.0+06      0.183+06         17.6          2.38
   1.5066+06     1.7947+03     6.472+00      6.339-02
    6.434-10      2.489-08     1.551-06      1.022-05
      0.0127        0.0317         0.12          0.315         1.36          3.9
0
0
0
 105   10510    1   0  10      SELF SH. BP
       10.013
0
0
0
0
0
0
0
0
0
  4.79423-01   0.0           0.0           0.0           0.0
  2.77019+01   0.0           0.0           0.0           0.0
  2.47948+02   0.0           0.0           0.0           0.0
  1.36655+03                                           2.33934-07
 125   12510    2   0   0      CH2
       10.811
0
0
0
0
0
0
0
0
0
       0.10+00
       2.02+00
       4.11+00
       3.79+00
```

```
  83    2612   0   0   0      CREF
       12.011
0
0
0
0
0
0
0
0
0
  7.59580-07  0.0          1.98076+00  0.0
  3.35931-05  0.0          4.38728+00  0.0
  2.54030-04  0.0          4.12727+00  0.0
  1.95200-03  0.0          4.88376+00  0.0
  1.76473+00  2.16030-01   0.0         0.0          0.0          4.60731+00
  8.76041-02  0.0          0.0         0.0          3.73898+00   3.88029-01
  0.0         0.0          0.0         4.88181+00
  4
001
  1                                                              3
  1  1                      1  1     1     1  1                          2          4
                      1.0
002
  1 13        1  2                              105                  1
       2000.0
         60.0        90.0        150.0
  1  1                      1  1     1     1  1
003
  0  2        7                    1  0  0  0
0
                                  300.0
004
  4     50.0  8     82.3  8     85.7  6    100.0
  6    118.9  8    79.25  8    79.25  8    79.25 12    79.25  4     36.3
  4     82.6
005
 16 16 16 18
  1  5  9 18
  2  6 10 18
  3  7 11 18
  4  8 12 18
 13 14 15 18
 17 17 17 18
012
  1 12     1              CORE
 13 15     2              BUFFER
 16 18     2      -01     REFLECTOR
  0
018
  8 10 14 16     6  9 12 15     7 82 13 11    17 18105125     5 83 84
   39 85 50 53 58 55 60 61 63 65 67 68 70 71 72 72 73 86 87
020
  1 12  0  0
 10 4.200-05 12  .316-05  6 34.68-05 84  73.7-05  5 6190.-05105 .2800-05
 58   3.5-10
 13 15  0  0
105 .1096-05 83 7107.-05
 16 16  0  0
```

```
 83 6663.-05125 30.43-05
 17 18  0  0
 83 7107.-05
  0
034
  1
 85 1.040-12 58 2.102-05 63 8.378-09 65 1.480-06 69 2.361-10 72 2.813-09
 73 1.210-08  7 2.971-07 13 3.414-06 16 1.539-09
  0
  1
  8 10 14 16  6  9 12 15  7 82 13 11 17 18
         39          .062        .0627
       .057          .057          .057        .057        .057        .057
       .057          .057          .057        .057        .057        .057
         85          .048
       .027          .063        .0606
       .063          .063          .063        .061        .061        .027
         50          .016          .063        .027        .027        .063
     .0016          .-66          .030
       .066          .066          .066        .057        .057        .0016
         53          .037          .0293       .0016       .0016       .066
       .016          .032          .032        .032        .032        .016
       .032          .032          .032        .016        .016        .032
         58          .060          .064
       .065          .069          .069        .072        .072        .065
       .069          .069          .069        .065        .065        .069
         55          .062          .0659
       .052          .055          .055        .054        .054        .052
       .055          .055          .055        .052        .052        .055
         60          .052          .0598
     .0372        .0372          .0372       .061        .061        .0372
     .0372        .0372          .0372       .0372       .0372       .0372
         61          .030          .0395       .0372
       .030          .041          .041        .041        .041        .030
       .041          .041          .041        .030        .030        .041
         63          .017          .0238
       .017          .026          .026        .026        .026        .017
       .026          .026          .026        .017        .017        .026
         67        .0062          .0113
     .0062          .017          .017        .017        .017        .0062
       .017          .017          .017        .0062       .0062       .017
         69        .0026          .0045
     .0026          .010          .010        .010        .010        .0026
       .010          .010          .010        .0026       .0026       .010
         70          .0017       .00285
       .0017          .0075       .0075       .0075       .0075       .0017
       .0075          .0075       .0075       .0017       .0017       .0075
         71       .00095          .0015
     .00095          .0043       .0043       .0043       .0043       .00095
       .0043          .0043       .0043     .00095      .00095       .0043
         86          1.0           .0
          .0           .0          .0          .0          .0          .0
          .0           .0          .0          .0          .0          .0
         87           .0          .0
          .0           .0        1.0           .0          .0          .0
          .0           .0          .0          .0          .0          .0
0
0
036
  1  1 18
```

```
      7   6  -7   8   9  10  11  18
      6   6   7 209 210 211 218
      3 506-110  82
      6  12 -13  14  15  16  17
      5  12  13 215 216 217
      2  63  65
      4  67  68  69  70
      3  71  72  73
      1  39
      1  85
      1  50
      1  53
      1  58
      1  55
      1  60
      1  61
      1  86
      1  87
    2  2  1
     1  83
0
999
0
/*ENDDATASET
/*
/*EOJ ********
```

EXCERPTS FROM THE FRD CITATION OUTPUT

**********CITATION - REVISION 2 (JULY 1971) - SUPPLEMENT 3 (JULY 1972)**********

*********THIS JOB WAS RUN ON 9/06/75 ON THE IBM 370/165*********

ARMY REACTOR DEPLETION RUNS
DATE : MAY 14 , 1975

MICROSCOPIC CROSS-SECTION UPDATING FOLLOWS

*******CONTROL OPTION IS 8*******

NEW CROSS SECTION TAPE 8 MADE

MICROSCOPIC CROSS-SECTION UPDATING FOLLOWS

*******CONTROL OPTION IS 9*******

CROSS SECTION SET ADDED TO TAPE 8

MICROSCOPIC CROSS-SECTION UPDATING FOLLOWS

*******CONTROL OPTION IS 4*******

THE TITLES OF THE CROSS SECTION SETS PRESENTLY ON THIS CITATION
CROSS SECTION LIBRARY TAPE ARE-

FOUR GE MOSCOPIC CS SET 1, HOT CORE
TYPE,NUCS,GRPS,DWS,UPS,X -2 37 4 1 0 0

FOUR GE MOSCOPIC CS SET 2, HOT REFLECTOR
TYPE,NUCS,GRPS,DWS,UPS,X -2 3 4 1 0 0

GENERAL CONTROL INPUT - SECTION 001

```
  1   0   0   0   0   0   0   0   0   0   0   0   0   0   0   0   0   0   0   3   0   0   0
  1   1   0   0   0   0   0   0   1   1   0   1   0   1   1   0   0   0   0   0   0   0   0
200 100  10   2   3   0   0   0   0   0   0   0   0   0   0   0   0   0  30   2  30  15  15   4
 1.500000E+00  1.000000E+00  9.999999E+09  9.999999E+23  0.0          1.000000E+00
```

DEPLETION HISTORY INPUT - SECTION 002

```
 1  13   C   0   1   2   0   0   0   0   0   0   0   0   0 105   0   0   C   0   0   1   0   0
2.000000E+03  0.0           0.0           1.000000E+00  9.999993E-31  1.000000E+00
6.000000E+01  9.000000E+01  1.500000E+02  0.0           0.0           0.0
 1   1   0   0   C   0   0   0   1   1   0   1   0   1   1   0   0   0   0   0   0   0   C   0
```

NEUTRON FLUX PROBLEM DESCRIPTION - SECTION 003

```
 0   2   C   0   7   C   0   0   0   0   1   0   0   0   0   0   C   0   C   0   0   0   0   0
9.999999E-05  1.000000E-05  9.999999E-05  9.999999E-05  9.999999E-05  0.0
0.0           0.0           3.000000E+02  1.000000E+00  1.000000E+00  0.0
```

LEFT,TOP,RIGHT,BOTTOM,FRONT,BACK BOUNDARY CONDITIONS ARE

```
0.0           4.692000E-01  4.692000E-01  4.692000E-01  4.692000E-01  4.692000E-01
```

TWO DIMENSIONAL CYLINDRICAL GEOMETRY (R,Z) WIDTH 3.179998E+02 HEIGHT 5.547998E+02

REGION SPECIFICATIONS

PTS	REGION WIDTH											
4	5.000000E+01	8	8.230000E+01	8	8.570000E+01	6	1.000000E+02					

PTS	REGION HEIGHT									
6	1.189000E+02	8	7.925000E+01	8	7.925000E+01	8	7.925000E+01	12	7.925000E+01	4	3.630000E+01
4	8.260001E+01									

X-DIR. POINTS 26 Y-DIR. POINTS 50

DISTANCES TO MESH INTERVAL INTERFACES

J	DIST.																			
2	25.000	3	35.355	4	43.301	5	50.000	6	66.147	7	79.062	8	90.146	9	100.008	10	108.982			
11	117.271	12	125.011	13	132.300	14	145.794	15	158.141	16	169.591	17	180.315	18	190.437	19	200.047			
20	209.216	21	218.000	22	237.607	23	255.716	24	272.624	25	288.543	26	303.629	27	318.000					

I	DIST.																			
2	19.817	3	39.633	4	59.450	5	79.267	6	99.083	7	118.900	8	128.806	9	138.712	10	148.619			
11	158.525	12	168.431	13	178.337	14	188.244	15	198.150	16	208.056	17	217.962	18	227.869	19	237.775			
20	247.681	21	257.587	22	267.494	23	277.400	24	287.306	25	297.212	26	307.119	27	317.025	28	326.931			
29	336.837	30	346.744	31	356.650	32	363.254	33	369.858	34	376.462	35	383.067	36	389.671	37	396.275			
38	402.879	39	409.483	40	416.087	41	422.692	42	429.296	43	435.900	44	444.975	45	454.050	46	463.125			
47	472.200	48	492.850	49	513.500	50	534.150	51	554.800											

DISTANCES TO FLUX POINTS

J	DIST.																			
1	17.678	2	30.619	3	39.528	4	46.771	5	58.632	6	72.891	7	84.785	8	95.205	9	104.591			
10	113.202	11	121.203	12	128.707	13	139.211	14	152.093	15	163.966	16	175.035	17	185.445	18	195.301			
19	204.683	20	213.653	21	228.015	22	246.828	23	264.305	24	280.696	25	296.182	26	310.897					

I	DIST.																			
1	9.908	2	29.725	3	49.542	4	69.358	5	89.175	6	108.992	7	123.853	8	133.759	9	143.666			
10	153.572	11	163.478	12	173.384	13	183.291	14	193.197	15	203.103	16	213.009	17	222.916	18	232.822			
19	242.728	20	252.634	21	262.541	22	272.447	23	282.353	24	292.259	25	302.166	26	312.072	27	321.978			
28	331.884	29	341.791	30	351.697	31	359.952	32	366.556	33	373.160	34	379.764	35	386.369	36	392.973			
37	399.577	38	406.181	39	412.785	40	419.389	41	425.994	42	432.598	43	440.437	44	449.512	45	458.587			
46	467.662	47	482.525	48	503.175	49	523.825	50	544.475											

ZONE INPUT BY REGION

16	16	16	18
1	5	9	18
2	6	10	18
3	7	11	18
4	8	12	18
13	14	15	18
17	17	17	18

ZONE NUMBER AT EACH MESH INTERVAL

	1	2	3	4	5	6	7	8	9	10	11	12	13	14	15	16	17	18	19	20	21	22	23	24	25	26
1	16	16	16	16	16	16	16	16	16	16	16	16	16	16	16	16	16	16	16	16	18	18	18	18	18	18
2	16	16	16	16	16	16	16	16	16	16	16	16	16	16	16	16	16	16	16	16	18	18	18	18	18	18
3	16	16	16	16	16	16	16	16	16	16	16	16	16	16	16	16	16	16	16	16	18	18	18	18	18	18
4	16	16	16	16	16	16	16	16	16	16	16	16	16	16	16	16	16	16	16	16	18	18	18	18	18	18
5	16	16	16	16	16	16	16	16	16	16	16	16	16	16	16	16	16	16	16	16	18	18	18	18	18	18
6	16	16	16	16	16	16	16	16	16	16	16	16	16	16	16	16	16	16	16	16	18	18	18	18	18	18
7	1	1	1	1	5	5	5	5	5	5	5	5	9	9	9	9	9	9	9	9	18	18	18	18	18	18
8	1	1	1	1	5	5	5	5	5	5	5	5	9	9	9	9	9	9	9	9	18	18	18	18	18	18
9	1	1	1	1	5	5	5	5	5	5	5	5	9	9	9	9	9	9	9	9	18	18	18	18	18	18
10	1	1	1	1	5	5	5	5	5	5	5	5	9	9	9	9	9	9	9	9	18	18	18	18	18	18
11	1	1	1	1	5	5	5	5	5	5	5	5	9	9	9	9	9	9	9	9	18	18	18	18	18	18
12	1	1	1	1	5	5	5	5	5	5	5	5	9	9	9	9	9	9	9	9	18	18	18	18	18	18
13	1	1	1	1	5	5	5	5	5	5	5	5	9	9	9	9	9	9	9	9	18	18	18	18	18	18
14	1	1	1	1	5	5	5	5	5	5	5	5	9	9	9	9	9	9	9	9	18	18	18	18	18	18
15	2	2	2	2	6	6	6	6	6	6	6	6	10	10	10	10	10	10	10	10	18	18	18	18	18	18
16	2	2	2	2	6	6	6	6	6	6	6	6	10	10	10	10	10	10	10	10	18	18	18	18	18	18
17	2	2	2	2	6	6	6	6	6	6	6	6	10	10	10	10	10	10	10	10	18	18	18	18	18	18
18	2	2	2	2	6	6	6	6	6	6	6	6	10	10	10	10	10	10	10	10	18	18	18	18	18	18
19	2	2	2	2	6	6	6	6	6	6	6	6	10	10	10	10	10	10	10	10	18	18	18	18	18	18
20	2	2	2	2	6	6	6	6	6	6	6	6	10	10	10	10	10	10	10	10	18	18	18	18	18	18
21	2	2	2	2	6	6	6	6	6	6	6	6	10	10	10	10	10	10	10	10	18	18	18	18	18	18
22	2	2	2	2	6	6	6	6	6	6	6	6	10	10	10	10	10	10	10	10	18	18	18	18	18	18
23	3	3	3	3	7	7	7	7	7	7	7	7	11	11	11	11	11	11	11	11	18	18	18	18	18	18
24	3	3	3	3	7	7	7	7	7	7	7	7	11	11	11	11	11	11	11	11	18	18	18	18	18	18
25	3	3	3	3	7	7	7	7	7	7	7	7	11	11	11	11	11	11	11	11	18	18	18	18	18	18
26	3	3	3	3	7	7	7	7	7	7	7	7	11	11	11	11	11	11	11	11	18	18	18	18	18	18
27	3	3	3	3	7	7	7	7	7	7	7	7	11	11	11	11	11	11	11	11	18	18	18	18	18	18
28	3	3	3	3	7	7	7	7	7	7	7	7	11	11	11	11	11	11	11	11	18	18	18	18	18	18
29	3	3	3	3	7	7	7	7	7	7	7	7	11	11	11	11	11	11	11	11	18	18	18	18	18	18
30	3	3	3	3	7	7	7	7	7	7	7	7	11	11	11	11	11	11	11	11	18	18	18	18	18	18
31	4	4	4	4	8	8	8	8	8	8	8	8	12	12	12	12	12	12	12	12	18	18	18	18	18	18
32	4	4	4	4	8	8	8	8	8	8	8	8	12	12	12	12	12	12	12	12	18	18	18	18	18	18
33	4	4	4	4	8	8	8	8	8	8	8	8	12	12	12	12	12	12	12	12	18	18	18	18	18	18
34	4	4	4	4	8	8	8	8	8	8	8	8	12	12	12	12	12	12	12	12	18	18	18	18	18	18
35	4	4	4	4	8	8	8	8	8	8	8	8	12	12	12	12	12	12	12	12	18	18	18	18	18	18
36	4	4	4	4	8	8	8	8	8	8	8	8	12	12	12	12	12	12	12	12	18	18	18	18	18	18
37	4	4	4	4	8	8	8	8	8	8	8	8	12	12	12	12	12	12	12	12	18	18	18	18	18	18
38	4	4	4	4	8	8	8	8	8	8	8	8	12	12	12	12	12	12	12	12	18	18	18	18	18	18
39	4	4	4	4	8	8	8	8	8	8	8	8	12	12	12	12	12	12	12	12	18	18	18	18	18	18
40	4	4	4	4	8	8	8	8	8	8	8	8	12	12	12	12	12	12	12	12	18	18	18	18	18	18
41	4	4	4	4	8	8	8	8	8	8	8	8	12	12	12	12	12	12	12	12	18	18	18	18	18	18
42	4	4	4	4	8	8	8	8	8	8	8	8	12	12	12	12	12	12	12	12	18	18	18	18	18	18
43	13	13	13	13	14	14	14	14	14	14	14	14	15	15	15	15	15	15	15	15	18	18	18	18	18	18
44	13	13	13	13	14	14	14	14	14	14	14	14	15	15	15	15	15	15	15	15	18	18	18	18	18	18
45	13	13	13	13	14	14	14	14	14	14	14	14	15	15	15	15	15	15	15	15	18	18	18	18	18	18
46	13	13	13	13	14	14	14	14	14	14	14	14	15	15	15	15	15	15	15	15	18	18	18	18	18	18
47	17	17	17	17	17	17	17	17	17	17	17	17	17	17	17	17	17	17	17	17	18	18	18	18	18	18
48	17	17	17	17	17	17	17	17	17	17	17	17	17	17	17	17	17	17	17	17	18	18	18	18	18	18
49	17	17	17	17	17	17	17	17	17	17	17	17	17	17	17	17	17	17	17	17	18	18	18	18	18	18
50	17	17	17	17	17	17	17	17	17	17	17	17	17	17	17	17	17	17	17	17	18	18	18	18	18	18

DESCRIPTION OF REACTOR ZONES

ZN	TC	ZN	SUB-ZNS	SIGMA-SET	ID	CLASS	DPL	NEX	NAME
1		12	0	1	0	0	0	0	CORE
13		15	0	2	0	0	0	0	BUFFER
16		18	0	2	0	0	-1	0	REFLECTOR

DESCRIPTION OF MICROSCOPIC CROSS SECTIONS

SET	NUCS	GRPS	UPSC	DWSC	,	TITLE
1	37	4	0	1	FOUR GP MCSCOPIC CS SET 1, HOT CORE	
GROUP	UPPER ENERGY	MEAN ENERGY	1/V X-SECTION	DIST.FUNCT		
1	1.500000E+07	1.506600E+06	6.434000E-10	0.976000		
2	1.830000E+05	1.794700E+03	2.489000E-08	0.024000		
3	1.760001E+01	6.472000E+00	1.551000E-06	0.0		
4	2.380000E+00	6.339002E-02	1.022000E-05	0.0		
SUM				1.000000		

SET	NUCS	GRPS	UPSC	DWSC	,	TITLE
2	3	4	0	1	FOUR GP MCSCOPIC CS SET 2, HOT REFLECTOR	
GROUP	UPPER ENERGY	MEAN ENERGY	1/V X-SECTION	DIST.FUNCT		
1	1.500000E+07	1.506600E+06	6.434000E-10	0.976000		
2	1.830000E+05	1.794700E+03	2.489000E-08	0.024000		
3	1.760001E+01	6.472000E+00	1.551000E-06	0.0		
4	2.380000E+00	6.339002E-02	1.022000E-05	0.0		
SUM				1.000000		

NC FUEL NUCLIDES IN SET 2

INPUT NUCLIDE DENSITIES(NUCLIDE NUMBER - DENSITY)

ZONES 1- 12 SUB-ZONE INDICATOR 0 AND CONTROL OPTION 0

10	4.200000E-05	12	3.160000E-06	6	3.468000E-04	84	7.370000E-04	5	6.190000E-02	105	2.800000E-06
58	3.500000E-10										

ZONES 13- 15 SUB-ZONE INDICATOR 0 AND CONTROL OPTION 0

105	1.096000E-06	83	7.107000E-02

ZONES 16- 16 SUB-ZONE INDICATOR 0 AND CONTROL OPTION 0

83	6.663000E-02	125	3.043000E-04

ZONES 17- 18 SUB-ZONE INDICATOR 0 AND CONTROL OPTION 0

83	7.107000E-02

DECAY CONSTANTS INPUT FROM CARDS

SIGMA-SETS 1- 1

NUC DECAY CNST.

85	1.040000E-12	58	2.102000E-05	63	8.378000E-09	65	1.480000E-06	69	2.361000E-10	72	2.813000E-09
73	1.210000E-08	7	2.971000E-07	13	3.414000E-06	16	1.539000E-09	0	0.0	0	0.0

CARD INPUT OF YIELD DATA

SIGMA-SETS 1- 1

FISS. NUCS

8	10	14	16	6	9	12	15	7	82	13	11	17	18	0	0	0	0	0	0

YIELD FRACTIONS TO NUCLIDE 39

6.200000E-02 6.269997E-02 5.700000E-02 5.700000E-02 5.700000E-02 5.700000E-02 5.700000E-02 5.700000E-02
5.700000E-02 5.700000E-02 5.700000E-02 5.700000E-02 5.700000E-02 5.700000E-02

YIELD FRACTIONS TO NUCLIDE 85

4.800000E-02 6.060000E-02 6.100000E-02 6.100000E-02 2.700000E-02 2.700000E-02 6.300002E-02 6.300002E-02

2.7CCCCCE-02 2.70C000E-02 6.300002E-02 6.300002E-02 6.300002E-02 6.300002E-02

YIELD FRACTIONS TO NUCLIDE 50
1.6CCCCCE-02 3.000000E-02 5.700000E-02 5.700000E-02 1.600000E-03 1.600000E-03 0.0 6.599998E-02
1.6CCCCCE-03 1.60CCCCE-03 6.599998E-02 6.599998E-02 6.599998E-02 6.599998E-02

YIELD FRACTIONS TO NUCLIDE 53
3.700000E-02 2.93CC00E-02 3.200000E-02 3.200000E-02 1.600000E-02 1.600000E-02 3.200000E-02 3.200C00E-02
1.6CC000E-02 1.600000E-02 3.200000E-02 3.200C00E-02 3.200C00E-02 3.2CC0C0E-02

YIELD FRACTIONS TC NUCLIDE 58
6.CCC000E-02 6.400001E-02 7.200003E-02 7.200003E-02 6.5CC0C0E-02 6.500000E-02 6.900001E-02 6.900001E-02
6.5CCCCCE-02 6.500000E-02 6.900001E-02 6.900001E-02 6.900001E-02 6.900001E-02

YIELD FRACTIONS TC NUCLIDE 59
6.2CCJCCE-02 6.599003E-02 5.400000E-02 5.400000E-02 5.200000E-02 5.200000E-02 5.500000E-02 5.500000E-02
5.2000C0E-02 5.2JC0CCE-02 5.500000E-02 5.500000E-02 5.500000E-02 5.500000E-02

YIELD FRACTIONS TO NUCLIDE 60
5.2CCCCCE-02 5.98CCCCE-02 6.100000E-02 6.100000E-02 3.720000E-02 3.720000E-02 3.720000E-02 3.720000E-02
3.72CCCCE-02 3.72CCCCE-02 3.720000E-02 3.72CC00E-02 3.72C000E-02 3.720000E-02

YIELD FRACTIONS TO NUCLIDE 61
3.0CCCCCE-02 3.95C000E-02 4.100000E-02 4.100000E-02 3.000000E-02 3.000000E-02 4.100000E-02 4.100000E-02
3.0CCCCCE-02 3.0JC000E-02 4.100000E-02 4.100000E-02 4.1CC000E-02 4.1CC000E-02

YIELD FRACTIONS TC NUCLIDE 63
1.7CCCCCE-02 2.380C0CE-02 2.600000E-02 2.600000E-02 1.700000E-02 1.700000E-02 2.600000E-02 2.600000E-02
1.7CCCCCE-02 1.70CCCCE-02 2.600000E-02 2.600000E-02 2.6CJ000E-02 2.600000E-02

YIELD FRACTIONS TC NUCLIDE 67
6.2JC001E-03 1.130000E-02 1.700000E-02 1.700000E-02 6.200001E-03 6.200001E-03 1.700000E-02 1.700000E-02
6.2JC001E-03 6.2JC001E-03 1.700J00E-02 1.700000E-02 1.700000E-02 1.700000E-02

YIELD FRACTIONS TO NUCLIDE 69
2.6CCCCCE-03 4.500002E-03 1.000J0JE-02 1.000000E-02 2.600000E-03 2.600000E-03 1.CC0000E-02 1.000000E-02
2.60C00JE-03 2.60CCCCE-03 1.000000E-02 1.00C000E-02 1.000000E-02 1.000000E-02

YIELD FRACTIONS TO NUCLIDE 70
1.7CCCCCE-03 2.85C000E-03 7.500000E-03 7.500000E-03 1.700000E-03 1.700000E-03 7.500000E-03 7.500000E-03
1.7CCCCCE-03 1.709000E-03 7.500000E-03 7.500000E-03 7.500000E-03 7.5C0C0CE-03

YIELD FRACTIONS TC NUCLIDE 71
9.5CCCCCE-04 1.500000E-03 4.299998E-03 4.299998E-03 9.500000E-04 9.500000E-04 4.299998E-03 4.299998E-03
9.5CCCCCE-04 9.5CC000E-04 4.299998E-03 4.299998E-03 4.299998E-03 4.299998E-03

YIELD FRACTIONS TC NUCLIDE 86
1.CCCCCCE+00 0.0 0.0 0.0 0.0 0.0 0.0 0.0
0.0 0.0 0.0 0.0 0.0 0.0

YIELD FRACTIONS TO NUCLIDE 87
0.0 1.00CCCCE+00 0.0 0.0 0.0 0.0 0.0 0.0
C.0 0.0 0.0 C.0 0.0 0.0

NUCLIDE CHAIN DESCRIPTIONS

SIG.SET 1 THROUGH 1 CCNTAIN 18 CHAINS

DECAY CAPTURE / YIELD NUCLIDE 8 10 14 16 6 9 12 15 7
82 13 11 17 18

NEW CHAIN STARTS
6 0.0 0.0 0.0 0.0 0.0 0.0 0.0 0.0 0.0
C.0 0.0 0.0 0.0 0.0
7 0.0 0.0 0.0 0.0 0.0 0.0 0.0 0.0 0.0

```
                C.0       0.0       0.0       0.0       0.0
       8                0.0       0.0       0.0       0.0       0.0       0.0       0.0       0.0       0.0       0.0
                C.0       0.0       0.0       0.0       0.0
       9                0.0       0.0       0.0       0.0       0.0       0.0       0.0       0.0       0.0       0.0
                C.0       0.0       0.0       0.0       0.0
      10                0.0       0.0       0.0       0.0       0.0       0.0       0.0       0.0       0.0       0.0
                C.0       0.0       0.0       0.0       0.0
      11                0.0       0.0       0.0       0.0       0.0       0.0       0.0       0.0       0.0       0.0
                0.0       0.0       0.0       0.0       0.0
      18                0.0       0.0       0.0       0.0       0.0       0.0       0.0       0.0       0.0       0.0
                0.0       0.0       0.0       0.0       0.0
 NEW CHAIN STARTS
       6                0.0       0.0       0.0       0.0       0.0       0.0       0.0       0.0       0.0       0.0
                0.0       0.0       0.0       0.0       0.0
       7                0.0       0.0       0.0       0.0       0.0       0.0       0.0       0.0       0.0       0.0
                0.0       0.0       0.0       0.0       0.0
     209
     210
     211
     218
 NEW CHAIN STARTS
     506FN FISS *1000  110   0.0       0.0       0.0       0.0       0.0       0.0       0.0       0.0       0.0       0.0
                0.C       0.0       0.0       0.0       0.0
      82                0.0       C.C       0.0       0.0       0.0       0.0       0.0       0.0       0.0       0.0
                0.0       0.0       0.0       0.0       0.0
 NEW CHAIN STARTS
      12                0.0       0.0       0.0       0.0       0.0       0.0       0.0       0.0       0.0       0.0
                0.0       0.0       0.0       0.0       0.0
      13                0.0       C.0       0.0       0.0       0.0       0.0       0.0       0.0       0.0       0.0
                0.0       0.0       0.0       0.0       0.0
      14                0.0       0.0       0.0       0.0       0.0       0.0       0.0       0.0       0.0       0.0
                0.0       0.0       0.0       0.0       0.0
      15                0.0       0.0       0.0       0.0       0.0       0.0       0.0       0.0       0.0       0.0
                C.0       0.0       0.0       0.0       0.0
      16                0.0       0.0       0.0       0.0       0.0       0.0       0.0       0.0       0.0       0.0
                C.0       0.0       0.0       0.0       0.0
      17                0.0       0.0       0.0       0.0       0.0       0.0       0.0       0.0       0.0       0.0
                0.0       0.0       0.0       0.0       0.0
 NEW CHAIN STARTS
      12                0.0       0.0       0.0       0.0       0.0       0.0       0.0       0.0       0.0       0.0
                C.0       0.0       0.0       0.0       0.0
      13                0.0       C.0       0.0       0.0       0.0       0.0       0.0       0.0       0.0       0.0
                0.0       0.0       0.0       0.0       0.0
     215
     216
     217
 NEW CHAIN STARTS
      63                0.0170000 0.0238000 0.0260000 0.0260000 0.0170000 0.0170000 0.0260000 0.0260000 0.0170000
 C.0170000 0.0260000 0.0260000 0.0260000 0.0260000
      65                0.0       0.0       0.0       0.0       0.0       0.0       0.0       0.0       0.0       0.0
                0.0       0.0       0.0       0.0       0.0
 NEW CHAIN STARTS
      67                0.0062000 0.0113000 0.0170000 0.0170000 0.0062000 0.0062000 0.0170000 0.0170000 0.0062000
 0.0062000 0.0170000 0.0170000 0.0170000 0.0170000
      68                0.0       0.0       0.0       0.0       0.0       0.0       0.0       0.0       0.0       0.0
 0.0       0.0       0.0       0.0       0.0
      69                0.0026000 0.0045000 0.0100000 0.0100000 0.0026000 0.0026000 0.0100000 0.0100000 0.0026000
 C.0026000 C.0100000 0.0100000 0.0100000 0.0100000
      70                0.0017000 0.0028500 0.0075000 0.0075000 0.0017000 0.0017000 0.0075000 0.0075000 0.0017000
 0.0017000 0.0075000 0.0075000 0.0075000 0.0075000
```

```
 W CHAIN STARTS
          71                    0.0009500 0.0015000 0.0043000 0.0043000 0.0009500 0.0009500 0.0043000 0.0043000 0.0009500
                   0.0009500 0.0043000 0.0043000 0.0043000 0.0043000
          72                    0.0       0.0       0.0       0.0       0.0       0.0       0.0       0.0       0.0
                   0.0       0.0       0.0       0.0       0.0
          73                    0.0       0.0       0.0       0.0       0.0       0.0       0.0       0.0       0.0
                   0.0       0.0       0.0       0.0       0.0

 NEW CHAIN STARTS
          39                    0.0620000 0.0627000 0.0570000 0.0570000 0.0570000 0.0570000 0.0570000 0.0570000 0.0570000
                   0.0570000 0.0570000 0.0570000 0.0570000 0.0570000

 NEW CHAIN STARTS
          85                    0.0480000 0.0606000 0.0610000 0.0610000 0.0270000 0.0270000 0.0630000 0.0630000 0.0270000
                   0.0270000 0.0630000 0.0630000 0.0630000 0.0630000

 NEW CHAIN STARTS
          50                    0.0160000 0.0300000 0.0570000 0.0570000 0.0016000 0.0016000 0.0       0.0660000 0.0016000
                   0.0016000 0.0660000 0.0660000 0.0660000 0.0660000

 NEW CHAIN STARTS
          53                    0.0370000 0.0293000 0.0320000 0.0320000 0.0160000 0.0160000 0.0320000 0.0320000 0.0160000
                   0.0160000 0.0320000 0.0320000 0.0320000 0.0320000

 NEW CHAIN STARTS
          58                    0.0600000 0.0640000 0.0720000 0.0720000 0.0650000 0.0650000 0.0690000 0.0690000 0.0650000
                   0.0650000 0.0690000 0.0690000 0.0690000 0.0690000

 NEW CHAIN STARTS
          55                    0.0620000 0.0659000 0.0540000 0.0540000 0.0520000 0.0520000 0.0550000 0.0550000 0.0520000
                   0.0520000 0.0550000 0.0550000 0.0550000 0.0550000

 NEW CHAIN STARTS
          60                    0.0520000 0.0598000 0.0610000 0.0610000 0.0372000 0.0372000 0.0372000 0.0372000 0.0372000
                   0.0372000 0.0372000 0.0372000 0.0372000 0.0372000

 NEW CHAIN STARTS
          61                    0.0300000 0.0395000 0.0410000 0.0410000 0.0300000 0.0300000 0.0410000 0.0410000 0.0300000
                   0.0300000 0.0410000 0.0410000 0.0410000 0.0410000

 NEW CHAIN STARTS
          86                    1.0000000 0.0       0.0       0.0       0.0       0.0       0.0       0.0       0.0
                   0.0       0.0       0.0       0.0       0.0

 NEW CHAIN STARTS
          87                    0.0       1.0000000 0.0       0.0       0.0       0.0       0.0       0.0       0.0
                   0.0       0.0       0.0       0.0       0.0

 CHAIN ARRAY (   1)  18   5  -9   1   6   2  12  14   0   5   9 206 202 212 214   0-505-110  10   0   7 -11   3   8   4
   13   0   7  11 208 204 213   0  27  28   0  29  30  31  32   0  33  34  35   0  19   0  20   0  21   0  22   0
   23   0  24   0  25   0  26   0  36   0  37   0   0

 SIG.SET     2 THROUGH     2 CONTAIN     1 CHAINS


 DECAY   CAPTURE / YIELD NUCLIDE     0

 NEW CHAIN STARTS
          83                    0.0

 CHAIN ARRAY (  67)  18   5  -9   1   6   2  12  14   0   5   9 206 202 212 214   0-505-110  10   0   7 -11   3   8   4
   13   0   7  11 208 204 213   0  27  28   0  29  30  31  32   0  33  34  35   0  19   0  20   0  21   0  22   0
   23   0  24   0  25   0  26   0  36   0  37   0   0   1   3   0   0
```

FISSILE NUCLIDES--- 8 10 14 16
FERTILE NUCLIDES--- 6 9 12 15
INTERMEDIATE NUCLIDES--- 7 82 13 11
OTHER NUCLIDES--- 17 18 105 125
STRUCTURAL NUCLIDES--- 5 83 84
SPECIAL NUCLIDES---NONE SPECIFIED
FISSION PRODUCT NUCLIDES--- 39 85 50 53 58 55 60 61 63 65 67 68 70 71 72 72 73 86 87

CORE STORAGE DIFFERENCE (WORDS) EQUATION CONSTANTS I/O INSTEAD OF STORED 11429

EQUATION CONSTANTS WILL BE STORED IN CORE

NUMBER OF---COLUMNS, ROWS, PLANES, GROUPS, UPSCAT, DOWNSCAT, REGIONS, AND ZONES 26 50 1 4 0 1 28 18

MEMORY LOCATIONS RESERVED FOR DATA STORAGE--- 40000
MEMORY LOCATIONS USED FOR THIS PROBLEM------- 39946
MEMORY LOCATIONS NOT USED------------------- 54

ARMY REACTOR DEPLETION RUNS
DATE : MAY 14 , 1975

SUMMARY OF NEUTRON LOSSES, ETC. FOR STEP 1 CYCLE 1 AT CYCLE DEPLETION TIME 30.00 DAYS. FISSILE KG IS AT 60.00 DAYS

ZONE CLASS	FISSILE	FERTILE	INTERMEDIATE	OTHER	STRUCTURAL	SPECIAL	UNSPECIFIED	SUMS	CONV. RATIO	POWER(MW)	FISSILE(KG)
CORE	0.54259	0.24808	0.00226	0.11570	0.00765	0.0	0.01638	0.93275	0.45131	2.98196E+02	7.67915E+02
BUFFER	0.0	0.0	0.0	0.00856	0.00132	0.0	0.0	0.00987	0.0	0.0	0.0
REFLECTOR	0.0	0.0	0.0	0.01220	0.01660	0.0	-0.00000	0.02880	0.0	0.0	0.0
OTHER LOSSES' BASED ON START-OF-STEP TOTAL LOSSES								0.02858			
OVERALL	0.54269	0.24808	0.00226	0.13645	0.02557	0.0	0.01638	1.00000	0.45131	2.98196E+02	7.67915E+02

TIME STEP THERMAL ENERGY, MW-HRS 4.29402E+05 AND TOTAL IS 4.29402E+05

NUCLIDE DENSITIES BY ZONE AND SUB-ZONE(NUCLIDE NUMBER - DENSITY) AT DEPLETION TIME 6.000000E+01DAYS

ZONE NUMBER 1-- CORE

8	2.63262E-07	10	4.07851E-05	14	2.04514E-08	16	2.30358E-11	6	3.46249E-04	9	3.60540E-09	
12	3.13679E-06	15	5.29977E-10	7	2.78724E-07	82	2.20041E-10	13	1.31186E-09	11	2.74101E-07	
17	1.87299E-13	18	1.13575E-09	105	2.44799E-06	125	0.0	5	6.19000E-02	84	7.37000E-04	
39	5.91960E-08	85	5.70632E-08	50	2.79955E-08	53	2.73931E-08	58	3.37908E-10	55	6.19802E-08	
60	5.61123E-08	61	3.71293E-08	63	2.13302E-08	65	1.35344E-10	67	4.42007E-09	68	6.22266E-09	
69	3.66506E-09	70	3.01606E-09	71	1.38148E-09	72	3.57450E-11	73	1.24293E-12	86	3.73641E-09	
87	9.39329E-07											

ZONE NUMBER 2-- CORE

8	4.26235E-07	10	4.00934E-05	14	3.24870E-08	16	8.75145E-11	6	3.45897E-04	9	9.41441E-09	
12	3.12176E-06	15	1.29940E-09	7	4.54398E-07	82	3.54470E-10	13	2.15558E-09	11	4.34681E-07	
17	1.12015E-12	18	2.96911E-09	105	2.30786E-06	125	0.0	5	6.19000E-02	84	7.37000E-04	
39	9.27153E-08	85	8.92788E-08	50	4.36106E-08	53	4.26599E-08	58	4.34798E-10	55	9.68535E-08	
60	8.76212E-08	61	5.80042E-08	63	3.27735E-08	65	3.20390E-10	67	4.87334E-09	68	1.17597E-08	
69	5.77135E-09	70	4.96291E-09	71	2.13152E-09	72	8.79001E-11	73	4.45591E-12	86	9.57538E-09	
87	1.46827E-06											

ZONE NUMBER 3-- CORE

8	4.46511E-07	10	4.00019E-05	14	3.39059E-08	16	1.00358E-10	6	3.45853E-04	9	1.03528E-08	
12	3.11989E-06	15	1.42075E-09	7	4.76459E-07	82	3.71182E-10	13	2.26021E-09	11	4.55396E-07	
17	1.34912E-12	18	3.26335E-09	105	2.29048E-06	125	0.0	5	6.19000E-02	84	7.37000E-04	
39	9.71888E-08	85	9.35742E-08	50	4.56807E-08	53	4.46859E-08	58	4.44736E-10	55	1.01498E-07	
60	9.18104E-08	61	6.07831E-08	63	3.42721E-08	65	3.48599E-10	67	4.89525E-09	68	1.25349E-08	
69	6.01130E-09	70	5.23535E-09	71	2.23006E-09	72	9.62791E-11	73	5.07304E-12	86	1.05275E-08	
87	1.53875E-06											

ZONE NUMBER 4-- CORE

8	3.17671E-07	10	4.04958E-05	14	2.42597E-08	16	4.28405E-11	6	3.46131E-04	9	5.36602E-09	
12	3.13200E-06	15	7.84572E-10	7	3.37550E-07	82	2.65203E-10	13	1.58108E-09	11	3.36154E-07	
17	4.38071E-13	18	1.68304E-09	105	2.38219E-06	125	0.0	5	6.19000E-02	84	7.37000E-04	
39	7.35225E-08	85	7.08501E-08	50	3.46833E-08	53	3.39560E-08	58	3.80483E-10	55	7.69228E-08	
60	6.95919E-08	61	4.60743E-08	63	2.63238E-08	65	1.96840E-10	67	4.60550E-09	68	8.60251E-09	
69	4.69545E-09	70	3.84081E-09	71	1.70649E-09	72	5.36524E-11	73	2.26221E-12	86	5.61907E-09	
87	1.16597E-06											

ZONE NUMBER 5-- CORE

8	2.36943E-07	10	4.09072E-05	14	1.84996E-08	16	1.68541E-11	6	3.46305E-04	9	2.91265E-09	
12	3.13915E-06	15	4.31477E-10	7	2.50551E-07	82	1.98157E-10	13	1.17923E-09	11	2.46674E-07	
17	1.22922E-13	18	9.18152E-10	105	2.47622E-06	125	0.0	5	6.19000E-02	84	7.37000E-04	
39	5.32361E-08	85	5.13265E-08	50	2.52020E-08	53	2.46578E-08	58	3.16621E-10	55	5.57602E-08	
60	5.04912E-08	61	3.34049E-08	63	1.92413E-08	65	1.10971E-10	67	4.28144E-09	68	5.29279E-09	
69	3.50722E-09	70	2.68498E-09	71	1.24547E-09	72	2.90302E-11	73	9.18697E-13	86	3.01952E-09	
87	8.45019E-07											

ZONE NUMBER 6-- CORE

8	3.83664E-07	10	4.02854E-05	14	2.94716E-08	16	6.41566E-11	6	3.45990E-04	9	7.51483E-09
12	3.12567E-06	15	1.06091E-09	7	4.08217E-07	82	3.19338E-10	13	1.93655E-09	11	3.91198E-07
17	7.35174E-13	18	2.35788E-09	105	2.34540E-06	125	0.0	5	6.19000E-02	84	7.37000E-04
39	8.33418E-08	85	8.02748E-08	50	3.92629E-08	53	3.84051E-08	58	4.12208E-10	55	8.71140E-08
60	7.88318E-08	61	5.21756E-08	63	2.96089E-08	65	2.64331E-10	67	4.81013E-09	68	1.01509E-08
69	5.25821E-09	70	4.40071E-09	71	1.92377E-09	72	7.15013E-11	73	3.31693E-12	86	7.72831E-09
87	1.32050E-06										

ZONE NUMBER 7-- CORE

8	4.01655E-07	10	4.02043E-05	14	3.07521E-08	16	7.34504E-11	6	3.45951E-04	9	8.33904E-09
12	3.12402E-06	15	1.15898E-09	7	4.27712E-07	82	3.34194E-10	13	2.02502E-09	11	4.09572E-07
17	8.83150E-13	18	2.63163E-09	105	2.32936E-06	125	0.0	5	6.19000E-02	84	7.37000E-04
39	8.72998E-08	85	8.40774E-08	50	4.11005E-08	53	4.02013E-08	58	4.22054E-10	55	9.12280E-08
60	8.25451E-08	61	5.46378E-08	63	3.09492E-08	65	2.87487E-10	67	4.84004E-09	68	1.08273E-08
69	5.47663E-09	70	4.63665E-09	71	2.01170E-09	72	7.82332E-11	73	3.77290E-12	86	8.48390E-09
87	1.38292E-06										

ZONE NUMBER 8-- CORE

8	2.85367E-07	10	4.06506E-05	14	2.19213E-08	16	3.11291E-11	6	3.46201E-04	9	4.30941E-09
12	3.13492E-06	15	6.36379E-10	7	3.02556E-07	82	2.38259E-10	13	1.41717E-09	11	3.01716E-07
17	2.84471E-13	18	1.35288E-09	105	2.41561E-06	125	0.0	5	6.19000E-02	84	7.37000E-04
39	6.59285E-08	85	6.35454E-08	50	3.11413E-08	53	3.04839E-08	58	3.58152E-10	55	6.90087E-08
60	6.24495E-08	61	4.13369E-08	63	2.36948E-08	65	1.61043E-10	67	4.50459E-09	68	7.34450E-09
69	4.25851E-09	70	3.40186E-09	71	1.53500E-09	72	4.33761E-11	73	1.66486E-12	86	4.51436E-09
87	1.04594E-06										

ZONE NUMBER 9-- CORE

8	1.72416E-07	10	4.11362E-05	14	1.32481E-08	16	8.11232E-12	6	3.46441E-04	9	1.60806E-09
12	3.14523E-06	15	2.52460E-10	7	1.81922E-07	82	1.46158E-10	13	8.36259E-10	11	1.89104E-07
17	4.79138E-14	18	4.99122E-10	105	2.52581E-06	125	0.0	5	6.19000E-02	84	7.37000E-04
39	4.24250E-08	85	4.09229E-08	50	2.01165E-08	53	1.96945E-08	58	2.69473E-10	55	4.44778E-08
60	4.02720E-08	61	2.66475E-08	63	1.54511E-08	65	6.53203E-11	67	3.84832E-09	68	3.78602E-09
69	2.83694E-09	70	2.10685E-09	71	9.98068E-10	72	1.74160E-11	73	4.56370E-13	86	1.73883E-09
87	6.74010E-07										

ZONE NUMBER 10-- CORE

8	2.78126E-07	10	4.06512E-05	14	2.11448E-08	16	3.07203E-11	6	3.46216E-04	9	4.14621E-09
12	3.13579E-06	15	6.19834E-10	7	2.94896E-07	82	2.34718E-10	13	1.36830E-09	11	2.98536E-07
17	2.83326E-13	18	1.29121E-09	105	2.41319E-06	125	0.0	5	6.19000E-02	84	7.37000E-04
39	6.60927E-08	85	6.37081E-08	50	3.12138E-08	53	3.05687E-08	58	3.56693E-10	55	6.91901E-08
60	6.25983E-08	61	4.14443E-08	63	2.37784E-08	65	1.56293E-10	67	4.48528E-09	68	7.41354E-09
69	4.26470E-09	70	3.41738E-09	71	1.53959E-09	72	4.26545E-11	73	1.64871E-12	86	4.40393E-09
87	1.04667E-06										

ZONE NUMBER 11-- CORE

8	2.90592E-07	10	4.05906E-05	14	2.20373E-08	16	3.49574E-11	6	3.46190E-04	9	4.53193E-09
12	3.13468E-06	15	6.74745E-10	7	3.08304E-07	82	2.45154E-10	13	1.43062E-09	11	3.11899E-07
17	3.37351E-13	18	1.41089E-09	105	2.39994E-06	125	0.0	5	6.19000E-02	84	7.37000E-04
39	6.90676E-08	85	6.65704E-08	50	3.26020E-08	53	3.19305E-08	58	3.65608E-10	55	7.22920E-08
60	6.53969E-08	61	4.33011E-08	63	2.48128E-08	65	1.69573E-10	67	4.50729E-09	68	7.90408E-09
69	4.43671E-09	70	3.58886E-09	71	1.60696E-09	72	4.64909E-11	73	1.86666E-12	86	4.81229E-09
87	1.09571E-06										

ZONE NUMBER 12-- CORE

8	2.05212E-07	10	4.09514E-05	14	1.55716E-08	16	1.42697E-11	6	3.46371E-04	9	2.31444E-09
12	3.14244E-06	15	3.62211E-10	7	2.16942E-07	82	1.73553E-10	13	9.53227E-10	11	2.27950E-07
17	1.03357E-13	18	7.16013E-10	105	2.47809E-06	125	0.0	5	6.19000E-02	84	7.37000E-04
39	5.16093E-08	85	4.97724E-08	50	2.44311E-08	53	2.39301E-08	58	3.05012E-10	55	5.40828E-08
60	4.89439E-08	61	3.23990E-08	63	1.87253E-08	65	9.27156E-11	67	4.11075E-09	68	5.17263E-09
69	3.40050E-09	70	2.60918E-09	71	1.21011E-09	72	2.52791E-11	73	7.93200E-13	86	2.52203E-09
87	8.19661E-07										

ZONE NUMBER 13-- BUFFER

105	1.08549E-06	125	0.0	83	7.10699E-02

ZONE NUMBER 14-- BUFFER

105	1.08659E-06	125	0.0	83	7.10699E-02

ZONE NUMBER 15-- BUFFER

105	1.08952E-06	125	0.0	83	7.10699E-02

ZONE NUMBER 16-- REFLECTOR

105	0.0	125	3.04300E-04	83	6.66300E-02

ZONE NUMBER 17-- REFLECTOR

105	0.0	125	0.0	83	7.10700E-02

ZONE NUMBER 18-- REFLECTOR

```
 105  0.0          125  0.0          83  7.10700E-02

 TIME STEP  1  REQUIRED  0.789  MINUTES CPU TIME, AND  1.112  MINUTES CLOCK TIME

 A FLUX - EIGENVALUE PROBLEM FOLLOWS FOR CYCLE  1 CYCLE TIME    60.0000 DAYS   TOTAL TIME    60.0000 DAYS

 ITERATION  FLUX CHANGE     BETA      MU-1      MU-2      MU-3          K
     1      2.07348E-02   1.00000   0.04147   0.0       0.0       1.028752
     2      2.09675E+00   1.76982 103.21893 103.21893   0.00236   1.029813
     3      1.17534E+00   1.62578   1.73590   0.23909   0.09118   1.029865
     4      1.60736E+00   1.54699   2.97493   0.48725  -0.39215   1.029790
     5      3.14887E-01   1.50704   0.51079   0.45472   1.17277   1.029741
     6     -2.39974E-01   1.48756  -1.00207  -0.10710   1.00441   1.029695
     7     -1.62367E-01   1.47825   0.51423   0.53409   0.89780   1.029655
     8     -4.18246E-02   1.47383   0.21577   0.90363   0.87855   1.029619
     9      1.09978E-02   1.47175  -0.25195  -0.32692   0.86633   1.029589
    10     -6.52091E-03   1.47077  -0.59944  -0.72240   0.86123   1.029562
    11      3.87001E-03   1.47031  -0.58962  -0.42859   0.85772   1.029540
    12      2.85149E-03   1.47009   0.73967   0.48171   0.85525   1.029520
    13      2.21348E-03   1.46999   0.77847   0.87284   0.85304   1.029504
    14      1.78432E-03   1.46994   0.80790   0.87328   0.85088   1.029490
    15      1.46770E-03   1.46992   0.82402   0.87459   0.84854   1.029477
    16      1.21890E-03   1.46991   0.83163   0.87542   0.84580   1.029467
    17      1.01757E-03   1.46991   0.83592   0.87759   0.84249   1.029457
    18      8.52595E-04   1.46990   0.83872   0.87857   0.83838   1.029449
    19      7.15256E-04   1.46990   0.83964   0.87904   0.83323   1.029443
    20      5.99661E-04   1.46990   0.83927   0.88166   0.82670   1.029437
    21      5.03540E-04   1.46990   0.83993   0.88274   0.81833   1.029432
    22      4.22478E-04   1.46990   0.83944   0.88521   0.80743   1.029428
    23      3.54767E-04   1.46990   0.84008   0.88663   0.79293
            2.24077E-03   EXTRAPOLATION WITH        6.3183          1.029399
    24     -4.75407E-04   1.00000  -1.34053  -0.81459   5.63865   1.029400
    25     -3.46065E-04   1.46990   0.72759   1.12287  -0.09996   1.029399
    26      1.00136E-04   1.46990  -0.28926  -0.40293   1.16986   1.029399
    27      8.20160E-05   1.46990   0.81913   0.76981   1.03760   1.029399

 END OF EIGENVALUE CALCULATION - ITERATION TIME  0.294 MINUTES

 CONVERGENCE INDICATION BY MINIMIZING THE SUM OF THE SQUARES OF THE RESIDUES - RELATIVE ABSORPTION  1.0000000   K  1.0294075

    LEAKAGE  6.27435E+17  TOTAL LOSSES  2.19543E+19  TOTAL PRODUCTIONS  2.25997E+19  REACTOR POWER(WATTS)  3.00000E+08


 AVERAGE FLUXES BY ZONE AND GROUP

 ZONE   1-- CORE
    3.17513E+13  6.35325E+13  9.32920E+12  2.06395E+13

 ZONE   2-- CORE
    5.07575E+13  1.03117E+14  1.51301E+13  3.15029E+13

 ZONE   3-- CORE
    5.30004E+13  1.07717E+14  1.58050E+13  3.29353E+13

 ZONE   4-- CORE
    3.80132E+13  7.56694E+13  1.11401E+13  2.57750E+13

 ZONE   5-- CORE
    2.88069E+13  5.75995E+13  8.45739E+12  1.86978E+13

 ZONE   6-- CORE
    4.60507E+13  9.34655E+13  1.37140E+13  2.85118E+13

 ZONE   7-- CORE
```

4.80522E+13 9.75640E+13 1.43154E+13 2.57826E+13

ZONE 8-- CORE
3.43894E+13 6.84050E+13 1.00701E+13 2.32646E+13

ZONE 9-- CORE
2.14887E+13 4.13051E+13 6.04361E+12 1.56811E+13

ZONE 10-- CORE
3.42293E+13 6.68168E+13 9.77571E+12 2.38655E+13

ZONE 11-- CORE
3.56453E+13 6.96072E+13 1.01844E+13 2.48679E+13

ZONE 12-- CORE
2.53176E+13 4.84658E+13 7.11375E+12 1.90837E+13

ZONE 13-- BUFFER
5.65306E+12 1.92723E+13 4.25573E+12 5.01495E+13

ZONE 14-- BUFFER
5.10510E+12 1.73953E+13 3.84079E+12 4.51498E+13

ZONE 15-- BUFFER
3.62388E+12 1.20268E+13 2.64318E+12 3.35691E+13

ZONE 16-- REFLECTOR
9.21943E+11 3.31505E+12 7.38458E+11 1.07258E+13

ZONE 17-- REFLECTOR
9.63608E+10 7.38860E+11 1.95791E+11 1.92901E+13

ZONE 18-- REFLECTOR
7.86958E+11 3.00837E+12 6.97966E+11 2.37935E+13

ZONE AVERAGE POWER DENSITIES (WATTS/CC)

5.90575E+00	9.07495E+00	9.47263E+00	7.25319E+00	5.36086E+00	8.23990E+00	8.59531E+00	6.56465E+00	4.33612E+00
6.64838E+00	6.92082E+00	5.21831E+00	0.0	0.0	0.0	0.0	0.0	0.0

ARRY REACTOR DEPLETION RUNS
DATE : MAY 14 , 1975

GROUP 1 FLUX

	1	2	3	4	5	6	7	8	9	10	11
1	4.690D+09	4.657D+09	4.625D+09	4.594D+09	4.534D+09	4.439D+09	4.345D+09	4.251D+09	4.157D+09	4.063D+09	3.968D+09
2	2.137D+10	2.122D+10	2.107D+10	2.093D+10	2.066D+10	2.023D+10	1.980D+10	1.937D+10	1.895D+10	1.852D+10	1.810D+10
3	8.632D+10	8.572D+10	8.514D+10	8.456D+10	8.347D+10	8.173D+10	8.000D+10	7.828D+10	7.658D+10	7.489D+10	7.320D+10
4	3.463D+11	3.439D+11	3.416D+11	3.393D+11	3.349D+11	3.280D+11	3.210D+11	3.142D+11	3.073D+11	3.006D+11	2.939D+11
5	1.389D+12	1.379D+12	1.370D+12	1.361D+12	1.343D+12	1.315D+12	1.288D+12	1.260D+12	1.233D+12	1.206D+12	1.179D+12
6	5.570D+12	5.531D+12	5.494D+12	5.458D+12	5.388D+12	5.276D+12	5.165D+12	5.054D+12	4.945D+12	4.836D+12	4.729D+12
7	1.853D+13	1.841D+13	1.828D+13	1.816D+13	1.793D+13	1.756D+13	1.719D+13	1.682D+13	1.646D+13	1.609D+13	1.574D+13
8	2.365D+13	2.349D+13	2.333D+13	2.318D+13	2.289D+13	2.241D+13	2.194D+13	2.147D+13	2.100D+13	2.054D+13	2.008D+13
9	2.758D+13	2.739D+13	2.721D+13	2.703D+13	2.669D+13	2.613D+13	2.558D+13	2.503D+13	2.449D+13	2.395D+13	2.342D+13
10	3.112D+13	3.091D+13	3.070D+13	3.049D+13	3.011D+13	2.949D+13	2.886D+13	2.824D+13	2.763D+13	2.702D+13	2.642D+13
11	3.445D+13	3.422D+13	3.399D+13	3.376D+13	3.334D+13	3.265D+13	3.195D+13	3.127D+13	3.058D+13	2.991D+13	2.924D+13
12	3.759D+13	3.734D+13	3.709D+13	3.684D+13	3.638D+13	3.562D+13	3.487D+13	3.411D+13	3.337D+13	3.263D+13	3.190D+13
13	4.051D+13	4.023D+13	3.996D+13	3.970D+13	3.920D+13	3.839D+13	3.757D+13	3.676D+13	3.596D+13	3.516D+13	3.439D+13
14	4.316D+13	4.287D+13	4.258D+13	4.230D+13	4.177D+13	4.090D+13	4.003D+13	3.917D+13	3.832D+13	3.747D+13	3.663D+13
15	4.559D+13	4.529D+13	4.499D+13	4.469D+13	4.415D+13	4.323D+13	4.231D+13	4.140D+13	4.050D+13	3.961D+13	3.872D+13
16	4.765D+13	4.733D+13	4.701D+13	4.670D+13	4.613D+13	4.517D+13	4.421D+13	4.326D+13	4.231D+13	4.137D+13	4.045D+13
17	4.957D+13	4.923D+13	4.890D+13	4.858D+13	4.799D+13	4.699D+13	4.599D+13	4.500D+13	4.401D+13	4.304D+13	4.207D+13
18	5.124D+13	5.089D+13	5.055D+13	5.022D+13	4.960D+13	4.857D+13	4.753D+13	4.651D+13	4.549D+13	4.448D+13	4.349D+13
19	5.264D+13	5.228D+13	5.193D+13	5.159D+13	5.096D+13	4.990D+13	4.883D+13	4.778D+13	4.673D+13	4.570D+13	4.467D+13
20	5.377D+13	5.340D+13	5.305D+13	5.270D+13	5.205D+13	5.097D+13	4.988D+13	4.880D+13	4.773D+13	4.667D+13	4.563D+13
21	5.462D+13	5.425D+13	5.389D+13	5.353D+13	5.287D+13	5.177D+13	5.067D+13	4.957D+13	4.849D+13	4.741D+13	4.635D+13
22	5.519D+13	5.481D+13	5.444D+13	5.409D+13	5.342D+13	5.231D+13	5.119D+13	5.008D+13	4.899D+13	4.790D+13	4.682D+13
23	5.546D+13	5.508D+13	5.471D+13	5.435D+13	5.368D+13	5.256D+13	5.144D+13	5.033D+13	4.922D+13	4.813D+13	4.705D+13
24	5.546D+13	5.508D+13	5.471D+13	5.435D+13	5.368D+13	5.256D+13	5.144D+13	5.032D+13	4.922D+13	4.812D+13	4.704D+13
25	5.519D+13	5.481D+13	5.444D+13	5.408D+13	5.341D+13	5.230D+13	5.118D+13	5.007D+13	4.896D+13	4.787D+13	4.680D+13
26	5.463D+13	5.426D+13	5.389D+13	5.353D+13	5.288D+13	5.177D+13	5.066D+13	4.956D+13	4.847D+13	4.738D+13	4.632D+13
27	5.380D+13	5.343D+13	5.307D+13	5.272D+13	5.207D+13	5.098D+13	4.988D+13	4.880D+13	4.772D+13	4.666D+13	4.560D+13
28	5.271D+13	5.234D+13	5.199D+13	5.164D+13	5.101D+13	4.993D+13	4.886D+13	4.779D+13	4.674D+13	4.569D+13	4.466D+13
29	5.135D+13	5.099D+13	5.065D+13	5.031D+13	4.969D+13	4.864D+13	4.759D+13	4.655D+13	4.552D+13	4.450D+13	4.349D+13
30	4.975D+13	4.940D+13	4.907D+13	4.874D+13	4.813D+13	4.711D+13	4.610D+13	4.509D+13	4.408D+13	4.309D+13	4.211D+13
31	4.823D+13	4.790D+13	4.757D+13	4.725D+13	4.666D+13	4.567D+13	4.468D+13	4.370D+13	4.273D+13	4.176D+13	4.081D+13
32	4.688D+13	4.656D+13	4.624D+13	4.593D+13	4.535D+13	4.439D+13	4.342D+13	4.247D+13	4.152D+13	4.058D+13	3.966D+13
33	4.541D+13	4.509D+13	4.478D+13	4.448D+13	4.392D+13	4.298D+13	4.205D+13	4.112D+13	4.020D+13	3.929D+13	3.840D+13
34	4.383D+13	4.352D+13	4.322D+13	4.293D+13	4.238D+13	4.148D+13	4.058D+13	3.968D+13	3.879D+13	3.791D+13	3.704D+13
35	4.214D+13	4.184D+13	4.156D+13	4.128D+13	4.075D+13	3.988D+13	3.901D+13	3.815D+13	3.729D+13	3.644D+13	3.560D+13
36	4.037D+13	4.008D+13	3.981D+13	3.954D+13	3.903D+13	3.820D+13	3.736D+13	3.653D+13	3.571D+13	3.490D+13	3.409D+13
37	3.851D+13	3.824D+13	3.798D+13	3.772D+13	3.724D+13	3.644D+13	3.564D+13	3.485D+13	3.406D+13	3.328D+13	3.251D+13
38	3.657D+13	3.631D+13	3.606D+13	3.581D+13	3.535D+13	3.459D+13	3.384D+13	3.308D+13	3.233D+13	3.159D+13	3.086D+13
39	3.448D+13	3.423D+13	3.400D+13	3.376D+13	3.333D+13	3.261D+13	3.189D+13	3.118D+13	3.047D+13	2.977D+13	2.908D+13
40	3.205D+13	3.182D+13	3.160D+13	3.139D+13	3.098D+13	3.031D+13	2.965D+13	2.898D+13	2.832D+13	2.767D+13	2.702D+13
41	2.882D+13	2.861D+13	2.842D+13	2.822D+13	2.786D+13	2.725D+13	2.665D+13	2.605D+13	2.546D+13	2.487D+13	2.428D+13
42	2.365D+13	2.348D+13	2.331D+13	2.315D+13	2.285D+13	2.236D+13	2.186D+13	2.137D+13	2.088D+13	2.040D+13	1.992D+13
43	1.234D+13	1.226D+13	1.217D+13	1.209D+13	1.193D+13	1.167D+13	1.141D+13	1.116D+13	1.090D+13	1.065D+13	1.040D+13
44	6.035D+12	5.992D+12	5.950D+12	5.909D+12	5.831D+12	5.705D+12	5.578D+12	5.453D+12	5.328D+12	5.204D+12	5.082D+12
45	2.970D+12	2.949D+12	2.929D+12	2.908D+12	2.870D+12	2.807D+12	2.745D+12	2.683D+12	2.622D+12	2.561D+12	2.500D+12
46	1.502D+12	1.492D+12	1.481D+12	1.471D+12	1.451D+12	1.420D+12	1.388D+12	1.357D+12	1.326D+12	1.295D+12	1.264D+12
47	4.213D+11	4.183D+11	4.154D+11	4.125D+11	4.069D+11	3.981D+11	3.892D+11	3.804D+11	3.717D+11	3.630D+11	3.544D+11
48	9.226D+10	9.161D+10	9.096D+10	9.032D+10	8.910D+10	8.715D+10	8.522D+10	8.329D+10	8.137D+10	7.945D+10	7.754D+10
49	2.011D+10	1.996D+10	1.982D+10	1.968D+10	1.941D+10	1.899D+10	1.856D+10	1.814D+10	1.772D+10	1.730D+10	1.688D+10
50	3.921D+09	3.893D+09	3.865D+09	3.837D+09	3.785D+09	3.702D+09	3.619D+09	3.537D+09	3.454D+09	3.371D+09	3.288D+09

	12	13	14	15	16	17	18	19	20	21	22
1	3.872D+09	3.728D+09	3.520D+09	3.291D+09	3.035D+09	2.743D+09	2.415D+09	2.055D+09	1.677D+09	1.012D+09	4.850D+08
2	1.767D+10	1.703D+10	1.612D+10	1.513D+10	1.401D+10	1.272D+10	1.124D+10	9.571D+09	7.780D+09	4.610D+09	2.116D+09
3	7.253D+10	6.999D+10	6.599D+10	6.171D+10	5.748D+10	5.255D+10	4.670D+10	3.985D+10	3.222D+10	1.841D+10	7.901D+09

4	2.872D+11	2.774D+11	2.639D+11	2.497D+11	2.342D+11	2.161D+11	1.938D+11	1.662D+11	1.336D+11	7.194D+10	2.817D+10
5	1.153D+12	1.114D+12	1.061D+12	1.008D+12	9.522D+11	8.883D+11	8.084D+11	7.021D+11	5.621D+11	2.734D+11	9.427D+10
6	4.624D+12	4.470D+12	4.263D+12	4.060D+12	3.858D+12	3.644D+12	3.387D+12	3.021D+12	2.445D+12	9.773D+11	2.821D+11
7	1.539D+13	1.488D+13	1.419D+13	1.353D+13	1.289D+13	1.230D+13	1.172D+13	1.096D+13	9.410D+12	2.453D+12	5.751D+11
8	1.964D+13	1.899D+13	1.811D+13	1.725D+13	1.644D+13	1.568D+13	1.494D+13	1.397D+13	1.195D+13	3.216D+12	7.517D+11
9	2.289D+13	2.213D+13	2.110D+13	2.010D+13	1.915D+13	1.825D+13	1.737D+13	1.622D+13	1.386D+13	3.818D+12	9.019D+11
10	2.582D+13	2.496D+13	2.380D+13	2.266D+13	2.158D+13	2.056D+13	1.955D+13	1.823D+13	1.558D+13	4.333D+12	1.032D+12
11	2.859D+13	2.763D+13	2.633D+13	2.507D+13	2.386D+13	2.273D+13	2.160D+13	2.013D+13	1.719D+13	4.799D+12	1.148D+12
12	3.119D+13	3.014D+13	2.872D+13	2.734D+13	2.601D+13	2.477D+13	2.353D+13	2.192D+13	1.872D+13	5.230D+12	1.253D+12
13	3.360D+13	3.247D+13	3.094D+13	2.945D+13	2.801D+13	2.666D+13	2.532D+13	2.359D+13	2.014D+13	5.628D+12	1.349D+12
14	3.583D+13	3.460D+13	3.297D+13	3.137D+13	2.984D+13	2.840D+13	2.696D+13	2.511D+13	2.143D+13	5.991D+12	1.437D+12
15	3.775D+13	3.649D+13	3.477D+13	3.308D+13	3.146D+13	2.994D+13	2.842D+13	2.647D+13	2.258D+13	6.317D+12	1.516D+12
16	3.954D+13	3.822D+13	3.641D+13	3.464D+13	3.294D+13	3.134D+13	2.975D+13	2.770D+13	2.364D+13	6.613D+12	1.587D+12
17	4.113D+13	3.975D+13	3.787D+13	3.603D+13	3.426D+13	3.260D+13	3.094D+13	2.881D+13	2.458D+13	6.876D+12	1.650D+12
18	4.251D+13	4.109D+13	3.914D+13	3.724D+13	3.541D+13	3.368D+13	3.197D+13	2.977D+13	2.540D+13	7.104D+12	1.705D+12
19	4.367D+13	4.221D+13	4.021D+13	3.825D+13	3.637D+13	3.460D+13	3.284D+13	3.057D+13	2.608D+13	7.296D+12	1.751D+12
20	4.460D+13	4.311D+13	4.106D+13	3.906D+13	3.714D+13	3.533D+13	3.353D+13	3.122D+13	2.663D+13	7.450D+12	1.788D+12
21	4.530D+13	4.378D+13	4.171D+13	3.967D+13	3.772D+13	3.588D+13	3.405D+13	3.170D+13	2.705D+13	7.565D+12	1.816D+12
22	4.576D+13	4.423D+13	4.213D+13	4.007D+13	3.810D+13	3.624D+13	3.439D+13	3.202D+13	2.732D+13	7.641D+12	1.834D+12
23	4.598D+13	4.444D+13	4.233D+13	4.026D+13	3.828D+13	3.641D+13	3.455D+13	3.217D+13	2.744D+13	7.676D+12	1.843D+12
24	4.598D+13	4.444D+13	4.232D+13	4.025D+13	3.827D+13	3.640D+13	3.454D+13	3.215D+13	2.743D+13	7.673D+12	1.842D+12
25	4.574D+13	4.420D+13	4.210D+13	4.004D+13	3.806D+13	3.620D+13	3.435D+13	3.198D+13	2.728D+13	7.630D+12	1.831D+12
26	4.527D+13	4.375D+13	4.166D+13	3.962D+13	3.766D+13	3.582D+13	3.399D+13	3.164D+13	2.698D+13	7.548D+12	1.812D+12
27	4.457D+13	4.307D+13	4.101D+13	3.900D+13	3.707D+13	3.525D+13	3.345D+13	3.113D+13	2.655D+13	7.428D+12	1.783D+12
28	4.364D+13	4.217D+13	4.016D+13	3.818D+13	3.629D+13	3.450D+13	3.274D+13	3.047D+13	2.599D+13	7.269D+12	1.745D+12
29	4.250D+13	4.106D+13	3.910D+13	3.717D+13	3.532D+13	3.358D+13	3.186D+13	2.965D+13	2.528D+13	7.073D+12	1.698D+12
30	4.115D+13	3.975D+13	3.785D+13	3.598D+13	3.419D+13	3.250D+13	3.082D+13	2.868D+13	2.446D+13	6.842D+12	1.642D+12
31	3.988D+13	3.852D+13	3.666D+13	3.485D+13	3.311D+13	3.147D+13	2.985D+13	2.777D+13	2.368D+13	6.620D+12	1.588D+12
32	3.874D+13	3.742D+13	3.561D+13	3.384D+13	3.215D+13	3.056D+13	2.898D+13	2.696D+13	2.299D+13	6.425D+12	1.541D+12
33	3.751D+13	3.622D+13	3.447D+13	3.275D+13	3.111D+13	2.957D+13	2.803D+13	2.608D+13	2.223D+13	6.213D+12	1.489D+12
34	3.618D+13	3.494D+13	3.324D+13	3.159D+13	3.000D+13	2.850D+13	2.702D+13	2.513D+13	2.142D+13	5.985D+12	1.433D+12
35	3.478D+13	3.358D+13	3.194D+13	3.035D+13	2.881D+13	2.737D+13	2.594D+13	2.412D+13	2.056D+13	5.740D+12	1.373D+12
36	3.330D+13	3.215D+13	3.058D+13	2.904D+13	2.757D+13	2.618D+13	2.481D+13	2.306D+13	1.965D+13	5.477D+12	1.307D+12
37	3.175D+13	3.065D+13	2.915D+13	2.768D+13	2.627D+13	2.494D+13	2.362D+13	2.195D+13	1.869D+13	5.193D+12	1.234D+12
38	3.013D+13	2.908D+13	2.765D+13	2.625D+13	2.491D+13	2.364D+13	2.238D+13	2.078D+13	1.769D+13	4.880D+12	1.152D+12
39	2.839D+13	2.740D+13	2.605D+13	2.472D+13	2.344D+13	2.224D+13	2.104D+13	1.953D+13	1.661D+13	4.523D+12	1.058D+12
40	2.638D+13	2.546D+13	2.419D+13	2.295D+13	2.176D+13	2.062D+13	1.950D+13	1.809D+13	1.537D+13	4.095D+12	9.484D+11
41	2.371D+13	2.287D+13	2.173D+13	2.061D+13	1.952D+13	1.849D+13	1.746D+13	1.618D+13	1.375D+13	3.555D+12	8.196D+11
42	1.944D+13	1.876D+13	1.781D+13	1.689D+13	1.599D+13	1.512D+13	1.425D+13	1.316D+13	1.117D+13	2.857D+12	6.722D+11
43	1.015D+13	9.787D+12	9.296D+12	8.811D+12	8.333D+12	7.849D+12	7.305D+12	6.555D+12	5.305D+12	1.855D+12	4.872D+11
44	4.960D+12	4.782D+12	4.542D+12	4.302D+12	4.060D+12	3.801D+12	3.491D+12	3.064D+12	2.435D+12	1.040D+12	3.097D+11
45	2.441D+12	2.352D+12	2.233D+12	2.113D+12	1.988D+12	1.850D+12	1.680D+12	1.453D+12	1.151D+12	5.603D+11	1.863D+11
46	1.234D+12	1.189D+12	1.128D+12	1.066D+12	1.000D+12	9.249D+11	8.325D+11	7.142D+11	5.680D+11	3.011D+11	1.093D+11
47	3.458D+11	3.330D+11	3.155D+11	2.971D+11	2.771D+11	2.539D+11	2.262D+11	1.930D+11	1.553D+11	9.088D+10	3.754D+10
48	7.563D+10	7.277D+10	6.879D+10	6.454D+10	5.983D+10	5.443D+10	4.818D+10	4.110D+10	3.350D+10	2.100D+10	9.622D+09
49	1.645D+10	1.581D+10	1.491D+10	1.394D+10	1.286D+10	1.164D+10	1.027D+10	8.781D+09	7.240D+09	4.755D+09	2.356D+09
50	3.203D+09	3.076D+09	2.894D+09	2.697D+09	2.479D+09	2.237D+09	1.972D+09	1.691D+09	1.406D+09	9.524D+08	4.981D+08

	23	24	25	26
1	2.218D+08	9.817D+07	4.152D+07	1.431D+07
2	9.227D+08	3.903D+08	1.588D+08	5.330D+07
3	3.216D+09	1.277D+09	4.924D+08	1.593D+08
4	1.051D+10	3.964D+09	1.399D+09	4.336D+08
5	3.155D+10	1.061D+10	3.581D+09	1.058D+09
6	8.288D+10	2.529D+10	7.935D+09	2.237D+09
7	1.505D+11	4.275D+10	1.279D+10	3.500D+09
8	1.943D+11	5.446D+10	1.610D+10	4.370D+09
9	2.339D+11	6.540D+10	1.928D+10	5.217D+09
10	2.667D+11	7.532D+10	2.221D+10	6.009D+09
11	2.998D+11	8.424D+10	2.488D+10	6.735D+09
12	3.279D+11	9.231D+10	2.729D+10	7.395D+09
13	3.535D+11	9.961D+10	2.948D+10	7.994D+09
14	3.767D+11	1.062D+11	3.146D+10	8.534D+09
15	3.977D+11	1.122D+11	3.324D+10	9.019D+09
16	4.164D+11	1.175D+11	3.482D+10	9.451D+09
17	4.330D+11	1.222D+11	3.622D+10	9.831D+09

28	1.697D+11	2.799D+11	9.989D+10	2.801E+10
29	7.486D+11	2.721D+11	9.710D+10	2.722E+10
30	7.233D+11	2.628D+11	9.376D+10	2.628D+10
31	6.587D+11	2.537E+11	9.047D+10	2.535E+10
32	6.769D+11	2.457D+11	8.756D+10	2.452D+10
33	6.530D+11	2.368D+11	8.434D+10	2.361D+10
34	6.267D+11	2.271D+11	8.081D+10	2.261E+10
35	5.978D+11	2.164D+11	7.693D+10	2.152E+10
36	5.660D+11	2.046D+11	7.268D+10	2.032E+10
37	5.309D+11	1.917D+11	6.805D+10	1.902E+10
38	4.923E+11	1.776D+11	6.302D+10	1.761D+10
39	4.499D+11	1.623E+11	5.763D+10	1.611E+10
40	4.039D+11	1.459D+11	5.192D+10	1.454D+10
41	3.549D+11	1.288D+11	4.599D+10	1.291D+10
42	3.043D+11	1.113E+11	3.999D+10	1.127D+10
43	2.447D+11	9.080D+10	3.299D+10	9.361D+09
44	1.815D+11	6.895D+10	2.550D+10	7.310E+09
45	1.288D+11	5.032D+10	1.900D+10	5.514D+09
46	8.825E+10	3.549D+10	1.369D+10	4.029D+09
47	4.042D+10	1.726E+10	6.981D+09	2.113E+09
48	1.372D+10	6.228D+09	2.648D+09	8.268E+08
49	4.256D+09	2.035D+09	9.026D+08	2.893D+08
50	1.012D+09	5.012E+08	2.289D+08	7.469D+07

GROUP 4 FLUX

	1	2	3	4	5	6	7	8	9	10	11
1	1.274D+12	1.265D+12	1.256D+12	1.247D+12	1.231D+12	1.206D+12	1.181D+12	1.157E+12	1.133D+12	1.110D+12	1.089D+12
2	3.898D+12	3.870D+12	3.844D+12	3.817E+12	3.768D+12	3.690D+12	3.613D+12	3.538D+12	3.465D+12	3.394D+12	3.325D+12
3	8.031D+12	7.974D+12	7.919D+12	7.865D+12	7.762D+12	7.601D+12	7.442D+12	7.285D+12	7.131D+12	6.981D+12	6.834D+12
4	1.465D+13	1.455D+13	1.445D+13	1.435D+13	1.416D+13	1.387D+13	1.357D+13	1.329D+13	1.300D+13	1.272D+13	1.244D+13
5	2.366D+13	2.349D+13	2.333D+13	2.317D+13	2.286D+13	2.239D+13	2.191D+13	2.144D+13	2.098D+13	2.052D+13	2.007D+13
6	2.977D+13	2.956D+13	2.936D+13	2.915D+13	2.877D+13	2.817D+13	2.757D+13	2.698D+13	2.640D+13	2.582D+13	2.524D+13
7	1.774E+13	1.761D+13	1.749D+13	1.737E+13	1.714D+13	1.678D+13	1.643D+13	1.607D+13	1.572D+13	1.538D+13	1.504D+13
8	1.644D+13	1.632D+13	1.621D+13	1.610E+13	1.588D+13	1.555D+13	1.522D+13	1.489D+13	1.457D+13	1.425D+13	1.393D+13
9	1.746D+13	1.734D+13	1.722D+13	1.710D+13	1.687D+13	1.652D+13	1.617D+13	1.582D+13	1.548D+13	1.513D+13	1.479D+13
10	1.925D+13	1.911E+13	1.898D+13	1.885E+13	1.860D+13	1.821D+13	1.783D+13	1.744E+13	1.706D+13	1.668D+13	1.631D+13
11	2.121D+13	2.107D+13	2.092D+13	2.078E+13	2.050D+13	2.007D+13	1.965D+13	1.922D+13	1.880D+13	1.839D+13	1.797D+13
12	2.314D+13	2.298D+13	2.282D+13	2.267D+13	2.237D+13	2.190D+13	2.143D+13	2.097E+13	2.051D+13	2.005D+13	1.960D+13
13	2.496D+13	2.479D+13	2.462D+13	2.445D+13	2.412D+13	2.361D+13	2.311D+13	2.261D+13	2.212D+13	2.163D+13	2.114D+13
14	2.664D+13	2.646D+13	2.627D+13	2.609D+13	2.574D+13	2.520D+13	2.467E+13	2.413D+13	2.360D+13	2.308D+13	2.256D+13
15	2.820D+13	2.800E+13	2.781D+13	2.761E+13	2.724D+13	2.666D+13	2.610D+13	2.553D+13	2.497D+13	2.442D+13	2.387D+13
16	2.957D+13	2.937D+13	2.916D+13	2.896E+13	2.856D+13	2.796D+13	2.737D+13	2.677D+13	2.619D+13	2.560D+13	2.502D+13
17	3.078D+13	3.056E+13	3.035D+13	3.014D+13	2.973D+13	2.910D+13	2.848D+13	2.786D+13	2.725D+13	2.665D+13	2.604D+13
18	3.182D+13	3.160D+13	3.138D+13	3.116E+13	3.073D+13	3.009D+13	2.944D+13	2.880D+13	2.817D+13	2.754D+13	2.692D+13
19	3.269D+13	3.246D+13	3.224D+13	3.201D+13	3.158D+13	3.091D+13	3.025E+13	2.959D+13	2.894D+13	2.830D+13	2.766D+13
20	3.340D+13	3.316D+13	3.293D+13	3.270D+13	3.225D+13	3.157E+13	3.090D+13	3.023D+13	2.956D+13	2.890D+13	2.825D+13
21	3.393D+13	3.369D+13	3.346D+13	3.322D+13	3.277D+13	3.207D+13	3.139D+13	3.071D+13	3.003D+13	2.936D+13	2.869D+13
22	3.429D+13	3.405D+13	3.381D+13	3.357D+13	3.311D+13	3.241D+13	3.172D+13	3.103E+13	3.035D+13	2.967D+13	2.899D+13
23	3.448E+13	3.424D+13	3.400D+13	3.376E+13	3.329D+13	3.259D+13	3.189D+13	3.120D+13	3.051D+13	2.983D+13	2.915D+13
24	3.449D+13	3.424D+13	3.401D+13	3.377D+13	3.330D+13	3.259D+13	3.189D+13	3.120D+13	3.051D+13	2.983D+13	2.915D+13
25	3.432D+13	3.408D+13	3.384D+13	3.360D+13	3.314D+13	3.243D+13	3.173D+13	3.104D+13	3.036D+13	2.968D+13	2.900D+13
26	3.397D+13	3.373E+13	3.350D+13	3.326E+13	3.280D+13	3.210D+13	3.141D+13	3.073D+13	3.005D+13	2.937D+13	2.870D+13
27	3.346D+13	3.322E+13	3.299D+13	3.275D+13	3.230D+13	3.161D+13	3.093D+13	3.026E+13	2.959D+13	2.892D+13	2.826D+13
28	3.277D+13	3.254D+13	3.231D+13	3.208D+13	3.164D+13	3.096D+13	3.029D+13	2.963D+13	2.897D+13	2.832D+13	2.767D+13
29	3.191D+13	3.169D+13	3.147D+13	3.124D+13	3.081D+13	3.015D+13	2.950D+13	2.885D+13	2.821D+13	2.757D+13	2.694D+13
30	3.089D+13	3.067D+13	3.045D+13	3.024D+13	2.982D+13	2.918D+13	2.855D+13	2.792E+13	2.730D+13	2.668D+13	2.606D+13
31	2.988D+13	2.967E+13	2.946D+13	2.925E+13	2.885D+13	2.823D+13	2.762D+13	2.701D+13	2.640D+13	2.581D+13	2.521D+13
32	2.901D+13	2.881D+13	2.860D+13	2.840D+13	2.801D+13	2.741D+13	2.681D+13	2.622E+13	2.563D+13	2.505D+13	2.447D+13
33	2.808D+13	2.788D+13	2.768D+13	2.749E+13	2.711D+13	2.652D+13	2.595D+13	2.537D+13	2.480D+13	2.424D+13	2.368D+13
34	2.708D+13	2.689E+13	2.670D+13	2.651D+13	2.614D+13	2.558D+13	2.502D+13	2.447D+13	2.392D+13	2.337D+13	2.283D+13
35	2.604D+13	2.585D+13	2.567D+13	2.548D+13	2.513D+13	2.459D+13	2.405D+13	2.352D+13	2.299D+13	2.246D+13	2.194D+13
36	2.496D+13	2.478E+13	2.461D+13	2.443E+13	2.409D+13	2.357D+13	2.305D+13	2.254D+13	2.203D+13	2.153D+13	2.102D+13
37	2.392D+13	2.375D+13	2.358D+13	2.341E+13	2.308D+13	2.258D+13	2.209D+13	2.159D+13	2.110D+13	2.062D+13	2.014D+13

38	2.302D+13	2.285D+13	2.269D+13	2.253D+13	2.221D+13	2.173D+13	2.125D+13	2.078D+13	2.030D+13	1.984D+13	1.937D+13
39	2.250D+13	2.234D+13	2.218D+13	2.202D+13	2.171D+13	2.124D+13	2.077D+13	2.030D+13	1.984D+13	1.938D+13	1.892D+13
40	2.283D+13	2.267D+13	2.250D+13	2.234D+13	2.203D+13	2.154D+13	2.107D+13	2.059D+13	2.012D+13	1.965D+13	1.919D+13
41	2.491D+13	2.473D+13	2.455D+13	2.437D+13	2.403D+13	2.350D+13	2.298D+13	2.246D+13	2.194D+13	2.143D+13	2.092D+13
42	3.041D+13	3.019D+13	2.997D+13	2.975D+13	2.934D+13	2.869D+13	2.805D+13	2.741D+13	2.678D+13	2.615D+13	2.552D+13
43	4.606D+13	4.566D+13	4.533D+13	4.500D+13	4.438D+13	4.340D+13	4.243D+13	4.146D+13	4.050D+13	3.954D+13	3.859D+13
44	5.311D+13	5.272D+13	5.234D+13	5.196D+13	5.124D+13	5.010D+13	4.897D+13	4.785D+13	4.674D+13	4.563D+13	4.452D+13
45	5.324D+13	5.285D+13	5.246D+13	5.208D+13	5.136D+13	5.021D+13	4.908D+13	4.795D+13	4.682D+13	4.570D+13	4.459D+13
46	5.047D+13	5.009D+13	4.973D+13	4.936D+13	4.867D+13	4.758D+13	4.650D+13	4.543D+13	4.435D+13	4.329D+13	4.222D+13
47	4.550D+13	4.515D+13	4.482D+13	4.449D+13	4.386D+13	4.287D+13	4.189D+13	4.091D+13	3.994D+13	3.897D+13	3.800D+13
48	3.253D+13	3.229D+13	3.205D+13	3.181D+13	3.136D+13	3.064D+13	2.993D+13	2.922D+13	2.852D+13	2.782D+13	2.712D+13
49	1.941D+13	1.927D+13	1.912D+13	1.898D+13	1.871D+13	1.828D+13	1.785D+13	1.742D+13	1.700D+13	1.658D+13	1.616D+13
50	7.117D+12	7.063D+12	7.009D+12	6.956D+12	6.857D+12	6.698D+12	6.541D+12	6.385D+12	6.229D+12	6.075D+12	5.921D+12

	12	13	14	15	16	17	18	19	20	21	22
1	1.068D+12	1.039D+12	1.005D+12	9.806D+11	9.669D+11	9.674D+11	9.857D+11	1.026D+12	1.091D+12	1.257D+12	1.219D+12
2	3.259D+12	3.165D+12	3.055D+12	2.968D+12	2.910D+12	2.892D+12	2.924D+12	3.020D+12	3.192D+12	3.648D+12	3.495D+12
3	6.691D+12	6.487D+12	6.237D+12	6.023D+12	5.859D+12	5.764D+12	5.761D+12	5.875D+12	6.135D+12	6.891D+12	6.468D+12
4	1.217D+13	1.178D+13	1.129D+13	1.084D+13	1.046D+13	1.019D+13	1.006D+13	1.013D+13	1.045D+13	1.155D+13	1.058D+13
5	1.962D+13	1.897D+13	1.813D+13	1.734D+13	1.664D+13	1.608D+13	1.575D+13	1.575D+13	1.620D+13	1.791D+13	1.614D+13
6	2.467D+13	2.384D+13	2.274D+13	2.170D+13	2.075D+13	1.999D+13	1.957D+13	1.979D+13	2.098D+13	2.521D+13	2.303D+13
7	1.470D+13	1.420D+13	1.354D+13	1.290D+13	1.232D+13	1.189D+13	1.183D+13	1.265D+13	1.553D+13	2.957D+13	2.870D+13
8	1.361D+13	1.315D+13	1.253D+13	1.193D+13	1.139D+13	1.099D+13	1.102D+13	1.212D+13	1.576D+13	3.316D+13	3.269D+13
9	1.446D+13	1.397D+13	1.330D+13	1.266D+13	1.207D+13	1.165D+13	1.171D+13	1.299D+13	1.722D+13	3.719D+13	3.678D+13
10	1.594D+13	1.539D+13	1.466D+13	1.394D+13	1.329D+13	1.281D+13	1.288D+13	1.432D+13	1.905D+13	4.137D+13	4.088D+13
11	1.756D+13	1.696D+13	1.615D+13	1.535D+13	1.463D+13	1.410D+13	1.416D+13	1.574D+13	2.094D+13	4.549D+13	4.499D+13
12	1.915D+13	1.850D+13	1.761D+13	1.674D+13	1.594D+13	1.536D+13	1.542D+13	1.713D+13	2.278D+13	4.945D+13	4.874D+13
13	2.065D+13	1.994D+13	1.898D+13	1.804D+13	1.718D+13	1.655D+13	1.660D+13	1.844D+13	2.450D+13	5.317D+13	5.236D+13
14	2.204D+13	2.128D+13	2.025D+13	1.925D+13	1.832D+13	1.765D+13	1.770D+13	1.965D+13	2.611D+13	5.663D+13	5.573D+13
15	2.332D+13	2.251D+13	2.142D+13	2.035D+13	1.937D+13	1.865D+13	1.871D+13	2.077D+13	2.758D+13	5.978D+13	5.881D+13
16	2.445D+13	2.360D+13	2.245D+13	2.134D+13	2.030D+13	1.955D+13	1.961D+13	2.176D+13	2.890D+13	6.262D+13	6.159D+13
17	2.544D+13	2.455D+13	2.336D+13	2.220D+13	2.112D+13	2.034D+13	2.040D+13	2.263D+13	3.006D+13	6.513D+13	6.405D+13
18	2.630D+13	2.538D+13	2.415D+13	2.295D+13	2.183D+13	2.102D+13	2.108D+13	2.339D+13	3.106D+13	6.730D+13	6.619D+13
19	2.702D+13	2.607D+13	2.481D+13	2.357D+13	2.243D+13	2.159D+13	2.165D+13	2.402D+13	3.190D+13	6.912D+13	6.797D+13
20	2.760D+13	2.663D+13	2.534D+13	2.407D+13	2.290D+13	2.205D+13	2.211D+13	2.453D+13	3.257D+13	7.058D+13	6.940D+13
21	2.803D+13	2.705D+13	2.574D+13	2.445D+13	2.326D+13	2.240D+13	2.245D+13	2.491D+13	3.308D+13	7.167D+13	7.047D+13
22	2.832D+13	2.733D+13	2.600D+13	2.470D+13	2.350D+13	2.262D+13	2.268D+13	2.517D+13	3.341D+13	7.239D+13	7.118D+13
23	2.847D+13	2.747D+13	2.614D+13	2.483D+13	2.362D+13	2.274D+13	2.280D+13	2.529D+13	3.358D+13	7.274D+13	7.152D+13
24	2.847D+13	2.747D+13	2.614D+13	2.483D+13	2.362D+13	2.273D+13	2.279D+13	2.529D+13	3.357D+13	7.271D+13	7.149D+13
25	2.833D+13	2.733D+13	2.600D+13	2.469D+13	2.349D+13	2.261D+13	2.267D+13	2.515D+13	3.338D+13	7.230D+13	7.109D+13
26	2.804D+13	2.705D+13	2.573D+13	2.444D+13	2.324D+13	2.237D+13	2.243D+13	2.488D+13	3.302D+13	7.152D+13	7.031D+13
27	2.760D+13	2.663D+13	2.533D+13	2.405D+13	2.288D+13	2.202D+13	2.207D+13	2.448D+13	3.249D+13	7.036D+13	6.917D+13
28	2.703D+13	2.607D+13	2.479D+13	2.355D+13	2.239D+13	2.155D+13	2.160D+13	2.395D+13	3.179D+13	6.884D+13	6.766D+13
29	2.631D+13	2.538D+13	2.413D+13	2.292D+13	2.179D+13	2.097D+13	2.101D+13	2.330D+13	3.092D+13	6.695D+13	6.580D+13
30	2.545D+13	2.455D+13	2.334D+13	2.216D+13	2.107D+13	2.027D+13	2.031D+13	2.252D+13	2.988D+13	6.470D+13	6.358D+13
31	2.462D+13	2.374D+13	2.257D+13	2.143D+13	2.037D+13	1.960D+13	1.963D+13	2.176D+13	2.887D+13	6.253D+13	6.144D+13
32	2.390D+13	2.305D+13	2.191D+13	2.079D+13	1.977D+13	1.901D+13	1.905D+13	2.111D+13	2.800D+13	6.064D+13	5.959D+13
33	2.312D+13	2.229D+13	2.119D+13	2.011D+13	1.912D+13	1.839D+13	1.841D+13	2.041D+13	2.706D+13	5.860D+13	5.759D+13
34	2.223D+13	2.149D+13	2.043D+13	1.938D+13	1.842D+13	1.771D+13	1.774D+13	1.965D+13	2.606D+13	5.643D+13	5.545D+13
35	2.142D+13	2.065D+13	1.962D+13	1.862D+13	1.769D+13	1.701D+13	1.703D+13	1.886D+13	2.501D+13	5.412D+13	5.319D+13
36	2.053D+13	1.979D+13	1.880D+13	1.783D+13	1.694D+13	1.629D+13	1.630D+13	1.804D+13	2.391D+13	5.171D+13	5.081D+13
37	1.966D+13	1.895D+13	1.800D+13	1.707D+13	1.621D+13	1.558D+13	1.558D+13	1.723D+13	2.279D+13	4.921D+13	4.834D+13
38	1.891D+13	1.822D+13	1.731D+13	1.641D+13	1.558D+13	1.496D+13	1.494D+13	1.648D+13	2.172D+13	4.667D+13	4.579D+13
39	1.847D+13	1.780D+13	1.690D+13	1.602D+13	1.520D+13	1.458D+13	1.453D+13	1.593D+13	2.079D+13	4.416D+13	4.320D+13
40	1.872D+13	1.804D+13	1.712D+13	1.622D+13	1.539D+13	1.474D+13	1.461D+13	1.582D+13	2.023D+13	4.178D+13	4.059D+13
41	2.041D+13	1.966D+13	1.865D+13	1.766D+13	1.674D+13	1.599D+13	1.572D+13	1.665D+13	2.045D+13	3.965D+13	3.801D+13
42	2.490D+13	2.397D+13	2.274D+13	2.153D+13	2.038D+13	1.940D+13	1.887D+13	1.941D+13	2.235D+13	3.789D+13	3.547D+13
43	3.764D+13	3.623D+13	3.435D+13	3.251D+13	3.074D+13	2.916D+13	2.804D+13	2.785D+13	2.939D+13	3.620D+13	3.252D+13
44	4.342D+13	4.179D+13	3.960D+13	3.746D+13	3.539D+13	3.351D+13	3.198D+13	3.112D+13	3.128D+13	3.360D+13	2.912D+13
45	4.348D+13	4.183D+13	3.964D+13	3.748D+13	3.539D+13	3.345D+13	3.178D+13	3.057D+13	3.001D+13	3.041D+13	2.577D+13
46	4.116D+13	3.960D+13	3.751D+13	3.545D+13	3.346D+13	3.159D+13	2.991D+13	2.854D+13	2.761D+13	2.701D+13	2.255D+13
47	3.734D+13	3.562D+13	3.372D+13	3.186D+13	3.005D+13	2.830D+13	2.666D+13	2.515D+13	2.376D+13	2.155D+13	1.757D+13
48	2.643D+13	2.541D+13	2.404D+13	2.270D+13	2.139D+13	2.012D+13	1.888D+13	1.768D+13	1.652D+13	1.460D+13	1.174D+13
49	1.575D+13	1.513D+13	1.432D+13	1.351D+13	1.273D+13	1.195D+13	1.120D+13	1.046D+13	9.728D+12	8.525D+12	6.821D+12
50	5.768D+12	5.543D+12	5.243D+12	4.948D+12	4.657D+12	4.372D+12	4.092D+12	3.817D+12	3.546D+12	3.099D+12	2.475D+12

APPY REACTOR DEPLETION RUNS
DATE : MAY 14 , 1975

POINT POWER DISTRIBUTION (WATTS/CC)

	1	2	3	4	5	6	7	8	9	10	11
1	0.0	0.0	0.0	0.0	0.0	0.0	0.0	0.0	0.0	0.0	0.0
2	0.0	0.0	0.0	0.0	0.0	0.0	0.0	0.0	0.0	0.0	0.0
3	0.0	0.0	0.0	0.0	0.0	0.0	0.0	0.0	0.0	0.0	0.0
4	0.0	0.0	0.0	0.0	0.0	0.0	0.0	0.0	0.0	0.0	0.0
5	0.0	0.0	0.0	0.0	0.0	0.0	0.0	0.0	0.0	0.0	0.0
6	0.0	0.0	0.0	0.0	0.0	0.0	0.0	0.0	0.0	0.0	0.0
7	4.618E+00	4.586E+00	4.555E+00	4.523E+00	4.472E+00	4.378E+00	4.285E+00	4.193E+00	4.102E+00	4.012E+00	3.922E+00
8	4.587E+00	4.555E+00	4.524E+00	4.493E+00	4.442E+00	4.349E+00	4.257E+00	4.165E+00	4.074E+00	3.985E+00	3.896E+00
9	5.016E+00	4.981E+00	4.947E+00	4.913E+00	4.858E+00	4.756E+00	4.655E+00	4.555E+00	4.455E+00	4.357E+00	4.260E+00
10	5.584E+00	5.545E+00	5.507E+00	5.469E+00	5.407E+00	5.294E+00	5.182E+00	5.070E+00	4.959E+00	4.850E+00	4.741E+00
11	6.172E+00	6.129E+00	6.087E+00	6.045E+00	5.977E+00	5.851E+00	5.727E+00	5.604E+00	5.481E+00	5.360E+00	5.239E+00
12	6.733E+00	6.691E+00	6.645E+00	6.600E+00	6.525E+00	6.388E+00	6.252E+00	6.117E+00	5.983E+00	5.851E+00	5.719E+00
13	7.267E+00	7.217E+00	7.167E+00	7.118E+00	7.037E+00	6.889E+00	6.743E+00	6.597E+00	6.453E+00	6.310E+00	6.168E+00
14	7.755E+00	7.701E+00	7.649E+00	7.596E+00	7.509E+00	7.351E+00	7.195E+00	7.040E+00	6.885E+00	6.733E+00	6.581E+00
15	8.125E+00	8.069E+00	8.013E+00	7.958E+00	7.874E+00	7.708E+00	7.544E+00	7.381E+00	7.219E+00	7.059E+00	6.899E+00
16	8.519E+00	8.460E+00	8.402E+00	8.344E+00	8.255E+00	8.081E+00	7.909E+00	7.738E+00	7.569E+00	7.400E+00	7.233E+00
17	8.866E+00	8.804E+00	8.744E+00	8.683E+00	8.591E+00	8.410E+00	8.231E+00	8.053E+00	7.876E+00	7.701E+00	7.527E+00
18	9.165E+00	9.101E+00	9.039E+00	8.976E+00	8.881E+00	8.694E+00	8.508E+00	8.324E+00	8.141E+00	7.960E+00	7.780E+00
19	9.417E+00	9.351E+00	9.287E+00	9.222E+00	9.124E+00	8.932E+00	8.741E+00	8.552E+00	8.364E+00	8.178E+00	7.993E+00
20	9.613E+00	9.552E+00	9.487E+00	9.421E+00	9.320E+00	9.124E+00	8.929E+00	8.736E+00	8.544E+00	8.353E+00	8.164E+00
21	9.772E+00	9.704E+00	9.637E+00	9.570E+00	9.468E+00	9.268E+00	9.070E+00	8.874E+00	8.679E+00	8.485E+00	8.293E+00
22	9.875E+00	9.806E+00	9.739E+00	9.671E+00	9.568E+00	9.366E+00	9.165E+00	8.967E+00	8.769E+00	8.574E+00	8.379E+00
23	9.916E+00	9.846E+00	9.779E+00	9.710E+00	9.608E+00	9.405E+00	9.203E+00	9.004E+00	8.805E+00	8.609E+00	8.413E+00
24	9.917E+00	9.848E+00	9.780E+00	9.712E+00	9.609E+00	9.406E+00	9.204E+00	9.004E+00	8.806E+00	8.609E+00	8.413E+00
25	9.869E+00	9.800E+00	9.732E+00	9.664E+00	9.561E+00	9.359E+00	9.158E+00	8.959E+00	8.761E+00	8.565E+00	8.370E+00
26	9.770E+00	9.701E+00	9.634E+00	9.567E+00	9.465E+00	9.264E+00	9.065E+00	8.868E+00	8.672E+00	8.477E+00	8.284E+00
27	9.621E+00	9.554E+00	9.488E+00	9.421E+00	9.321E+00	9.123E+00	8.926E+00	8.732E+00	8.539E+00	8.347E+00	8.156E+00
28	9.424E+00	9.358E+00	9.293E+00	9.228E+00	9.129E+00	8.935E+00	8.742E+00	8.551E+00	8.362E+00	8.173E+00	7.987E+00
29	9.179E+00	9.114E+00	9.050E+00	8.987E+00	8.891E+00	8.701E+00	8.513E+00	8.327E+00	8.142E+00	7.958E+00	7.776E+00
30	8.885E+00	8.822E+00	8.760E+00	8.699E+00	8.606E+00	8.422E+00	8.239E+00	8.059E+00	7.879E+00	7.701E+00	7.524E+00
31	8.652E+00	8.591E+00	8.531E+00	8.471E+00	8.375E+00	8.196E+00	8.018E+00	7.842E+00	7.667E+00	7.493E+00	7.321E+00
32	8.402E+00	8.342E+00	8.284E+00	8.226E+00	8.133E+00	7.959E+00	7.786E+00	7.614E+00	7.444E+00	7.275E+00	7.107E+00
33	8.132E+00	8.074E+00	8.018E+00	7.961E+00	7.871E+00	7.702E+00	7.534E+00	7.368E+00	7.203E+00	7.039E+00	6.876E+00
34	7.842E+00	7.786E+00	7.732E+00	7.677E+00	7.590E+00	7.427E+00	7.265E+00	7.104E+00	6.945E+00	6.786E+00	6.629E+00
35	7.535E+00	7.482E+00	7.429E+00	7.376E+00	7.293E+00	7.136E+00	6.980E+00	6.825E+00	6.671E+00	6.519E+00	6.367E+00
36	7.216E+00	7.164E+00	7.114E+00	7.063E+00	6.983E+00	6.832E+00	6.683E+00	6.534E+00	6.387E+00	6.240E+00	6.095E+00
37	6.894E+00	6.845E+00	6.797E+00	6.748E+00	6.671E+00	6.527E+00	6.384E+00	6.241E+00	6.100E+00	5.960E+00	5.821E+00
38	6.593E+00	6.545E+00	6.499E+00	6.453E+00	6.379E+00	6.240E+00	6.103E+00	5.967E+00	5.831E+00	5.697E+00	5.563E+00
39	6.357E+00	6.312E+00	6.267E+00	6.222E+00	6.151E+00	6.017E+00	5.884E+00	5.752E+00	5.621E+00	5.491E+00	5.362E+00
40	6.202E+00	6.236E+00	6.192E+00	6.148E+00	6.077E+00	5.944E+00	5.812E+00	5.682E+00	5.552E+00	5.423E+00	5.295E+00
41	6.550E+00	6.503E+00	6.456E+00	6.410E+00	6.335E+00	6.197E+00	6.059E+00	5.922E+00	5.786E+00	5.651E+00	5.517E+00
42	7.517E+00	7.462E+00	7.409E+00	7.355E+00	7.270E+00	7.110E+00	6.951E+00	6.794E+00	6.637E+00	6.481E+00	6.326E+00
43	0.0	0.0	0.0	0.0	0.0	0.0	0.0	0.0	0.0	0.0	0.0
44	0.0	0.0	0.0	0.0	0.0	0.0	0.0	0.0	0.0	0.0	0.0
45	0.0	0.0	0.0	0.0	0.0	0.0	0.0	0.0	0.0	0.0	0.0
46	0.0	0.0	0.0	0.0	0.0	0.0	0.0	0.0	0.0	0.0	0.0
47	0.0	0.0	0.0	0.0	0.0	0.0	0.0	0.0	0.0	0.0	0.0
48	0.0	0.0	0.0	0.0	0.0	0.0	0.0	0.0	0.0	0.0	0.0
49	0.0	0.0	0.0	0.0	0.0	0.0	0.0	0.0	0.0	0.0	0.0
50	0.0	0.0	0.0	0.0	0.0	0.0	0.0	0.0	0.0	0.0	0.0

	12	13	14	15	16	17	18	19	20	21	22
1	0.0	0.0	0.0	0.0	0.0	0.0	0.0	0.0	0.0	0.0	0.0
2	0.0	0.0	0.0	0.0	0.0	0.0	0.0	0.0	0.0	0.0	0.0
3	0.0	0.0	0.0	0.0	0.0	0.0	0.0	0.0	0.0	0.0	0.0

4	0.0	0.0	0.0	0.0	0.0	0.0	0.0	0.0	0.0	0.0	0.0
5	C.C	0.0	0.0	0.0	0.0	0.0	0.0	0.0	C.C	0.0	0.0
6	0.0	0.0	0.0	0.C	C.0	0.0	C.0	0.0	0.0	0.0	0.0
7	3.934E+00	3.714E+00	3.540E+00	3.371E+00	3.213E+00	3.083E+00	3.024E+00	3.139E+00	3.670E+00	0.0	C.0
8	3.807E+00	3.688E+00	3.514E+00	3.344E+00	3.183E+00	3.051E+00	2.999E+00	3.156E+00	3.828E+00	0.0	0.0
9	4.163E+00	4.032E+00	3.840E+00	3.652E+00	3.474E+00	3.327E+00	3.270E+00	3.454E+00	4.230E+00	0.0	0.0
10	4.633E+00	4.486E+00	4.272E+00	4.062E+00	3.861E+00	3.695E+00	3.629E+00	3.833E+00	4.700E+00	0.0	0.0
11	5.120E+00	4.957E+00	4.720E+00	4.486E+00	4.263E+00	4.077E+00	4.002E+00	4.223E+00	5.174E+00	0.0	0.0
12	5.589E+00	5.411E+00	5.151E+00	4.894E+00	4.65CE+00	4.445E+00	4.361E+00	4.599E+00	5.630E+00	0.0	0.0
13	6.026E+00	5.834E+00	5.553E+00	5.276E+00	5.011E+00	4.789E+00	4.697E+00	4.951E+00	6.059E+00	0.0	0.0
14	6.430E+00	6.224E+00	5.924E+00	5.627E+00	5.344E+00	5.107E+00	5.007E+00	5.276E+00	6.455E+00	0.0	0.0
15	6.741E+00	6.534E+00	6.219E+00	5.907E+00	5.609E+00	5.359E+00	5.253E+00	5.535E+00	6.770E+00	0.0	0.0
16	7.067E+00	6.850E+00	6.518E+00	6.191E+00	5.878E+00	5.616E+00	5.504E+00	5.800E+00	7.093E+00	0.0	0.0
17	7.353E+00	7.127E+00	6.782E+00	6.441E+00	6.115E+00	5.842E+00	5.726E+00	6.033E+00	7.378E+00	0.0	0.0
18	7.601E+00	7.367E+00	7.010E+00	6.657E+00	6.320E+00	6.037E+00	5.917E+00	6.234E+00	7.623E+00	0.0	0.0
19	7.809E+00	7.568E+00	7.201E+00	6.838E+00	6.492E+00	6.201E+00	6.078E+00	6.403E+00	7.830E+00	0.0	0.0
20	7.976E+00	7.730E+00	7.355E+00	6.984E+00	6.630E+00	6.333E+00	6.206E+00	6.538E+00	7.995E+00	0.0	0.0
21	8.101E+00	7.852E+00	7.470E+00	7.094E+00	6.734E+00	6.432E+00	6.303E+00	6.640E+00	8.119E+00	0.0	0.0
22	8.186E+00	7.933E+00	7.547E+00	7.166E+00	6.803E+00	6.497E+00	6.367E+00	6.707E+00	8.202E+00	0.0	0.0
23	8.219E+00	7.967E+00	7.579E+00	7.196E+00	6.831E+00	6.524E+00	6.393E+00	6.734E+00	8.234E+00	0.0	0.0
24	8.218E+00	7.966E+00	7.578E+00	7.195E+00	6.829E+00	6.522E+00	6.391E+00	6.732E+00	8.231E+00	0.0	0.0
25	8.176E+00	7.925E+00	7.539E+00	7.157E+00	6.793E+00	6.487E+00	6.356E+00	6.695E+00	8.186E+00	0.0	0.0
26	8.092E+00	7.843E+00	7.460E+00	7.082E+00	6.722E+00	6.419E+00	6.289E+00	6.624E+00	8.098E+00	0.0	0.0
27	7.967E+00	7.721E+00	7.344E+00	6.971E+00	6.616E+00	6.317E+00	6.189E+00	6.518E+00	7.968E+00	0.0	0.0
28	7.801E+00	7.560E+00	7.190E+00	6.824E+00	6.476E+00	6.183E+00	6.057E+00	6.378E+00	7.796E+00	0.0	0.0
29	7.594E+00	7.359E+00	6.998E+00	6.642E+00	6.302E+00	6.016E+00	5.893E+00	6.205E+00	7.583E+00	0.0	0.0
30	7.348E+00	7.120E+00	6.770E+00	6.424E+00	6.095E+00	5.818E+00	5.698E+00	5.998E+00	7.329E+00	0.0	0.0
31	7.149E+00	6.922E+00	6.580E+00	6.244E+00	5.923E+00	5.653E+00	5.536E+00	5.826E+00	7.118E+00	0.0	0.0
32	6.940E+00	6.719E+00	6.387E+00	6.060E+00	5.747E+00	5.485E+00	5.370E+00	5.651E+00	6.904E+00	0.0	0.0
33	6.714E+00	6.500E+00	6.178E+00	5.861E+00	5.558E+00	5.304E+00	5.192E+00	5.463E+00	6.673E+00	0.0	0.0
34	6.473E+00	6.265E+00	5.954E+00	5.648E+00	5.355E+00	5.109E+00	5.001E+00	5.261E+00	6.426E+00	0.0	0.0
35	6.217E+00	6.017E+00	5.717E+00	5.422E+00	5.141E+00	4.904E+00	4.799E+00	5.048E+00	6.164E+00	0.0	0.0
36	5.950E+00	5.758E+00	5.471E+00	5.188E+00	4.918E+00	4.690E+00	4.589E+00	4.825E+00	5.889E+00	0.0	0.0
37	5.682E+00	5.498E+00	5.223E+00	4.951E+00	4.693E+00	4.474E+00	4.376E+00	4.599E+00	5.609E+00	0.0	0.0
38	5.431E+00	5.254E+00	4.990E+00	4.729E+00	4.481E+00	4.271E+00	4.174E+00	4.381E+00	5.331E+00	0.0	0.0
39	5.233E+00	5.062E+00	4.807E+00	4.554E+00	4.314E+00	4.109E+00	4.011E+00	4.196E+00	5.079E+00	0.0	0.0
40	5.167E+00	4.997E+00	4.743E+00	4.493E+00	4.254E+00	4.048E+00	3.941E+00	4.096E+00	4.896E+00	0.0	0.0
41	5.383E+00	5.205E+00	4.938E+00	4.676E+00	4.424E+00	4.205E+00	4.077E+00	4.184E+00	4.869E+00	0.0	0.0
42	6.172E+00	5.966E+00	5.659E+00	5.356E+00	5.064E+00	4.805E+00	4.631E+00	4.665E+00	5.185E+00	0.0	0.0
43	0.0	0.0	0.0	0.0	0.0	0.0	0.0	0.0	0.0	0.0	0.0
44	0.0	0.0	0.0	0.0	0.0	0.0	0.0	0.0	0.0	0.0	0.0
45	0.0	0.0	0.0	0.0	0.0	0.0	0.0	0.0	0.0	0.0	0.0
46	0.0	0.0	0.0	0.0	0.0	0.0	0.0	0.0	0.0	0.0	0.0
47	C.C	0.0	0.0	0.0	0.0	0.0	0.0	0.0	0.0	0.0	0.0
48	0.0	0.0	0.0	0.0	0.0	0.0	0.0	0.0	0.0	0.0	0.0
49	0.0	0.0	0.0	0.0	0.0	0.0	0.0	0.0	0.0	0.0	0.0
50	0.0	0.0	0.0	0.0	0.0	0.0	0.0	0.0	0.0	0.0	0.0

	23	24	25	26
1	C.C	0.0	0.0	0.0
2	C.0	0.0	0.0	0.0
3	0.0	0.0	0.0	0.0
4	C.C	0.0	0.0	0.0
5	C.0	0.0	C.0	0.0
6	0.0	0.0	0.0	0.0
7	C.0	0.0	0.0	0.0
8	C.0	0.0	0.0	0.0
9	C.0	0.0	0.0	0.0
10	0.0	0.0	0.0	0.0
11	0.0	0.0	0.0	0.0
12	C.C	0.0	0.0	0.0
13	C.0	0.0	0.0	0.0
14	0.0	0.0	0.0	0.0
15	0.C	0.0	0.0	C.0
16	0.C	0.0	0.0	0.0
17	C.C	0.0	0.C	0.0

ARMY REACTOR DEPLETION RUNS
DATE : MAY 14 , 1975

SUMMARY OF NEUTRON LOSSES, ETC. FOR STEP 5 CYCLE 1 AT CYCLE DEPLETION TIME 525.00 DAYS. FISSILE KG IS AT 600.00 DAYS

ZONE CLASS	FISSILE	FERTILE	INTERMEDIATE	OTHER STRUCTURAL	SPECIAL	UNSPECIFIED	SUMS	CONV. RATIO	POWER(MW)	FISSILE(KG)
CORE	0.53631	0.25629	0.01193	0.07011	0.00851	0.0	0.04371	0.92686	0.45395	2.97656E+02	6.92844E+02
BUFFER	0.0	0.0	0.0	0.00867	0.00139	0.0	0.0	0.01006	0.0	0.0	0.0
REFLECTOR	0.0	0.0	0.0	0.01279	0.01727	0.0	-0.00000	0.03007	0.0	0.0	0.0
				OTHER LOSSES* BASED ON START-OF-STEP TOTAL LOSSES				0.03301			
OVERALL	0.53631	0.25629	0.01193	0.09157	0.02718	0.0	0.04371	1.00000	0.45395	2.97656E+02	6.92844E+02

THIS STEP THERMAL ENERGY, MW-HRS 1.07156E+06 AND TOTAL IS 4.29109E+06

NUCLIDE DENSITIES BY ZONE AND SUB-ZONE(NUCLIDE NUMBER - DENSITY) AT DEPLETION TIME 6.000000E+02DAYS

ZONE NUMBER 1-- CORE

8	4.22258E-06	10	3.08944E-05	14	1.14452E-07	16	1.17479E-08	6	3.41239E-04	9	1.56864E-07
12	2.93373E-06	15	2.61579E-08	7	3.60524E-07	82	1.73170E-09	13	1.24993E-09	11	2.38524E-06
17	1.20809E-09	18	9.73847E-08	105	1.09645E-06	125	0.0	5	6.19000E-02	84	7.37000E-04
39	5.82709E-07	85	5.48741E-07	50	2.45029E-07	53	2.51862E-07	58	3.22699E-10	55	5.89934E-07
60	5.20615E-07	61	3.48535E-07	63	1.34948E-07	65	9.65932E-10	67	4.21220E-09	68	9.41875E-08
69	1.92816E-08	70	4.16638E-08	71	1.07406E-08	72	2.08707E-09	73	3.02534E-10	86	7.85705E-07
87	8.59866E-06										

ZONE NUMBER 2-- CORE

8	6.07824E-06	10	2.59040E-05	14	1.32588E-07	16	2.72978E-08	6	3.37647E-04	9	3.65607E-07
12	2.80022E-06	15	4.09783E-08	7	5.71043E-07	82	2.40470E-09	13	1.92573E-09	11	3.39909E-06
17	4.75417E-09	18	2.22572E-07	105	7.46941E-07	125	0.0	5	6.19000E-02	84	7.37000E-04
39	8.79189E-07	85	8.15527E-07	50	3.43956E-07	53	3.62530E-07	58	3.88748E-10	55	8.69970E-07
60	7.57539E-07	61	5.09723E-07	63	1.72711E-07	65	1.83294E-09	67	3.87431E-09	68	1.38524E-07
69	2.19668E-08	70	6.21964E-08	71	1.39370E-08	72	3.73305E-09	73	6.14851E-10	86	1.85192E-06
87	1.24232E-05										

ZONE NUMBER 3-- CORE

8	6.26250E-06	10	2.53241E-05	14	1.32862E-07	16	2.92560E-08	6	3.37444E-04	9	3.95585E-07
12	2.78499E-06	15	4.21965E-08	7	5.94604E-07	82	2.46561E-09	13	1.99621E-09	11	3.50867E-06
17	5.39871E-09	18	2.39649E-07	105	7.12346E-07	125	0.0	5	6.19000E-02	84	7.37000E-04
39	9.15547E-07	85	8.47785E-07	50	3.54650E-07	53	3.75405E-07	58	3.93467E-10	55	9.03439E-07
60	7.85033E-07	61	5.28846E-07	63	1.76466E-07	65	1.91337E-09	67	3.82206E-09	68	1.43719E-07
69	2.21425E-08	70	6.45420E-08	71	1.42525E-08	72	3.91562E-09	73	6.51611E-10	86	2.00843E-06
87	1.28730E-05										

ZONE NUMBER 4-- CORE

8	4.84120E-06	10	2.86933E-05	14	1.16851E-07	16	1.74684E-08	6	3.40114E-04	9	2.25102E-07
12	2.69135E-06	15	3.14200E-08	7	4.23903E-07	82	1.94805E-09	13	1.46380E-09	11	2.80372E-06
17	2.35251E-09	18	1.36167E-07	105	9.24691E-07	125	0.0	5	6.19000E-02	84	7.37000E-04
39	7.10600E-07	85	6.65566E-07	50	2.89025E-07	53	3.01999E-07	58	3.50154E-10	55	7.13801E-07
60	6.23833E-07	61	4.20311E-07	63	1.55541E-07	65	1.28451E-09	67	3.96638E-09	68	1.14207E-07
69	2.03334E-08	70	5.16844E-08	71	1.23830E-08	72	2.72760E-09	73	4.23524E-10	86	1.14028E-06
87	1.03321E-05										

ZONE NUMBER 5-- CORE

8	3.88921E-06	10	3.18501E-05	14	1.10241E-07	16	9.45657E-09	6	3.41779E-04	9	1.29564E-07
12	2.95496E-06	15	2.32445E-08	7	3.26113E-07	82	1.60575E-09	13	1.13722E-09	11	2.19050E-06
17	8.61492E-10	18	8.09353E-08	105	1.17810E-06	125	0.0	5	6.19000E-02	84	7.37000E-04
39	5.28976E-07	85	4.99169E-07	50	2.25239E-07	53	2.30296E-07	58	3.06525E-10	55	5.37282E-07
60	4.75548E-07	61	3.17878E-07	63	1.25792E-07	65	8.25193E-10	67	4.29178E-09	68	8.56112E-08
69	1.85839E-08	70	3.74794E-08	71	9.99495E-09	72	1.80147E-09	73	2.51535E-10	86	6.47010E-07
87	7.65816E-06										

ZONE NUMBER 6-- CORE

8	5.66183E-06	10	2.71789E-05	14	1.31145E-07	16	2.30600E-08	6	3.36710E-04	9	3.04628E-07		
12	2.83316E-06	15	3.79732E-08	7	5.17998E-07	82	2.26227E-09	13	1.76306E-09	11	3.15407E-06		
17	3.52711E-09	18	1.87268E-07	105	8.27304E-07	125	0.0	5	6.19000E-02	84	7.37000E-04		
39	8.00736E-07	85	7.45523E-07	50	3.19581E-07	53	3.34198E-07	58	3.76092E-10	55	7.96788E-07		
60	6.97946E-07	61	4.67929E-07	63	1.63883E-07	65	1.60783E-09	67	3.98554E-09	68	1.27110E-07		
69	2.15070E-08	70	5.69628E-08	71	1.31977E-08	72	3.32335E-09	73	5.33593E-10	86	1.53563E-06		
87	1.14362E-05												
ZONE NUMBER 7-- CORE													
8	5.83945E-06	10	2.66380E-05	14	1.31814E-07	16	2.48418E-08	6	3.38350E-04	9	3.29613E-07		
12	2.81946E-06	15	3.92869E-08	7	5.39376E-07	82	2.32317E-09	13	1.82847E-09	11	3.25849E-06		
17	4.01810E-09	18	2.01758E-07	105	7.92459E-07	125	0.0	5	6.19000E-02	84	7.37000E-04		
39	8.33803E-07	85	7.75102E-07	50	3.29963E-07	53	3.46246E-07	58	3.81441E-10	55	8.27720E-07		
60	7.22716E-07	61	4.85645E-07	63	1.67738E-07	65	1.70027E-09	67	3.93755E-09	68	1.31959E-07		
69	2.17103E-08	70	5.92077E-08	71	1.35207E-08	72	3.49698E-09	73	5.67845E-10	86	1.66504E-06		
87	1.18552E-05												
ZONE NUMBER 8-- CORE													
8	4.47187E-06	10	2.98318E-05	14	1.13968E-07	16	1.42938E-08	6	3.40777E-04	9	1.85588E-07		
12	2.91654E-06	15	2.84094E-08	7	3.88434E-07	82	1.81529E-09	13	1.33225E-09	11	2.57931E-06		
17	1.69160E-09	18	1.13202E-07	105	1.00880E-06	125	0.0	5	6.19000E-02	84	7.37000E-04		
39	6.44199E-07	85	6.05152E-07	50	2.66442E-07	53	2.76368E-07	58	3.35477E-10	55	6.49961E-07		
60	5.70410E-07	61	3.83408E-07	63	1.45679E-07	65	1.10511E-09	67	4.06368E-09	68	1.03976E-07		
69	1.97685E-08	70	4.66878E-08	71	1.15813E-08	72	2.37732E-09	73	3.57497E-10	86	9.36685E-07		
87	9.44661E-06												
ZONE NUMBER 9-- CORE													
8	2.95035E-06	10	3.37338E-05	14	8.78101E-08	16	5.35012E-09	6	3.43130E-04	9	7.63490E-08		
12	3.01256E-06	15	1.57427E-08	7	2.38985E-07	82	1.24334E-09	13	8.24790E-10	11	1.74947E-06		
17	3.89307E-10	18	4.62781E-08	105	1.34393E-06	125	0.0	5	6.19000E-02	84	7.37000E-04		
39	4.26834E-07	85	4.05249E-07	50	1.85664E-07	53	1.89263E-07	58	2.64665E-10	55	4.37614E-07		
60	3.87585E-07	61	2.59623E-07	63	1.08739E-07	65	5.29107E-10	67	4.25510E-09	68	6.94163E-08		
69	1.65732E-08	70	3.00879E-08	71	8.54181E-09	72	1.20826E-09	73	1.54774E-10	86	3.85527E-07		
87	6.45740E-06												
ZONE NUMBER 10-- CORE													
8	4.37346E-06	10	2.97842E-05	14	1.09485E-07	16	1.41123E-08	6	3.40903E-04	9	1.81774E-07		
12	2.92413E-06	15	2.75505E-08	7	3.80248E-07	82	1.78998E-09	13	1.29367E-09	11	2.56646E-06		
17	1.70248E-09	18	1.09056E-07	105	1.00250E-06	125	0.0	5	6.19000E-02	84	7.37000E-04		
39	6.47449E-07	85	6.08591E-07	50	2.67202E-07	53	2.78280E-07	58	3.33223E-10	55	6.53995E-07		
60	5.72429E-07	61	3.85728E-07	63	1.47488E-07	65	1.08570E-09	67	4.00079E-09	68	1.04681E-07		
69	1.96232E-08	70	4.73744E-08	71	1.16799E-08	72	2.35105E-09	73	3.54552E-10	86	9.21987E-07		
87	9.51124E-06												
ZONE NUMBER 11-- CORE													
8	4.51660E-06	10	2.93364E-05	14	1.10651E-07	16	1.53052E-08	6	3.40651E-04	9	1.96463E-07		
12	2.91443E-06	15	2.87087E-08	7	3.95645E-07	82	1.84185E-09	13	1.34228E-09	11	2.65458E-06		
17	1.94462E-09	18	1.17478E-07	105	9.68942E-07	125	0.0	5	6.19000E-02	84	7.37000E-04		
39	6.73401E-07	85	6.32275E-07	50	2.76088E-07	53	2.88401E-07	58	3.38655E-10	55	6.79076E-07		
60	5.93361E-07	61	4.00238E-07	63	1.51497E-07	65	1.15299E-09	67	3.96264E-09	68	1.08709E-07		
69	1.98473E-08	70	4.93701E-08	71	1.20033E-08	72	2.48582E-09	73	3.79781E-10	86	9.97837E-07		
87	9.86603E-06												
ZONE NUMBER 12-- CORE													
8	3.39227E-06	10	3.21832E-05	14	9.29342E-08	16	8.09828E-09	6	3.42448E-04	9	1.07256E-07		
12	2.98674E-06	15	1.95913E-08	7	2.82020E-07	82	1.40952E-09	13	9.61287E-10	11	2.05123E-06		
17	7.42320E-10	18	6.38422E-08	105	1.19370E-06	125	0.0	5	6.19000E-02	84	7.37000E-04		
39	5.12478E-07	85	4.85040E-07	50	2.18236E-07	53	2.24955E-07	58	2.92308E-10	55	5.23050E-07		
60	4.60174E-07	61	3.09647E-07	63	1.26085E-07	65	7.08162E-10	67	4.08781E-09	68	8.35554E-08		
69	1.78274E-08	70	3.72460E-08	71	9.90270E-09	72	1.59918E-09	73	2.21856E-10	86	5.45569E-07		
87	7.68343E-06												
ZONE NUMBER 13-- BUFFER													
105	9.95307E-07	125	0.0	83	7.10694E-02								
ZONE NUMBER 14-- BUFFER													
105	1.00504E-06	125	0.0	83	7.10694E-02								
ZONE NUMBER 15-- BUFFER													
105	1.03224E-06	125	0.0	83	7.10694E-02								
ZONE NUMBER 16-- REFLECTOR													
105	0.0	125	3.04300E-04	83	6.66300E-02								
ZONE NUMBER 17-- REFLECTOR													
105	0.0	125	0.0	83	7.10700E-02								
ZONE NUMBER 18-- REFLECTOR													

```
 105  C.C          125  0.0          83  7.10700E-02

 TIME STEP  5  REQUIRED  0.282  MINUTES CPU TIME, AND  0.524  MINUTES CLOCK TIME

 A FLUX - EIGENVALUE PROBLEM FOLLOWS FOR CYCLE  1 CYCLE TIME   600.0000 DAYS   TOTAL TIME   600.0000 DAYS

 ITERATION   FLUX CHANGE     BETA       MU-1       MU-2       MU-3          K
     1      3.96614E-02   1.00000    0.07932    0.0        0.0        1.049512
     2      2.33567E+00   1.76982   61.22597   61.22597    0.00502    1.052058
     3      1.92859E+00   1.62578    2.75429    0.31755    0.09387    1.052186
     4      2.12163E+00   1.54699    3.22172    0.29921    0.11908    1.052150
     5      5.34964E-01   1.50704    0.78711    0.37072    0.19224    1.052140
     6     -2.61878E-01   1.48756   -0.75140   -0.17325   -1.24224    1.052123
     7     -1.97275E-01   1.47825    0.55603    0.52522    1.23103    1.052107
     8     -8.11335E-02   1.47383    0.33014    0.97629    0.95145    1.052093
     9     -2.28572E-02   1.47175    0.25887    0.50896    0.85548    1.052081
    10     -1.25344E-02   1.47077    0.53584    0.34070    0.81999    1.052071
    11     -5.10472E-03   1.47031    0.40215    0.22458    0.79035    1.052061
    12     -1.00350E-03   1.47009    0.19558    0.42029    0.76160    1.052054
    13      4.49181E-04   1.46999   -0.44716   -0.47944    0.72525    1.052048
    14      3.76701E-04   1.46994    0.83902    0.83721    0.67329    1.052042
    15      3.24249E-04   1.46992    0.86108    0.84328    0.58602    1.052037
    16      2.83241E-04   1.46991    0.87381    0.84732    0.40120    1.052033
    17      2.47955E-04   1.46990    0.87567    0.85245   -0.25956    1.052031
    18      2.18391E-04   1.46990    0.88099    0.85888    5.08362    1.052028
    19      1.92642E-04   1.46990    0.88229    0.86653    1.67457    1.052025
    20      1.71661E-04   1.46990    0.89126    0.87308    1.33777    1.052023
    21      1.52588E-04   1.46990    0.88904    0.88307    1.21143    1.052021
    22      1.36375E-04   1.46990    0.89389    0.89247    1.14598    1.052020
    23      1.22070E-04   1.46990    0.89523    0.90165    1.10641    1.052019
    24      1.09673E-04   1.46990    0.89855    0.91910    1.08024    1.052017
    25      9.91921E-05   1.46990    0.90445    0.92880    1.06188    1.052016

 END OF EIGENVALUE CALCULATION - ITERATION TIME  0.271 MINUTES

 CONVERGENCE INDICATION BY MINIMIZING THE SUM OF THE SQUARES OF THE RESIDUES - RELATIVE ABSORPTION  0.9999990   K  1.0520239

     LEAKAGE  6.37102E+17   TOTAL LOSSES  2.16856E+19   TOTAL PRODUCTIONS  2.28137E+19   REACTOR POWER(WATTS)  3.00000E+08


 AVERAGE FLUXES BY ZONE AND GROUP

 ZONE   1-- CORE
    3.19269E+13  6.50193E+13  9.47714E+12  2.37047E+13

 ZONE   2-- CORE
    4.98336E+13  1.04007E+14  1.50570E+13  3.70625E+13

 ZONE   3-- CORE
    5.16535E+13  1.07985E+14  1.56233E+13  3.87570E+13

 ZONE   4-- CORE
    3.75233E+13  7.63351E+13  1.11372E+13  2.99468E+13

 ZONE   5-- CORE
    2.89895E+13  5.88943E+13  8.59280E+12  2.12786E+13

 ZONE   6-- CORE
    4.54385E+13  9.44701E+13  1.36961E+13  3.32417E+13

 ZONE   7-- CORE
    4.71166E+13  9.81019E+13  1.42145E+13  3.47428E+13

 ZONE   8-- CORE
```

3.407642E+13 6.91121E+13 1.00946E+13 2.67790E+13

ZCBE 9-- CORE
2.15037E+13 4.19183E+13 6.11495E+12 1.75401E+13

ZCBE 10-- CORE
3.37534E+13 6.72605E+13 9.77105E+12 2.73910E+13

ZCBE 11-- CORE
3.49876E+13 6.98012E+13 1.01362E+13 2.85754E+13

ZCBE 12-- CORE
2.50598E+13 4.87658E+13 7.12882E+12 2.15616E+13

ZCBE 13-- BUFFER
5.58119E+12 1.92742E+13 4.25822E+12 5.30738E+13

ZCBE 14-- BUFFER
5.05367E+12 1.74188E+13 3.84765E+12 4.76022E+13

ZCBE 15-- BUFFER
3.57721E+12 1.19938E+13 2.63784E+12 3.50378E+13

ZCBE 16-- REFLECTOR
9.23872E+11 3.35082E+12 7.46622E+11 1.10959E+13

ZCBE 17-- REFLECTOR
9.52383E+10 7.34457E+11 1.94758E+11 1.98858E+13

ZCBE 18-- REFLECTOR
7.71577E+11 2.97910E+12 6.91417E+11 2.42805E+13

ZCBE AVERAGE POWER DENSITIES(WATTS/CC)
6.02660E+00 8.95323E+00 9.26862E+00 7.23795E+00 5.48350E+00 8.19758E+00 8.49150E+00 6.59081E+00 4.41186E+00
6.62517E+00 6.86153E+00 5.24204E+00 0.0 0.0 0.0 0.0 0.0 0.0

ARMY REACTOR DIFFUSION RUNS
DATE : MAY 14 , 1975

GROUP 1 FLUX

	1	2	3	4	5	6	7	8	9	10	11
1	4.719D+09	4.667D+09	4.655D+09	4.624D+09	4.564D+09	4.467D+09	4.370D+09	4.273D+09	4.177D+09	4.080D+09	3.983D+09
2	2.150D+10	2.135D+10	2.121D+10	2.107D+10	2.079D+10	2.036D+10	1.992D+10	1.948D+10	1.904D+10	1.860D+10	1.817D+10
3	8.685D+10	8.627D+10	8.570D+10	8.512D+10	8.404D+10	8.227D+10	8.050D+10	7.873D+10	7.697D+10	7.522D+10	7.348D+10
4	3.484D+11	3.461D+11	3.438D+11	3.416D+11	3.373D+11	3.302D+11	3.231D+11	3.160D+11	3.089D+11	3.020D+11	2.950D+11
5	1.397D+12	1.388D+12	1.379D+12	1.370D+12	1.353D+12	1.325D+12	1.296D+12	1.268D+12	1.239D+12	1.211D+12	1.184D+12
6	5.602D+12	5.564D+12	5.528D+12	5.493D+12	5.429D+12	5.316D+12	5.201D+12	5.086D+12	4.972D+12	4.859D+12	4.748D+12
7	1.864D+13	1.851D+13	1.839D+13	1.827D+13	1.808D+13	1.770D+13	1.731D+13	1.693D+13	1.655D+13	1.617D+13	1.580D+13
8	2.396D+13	2.369D+13	2.354D+13	2.339D+13	2.314D+13	2.265D+13	2.216D+13	2.167D+13	2.118D+13	2.070D+13	2.022D+13
9	2.783D+13	2.764D+13	2.746D+13	2.729D+13	2.699D+13	2.643D+13	2.585D+13	2.528D+13	2.471D+13	2.415D+13	2.359D+13
10	3.138D+13	3.117D+13	3.096D+13	3.077D+13	3.044D+13	2.980D+13	2.915D+13	2.851D+13	2.787D+13	2.723D+13	2.660D+13
11	3.470D+13	3.446D+13	3.424D+13	3.403D+13	3.366D+13	3.296D+13	3.224D+13	3.153D+13	3.082D+13	3.012D+13	2.942D+13
12	3.780D+13	3.754D+13	3.730D+13	3.707D+13	3.667D+13	3.591D+13	3.513D+13	3.436D+13	3.359D+13	3.282D+13	3.207D+13
13	4.063D+13	4.036D+13	4.010D+13	3.986D+13	3.943D+13	3.862D+13	3.778D+13	3.695D+13	3.613D+13	3.530D+13	3.449D+13
14	4.311D+13	4.282D+13	4.255D+13	4.229D+13	4.186D+13	4.100D+13	4.012D+13	3.924D+13	3.836D+13	3.749D+13	3.663D+13
15	4.499D+13	4.469D+13	4.442D+13	4.416D+13	4.375D+13	4.286D+13	4.194D+13	4.102D+13	4.011D+13	3.920D+13	3.831D+13
16	4.692D+13	4.662D+13	4.633D+13	4.607D+13	4.565D+13	4.473D+13	4.378D+13	4.282D+13	4.187D+13	4.093D+13	4.000D+13
17	4.870D+13	4.839D+13	4.810D+13	4.783D+13	4.740D+13	4.645D+13	4.546D+13	4.447D+13	4.348D+13	4.251D+13	4.154D+13
18	5.026D+13	4.994D+13	4.964D+13	4.937D+13	4.893D+13	4.795D+13	4.693D+13	4.591D+13	4.489D+13	4.389D+13	4.289D+13
19	5.157D+13	5.125D+13	5.094D+13	5.066D+13	5.021D+13	4.921D+13	4.816D+13	4.712D+13	4.608D+13	4.504D+13	4.403D+13
20	5.262D+13	5.229D+13	5.198D+13	5.169D+13	5.123D+13	5.021D+13	4.915D+13	4.808D+13	4.702D+13	4.597D+13	4.493D+13
21	5.340D+13	5.306D+13	5.274D+13	5.246D+13	5.199D+13	5.095D+13	4.988D+13	4.880D+13	4.772D+13	4.665D+13	4.560D+13
22	5.388D+13	5.354D+13	5.322D+13	5.293D+13	5.247D+13	5.142D+13	5.034D+13	4.925D+13	4.816D+13	4.708D+13	4.602D+13
23	5.403D+13	5.369D+13	5.338D+13	5.309D+13	5.263D+13	5.158D+13	5.049D+13	4.940D+13	4.831D+13	4.723D+13	4.617D+13
24	5.398D+13	5.364D+13	5.332D+13	5.304D+13	5.258D+13	5.153D+13	5.045D+13	4.935D+13	4.826D+13	4.719D+13	4.612D+13
25	5.368D+13	5.335D+13	5.303D+13	5.275D+13	5.229D+13	5.125D+13	5.017D+13	4.908D+13	4.800D+13	4.692D+13	4.587D+13
26	5.314D+13	5.280D+13	5.249D+13	5.221D+13	5.175D+13	5.072D+13	4.965D+13	4.857D+13	4.750D+13	4.643D+13	4.539D+13
27	5.233D+13	5.200D+13	5.169D+13	5.141D+13	5.097D+13	4.995D+13	4.889D+13	4.783D+13	4.677D+13	4.572D+13	4.468D+13
28	5.128D+13	5.096D+13	5.065D+13	5.038D+13	4.994D+13	4.894D+13	4.790D+13	4.685D+13	4.581D+13	4.478D+13	4.377D+13
29	5.001D+13	4.968D+13	4.939D+13	4.912D+13	4.868D+13	4.770D+13	4.669D+13	4.566D+13	4.465D+13	4.364D+13	4.265D+13
30	4.855D+13	4.823D+13	4.794D+13	4.767D+13	4.724D+13	4.629D+13	4.529D+13	4.430D+13	4.331D+13	4.233D+13	4.136D+13
31	4.728D+13	4.697D+13	4.668D+13	4.642D+13	4.599D+13	4.504D+13	4.407D+13	4.310D+13	4.213D+13	4.117D+13	4.023D+13
32	4.605D+13	4.575D+13	4.547D+13	4.521D+13	4.477D+13	4.385D+13	4.291D+13	4.196D+13	4.101D+13	4.008D+13	3.916D+13
33	4.467D+13	4.438D+13	4.410D+13	4.384D+13	4.342D+13	4.252D+13	4.160D+13	4.068D+13	3.976D+13	3.885D+13	3.795D+13
34	4.317D+13	4.289D+13	4.261D+13	4.236D+13	4.195D+13	4.108D+13	4.018D+13	3.929D+13	3.840D+13	3.752D+13	3.665D+13
35	4.156D+13	4.128D+13	4.102D+13	4.078D+13	4.038D+13	3.954D+13	3.867D+13	3.781D+13	3.695D+13	3.610D+13	3.526D+13
36	3.987D+13	3.960D+13	3.935D+13	3.911D+13	3.872D+13	3.791D+13	3.708D+13	3.625D+13	3.542D+13	3.460D+13	3.379D+13
37	3.809D+13	3.783D+13	3.759D+13	3.736D+13	3.699D+13	3.621D+13	3.541D+13	3.462D+13	3.382D+13	3.303D+13	3.226D+13
38	3.621D+13	3.596D+13	3.573D+13	3.552D+13	3.516D+13	3.442D+13	3.366D+13	3.289D+13	3.214D+13	3.139D+13	3.065D+13
39	3.417D+13	3.393D+13	3.371D+13	3.351D+13	3.317D+13	3.247D+13	3.175D+13	3.103D+13	3.031D+13	2.960D+13	2.889D+13
40	3.176D+13	3.154D+13	3.134D+13	3.115D+13	3.083D+13	3.018D+13	2.951D+13	2.883D+13	2.816D+13	2.750D+13	2.684D+13
41	2.852D+13	2.832D+13	2.813D+13	2.796D+13	2.768D+13	2.709D+13	2.649D+13	2.588D+13	2.528D+13	2.468D+13	2.409D+13
42	2.332D+13	2.316D+13	2.301D+13	2.287D+13	2.264D+13	2.216D+13	2.166D+13	2.117D+13	2.067D+13	2.018D+13	1.969D+13
43	1.218D+13	1.209D+13	1.202D+13	1.194D+13	1.181D+13	1.156D+13	1.131D+13	1.105D+13	1.079D+13	1.053D+13	1.028D+13
44	5.954D+12	5.914D+12	5.877D+12	5.841D+12	5.774D+12	5.652D+12	5.526D+12	5.399D+12	5.273D+12	5.149D+12	5.027D+12
45	2.931D+12	2.911D+12	2.893D+12	2.875D+12	2.841D+12	2.781D+12	2.719D+12	2.657D+12	2.595D+12	2.534D+12	2.474D+12
46	1.483D+12	1.473D+12	1.464D+12	1.454D+12	1.437D+12	1.406D+12	1.375D+12	1.344D+12	1.312D+12	1.281D+12	1.251D+12
47	4.160D+11	4.132D+11	4.105D+11	4.079D+11	4.027D+11	3.942D+11	3.854D+11	3.766D+11	3.679D+11	3.592D+11	3.506D+11
48	9.112D+10	9.052D+10	8.992D+10	8.932D+10	8.818D+10	8.629D+10	8.437D+10	8.245D+10	8.054D+10	7.863D+10	7.673D+10
49	1.966D+10	1.973D+10	1.960D+10	1.946D+10	1.921D+10	1.880D+10	1.838D+10	1.796D+10	1.754D+10	1.712D+10	1.670D+10
50	3.874D+09	3.848D+09	3.822D+09	3.795D+09	3.746D+09	3.664D+09	3.583D+09	3.501D+09	3.418D+09	3.336D+09	3.253D+09

	12	13	14	15	16	17	18	19	20	21	22
1	3.885D+09	3.736D+09	3.525D+09	3.293D+09	3.034D+09	2.740D+09	2.410D+09	2.050D+09	1.671D+09	1.308D+09	4.825D+08
2	1.773D+10	1.707D+10	1.614D+10	1.513D+10	1.400D+10	1.270D+10	1.121D+10	9.543D+09	7.753D+09	4.589D+09	2.105D+09
3	7.174D+10	6.916D+10	6.557D+10	6.174D+10	5.745D+10	5.248D+10	4.659D+10	3.972D+10	3.209D+10	1.831D+10	7.854D+09

4	2.892D+11	2.780D+11	2.642D+11	2.498D+11	2.341D+11	2.157D+11	1.933D+11	1.656D+11	1.340D+11	7.152D+10	2.798D+10
5	1.156D+12	1.117D+12	1.063D+12	1.009D+12	9.518D+11	8.870D+11	8.062D+11	6.991D+11	5.590D+11	2.716D+11	9.360D+10
6	4.639D+12	4.481D+12	4.269D+12	4.062D+12	3.856D+12	3.639D+12	3.378D+12	3.007D+12	2.429D+12	9.699D+11	2.800D+11
7	1.544D+13	1.492D+13	1.421D+13	1.353D+13	1.289D+13	1.229D+13	1.169D+13	1.091D+13	9.319D+12	2.433D+12	5.708D+11
8	1.975D+13	1.909D+13	1.818D+13	1.731D+13	1.648D+13	1.572D+13	1.495D+13	1.394D+13	1.187D+13	3.194D+12	7.465D+11
9	2.304D+13	2.226D+13	2.120D+13	2.018D+13	1.921D+13	1.831D+13	1.740D+13	1.620D+13	1.378D+13	3.794D+12	8.960D+11
10	2.599D+13	2.511D+13	2.391D+13	2.275D+13	2.165D+13	2.062D+13	1.958D+13	1.822D+13	1.549D+13	4.306D+12	1.025D+12
11	2.874D+13	2.777D+13	2.644D+13	2.515D+13	2.393D+13	2.278D+13	2.163D+13	2.011D+13	1.709D+13	4.768D+12	1.140D+12
12	3.133D+13	3.026D+13	2.881D+13	2.741D+13	2.607D+13	2.481D+13	2.355D+13	2.189D+13	1.860D+13	5.192D+12	1.243D+12
13	3.378D+13	3.256D+13	3.100D+13	2.949D+13	2.805D+13	2.669D+13	2.532D+13	2.353D+13	1.999D+13	5.578D+12	1.336D+12
14	3.579D+13	3.459D+13	3.294D+13	3.133D+13	2.980D+13	2.835D+13	2.690D+13	2.499D+13	2.123D+13	5.920D+12	1.419D+12
15	3.744D+13	3.621D+13	3.449D+13	3.280D+13	3.120D+13	2.969D+13	2.815D+13	2.614D+13	2.217D+13	6.212D+12	1.492D+12
16	3.909D+13	3.782D+13	3.602D+13	3.427D+13	3.259D+13	3.101D+13	2.941D+13	2.730D+13	2.315D+13	6.484D+12	1.558D+12
17	4.061D+13	3.929D+13	3.742D+13	3.560D+13	3.386D+13	3.222D+13	3.056D+13	2.836D+13	2.405D+13	6.732D+12	1.617D+12
18	4.193D+13	4.056D+13	3.864D+13	3.676D+13	3.497D+13	3.327D+13	3.156D+13	2.929D+13	2.484D+13	6.950D+12	1.669D+12
19	4.304D+13	4.164D+13	3.967D+13	3.774D+13	3.590D+13	3.416D+13	3.239D+13	3.007D+13	2.550D+13	7.133D+12	1.712D+12
20	4.392D+13	4.250D+13	4.049D+13	3.852D+13	3.664D+13	3.486D+13	3.306D+13	3.069D+13	2.603D+13	7.279D+12	1.747D+12
21	4.458D+13	4.313D+13	4.109D+13	3.909D+13	3.719D+13	3.538D+13	3.356D+13	3.115D+13	2.642D+13	7.388D+12	1.773D+12
22	4.499D+13	4.353D+13	4.148D+13	3.946D+13	3.754D+13	3.571D+13	3.387D+13	3.144D+13	2.666D+13	7.456D+12	1.789D+12
23	4.513D+13	4.369D+13	4.161D+13	3.959D+13	3.766D+13	3.583D+13	3.398D+13	3.154D+13	2.674D+13	7.483D+12	1.796D+12
24	4.509D+13	4.364D+13	4.158D+13	3.955D+13	3.762D+13	3.580D+13	3.395D+13	3.151D+13	2.672D+13	7.474D+12	1.794D+12
25	4.484D+13	4.339D+13	4.134D+13	3.933D+13	3.741D+13	3.559D+13	3.375D+13	3.132D+13	2.656D+13	7.430D+12	1.784D+12
26	4.437D+13	4.293D+13	4.090D+13	3.891D+13	3.701D+13	3.521D+13	3.339D+13	3.098D+13	2.627D+13	7.349D+12	1.764D+12
27	4.368D+13	4.227D+13	4.026D+13	3.830D+13	3.642D+13	3.465D+13	3.285D+13	3.049D+13	2.585D+13	7.231D+12	1.736D+12
28	4.278D+13	4.139D+13	3.943D+13	3.750D+13	3.566D+13	3.392D+13	3.216D+13	2.984D+13	2.529D+13	7.078D+12	1.700D+12
29	4.168D+13	4.033D+13	3.840D+13	3.652D+13	3.472D+13	3.302D+13	3.130D+13	2.904D+13	2.462D+13	6.892D+12	1.655D+12
30	4.042D+13	3.910D+13	3.723D+13	3.540D+13	3.365D+13	3.200D+13	3.033D+13	2.813D+13	2.385D+13	6.677D+12	1.603D+12
31	3.902D+13	3.803D+13	3.620D+13	3.441D+13	3.271D+13	3.109D+13	2.947D+13	2.734D+13	2.319D+13	6.476D+12	1.553D+12
32	3.826D+13	3.700D+13	3.522D+13	3.348D+13	3.181D+13	3.024D+13	2.865D+13	2.659D+13	2.255D+13	6.296D+12	1.509D+12
33	3.708D+13	3.586D+13	3.413D+13	3.243D+13	3.081D+13	2.928D+13	2.774D+13	2.573D+13	2.182D+13	6.095D+12	1.463D+12
34	3.581D+13	3.462D+13	3.294D+13	3.129D+13	2.973D+13	2.824D+13	2.675D+13	2.481D+13	2.104D+13	5.875D+12	1.406D+12
35	3.444D+13	3.330D+13	3.168D+13	3.009D+13	2.857D+13	2.714D+13	2.570D+13	2.383D+13	2.020D+13	5.638D+12	1.348D+12
36	3.301D+13	3.191D+13	3.034D+13	2.881D+13	2.736D+13	2.598D+13	2.459D+13	2.279D+13	1.931D+13	5.382D+12	1.283D+12
37	3.151D+13	3.045D+13	2.895D+13	2.748D+13	2.608D+13	2.476D+13	2.343D+13	2.170D+13	1.838D+13	5.104D+12	1.212D+12
38	2.993D+13	2.892D+13	2.748D+13	2.608D+13	2.474D+13	2.348D+13	2.220D+13	2.056D+13	1.740D+13	4.797D+12	1.132D+12
39	2.829D+13	2.725D+13	2.590D+13	2.457D+13	2.329D+13	2.209D+13	2.088D+13	1.932D+13	1.633D+13	4.446D+12	1.040D+12
40	2.662D+13	2.561D+13	2.434D+13	2.308D+13	2.188D+13	2.075D+13	1.961D+13	1.814D+13	1.533D+13	4.172D+12	9.744D+11
41	2.491D+13	2.395D+13	2.276D+13	2.158D+13	2.045D+13	1.938D+13	1.830D+13	1.691D+13	1.428D+13	3.879D+12	9.046D+11
42	2.317D+13	2.226D+13	2.114D+13	2.004D+13	1.898D+13	1.797D+13	1.695D+13	1.565D+13	1.321D+13	3.581D+12	8.341D+11
43	2.140D+13	2.054D+13	1.950D+13	1.847D+13	1.748D+13	1.653D+13	1.557D+13	1.436D+13	1.211D+13	3.279D+12	7.631D+11
44	1.960D+13	1.880D+13	1.783D+13	1.687D+13	1.595D+13	1.507D+13	1.418D+13	1.306D+13	1.100D+13	2.975D+12	6.916D+11
45	1.778D+13	1.704D+13	1.615D+13	1.526D+13	1.441D+13	1.359D+13	1.277D+13	1.175D+13	9.880D+12	2.670D+12	6.197D+11
46	1.594D+13	1.526D+13	1.445D+13	1.364D+13	1.286D+13	1.211D+13	1.136D+13	1.044D+13	8.768D+12	2.366D+12	5.476D+11
47	1.408D+13	1.347D+13	1.274D+13	1.201D+13	1.130D+13	1.062D+13	9.947D+12	9.132D+12	7.651D+12	2.063D+12	4.756D+11
48	1.221D+13	1.167D+13	1.102D+13	1.037D+13	9.741D+12	9.142D+12	8.552D+12	7.843D+12	6.561D+12	1.764D+12	4.040D+11
49	1.033D+13	9.862D+12	9.300D+12	8.734D+12	8.189D+12	7.677D+12	7.173D+12	6.570D+12	5.490D+12	1.471D+12	3.331D+11
50	8.446D+12	8.054D+12	7.586D+12	7.113D+12	6.663D+12	6.241D+12	5.825D+12	5.329D+12	4.447D+12	1.187D+12	2.631D+11

	23	24	25	26
1	2.205D+08	9.758D+07	4.126D+07	1.422D+07
2	9.171D+08	3.878D+08	1.577D+08	5.295D+07
3	3.195D+09	1.268D+09	4.891D+08	1.582D+08
4	1.044D+10	3.837D+09	1.389D+09	4.365D+08
5	3.132D+10	1.054D+10	3.555D+09	1.051D+09
6	8.226D+10	2.510D+10	7.878D+09	2.221D+09
7	1.495D+11	4.244D+10	1.269D+10	3.474D+09
8	1.930D+11	5.407D+10	1.598D+10	4.338D+09
9	2.322D+11	6.493D+10	1.913D+10	5.177D+09
10	2.668D+11	7.475D+10	2.203D+10	5.959D+09
11	2.975D+11	8.355D+10	2.466D+10	6.674D+09
12	3.250D+11	9.143D+10	2.702D+10	7.318D+09
13	3.497D+11	9.848D+10	2.913D+10	7.897D+09
14	3.717D+11	1.048D+11	3.102D+10	8.414D+09
15	3.913D+11	1.104D+11	3.270D+10	8.874D+09
16	4.088D+11	1.154D+11	3.419D+10	9.282D+09
17	4.243D+11	1.198D+11	3.551D+10	9.640D+09

28	7.563D+11	2.747D+11	9.797D+10	2.746D+10
29	7.360D+11	2.672D+11	9.530D+10	2.671D+10
30	7.116D+11	2.583D+11	9.208D+10	2.580D+10
31	6.881D+11	2.496D+11	8.892D+10	2.490D+10
32	6.672D+11	2.419D+11	8.611D+10	2.411D+10
33	6.440D+11	2.333D+11	8.300D+10	2.323D+10
34	6.185D+11	2.238D+11	7.957D+10	2.226D+10
35	5.903D+11	2.134D+11	7.579D+10	2.119D+10
36	5.591D+11	2.018D+11	7.163D+10	2.001D+10
37	5.246D+11	1.891D+11	6.708D+10	1.874D+10
38	4.865D+11	1.753D+11	6.214D+10	1.736D+10
39	4.446D+11	1.602D+11	5.683D+10	1.588D+10
40	3.991D+11	1.440D+11	5.120D+10	1.433D+10
41	3.506D+11	1.271D+11	4.535D+10	1.273D+10
42	3.006D+11	1.098D+11	3.944D+10	1.111D+10
43	2.416D+11	8.957D+10	3.253D+10	9.226D+09
44	1.792D+11	6.800D+10	2.513D+10	7.203D+09
45	1.271D+11	4.961D+10	1.872D+10	5.433D+09
46	8.705D+10	3.498D+10	1.349D+10	3.969D+09
47	3.986D+10	1.701D+10	6.878D+09	2.082D+09
48	1.352D+10	6.137D+09	2.608D+09	8.144D+08
49	4.196D+09	2.005D+09	8.891D+08	2.850D+08
50	9.975D+08	4.939D+08	2.255D+08	7.357D+07

GROUP 4 FLUX

	1	2	3	4	5	6	7	8	9	10	11
1	1.310D+12	1.301D+12	1.292D+12	1.283D+12	1.266D+12	1.239D+12	1.213D+12	1.187D+12	1.162D+12	1.138D+12	1.115D+12
2	4.013D+12	3.984D+12	3.956D+12	3.928D+12	3.876D+12	3.794D+12	3.713D+12	3.634D+12	3.557D+12	3.481D+12	3.409D+12
3	8.279D+12	8.219D+12	8.162D+12	8.104D+12	7.996D+12	7.825D+12	7.657D+12	7.492D+12	7.329D+12	7.170D+12	7.015D+12
4	1.514D+13	1.504D+13	1.493D+13	1.482D+13	1.463D+13	1.431D+13	1.400D+13	1.370D+13	1.339D+13	1.310D+13	1.280D+13
5	2.458D+13	2.440D+13	2.423D+13	2.406D+13	2.374D+13	2.323D+13	2.272D+13	2.222D+13	2.172D+13	2.123D+13	2.075D+13
6	3.135D+13	3.116D+13	3.094D+13	3.071D+13	3.029D+13	2.963D+13	2.898D+13	2.834D+13	2.770D+13	2.707D+13	2.645D+13
7	2.002D+13	1.987D+13	1.972D+13	1.956D+13	1.923D+13	1.880D+13	1.839D+13	1.798D+13	1.757D+13	1.717D+13	1.676D+13
8	1.891D+13	1.877D+13	1.862D+13	1.847D+13	1.814D+13	1.774D+13	1.735D+13	1.696D+13	1.658D+13	1.619D+13	1.581D+13
9	2.015D+13	2.000D+13	1.984D+13	1.968D+13	1.933D+13	1.889D+13	1.848D+13	1.807D+13	1.766D+13	1.725D+13	1.684D+13
10	2.219D+13	2.202D+13	2.185D+13	2.167D+13	2.129D+13	2.081D+13	2.035D+13	1.990D+13	1.945D+13	1.900D+13	1.855D+13
11	2.441D+13	2.423D+13	2.405D+13	2.385D+13	2.343D+13	2.291D+13	2.240D+13	2.191D+13	2.141D+13	2.092D+13	2.042D+13
12	2.661D+13	2.642D+13	2.621D+13	2.600D+13	2.554D+13	2.497D+13	2.443D+13	2.389D+13	2.335D+13	2.281D+13	2.227D+13
13	2.872D+13	2.851D+13	2.830D+13	2.806D+13	2.757D+13	2.696D+13	2.637D+13	2.578D+13	2.520D+13	2.462D+13	2.404D+13
14	3.081D+13	3.059D+13	3.035D+13	3.010D+13	2.956D+13	2.891D+13	2.828D+13	2.765D+13	2.703D+13	2.641D+13	2.578D+13
15	3.312D+13	3.287D+13	3.262D+13	3.234D+13	3.174D+13	3.103D+13	3.035D+13	2.969D+13	2.902D+13	2.835D+13	2.768D+13
16	3.493D+13	3.463D+13	3.436D+13	3.406D+13	3.342D+13	3.267D+13	3.196D+13	3.126D+13	3.056D+13	2.986D+13	2.915D+13
17	3.632D+13	3.606D+13	3.578D+13	3.547D+13	3.480D+13	3.403D+13	3.329D+13	3.256D+13	3.183D+13	3.110D+13	3.036D+13
18	3.752D+13	3.725D+13	3.697D+13	3.665D+13	3.596D+13	3.516D+13	3.440D+13	3.364D+13	3.289D+13	3.214D+13	3.138D+13
19	3.852D+13	3.824D+13	3.794D+13	3.762D+13	3.691D+13	3.609D+13	3.531D+13	3.454D+13	3.377D+13	3.300D+13	3.222D+13
20	3.931D+13	3.903D+13	3.873D+13	3.839D+13	3.767D+13	3.684D+13	3.604D+13	3.525D+13	3.447D+13	3.368D+13	3.289D+13
21	3.991D+13	3.962D+13	3.932D+13	3.898D+13	3.825D+13	3.740D+13	3.659D+13	3.580D+13	3.500D+13	3.420D+13	3.339D+13
22	4.033D+13	4.004D+13	3.974D+13	3.939D+13	3.865D+13	3.780D+13	3.698D+13	3.617D+13	3.537D+13	3.456D+13	3.375D+13
23	4.062D+13	4.033D+13	4.002D+13	3.968D+13	3.892D+13	3.806D+13	3.724D+13	3.643D+13	3.561D+13	3.480D+13	3.398D+13
24	4.064D+13	4.035D+13	4.004D+13	3.970D+13	3.894D+13	3.808D+13	3.726D+13	3.644D+13	3.563D+13	3.481D+13	3.399D+13
25	4.044D+13	4.015D+13	3.984D+13	3.950D+13	3.875D+13	3.788D+13	3.707D+13	3.626D+13	3.545D+13	3.464D+13	3.382D+13
26	4.003D+13	3.974D+13	3.944D+13	3.910D+13	3.835D+13	3.750D+13	3.669D+13	3.588D+13	3.508D+13	3.428D+13	3.347D+13
27	3.942D+13	3.914D+13	3.883D+13	3.850D+13	3.776D+13	3.692D+13	3.612D+13	3.533D+13	3.454D+13	3.375D+13	3.294D+13
28	3.861D+13	3.833D+13	3.803D+13	3.770D+13	3.698D+13	3.615D+13	3.537D+13	3.459D+13	3.381D+13	3.304D+13	3.225D+13
29	3.758D+13	3.730D+13	3.701D+13	3.669D+13	3.599D+13	3.516D+13	3.442D+13	3.366D+13	3.290D+13	3.214D+13	3.137D+13
30	3.628D+13	3.601D+13	3.573D+13	3.542D+13	3.475D+13	3.397D+13	3.322D+13	3.249D+13	3.175D+13	3.102D+13	3.027D+13
31	3.486D+13	3.461D+13	3.434D+13	3.404D+13	3.340D+13	3.265D+13	3.193D+13	3.123D+13	3.052D+13	2.981D+13	2.909D+13
32	3.377D+13	3.352D+13	3.326D+13	3.297D+13	3.236D+13	3.163D+13	3.093D+13	3.024D+13	2.956D+13	2.887D+13	2.817D+13
33	3.266D+13	3.242D+13	3.217D+13	3.189D+13	3.129D+13	3.059D+13	2.991D+13	2.924D+13	2.857D+13	2.791D+13	2.723D+13
34	3.151D+13	3.128D+13	3.103D+13	3.076D+13	3.019D+13	2.950D+13	2.885D+13	2.820D+13	2.756D+13	2.691D+13	2.625D+13
35	3.032D+13	3.009D+13	2.986D+13	2.960D+13	2.904D+13	2.838D+13	2.775D+13	2.713D+13	2.650D+13	2.588D+13	2.524D+13
36	2.911D+13	2.889D+13	2.867D+13	2.842D+13	2.788D+13	2.724D+13	2.664D+13	2.603D+13	2.543D+13	2.483D+13	2.422D+13
37	2.795D+13	2.774D+13	2.752D+13	2.728D+13	2.676D+13	2.615D+13	2.556D+13	2.498D+13	2.440D+13	2.382D+13	2.323D+13

38	2.696D+13	2.676D+13	2.655D+13	2.631D+13	2.581D+13	2.[illegible]D+13	2.465D+13	2.408D+13	2.352D+13	2.296D+13	2.239D+13
39	2.640D+13	2.620D+13	2.599D+13	2.576D+13	2.526D+13	2.468D+13	2.412D+13	2.357D+13	2.302D+13	2.246D+13	2.190D+13
40	2.675D+13	2.655D+13	2.633D+13	2.610D+13	2.559D+13	2.501D+13	2.443D+13	2.387D+13	2.331D+13	2.274D+13	2.217D+13
41	2.889D+13	2.867D+13	2.844D+13	2.819D+13	2.766D+13	2.701D+13	2.640D+13	2.579D+13	2.517D+13	2.456D+13	2.394D+13
42	3.442D+13	3.415D+13	3.388D+13	3.360D+13	3.299D+13	3.223D+13	3.149D+13	3.076D+13	3.003D+13	2.929D+13	2.855D+13
43	4.957D+13	4.920D+13	4.882D+13	4.844D+13	4.769D+13	4.660D+13	4.553D+13	4.447D+13	4.341D+13	4.234D+13	4.127D+13
44	5.626D+13	5.584D+13	5.542D+13	5.499D+13	5.418D+13	5.295D+13	5.173D+13	5.051D+13	4.930D+13	4.809D+13	4.687D+13
45	5.601D+13	5.559D+13	5.517D+13	5.475D+13	5.395D+13	5.272D+13	5.150D+13	5.028D+13	4.907D+13	4.786D+13	4.664D+13
46	5.288D+13	5.247D+13	5.208D+13	5.168D+13	5.093D+13	4.976D+13	4.860D+13	4.745D+13	4.630D+13	4.515D+13	4.400D+13
47	4.739D+13	4.694D+13	4.659D+13	4.623D+13	4.556D+13	4.451D+13	4.347D+13	4.242D+13	4.139D+13	4.035D+13	3.932D+13
48	3.371D+13	3.345D+13	3.320D+13	3.294D+13	3.246D+13	3.171D+13	3.096D+13	3.021D+13	2.946D+13	2.872D+13	2.798D+13
49	2.009D+13	1.993D+13	1.978D+13	1.963D+13	1.934D+13	1.889D+13	1.844D+13	1.799D+13	1.754D+13	1.710D+13	1.666D+13
50	7.362D+12	7.304D+12	7.248D+12	7.192D+12	7.087D+12	6.920D+12	6.754D+12	6.589D+12	6.425D+12	6.262D+12	6.100D+12

	12	13	14	15	16	17	18	19	20	21	22
1	1.093D+12	1.063D+12	1.028D+12	1.002D+12	9.871D+11	9.870D+11	1.005D+12	1.046D+12	1.112D+12	1.281D+12	1.242D+12
2	3.339D+12	3.241D+12	3.125D+12	3.033D+12	2.972D+12	2.952D+12	2.984D+12	3.080D+12	3.254D+12	3.717D+12	3.561D+12
3	6.864D+12	6.650D+12	6.387D+12	6.162D+12	5.989D+12	5.889D+12	5.882D+12	5.996D+12	6.258D+12	7.025D+12	6.591D+12
4	1.252D+13	1.210D+13	1.158D+13	1.111D+13	1.072D+13	1.043D+13	1.029D+13	1.036D+13	1.068D+13	1.178D+13	1.078D+13
5	2.027D+13	1.958D+13	1.868D+13	1.785D+13	1.712D+13	1.653D+13	1.618D+13	1.616D+13	1.660D+13	1.830D+13	1.646D+13
6	2.583D+13	2.492D+13	2.374D+13	2.262D+13	2.161D+13	2.080D+13	2.036D+13	2.054D+13	2.170D+13	2.586D+13	2.352D+13
7	1.636D+13	1.573D+13	1.497D+13	1.425D+13	1.360D+13	1.312D+13	1.304D+13	1.388D+13	1.677D+13	3.049D+13	2.935D+13
8	1.542D+13	1.482D+13	1.409D+13	1.340D+13	1.279D+13	1.235D+13	1.236D+13	1.349D+13	1.717D+13	3.424D+13	3.343D+13
9	1.642D+13	1.579D+13	1.500D+13	1.426D+13	1.360D+13	1.313D+13	1.318D+13	1.451D+13	1.879D+13	3.841D+13	3.762D+13
10	1.809D+13	1.739D+13	1.652D+13	1.570D+13	1.496D+13	1.444D+13	1.449D+13	1.599D+13	2.078D+13	4.272D+13	4.181D+13
11	1.992D+13	1.914D+13	1.819D+13	1.728D+13	1.646D+13	1.588D+13	1.593D+13	1.757D+13	2.284D+13	4.697D+13	4.590D+13
12	2.172D+13	2.087D+13	1.983D+13	1.884D+13	1.794D+13	1.730D+13	1.735D+13	1.913D+13	2.484D+13	5.105D+13	4.981D+13
13	2.344D+13	2.253D+13	2.141D+13	2.033D+13	1.936D+13	1.867D+13	1.872D+13	2.062D+13	2.675D+13	5.490D+13	5.350D+13
14	2.514D+13	2.416D+13	2.295D+13	2.180D+13	2.076D+13	2.002D+13	2.007D+13	2.209D+13	2.860D+13	5.848D+13	5.692D+13
15	2.699D+13	2.592D+13	2.463D+13	2.339D+13	2.228D+13	2.148D+13	2.154D+13	2.370D+13	3.057D+13	6.178D+13	6.006D+13
16	2.843D+13	2.730D+13	2.593D+13	2.464D+13	2.346D+13	2.263D+13	2.269D+13	2.495D+13	3.214D+13	6.473D+13	6.287D+13
17	2.961D+13	2.844D+13	2.701D+13	2.566D+13	2.444D+13	2.357D+13	2.364D+13	2.598D+13	3.345D+13	6.732D+13	6.536D+13
18	3.060D+13	2.939D+13	2.792D+13	2.652D+13	2.526D+13	2.436D+13	2.443D+13	2.685D+13	3.456D+13	6.954D+13	6.751D+13
19	3.142D+13	3.018D+13	2.867D+13	2.723D+13	2.594D+13	2.502D+13	2.509D+13	2.757D+13	3.549D+13	7.139D+13	6.930D+13
20	3.207D+13	3.080D+13	2.926D+13	2.780D+13	2.648D+13	2.554D+13	2.561D+13	2.815D+13	3.623D+13	7.287D+13	7.073D+13
21	3.257D+13	3.128D+13	2.971D+13	2.823D+13	2.689D+13	2.593D+13	2.600D+13	2.858D+13	3.678D+13	7.397D+13	7.180D+13
22	3.291D+13	3.161D+13	3.003D+13	2.853D+13	2.717D+13	2.620D+13	2.628D+13	2.888D+13	3.716D+13	7.470D+13	7.250D+13
23	3.314D+13	3.182D+13	3.023D+13	2.872D+13	2.735D+13	2.638D+13	2.645D+13	2.907D+13	3.738D+13	7.514D+13	7.282D+13
24	3.315D+13	3.183D+13	3.023D+13	2.872D+13	2.736D+13	2.638D+13	2.646D+13	2.907D+13	3.738D+13	7.500D+13	7.277D+13
25	3.299D+13	3.166D+13	3.007D+13	2.857D+13	2.721D+13	2.624D+13	2.631D+13	2.891D+13	3.717D+13	7.457D+13	7.235D+13
26	3.263D+13	3.133D+13	2.976D+13	2.827D+13	2.692D+13	2.596D+13	2.603D+13	2.860D+13	3.676D+13	7.375D+13	7.155D+13
27	3.212D+13	3.084D+13	2.929D+13	2.782D+13	2.649D+13	2.554D+13	2.561D+13	2.813D+13	3.617D+13	7.255D+13	7.038D+13
28	3.145D+13	3.018D+13	2.866D+13	2.722D+13	2.592D+13	2.499D+13	2.505D+13	2.752D+13	3.538D+13	7.097D+13	6.885D+13
29	3.059D+13	2.936D+13	2.787D+13	2.647D+13	2.520D+13	2.429D+13	2.434D+13	2.674D+13	3.438D+13	6.901D+13	6.695D+13
30	2.951D+13	2.832D+13	2.688D+13	2.552D+13	2.429D+13	2.341D+13	2.345D+13	2.576D+13	3.315D+13	6.667D+13	6.469D+13
31	2.835D+13	2.719D+13	2.580D+13	2.449D+13	2.330D+13	2.245D+13	2.249D+13	2.470D+13	3.179D+13	6.440D+13	6.252D+13
32	2.745D+13	2.631D+13	2.496D+13	2.369D+13	2.254D+13	2.171D+13	2.174D+13	2.388D+13	3.081D+13	6.244D+13	6.064D+13
33	2.653D+13	2.543D+13	2.412D+13	2.288D+13	2.177D+13	2.096D+13	2.099D+13	2.306D+13	2.975D+13	6.035D+13	5.861D+13
34	2.558D+13	2.451D+13	2.324D+13	2.205D+13	2.097D+13	2.019D+13	2.021D+13	2.220D+13	2.864D+13	5.811D+13	5.645D+13
35	2.459D+13	2.356D+13	2.234D+13	2.119D+13	2.014D+13	1.939D+13	1.940D+13	2.130D+13	2.748D+13	5.575D+13	5.416D+13
36	2.359D+13	2.260D+13	2.142D+13	2.031D+13	1.930D+13	1.858D+13	1.858D+13	2.039D+13	2.628D+13	5.327D+13	5.175D+13
37	2.263D+13	2.167D+13	2.053D+13	1.946D+13	1.849D+13	1.779D+13	1.778D+13	1.949D+13	2.507D+13	5.072D+13	4.925D+13
38	2.180D+13	2.087D+13	1.977D+13	1.874D+13	1.780D+13	1.710D+13	1.707D+13	1.865D+13	2.391D+13	4.812D+13	4.666D+13
39	2.132D+13	2.041D+13	1.932D+13	1.830D+13	1.737D+13	1.668D+13	1.660D+13	1.803D+13	2.293D+13	4.555D+13	4.403D+13
40	2.159D+13	2.065D+13	1.954D+13	1.850D+13	1.755D+13	1.681D+13	1.665D+13	1.787D+13	2.226D+13	4.313D+13	4.138D+13
41	2.330D+13	2.229D+13	2.110D+13	1.996D+13	1.891D+13	1.807D+13	1.774D+13	1.867D+13	2.242D+13	4.089D+13	3.876D+13
42	2.779D+13	2.661D+13	2.518D+13	2.381D+13	2.253D+13	2.145D+13	2.085D+13	2.134D+13	2.420D+13	3.903D+13	3.617D+13
43	4.020D+13	3.858D+13	3.650D+13	3.450D+13	3.260D+13	3.092D+13	2.970D+13	2.942D+13	3.082D+13	3.720D+13	3.316D+13
44	4.565D+13	4.383D+13	4.147D+13	3.918D+13	3.699D+13	3.499D+13	3.336D+13	3.239D+13	3.242D+13	3.446D+13	2.969D+13
45	4.542D+13	4.361D+13	4.125D+13	3.896D+13	3.675D+13	3.471D+13	3.294D+13	3.162D+13	3.095D+13	3.114D+13	2.627D+13
46	4.285D+13	4.114D+13	3.890D+13	3.673D+13	3.463D+13	3.266D+13	3.089D+13	2.943D+13	2.840D+13	2.763D+13	2.298D+13
47	3.829D+13	3.678D+13	3.478D+13	3.282D+13	3.092D+13	2.910D+13	2.739D+13	2.580D+13	2.434D+13	2.202D+13	1.791D+13
48	2.725D+13	2.617D+13	2.474D+13	2.334D+13	2.197D+13	2.064D+13	1.935D+13	1.811D+13	1.690D+13	1.491D+13	1.198D+13
49	1.622D+13	1.558D+13	1.472D+13	1.388D+13	1.306D+13	1.226D+13	1.147D+13	1.070D+13	9.951D+12	8.710D+12	6.958D+12
50	5.939D+12	5.703D+12	5.389D+12	5.081D+12	4.779D+12	4.482D+12	4.192D+12	3.907D+12	3.627D+12	3.166D+12	2.525D+12

ARMY REACTOR DEPLETION RUNS
DATE : MAY 14 , 1975

POINT POWER DISTRIBUTION (WATTS/CC)

	1	2	3	4	5	6	7	8	9	10	11
1	0.0	0.0	0.0	0.0	0.0	0.0	0.0	0.0	0.0	0.0	0.0
2	0.0	0.0	0.0	0.0	0.0	0.0	0.0	0.0	0.0	0.0	0.0
3	0.0	0.0	0.0	0.0	0.0	0.0	0.0	0.0	0.0	0.0	0.0
4	0.0	0.0	0.0	0.0	0.0	0.0	0.0	0.0	0.0	0.0	0.0
5	0.0	0.0	0.0	0.0	0.0	0.0	0.0	0.0	0.0	0.0	0.0
6	0.0	0.0	0.0	0.0	0.0	0.0	0.0	0.0	0.0	0.0	0.0
7	4.681E+00	4.647E+00	4.613E+00	4.577E+00	4.554E+00	4.453E+00	4.356E+00	4.259E+00	4.163E+00	4.067E+00	3.972E+00
8	4.699E+00	4.665E+00	4.630E+00	4.593E+00	4.568E+00	4.467E+00	4.369E+00	4.272E+00	4.176E+00	4.079E+00	3.983E+00
9	5.139E+00	5.102E+00	5.064E+00	5.023E+00	4.997E+00	4.886E+00	4.779E+00	4.673E+00	4.568E+00	4.462E+00	4.357E+00
10	5.711E+00	5.669E+00	5.627E+00	5.583E+00	5.554E+00	5.431E+00	5.313E+00	5.195E+00	5.077E+00	4.960E+00	4.843E+00
11	6.302E+00	6.257E+00	6.210E+00	6.162E+00	6.130E+00	5.995E+00	5.864E+00	5.734E+00	5.605E+00	5.476E+00	5.346E+00
12	6.872E+00	6.823E+00	6.773E+00	6.720E+00	6.686E+00	6.539E+00	6.396E+00	6.255E+00	6.114E+00	5.973E+00	5.832E+00
13	7.412E+00	7.359E+00	7.305E+00	7.248E+00	7.211E+00	7.054E+00	6.900E+00	6.748E+00	6.596E+00	6.444E+00	6.293E+00
14	7.933E+00	7.876E+00	7.819E+00	7.757E+00	7.717E+00	7.548E+00	7.384E+00	7.222E+00	7.059E+00	6.898E+00	6.735E+00
15	8.418E+00	7.961E+00	7.903E+00	7.840E+00	7.842E+00	7.670E+00	7.504E+00	7.339E+00	7.175E+00	7.010E+00	6.846E+00
16	8.423E+00	8.368E+00	8.307E+00	8.240E+00	8.241E+00	8.061E+00	7.887E+00	7.714E+00	7.542E+00	7.369E+00	7.196E+00
17	8.769E+00	8.708E+00	8.644E+00	8.575E+00	8.576E+00	8.389E+00	8.208E+00	8.028E+00	7.849E+00	7.670E+00	7.490E+00
18	9.057E+00	8.994E+00	8.928E+00	8.857E+00	8.858E+00	8.666E+00	8.479E+00	8.294E+00	8.109E+00	7.924E+00	7.738E+00
19	9.295E+00	9.230E+00	9.163E+00	9.090E+00	9.092E+00	8.895E+00	8.704E+00	8.514E+00	8.324E+00	8.135E+00	7.944E+00
20	9.486E+00	9.420E+00	9.351E+00	9.277E+00	9.279E+00	9.078E+00	8.883E+00	8.689E+00	8.496E+00	8.303E+00	8.109E+00
21	9.629E+00	9.562E+00	9.493E+00	9.417E+00	9.420E+00	9.216E+00	9.018E+00	8.821E+00	8.625E+00	8.429E+00	8.232E+00
22	9.728E+00	9.661E+00	9.590E+00	9.514E+00	9.516E+00	9.310E+00	9.111E+00	8.912E+00	8.714E+00	8.516E+00	8.317E+00
23	9.710E+00	9.643E+00	9.572E+00	9.496E+00	9.507E+00	9.301E+00	9.101E+00	8.903E+00	8.705E+00	8.507E+00	8.309E+00
24	9.712E+00	9.645E+00	9.575E+00	9.498E+00	9.508E+00	9.302E+00	9.102E+00	8.904E+00	8.706E+00	8.508E+00	8.309E+00
25	9.561E+00	9.595E+00	9.526E+00	9.450E+00	9.459E+00	9.254E+00	9.055E+00	8.858E+00	8.661E+00	8.464E+00	8.265E+00
26	9.565E+00	9.498E+00	9.429E+00	9.353E+00	9.363E+00	9.159E+00	8.962E+00	8.767E+00	8.571E+00	8.376E+00	8.180E+00
27	9.419E+00	9.353E+00	9.285E+00	9.211E+00	9.220E+00	9.019E+00	8.825E+00	8.631E+00	8.439E+00	8.246E+00	8.052E+00
28	9.227E+00	9.162E+00	9.094E+00	9.021E+00	9.030E+00	8.833E+00	8.642E+00	8.452E+00	8.263E+00	8.074E+00	7.884E+00
29	8.994E+00	8.920E+00	8.855E+00	8.783E+00	8.791E+00	8.599E+00	8.413E+00	8.228E+00	8.043E+00	7.858E+00	7.673E+00
30	8.683E+00	8.622E+00	8.558E+00	8.489E+00	8.497E+00	8.310E+00	8.129E+00	7.950E+00	7.771E+00	7.592E+00	7.412E+00
31	8.628E+00	8.566E+00	8.503E+00	8.435E+00	8.417E+00	8.232E+00	8.052E+00	7.874E+00	7.696E+00	7.518E+00	7.339E+00
32	8.366E+00	8.306E+00	8.245E+00	8.179E+00	8.162E+00	7.982E+00	7.807E+00	7.634E+00	7.461E+00	7.288E+00	7.113E+00
33	8.095E+00	8.037E+00	7.977E+00	7.913E+00	7.897E+00	7.722E+00	7.553E+00	7.384E+00	7.216E+00	7.048E+00	6.879E+00
34	7.811E+00	7.755E+00	7.697E+00	7.634E+00	7.619E+00	7.449E+00	7.285E+00	7.122E+00	6.960E+00	6.797E+00	6.633E+00
35	7.513E+00	7.459E+00	7.402E+00	7.342E+00	7.326E+00	7.163E+00	7.005E+00	6.848E+00	6.691E+00	6.534E+00	6.376E+00
36	7.205E+00	7.152E+00	7.098E+00	7.040E+00	7.025E+00	6.867E+00	6.715E+00	6.564E+00	6.413E+00	6.262E+00	6.110E+00
37	6.897E+00	6.847E+00	6.795E+00	6.739E+00	6.723E+00	6.572E+00	6.426E+00	6.280E+00	6.135E+00	5.990E+00	5.844E+00
38	6.612E+00	6.563E+00	6.513E+00	6.459E+00	6.443E+00	6.298E+00	6.157E+00	6.017E+00	5.877E+00	5.738E+00	5.597E+00
39	6.393E+00	6.345E+00	6.296E+00	6.244E+00	6.228E+00	6.086E+00	5.949E+00	5.814E+00	5.678E+00	5.542E+00	5.405E+00
40	6.325E+00	6.278E+00	6.229E+00	6.177E+00	6.160E+00	6.020E+00	5.884E+00	5.749E+00	5.614E+00	5.479E+00	5.343E+00
41	6.571E+00	6.522E+00	6.471E+00	6.417E+00	6.400E+00	6.253E+00	6.111E+00	5.971E+00	5.830E+00	5.689E+00	5.546E+00
42	7.426E+00	7.372E+00	7.315E+00	7.255E+00	7.241E+00	7.075E+00	6.913E+00	6.753E+00	6.593E+00	6.433E+00	6.271E+00
43	0.0	0.0	0.0	0.0	0.0	0.0	0.0	0.0	0.0	0.0	0.0
44	0.0	0.0	0.0	0.0	0.0	0.0	0.0	0.0	0.0	0.0	0.0
45	0.0	0.0	0.0	0.0	0.0	0.0	0.0	0.0	0.0	0.0	0.0
46	0.0	0.0	0.0	0.0	0.0	0.0	0.0	0.0	0.0	0.0	0.0
47	0.0	0.0	0.0	0.0	0.0	0.0	0.0	0.0	0.0	0.0	0.0
48	0.0	0.0	0.0	0.0	0.0	0.0	0.0	0.0	0.0	0.0	0.0
49	0.0	0.0	0.0	0.0	0.0	0.0	0.0	0.0	0.0	0.0	0.0
50	0.0	0.0	0.0	0.0	0.0	0.0	0.0	0.0	0.0	0.0	0.0

	12	13	14	15	16	17	18	19	20	21	22
1	0.0	0.0	0.0	0.0	0.0	0.0	0.0	0.0	0.0	0.0	0.0
2	0.0	0.0	0.0	0.0	0.0	0.0	0.0	0.0	0.0	0.0	0.0
3	0.0	0.0	0.0	0.0	0.0	0.0	0.0	0.0	0.0	0.0	0.0

4	0.0	0.0	0.0	0.0	0.0	0.0	0.0	0.0	0.0	0.0	0.0
5	0.0	0.0	0.0	0.0	0.0	0.0	0.0	0.0	0.0	0.0	0.0
6	0.0	0.0	0.0	0.0	0.0	0.0	0.0	0.0	0.0	0.0	0.0
7	3.676E+00	3.766E+00	3.583E+00	3.408E+00	3.247E+00	3.116E+00	3.055E+00	3.163E+00	3.656E+00	0.0	0.0
8	3.886E+00	3.775E+00	3.589E+00	3.412E+00	3.247E+00	3.113E+00	3.061E+00	3.211E+00	3.838E+00	0.0	0.0
9	4.251E+00	4.128E+00	3.924E+00	3.728E+00	3.546E+00	3.397E+00	3.341E+00	3.517E+00	4.244E+00	0.0	0.0
10	4.725E+00	4.589E+00	4.361E+00	4.142E+00	3.939E+00	3.770E+00	3.705E+00	3.901E+00	4.713E+00	0.0	0.0
11	5.216E+00	5.066E+00	4.814E+00	4.571E+00	4.344E+00	4.157E+00	4.083E+00	4.296E+00	5.187E+00	0.0	0.0
12	5.690E+00	5.526E+00	5.251E+00	4.986E+00	4.737E+00	4.532E+00	4.449E+00	4.678E+00	5.644E+00	0.0	0.0
13	6.139E+00	5.962E+00	5.666E+00	5.379E+00	5.110E+00	4.888E+00	4.797E+00	5.042E+00	6.078E+00	0.0	0.0
14	6.571E+00	6.381E+00	6.064E+00	5.757E+00	5.469E+00	5.232E+00	5.135E+00	5.395E+00	6.495E+00	0.0	0.0
15	6.979E+00	6.518E+00	6.194E+00	5.881E+00	5.587E+00	5.345E+00	5.247E+00	5.512E+00	6.621E+00	0.0	0.0
16	7.021E+00	6.852E+00	6.511E+00	6.182E+00	5.873E+00	5.620E+00	5.517E+00	5.795E+00	6.954E+00	0.0	0.0
17	7.308E+00	7.132E+00	6.778E+00	6.435E+00	6.114E+00	5.851E+00	5.744E+00	6.032E+00	7.237E+00	0.0	0.0
18	7.552E+00	7.369E+00	7.003E+00	6.649E+00	6.318E+00	6.046E+00	5.935E+00	6.233E+00	7.477E+00	0.0	0.0
19	7.751E+00	7.565E+00	7.190E+00	6.827E+00	6.487E+00	6.207E+00	6.094E+00	6.400E+00	7.676E+00	0.0	0.0
20	7.912E+00	7.722E+00	7.339E+00	6.969E+00	6.621E+00	6.336E+00	6.221E+00	6.533E+00	7.836E+00	0.0	0.0
21	8.032E+00	7.840E+00	7.451E+00	7.075E+00	6.723E+00	6.433E+00	6.316E+00	6.633E+00	7.955E+00	0.0	0.0
22	8.115E+00	7.921E+00	7.527E+00	7.148E+00	6.792E+00	6.499E+00	6.381E+00	6.701E+00	8.036E+00	0.0	0.0
23	8.166E+00	7.921E+00	7.527E+00	7.148E+00	6.791E+00	6.499E+00	6.381E+00	6.700E+00	8.031E+00	0.0	0.0
24	8.167E+00	7.921E+00	7.527E+00	7.147E+00	6.791E+00	6.499E+00	6.380E+00	6.700E+00	8.031E+00	0.0	0.0
25	8.064E+00	7.879E+00	7.487E+00	7.109E+00	6.754E+00	6.463E+00	6.345E+00	6.663E+00	7.986E+00	0.0	0.0
26	7.960E+00	7.796E+00	7.409E+00	7.033E+00	6.682E+00	6.394E+00	6.277E+00	6.590E+00	7.899E+00	0.0	0.0
27	7.836E+00	7.674E+00	7.291E+00	6.922E+00	6.576E+00	6.292E+00	6.176E+00	6.484E+00	7.771E+00	0.0	0.0
28	7.691E+00	7.513E+00	7.137E+00	6.775E+00	6.435E+00	6.156E+00	6.042E+00	6.343E+00	7.602E+00	0.0	0.0
29	7.484E+00	7.309E+00	6.943E+00	6.589E+00	6.258E+00	5.986E+00	5.874E+00	6.166E+00	7.392E+00	0.0	0.0
30	7.229E+00	7.058E+00	6.702E+00	6.360E+00	6.039E+00	5.775E+00	5.666E+00	5.946E+00	7.129E+00	0.0	0.0
31	7.156E+00	6.987E+00	6.633E+00	6.293E+00	5.974E+00	5.711E+00	5.601E+00	5.878E+00	7.054E+00	0.0	0.0
32	6.935E+00	6.770E+00	6.426E+00	6.095E+00	5.785E+00	5.529E+00	5.422E+00	5.688E+00	6.829E+00	0.0	0.0
33	6.736E+00	6.545E+00	6.211E+00	5.891E+00	5.590E+00	5.342E+00	5.236E+00	5.493E+00	6.596E+00	0.0	0.0
34	6.466E+00	6.310E+00	5.987E+00	5.677E+00	5.386E+00	5.145E+00	5.043E+00	5.289E+00	6.350E+00	0.0	0.0
35	6.214E+00	6.063E+00	5.751E+00	5.452E+00	5.172E+00	4.940E+00	4.840E+00	5.075E+00	6.092E+00	0.0	0.0
36	5.954E+00	5.808E+00	5.508E+00	5.221E+00	4.951E+00	4.727E+00	4.630E+00	4.854E+00	5.824E+00	0.0	0.0
37	5.694E+00	5.554E+00	5.265E+00	4.989E+00	4.730E+00	4.515E+00	4.420E+00	4.630E+00	5.549E+00	0.0	0.0
38	5.453E+00	5.316E+00	5.039E+00	4.773E+00	4.523E+00	4.316E+00	4.222E+00	4.415E+00	5.279E+00	0.0	0.0
39	5.265E+00	5.132E+00	4.862E+00	4.604E+00	4.361E+00	4.158E+00	4.061E+00	4.233E+00	5.034E+00	0.0	0.0
40	5.203E+00	5.070E+00	4.801E+00	4.544E+00	4.302E+00	4.097E+00	3.990E+00	4.131E+00	4.852E+00	0.0	0.0
41	5.401E+00	5.261E+00	4.981E+00	4.712E+00	4.457E+00	4.238E+00	4.109E+00	4.202E+00	4.814E+00	0.0	0.0
42	6.106E+00	5.951E+00	5.632E+00	5.325E+00	5.034E+00	4.776E+00	4.602E+00	4.623E+00	5.078E+00	0.0	0.0
43	0.0	0.0	0.0	0.0	0.0	0.0	0.0	0.0	0.0	0.0	0.0
44	0.0	0.0	0.0	0.0	0.0	0.0	0.0	0.0	0.0	0.0	0.0
45	0.0	0.0	0.0	0.0	0.0	0.0	0.0	0.0	0.0	0.0	0.0
46	0.0	0.0	0.0	0.0	0.0	0.0	0.0	0.0	0.0	0.0	0.0
47	0.0	0.0	0.0	0.0	0.0	0.0	0.0	0.0	0.0	0.0	0.0
48	0.0	0.0	0.0	0.0	0.0	0.0	0.0	0.0	0.0	0.0	0.0
49	0.0	0.0	0.0	0.0	0.0	0.0	0.0	0.0	0.0	0.0	0.0
50	0.0	0.0	0.0	0.0	0.0	0.0	0.0	0.0	0.0	0.0	0.0

	23	24	25	26
1	0.0	0.0	0.0	0.0
2	0.0	0.0	0.0	0.0
3	0.0	0.0	0.0	0.0
4	0.0	0.0	0.0	0.0
5	0.0	0.0	0.0	0.0
6	0.0	0.0	0.0	0.0
7	0.0	0.0	0.0	0.0
8	0.0	0.0	0.0	0.0
9	0.0	0.0	0.0	0.0
10	0.0	0.0	0.0	0.0
11	0.0	0.0	0.0	0.0
12	0.0	0.0	0.0	0.0
13	0.0	0.0	0.0	0.0
14	0.0	0.0	0.0	0.0
15	0.0	0.0	0.0	0.0
16	0.0	0.0	0.0	0.0
17	0.0	0.0	0.0	0.0

ARMY REACTOR DEPLETION RUNS
DATE : MAY 14 , 1975

SUMMARY OF NEUTRON LOSSES, ETC. FOR STEP 12 CYCLE 1 AT CYCLE DEPLETION TIME 1575.00 DAYS. FISSILE KG IS AT 1650.00 DAYS

ZONE CLASS	FISSILE	FERTILE	INTERMEDIATE	OTHER STRUCTURAL	SPECIAL	UNSPECIFIED	SUMS	CONV. RATIO	POWER(MW)	FISSILE(KG)
CORE	0.49293	0.27412	0.02297	0.03523	0.01063	0.0	0.08565	0.92153	0.50763	2.96715E+02	5.42059E+02
BUFFER	0.0	0.0	0.0	0.00894	0.00159	0.0	0.0	0.01053	0.0	0.0	0.0
REFLECTOR	0.0	0.0	0.0	0.01535	0.01933	0.0	0.0	0.03468	0.0	0.0	0.0
			OTHER LOSSES' BASED ON START-OF-STEP TOTAL LOSSES					0.03326			
OVERALL	0.49293	0.27412	0.02297	0.05952	0.03155	0.0	0.08565	1.00000	0.50763	2.96715E+02	5.42059E+02

TIME STEP THERMAL ENERGY, MW-HRS 1.06817E+06 AND TOTAL IS 1.17777E+07

NUCLIDE DENSITIES BY ZONE AND SUB-ZONE(NUCLIDE NUMBER - DENSITY) AT DEPLETION TIME 1.650000E+03DAYS

ZONE NUMBER 1-- CORE

8	8.47843E-06	10	1.62632E-05	14	1.07053E-07	16	4.94797E-08	6	3.30768E-04	9	8.34139E-07
12	2.55302E-06	15	8.41339E-08	7	4.06435E-07	82	2.91111E-09	13	1.21988E-09	11	4.98674E-06
17	2.27588E-08	18	5.47801E-07	105	2.84045E-07	125	0.0	5	6.19000E-02	84	7.37000E-04
39	1.57083E-06	85	1.40952E-06	50	4.92836E-07	53	5.87539E-07	58	2.85464E-10	55	1.48394E-06
60	1.20887E-06	61	8.48678E-07	63	1.79302E-07	65	1.40242E-09	67	2.77691E-09	68	2.27146E-07
69	2.23093E-08	70	9.99295E-08	71	1.77645E-08	72	5.69608E-09	73	1.01000E-09	86	6.02523E-06
87	2.00114E-05										

ZONE NUMBER 2-- CORE

8	9.76437E-06	10	9.96753E-06	14	9.11035E-08	16	5.20427E-08	6	3.22241E-04	9	1.53257E-06
12	2.26959E-06	15	3.91674E-08	7	5.67184E-07	82	3.05441E-09	13	1.54829E-09	11	5.80424E-06
17	4.33750E-08	18	9.33818E-07	105	1.12708E-07	125	0.0	5	6.19000E-02	84	7.37000E-04
39	2.16428E-06	85	1.87598E-06	50	5.43196E-07	53	7.19147E-07	58	2.86310E-10	55	1.93453E-06
60	1.48552E-06	61	1.08138E-06	63	1.80498E-07	65	1.85564E-09	67	2.15999E-09	68	2.81859E-07
69	2.21368E-08	70	1.14500E-07	71	1.72030E-08	72	6.10841E-09	73	1.12939E-09	86	1.19048E-05
87	2.49483E-05										

ZONE NUMBER 3-- CORE

8	9.78337E-06	10	9.50390E-06	14	8.88327E-08	16	5.12542E-08	6	3.21504E-04	9	1.59640E-06
12	2.24716E-06	15	3.82127E-08	7	5.69105E-07	82	3.02864E-09	13	1.53751E-09	11	5.84638E-06
17	4.55851E-08	18	9.61930E-07	105	1.03085E-07	125	0.0	5	6.19000E-02	84	7.37000E-04
39	2.21560E-06	85	1.91481E-06	50	5.43125E-07	53	7.28552E-07	58	2.82317E-10	55	1.97116E-06
60	1.50169E-06	61	1.09938E-06	63	1.80137E-07	65	1.84892E-09	67	2.10102E-09	68	2.85790E-07
69	2.19838E-08	70	1.15509E-07	71	1.70762E-08	72	6.05535E-09	73	1.12138E-09	86	1.24904E-05
87	2.53280E-05										

ZONE NUMBER 4-- CORE

8	8.72672E-06	10	1.33258E-05	14	9.34007E-08	16	4.94780E-08	6	3.28227E-04	9	1.06745E-06
12	2.47281E-06	15	3.95904E-08	7	4.40177E-07	82	2.84378E-09	13	1.26662E-09	11	5.37277E-06
17	3.11770E-08	18	6.61933E-07	105	1.95787E-07	125	0.0	5	6.19000E-02	84	7.37000E-04
39	1.81397E-06	85	1.60939E-06	50	5.15263E-07	53	6.52448E-07	58	2.76669E-10	55	1.68542E-06
60	1.32362E-06	61	9.54962E-07	63	1.85722E-07	65	1.52805E-09	67	2.40600E-09	68	2.53356E-07
69	2.15063E-08	70	1.09753E-07	71	1.80547E-08	72	5.85485E-09	73	1.05930E-09	86	7.92048E-06
87	2.23875E-05										

ZONE NUMBER 5-- CORE

8	8.16685E-06	10	1.77418E-05	14	1.11062E-07	16	4.72824E-08	6	3.32142E-04	9	7.22785E-07
12	2.60009E-06	15	4.47683E-08	7	3.80663E-07	82	2.85938E-09	13	1.16282E-09	11	4.76125E-06
17	1.83695E-08	18	4.82841E-07	105	3.35481E-07	125	0.0	5	6.19000E-02	84	7.37000E-04
39	1.45431E-06	85	1.31268E-06	50	4.75013E-07	53	5.54650E-07	58	2.83773E-10	55	1.38519E-06
60	1.14273E-06	61	7.96065E-07	63	1.75617E-07	65	1.30297E-09	67	2.92953E-09	68	2.13896E-07
69	2.23517E-08	70	9.51191E-08	71	1.75048E-08	72	5.46490E-09	73	9.56576E-10	86	5.15609E-06
87	1.88459E-05										

ZONE NUMBER 6-- CORE

8	9.63704E-06	10	1.13023E-05	14	9.65560E-08	16	4.84886E-08	6	3.24251E-04	9	1.36050E-06
12	2.33229E-06	15	4.14249E-08	7	5.36861E-07	82	3.09307E-09	13	1.50284E-09	11	5.66952E-06
17	3.90813E-08	18	8.50914E-07	105	1.42757E-07	125	0.0	5	6.19000E-02	84	7.37000E-04
39	2.02444E-06	85	1.76897E-06	50	5.39685E-07	53	6.92280E-07	58	2.91352E-10	55	1.83315E-06
60	1.43422E-06	61	1.03070E-06	63	1.81827E-07	65	1.79269E-09	67	2.31655E-09	68	2.70506E-07
69	2.24265E-08	70	1.11674E-07	71	1.75078E-08	72	6.17683E-09	73	1.13439E-09	86	1.03749E-05
87	2.38697E-05										

ZONE NUMBER 7-- CORE

8	9.68349E-06	10	1.08158E-05	14	9.43427E-08	16	5.29746E-08	6	3.23567E-04	9	1.41991E-06
12	2.31092E-06	15	4.05430E-08	7	5.39734E-07	82	3.07636E-09	13	1.49647E-09	11	5.72135E-06
17	4.08299E-08	18	8.79256E-07	105	1.31505E-07	125	0.0	5	6.19000E-02	84	7.37000E-04
39	2.07418E-06	85	1.80741E-06	50	5.41268E-07	53	7.02476E-07	58	2.87918E-10	55	1.87003E-06
60	1.45307E-06	61	1.04926E-06	63	1.81415E-07	65	1.79296E-09	67	2.25698E-09	68	2.74719E-07
69	2.23004E-08	70	1.12846E-07	71	1.74241E-08	72	6.15037E-09	73	1.13181E-09	86	1.09008E-05
87	2.42628E-05										

ZONE NUMBER 8-- CORE

8	9.49684E-06	10	1.48323E-05	14	9.82217E-08	16	4.90614E-08	6	3.29821E-04	9	9.30056E-07
12	2.52525E-06	15	4.11559E-08	7	4.13895E-07	82	2.83717E-09	13	1.21633E-09	11	5.16807E-06
17	2.65521E-08	18	5.89939E-07	105	2.38943E-07	125	0.0	5	6.19000E-02	84	7.37000E-04
39	1.68377E-06	85	1.50409E-06	50	5.03460E-07	53	6.19816E-07	58	2.78673E-10	55	1.58075E-06
60	1.26216E-06	61	9.00213E-07	63	1.83731E-07	65	1.44271E-09	67	2.56895E-09	68	2.40099E-07
69	2.17165E-08	70	1.05404E-07	71	1.80315E-08	72	5.75096E-09	73	1.02999E-09	86	6.80167E-06
87	2.11916E-05										

ZONE NUMBER 9-- CORE

8	6.72731E-06	10	2.10430E-05	14	1.02383E-07	16	3.61268E-08	6	3.35900E-04	9	4.70858E-07
12	2.74463E-06	15	3.85771E-08	7	2.93092E-07	82	2.43923E-09	13	9.12266E-10	11	4.12825E-06
17	1.11753E-08	18	3.07439E-07	105	4.66099E-07	125	0.0	5	6.19000E-02	84	7.37000E-04
39	1.20564E-06	85	1.10589E-06	50	4.21471E-07	53	4.83253E-07	58	2.61203E-10	55	1.17851E-06
60	9.78287E-07	61	6.82439E-07	63	1.69387E-07	65	9.79799E-10	67	3.07728E-09	68	1.84968E-07
69	2.11166E-08	70	8.62349E-08	71	1.68792E-08	72	4.50324E-09	73	7.60376E-10	86	3.28307E-06
87	1.64105E-05										

ZONE NUMBER 10-- CORE

8	8.31771E-06	10	1.45138E-05	14	9.34234E-08	16	4.74775E-08	6	3.29943E-04	9	9.35315E-07
12	2.53553E-06	15	3.91325E-08	7	4.21581E-07	82	2.78023E-09	13	1.22954E-09	11	5.18538E-06
17	2.70340E-08	18	5.79056E-07	105	2.29860E-07	125	0.0	5	6.19000E-02	84	7.37000E-04
39	1.70509E-06	85	1.52390E-06	50	5.02251E-07	53	6.28160E-07	58	2.77618E-10	55	1.60309E-06
60	1.26662E-06	61	9.11709E-07	63	1.87431E-07	65	1.47349E-09	67	2.48907E-09	68	2.43025E-07
69	2.12887E-08	70	1.07670E-07	71	1.81767E-08	72	5.69266E-09	73	1.02297E-09	86	6.84608E-06
87	2.14976E-05										

ZONE NUMBER 11-- CORE

8	8.33404E-06	10	1.40019E-05	14	9.17237E-08	16	4.76001E-08	6	3.29429E-04	9	9.80050E-07
12	2.51674E-06	15	3.85930E-08	7	4.25282E-07	82	2.78024E-09	13	1.23099E-09	11	5.25675E-06
17	2.85795E-08	18	6.01783E-07	105	2.15141E-07	125	0.0	5	6.19000E-02	84	7.37000E-04
39	1.74866E-06	85	1.55938E-06	50	5.06152E-07	53	6.39452E-07	58	2.75353E-10	55	1.63857E-06
60	1.28706E-06	61	9.30319E-07	63	1.87936E-07	65	1.48558E-09	67	2.43253E-09	68	2.47547E-07
69	2.12013E-08	70	1.09245E-07	71	1.81976E-08	72	5.72371E-09	73	1.03158E-09	86	7.20918E-06
87	2.19048E-05										

ZONE NUMBER 12-- CORE

8	7.14010E-06	10	1.84504E-05	14	9.42103E-08	16	4.01182E-08	6	3.34263E-04	9	6.05701E-07
12	2.69213E-06	15	3.75921E-08	7	3.19225E-07	82	2.49086E-09	13	9.64508E-10	11	4.53646E-06
17	1.61949E-08	18	3.80245E-07	105	3.60826E-07	125	0.0	5	6.19000E-02	84	7.37000E-04
39	1.38820E-06	85	1.26366E-06	50	4.54769E-07	53	5.42610E-07	58	2.62350E-10	55	1.34252E-06
60	1.08810E-06	61	7.72545E-07	63	1.80456E-07	65	1.11296E-09	67	2.78338E-09	68	2.08499E-07
69	2.07942E-08	70	9.67984E-08	71	1.78146E-08	72	4.95688E-09	73	8.60194E-10	86	4.29787E-06
87	1.84864E-05										

ZONE NUMBER 13-- BUFFER

105	8.37814E-07	125	0.0	83	7.10686E-02

ZONE NUMBER 14-- BUFFER

105	8.58150E-07	125	0.0	83	7.10686E-02

ZONE NUMBER 15-- BUFFER

105	9.22581E-07	125	0.0	83	7.10686E-02

ZONE NUMBER 16-- REFLECTOR

105	0.0	125	3.04300E-04	83	6.66300E-02

ZONE NUMBER 17-- REFLECTOR

105	0.0	125	0.0	83	7.10700E-02

105 C.C 125 0.0 83 7.10700E-02

TIME STEP 12 REQUIRED 0.389 MINUTES CPU TIME, AND 0.537 MINUTES CLOCK TIME

A FLUX - EIGENVALUE PROBLEM FOLLOWS FOR CYCLE 1 CYCLE TIME 1650.0000 DAYS TOTAL TIME 1650.0000 DAYS

ITERATION	FLUX CHANGE	BETA	MU-1	MU-2	MU-3	K
1	2.27642E-02	1.00000	0.04553	-0.04478	0.0	1.004385
2	6.22296E-01	1.76982	27.95889	6.04777	0.00468	1.007431
3	5.73844E-01	1.62578	1.49598	0.87100	-0.04672	1.007043
4	[illegible]E-01	1.54699	-0.70534	-1.33124	0.02707	1.007025
5	-2.[illegible]E-01	1.50704	0.78346	0.16690	4.80615	1.007006
6	-1.48863E-01	1.48756	0.39949	1.06699	1.25245	1.006984
7	-5.36947E-02	1.47825	0.30857	0.70168	0.94818	1.006964
8	-1.45517E-02	1.47383	0.25545	0.65251	0.86229	1.006945
9	6.69098E-03	1.47175	-0.45312	-0.30493	0.83110	1.006928
10	4.20380E-03	1.47077	0.63248	0.28561	0.80968	1.006915
11	2.17819E-03	1.47031	0.52033	0.53095	0.79001	1.006904
12	1.17683E-03	1.47009	0.54146	0.85639	0.76924	1.006893
13	8.41141E-04	1.46999	0.71559	0.85724	0.74368	1.006885
14	6.16074E-04	1.46994	0.73304	0.86337	0.70859	1.006878
15	4.84467E-04	1.46992	0.78686	0.86621	0.65468	1.006871
16	4.28200E-04	1.46991	0.88429	0.87266	0.55924	1.006866
17	3.79562E-04	1.46990	0.88679	0.87802	0.34385	1.006863
18	3.38554E-04	1.46990	0.89230	0.88715	-0.58397	1.006859
19	3.01361E-04	1.46990	0.89044	0.89335	3.24523	1.006856
20	2.69890E-04	1.46990	0.89584	0.90358	1.57116	1.006853
21	2.43187E-04	1.46990	0.90130	0.91388	1.29922	1.006851
22	2.18391E-04	1.46990	0.89826	0.92265	1.19895	1.006849
23	1.97411E-04	1.46990	0.90413	0.93103	1.12988	1.006847
24	1.79291E-04	1.46990	0.90839	0.93535	1.09351	1.006845
25	1.63078E-04	1.46990	0.90974	0.93658	1.06917	1.006845
26	1.47820E-04	1.46990	0.90658	0.93977	1.05197	
	1.77626E-03	EXTRAPOLATION WITH		12.0164		1.006831
27	-9.31084E-04	1.00000	-6.29972	-0.76937	12.98493	1.006831
28	1.82152E-04	1.46990	-0.19545	-1.32486	0.11993	1.006833
29	1.73569E-04	1.46990	0.95305	0.54128	0.91527	1.006833
30	5.34058E-05	1.46990	0.30775	0.60014	0.95933	1.006834

END OF EIGENVALUE CALCULATION - ITERATION TIME 0.325 MINUTES

CONVERGENCE INDICATION BY MINIMIZING THE SUM OF THE SQUARES OF THE RESIDUES - RELATIVE ABSORPTION 0.9999969 K 1.0068388

LEAKAGE 7.43347E+17 TOTAL LOSSES 2.29502E+19 TOTAL PRODUCTIONS 2.31071E+19 REACTOR POWER(WATTS) 3.00000E+09

AVERAGE FLUXES BY ZONE AND GROUP

ZONE 1-- CORE
3.52272E+13 7.34184E+13 1.05463E+13 3.33770E+13

ZONE 2-- CORE
4.71280E+13 1.02939E+14 1.47166E+13 4.92030E+13

ZONE 3-- CORE
4.68294E+13 1.02600E+14 1.46687E+13 4.88678E+13

ZONE 4-- CORE
3.67141E+13 7.71155E+13 1.11096E+13 3.95805E+13

ZONE 5-- CORE
3.33921E+13 6.91262E+13 9.93820E+12 3.66138E+13

ZONE 6-- CORE

4.52382E+13 9.78754E+13 1.39964E+13 4.53155E+13

ZONE 7-- CORE
4.50637E+13 9.77757E+13 1.39815E+13 4.59806E+13

ZONE 8-- CORE
3.50441E+13 7.30265E+13 1.05248E+13 3.62417E+13

ZONE 9-- CORE
2.61076E+13 5.15391E+13 7.42728E+12 2.58122E+13

ZONE 10-- CORE
3.55750E+13 7.39121E+13 1.06036E+13 3.67238E+13

ZONE 11-- CORE
3.59762E+13 7.40798E+13 1.06261E+13 3.93646E+13

ZONE 12-- CORE
2.75435E+13 5.46216E+13 7.88867E+12 2.99660E+13

ZONE 13-- BUFFER
5.57276E+12 1.96581E+13 4.34927E+12 6.13313E+13

ZONE 14-- BUFFER
5.26258E+12 1.85321E+13 4.09661E+12 5.64602E+13

ZONE 15-- BUFFER
3.96473E+12 1.34588E+13 2.95997E+12 4.28524E+13

ZONE 16-- REFLECTOR
1.12609E+12 4.12320E+12 9.18081E+11 1.43006E+13

ZONE 17-- REFLECTOR
1.02380E+11 7.95584E+11 2.11168E+11 2.31696E+13

ZONE 18-- REFLECTOR
8.40223E+11 3.29350E+12 7.64670E+11 2.86208E+13

ZONE AVERAGE POWER DENSITIES(WATTS/CC)
6.33027E+00 7.85205E+00 7.79301E+00 6.67898E+00 6.03983E+00 7.61835E+00 7.58004E+00 6.42529E+00 5.14211E+00
6.64522E+00 6.63829E+00 5.50051E+00 0.0 0.0 0.0 0.0 0.0 0.0

ARMY REACTOR DEPLETION RUNS
DATE : MAY 14 , 1975

GROUP 1 FLUX

	1	2	3	4	5	6	7	8	9	10	11
1	5.441D+09	5.422D+09	5.403D+09	5.382D+09	5.341D+09	5.267D+09	5.187D+09	5.103D+09	5.017D+09	4.927D+09	4.833D+09
2	2.474D+10	2.466D+10	2.458D+10	2.449D+10	2.431D+10	2.398D+10	2.362D+10	2.325D+10	2.286D+10	2.246D+10	2.204D+10
3	9.972D+10	9.943D+10	9.913D+10	9.880D+10	9.814D+10	9.684D+10	9.541D+10	9.390D+10	9.235D+10	9.077D+10	8.915D+10
4	3.99CD+11	3.980D+11	3.969D+11	3.958D+11	3.934D+11	3.884D+11	3.827D+11	3.766D+11	3.704D+11	3.642D+11	3.579D+11
5	1.596D+12	1.592D+12	1.588D+12	1.584D+12	1.577D+12	1.557D+12	1.534D+12	1.510D+12	1.485D+12	1.460D+12	1.435D+12
6	6.392D+12	6.365D+12	6.351D+12	6.340D+12	6.321D+12	6.243D+12	6.150D+12	6.052D+12	5.951D+12	5.851D+12	5.752D+12
7	2.119D+13	2.112D+13	2.106D+13	2.103D+13	2.105D+13	2.078D+13	2.046D+13	2.013D+13	1.979D+13	1.945D+13	1.912D+13
8	2.715D+13	2.706D+13	2.699D+13	2.695D+13	2.696D+13	2.662D+13	2.622D+13	2.579D+13	2.536D+13	2.493D+13	2.453D+13
9	3.150D+13	3.140D+13	3.132D+13	3.128D+13	3.128D+13	3.089D+13	3.043D+13	2.994D+13	2.945D+13	2.894D+13	2.845D+13
10	3.517D+13	3.506D+13	3.498D+13	3.493D+13	3.494D+13	3.451D+13	3.400D+13	3.346D+13	3.291D+13	3.235D+13	3.180D+13
11	3.833D+13	3.828D+13	3.819D+13	3.814D+13	3.815D+13	3.769D+13	3.714D+13	3.656D+13	3.596D+13	3.536D+13	3.477D+13
12	4.117D+13	4.105D+13	4.096D+13	4.091D+13	4.094D+13	4.046D+13	3.987D+13	3.926D+13	3.862D+13	3.798D+13	3.735D+13
13	4.341D+13	4.330D+13	4.321D+13	4.316D+13	4.321D+13	4.271D+13	4.210D+13	4.146D+13	4.080D+13	4.013D+13	3.948D+13
14	4.486D+13	4.475D+13	4.467D+13	4.464D+13	4.472D+13	4.422D+13	4.360D+13	4.295D+13	4.227D+13	4.159D+13	4.093D+13
15	4.487D+13	4.477D+13	4.471D+13	4.470D+13	4.487D+13	4.439D+13	4.379D+13	4.314D+13	4.247D+13	4.180D+13	4.115D+13
16	4.558D+13	4.549D+13	4.544D+13	4.545D+13	4.565D+13	4.519D+13	4.458D+13	4.393D+13	4.326D+13	4.259D+13	4.195D+13
17	4.644D+13	4.635D+13	4.630D+13	4.632D+13	4.654D+13	4.608D+13	4.548D+13	4.482D+13	4.415D+13	4.348D+13	4.283D+13
18	4.722D+13	4.714D+13	4.710D+13	4.712D+13	4.736D+13	4.690D+13	4.629D+13	4.563D+13	4.496D+13	4.428D+13	4.363D+13
19	4.787D+13	4.779D+13	4.775D+13	4.778D+13	4.802D+13	4.757D+13	4.696D+13	4.630D+13	4.562D+13	4.494D+13	4.429D+13
20	4.834D+13	4.826D+13	4.823D+13	4.826D+13	4.851D+13	4.806D+13	4.745D+13	4.679D+13	4.611D+13	4.543D+13	4.477D+13
21	4.863D+13	4.855D+13	4.852D+13	4.855D+13	4.881D+13	4.836D+13	4.776D+13	4.710D+13	4.641D+13	4.573D+13	4.507D+13
22	4.871D+13	4.863D+13	4.860D+13	4.864D+13	4.890D+13	4.846D+13	4.785D+13	4.719D+13	4.651D+13	4.583D+13	4.518D+13
23	4.85CD+13	4.842D+13	4.839D+13	4.843D+13	4.871D+13	4.827D+13	4.767D+13	4.701D+13	4.634D+13	4.567D+13	4.501D+13
24	4.826D+13	4.818D+13	4.816D+13	4.820D+13	4.847D+13	4.804D+13	4.744D+13	4.679D+13	4.612D+13	4.545D+13	4.481D+13
25	4.792D+13	4.784D+13	4.782D+13	4.786D+13	4.813D+13	4.770D+13	4.711D+13	4.646D+13	4.580D+13	4.513D+13	4.449D+13
26	4.745D+13	4.738D+13	4.735D+13	4.739D+13	4.766D+13	4.723D+13	4.664D+13	4.600D+13	4.534D+13	4.468D+13	4.405D+13
27	4.686D+13	4.679D+13	4.676D+13	4.680D+13	4.706D+13	4.663D+13	4.605D+13	4.541D+13	4.476D+13	4.410D+13	4.347D+13
28	4.615D+13	4.608D+13	4.605D+13	4.608D+13	4.634D+13	4.591D+13	4.533D+13	4.470D+13	4.405D+13	4.341D+13	4.278D+13
29	4.537D+13	4.529D+13	4.526D+13	4.529D+13	4.554D+13	4.511D+13	4.453D+13	4.391D+13	4.327D+13	4.262D+13	4.200D+13
30	4.463D+13	4.455D+13	4.451D+13	4.453D+13	4.476D+13	4.433D+13	4.375D+13	4.313D+13	4.250D+13	4.186D+13	4.124D+13
31	4.430D+13	4.422D+13	4.417D+13	4.418D+13	4.438D+13	4.394D+13	4.337D+13	4.274D+13	4.210D+13	4.147D+13	4.085D+13
32	4.364D+13	4.355D+13	4.350D+13	4.351D+13	4.369D+13	4.325D+13	4.267D+13	4.206D+13	4.142D+13	4.079D+13	4.018D+13
33	4.271D+13	4.263D+13	4.257D+13	4.257D+13	4.274D+13	4.230D+13	4.173D+13	4.112D+13	4.050D+13	3.987D+13	3.927D+13
34	4.160D+13	4.151D+13	4.146D+13	4.145D+13	4.161D+13	4.117D+13	4.061D+13	4.001D+13	3.940D+13	3.878D+13	3.819D+13
35	4.034D+13	4.025D+13	4.019D+13	4.019D+13	4.033D+13	3.990D+13	3.935D+13	3.877D+13	3.816D+13	3.756D+13	3.698D+13
36	3.895D+13	3.886D+13	3.881D+13	3.880D+13	3.893D+13	3.851D+13	3.797D+13	3.740D+13	3.681D+13	3.622D+13	3.566D+13
37	3.745D+13	3.736D+13	3.730D+13	3.729D+13	3.741D+13	3.700D+13	3.648D+13	3.592D+13	3.534D+13	3.477D+13	3.422D+13
38	3.588D+13	3.571D+13	3.565D+13	3.564D+13	3.575D+13	3.535D+13	3.484D+13	3.430D+13	3.375D+13	3.319D+13	3.266D+13
39	3.392D+13	3.383D+13	3.377D+13	3.376D+13	3.387D+13	3.348D+13	3.299D+13	3.247D+13	3.194D+13	3.141D+13	3.089D+13
40	3.159D+13	3.150D+13	3.145D+13	3.143D+13	3.154D+13	3.117D+13	3.071D+13	3.022D+13	2.972D+13	2.922D+13	2.873D+13
41	2.933D+13	2.824D+13	2.819D+13	2.818D+13	2.829D+13	2.795D+13	2.753D+13	2.709D+13	2.663D+13	2.617D+13	2.573D+13
42	2.306D+13	2.299D+13	2.295D+13	2.294D+13	2.304D+13	2.276D+13	2.242D+13	2.205D+13	2.168D+13	2.130D+13	2.094D+13
43	1.206D+13	1.203D+13	1.201D+13	1.201D+13	1.202D+13	1.188D+13	1.170D+13	1.151D+13	1.132D+13	1.113D+13	1.095D+13
44	5.904D+12	5.892D+12	5.885D+12	5.881D+12	5.874D+12	5.807D+12	5.722D+12	5.631D+12	5.538D+12	5.446D+12	5.357D+12
45	2.911D+12	2.906D+12	2.902D+12	2.899D+12	2.891D+12	2.858D+12	2.817D+12	2.772D+12	2.727D+12	2.682D+12	2.638D+12
46	1.475D+12	1.472D+12	1.470D+12	1.468D+12	1.463D+12	1.446D+12	1.425D+12	1.403D+12	1.380D+12	1.357D+12	1.335D+12
47	4.149D+11	4.141D+11	4.134D+11	4.125D+11	4.105D+11	4.056D+11	3.998D+11	3.936D+11	3.873D+11	3.809D+11	3.745D+11
48	9.114D+10	9.095D+10	9.074D+10	9.050D+10	8.998D+10	8.887D+10	8.760D+10	8.625D+10	8.486D+10	8.343D+10	8.197D+10
49	1.992D+10	1.987D+10	1.981D+10	1.975D+10	1.963D+10	1.938D+10	1.910D+10	1.880D+10	1.849D+10	1.818D+10	1.785D+10
50	3.893D+09	3.882D+09	3.871D+09	3.858D+09	3.832D+09	3.782D+09	3.726D+09	3.666D+09	3.607D+09	3.543D+09	3.477D+09

	12	13	14	15	16	17	18	19	20	21	22
1	4.736D+09	4.584D+09	4.352D+09	4.066D+09	3.776D+09	3.417D+09	3.008D+09	2.559D+09	2.086D+09	1.257D+09	6.010D+08
2	2.162D+10	2.095D+10	1.995D+10	1.880D+10	1.745D+10	1.586D+10	1.401D+10	1.192D+10	9.680D+09	5.722D+09	2.620D+09
3	8.749D+10	8.494D+10	8.112D+10	7.678D+10	7.168D+10	6.558D+10	5.824D+10	4.964D+10	4.006D+10	2.282D+10	9.769D+09

4	3.515D+11	3.417D+11	3.273D+11	3.112E+11	2.925D+11	2.699D+11	2.418D+11	2.070D+11	1.659D+11	8.933D+10	3.477D+10
5	1.410D+12	1.373D+12	1.318D+12	1.258D+12	1.191D+12	1.111D+12	1.010D+12	8.737D+11	6.969D+11	3.376D+11	1.161D+11
6	5.656D+12	5.518E+12	5.304D+12	5.075E+12	4.835D+12	4.569D+12	4.236D+12	3.756E+12	3.019D+12	1.203D+12	3.466D+11
7	1.880D+13	1.840D+13	1.769D+13	1.694E+13	1.619D+13	1.546D+13	1.469D+13	1.363D+13	1.153D+13	3.009D+12	7.047D+11
8	2.409D+13	2.357D+13	2.266D+13	2.170D+13	2.075D+13	1.982E+13	1.883D+13	1.745E+13	1.472D+13	3.947D+12	9.196D+11
9	2.798D+13	2.737D+13	2.631D+13	2.520E+13	2.409D+13	2.300D+13	2.184D+13	2.022D+13	1.704D+13	4.671D+12	1.099D+12
10	3.128D+13	3.061D+13	2.942D+13	2.818D+13	2.694E+13	2.572E+13	2.441E+13	2.259D+13	1.902D+13	5.267D+12	1.248D+12
11	3.420D+13	3.347E+13	3.218D+13	3.082E+13	2.947D+13	2.813D+13	2.669D+13	2.470D+13	2.080D+13	5.777D+12	1.374D+12
12	3.676D+13	3.598D+13	3.460D+13	3.315E+13	3.170D+13	3.026E+13	2.871D+13	2.657D+13	2.237D+13	6.213D+12	1.479D+12
13	3.895D+13	3.805D+13	3.661D+13	3.509D+13	3.356D+13	3.204D+13	3.041D+13	2.814E+13	2.370D+13	6.569D+12	1.565D+12
14	4.080D+13	3.950E+13	3.803D+13	3.646E+13	3.488D+13	3.331D+13	3.162D+13	2.927D+13	2.465D+13	6.823D+12	1.629D+12
15	4.055D+13	3.982D+13	3.837D+13	3.680E+13	3.522D+13	3.364D+13	3.191E+13	2.948E+13	2.473D+13	6.960D+12	1.673D+12
16	4.135D+13	4.064D+13	3.918D+13	3.760D+13	3.599D+13	3.439D+13	3.264D+13	3.014D+13	2.529D+13	7.111D+12	1.713D+12
17	4.223D+13	4.152D+13	4.005D+13	3.845E+13	3.682D+13	3.520D+13	3.341D+13	3.087D+13	2.591D+13	7.269D+12	1.750D+12
18	4.303D+13	4.232D+13	4.083D+13	3.921E+13	3.757E+13	3.592D+13	3.411D+13	3.152E+13	2.646D+13	7.415D+12	1.783D+12
19	4.368E+13	4.297E+13	4.147D+13	3.984E+13	3.817D+13	3.651D+13	3.468D+13	3.206D+13	2.692D+13	7.537D+12	1.812D+12
20	4.417D+13	4.345D+13	4.195D+13	4.030E+13	3.863D+13	3.695D+13	3.511D+13	3.246E+13	2.726D+13	7.630D+12	1.833D+12
21	4.447D+13	4.376D+13	4.226D+13	4.060D+13	3.893D+13	3.724E+13	3.539D+13	3.273E+13	2.748D+13	7.690D+12	1.847D+12
22	4.459D+13	4.388E+13	4.237D+13	4.072E+13	3.904D+13	3.735D+13	3.550D+13	3.283D+13	2.757D+13	7.714D+12	1.853D+12
23	4.443D+13	4.374E+13	4.224D+13	4.060D+13	3.893D+13	3.725D+13	3.539D+13	3.273E+13	2.748D+13	7.701D+12	1.851D+12
24	4.422D+13	4.354E+13	4.205D+13	4.042E+13	3.875D+13	3.708D+13	3.524D+13	3.258D+13	2.736D+13	7.666D+12	1.843D+12
25	4.391D+13	4.323D+13	4.176D+13	4.013E+13	3.848D+13	3.682D+13	3.498D+13	3.235D+13	2.716D+13	7.608D+12	1.830D+12
26	4.347D+13	4.280E+13	4.133D+13	3.972D+13	3.808D+13	3.643D+13	3.461E+13	3.200D+13	2.686D+13	7.527D+12	1.810D+12
27	4.290D+13	4.223E+13	4.078D+13	3.918E+13	3.756D+13	3.593D+13	3.413D+13	3.155D+13	2.648D+13	7.421D+12	1.785D+12
28	4.221D+13	4.155D+13	4.011D+13	3.853D+13	3.693D+13	3.531D+13	3.353D+13	3.099D+13	2.601D+13	7.294D+12	1.756D+12
29	4.144D+13	4.078D+13	3.936D+13	3.780D+13	3.621D+13	3.462E+13	3.286D+13	3.036D+13	2.547D+13	7.153D+12	1.722D+12
30	4.063D+13	4.004E+13	3.863D+13	3.708D+13	3.551D+13	3.393D+13	3.221D+13	2.975D+13	2.495D+13	7.011D+12	1.686D+12
31	4.030D+13	3.969D+13	3.827D+13	3.673D+13	3.516D+13	3.359D+13	3.188D+13	2.947D+13	2.478D+13	6.892D+12	1.650D+12
32	3.963D+13	3.902E+13	3.763D+13	3.610E+13	3.454D+13	3.299D+13	3.131D+13	2.894E+13	2.433D+13	6.763D+12	1.617D+12
33	3.873D+13	3.812D+13	3.675D+13	3.524E+13	3.372D+13	3.219D+13	3.053D+13	2.822D+13	2.371D+13	6.598D+12	1.576D+12
34	3.766E+13	3.706D+13	3.572D+13	3.424D+13	3.274D+13	3.124D+13	2.962E+13	2.736E+13	2.299E+13	6.400D+12	1.528D+12
35	3.646D+13	3.587E+13	3.455D+13	3.311E+13	3.165D+13	3.019D+13	2.861D+13	2.641D+13	2.218D+13	6.174D+12	1.472D+12
36	3.515D+13	3.456D+13	3.328D+13	3.188D+13	3.045D+13	2.903E+13	2.750E+13	2.537E+13	2.129D+13	5.920D+12	1.408D+12
37	3.372D+13	3.315D+13	3.191D+13	3.055D+13	2.917D+13	2.779D+13	2.631D+13	2.426D+13	2.034D+13	5.635D+12	1.335D+12
38	3.218D+13	3.162D+13	3.042D+13	2.911D+13	2.777E+13	2.645D+13	2.501D+13	2.305D+13	1.931D+13	5.311D+12	1.250D+12
39	3.043D+13	2.990E+13	2.875D+13	2.749D+13	2.621D+13	2.494D+13	2.357D+13	2.170D+13	1.817D+13	4.931D+12	1.150D+12
40	2.823D+13	2.760E+13	2.671D+13	2.553E+13	2.432D+13	2.312E+13	2.183D+13	2.008D+13	1.680D+13	4.465D+12	1.032D+12
41	2.533D+13	2.490D+13	2.391D+13	2.283D+13	2.174D+13	2.064D+13	1.946D+13	1.789D+13	1.497D+13	3.869D+12	8.916D+11
42	2.061D+13	2.027D+13	1.945D+13	1.856D+13	1.765D+13	1.674D+13	1.574D+13	1.443D+13	1.207D+13	3.102D+12	7.308D+11
43	1.076D+13	1.055E+13	1.014E+13	9.675D+12	9.190D+12	8.671D+12	8.055D+12	7.182D+12	5.761D+12	2.016D+12	5.296D+11
44	5.273D+12	5.151D+12	4.947D+12	4.719D+12	4.472D+12	4.193D+12	3.845D+12	3.358D+12	2.654D+12	1.131D+12	3.368D+11
45	2.596E+12	2.531E+12	2.430D+12	2.315E+12	2.187D+12	2.038D+12	1.848D+12	1.593D+12	1.258D+12	6.101D+11	2.027D+11
46	1.313D+12	1.279D+12	1.226D+12	1.167D+12	1.099D+12	1.018D+12	9.153D+11	7.833D+11	6.212D+11	3.282D+11	1.190D+11
47	3.679E+11	3.578E+11	3.423D+11	3.246D+11	3.039D+11	2.790D+11	2.484D+11	2.117E+11	1.700D+11	9.920D+10	4.091D+10
48	8.046D+10	7.812E+10	7.453D+10	7.061E+10	6.651D+10	5.971D+10	5.287D+10	4.507D+10	3.670D+10	2.294D+10	1.050D+10
49	1.750D+10	1.696D+10	1.614D+10	1.518E+10	1.406D+10	1.275D+10	1.126D+10	9.625E+09	7.931D+09	5.200D+09	2.572D+09
50	3.407D+09	3.297D+09	3.128D+09	2.933D+09	2.706D+09	2.448D+09	2.160D+09	1.852D+09	1.540D+09	1.042D+09	5.441D+08

	23	24	25	26
1	2.744E+08	1.213E+08	5.122D+07	1.765E+07
2	1.140D+09	4.816E+08	1.957D+08	6.565E+07
3	3.969D+09	1.574E+09	6.061D+08	1.960E+08
4	1.295D+10	4.754E+09	1.719D+09	5.323D+08
5	3.880D+10	1.303E+10	4.390D+09	1.296E+09
6	1.016D+11	3.096D+10	9.698D+09	2.730E+09
7	1.841D+11	5.213E+10	1.555D+10	4.249D+09
8	2.370D+11	6.618E+10	1.951D+10	5.282E+09
9	2.836D+11	7.905E+10	2.322D+10	6.265E+09
10	3.235D+11	9.030E+10	2.652D+10	7.155E+09
11	3.572D+11	9.990D+10	2.938D+10	7.930E+09
12	3.852D+11	1.079D+11	3.179D+10	8.539D+09
13	4.079D+11	1.145E+11	3.377D+10	9.136E+09
14	4.255D+11	1.197D+11	3.537D+10	9.581E+09
15	4.390D+11	1.238D+11	3.666D+10	9.943D+09
16	4.502D+11	1.272E+11	3.771D+10	1.024E+10
17	4.601E+11	1.300E+11	3.859D+10	1.048D+10

28	7.942D+11	2.883E+11	1.028D+11	2.881E+10
29	7.778D+11	2.821D+11	1.005D+11	2.817E+10
30	7.581D+11	2.747E+11	9.782D+10	2.739E+10
31	7.383D+11	2.672D+11	9.506D+10	2.660E+10
32	7.201E+11	2.604E+11	9.254D+10	2.588D+10
33	6.991D+11	2.525D+11	8.965D+10	2.506E+10
34	6.750D+11	2.435D+11	8.637D+10	2.412D+10
35	6.474D+11	2.332D+11	8.263D+10	2.306D+10
36	6.158D+11	2.215E+11	7.842D+10	2.188E+10
37	5.799D+11	2.084E+11	7.371D+10	2.055E+10
38	5.394E+11	1.937D+11	6.849D+10	1.910E+10
39	4.941D+11	1.774D+11	6.279D+10	1.752E+10
40	4.443D+11	1.598D+11	5.669D+10	1.584D+10
41	3.908D+11	1.413E+11	5.029D+10	1.409E+10
42	3.352D+11	1.222D+11	4.378D+10	1.232E+10
43	2.696D+11	9.973D+10	3.616D+10	1.024D+10
44	2.000D+11	7.577D+10	2.796D+10	8.006D+09
45	1.419E+11	5.529E+10	2.084D+10	6.042E+09
46	9.717D+10	3.899D+10	1.503D+10	4.416E+09
47	4.449D+10	1.897D+10	7.661D+09	2.318E+09
48	1.509D+10	6.843E+09	2.906D+09	9.070D+08
49	4.682D+09	2.236E+09	9.908D+08	3.174E+08
50	1.113D+09	5.507D+08	2.513D+08	8.195E+07

GROUP 4 FLUX

	1	2	3	4	5	6	7	8	9	10	11
1	1.592D+12	1.584D+12	1.576D+12	1.568D+12	1.552D+12	1.528D+12	1.502D+12	1.477D+12	1.452D+12	1.428D+12	1.403D+12
2	4.872D+12	4.848E+12	4.824D+12	4.800E+12	4.753D+12	4.677D+12	4.601D+12	4.523D+12	4.446D+12	4.369D+12	4.293D+12
3	1.005D+13	1.000D+13	9.954D+12	9.905D+12	9.811D+12	9.656D+12	9.498D+12	9.338E+12	9.176D+12	9.013D+12	8.852D+12
4	1.842E+13	1.833D+13	1.825D+13	1.816E+13	1.799D+13	1.771D+13	1.742D+13	1.713D+13	1.683D+13	1.653D+13	1.622D+13
5	3.010D+13	2.996D+13	2.982D+13	2.968D+13	2.941E+13	2.896D+13	2.849D+13	2.801D+13	2.752D+13	2.702D+13	2.652D+13
6	3.937D+13	3.919D+13	3.900D+13	3.881D+13	3.842D+13	3.783D+13	3.722D+13	3.660E+13	3.596D+13	3.531D+13	3.464D+13
7	2.816D+13	2.802E+13	2.786D+13	2.767E+13	2.719D+13	2.674D+13	2.631D+13	2.587D+13	2.542D+13	2.495D+13	2.446D+13
8	2.735D+13	2.721D+13	2.704D+13	2.684D+13	2.634D+13	2.590D+13	2.548D+13	2.506E+13	2.463D+13	2.417D+13	2.369D+13
9	2.908E+13	2.894D+13	2.876D+13	2.855E+13	2.802D+13	2.754D+13	2.711D+13	2.666D+13	2.620D+13	2.573D+13	2.522D+13
10	3.169D+13	3.153D+13	3.134D+13	3.111D+13	3.054D+13	3.003D+13	2.956D+13	2.908D+13	2.858D+13	2.806D+13	2.751D+13
11	3.442D+13	3.426E+13	3.406D+13	3.380D+13	3.319D+13	3.264D+13	3.214D+13	3.162E+13	3.109D+13	3.053D+13	2.993D+13
12	3.702D+13	3.685E+13	3.664D+13	3.637E+13	3.571D+13	3.513D+13	3.459D+13	3.404E+13	3.347D+13	3.288D+13	3.224D+13
13	3.943D+13	3.930D+13	3.908D+13	3.879E+13	3.809D+13	3.748D+13	3.691D+13	3.634D+13	3.574D+13	3.511D+13	3.444D+13
14	4.205D+13	4.186D+13	4.162D+13	4.132D+13	4.057D+13	3.992D+13	3.933D+13	3.872E+13	3.809D+13	3.742D+13	3.672D+13
15	4.540D+13	4.519E+13	4.494D+13	4.460E+13	4.377D+13	4.308D+13	4.244D+13	4.179D+13	4.112D+13	4.041D+13	3.965D+13
16	4.747D+13	4.726D+13	4.699D+13	4.663D+13	4.576D+13	4.504D+13	4.438D+13	4.371D+13	4.302D+13	4.228D+13	4.150D+13
17	4.887D+13	4.865E+13	4.838D+13	4.802E+13	4.712D+13	4.639D+13	4.572D+13	4.503D+13	4.433D+13	4.358D+13	4.278D+13
18	4.988D+13	4.966D+13	4.938D+13	4.902E+13	4.811D+13	4.737D+13	4.669D+13	4.600D+13	4.528D+13	4.453D+13	4.372D+13
19	5.063D+13	5.041D+13	5.013D+13	4.976D+13	4.884D+13	4.810D+13	4.742D+13	4.672E+13	4.600D+13	4.524D+13	4.442D+13
20	5.117D+13	5.095E+13	5.067D+13	5.030E+13	4.938D+13	4.863D+13	4.795D+13	4.725D+13	4.653D+13	4.576D+13	4.494D+13
21	5.154D+13	5.133D+13	5.104D+13	5.067D+13	4.975D+13	4.900D+13	4.832D+13	4.762E+13	4.689D+13	4.613D+13	4.530D+13
22	5.179D+13	5.157D+13	5.129D+13	5.092D+13	4.999D+13	4.924E+13	4.856D+13	4.786D+13	4.714D+13	4.637D+13	4.554D+13
23	5.196D+13	5.178D+13	5.150D+13	5.112D+13	5.019D+13	4.944D+13	4.875D+13	4.806D+13	4.733D+13	4.656D+13	4.573D+13
24	5.130D+13	5.169D+13	5.141D+13	5.103E+13	5.010D+13	4.935D+13	4.867D+13	4.797D+13	4.725D+13	4.648D+13	4.565D+13
25	5.16CE+13	5.138D+13	5.110D+13	5.073E+13	4.980E+13	4.906D+13	4.838D+13	4.769D+13	4.697D+13	4.620D+13	4.538D+13
26	5.111D+13	5.090D+13	5.062D+13	5.025E+13	4.933D+13	4.859D+13	4.791D+13	4.723D+13	4.651D+13	4.575D+13	4.494D+13
27	5.044D+13	5.023D+13	4.996D+13	4.959D+13	4.868D+13	4.795D+13	4.728D+13	4.66CE+13	4.589D+13	4.514D+13	4.433D+13
28	4.959D+13	4.937E+13	4.910D+13	4.874E+13	4.784D+13	4.712D+13	4.646D+13	4.579D+13	4.508D+13	4.434D+13	4.354D+13
29	4.847D+13	4.826D+13	4.799D+13	4.764D+13	4.675D+13	4.604D+13	4.539D+13	4.473E+13	4.404D+13	4.330D+13	4.252D+13
30	4.694D+13	4.674E+13	4.648D+13	4.613E+13	4.527D+13	4.457D+13	4.394D+13	4.329D+13	4.261D+13	4.190D+13	4.112D+13
31	4.506D+13	4.487D+13	4.461D+13	4.428E+13	4.344D+13	4.277D+13	4.215D+13	4.152D+13	4.087D+13	4.017D+13	3.942D+13
32	4.375D+13	4.355E+13	4.331D+13	4.298D+13	4.216D+13	4.150D+13	4.090D+13	4.029E+13	3.964D+13	3.896D+13	3.822D+13
33	4.249D+13	4.230E+13	4.205D+13	4.173E+13	4.094D+13	4.029D+13	3.970D+13	3.910D+13	3.847D+13	3.780D+13	3.707D+13
34	4.121D+13	4.103D+13	4.079D+13	4.047E+13	3.970D+13	3.906D+13	3.849D+13	3.790D+13	3.728D+13	3.663D+13	3.591D+13
35	3.991D+13	3.972D+13	3.949D+13	3.918D+13	3.843D+13	3.780D+13	3.724D+13	3.666D+13	3.606D+13	3.542D+13	3.472D+13
36	3.859D+13	3.840E+13	3.817D+13	3.787D+13	3.714D+13	3.653D+13	3.598D+13	3.541D+13	3.482D+13	3.420D+13	3.352D+13
37	3.732D+13	3.714D+13	3.692D+13	3.662D+13	3.590D+13	3.531D+13	3.476D+13	3.421D+13	3.364D+13	3.302D+13	3.236D+13

38	3.627D+13	3.609D+13	3.587D+13	3.558D+13	3.487D+13	[illegible]	[illegible]	[illegible]	[illegible]	[illegible]	[illegible]
39	3.571D+13	3.553D+13	3.531D+13	3.502D+13	3.431D+13	3.373D+13	3.319D+13	3.265D+13	3.208D+13	3.148D+13	3.082D+13
40	3.615D+13	3.597D+13	3.574D+13	3.545D+13	3.473D+13	3.413D+13	3.358D+13	3.302D+13	3.244D+13	3.182D+13	3.115D+13
41	3.947D+13	3.827D+13	3.803D+13	3.773D+13	3.700D+13	3.635D+13	3.576D+13	3.516D+13	3.452D+13	3.386D+13	3.313D+13
42	4.409D+13	4.386D+13	4.361D+13	4.329D+13	4.253D+13	4.181D+13	4.112D+13	4.041D+13	3.968D+13	3.890D+13	3.807D+13
43	5.971D+13	5.942D+13	5.911D+13	5.776D+13	5.705D+13	5.611D+13	5.518D+13	5.422D+13	5.322D+13	5.218D+13	5.108D+13
44	6.477D+13	6.445D+13	6.412D+13	6.377D+13	6.307D+13	6.203D+13	6.098D+13	5.990D+13	5.878D+13	5.761D+13	5.639D+13
45	6.382D+13	6.350D+13	6.317D+13	6.283D+13	6.215D+13	6.112D+13	6.007D+13	5.898D+13	5.785D+13	5.668D+13	5.546D+13
46	5.994D+13	5.963D+13	5.932D+13	5.899D+13	5.835D+13	5.736D+13	5.635D+13	5.530D+13	5.423D+13	5.311D+13	5.196D+13
47	5.310D+13	5.281D+13	5.252D+13	5.223D+13	5.167D+13	5.076D+13	4.983D+13	4.887D+13	4.789D+13	4.688D+13	4.584D+13
48	3.778D+13	3.757D+13	3.735D+13	3.714D+13	3.672D+13	3.605D+13	3.536D+13	3.465D+13	3.393D+13	3.320D+13	3.245D+13
49	2.254D+13	2.240D+13	2.227D+13	2.214D+13	2.188D+13	2.147D+13	2.105D+13	2.061D+13	2.018D+13	1.973D+13	1.928D+13
50	8.266D+12	8.216D+12	8.166D+12	8.116D+12	8.021D+12	7.867D+12	7.709D+12	7.549D+12	7.387D+12	7.223D+12	7.057D+12

	12	13	14	15	16	17	18	19	20	21	22
1	1.330D+12	1.347D+12	1.309D+12	1.280D+12	1.264D+12	1.266D+12	1.290D+12	1.342D+12	1.427D+12	1.642D+12	1.589D+12
2	4.219D+12	4.113D+12	3.985D+12	3.880D+12	3.811D+12	3.790D+12	3.833D+12	3.956D+12	4.177D+12	4.766D+12	4.556D+12
3	8.691D+12	8.459D+12	8.164D+12	7.905D+12	7.703D+12	7.583D+12	7.576D+12	7.719D+12	8.049D+12	9.016D+12	8.433D+12
4	1.592D+13	1.547D+13	1.488D+13	1.433D+13	1.385D+13	1.350D+13	1.332D+13	1.339D+13	1.378D+13	1.514D+13	1.380D+13
5	2.601D+13	2.525D+13	2.423D+13	2.325D+13	2.235D+13	2.161D+13	2.114D+13	2.107D+13	2.156D+13	2.360D+13	2.106D+13
6	3.396D+13	3.293D+13	3.155D+13	3.020D+13	2.895D+13	2.790D+13	2.728D+13	2.741D+13	2.870D+13	3.352D+13	3.006D+13
7	2.393D+13	2.305D+13	2.203D+13	2.108D+13	2.020D+13	1.954D+13	1.939D+13	2.040D+13	2.387D+13	3.974D+13	3.738D+13
8	2.317D+13	2.228D+13	2.129D+13	2.036D+13	1.951D+13	1.889D+13	1.888D+13	2.029D+13	2.474D+13	4.456D+13	4.243D+13
9	2.466D+13	2.372D+13	2.266D+13	2.166D+13	2.075D+13	2.010D+13	2.015D+13	2.182D+13	2.700D+13	4.976D+13	4.750D+13
10	2.691D+13	2.599D+13	2.474D+13	2.364D+13	2.265D+13	2.194D+13	2.200D+13	2.387D+13	2.965D+13	5.497D+13	5.244D+13
11	2.928D+13	2.818D+13	2.693D+13	2.574D+13	2.466D+13	2.389D+13	2.395D+13	2.600D+13	3.230D+13	5.994D+13	5.712D+13
12	3.155D+13	3.036D+13	2.903D+13	2.775D+13	2.659D+13	2.576D+13	2.583D+13	2.803D+13	3.481D+13	6.455D+13	6.145D+13
13	3.370D+13	3.244D+13	3.102D+13	2.967D+13	2.843D+13	2.755D+13	2.763D+13	2.997D+13	3.717D+13	6.874D+13	6.539D+13
14	3.593D+13	3.460D+13	3.310D+13	3.16[illegible]D+13	3.036D+13	2.944D+13	2.953D+13	3.201D+13	3.955D+13	7.252D+13	6.891D+13
15	3.882D+13	3.739D+13	3.578D+13	3.425D+13	3.285D+13	3.188D+13	3.200D+13	3.464D+13	4.250D+13	7.592D+13	7.200D+13
16	4.063D+13	3.915D+13	3.748D+13	3.589D+13	3.444D+13	3.344D+13	3.358D+13	3.633D+13	4.444D+13	7.879D+13	7.466D+13
17	4.199D+13	4.037D+13	3.866D+13	3.703D+13	3.555D+13	3.454D+13	3.470D+13	3.753D+13	4.587D+13	8.116D+13	7.691D+13
18	4.282D+13	4.127D+13	3.953D+13	3.788D+13	3.638D+13	3.535D+13	3.553D+13	3.844D+13	4.697D+13	8.308D+13	7.875D+13
19	4.351D+13	4.195D+13	4.020D+13	3.853D+13	3.701D+13	3.597D+13	3.616D+13	3.913D+13	4.793D+13	8.460D+13	8.023D+13
20	4.403D+13	4.245D+13	4.068D+13	3.900D+13	3.748D+13	3.643D+13	3.664D+13	3.965D+13	4.857D+13	8.575D+13	8.135D+13
21	4.433D+13	4.280D+13	4.103D+13	3.934D+13	3.780D+13	3.676D+13	3.697D+13	4.002D+13	4.892D+13	8.653D+13	8.211D+13
22	4.462D+13	4.303D+13	4.125D+13	3.956D+13	3.802D+13	3.697D+13	3.719D+13	4.026D+13	4.920D+13	8.697D+13	8.253D+13
23	4.481D+13	4.321D+13	4.142D+13	3.972D+13	3.818D+13	3.714D+13	3.736D+13	4.044D+13	4.939D+13	8.737D+13	8.261D+13
24	4.473D+13	4.314D+13	4.135D+13	3.966D+13	3.812D+13	3.708D+13	3.730D+13	4.037D+13	4.928D+13	8.681D+13	8.236D+13
25	4.446D+13	4.288D+13	4.110D+13	3.942D+13	3.789D+13	3.685D+13	3.707D+13	4.011D+13	4.896D+13	8.621D+13	8.178D+13
26	4.403D+13	4.245D+13	4.069D+13	3.902D+13	3.750D+13	3.647D+13	3.668D+13	3.968D+13	4.843D+13	8.527D+13	8.087D+13
27	4.343D+13	4.187D+13	4.013D+13	3.847D+13	3.697D+13	3.594D+13	3.614D+13	3.910D+13	4.771D+13	8.399D+13	7.963D+13
28	4.265D+13	4.111D+13	3.939D+13	3.776D+13	3.627D+13	3.526D+13	3.544D+13	3.833D+13	4.677D+13	8.235D+13	7.805D+13
29	4.164D+13	4.012D+13	3.843D+13	3.682D+13	3.536D+13	3.435D+13	3.452D+13	3.733D+13	4.557D+13	8.033D+13	7.613D+13
30	4.025D+13	3.876D+13	3.710D+13	3.553D+13	3.410D+13	3.312D+13	3.326D+13	3.597D+13	4.399D+13	7.790D+13	7.383D+13
31	3.856D+13	3.704D+13	3.543D+13	3.392D+13	3.254D+13	3.157D+13	3.169D+13	3.429D+13	4.206D+13	7.550D+13	7.160D+13
32	3.737D+13	3.587D+13	3.429D+13	3.281D+13	3.146D+13	3.052D+13	3.062D+13	3.313D+13	4.071D+13	7.342D+13	6.965D+13
33	3.624D+13	3.476D+13	3.322D+13	3.177D+13	3.045D+13	2.952D+13	2.961D+13	3.203D+13	3.939D+13	7.118D+13	6.754D+13
34	3.510D+13	3.366D+13	3.214D+13	3.073D+13	2.945D+13	2.853D+13	2.860D+13	3.093D+13	3.804D+13	6.878D+13	6.525D+13
35	3.393D+13	3.252D+13	3.105D+13	2.967D+13	2.842D+13	2.752D+13	2.757D+13	2.980D+13	3.663D+13	6.621D+13	6.280D+13
36	3.274D+13	3.137D+13	2.993D+13	2.860D+13	2.737D+13	2.650D+13	2.652D+13	2.864D+13	3.517D+13	6.349D+13	6.019D+13
37	3.160D+13	3.026D+13	2.886D+13	2.756D+13	2.636D+13	2.550D+13	2.549D+13	2.748D+13	3.369D+13	6.064D+13	5.744D+13
38	3.063D+13	2.932D+13	2.794D+13	2.666D+13	2.549D+13	2.463D+13	2.458D+13	2.641D+13	3.223D+13	5.771D+13	5.458D+13
39	3.006D+13	2.877D+13	2.741D+13	2.613D+13	2.496D+13	2.408D+13	2.395D+13	2.559D+13	3.096D+13	5.477D+13	5.162D+13
40	3.039D+13	2.906D+13	2.765D+13	2.635D+13	2.513D+13	2.419D+13	2.394D+13	2.531D+13	3.011D+13	5.192D+13	4.862D+13
41	3.232D+13	3.091D+13	2.940D+13	2.799D+13	2.666D+13	2.557D+13	2.511D+13	2.609D+13	3.014D+13	4.930D+13	4.561D+13
42	3.716D+13	3.559D+13	3.385D+13	3.220D+13	3.062D+13	2.926D+13	2.845D+13	2.889D+13	3.187D+13	4.701D+13	4.262D+13
43	4.330D+13	4.805D+13	4.573D+13	4.346D+13	4.125D+13	3.924D+13	3.772D+13	3.720D+13	3.844D+13	4.464D+13	3.910D+13
44	5.511D+13	5.311D+13	5.053D+13	4.799D+13	4.549D+13	4.314D+13	4.115D+13	3.984D+13	3.957D+13	4.118D+13	3.503D+13
45	5.419D+13	5.222D+13	4.966D+13	4.713D+13	4.462D+13	4.224D+13	4.010D+13	3.842D+13	3.742D+13	3.711D+13	3.100D+13
46	5.076D+13	4.891D+13	4.649D+13	4.409D+13	4.171D+13	3.942D+13	3.730D+13	3.549D+13	3.413D+13	3.286D+13	2.713D+13
47	4.479D+13	4.321D+13	4.105D+13	3.890D+13	3.676D+13	3.466D+13	3.265D+13	3.075D+13	2.897D+13	2.611D+13	2.114D+13
48	3.173D+13	3.057D+13	2.903D+13	2.748D+13	2.594D+13	2.442D+13	2.292D+13	2.146D+13	2.002D+13	1.764D+13	1.413D+13
49	1.883D+13	1.815D+13	1.723D+13	1.630D+13	1.537D+13	1.446D+13	1.355D+13	1.265D+13	1.176D+13	1.029D+13	8.210D+12
50	6.989D+12	6.640D+12	6.299D+12	5.958D+12	5.618D+12	5.279D+12	4.944D+12	4.611D+12	4.282D+12	3.738D+12	2.979D+12

0.0 0.0 0.0 0.0 0.0 0.0 0.0 0.0 0.0 0.0

ARMY REACTOR DEPLETION RUNS
DATE : MAY 14 , 1975

POINT POWER DISTRIBUTION (WATTS/CC)

	1	2	3	4	5	6	7	8	9	10	11
1	0.0	0.0	0.0	0.0	0.0	0.0	0.0	0.0	0.0	0.0	0.0
2	0.0	0.0	0.0	0.0	0.0	0.0	0.0	0.0	0.0	0.0	0.0
3	0.0	0.0	0.0	0.0	0.0	0.0	0.0	0.0	0.0	0.0	0.0
4	0.0	0.0	0.0	0.0	0.0	0.0	0.0	0.0	0.0	0.0	0.0
5	0.0	0.0	0.0	0.0	0.0	0.0	0.0	0.0	0.0	0.0	0.0
6	0.0	0.0	0.0	0.0	0.0	0.0	0.0	0.0	0.0	0.0	0.0
7	4.998E+00	4.975E+00	4.949E+00	4.917E+00	5.010E+00	4.930E+00	4.851E+00	4.771E+00	4.688E+00	4.603E+00	4.515E+00
8	5.089E+00	5.065E+00	5.038E+00	5.005E+00	5.095E+00	5.013E+00	4.934E+00	4.853E+00	4.770E+00	4.683E+00	4.593E+00
9	5.531E+00	5.506E+00	5.477E+00	5.441E+00	5.540E+00	5.452E+00	5.367E+00	5.279E+00	5.189E+00	5.096E+00	4.998E+00
10	6.076E+00	6.049E+00	6.017E+00	5.979E+00	6.089E+00	5.993E+00	5.900E+00	5.805E+00	5.707E+00	5.605E+00	5.498E+00
11	6.616E+00	6.588E+00	6.554E+00	6.513E+00	6.634E+00	6.531E+00	6.431E+00	6.329E+00	6.223E+00	6.113E+00	5.997E+00
12	7.115E+00	7.085E+00	7.050E+00	7.006E+00	7.137E+00	7.028E+00	6.922E+00	6.813E+00	6.700E+00	6.583E+00	6.460E+00
13	7.571E+00	7.540E+00	7.503E+00	7.457E+00	7.597E+00	7.482E+00	7.371E+00	7.256E+00	7.138E+00	7.014E+00	6.884E+00
14	8.021E+00	7.988E+00	7.949E+00	7.900E+00	8.049E+00	7.928E+00	7.812E+00	7.692E+00	7.568E+00	7.439E+00	7.302E+00
15	7.287E+00	7.258E+00	7.223E+00	7.178E+00	7.395E+00	7.286E+00	7.180E+00	7.071E+00	6.959E+00	6.841E+00	6.717E+00
16	7.582E+00	7.553E+00	7.516E+00	7.469E+00	7.695E+00	7.582E+00	7.474E+00	7.362E+00	7.246E+00	7.125E+00	6.998E+00
17	7.789E+00	7.759E+00	7.722E+00	7.674E+00	7.907E+00	7.793E+00	7.683E+00	7.569E+00	7.452E+00	7.329E+00	7.198E+00
18	7.943E+00	7.913E+00	7.876E+00	7.827E+00	8.066E+00	7.950E+00	7.840E+00	7.725E+00	7.606E+00	7.482E+00	7.350E+00
19	8.059E+00	8.029E+00	7.992E+00	7.943E+00	8.186E+00	8.070E+00	7.959E+00	7.844E+00	7.724E+00	7.599E+00	7.466E+00
20	8.143E+00	8.113E+00	8.076E+00	8.027E+00	8.271E+00	8.157E+00	8.046E+00	7.931E+00	7.811E+00	7.685E+00	7.552E+00
21	8.200E+00	8.170E+00	8.133E+00	8.084E+00	8.333E+00	8.217E+00	8.105E+00	7.990E+00	7.870E+00	7.744E+00	7.610E+00
22	8.234E+00	8.205E+00	8.168E+00	8.119E+00	8.369E+00	8.253E+00	8.141E+00	8.026E+00	7.906E+00	7.780E+00	7.646E+00
23	8.114E+00	8.085E+00	8.049E+00	8.000E+00	8.256E+00	8.142E+00	8.033E+00	7.919E+00	7.801E+00	7.677E+00	7.545E+00
24	8.096E+00	8.067E+00	8.030E+00	7.982E+00	8.238E+00	8.124E+00	8.015E+00	7.902E+00	7.784E+00	7.660E+00	7.529E+00
25	8.046E+00	8.018E+00	7.981E+00	7.933E+00	8.187E+00	8.074E+00	7.965E+00	7.853E+00	7.736E+00	7.613E+00	7.482E+00
26	7.970E+00	7.941E+00	7.905E+00	7.858E+00	8.109E+00	7.996E+00	7.888E+00	7.777E+00	7.661E+00	7.539E+00	7.409E+00
27	7.867E+00	7.839E+00	7.803E+00	7.756E+00	8.003E+00	7.892E+00	7.785E+00	7.675E+00	7.559E+00	7.438E+00	7.310E+00
28	7.737E+00	7.709E+00	7.673E+00	7.627E+00	7.869E+00	7.759E+00	7.653E+00	7.544E+00	7.430E+00	7.310E+00	7.183E+00
29	7.571E+00	7.543E+00	7.508E+00	7.462E+00	7.699E+00	7.590E+00	7.485E+00	7.377E+00	7.265E+00	7.147E+00	7.022E+00
30	7.351E+00	7.323E+00	7.289E+00	7.244E+00	7.473E+00	7.366E+00	7.264E+00	7.158E+00	7.048E+00	6.932E+00	6.809E+00
31	7.730E+00	7.700E+00	7.664E+00	7.616E+00	7.825E+00	7.712E+00	7.604E+00	7.492E+00	7.375E+00	7.253E+00	7.122E+00
32	7.521E+00	7.492E+00	7.456E+00	7.409E+00	7.612E+00	7.501E+00	7.394E+00	7.285E+00	7.170E+00	7.050E+00	6.921E+00
33	7.313E+00	7.284E+00	7.249E+00	7.203E+00	7.399E+00	7.290E+00	7.186E+00	7.079E+00	6.966E+00	6.848E+00	6.722E+00
34	7.097E+00	7.069E+00	7.034E+00	6.989E+00	7.179E+00	7.072E+00	6.970E+00	6.864E+00	6.755E+00	6.639E+00	6.515E+00
35	6.871E+00	6.843E+00	6.808E+00	6.765E+00	6.947E+00	6.842E+00	6.742E+00	6.639E+00	6.532E+00	6.419E+00	6.298E+00
36	6.635E+00	6.608E+00	6.574E+00	6.531E+00	6.706E+00	6.604E+00	6.506E+00	6.405E+00	6.300E+00	6.190E+00	6.072E+00
37	6.399E+00	6.372E+00	6.339E+00	6.297E+00	6.464E+00	6.364E+00	6.269E+00	6.170E+00	6.068E+00	5.961E+00	5.845E+00
38	6.182E+00	6.155E+00	6.123E+00	6.081E+00	6.241E+00	6.143E+00	6.049E+00	5.953E+00	5.853E+00	5.748E+00	5.635E+00
39	6.021E+00	5.994E+00	5.961E+00	5.920E+00	6.074E+00	5.977E+00	5.884E+00	5.789E+00	5.690E+00	5.586E+00	5.475E+00
40	5.930E+00	5.903E+00	5.920E+00	5.878E+00	6.030E+00	5.932E+00	5.839E+00	5.743E+00	5.643E+00	5.538E+00	5.426E+00
41	6.178E+00	6.149E+00	6.115E+00	6.073E+00	6.231E+00	6.129E+00	6.030E+00	5.930E+00	5.825E+00	5.715E+00	5.597E+00
42	6.813E+00	6.781E+00	6.745E+00	6.700E+00	6.885E+00	6.772E+00	6.662E+00	6.548E+00	6.431E+00	6.307E+00	6.176E+00
43	0.0	0.0	0.0	0.0	0.0	0.0	0.0	0.0	0.0	0.0	0.0
44	0.0	0.0	0.0	0.0	0.0	0.0	0.0	0.0	0.0	0.0	0.0
45	0.0	0.0	0.0	0.0	0.0	0.0	0.0	0.0	0.0	0.0	0.0
46	0.0	0.0	0.0	0.0	0.0	0.0	0.0	0.0	0.0	0.0	0.0
47	0.0	0.0	0.0	0.0	0.0	0.0	0.0	0.0	0.0	0.0	0.0
48	0.0	0.0	0.0	0.0	0.0	0.0	0.0	0.0	0.0	0.0	0.0
49	0.0	0.0	0.0	0.0	0.0	0.0	0.0	0.0	0.0	0.0	0.0
50	0.0	0.0	0.0	0.0	0.0	0.0	0.0	0.0	0.0	0.0	0.0

	12	13	14	15	16	17	18	19	20	21	22
1	0.0	0.0	0.0	0.0	0.0	0.0	0.0	0.0	0.0	0.0	0.0
2	0.0	0.0	0.0	0.0	0.0	0.0	0.0	0.0	0.0	0.0	0.0
3	0.0	0.0	0.0	0.0	0.0	0.0	0.0	0.0	0.0	0.0	0.0

4	0.0	0.0	0.0	0.0	0.0	0.0	0.0	0.0	0.0	0.0	0.0	0.0
5	0.0	0.0	0.0	0.0	0.0	0.0	0.0	0.0	0.0	0.0	0.0	0.0
6	0.0	0.0	0.0	0.0	0.0	0.0	0.0	0.0	0.0	0.0	0.0	0.0
7	4.420E+00	4.413E+00	4.221E+00	4.036E+00	3.861E+00	3.715E+00	3.643E+00	3.744E+00	4.221E+00	0.0	0.0	
8	4.495E+00	4.485E+00	4.289E+00	4.099E+00	3.919E+00	3.770E+00	3.708E+00	3.855E+00	4.469E+00	0.0	0.0	
9	4.993E+00	4.882E+00	4.668E+00	4.461E+00	4.263E+00	4.101E+00	4.036E+00	4.211E+00	4.922E+00	0.0	0.0	
10	5.383E+00	5.372E+00	5.139E+00	4.910E+00	4.692E+00	4.511E+00	4.440E+00	4.635E+00	5.426E+00	0.0	0.0	
11	5.873E+00	5.862E+00	5.608E+00	5.359E+00	5.121E+00	4.923E+00	4.844E+00	5.056E+00	5.919E+00	0.0	0.0	
12	6.327E+00	6.317E+00	6.045E+00	5.777E+00	5.521E+00	5.308E+00	5.223E+00	5.451E+00	6.378E+00	0.0	0.0	
13	6.744E+00	6.735E+00	6.447E+00	6.163E+00	5.892E+00	5.666E+00	5.576E+00	5.819E+00	6.804E+00	0.0	0.0	
14	7.155E+00	7.148E+00	6.844E+00	6.546E+00	6.260E+00	6.024E+00	5.932E+00	6.190E+00	7.223E+00	0.0	0.0	
15	6.583E+00	6.646E+00	6.367E+00	6.092E+00	5.829E+00	5.614E+00	5.533E+00	5.773E+00	6.704E+00	0.0	0.0	
16	6.859E+00	6.927E+00	6.638E+00	6.354E+00	6.082E+00	5.862E+00	5.781E+00	6.032E+00	6.994E+00	0.0	0.0	
17	7.057E+00	7.129E+00	6.834E+00	6.544E+00	6.267E+00	6.042E+00	5.961E+00	6.222E+00	7.212E+00	0.0	0.0	
18	7.207E+00	7.283E+00	6.983E+00	6.689E+00	6.407E+00	6.180E+00	6.100E+00	6.368E+00	7.382E+00	0.0	0.0	
19	7.322E+00	7.400E+00	7.097E+00	6.800E+00	6.516E+00	6.286E+00	6.206E+00	6.482E+00	7.515E+00	0.0	0.0	
20	7.406E+00	7.487E+00	7.182E+00	6.882E+00	6.596E+00	6.365E+00	6.286E+00	6.566E+00	7.615E+00	0.0	0.0	
21	7.464E+00	7.546E+00	7.240E+00	6.939E+00	6.652E+00	6.420E+00	6.341E+00	6.625E+00	7.684E+00	0.0	0.0	
22	7.500E+00	7.583E+00	7.276E+00	6.975E+00	6.686E+00	6.454E+00	6.376E+00	6.662E+00	7.726E+00	0.0	0.0	
23	7.401E+00	7.495E+00	7.192E+00	6.894E+00	6.610E+00	6.381E+00	6.305E+00	6.588E+00	7.636E+00	0.0	0.0	
24	7.385E+00	7.473E+00	7.177E+00	6.880E+00	6.596E+00	6.368E+00	6.292E+00	6.574E+00	7.618E+00	0.0	0.0	
25	7.339E+00	7.432E+00	7.132E+00	6.836E+00	6.554E+00	6.327E+00	6.251E+00	6.531E+00	7.568E+00	0.0	0.0	
26	7.267E+00	7.358E+00	7.060E+00	6.767E+00	6.487E+00	6.262E+00	6.186E+00	6.462E+00	7.487E+00	0.0	0.0	
27	7.169E+00	7.259E+00	6.964E+00	6.673E+00	6.396E+00	6.173E+00	6.097E+00	6.368E+00	7.376E+00	0.0	0.0	
28	7.044E+00	7.131E+00	6.839E+00	6.553E+00	6.279E+00	6.058E+00	5.982E+00	6.245E+00	7.233E+00	0.0	0.0	
29	6.895E+00	6.967E+00	6.680E+00	6.398E+00	6.129E+00	5.910E+00	5.833E+00	6.089E+00	7.052E+00	0.0	0.0	
30	6.674E+00	6.749E+00	6.467E+00	6.192E+00	5.928E+00	5.714E+00	5.636E+00	5.881E+00	6.817E+00	0.0	0.0	
31	6.977E+00	7.091E+00	6.792E+00	6.499E+00	6.220E+00	5.991E+00	5.905E+00	6.161E+00	7.158E+00	0.0	0.0	
32	6.778E+00	6.884E+00	6.590E+00	6.304E+00	6.031E+00	5.806E+00	5.720E+00	5.966E+00	6.937E+00	0.0	0.0	
33	6.581E+00	6.691E+00	6.393E+00	6.113E+00	5.846E+00	5.625E+00	5.539E+00	5.776E+00	6.717E+00	0.0	0.0	
34	6.377E+00	6.478E+00	6.190E+00	5.917E+00	5.656E+00	5.440E+00	5.354E+00	5.580E+00	6.490E+00	0.0	0.0	
35	6.163E+00	6.253E+00	5.978E+00	5.712E+00	5.458E+00	5.247E+00	5.161E+00	5.377E+00	6.250E+00	0.0	0.0	
36	5.941E+00	6.025E+00	5.758E+00	5.499E+00	5.252E+00	5.046E+00	4.961E+00	5.164E+00	5.998E+00	0.0	0.0	
37	5.717E+00	5.796E+00	5.536E+00	5.285E+00	5.044E+00	4.844E+00	4.758E+00	4.947E+00	5.738E+00	0.0	0.0	
38	5.510E+00	5.583E+00	5.329E+00	5.084E+00	4.850E+00	4.654E+00	4.566E+00	4.738E+00	5.480E+00	0.0	0.0	
39	5.351E+00	5.419E+00	5.169E+00	4.928E+00	4.697E+00	4.503E+00	4.409E+00	4.558E+00	5.242E+00	0.0	0.0	
40	5.301E+00	5.365E+00	5.113E+00	4.871E+00	4.639E+00	4.440E+00	4.333E+00	4.450E+00	5.060E+00	0.0	0.0	
41	5.467E+00	5.531E+00	5.269E+00	5.015E+00	4.771E+00	4.556E+00	4.425E+00	4.493E+00	5.000E+00	0.0	0.0	
42	6.033E+00	6.111E+00	5.818E+00	5.534E+00	5.258E+00	5.008E+00	4.833E+00	4.828E+00	5.189E+00	0.0	0.0	
43	0.0	0.0	0.0	0.0	0.0	0.0	0.0	0.0	0.0	0.0	0.0	
44	0.0	0.0	0.0	0.0	0.0	0.0	0.0	0.0	0.0	0.0	0.0	
45	0.0	0.0	0.0	0.0	0.0	0.0	0.0	0.0	0.0	0.0	0.0	
46	0.0	0.0	0.0	0.0	0.0	0.0	0.0	0.0	0.0	0.0	0.0	
47	0.0	0.0	0.0	0.0	0.0	0.0	0.0	0.0	0.0	0.0	0.0	
48	0.0	0.0	0.0	0.0	0.0	0.0	0.0	0.0	0.0	0.0	0.0	
49	0.0	0.0	0.0	0.0	0.0	0.0	0.0	0.0	0.0	0.0	0.0	
50	0.0	0.0	0.0	0.0	0.0	0.0	0.0	0.0	0.0	0.0	0.0	

	23	24	25	26
1	0.0	0.0	0.0	0.0
2	0.0	0.0	0.0	0.0
3	0.0	0.0	0.0	0.0
4	0.0	0.0	0.0	0.0
5	0.0	0.0	0.0	0.0
6	0.0	0.0	0.0	0.0
7	0.0	0.0	0.0	0.0
8	0.0	0.0	0.0	0.0
9	0.0	0.0	0.0	0.0
10	0.0	0.0	0.0	0.0
11	0.0	0.0	0.0	0.0
12	0.0	0.0	0.0	0.0
13	0.0	0.0	0.0	0.0
14	0.0	0.0	0.0	0.0
15	0.0	0.0	0.0	0.0
16	0.0	0.0	0.0	0.0
17	0.0	0.0	0.0	0.0

B.2 ANISN

ANISN solves the one-dimensional multigroup neutron transport equation in slab, cylindrical and spherical geometry using the S_N method. It has a large number of options, including higher order anisotropic scattering and the ability to use any order of S_N calculation desired. Boundary conditions include vacuum, reflection, periodic and white/albedo options. A complete shell source option description by group ,position, and angle is available, and mid streaming corrections can be made. Fixed source, k_{eff} calculation, concentration search, zone width search, outer radius search and buckling search for criticality options are available. Cross-sections (cs) can be input on cards or from a tape prepared by a supplementary program , and the code will collapse cs's to any desired few-group scheme.

There follows an input example for the use of ANISN to obtain the fast neutron flux and gamma heating on the reactor vessel wall (see Section 2.2).

```
//JG0168  JOB 1,
// 'ARNALDO A T RIBEIRO',CLASS=C,REGION=450K
/*MITID USER=(M12303,12680,,DENISE)
/*SRI LOW
/*MAIN    TIME=10,LINES=80,CARDS=50
//STEP4 EXEC FORG,PROG='U.M7384.10581.ANISN.LOAD90K(NELIB)'
//G.FT02F001 DD UNIT=SYSDA,DISP=(NEW,PASS),SPACE=(TRK,(10,5)),          X
//        DCB=(RECFM=VS,LRECL=1504,BLKSIZE=1608)
//G.FT03F001 DD UNIT=SYSDA,DISP=(NEW,PASS),SPACE=(TRK,(10,5)),          X
//        DCB=(RECFM=VS,LRECL=1504,BLKSIZE=1608)
//G.FT01F001 DD UNIT=SYSDA,DISP=(NEW,PASS),SPACE=(TRK,(10,5)),          X
//        DCB=(RECFM=VS,LRECL=1004,BLKSIZE=1008)
//G.FT04F001 DD UNIT=SYSDA,DISP=(NEW,PASS),SPACE=(TRK,(10,5)),          X
//        DCB=(RECFM=VS,LRECL=1004,BLKSIZE=1008)
//G.FT08F001 DD DSNAME=U.M7384.10581.ANISN.XS22N18G,
//        DISP=(OLD,PASS),LABEL=(,,,IN)
//G.SYSIN DD *
HTGR/GT REF DESIGN 2
1$$                     1         0         1         8         2
                        1         0         6        70         0        40
                        3         4        43        30         0        10
                       22         0         0         1         0         0
                       10         0         0         0         0        10
                        1         0         0         0         1         1
                        0
 16*             0.0       0.0       1.0   -03   1.421      317.0
   -0.0          0.0     1.1304+17   0.0         0.5        5.0   -04
    0.0          0.0       0.0       T
 13$
             1000      1001
             6000      6001
             8000      8001
            14000     14001
            26000     26001
  T
 17*
30R0.000127940R0.0    30R0.000781440R0.0    30R0.003211040R0.0
30R0.01306  40R0.0    30R0.03295  40R0.0    30R0.047    40R0.0
30R0.1047   40R0.0    30R0.08888  40R0.0    30R0.02136  40R0.0
30R0.1189   40R0.0    30R0.2171   40R0.0    30R0.196    40R0.0
30R0.1389   40R0.0    30R0.017    F0.0
  T
  T
  1*
    0.0001279   0.0007814   0.0032110   0.01306   0.03295   0.047
    0.1047      0.08888     0.02136     0.1189    0.2171    0.196
    0.1389      0.017       F0.0
  4*
2910.0    9I218.0    11291.15   3I298.77   3I319.09   19I334.33
  534.33
  5*          F1.0
  6*            0.0       2R0.0533004     0.0       4R0.0505859     0.0
    0.0505859   0.0365831 2R0.0505859   0.0365831     0.0505859     0.0        6*-2
    0.0533004 2R0.0505859 2R0.0533004 2R0.0505859     0.0533004                6*-3
  7*          -0.308607   -0.218218     0.218218    -0.617213   -0.577350
   -0.218218    0.218218    0.577350    -0.816497   -0.786796   -0.577350     7*-2
   -0.218218    0.218218    0.577350     0.786796   -0.975900   -0.951190     7*-3
   -0.786796   -0.577350   -0.218218     0.218218    0.577350    0.786796     7*-4
    0.951190                                                                  7*-5
 8$          30R        110R        2 2R        3 4R        4 4R        5
```

```
20R     6
 9$                 11          13          15          17          19
        21
10$
 3R    11 3R       12 2R       13 2R       14 2R       15 2R       16
 2R    17 2R       18 2R       19 2R       20 4R       21 4R       22
11$
            0          3           7
            0          4           8
            0          3
            0          4
            0          9
            0         10
            0          3
            0          4
            0          9
            0         10
            0          1           5           7
            0          2           6           8
12*
   0.0        0.06190     0.000737
   0.0        0.06190     0.000737
   0.0        0.05330
   0.0        0.05330
   0.0        0.08487
   0.0        0.08487
   0.0        0.08884
   0.0        0.08884
   0.0        0.08487
   0.0        0.08487
   0.0        0.006931    0.0229      0.02
   0.0        0.006931    0.0229      0.02
19$      6R        1
 T          T
/*
/*EOJ ********
```

B.3 2DB

2DB is a two-dimensional (XY, RZ, RΘ, triangular), multigroup diffusion code for use in fast reactor criticality or burnup analysis.

Depletion is done zone by zone. At present, the technique used to solve the burnup equations does not handle thermal reactor problems very well. It uses only a lumped fictitious fission product, not having a provision for yields from fission. In a thermal reactor where the role of the fission products is more important this approximation is not adequate. For that reason 2DB was used only in static runs in the HTGR/GT design calculations.

In comparing 2DB with CITATION for the treatment of static cases it was found that 2DB requires less memory (~25% cheaper runs), has a much simpler input requiring much less cards than CITATION and has 3 difficiencies that can be partially compensated by tricking the code or by minor modifications in the cs set: (a) it uses 215 MeV/fission to normalize the power while CITATION treats separately each fissile nuclide; (b) it does not have a provision for $\sigma(n,2n)$; (c) it does not have a provision for upscattering. The power normalization can be easily compensated by hand calculations; the problem with $\sigma(n,2n)$ and upscattering are compensated by changes in the cs.

Upscattering:

In a four group scheme (1 thermal group and 3 epithermal groups), upscattering from group 4 to group 3 is just a small contribution whose absence can be partially compensated with the use of an effective σ_{23} for the moderator. Consider the diffusion equation applied to groups 3 and 4:

$$-\Sigma_{23}\,\phi_2 + (D_3B^2 + \Sigma_{a3} + \Sigma_{34})\phi_3 - \Sigma_{43}\phi_4 = 0, \qquad \text{(B.3-1)}$$

and

$$-\Sigma_{34}\,\phi_3 + (D_4B^2 + \Sigma_{a4} + \Sigma_{43})\phi_4 = 0. \qquad \text{(B.3-2)}$$

Suppose now that Σ_{43} is null: Eqs. B.3-1 and B.3-2 would have been respectively:

$$\phi_3/\phi_2 = \Sigma_{23}/(D_3B^2 + \Sigma_{a3} + \Sigma_{34}), \qquad \text{(B.3-3)}$$

and

$$\phi_3/\phi_4 = (D_4B^2 + \Sigma_{a4})/\Sigma_{34}. \qquad \text{(B.3-4)}$$

The two ratios above are smaller than the correct ones including Σ_{43}. These two ratios can be made equal to the correct ones with the use of effective σ_{23} and σ_{24}. Since

$$[(D_3B^2 + \Sigma_{a3} + \Sigma_{34})(\phi_3/\phi_2)]_{correct} = \Sigma_{23} + \Sigma_{43}(\phi_4/\phi_2), \qquad \text{(B.3-5)}$$

$$(\Sigma_{23})_{eff} = \Sigma_{23} + \Sigma_{43}\,(\phi_4/\phi_2). \qquad \text{(B.3-6)}$$

Since carbon is the only nuclide with a non-zero σ_{43}, $(\sigma_{23})_{eff} = \sigma_{23}$ for all nuclides except carbon and

$$(\sigma_{23})_{eff} = \sigma_{23} + \sigma_{43}\,(\phi_4/\phi_2) \qquad \text{(B.3-7)}$$

for carbon. Analogously, since

$$[\Sigma_{34}\ \phi_3/\phi_4]_{\text{correct}} = D_4 B^2 + \Sigma_{a4} + \Sigma_{43} = D_4 B^2 + (\Sigma_{a^4})_{\text{eff}}, \quad \text{(B.3-8)}$$

$$(\sigma_{a4})_{\text{eff}} = \sigma_{a4} + \sigma_{43} \quad \text{(B.3-9)}$$

for carbon. This $(\sigma_{a4})_{\text{eff}}$ cannot be used though because its effect in the total absorption is too large. The use of an effective σ_{23}, $(\sigma_{23})_{\text{eff}}$, as in Equation B.3-7 was made in all 2DB runs and all CITATION runs after consulting Dr. Davison (see Section 2.1.1.2.2).

Lack of $\sigma(n,2n)$:

The absence of $\sigma(n,2n)$ brings two problems: (a) No U^{232} will appear from the n,2n interaction of U^{233}; (b) criticality.

The concentration of U^{232} is about 10^5 times smaller than that of U^{233} and its value does not have any noticeable influence in k_{eff}; it is calculated at GA because U^{232} is radioactive and its content in the U^{233} is important in U^{233} recycle; for the HTGR/GT case where no recycle will be made, the U^{232} content is irrelevant. The lack of $\sigma(n,2n)$ influence on k_{eff} can be compensated for by the use of effective absorption cs's. Consider the equation to calculate k_{eff}:

$$k_{eff} = \frac{\text{Production Rate}}{\text{Destruction Rate}} = \frac{\sum_j \nu^j \sum_{i=1}^{4} N^j \sigma_{fi}^i \phi_i + 2 \sum_{i=1}^{4} \sum_k N^k \sigma_i^k (n,2n) \phi_i}{\sum_{i=1}^{4} \sum_k N^k \sigma_{ai}^k \phi_i}$$

$$= \frac{\sum_j \nu^j \sum_{i=1}^{4} N^j \sigma_{fi}^i \phi_i}{\sum_{i=1}^{4} \sum_k N^k (\sigma_{ai}^k)_{\text{eff}} \phi_i}, \quad \text{(B.3-10)}$$

where the summation over j is for fissile nuclides and over k is for all nuclides. Since near criticality $k_{eff} \sim 1$,

$$\sum_k \sum_{i=1}^{4} N^k \sigma_{ai}^k \phi_i = \sum_k \sum_{i=1}^{4} N^k [2\sigma_i^k(n,2n) + (\sigma_{ai}^k)_{eff}]\phi_i . \qquad \text{(B.3-11)}$$

Since the fluxes of each neutron group i and each individual nuclide are independent, it follows that

$$(\sigma_{ai}^k)_{eff} = \sigma_{ai}^k - 2\sigma_i^k(n,2n). \qquad \text{(B.3-12)}$$

This equation can also be written as

$$(\sigma_{ai}^k)_{eff} = \sigma_{fi}^k + \sigma_{\gamma i}^k - \sigma_i^k(n,2n) \ , \qquad \text{(B.3-13)}$$

if one remembers that

$$\sigma_{ai}^k = \sigma_{fi}^k + \sigma_{\gamma i}^k + \sigma_i^k(n,2n) \ . \qquad \text{(B.3-14)}$$

It is important to mention that although CITATION has an option for the use of $\sigma(n,2n)$, this option can not be used together with the option for the resonance shielding correlation (Appendix A.3.3). For that reason the effective absorption cs's given by Eq. B.3-12 or B.3-13 were used in all the runs, with 2DB or CITATION. The value of $\sigma_i^k(n,2n)$ is of the order of 10^{-3} barns for i = 1 and zero for any other group, so $(\sigma_{ai}^k)_{eff} = \sigma_{ai}^k$ for $i \neq 1$ and not much lower than σ_{ai} for i = 1.

There follows an illustration for a typical 2DB input.

```
// *ANALYSIS RIBET-3,CLASS=A,REGION=200K
/*MITID USER=(M11535,12680,,DENISE)
/*SRI LOW
/*MAIN TIME=1,LINES=6
//STEP1 EXEC FORG,PROG='U.M11535.1054L.2DHFAST.NEWLOAD(NELIB)'
//G.FT03F001 DD UNIT=SYSDA,DISP=(NEW,DELETE),SPACE=(TRK,(10,10)),      X
//        DCB=(RECFM=VS,LRECL=1604,BLKSIZE=1608)
//G.FT04F001 DD UNIT=SYSDA,DISP=(NEW,DELETE),SPACE=(TRK,(10,10)),      X
//        DCB=(RECFM=VS,LRECL=2004,BLKSIZE=2008)
//G.FT08F001 DD UNIT=SYSDA,DISP=(NEW,DELETE),SPACE=(TRK,(10,10)),      X
//        DCB=(RECFM=VS,LRECL=2004,BLKSIZE=2008)
//G.FT09F001 DD UNIT=SYSDA,DISP=(NEW,DELETE),SPACE=(TRK,(10,10)),      X
//        DCB=(RECFM=VS,LRECL=2004,BLKSIZE=2008)
//G.FT10F001 DD UNIT=SYSDA,DISP=(NEW,DELETE),SPACE=(TRK,(10,10)),      X
//        DCB=(RECFM=VS,LRECL=1604,BLKSIZE=1608)
//G.SYSIN DD *
ARMY HTGR R-Z BOL STATIC 2DB FIRST RUN UNRODDED-SEP.,1974              2    CD01
     0     1     0     4     3     5          50    10     0
     1     6     5     2     7     7     1     0     0     1     0     0    CD03
         0.0         0.0         0.0         0.0         0.5         0.5    CD04
     0.00003         0.0003        0.0         1.0         1.4      -304.2    CD05
U238  238.05              CORE,HOT,C/U=4000                                 CD06
  6.76320-02  1.81243-01  1.96721-01  5.45743     5.02175     0.0
  0.0         0.0
  5.25206-11  1.22929+01  0.0         3.59861+01  2.36330+01  2.50637-01
  0.0         0.0
  9.95458-11  6.53815+01  0.0         7.78183+01  1.24010+01  6.01594-02
  0.0         0.0
  0.0         1.05319+00  0.0         1.17433+01  1.06901+01  3.57869-02
  0.0         0.0
U235  235.05              CORE,HOT,C/U=4000                                 CD06
  1.27033     1.39898     3.25238     5.40597     3.83927     0.0
  0.0         0.0
  1.25851+01  1.89305+01  3.05838+01  2.92793+01  1.03392+01  1.62185-01
  0.0         0.0
  3.43436+01  6.27115+01  8.34549+01  7.77132+01  1.49475+01  9.56718-03
  0.0         0.0
  1.84431+02  2.19357+02  4.48167+02  2.32064+02  1.27070+01  5.41935-02
  0.0         0.0
TH232 232.04              CORE,HOT,C/U=4000                                 CD06
  3.57550-02  1.67250-01  8.58610-02  5.34430     4.98730     0.0
  0.0         0.0
  5.58306-15  4.00577     0.0         2.24742+01  1.84571+01  1.81911-01
  0.0         0.0
  0.0         1.77361-01  0.0         1.18115+01  1.15838+01  1.13191-02
  0.0         0.0
  0.0         2.56462     0.0         1.45630+01  1.19984+01  5.03630-02
  0.0         0.0
CARBON12.011              CORE,C/U=4000                                     CD06
  0.0         1.58789-04  0.0         2.26492     2.06809     0.0
  0.0         0.0
  0.0         2.45014-05  0.0         4.39658     4.33582     1.96672-01
  0.0         0.0
  0.0         2.20025-04  0.0         4.48714     4.12032     6.22787-02
  3.18371-11  0.0
  0.0         1.27191-03  0.0         4.54142     4.54015     3.66596-01
  0.0         0.0
CREF  12.011              REFLECTOR,HOT                                     CD06
  0.0         7.59580-07  0.0         1.98076     1.76473     0.0
  0.0         0.0
```

```
   0.0          3.35931-05  0.0          4.38728      4.29964      2.16030-01
   0.0          0.0
   0.0          2.54030-04  0.0          4.12727      3.73899      8.76041-02
   0.0          0.0
   0.0          1.45200-03  0.0          4.48376      4.88181      3.88029-01
   0.0          0.0
2 3      0.02 1     215.5        384.53                                        CD10
2 2      0.02 1     157.5        276.53                                        CD11
1 4        11 2          24 2         61 6          24 1         63           CD12
           6              73                                                  CD13
         0.976        0.024          0.0          0.03                       CD15
1 4      1.0003                                                               CD16
1 5        61 2          73                                                  CD17
           0              1            2            3            4          0 CD18
           53
           0    0.0000013    0.0000174    0.0003514       0.0632          0 CD19
      0.088763
      0     2     0     0            0                                        CD24
```

B.4 HELIUM

HELIUM is a computer program to calculate the thermodynamical and transport properties of helium at any given pressure and temperature condition. There follows a HELIUM printout of 400 psi for temperatures from 950 to 1500°F.

TABLES OF HELIUM THERMODYNAMIC AND TRANSPORT PROPERTIES IN ENGLISH UNITS X

EACH TABLE GIVES PROPERTIES OVER THE TEMPERATURE RANGE OF INTEREST FOR THE PRESSURE SPECIFIED

THE UNITS FOR THE OUTPUT ARE SPECIFIED BELOW - -

P = PRESSURE (PSIA)
T = TEMPERATURE (F)
R = HELIUM GAS CONSTANT (BTU/LBM-F)
Z = COMPRESSIBILITY FACTOR (-)
RHO = DENSITY (LBM/FT3)
V = SPECIFIC VOLUME (FT3/LBM)
CP = SPECIFIC HEAT AT CONSTANT PRESSURE (BTU/LBM-F)
CV = SPECIFIC HEAT AT CONSTANT VOLUME (BTU/LBM-F)
CP/CV = RATIO OF SPECIFIC HEATS (-)
H = ENTHALPY (BTU/LBM)
S = ENTROPY (BTU/LBM-F)
VISCD = DYNAMIC VISCOSITY (LBM/HR-FT)
VISCK = KINEMATIC VISCOSITY (FT2/HR)
K = THERMAL CONDUCTIVITY (BTU/HR-FT2-F)
PR = PRANDTL NUMBER (-)
C* = SONIC VELOCITY (FT/SEC

THE EQUATIONS USED ARE IDENTIFIED BY 3 WHERE
1 = EIR TM-IN-410, VARADI,
2 = RISO - 224, PETERSEN,
3 = GA-1355, WILSON,
4 = MISCELLANEOUS, SEE TEXT IN SUBROUTINE MISC.

Information Processing Center
Information Processing Center
Information Processing Center

PRESSURE = 400.0 PSIA

T	RHO	V	Z	H	S	CP	CV	CP/CV	VISCD	VISCK	K	PR	C*	T
950.0	0.1053	9.50	1.0057	1765.4	6.357	1.2417	0.7455	1.66554	0.0928	0.8815	0.1772	0.64999	5430.8	950.0
1000.0	0.1017	9.84	1.0055	1827.5	6.400	1.2416	0.7455	1.66553	0.0950	0.9345	0.1814	0.65036	5525.2	1000.0
1050.0	0.0983	10.17	1.0054	1889.5	6.442	1.2416	0.7455	1.66551	0.0972	0.9887	0.1855	0.65070	5618.0	1050.0
1100.0	0.0952	10.51	1.0052	1951.6	6.483	1.2416	0.7455	1.66550	0.0994	1.0442	0.1896	0.65103	5709.3	1100.0
1150.0	0.0922	10.84	1.0050	2013.7	6.522	1.2416	0.7455	1.66549	0.1015	1.1009	0.1936	0.65134	5799.2	1150.0
1200.0	0.0895	11.18	1.0049	2075.8	6.560	1.2416	0.7455	1.66547	0.1037	1.1588	0.1975	0.65163	5887.7	1200.0
1250.0	0.0869	11.51	1.0048	2137.8	6.597	1.2416	0.7455	1.66546	0.1058	1.2178	0.2015	0.65192	5974.9	1250.0
1300.0	0.0844	11.85	1.0046	2199.9	6.632	1.2416	0.7455	1.66545	0.1079	1.2781	0.2054	0.65218	6060.8	1300.0
1350.0	0.0821	12.18	1.0045	2262.0	6.667	1.2416	0.7455	1.66544	0.1100	1.3395	0.2093	0.65244	6145.6	1350.0
1400.0	0.0799	12.52	1.0044	2324.1	6.701	1.2416	0.7455	1.66544	0.1120	1.4021	0.2131	0.65268	6229.1	1400.0
1450.0	0.0778	12.85	1.0043	2386.1	6.734	1.2416	0.7455	1.66543	0.1141	1.4659	0.2169	0.65292	6311.6	1450.0
1500.0	0.0758	13.19	1.0042	2448.2	6.766	1.2416	0.7455	1.66542	0.1161	1.5308	0.2207	0.65314	6393.0	1500.0

Information Processing Center
Information Processing Center
Information Processing Center

APPENDIX C

SOME TRIALS TO ADJUST LE CS TO REPRODUCE HE RESULTS IN RUNS WITHOUT Th^{232} and U^{238}

Table C-1 reproduces some important cs at operating temperature as received from Dragon (LE) and GA(HE). This original LE cs set received from Dragon is called LE1.

A second LE cs set, called LE2, was obtained by substituting the LE1 nat. B abs cs from each group by another one calculated from

$$(\sigma^B_{ai})_{LE2} = (\sigma^B_{ai}/\sigma^{25}_{fi})_{HE}\ (\sigma^{25}_{fi})_{LE1} \quad , \qquad \text{(C-1)}$$

for all the groups, that is, i = 1 to 4. The new values obtained (in barns) were: $(\sigma^B_{a1})_{LE2} = .11781$, $(\sigma^B_{a2})_{LE2} = 2.6117$, $(\sigma^B_{a3})_{LE2} = 38.292$ and $(\sigma^B_{a4})_{LE2} = 294.13$.

The LE run of Table 2.1.1.2.3-1 was repeated with the LE2 set and Table C-2 summarize the CITATION depletion output using this new set.

This modification in the nat. B cs made $(\Delta K_{eff}/\Delta t)_{LE2}$ almost as small as that of HE, but it increased the BOL difference in k_{eff}.

With the objective of getting a new set $(\sigma^B_{ai})_{LE3}$ with values slightly different from those of LE2 and such that $(k_{eff})_{LE} \equiv (k_{off})_{HE}$ at BOL, the following derivation was made. For the mentioned run without U^{238} and Th^{232} at BOL:

$$\left\{\frac{V\, N_{25} \sum_{i=1}^{4} \nu^{25}_i\, \sigma^{25}_{fi}\, \phi_i}{V \sum_{i=1}^{4} [N_B(\sigma^B_{ai})_{LE3} + N_{25}\sigma^{25}_{ai} + N_{xe}\sigma^{xe}_{ai} + N_c\sigma^c_{ai} + N_{Si}\sigma^{Si}_{ai}]\phi_i + L}\right\}_{LE3} = (k_{eff})_{HE} \quad , \qquad \text{(C-2)}$$

TABLE C-1

SOME IMPORTANT CS FROM THE LE AND HE SETS

Group	σ_a^{25}(LE)	σ_a^{25}(HE)	σ_f^{25}(LE)	σ_f^{25}(HE)	σ_a^{B}(LE)	σ_a^{B}(HE)	$(\sigma_a^B/\sigma_f^{25})_{LE}$	$(\sigma_a^B/\sigma_f^{25})_{HE}$
1	1.4121	1.3990	1.2680	1.2703	.11754	.11802	.09270	.09291
2	5.0980	18.9305	3.6623	12.5851	1.4967	5.5534	.40868	.44127
3	46.630	62.7115	26.788	34.3436	24.930	49.0918	.93064	1.4294
4	226.59	219.357	190.98	184.431	309.86	284.048	1.6225	1.5401

TABLE C-2

DEPLETION RESULTS FOR LE2 WITHOUT U^{238} AND Th^{232}, USING THE NAT. B ABS. CS AS GIVEN BY EQ. C-1

Time (days)	$(N_{25}$	$N_B)$ x 10^5 atoms/bcm	$(k_{eff})_{LE}$	$(k_{eff})_{HE}$-$(k_{eff})_{HE}$
0	4.860	1.709	1.2360	.0497
100	4.617	1.615	1.1921	.0570
360	3.996	1.377	1.1482	.0561
720	3.143	1.052	1.0902	.0535

where V is the volume of the core and L the leakage. With the values of ϕ_i from LE2 run and making

$$(\sigma^B_{ai})_{LE3} = \alpha(\sigma^B_{ai})_{LE2} \quad , \qquad \text{(C-3)}$$

it was possible to determine α = .98621 and obtain $(\sigma^B_{ai})_{LE3}$. A new computer run without U^{238} and Th^{232} was made; the $(k_{eff})_{LE3}$ obtained was still much lower than $(k_{eff})_{HE}$, though. With the exception of the last trial, called LE4, all the others caused a significant change in spectrum (see Table C-3) to invalidated the trial. In the case of LE4 (described below) no spectrum change occured but the result nonetheless was a surprise.

LE4 trial: It was observed that $(\text{Prod./abs.})^{25}_{HE}$ = 1.8503 and $(\text{Prod./abs.})^{25}_{LE3}$ = 1.8231 in the CITATION outputs. By inspection in the ratio $\nu\sigma^{25}_{fi}/\sigma^{25}_{ai}$ for LE and HE (see Table C-4) it can be seen that this ratio is always larger for LE except in group 1; it was then thought that if $(\nu\sigma^{25}_{fi}/\sigma^{25}_{ai})_{LE} \geq (\nu\sigma^{25}_{fi}/\sigma^{25}_{ai})_{HE}$ for an i, $(\text{Prod./abs})^{25}_{LE4}$ would be larger than $(\text{Prod./abs})^{25}_{HE}$. The LE4 trial was then: LE3 with $(\sigma^{25}_{a1})_{LE4} = (\nu\sigma^{25}_{f1})_{LE}/(\nu\sigma^{25}_{f1}/\sigma^{25}_{a1})_{HE}$.

Surprisingly enough the output with LE4 cs had still a $(\text{Prod./abs})^{25}_{LE4}$ = 1.8233 < 1.8503.

To check the possibility of a mistake in the cs (highly improbable after several earlier checks) the ratio $(\text{Prod./abs})^{25}$ was calculated by hand for LE4 and HE using the fluxes from the CITATION outputs and the equation below:

TABLE C-3

NEUTRON SPECTRUM AT BOL FOR SEVERAL COMPOSITIONS & CS

Description of run	C/HM	(ϕ_1	ϕ_2	ϕ_3	ϕ_4)x10^{-13} n/sec cc
LE w/out U^{238}, Th^{232} and nat B	15,550	3.36	4.75	6.18	26.9
LW w/out U^{238} and Th^{232} (LE1)	1,280	3.23	4.45	4.19	1.60
LE w/out U^{238} and Th^{232} (LE2)	1,280	3.38	4.51	4.14	1.60
LE w/out U^{238} and Th^{232} (LE3)	1,280	3.27	4.49	4.13	1.60
LE w/out U^{238} and Th^{232} (LE4)	1,280	3.27	4.49	4.13	1.60
LE complete unrodded	397	3.67	5.03	4.30	1.74
HE w/out U^{238}, Th^{232} and nat B	15,550	3.28	10.3	1.69	27.8
HE w/out U^{238} and Th^{232}	1,280	3.05	7.79	1.10	1.62
HE complete unrodded	158	3.59	7.35	1.06	2.02

TABLE C-4

$\nu\sigma_f^{25}/\sigma_a^{25}$ FOR LE AND HE

Group	1	2	3	4
LE	2.300	1.746	1.396	2.048
HE	2.325	1.616	1.331	2.043

$$\frac{(\text{Prod/abs})^{25}_{HE}}{(\text{Prod/abs})^{25}_{LE}} = \frac{\sum_i (\nu_i \sigma^{25}_{fi} \phi_i)_{HE}}{\sum_i (\sigma^{25}_{ai} \phi_i)_{HE}} \Big/ \frac{\sum_i (\nu_i \sigma^{25}_{fi} \phi_i)_{LE4}}{\sum_i (\sigma^{25}_{ai} \phi_i)_{LE4}} = \frac{\sum_i [(\nu_i \sigma^{25}_{fi}/\sigma^{25}_{ai})\sigma^{25}_{ai} \phi_i]_{HE}}{\sum_i (\sigma^{25}_{ai} \phi_i)_{HE}} \Big/ \frac{\sum_i [(\nu_i \sigma^{25}_{fi}/\sigma^{25}_{ai})\sigma^{25}_{ai} \phi_i]_{LE4}}{\sum_i (\sigma^{25}_{ai} \phi_i)_{LE4}}$$

(C-4)

After substitution by numerical values, although $(\nu_i \sigma^{25}_{fi}/\sigma^{25}_{ai})_{LE4} \geq (\nu_i \sigma^{25}_{fi}/\sigma^{25}_{ai})_{HE}$ for any i, $(\text{Prod/abs})^{25}_{HE} > (\text{Prod/abs})^{25}_{LE}$ checking exactly with the CITATION output:

$$\frac{(P/A)^{25}_{HE}}{(P/A)^{25}_{LE4}} = \frac{(2.325)(4.2610)+(1.616)(147.40)+(1.331)(68.919)+(2.043)(354.60)}{4.2610 + 147.40 + 68.919 + 354.60} \Big/ \frac{(2.325)(4.6110)+(1.746)(22.885)+(1.396)(192.57)+(2.048)(363.67)}{4.6110 + 22.885 + 192.57 + 363.67} =$$

$$\frac{1.8503}{1.8233};$$

this result is caused entirely by the spectrum differences.

APPENDIX D

SYMBOLS AND ABBREVIATIONS

abs.	absorption
AEC	Atomic Energy Commission
BP	Burnable poison
BU	Burnup
conc.	concentration
CR	Control rod
cs	cross section
c/u	carbon-to-uranium ratio (atom densities)
Eq.	Equation
Fig.	Figure
FIMA	Fissions per initial heavy metal atom
FP	Fission products
FRD	Final reference design
FSV	Fort Saint Vrain
GA	General Atomic
GT	Gas turbine
HE	High enrichment
HM	Heavy metal
HTGR	High Temperature Gas-Cooled Reactor
HTGR/GT	High Temperature Gas-Cooled Reactor/Gas Turbine
LBP	Lumped burnable poison
LMFBR	Liquid Metal Fast Breeder Reactor
LWR	Light Water Reactor
max.	maximum
MWD/T,GWD/T	10^6 watt-days/ton, 10^9 watt-days/ton

MIT	Massachusetts Institute of Technology
nat.	natural
nvt	neutron fluence
PARF	Parfait configuration
PCRV	Prestressed concrete reactor vessel
RD	Reference design
Ref.	Reference (bibliographic)
SNG	Synthetic natural gas
T_{CL}	Center line temperature

BIOGRAPHICAL NOTE

The author was born in the city of Rio de Janeiro, Brazil, on the second day of June, 1943.

In 1960 he entered the Federal School of Technical Chemistry, receiving the degree of Chemistry Technician in 1962. During the next five years he attended classes at the School of Chemistry of the Federal University of Rio de Janeiro (SCh FURJ), graduating as a Chemical Engineer in December, 1967. To help maintain his studies while in the SCh FURJ he participated in several renumerated activities: (a) Technical Drawer; (b) Lecturer of Chemistry; (c) Precis writter of conferences; (d) one year fellowship at the Radioisotopes Laboratory of the SCh FURJ sponsored by the Brazilian National Nuclear Energy Commission (CNEN) in 1964; (e) one year of industrial training at "Companhia de Petroleos de Manguinhos" during 1966; (f) one year of industrial training at "Solutec S/A" (an EXXON subsidiary) during 1967.

In the next two years after graduation the author worked as a Chemical Engineer for CNEN in the Heavy Water Group. In 1970 he was selected to take part in an especial CNEN program whose objective was to sponsor doctorate studies in nuclear engineering in outstanding universities abroad. After attending some introductory courses in Brazil, he applied for admission to MIT and was accepted to start in February, 1972. In May, 1974 he received an MS in Nuclear Engineering and started working on the present Ph.D. thesis.

The author has been married to Denise Telles Ribeiro since December, 1966 and has a 5 year old son named Andre.

REFERENCES

1. Nida, A. von, "Nuclear Total Utility System for Military Installations", M.S. Thesis, M.I.T., January 1974.

2. Feher, R.D., "A Brayton-Cycle HTGR for a total Energy Application", Nuclear Engineering Thesis, M.I.T., May 1974.

3. Hoppes, D.F., "Investigations of Axial Fuel Shuffling Schemes for a High-Temperature Gas-Cooled Reactor", M.S. Thesis presented at Georgia Institute of Technology, March 1972.

4. Hansen, U., "Fuel Management Strategies for the Low Enriched 600 MWe Dragon-HHT Reactor", Dragon Project Report 862, England, November 1973.

5. Merril, M.H., "Nuclear Methods and Experimental Data in Use at Gulf Central Atomic", Gulf-GA-A12652 (GA-LTR-2), July 1973.

6. Driscoll, M.J., "Nuclear Reactor Design", Course 22.33 at M.I.T., Fall 1973.

7. General Atomic, "Nuclear Design Methods in Use at General Atomic", General Atomic, June 1967.

8. Ducat, G.A., M.J. Driscoll and N.E.Todreas, "Evaluation of the Parfait Blanket Concept for Fast Breeder Reactors", COO-2250-5, MITNE-157, January 1974.

9. Maly, V. and E. Teuchert, "Power Profile Manipulation in Block-Fuel HTGRS", Nuclear Technology Vol. 22, June 1974.

10. Fowler, T.B., D.R. Vondy and G.W. Cunningham, "Nuclear Reactor Core Analysis Code: CITATION", ORNL-TM-2496, Rev. 2, July 1971.

11. Birely, W.C., "Operating Experience of the Peach Bottom Atomic Power Station", CONF-740501, May 1974.

12. Gutman, H., U. Hansen, H. Larsen, H.J. Neff and R.H. Brogli, "Alternative Fuel Cycles for HTGR's", ANS-Symp. HTGR & GCFR, CONF 740501, Gatlinburg, May 1974.

13. Hansen, U., "KPD Present Worth Fuel Cycle Calculation Methods and Codes", D.P. Report 811, England, September 1972.

14. Hick, H., "Status of Models Describing the Mechanical Performance of Coated Particles Fuels", 2nd Int.Conf. on Structural Mechanics in Reactor Tech., Berlin, September 1973, paper C1/1.

15. Martin, D.G., "A Simple, Reasonable Accurate Model for Calculating Stresses in the Layers of Coated Fuel Particles During Irradiation", 2nd Int. Conf. on Structural Mechanics in Reactor Tech., Berlin, September 1973, paper C1/5.

16. Bennet, L.L., and R.K. Lane, "Fuel Management Flexibilities of the Th-U^{233} Cycle", CONF-740501, Gatlinburg, May 1974.

17. Nordwall, H.J., and W.E. Bell, "Fission Product Control in HTGR Plants", CONF-740501, Catlinburg, May 1974.

18. Ribeiro, A.A.T., "Flow Orificing in Nuclear Power Reactors", M.S. Thesis presented at M.I.T., May 1974.

19. Stansfield, O.M., T.D. Gulden and D.P. Harmon, "Fuel Kernel Materials for the Th Cycle HTGR", Gulf-GA-A12632, June 29, 1973.

20. General Atomic, "HTGR Fact Sheet", 1973.

21. Gulden, T.D., J.L. Scott and C. Moreau, "Present Th-Cycle Concepts and Performance Limitations", CONF-740501, Gatlinburg, May 1974.

22. Little, Jr., W.W. and R.W. Hardie, "2DB Users Manual-Revision1", BNWL-831 REV1 UC-32, August 1969.

23. Walker, R.E. and T.A. Johnston, "Fort Saint Vrain Nuclear Power Station", Nuc. Eng'g International, December 1969.

24. Dahlberg, R.C., R.F. Turner and W.V. Goeddel, "Core Design Characteristics, "Nuclear Eng'g International, December 1969.

25. Brogli, R.H., R.C. Dahlberg and C.H. George, "Plutonium Utilization in the HTGR", Trans. Am. Nucl. Soc. Vol. 17, November 1973.

26. Marshall, A.C., "Cross Sections for the Fort Saint Vrain Initial Core", Gulf-GA-B12406, November 1972.

27. Glasstone,S. and A. Sesonske, "Nuclear Reactor Engineering", International Student Editions, 1967.

28. Soodak, H., "Reactor Handbook", Vol. III, Part A, Physics, 1962.

29. Lamarsh, J.R., "Introduction to Nuclear Reactor Theory", Addison-Wesley Pub. Co., Inc., 1966.

30. Prados, J.W. and J.L. Scott, "Mathematical Model for Predicting Coated-Particle Behavior", Nuclear Applications, Vol. 2, October 1966.

31. Rockenhauser, W., "Prestressed Concrete Pressure Vessels for Power Reactors", GA-7162, June 8, 1966.

32. Delmarva Power & Light Co., "PSAR Summit Power Station".

33. Fischer, P.U., S. Jaye and H.B. Stewart, "Alternate Fuel Cycles for the HTGR", pp. 745-60 of Advanced and High-Temperature Gas-Cooled Reactors, Vienna, Int. Atomic Energy Agency, 1969. See STI/PUB-197; CONF-681008

34. Shepherd, L.R., "Development of Coated Particle Fuels for High Temperature Reactors", JBNES, 1970.

35. Phyladelphia Electric Co., PSAR Fulton Generating Station, Units 1 and 2", Docket-50463-6 Unclas., 1973.

36. Garrison, J.D. and B.W. Roos, "Fission-Product Capture Cross Sections", Nuclear Science and Engineering: 12, 115-134, 1962.

37. USAEC, "Reactor Physics Constants", ANL-5800, 2nd edition, July 1963.

38. Davison, W., "HTGR Cross Sections for Transmittal to M.I.T.," Internal Correspondence Gulf 973, General Atomic, July 24, 1974.

39. Private correspondence with Dr. H. Gutmann, Head of the Physics Branch, O.E.C.D. High Temperature Reactor Project, July, 1974.

40. Insch, G.M. and A.J. Joyce, "The Low Enriched HTG", CONF-740501, pages 146-161, May, 1974.

41. Melese-d'Hospital, G., "Simplified Analysis of Coolant Flow and Outlet Temperature in Gas-Cooled Nuclear Reactor Cores", Nuc. Sci. and Eng'g: 35,165-175, (1969).

42. Hansen, U., R. Shulten and E. Teuchert, "Physical Properties of the Once Through Then Out Pebble-Bed Reactor", Nuc. Sci. and Eng'g: 47,132-139 (1972).

43. Kaae, J.L., D.W. Stevens and C.S. Luby, "Prediction of the Irradiation Performance of Coated Particle Fuels by Means of Stress-Analysis Models", Nuclear Technology Vol. 10, January, 1971.

44. Kaae, J.L., "Mathematical Model for Calculating Stress in a Pyrocarbon and Silicon Carbide-Coated Fuel Particle", Journal of Nuclear Materials 29 (1969), 249-266.

45. Oehme, H., "Comparative HTGR-Designs", CONF-740501, pages 72-91, Gatlinburg, May 1974.

46. Graham, L.W., M.S.T. Price, R.A. Saunders and E. Smith, "HTR Fuel Development and Testing in the Dragon Project," CONF-740501, Gatlinburg, May 1974.

47. Engle, G.B., M.R. Everett and W.P. Eatherly, "Status of Graphite Technology and Requirements for HTGR's, CONF-740501, Gatlinburg, May 1974.

48. Dahlberg, R.C., K. Asmussen, D.Lee, L. Brooks and R.K. Lane, "HTGR Fuel and Fuel Cycle", Nuc. Eng'g and Design 26(1974) 58-77.

49. Dahlberg, R.C., "Comparison of HTGR Fuel Cycles for Large Reactors, GA-10069, April 1970.

50. Boyer, V.S., J.P. Gibbons, T.A. Johnston, R.H. Hoe, K.D. Feldtmose and W.C. Drotleff, "Fulton Station HTGR", Nuc. Eng'g International, August 1974.

51. Dahlberg, R.C., R.F. Turner and W.V. Goeddel, "HTGR Fuel and Fuel Cycle Summary Description", GA-A12801 (Rev), January 1974.

52. Dahlberg, R.C., "Nuclear Fuel and Power Management", HTGR Fuel Management - Class Notes, General Atomic Co.

53. Lane, R.K., C.H. George and R.C. Dahlberg, "Comparative Fuel Utilization in the HTGR and PWR", Gulf GA-A12592, April 1973.

54. Driscoll, M.J., "Nuclear Reactor Design", Course 22.33, at M.I.T., Fall 1974.

55. El-Wakil, M.M., "Nuclear Heat Transport", International Textbook Co., 1971.

56. Gutmann, H. and F. Woloch, "Temperature Coefficients of the First Dragon Charge", D.P. Report 703, September 1970.

57. Goodjohn, A.J. and G.C. Pomraning, "Reactor Physics in the Resonance and Thermal Regions, Vol II Resonance Absorption", The MIT Press, 1966.

58. Bondarenko, I.I., et al., "Group Constants for Nuclear Reactor Calculations", Consultants Bureau, New York, 1964.

59. Hughes, D.J., et al., "Neutron Cross Sections", BNL-325, Second Edition (1958) plus supplements (1960, 1964 and 1965).

60. Patterson, R.M., R.P. Christman and E.J. Hennelly, "Resonance Self Shielding Factors for Heavy Actinides", Journal of Nuclear Energy, Vol. 24, pp 53-56. Pergamon Press 1970.

61. Benedict, Manson, "Economics of Nuclear Power", Course 22.34 at MIT, Spring 1973.

62. DaSilva, R.A., "An Analytical Model for Study of Plutonium Recycle in PWR Core", M.S. Thesis submitted at MIT, June 1974.

63. Nirsche, R.J., E.M. Gillett and J.R. Brown, "Experimental and Analytical Results for HTGR Type Control Rods of Hf and B in the HTGR Critical Facility", Gulf-GA-A9354 Jan. 1973.

64. Sha, W.T., "An Analysis of Reactivity Worth of the Rod Cluster Control (RCC) Elements and Local Water-Hole Power Density", WCAP-3269-47, May 1965.

65. Spiegel, M.R., "Mathematical Handbook of Formulas and Tables", McGraw-Hill Book Co., 1968.

66. G.A., "Public Service Co. of Colorado 330 MWe HTGR R&D Program Quaterly Progress Report for the Period Ending in June 1966", GA-7314.

67. Meghreblian, R.V. and D.K. Holmes, "Reactor Analysis", McGraw-Hill Book Co., Inc., 1960.

68. G.A. "Pub. Serv. Co. of Colorado 330MWeHTGR R&D Program QPR for the Period Ending in March 31, 1971", GA-10560, April 1971.

69. G.A., "Pub Serv. Co. of Colorado 330MWe HTGR R&D Program QPR for the Period Ending June 1971", GULF-GA-10754, July 1971.

70. G.A., "Pub. Serv. Co. of Colorado 330 MWe HTGR R&D Program QPR for the period ending in December 1970", GA-10444, Jan. 1971.

71. G.A., "Pub. Serv. Co. of Colorado 330 MWe HTGR R&D Program QPR for the period ending in June 30, 1970", GA-10202, July, 1970.

72. Private correspondence with Dr. Albert C. Marshall, from GA, on Feb. 20, 1975.

73. Public Service Co. of Colorado, "Fort St. Vrain Nuclear Power Station PSAR", Pub. Serv. Co. of Colorado, September 1966.

74. Piccinini, N., "Coated Nuclear Fuel Particles", Advances in Nuclear Sciences and Technology, Vol. 8, 1974.

75. Shepherd, L.R., "Reactor Developments for High Temperature Processes", Energia Nucleare, Vol. 22/n.3/Marzo 1975.

76. AEC, "Current Status & Future Technical & Economic Potential of Light Water Reactors", WASH -1082, March 1968.

77. Wilson, Jr., M.P., "Thermodynamic and Transport Properties of Helium", GA-1355, January 1960 .

78. Eaton, Thomas E., "Comments on the Calculation of Thermodynamic and Transport Properties of Helium", MITNE-166, November 1974.

79. Engle, Jr., W.W., "ANISN", A1-66-MEMO-171, NAA-SR 10951 .

80. Morrison, G.W., G.A. Straker, and R.H. Odi Garden, "A Coupled Neutron and Gamma Ray Multigroup Cross Section Library for Use in Shielding Calculation", Trans. Am. Nuc. Soc., 15, 1, pp 535, (June 1972).

81. Scheinert, P.A. and M.J. Driscoll, "Gamma Heating Measurements in Fast Breeder Reactor Blankets", COO-2250-10, MITNE-164, August 1974.

82. Shin, J.I., and M.J. Driscoll, "Conceptual Design of a Small HTGR for Total Energy Applications at Military Installations", Nuc. Engineering Thesis, M.I.T., May 1975.

83. Ikawa, K and K. Iwamoto, J. Nucl. Mater. 45, 67 (1972).

84. Shimokawa, J., T. Yasuno, S. Yasukawa and H. Ishikawa, "Design Concept of Experimental Multi-Purpose VHTR", Paper No. 89 Presented at European Nuclear Conference, Paris, April 22, 1975.

85. Private meeting with H. Hick, C. Hunt, H. Larsen and T.C. Steemers from O.E.C.D. HTR Project, May 1975, M.I.T..

86. Metcalfe, L.J., "Economic Assessment of Alternative Total Energy Systems for Large Military Installations", M.S. Thesis at M.I.T. August 1975.

87. Stengle, R.G., "Thermal-Hydraulic Analysis of a 100 MW(e) HTGR, M.S. Thesis at M.I.T., August 1975.

88. Barry, R.F., "LEOPARD - A Spectrum Dependent, Non-Spatial Depletion Code for the IBM-7094", WCAP-3269-26, Westinghouse Electric Corp. (1973).

89. Poncelet, C.G., "LASER - A Depletion Program for Lattice Calculations Based on MUFT and THERMOS", WCAP-6073, Westinghouse Electric Corp (1966).

90. "Conference on Prestressed Concrete Pressure Vessels", Group A Paper 1, p. 2, Church House, Westminster S.W.I, 13-17 March 1967.

91. Public Service Co. of Colorado, "Fort Saint Vrain Nuclear Generating Station, Final Safety Analysis Report", Docket 50267-17, Vol. 4, Nov. 1969.

92. United Engineers and Constructors Inc., "Boiling Water Reactor Plant, 1000 MWe, Central Station Power Plant Investment Cost Study", WASH-1230, Vol. 2, June, 1972 .

93. Rohsenow, W.M. and H. Choi, "Heat, Mass and Momentum Transfer", Prentice-Hall, Inc., 1961 .

94. McLain, S. and J.H. Martens, "Reactor Handbood, Vol. IV Engineering", Interscience Publishers, 1964.

95. Bowers, H.I., et al, "CONCEPT-III Computerized Conceptual Estimates for Steam-Electric Power Plants, Phase II Users Manual", ORNL-4809, April 1973.

96. Pilat, E.E., H. Guéron and D.D. Lanning, "Measurement of the Diffusion Coefficient in a Highly Anisotropic Medium", Trans. Am. Nucl. Soc., 8, 446 (1965).

97. Steele, L. E., "Neutron Irradiation Embrittlement of Reactor Pressure Vessel Steels", I.A.E.A., Vienna, 1975.

98. Public Service Co. of Colorado, "Fort Saint Vrain Nuclear Generating Station, FSAR", Docket 50267-17, Vol. 4, 1969.

99. Philadelphia Electric Co., "Final Hazards Summary Report: Peach Bottom Atomic Power Station", NP-9115, 1963; Docket-50171-1-7, 1964.

100. Yellowlees, J. M. and R. Scheider, "Safety of the HTR", in "Advanced and High Temperature Gas Cooled Reactors", IAEA, Vienna, 1969.

101. Adir, J. and R. D. Larthrop, "Theory of Methods used in the GGC-3 Multigroup Cross Section Code", GA-7156, July 1967.